



UNIL | Université de Lausanne

Unicentre

CH-1015 Lausanne

<http://serval.unil.ch>

Year : 2021

A MULTIDISCIPLINARY APPROACH TO UNRAVEL THE ENVIRONMENTAL AND CLIMATIC HISTORY OF LAKE LIAMBEZI IN THE CAPRIVI, NAMIBIA

Lehmann Anaël Jonas

Lehmann Anaël Jonas, 2021, A MULTIDISCIPLINARY APPROACH TO UNRAVEL THE ENVIRONMENTAL AND CLIMATIC HISTORY OF LAKE LIAMBEZI IN THE CAPRIVI, NAMIBIA

Originally published at : Thesis, University of Lausanne

Posted at the University of Lausanne Open Archive <http://serval.unil.ch>

Document URN : urn:nbn:ch:serval-BIB_70D3B3A2D5B18

Droits d'auteur

L'Université de Lausanne attire expressément l'attention des utilisateurs sur le fait que tous les documents publiés dans l'Archive SERVAL sont protégés par le droit d'auteur, conformément à la loi fédérale sur le droit d'auteur et les droits voisins (LDA). A ce titre, il est indispensable d'obtenir le consentement préalable de l'auteur et/ou de l'éditeur avant toute utilisation d'une oeuvre ou d'une partie d'une oeuvre ne relevant pas d'une utilisation à des fins personnelles au sens de la LDA (art. 19, al. 1 lettre a). A défaut, tout contrevenant s'expose aux sanctions prévues par cette loi. Nous déclinons toute responsabilité en la matière.

Copyright

The University of Lausanne expressly draws the attention of users to the fact that all documents published in the SERVAL Archive are protected by copyright in accordance with federal law on copyright and similar rights (LDA). Accordingly it is indispensable to obtain prior consent from the author and/or publisher before any use of a work or part of a work for purposes other than personal use within the meaning of LDA (art. 19, para. 1 letter a). Failure to do so will expose offenders to the sanctions laid down by this law. We accept no liability in this respect.



UNIL | Université de Lausanne

Faculté des Géosciences et de l'Environnement
Institut des Dynamiques de la Surface Terrestre
Université de Lausanne

**A MULTIDISCIPLINARY APPROACH TO UNRAVEL THE ENVIRONMENTAL AND CLIMATIC
HISTORY OF LAKE LIAMBEZI IN THE CAPRIVI, NAMIBIA**

Thèse de Doctorat

Présentée à la

Faculté des Géosciences et de l'Environnement de l'Université de Lausanne

Pour l'obtention du grade de

Docteur en Sciences de la Terre

par

Anaël Jonas LEHMANN

Maîtrise universitaire ès Sciences en Géologie à l'École Lémanique des Sciences de la Terre et
de l'Environnement (ELSTE) conjointe aux Universités de Genève et Lausanne

Directeur de thèse

Prof. Dr. Torsten Vennemann

Jury

Prof. Dr. Torsten Vennemann	Président
Prof. Dr. Christian Kull	Rapporteur
Prof. Dr. Pilar Junier	Expert
Prof. Dr. Eric Verrecchia	Expert
Prof. Dr. Daniel Ariztegui	Expert
Dr. Jakob Zopfi	Expert

Université de Lausanne

2021

La Reprographie – UNIL

Lausanne

2021

IMPRIMATUR

Vu le rapport présenté par le jury d'examen, composé de

Président de la séance publique :	M. le Professeur Christian Kull
Président du colloque :	M. le Professeur Christian Kull
Directeur de thèse :	M. le Professeur Torsten Vennemann
Expert interne :	M. le Professeur Eric Verrecchia
Expert externe :	M. le Professeur Daniel Ariztegui
Experte externe :	Mme la Professeure Pilar Junier
Expert externe :	M. le Professeur Jakob Zopfi

Le Doyen de la Faculté des géosciences et de l'environnement autorise l'impression de la thèse de

Monsieur Anaël Lehmann

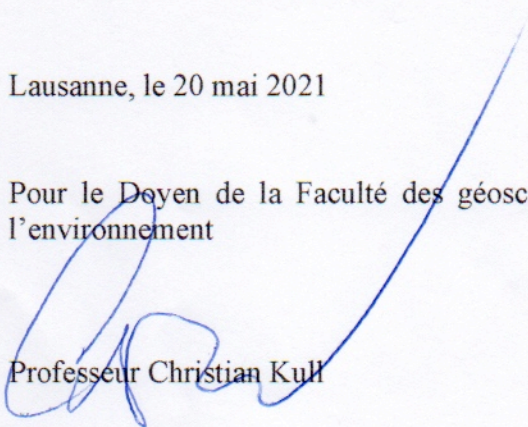
*Titulaire d'un
Master ès Sciences en géologie
de l'Université de Lausanne*

intitulée

**A multidisciplinary approach to unravel the
environmental and climatic history of Lake Liambezi in
northern Botswana**

Lausanne, le 20 mai 2021

Pour le Doyen de la Faculté des géosciences et de
l'environnement


Professeur Christian Kull



UNIL | Université de Lausanne

Faculty of Geosciences and Environment
Institute of Earth Surface Dynamics
University of Lausanne

**A MULTIDISCIPLINARY APPROACH TO UNRAVEL THE ENVIRONMENTAL AND CLIMATIC
HISTORY OF LAKE LIAMBEZI IN THE CAPRIVI, NAMIBIA**

Ph.D. thesis

Presented at the
Faculty of Geosciences and Environment of the University of Lausanne

To obtain the grade of
Ph.D. in Earth Sciences

by

Anaël Jonas LEHMANN

M.Sc. of Science in Geology at joint School of Earth and Environmental Sciences
of the Geneva and Lausanne Universities (ELSTE)

Thesis director

Prof. Dr. Torsten Vennemann

Jury

Prof. Dr. Torsten Vennemann	President
Prof. Dr. Christian Kull	Rapporteur
Prof. Dr. Pilar Junier	Expert
Prof. Dr. Eric Verrecchia	Expert
Prof. Dr. Daniel Ariztegui	Expert
Dr. Jakob Zopfi	Expert

University of Lausanne
2021

La Reprographie – UNIL
Lausanne
2021



UNIL | Université de Lausanne

Unicentre
CH-1015 Lausanne
<http://serval.unil.ch>

2021

A multidisciplinary approach to unravel the environmental and climatic history of Lake Liambezi in the Caprivi, Namibia

Anaël Jonas LEHMANN

Anaël Jonas LEHMANN, 2021, "A multidisciplinary approach to unravel the environmental and climatic history of Lake Liambezi in the Caprivi, Namibia"

Originally published at: Thesis, University of Lausanne

Posted at the University of Lausanne Open Archive <http://serval.unil.ch>

Document URN:

Droits d'auteur

L'Université de Lausanne attire expressément l'attention des utilisateurs sur le fait que tous les documents publiés dans l'Archive SERVAL sont protégés par le droit d'auteur, conformément à la loi fédérale sur le droit d'auteur et les droits voisins (LDA). A ce titre, il est indispensable d'obtenir le consentement préalable de l'auteur et/ou de l'éditeur avant toute utilisation d'une œuvre ou d'une partie d'une œuvre ne relevant pas d'une utilisation à des fins personnelles au sens de la LDA (art. 19, al. 1 lettre a). A défaut, tout contrevenant s'expose aux sanctions prévues par cette loi. Nous déclinons toute responsabilité en la matière.

Copyright

The University of Lausanne expressly draws the attention of users to the fact that all documents published in the SERVAL Archive are protected by copyright in accordance with federal law on copyright and similar rights (LDA). Accordingly it is indispensable to obtain prior consent from the author and/or publisher before any use of a work or part of a work for purposes other than personal use within the meaning of LDA (art. 19, para. 1 letter a). Failure to do so will expose offenders to the sanctions laid down by this law. We accept no liability in this respect.



Lake Liambezi, northern basin, March 2017
Fishermen on their mokoro

Acknowledgements

- Torsten Vennemann, my supervisor, for his confidence, help, support, enthusiasm, great ideas, great field experiences. Thank you for giving me the opportunity of realising this incredible job and this exceptional adventure.
- Christophe Paul, my friend and colleague. Thank you for the long discussions and the detail corrections. Thank you also for having shared your profession of heart with your music group and for making me discover this wonderful music.
- Sevasti Filippidou, my lab colleague, for having shared your lab experience with me.
- Mathilda Fatton, my field assistant, for accompanying me during the second field campaign.
- Shannon Dyer and Léandre Ballif, my field assistants, for accompanying me during the first (and the second for Shannon as well) field campaign.
- John VanThuyne, founder and director of the VanThuyne-Ridge Research Center, friend and colleague, for the ideas, the development and the realization of the present project.
- The VTR Research Center Team, for their welcome and the organization of our stay at the center.
- Ali Mainga, guide of the VTR Research Center, for his experience and exceptional knowledge of the field.
- Eric Verrecchia, for his knowledge and his help for laboratories and data's interpretations.
- David Sebag, Thierry Adatte, Jorge Spangenberg, Laetitia Monbaron and Micaela Faria for their help in the laboratories and some data treatment.
- Pilar Junier and Daniel Ariztegui, for the discussion about the project.
- Michael Rowley and Zoneibe Luz, exceptional friends, for having shared all those years together in our reputable and recognized office. Your friendship is precious.
- My parents Isabelle and Jacques-Alain Lehmann and Laurence's parents, for their unconditional support.
- All my friends from the ski team, diving team and VTT friends, for allowing me to clear my spirits in outdoor activities and thus share exceptional moments.
- And last but not least! My wife Laurence and my son Camille, for everything and more.
THANK YOU!!!

Table of contents

Acknowledgements	iii
Table of contents	iv
Summaries	1
Summary	2
Résumé	3
Preface	5
References.....	8
Foreword to the main chapters	9
1. General Introduction	12
1.1. Introduction.....	12
1.2. Regional settings	14
1.2.1. Linyanti-Chobe Basin	14
1.2.2. Geology and tectonism.....	15
1.2.3. Hydrothermal activity.....	24
1.2.4. Cuando, Kwando, Linyanti, Chobe and Zambezi Rivers	24
1.2.5. Climate and flood system.....	25
1.2.6. Soils.....	26
1.2.7. Vegetation	28
1.2.8. Lake Liambezi and its ecology	29
1.3. Objectives of the project	30
1.4. Prior description of the secondary sites sampled	32
1.4.1. BO01: Thamalakane	32
1.4.2. BO02: Rileys Cresta.....	32
1.4.3. BO03: Khwai River (Kudumane)	32
1.4.4. BO04: Mababe Bridge	32
1.4.5. BO05 and BO06: Linyanti.....	32
1.4.6. BO07: Chobe.....	32
1.4.7. BO08: Kavimba	33
1.4.8. BO09: Lake Liambezi.....	33
1.5. Additional projects:	33
1.6. References.....	34
2. Vegetation and soil carbon and nitrogen contents and stable isotope compositions in savannas of northern Botswana as environmental proxies	38
2.1. Abstract	38
2.2. Introduction.....	39

2.3.	Material and methods	40
2.3.1.	Regional settings of northern Botswana	40
2.3.2.	Bioclimatic data	41
2.3.3.	Sampling	42
2.3.4.	Geochemical analyses	43
2.4.	Results	43
2.5.	Discussion	48
2.5.1.	Geographical distribution of vegetation zones in the Linyanti-Chobe basin	48
2.5.2.	Vegetation classes and isotopic compositions	50
2.5.2.1.	Reed beds	50
2.5.2.2.	Sedgeland	50
2.5.2.3.	Floodplain grassland	50
2.5.2.4.	<i>Combretum</i> /Kalahari shrubland 5b and <i>Acacia-Combretum</i> /mixed marginal/riverine woodland 6b.....	51
2.5.2.5.	Dry grassland	51
2.5.2.6.	Mopane shrubland 5a and Mopane woodland 6a	51
2.5.3.	Estimation of water stress using isotope composition	52
2.5.4.	Plant-soil-sediment isotopic relationships	55
2.5.5.	Nitrogen isotopes	56
2.6.	Conclusions.....	58
2.7.	References.....	60
3.	Sedimentology, mineralogy and geochemistry of sediments from Lake Liambezi, Namibia-Botswana	62
3.1.	Abstract	62
3.2.	Introduction.....	63
3.3.	Material and methods	64
3.3.1.	Regional and lake settings.....	64
3.3.2.	Coring	65
3.3.3.	Mineralogical and geochemical analyses	65
3.4.	Results	66
3.5.	Discussion	81
3.5.1.	Origin of the organic matter.....	81
3.5.2.	Grain-size: End-member analysis	85
3.5.3.	Silica – abundance and origin	88
3.5.4.	Origin of the sediment components and importance of clays.....	89
3.5.5.	Discussion of the sulphur content and the pyrite occurrence and their implication to the redox conditions: a complementary presence	90

Table of contents

3.5.6.	Barium origin	91
3.5.7.	Characterization of type of deposit.....	92
3.6.	Conclusion	92
	Acknowledgments.....	93
3.7.	References.....	94
4.	Cross correlation of bacterial communities and geological proxies in paleoecology: a holistic approach for the study of past environmental history.....	96
4.1.	Abstract	96
4.2.	Introduction.....	97
4.3.	Material and methods.....	98
4.3.1.	Regional settings and lake description.....	98
4.3.2.	Sampling	99
4.3.3.	Use of data obtained by the RockEval method as environmental tracer	100
4.3.4.	DNA extraction	100
4.3.5.	Sequencing and date analysis.....	101
4.3.6.	Statistical and multivariate analysis	101
4.4.	Results	102
4.4.1.	North Core	106
4.4.2.	Center Core.....	106
4.4.3.	South Core	106
4.5.	Discussion	106
4.5.1.	Applicability of using bacterial DNA for sediments: Bacterial Community Composition (BCC) changes as environmental tracer	106
4.5.2.	Hydrothermalism and Sulphur oxidation	107
4.5.3.	Importance of the climate facing the sites.....	110
4.5.4.	Cores interpretation	111
4.5.4.1.	North Core	111
4.5.4.1.1.	Lower section (NC23-NC15)	112
4.5.4.1.2.	Mid-section (NC14-NC04).....	112
4.5.4.1.3.	Upper section (NC02)	113
4.5.4.2.	Center Core.....	113
4.5.4.2.1.	Lower section (CC29-CC20)	114
4.5.4.2.2.	Mid-section (CC17-CC12).....	114
4.5.4.2.3.	CC10-CC08	115
4.5.4.2.4.	Upper section (CC05-CC02)	115
4.5.4.3.	South Core	116

4.5.4.3.1.	Lower section (SC23-SC17)	116
4.5.4.3.2.	Upper section (SC16-SC01)	117
4.6.	Conclusion	119
4.7.	References	120
4.8.	Supplementary material	124
4.8.1.	Detailed description of the cores	124
4.8.1.1.	North Core	124
4.8.1.1.1.	Sedimentology and texture	124
4.8.1.1.2.	Geochemistry	124
4.8.1.1.3.	Microbiology	124
4.8.1.2.	Center Core	125
4.8.1.2.1.	Sedimentology and texture	125
4.8.1.2.2.	Geochemistry	125
4.8.1.2.3.	Microbiology	126
4.8.1.3.	South Core	127
4.8.1.3.1.	Sedimentology and texture	127
4.8.1.3.2.	Geochemistry	127
4.8.1.3.3.	Microbiology	127
5.	Dating the sediments of Lake Liambezi, Namibia-Botswana	129
5.1.	Abstract	129
5.2.	Introduction	130
5.3.	Material and methods	130
5.3.1.	Regional settings and lake description	130
5.3.2.	Sampling	131
5.4.	Results	132
5.4.1.	Radiocarbon dating	132
5.5.	Discussion	132
5.5.1.	Sources of the organic matter	132
5.5.2.	Dating	133
5.5.2.1.	Limitations of ¹⁴ C dating in this lake	134
5.5.3.	Correlation using clay minerals	134
5.5.4.	Correlation using microbiological communities	136
5.5.5.	Average vertical accretion rate	141
5.6.	Conclusion	141
5.7.	References	142

Table of contents

6.	Lake Liambezi: a climatic and environmental record for the last 5500 years BP through a multidisciplinary study.....	143
6.1.	Abstract	143
6.2.	Introduction.....	144
6.3.	Material and methods.....	145
6.3.1.	Regional settings and lake description.....	145
6.3.2.	Sampling.....	146
6.4.	Results	146
6.5.	Discussion.....	146
6.5.1.	General remarks on sediment characteristics.....	146
6.5.2.	General climatic reconstruction and comparison to other studies.....	147
6.5.3.	Understanding the environmental evolution of Lake Liambezi.....	150
6.5.4.	General history of Lake Liambezi: from its supposed tectonic origin to its filling with lacustrine sediments according to climatic and environmental evolutions	151
6.5.5.	Grain-sizes: geomorphological evolution in relationship with the evolution of the end-member analysis	154
6.5.6.	Bacterial Community Composition (BCC) evolution and characteristics	156
6.5.7.	Mineralogy and hydrothermalism.....	161
6.5.8.	Reviews and discussion of a potential reworking of top part for North and Center Cores	161
6.6.	Conclusion	162
6.7.	References.....	163
7.	General conclusion	165
7.1.	Initial questions	167
7.2.	Weaknesses of present work	171
7.3.	Evolution of the region.....	171
7.4.	Perspectives.....	172
7.5.	References.....	174
8.	Appendix: Poster presentations, data and collaborations.....	176
8.1.	Poster presentations	176
8.2.	Water data.....	182
8.2.1.	Samples name, location and other details.....	182
8.2.2.	Data for the dry season	183
8.2.3.	Data for the wet season	184
8.3.	Vegetation data:.....	185
8.3.1.	Species and mean geochemical values	185
8.3.2.	Geochemical data of different parts of four reference trees.....	186

8.4.	Soils data	187
8.5.	Tributaries data	189
8.5.1.	Samples name, location and other details	189
8.5.2.	Mineralogy data	189
8.5.3.	Major elements data	189
8.5.4.	Trace elements data	190
8.5.5.	Organic matter data	190
8.5.1.	Grain-size data	191
8.6.	Lake Liambezi sediments data	192
8.6.1.	Samples name, location and other details	192
8.6.2.	Radiocarbon data and estimated climatic and environmental data for estimated age model	192
8.6.3.	Mineralogy data	193
8.6.4.	Major elements data	194
8.6.5.	Trace elements data	195
8.6.6.	Organic matter data	196
8.6.7.	Grain-size data	197
8.6.8.	SEM images	200
8.6.9.	Selection of photos of Lake Liambezi and its tributaries as well as sampling and laboratory work	204
8.7.	Joeri Lakes data	207
8.7.1.	Water data	207
8.7.2.	Radiocarbon data	207
8.7.3.	Grain-size data	208
8.7.4.	Major elements data	217
8.7.1.	Organic matter data	219
8.8.	Bacterial spores, from ecology to biotechnology	221
9.	Curriculum vitæ	254

Summaries

A multidisciplinary approach to unravel the environmental and climatic history of Lake Liambezi in the Caprivi, Namibia

Keywords: multidisciplinary studies, paleoenvironment, paleoecology, sediment, geochemistry, organic matter, microbiology

Approche multidisciplinaire pour une meilleure compréhension de l'histoire environnementale et climatique du lac Liambezi dans la région de Caprivi en Namibie

Mots-clés: études multidisciplinaires, paléo-environnement, paléoécologie, sédiment, géochimie, matière organique, microbiologie

Summary

Paleoecology is the study of the history of an ecosystem using sedimentary records. Analyses of the mineralogical, chemical, isotopic and biological composition of the sediment can provide clues on the past environmental conditions of a particular ecosystem. The topic is of particular importance today since many lakes, river deltas or marshlands are subjected to increasing anthropogenic influence related to population growth and a parallel increase in agricultural and industrial activity. In many cases, these ecosystems are of important social, ecological, and economic value to the population living within the watershed of this precious water resource. Wetlands in arid climates represent unique ecosystems and are of major importance for an often specialized flora and fauna. They represent a life-supporting water source in an otherwise inhospitable environment. These environments are, however, particularly fragile ecosystems as they respond sensitively to any climatic or environmental changes.

The present study focuses on the regions of the Caprivi in Namibia and of northern Botswana. These regions hold the second largest endorheic delta system in the world. This specific landscape is the result of an active tectonic activity related to the East African Rift system and accommodating differential movements between different plates and rigid cratons. It results in a deformation zone called Okavango Graben that presents normal faults all along these two regions. These normal faults affect and control the course of the Okavango, Kwando and Zambezi Rivers and form a complex system of rivers and waterbodies. A minor change in tectonism and faulting can influence the morphology and hence the drainage pattern of the entire system. The Okavango Delta has been described through numerous studies already. In contrast, the region of the Linyanti-Chobe Basin with Lake Liambezi in its middle remains poorly studied or understood. Moreover, studies on the Quaternary climate evolution in northern Namibia and Botswana demonstrated the difficulty to find or target paleo-environmental archives with well-dated proxies and results might show inconsistencies or even contradictions. Therefore, the choice was made to focus on this extraordinary region, showing a high complexity of connection between the different rivers and waterbodies.

Lake Liambezi has been investigated through a number of sediment cores using a multidisciplinary approach including mineralogy, geochemistry, organic matter composition and a novel use of bacterial DNA populations. A climatic and environmental evolution of the lake and its surroundings is proposed for the last 5400 years BP. This highlighted an alternation of relatively dry and wet periods, and changes in the hydrological lake regime. However, major evolutions and changes in shape and environmental settings of the lake can also be related to the tectonic activity linked to the Okavango Graben. This was supported by the marked presence of thermophilic bacteria. A first sediment record is estimated at about 5420 years BP and is described as the tectonic opening of Lake Liambezi's north basin. An extension of this basin was likely developed at around 1650 years BP. The second basin of the lake was probably created during the last known tectonic event dated at around 1000 years BP. Successively, the resulting depressions are filled with lacustrine and fluvio-deltaic sediments. The watershed, the climate and the morphology of the site define the environmental conditions of the lake and therefore control the sediment types and content.

To target paleo-environmental archives with well-dated proxies is challenging, certainly in tectonically active continental systems. The present work demonstrates the relevance of using a multidisciplinary approach in such complex systems. The integrated approach of using multidisciplinary methods does allow for an elaboration of a coherent age model for Lake Liambezi with a coherent environmental and climatic evolution. This approach also demonstrated the potential of using bacterial DNA (total and/or lysis-resistant) to identify changes and variability in the environmental conditions of such an environment. The multidisciplinary approach including characterization of bacterial DNA populations might therefore be developed for future projects in diverse types of environments.

Résumé

La paléoécologie est l'étude de l'histoire d'un écosystème à l'aide d'enregistrements sédimentaires. L'étude des conditions environnementales passées d'un écosystème particulier se fait grâce à l'analyse de la composition minéralogique, chimique, isotopique et biologique de ses sédiments. Le sujet revêt aujourd'hui une importance particulière avec un impact grandissant de l'influence anthropique liée à la croissance démographique et à l'augmentation parallèle de l'activité agricole et industrielle subie par de nombreux lacs, deltas ou marais. En plus de représenter une précieuse ressource en eau, ces écosystèmes se révèlent également être importants pour le tissu social, écologique et économique des populations présentes au sein du bassin versant. Les milieux humides en climat aride représentent un type d'écosystème particulier d'importance majeure pour une flore et une faune souvent spécialisées dont la présence d'eau dans ce milieu inhospitalier représente une source vitale. Cependant, ces milieux représentent des écosystèmes particulièrement fragiles car ils réagissent de manière sensible à tout changement climatique ou environnemental.

L'étude présente se concentre sur les régions de Caprivi, en Namibie ainsi que du nord Botswana. Ces régions contiennent le deuxième plus grand delta endoréique du monde. La spécificité de ce paysage est le résultat d'une activité tectonique active liée au rift est-africain et de l'accommodation de cette dernière avec les mouvements différentiels entre plaques tectoniques et cratons rigides. Il en résulte une zone de déformation appelée Okavango Graben qui se traduit par la présence de failles normales sur toute la surface de ces deux régions. Ce réseau de failles affecte et contrôle le cours des rivières Okavango, Kwando et Zambèze. Il en résulte un réseau complexe de chenaux et de plans d'eau. Un mouvement de faille liée à l'activité tectonique de la région, même mineur, peut démontrer une redistribution complète du réseau de rivières suite à l'impact géomorphologique. De nombreuses études se sont concentrées sur le delta de l'Okavango. En revanche, le bassin de Linyanti-Chobe ainsi que le lac Liambezi situé en son centre n'ont été que peu étudiés et de nombreux sujets restent à découvrir. De plus, les études sur le climat du Quaternaire dans les régions du nord de la Namibie et du Botswana ont démontré la difficulté d'obtenir des archives paléo-environnementales contenant un matériel permettant une datation fiable et précise. Les résultats obtenus présentent parfois des incohérences, voire même des contradictions. Le choix s'est donc porté sur cette région d'une richesse naturelle exceptionnelle, montrant une grande complexité de connexion entre les rivières et les différents plans d'eau.

Le lac Liambezi a été étudié à l'aide de carottes de sédiments en utilisant une approche multidisciplinaire incluant la minéralogie, la géochimie, la composition de la matière organique ainsi qu'une méthode novatrice visant à l'utilisation de l'ADN de populations de bactéries. Une reconstruction de l'évolution climatique et environnementale pour la région du lac Liambezi comprenant les derniers 5400 ans AP est proposée. Il en résulte la description de l'alternance de périodes relativement sèches et humides ainsi que l'observation de changements dans le régime hydrologique du lac Liambezi. Toutefois, les modifications majeures au sein du lac, tel que l'évolution de sa forme ainsi que l'évolution de ses conditions environnementales, semblent être reliées à l'activité tectonique liée au graben de l'Okavango. La présence importante de bactéries thermophiles soutient cette hypothèse. Une première datation estimée à 5420 ans AP semble démontrer l'ouverture tectonique du bassin nord du lac Liambezi. L'extension de ce premier bassin intervient probablement aux alentours de 1650 ans AP. Le bassin sud se forme lors du dernier événement tectonique enregistré, daté à environ 1000 ans AP. Les dépressions ainsi formées se remplissent dès lors de sédiments de types lacustres et fluvio-deltaïques. Le type de sédiment est contrôlé par les conditions environnementales qui découlent du bassin versant, du climat et de la géomorphologie du site.

Les matériaux permettant une datation précise au sein d'archives paléo-environnementales de milieux continentaux avec une activité tectonique sont difficiles à cibler. Le travail présent démontre la pertinence d'une approche multidisciplinaire dans un milieu aussi complexe. L'utilisation intégrée

Summaries

des diverses méthodes a permis la construction d'un modèle d'âge cohérent pour les sédiments du lac Liambezi ainsi qu'une reconstruction paléo-environnementale et paléo-climatique pertinentes. Cette approche a permis en outre de démontrer le potentiel indéniable de l'utilisation d'ADN de bactérie (populations totales et/ou sporulantes) pour identifier les changements et la variabilité des conditions environnementales d'un tel milieu. Une telle approche, y incluant l'utilisation d'ADN de bactérie est tout-à-fait pertinente pour une utilisation à plus large spectre d'environnements.

Preface

Paleoecology is of particular importance today since many lakes, river deltas or marshlands are subjected to increasing anthropogenic influence related to population growth and a parallel increase in agricultural and industrial activity. In order to be relevant, paleoecology may ask to use methods from a wide variety of fields. This multidisciplinary approach requires the coordination of sometimes distant fields with methods specific to each. Technical and scientific progress also makes it possible to develop new methods or new perspectives on known methods. This makes it possible to highlight aspects previously unheard of or to observe a given site from a new angle. This reflection is at the origin of the current project and aims at the development and validation of a new approach in microbiology and was funded by the SNF.

Spore-forming bacteria have been recently proposed as an innovative proxy for the reconstruction of past environments by the laboratory of Microbiology at the University of Neuchâtel. The method has been developed with samples from Lake Geneva and from Lake Baikal. The results for Lake Geneva demonstrated a direct and identifiable link in the evolution of microbiological communities and the environmental evolution of the lake. Thus, major climatic events such as a particularly cold winter or technological development in wastewater treatment or even a political decision to ban the use of certain products are reflected in the composition of the microbiological communities of the lake (see the description of the project in the Appendix). The development of such a new method ask therefore for a well-documented and known environmental history to allow an easier understanding of the microbiological results. The extension of the project was then to evaluate the potential of generalizing the combined approach of endospores and complimentary chemical methods to lakes of diverse environmental settings. In this context, the choice of the site was crucial. The site had to demonstrate a different environment type and climate. However, even with different settings, the choice for a lake with well understood environmental settings and well-described environmental history was important in order to facilitate the evaluation of generalizing the combined approach endospores and complimentary chemical methods. Therefore, the choice fell on a lake in India as well as a group of lakes in Graubünden. The Indian lake was supposed to be the main topic of my thesis work where the group of lakes in Graubünden was a side project and has been in fact covered in a Master thesis (Fatton-Hayoz, 2018).

The choice of the lake in India was made through the development of an exchange program for researchers between the Faculty of Geosciences and Environment at the University of Lausanne and the School of Biotechnology, KIIT University (Kalinga Institute of Industrial Technology) in Bhubaneswar, headed by Prof. M. Suar, and in agreement with the Chilika Development Authority (CDA), headed by Dr. A.K. Pattnaik. In this context, the research group of the Stable Isotope Laboratory at the University of Lausanne has conducted an exploratory work on that lake through numerous Master thesis. These various projects aimed at a better understanding of the hydrological cycle, geochemical cycle as well as the sedimentologic and ecological evolution of Chilika Lake in the county of Orissa in India (Bourgeois, 2015; Delavy & Ecuyer, 2014; Hostettler, 2015; Lange, 2014). It did permit to bring additional information to existing works aiming at the ecological evolution and environmental history of the lake (e.g., Khandelwal et al., 2008). Chilika Lake, the largest lagoon on the Asian continent and second-largest lagoon on Earth, is located on the east coast of India, just south of the Bay of Bengal. This lagoon has been selected for the present study as it is situated in a completely different climatic zone and has quite different hydrologic conditions compared to Lake Geneva but, analogous to Lake Geneva or other lakes and estuarine systems, the anthropogenic influence on Chilika Lake has substantially changed over the past century (e.g., Ghosh and Pattnaik, 2005). It is thus of interest to examine the use of spore-forming bacteria as paleolimnological proxies under these different conditions. The aim was to collect three sediment cores at specific sites of about 2.5 to 3 m corresponding ideally to the last 2'000 to 4'000 years following estimation made after previous works

of Khandelwal et al. (2008) and Zachmann et al. (2009). The last several thousand of years are of particular interest to the microbiological and biogeochemical studies as the previous work on pollen by Khandelwal et al. (2008) has shown substantial biological changes, some of them likely anthropogenic in origin. In addition, the agricultural practices have changed drastically and as a result processes of siltation and the nutrient cycles have been impacted (Ghosh & Pattnaik, 2005).

At the same time, under my impulse and the support of my supervisor, a collaboration was undertaken between the research group of the Stable Isotope Laboratory at the University of Lausanne and the VanThuyne-Ridge Research Center in Botswana in order to conduct scientific missions in the region that covers northern Botswana. The collaboration focused on various environmental aspects related to hydrology as well as the geochemistry of plant cover and its relationship to soils. This collaboration was built through two MSc thesis, which were to serve as a basis for future work (Ballif, 2018; Dyer, 2017). As part of this exploratory work carried out in August 2016, one of the main missions was also to assess the potential of the northern Botswana region for future work. To do this, the two MSc thesis covered a wide region. However, human stories triggered a total overhaul of the project and a drastic redirection of the original goals.

Following changes at the head of several working groups on the Indian side (including the regional government of the state of Orissa as well as at the School of Biotechnology, KIIT University in Bhubaneswar), the exchange program as well as current projects were stopped immediately and the collaboration unilaterally cancelled by the Indian side. This happened only two months before our team was supposed to fly to India. Material, day-to-day program, visa applications and team were booked and ready to go. These cancellations led to an urgent overhaul of the project. Carrying out exploratory work in parallel in the northern region of Botswana, a redirection of the initial project in this region was evaluated. In the urgency of a project redirection, Lake Liambezi, drawing the border between Namibia and Botswana was chosen as a replacement site.

As the thesis will describe in the following chapters, with the exception of a study on the limnology of Lake Liambezi (Seaman et al., 1978) as well as a study on its fish population (Peel et al., 2015), Lake Liambezi and its direct region have only been very little studied. In addition, the environmental history of the North Botswana region is debated and the various studies concerned are not all in agreement (e.g., Thomas et al., 2012) and many studies remain to be done. The work in this region is therefore completely exploratory and the use of spore-forming bacteria is also carried out as an exploratory method. The conclusions obtained from the results of the present work can therefore be subject to discussion and above all, to evolution. It is legitimate that future work on the region will make it possible to complete and provide details on certain sedimentation mechanisms as well as on the interpretation of the sediments and the environmental history of Lake Liambezi site.

The present work offers a description of the sedimentology of the lake as well as an estimation of the environmental history of the lake. It provides a solid description of the sediment and its different components. It provides also a large panel of methods and demonstrates what utility for each method. This thus facilitates planning for future studies on this site, or at least on the Lake Liambezi region in the choice of methods and subjects.

The present study has demonstrated a Lake Liambezi preserved from a measurable anthropogenic impact. This study therefore makes it possible to draw up an inventory before anthropogenic modification of this environment. This is very interesting information because it shows that the surrounding populations have a way of life that do not show a measurable impact on water or on sediments with the methods used by the present study. It will therefore be interesting to come back to these results in a few years in order to see if the current economic development of Angola will be sufficiently important to be observed in the water and sediments of Lake Liambezi. Being an environment allowing the development of a lake in an arid environment, the site of Lake Liambezi is

unique, with the development of a specific flora and fauna. However, due to these characteristics, it is also a very fragile environment and extremely sensitive to the climatic and environmental evolution (as demonstrated by the present work). It is therefore also interesting to be able to offer a current inventory in order to better understand the future evolution linked to the current climate change.

The Lake Liambezi sampling campaign was therefore carried out in March 2017. New field, new issues... The fate seeming to be bitter about the field authorizations, three weeks before leaving, the expected permits were refused to us. The reason was that the authorities in Botswana wished to reform the issuance of permits and in the meantime, all permits have been suspended. The lake being located between Namibia and Botswana, we therefore urgently took steps to obtain a sampling permit from the Namibian authorities (thank you Torsten!). These steps finally allowed us to leave as planned. Regarding the field campaign itself, we faced a hardware problem with unsuitable pipes. It was agreed that we would get some on site and unfortunately this could not be the case. So we had to use replacement pipes. Despite these various misadventures (probably typical in the organization of an explorative work), the field campaign was completed and allowed us to bring back three sediment cores. The material problems we faced did not allow us to take any additional one. Furthermore, the sediment depth was much shallower than expected and sediment cores were thus shorter than expected. However, these various disappointments are part of the game and will serve as an experience for the organization of future work in this region.

As a final preamble, this project was built to lie at the intersection of several independent disciplines: limnogeology, aqueous geochemistry and microbiology. It was then meant to be an interdisciplinary research. Indeed, although the study of microbial community composition in sediments can be done in an isolated way, only when the environmental context is considered, can the interpretation of the changes observed take its full dimension. In this case, the interdisciplinary approach will allow not only the valorisation of a significant sampling effort of sediment cores, but also the global validation of a novel biological approach for the reconstruction of the environmental history of freshwater bodies. Each approach to be used has its own strengths and weaknesses in terms of being able to trace the original ecological conditions that may have existed in the past. The data are complementary and each method did permit to refine the possible interpretations that can be made. The work presented below is therefore a total success from this perspective.

References

- Ballif, L. 2018. Carbon and nitrogen stable isotope compositions as environmental proxies in savannas of northern Botswana. Unpubl. Master of Science in Biogeosciences, UNIL.
- Bourgeois, G., 2015. Historical sediment record in Chilika Lake, India: geochemical, mineralogical and micropaleontological study. Unpubl. Master of Science in Biogeosciences, University of Lausanne.
- Delavy, K. & Ecuyer, M., 2014. Isotopic study of the spatial and temporal origin, source and dynamic of organic matter in Chilika Lake's estuarine ecosystem. Unpubl. Master of Science in Biogeosciences, University of Lausanne.
- Dyer, S. 2017. Water cycle in the Northern Kalahari. Unpubl. Master of Science in Biogeosciences, UNIL.
- Fatton-Hayoz, M. 2018. Investigation of bacterial communities in high mountain lakes: Total versus spores's fractions. Unpubl. Master of Science in Biogeosciences, UNINE.
- Ghosh, A.K. & Pattnaik, A.K. 2005. Chilika Lagoon, experience and lessons learned brief.
- Hostettler, C., 2015. Ecology and geochemistry of living ostracods in Chilika Lake, India. Unpubl. Master of Science in the Institute of Earth Dynamic, University of Lausanne.
- Khandelwal, A., Mohanti, M., García-Rodríguez, F. and Scharf, B.W. 2008. Vegetation history and sea level variations during the last 13,500 years inferred from a pollen record at Chilika Lake, Orissa, India. *Veget Hist Archaeobot* 17, 335-344.
- Lange, P., 2014. Water dynamics in Cjilika Lake (India). Unpubl. Master of Science in Geosciences of the Environment, University of Lausanne.
- Peel, R.A., Tweddle, D., Simasiku, E.K., Martin, G.D., Lubanda, J., Hay, C.J., Weyl, O.L.F. 2015: Ecology, fish and fishery of Lake Liambezi, a recently refilled floodplain lake in the Zambezi Region, Namibia. *African Journal of Aquatic Science* 40:4, 417-424.
- Seaman, M.T., Scott, W.E., Walmsley, R.D., van der Waal, B.C.W., & Toerien, D.F. 1978: A limnological investigation of Lake Liambezi, Caprivi. *Journal of the Limnological Society of Southern Africa* 4:2, 129-144.
- Thomas, D.S.G. & Burrough, S.L, 2012. Interpreting geoproxies of late Quaternary climate change in African drylands: Implications for understanding environmental change and early human behaviour. *Quaternary International*, 253, 5-17.
- Zachmann, D.W., Mohanti, M., Treutler, H.C., Scharf, B. 2009. Assessment of element distribution and heavy metal contamination in Chilika Lake sediments (India). *Lakes & Reservoirs: Research & Management* 14, 105-125.

Foreword to the main chapters

Vegetation and soil carbon and nitrogen contents and stable isotope compositions in savannas of northern Botswana as environmental proxies

This chapter aims at the geochemical investigation of the soils and vegetation of the Linyanti-Chobe Basin. A few rivers are investigated as well and bring additional information about the geochemistry of sediments coming from the watershed of Lake Liambezi.

This chapter partly takes up the work presented by Léandre Ballif in his master's thesis entitled "Carbon and nitrogen stable isotope compositions as environmental proxies in savannas of northern Botswana (unpubl. Master of Science in Biogeosciences, UNIL)". The project was thought out, written and organized by T. Vennemann and myself. The field was then designed in a collaborative way between T. Vennemann, L. Ballif and myself. Field work and sampling has been made with the same team in August 2016. The analyses as well as the interpretation of the results were then carried out by L. Ballif and are summarized in his master's thesis (Ballif, 2018). I subsequently took up his writings and summarized them in the present chapter. However, I added a number of sub-chapters to them. These sub-chapters notably contain the results and interpretations of river sediments as well as work on the construction of a regional vegetation transect and a humidity gradient. I therefore reorganized the work of L. Ballif into a thesis chapter and estimate my share of work for this chapter at one third of the total work.

Sedimentology, mineralogy and geochemistry of sediments from Lake Liambezi, Namibia-Botswana

This chapter aims at the first investigation on Lake Liambezi's sedimentology. A precise description of the material found in the sediments is made with a discussion on their origin and quality.

The storyline of the chapter as well as all the different descriptions and discussions were written by myself. These discussions were then discussed and improved with the co-authors. Prof. Eric Verrecchia has also largely contributed to a few specific subjects such as the descriptions made using SEM as well as the grain-size distribution.

Cross correlation of bacterial communities and geological proxies in paleoecology: a holistic approach for the study of past environmental history

This chapter introduces the novel approach using microbiology. It is made through a precise description of the evolution of the sediments through depth. In this context, data acquired with more classical methods are added to obtain a direct comparison of the results and to build a global discussion of the evolution of each sampled site. This chapter allows the validation of the use of the microbiology as an environmental tracer in lake sediments; not only in actual sediments, but also in older sediments corresponding to past environmental conditions. Thus, the microbiological approach used in the present work did permit to trace and characterize past environmental conditions.

Description of the bacterial communities were produced by Dr. Christophe Paul and already presented in his Ph.D. thesis. However, many improvements have been made to the first text and this is an improved version written by myself and subsequently edited by the co-authors of this chapter.

Dating the sediments of Lake Liambezi, Namibia-Botswana

After a precise description on the sediment sources and the evolution of the cored sites regarding the sedimentology, this chapter aims at giving a chronological framework to the sediments. The chosen multidisciplinary method shows all its strength in this exercise. The age model is built after a combination of multiple methods. Radiocarbon dating is complemented with diverse relative dating methods using clay mineralogy and microbiology datasets.

Foreword to the main chapters

The storyline of the chapter as well as the different descriptions and discussions were written by myself. A few sections have been reworked and improved by Dr. Christophe Paul. It was then also discussed and improved with the co-authors.

Lake Liambezi: a climatic and environmental record for the last 5500 years BP through a multidisciplinary study

This chapter is a compilation of all the previous studies and aims at giving a precise environmental and climatic history for Lake Liambezi.

Dr. Christophe Paul helped in the discussion of some sections of the chapter. It was then also subsequently edited by the co-authors of this chapter.

General conclusion

The general conclusion aims at summarising all results and main findings. It provides a general view of the environmental and climatic context of northern Botswana. It also reviews the initial questions. It concludes with various perspectives for further possible investigations.

Appendix: Poster presentations, data and collaborations

This chapter brings together the posters and their summaries of the two conferences to which I presented my work. These are the poster presentation session of the 16th Swiss Geoscience Meeting in Bern, Switzerland, 1st December 2018 and the poster presentation session of the EGU General Assembly in Vienna, Austria, 7–12 April 2019.

All the analyses carried out within the framework of this thesis are to be found next. First, there is the data from water analyses collected in northern Botswana and presented in the work of Dyer (2017). Then there are data on vegetation, soils and sedimentological analyses of rivers in northern Botswana. Data on the sedimentology of Lake Liambezi are presented next. A chapter also presents a selection of photos taken at Lake Liambezi during the two field campaigns. The chapter also offers a photo of the two tributaries Linyanti and Chobe Rivers as well as a photo of the sample collection work for the microbiology and sedimentology laboratories in controlled atmosphere and sterilized equipment at the VanThuyne-Ridge Research Center. The photos of all the other sampling sites can be found in the digital version of the thesis. A final data chapter brings together the data from all the water and sediment analyses that were carried out for the Joeri Lakes. Part of this data is used in the work of Fatton-Hayoz (2018). Microbiological data for the rivers of northern Botswana, for Lake Liambezi as well as for the Joeri Lakes can be found in more detail in the work of Paul (2019) and Fatton-Hayoz (2018). The details of the data carried out in XRD analyses can be found in the digital version of the present work (calculations of peaks, mineralogical curves, etc.).

The paper from the collaboration between the microbiology and isotope teams is added in this appendix chapter. Its title is “Bacterial spores, from ecology to biotechnology” and is a review summarizing the current knowledge on bacterial spores, with a particular emphasis on their environmental significance and their application in biotechnology. It was published as a book chapter. Spore formation is a common feature widespread among the tree of life. It consists on the ability of an organism to enter a dormant state to withstand unfavorable environmental conditions. As a review, this paper went over the different types of spores known among bacteria, and their cellular process, but also present new discoveries such as an unsuspected diversity of potential spore-formers, and propose different possible applications, from ARG tracking to sustainable agriculture.” As explained in Paul, 2019 – Ph.D. Thesis.

As member of the doctoral program in Earth Surface Processes & Paleobiosphere of the Conférence Universitaire de Suisse Orientale (CUSO), I get the opportunity to participate in an ecological survey campaign in the Maldives. This campaign was then fixed in three publications. My

participation in these publications lies in data collection as well as group discussions aimed at understanding the data and their interpretation. A first paper is entitled “Responses of reef bioindicators to recent temperature anomalies in distinct areas of the North Ari and Rasdhoo atolls (Maldives)” from Beccari et al. (2020). It aims at the survey of environmental evolution of reef sediments in the North Ari Atoll in the Maldives. It uses the survey of various indicators of water quality, community structure, and processes such as grazing and bioerosion. A second paper is entitled “Photic stress on coral reefs in the Maldives: The *Amphistegina* bleaching index” from Stainbank et al. (2020). It aims at the verification and application of a bleaching index developed in the Florida Reef Tract. It targets to measure the photoinhibitory stress status of coral reefs on coral reefs in the Rasdhoo and North Ari Atolls in the Maldives. The last paper of these three is entitled “A snapshot of reef conditions in North Ari Atoll (Maldives) following the 2016 bleaching event and *Acanthaster planci* outbreak” from Caragnano et al. (2021). This study explored the benthic community structure (biotic and abiotic benthic cover and coral composition) at three islands (Rasdhoo, Maayafushi and Vihamaafaru) in the central Maldivian archipelago, 2 years after the 2016 El Niño–Southern Oscillation (ENSO) and the associated mass-bleaching events. These three publications can be found in the computer version of my thesis.

References cited above are to be found in the respective chapters.

1. General Introduction

1.1. Introduction

Wetlands in arid climates represent unique ecosystems and are of major importance for an often specialized flora and fauna. They represent a source of life-supporting water in an otherwise inhospitable environment. These environments are, however, particularly fragile ecosystems as they respond sensitively to any climatic or environmental change. The region located in the north of Botswana offers a unique example of this type of environment, being the second largest endorheic delta system in the world. This unique ecosystem is established by the two endorheic Okavango and Kwando rivers, but also with changing contributions from the Zambezi River. These three rivers form a complex network controlled by tectonic faults (Haddon & McCarthy, 2005). A minor change in tectonism and faulting can significantly influence the morphology and hence the drainage pattern of the entire system. This has been clearly demonstrated by the work of Burrough & Thomas, 2008 for the evolution of the paleolakes of the middle Kalahari, also considered to be the cradle of humanity (Cavaillé-Fol, 2020).

The Quaternary period shows oscillations between glacial and interglacial states in the global climatic system (e.g., Walker et al., 2005). Climate cyclicity in the tropics is driven by the variations in the latitudinal migration of the Intertropical Convergence Zone (ITCZ). As this zone is responsible for delivering moisture to the tropical areas (e.g., deMenocal et al., 2000; Truc *et al.*, 2013), these areas are very sensitive to the climatic oscillations (Pastouret et al., 1978). Climate variations during the Quaternary in northern Namibia and Botswana is poorly documented and understood (Thomas et al., 2012; Burrough et al., 2007; Chevalier et al., 2015). Paleo-environmental archives with well-dated proxies are difficult to find or target and results might show inconsistencies and even contradictions (Thomas et al., 2012; Burrough et al., 2007 but more specifically Chapter 4 of the present thesis). It is thus particularly important to find archives which are exploitable not only for questions of dating, but of climatic tracing as well. The archives must be well documented and contain the proxies that can be used for these purposes. The study of these different subjects is called paleoecology and represents the study of ecosystem history and evolution using sedimentary records.

As summarized by Wiese et al. (2020), interpretations of late Quaternary climate variation in the Kalahari are controversial. Tools as speleothem records are rare and dating of aeolian sediments to reconstruct aridity periods show considerable uncertainties. Furthermore, the complex tectonic activity of the region as well as the climate evolution in the catchment area much further in the north in another climate zone renders the exercise even more complex. Thus hydrological signals in paleolakes may not or only partly reflect Kalahari palaeoclimate (Wiese et al., 2020). The same statement might be true for actual lakes. Sediments description in Lake Liambezi fully reflect and agree with Wiese et al. (2020) considerations. Lake Liambezi offers a current environmental system that allows good comparison to paleolakes systems. We demonstrate in the present work the weak correlation between environmental evolution of Lake Liambezi (in its water level in particular) and the regional climate evolution. Furthermore, we describe efficient tools allowing for a better understanding of this weak correlation and the understanding of the difference between environmental and climatic considerations. The environmental evolution of Lake Liambezi is related to a group of factors including the shape of the lake basin (morphology), its evolution, its environmental condition, and the climate of the region.

This is particularly true as lakes are part of an environment of interactions and exchanges with the surrounding environmental systems. The geological substrate, the surrounding soils, the flora and fauna colonizing the lake and its surroundings, its tributaries and the regional climate form a set of environmental interactions. The sediments are recording in their content the components and the information of these interactions and constitute therefore unique archives. Fossil organic and

inorganic matter as well as microorganisms offer physicochemical parameters and biological indicators to read these archives and are therefore used for paleoecological studies in lake sediments. Lakes offer then precious and unique environments for recording morphological, climatic and environmental changes not only of the site itself, but of the region in which it is also located.

The understanding of Lake Liambezi as a whole system had to encompass all its environmental spheres as surrounding vegetation and soils and surrounding water sources. The geochemical interactions between vegetation, soils and sediments have been investigated and are resumed in Chapter 2. The water origin of the Linyanti-Chobe Basin and of the Okavango has been resumed in Dyer (2017).

All ecosystems, even the most extremes have been colonized by bacteria and they are involved in all biochemical cycles of elements. Their community are shaped by the environment, which is shaped by bacterial activity in response. However, to date, no general marker, representative for all bacteria, exists in paleoecology. This statement is of major importance since bacteria are the most abundant and diverse group of organisms among all domains of life. A biological marker targeting bacteria would be undoubtedly of main interest for paleoecological studies. In the past decades, due to advances in the field of metagenomics, the use of DNA have been proposed as a possible bio-indicator. However, DNA and vegetative cells are subjected to degradation, and therefore, their use remains uncertain. Due to their ability to withstand degradation for extended times, spores or other lysis-resistant structures might represent an ideal marker for paleoecology. A close collaboration has been conducted with the Laboratory of Microbiology at the Institute of Biology of the University of Neuchâtel.

Endospore-forming Firmicutes as paleoecological indicators in lake sediments is a novel approach for paleoecology studies. The current work is part of a more global project aiming to validate the application of this novel approach in comparison to other complimentary methods used for paleoecological and paleoenvironmental interpretations of aquatic systems. This work is more specifically in the generalization of the use of this method in various environmental settings. As the sedimentology of Lake Liambezi and in fact its environmental history have never been studied, the microbiology approach would therefore serve as an exploratory method, in the same way as the more traditional methods. The method has demonstrated its full potential in this exercise. Indeed, it made it possible to highlight aspects that would probably have gone unnoticed with the conventional methods chosen beforehand (e.g., the presence of hydrothermal activity). The types of analyses carried out could therefore be adapted in order to confirm, when possible, the observations made using microbiology. The microbiological approach has also helped to refine certain results such as the dating of sediments. The different uses of the method are described in the following chapters. The method has therefore fully found its place in the information it can provide in the study of a site devoid of any description.

1.2. Regional settings

1.2.1. Linyanti-Chobe Basin

A multitude of ecosystems with a large diversity in fauna and flora is found in the wetlands not only of the Okavango Delta (Milzow et al., 2009) but also in the different delta, swamps, lake and rivers of the Linyanti-Chobe basin. In addition to their natural wealth, this environment provides a traditional livelihood for the local communities (Figure 1) and are the basis of a tourism industry that generates substantial revenue for the whole of Botswana (Milzow et al., 2009). Local traditional subsistence fisheries as well as exporting fisheries to Zambia are of major importance for local communities of the Caprivi and Linyanti-Chobe Basin regions. Lake Liambezi produced more than 600 tonnes of fish in year 1973-74 (Van Der Waal, 1990). The annual yield for 2011-12 after yet several years of drying was estimated at 2'700 tonnes (Peel et al., 2015).

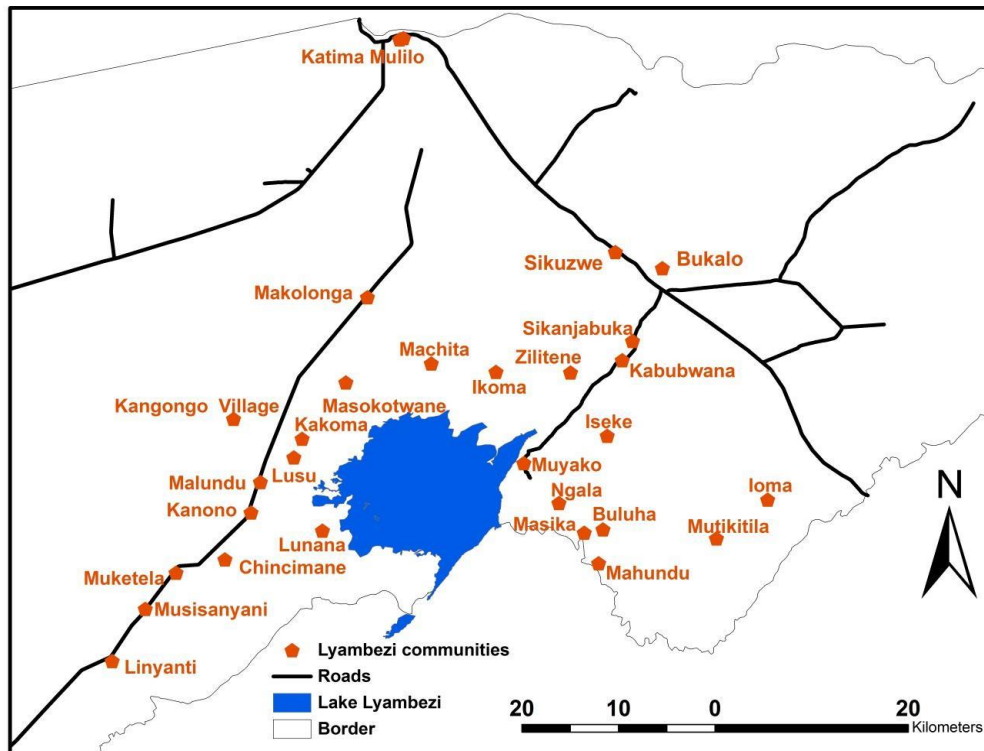


Figure 1 Community settlements around Lake Lyambezi (Mutelo, 2013).

The combination of a highly seasonal inflow and local dry and wet seasons offers a multitude of different environments and ecological niches. The special hydrological setting does permit the large biodiversity found in the wetlands of this region (Milzow et al., 2009). Linyanti-Chobe Basin includes in its western part the Kwando River terminal with the Mamili swamps, the Linyanti River and its Linyanti swamps, their terminal with Lake Liambezi in the center of the basin and finally, at its eastern side, the Chobe enclave and the Chobe River (Figure 2).

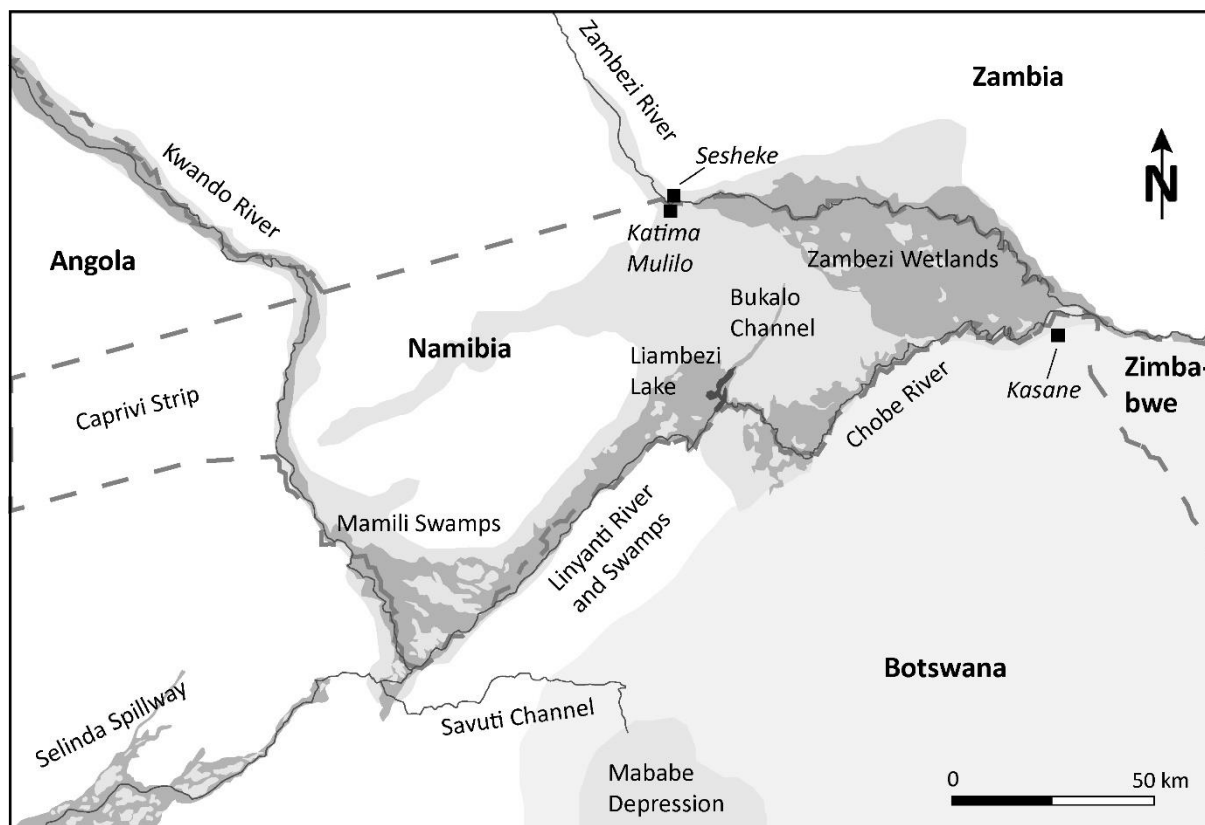


Figure 2 Map of the Linyanti-Chobe Basin. Rivers and their courses as well as their interactions are described in Chapter 1.2.4. Borders between the different countries are drawn in dashed lines.

1.2.2. Geology and tectonism

Southern African Subcontinent crust is made of two Archean cratonic units, the Kalahari and Congo cratons. These two units are surrounded and separated by a network of Proterozoic orogenic belts (Figure 3). However, the Phanerozoic cover occurring in the Kalahari region of Botswana and adjacent parts of Zimbabwe, Zambia, Angola, Namibia, and South Africa impedes the understanding of the tectonic evolution of these belts stems. Cover of this Precambrian basement in this region, located on the Kalahari Desert, is made of Carboniferous to Jurassic Karoo strata. Cenozoic units of the Kalahari Group are then overlaying with thin but extremely widespread deposits (Singletary et al., 2003). In Late Cretaceous, these different geologic units experienced a down-warp towards the interior of the subcontinent and an epeirogenic uplift. These structural changes formed a vast confined area called Kalahari basin (Figure 4 and Figure 5). This led to the erosion of units of the Kalahari Group and the consequent deposit of large amount of sediments in the Kalahari basin during Phanerozoic times (Haddon & McCarthy, 2005; Singletary et al., 2003; Jones *et al.*, 1980).

Introduction

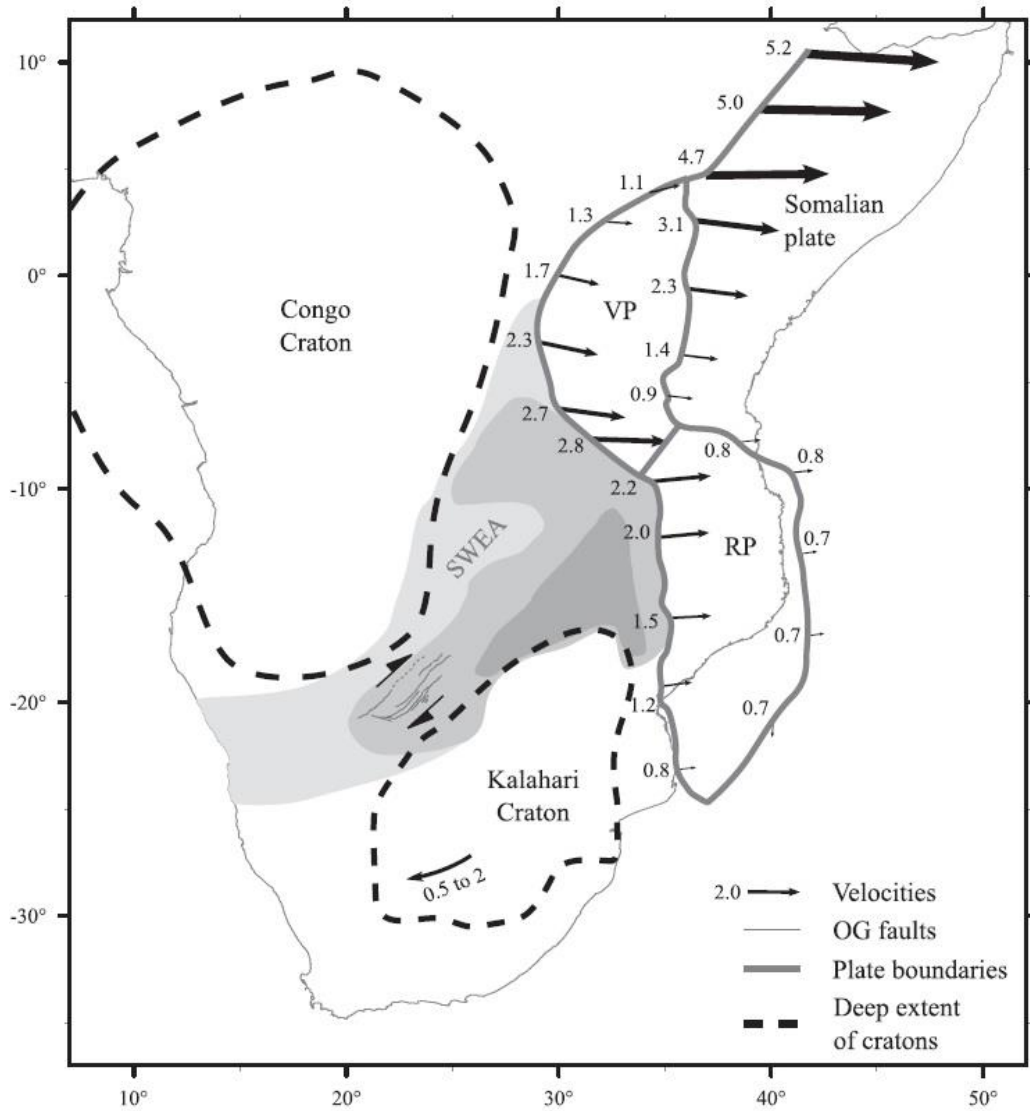


Figure 3 EARS block limits and velocities (in mm/year, relative to adjacent blocks), South Africa velocity relative to the Nubian plate. In the SWEA (South Western Extension Area), increasing saturation represents observed fault density and hence probably increased deformation, revealing the distribution of the lithospheric weakness and conjugated influences of the southern Africa displacement and the EARS opening. RP: Rovuma plate, VP: Victoria plate (Pastier et al., 2017).

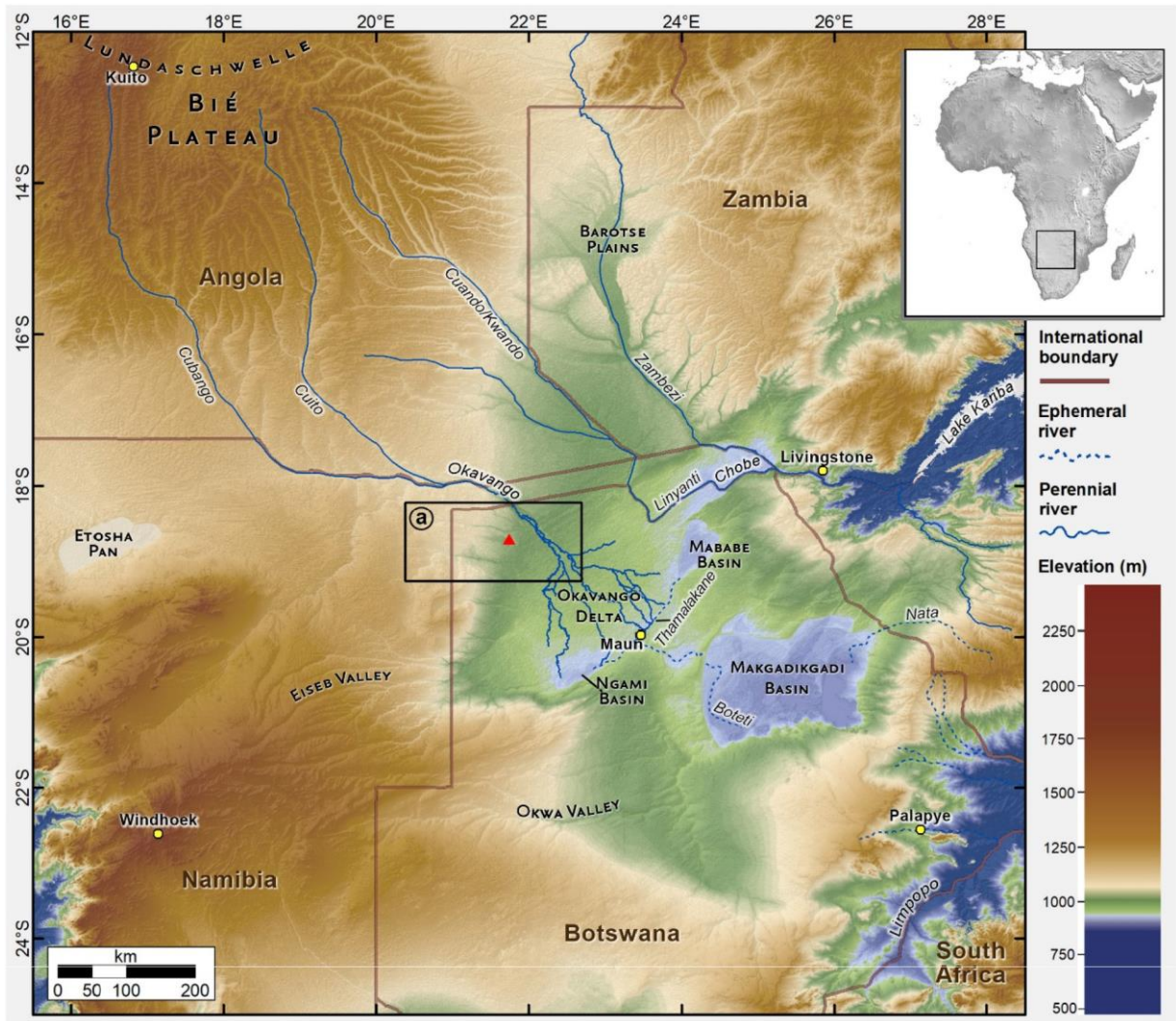


Figure 4 Elevation model with hydromorphological setting of the Kalahari in southern Africa (Wiese et al., 2020). It shows the high plateau forming a vast confined area called Kalahari basin.

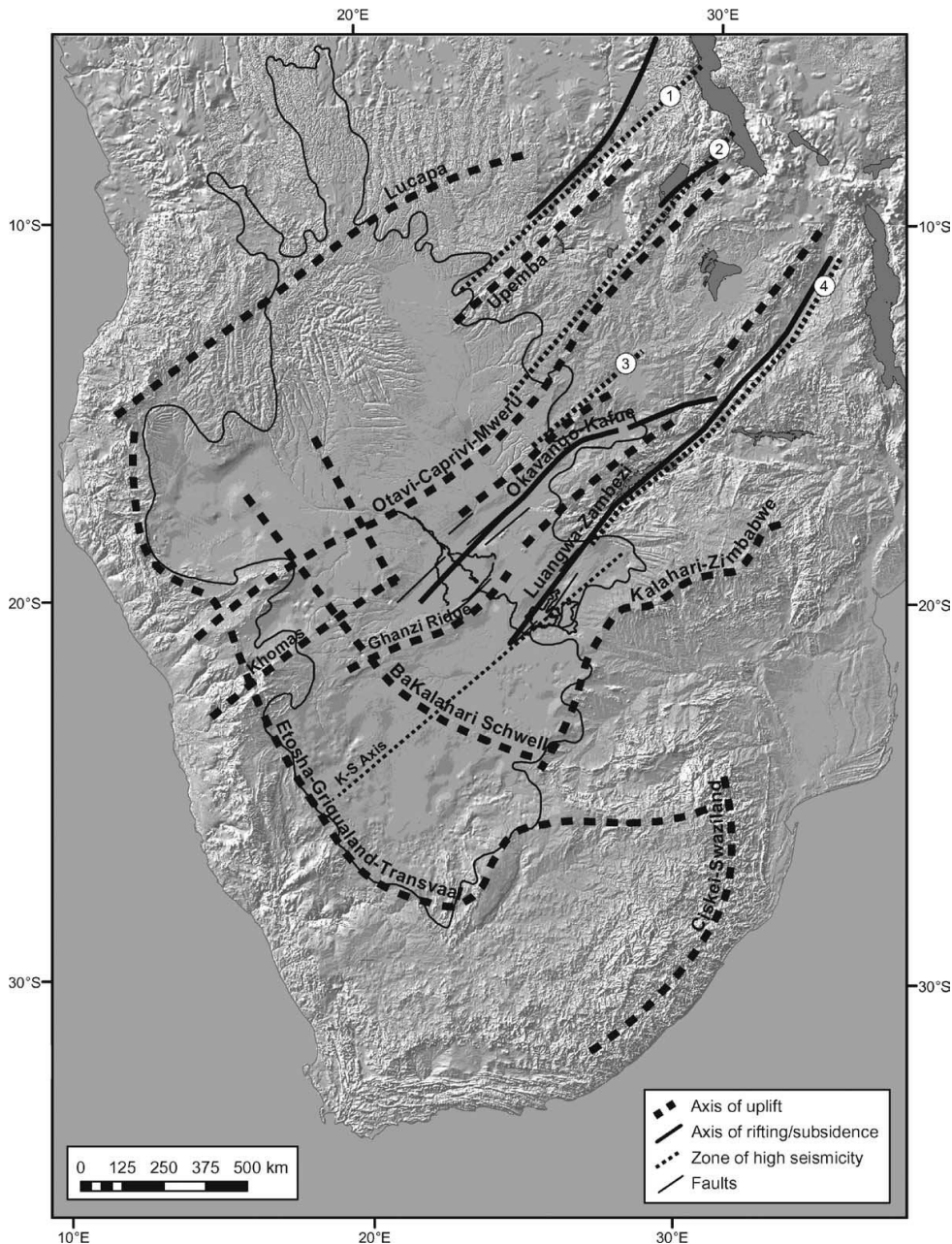


Figure 5 The axes of late Tertiary and Quaternary uplift, rifting/subsidence and seismicity in the Kalahari basin (Haddon & McCarthy, 2005).

The Kalahari Basin, as an epeirogenic feature which remained depressed as the marginal mountains of Southern Africa's Great Escarpment, rose during the Tertiary (Jones *et al.*, 1980). It forms a depression of about 2700 km long and 1800 km wide (McCarthy, 2013). This basin lies within the Proterozoic Damaran belt, which is bounded by the Congo Craton to the northwest and the Zimbabwe and Kaapvaal cratons to the southeast (Kinabo *et al.*, 2008; Jones *et al.*, 1980; Bufford *et al.*, 2012). The north part of the basin is crossed by an incipient continental graben found at the terminal of the southwestern branch of the East African Rift System (EARS) (Figure 6) (Pastier *et al.*, 2017, Bufford *et al.*, 2012; Haddon & McCarthy, 2005; Jones *et al.*, 1980). It forms a topographic depression filled with Quaternary lacustrine and fluvio-deltaic sediments and is bounded by northeast-trending normal faults (Figure 7). These faults affect the course of the rivers Okavango, Kwando and Zambezi and causes an endorheic basin for the two rivers Okavango and Kwando and the partial deviation of the Zambezi named Chobe (Bufford *et al.*, 2012). It forms a network of about 100 km long and 40 to 80 km wide Quaternary rift basins distributed along an approximately 250 km wide corridor extending for about

1700 km west of the Tanganyika and Malawi rifts (Bufford et al., 2012). This graben, situated all along the northwestern part of Botswana, is named Okavango Graben (Pastier et al., 2017). The presence of an incipient graben was highlighted by a significant tectonic activity and morphologic features that have been associated to the East African Rift system (Pastier et al., 2017). The tectonic activity as well as the faulting system (Figure 8 and Figure 9) of the Kalahari Basin have been interpreted as an incipient rifting zone described as an extension of the East Africa Rift system and called Okavango Rifting Zone (Pastier et al., 2017, Bufford et al., 2012; Haddon & McCarthy, 2005; Jones et al., 1980). It forms the extreme south-western extent of the southwestern branch of the East African Rift System (Bufford et al., 2012; Kinabo et al., 2008). It lies within the Proterozoic Damaran belt, which is bounded by the Congo Craton to the northwest and the Zimbabwe and Kaapvaal cratons to the southeast (Kinabo et al., 2008; Jones et al., 1980; Bufford et al., 2012). However, the region does not show similarities with classical definition of a rift system. There is no clear horizontal extension, no lithosphere thinning or neither no pronounced seismicity (Pastier et al., 2017). It is thought to be therefore not an incipient rifting zone, but more a deformation zone accommodating differential movements between different plates and rigid cratons (Figure 3) (Pastier et al., 2017). Therefore, Pastier et al. (2017) proposed to change the commonly used but genetically loaded name “Okavango Rifting Zone” to a more geologically neutral, descriptive, “Okavango Graben”.

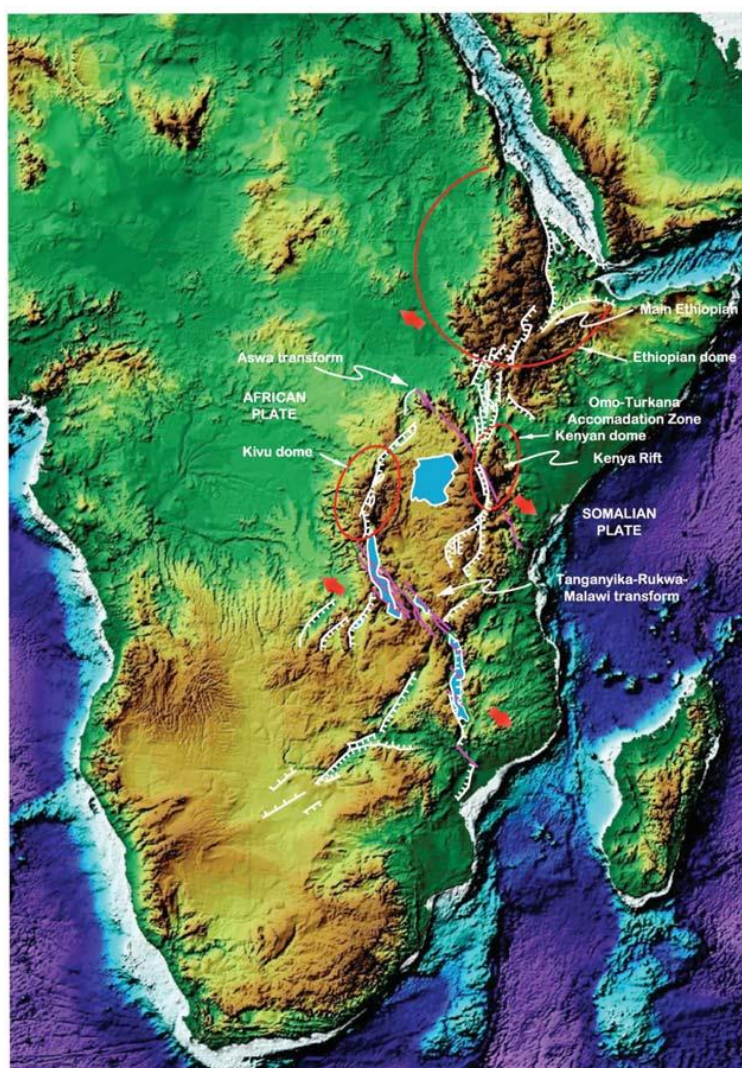


Figure 6 The East African Rift system (McCarthy, 2013).

Introduction

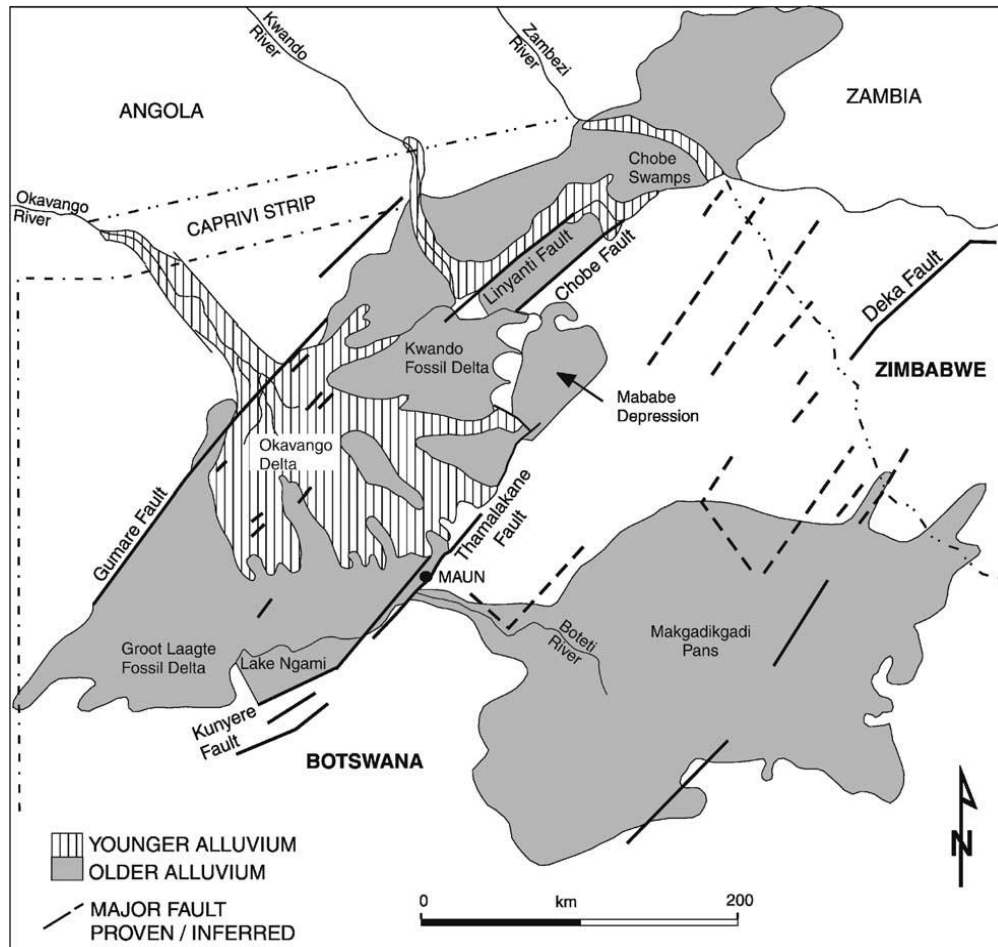


Figure 7 Distribution of alluvial sediments in the Okavango-Linyanti depression and their relationship to major faults in the region (Haddon & McCarthy, 2005).

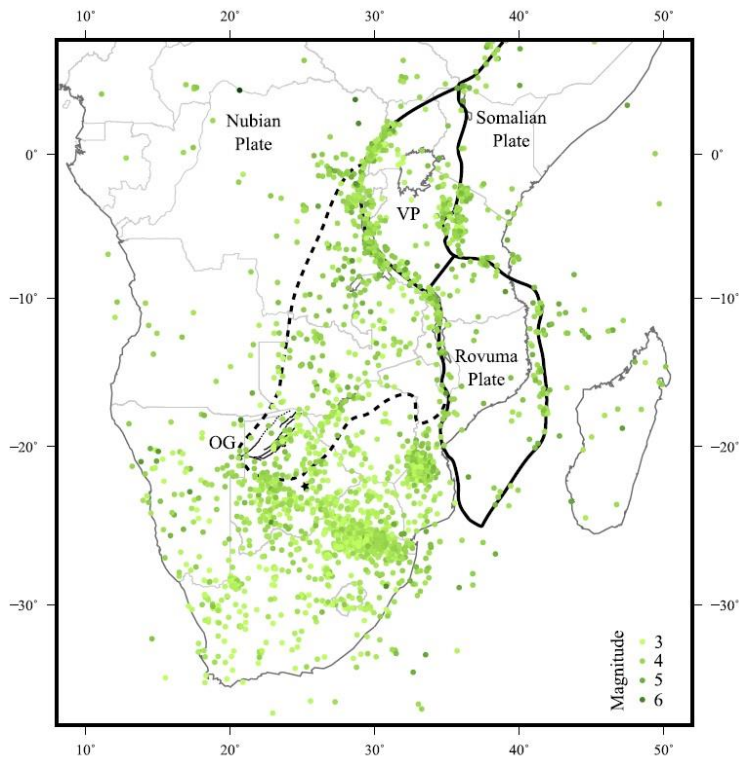


Figure 8 Recorded earthquakes from 2004 to 2016, with magnitude over 3 (International Seismological Centre, 2016). The black star indicates the location of the recent M6.5 earthquake (Pastier et al., 2017).

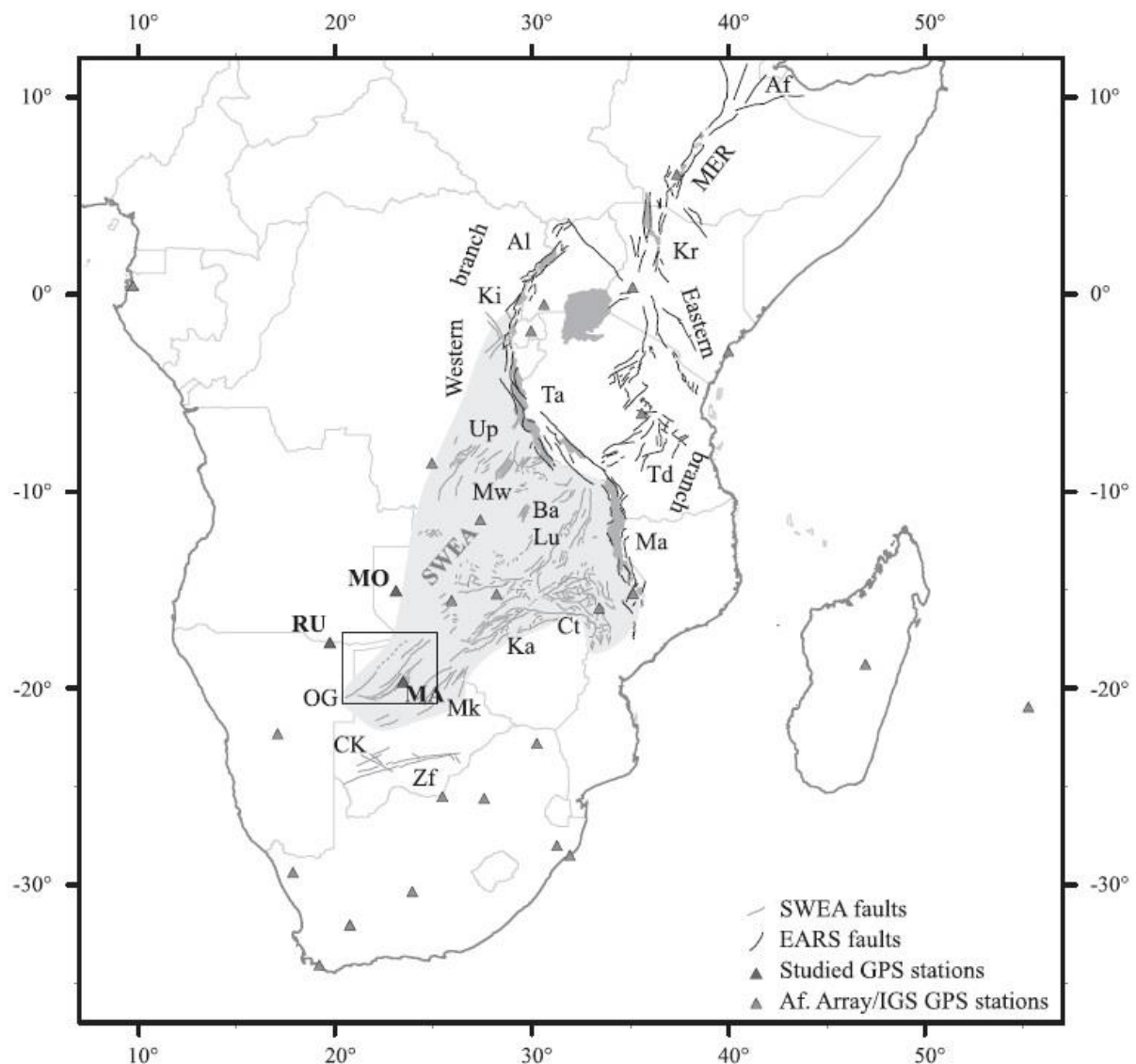


Figure 9 Location of the Okavango Graben and the three studied permanent AfricaArray GPS stations (MA: MAUA, MO: MONG, RU: RUND). 26 GPS stations complete the network. The EARS (East African Rift System) and SWEA (South Western Extension Area) main faults are compiled from different works referenced in Pastier et al. (2017). The SWEA extent is filled with light grey. Af: Afar Depression, Al: Lake Albert, Ba: Lake Bangweulu, Ct: Chicooa trough, CK: central Kalahari, Ka: Lake Kariba, Ki: Lake Kivu, Kr: Kenyan rifts, Lu: Luangwa Valley, Ma: Lake Malawi, MER: Main Ethiopian Rift, Mk: Makgadikgadi Pans, Mw: Lake Mweru, Ta: Lake Tanganyika, Td: Tanzanian divergence, Up: Upemba trough, Zf: Zoetfontein fault (Pastier et al., 2017).

Quaternary unconsolidated lacustrine and fluvio-deltaic sediments occurring around the Okavango Graben are underlain by lacustrine and fluvio-deltaic sediments of varying thickness (Bufford, 2012). These pre-Okavango geologic units include marls, clays, gravels, aeolian sands, calcrete, and silcretes and build the 230 meters-thick Cenozoic Kalahari beds (Kinabo et al., 2008). Bedrock is dominated by Precambrian crystalline rocks of the Damara and Ghanzi-Chobe orogenic belt and are exposed to the northwest and southeast of the southwestern end of the Okavango Graben (Bufford et al., 2012).

Drainage of the region is strongly influenced by the fault system (McCarthy, 2013). The basin contains the three drainage systems of the Okavango Delta, Kwando and Zambezi Rivers that flow to the southeast. The graben is composed of three depocenters represented by Ngami sub-basin in the southwest and the Mababe and Linyanti-Chobe sub-basins to the northeast (Figure 4 and Figure 7) (Bufford et al., 2012). If the Ngami and the Mababe sub-basins are well described, the Linyanti-Chobe

Introduction

basin is less studied and described (Bufford *et al.*, 2012; Burrough *et al.*, 2007; Burrough & Thomas, 2008). Faults escarpments of the East African Rift System are well developed and reach hundreds of meters. Faults escarpments of the Okavango Graben are very small and are in a range of 6 m along the Ngami sub-basin, 12-18 m around the Mababe sub-basin to a maximum of 44 m around the Linyanti-Chobe sub-basin (Kinabo *et al.*, 2008). The orientation of the Okavango Graben below the surface is influenced by the pre-existing regional fabric of the Precambrian Damara and Ghanzi-Chobe orogenic belt (Bufford *et al.*, 2012; Kinabo *et al.*, 2007; Kinabo *et al.*, 2008).

The age of initiation of the Okavango Graben remains unknown. Paleoenvironmental reconstruction from the sediments of the Ngami sub-basin suggests that southeast-flowing rivers related to the today's Okavango and Kwando Rivers network flowed to the southeast beyond the Thamalakane and Kunyere faults into the Makgadikgadi pans until ~120 Ka (Figure 10) (Bufford *et al.*, 2012; McCarthy, 2013). The uplift along the Zimbabwe-Kalahari axis and displacement along the northeast-trending faults of the Okavango Graben between ~120 Ka and ~40 Ka resulted in the development of the proto-Okavango, Kwando, and the upper Zambezi Rivers and the development of the proto-Linyanti-Chobe, Ngami, and Mababe sub-basins. The graben and its related faulting in the Okavango region may have been then initiated between ~40 Ka and ~27 Ka. This temporality is supported by paleo-environmental studies from the Mababe sub-basin which suggest neotectonic activity in this zone (Bufford *et al.*, 2012). Major changes in the sedimentation and hydrologic regime during the same period in the Mababe sub-basin is also attributed to possible movement along the Linyanti fault (Gamrod *et al.*, 2009).

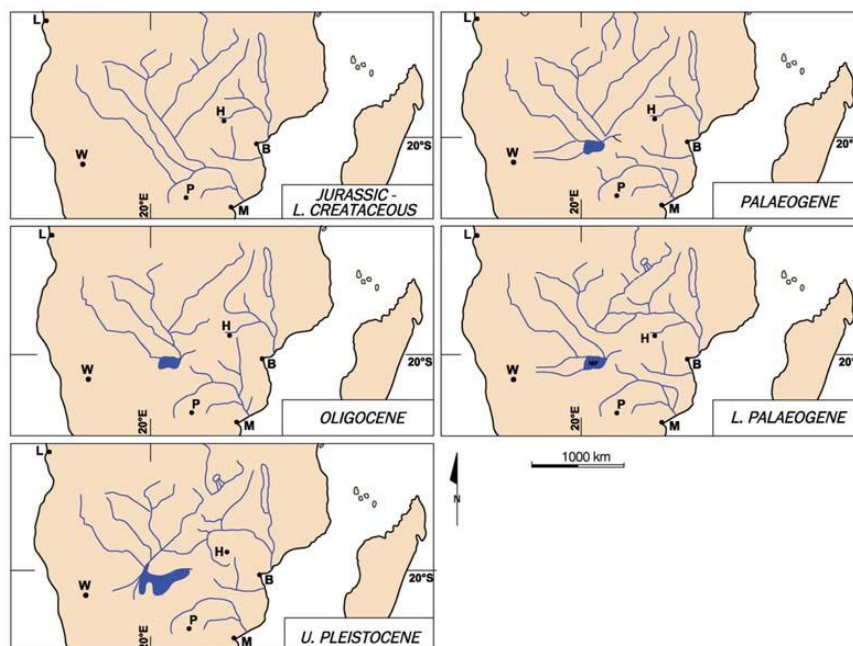


Figure 10 Schematic diagrams illustrating the evolution of the Okavango, Kwando and Zambezi Rivers system (McCarthy, 2013).

Kwando watershed is made of the Kalahari units (Figure 11). It brings in transported sediments a composition rich in quartz with an amount of K-feldspar up to 11% and a low abundance or even absence of plagioclase and calcite (Haddon and McCarthy, 2005; Setti *et al.*, 2014). Smaller streams are also transporting the Proterozoic Choma-Kalomo Block containing mostly granites and gneisses as well as metasedimentary rocks (Vainer *et al.*, 2020). Sediments issued of this watershed show variable phyllosilicate levels but up to 30%. Clays are composed of a significant amount of smectite (> 40%), 10-

40% of mica and kaolinite and the absence of chlorite. Calcite comes from continental (pedogenic) carbonates found locally along the Kalahari (Setti et al., 2014). Zambezi watershed is made of the Kalahari units as well but in addition with the Karoo basalts and some other mafic and sedimentary units (Figure 11) (Gärtner et al., 2013; Setti et al., 2014). Those different units are notably composed of the granite-greenstone Zimbabwe Craton and the Kasai Craton that lies to the north of the Okavango Basin and includes granulites, amphibolites, granitoids, and gabbros. It also drains the copper-bearing volcanics and metasediments of the Neoproterozoic Lufilian Belt (Vainer et al., 2020). Transported sediment then show a composition dominated by detrital quartz and feldspars (63-85%) and significant amounts of phyllosilicates (up to 40%). Calcite is found again in small amount (<5%) and comes again probably from local continental carbonates. Concerning clays, smectite is dominant where kaolinite varies from 4% to 36% and chlorite is minor or absent (Setti et al., 2014). In continental environments, if mica and chlorite are usually inherited from ancient rocks, modified by physical or moderate chemical weathering, kaolinite forms through long-term weathering processes. Smectite figure of intermediate stage (Setti et al., 2014, and references therein).

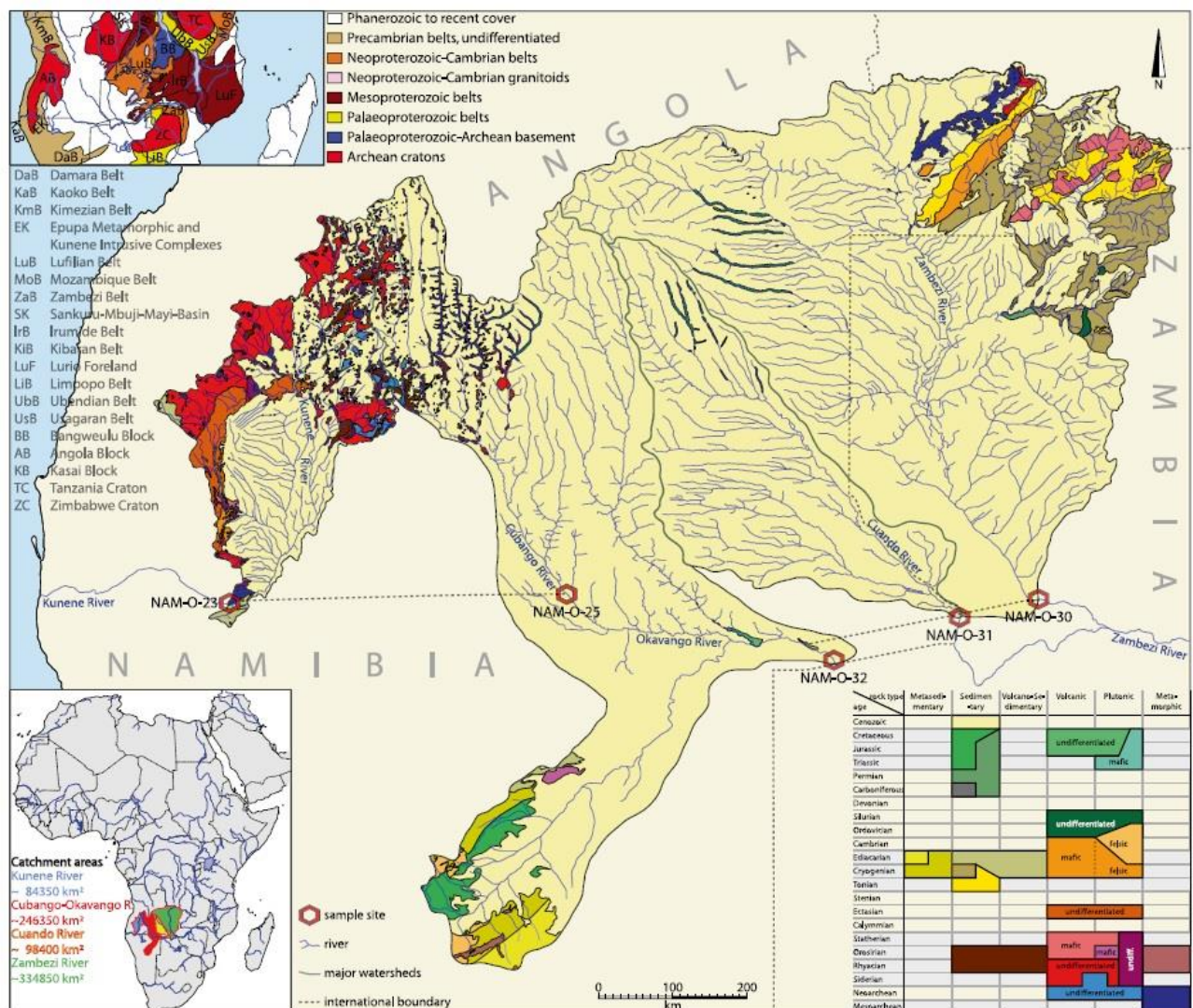


Figure 11 Overview of the areal distribution and surface geology of the catchment areas of the Kunene, Cubango–Okavango, Cuando and Zambezi River systems upstream of the sample localities (made after a compilation of various works referenced in Gärtner et al. (2013)). The legend specifies the main rock types in the working area by their estimated age and their petrologic characteristics (Gärtner et al., 2013).

1.2.3. Hydrothermal activity

The presence of a few water sources showing hydrothermal activity in the Linyanti-Chobe basin is known (personal communication from the guide Ali Mainga of the VanThuyne-Ridge Research Center, Chobe Enclave, Botswana). Furthermore, a low temperature hydrothermal activity (up to 50° C) is described for hydrothermal vents along the Chobe in Kasane (Mukwati *et al.*, 2018). The tectonic activity linked to the Okavango Graben seems to make the presence of hydrothermal vents plausible in this region.

1.2.4. Cuando, Kwando, Linyanti, Chobe and Zambezi Rivers

The Cuando River has its source in Angola (Figure 12). Numerous channels in a wide swamp corridor along the Angola and Zambia border characterize it until it enters into Namibia through the Caprivi Strip and takes the name of Kwando River (Kurugundla *et al.*, 2010). The Kwando River is then redirected by the Linyanti fault (Haddon & McCarthy, 2005; Burrough & Thomas, 2008; Kinabo *et al.*, 2007) and the water flow continues to the east through the Linyanti swamps (Figure 2). Some water may flow to the west through the Selinda Spillway as well as to the Savuti. Selinda Spillway may eventually connect the Okavango system to the Mamili swamps of the Kwando River depending on the water amount in the Okavango system. It may then run through the Savuti channel and may reach the small Mababe Marsh in the Mababe depression (Shaw, 1984). In the Linyanti swamps, Kwando River has the name of Linyanti River. It flows through the swamps to reach Lake Liambezi (Kurugundla *et al.*, 2010).

Zambezi River has its source in Zambia (Figure 12). After a short intrusion in Angola, it flows into Zambia again before marking the border with Namibia and then Botswana. It then flows along the Zimbabwe border, across Mozambique and finally into the Indian Ocean (Moore *et al.*, 2007). The Zambezi reaches the Namibian border up to Katima-Mulilo (Namibia) and Sesheke (Zambia), two villages facing each other (Figure 2). It then spreads into large wetlands. Some channels of these wetlands reach the Chobe fault and form the Chobe River. Chobe River and Zambezi River meet in Kazungula (Zambia), a rare quadruple border point (Zambia, Zimbabwe, Namibia and Botswana). During the peak flood, the Zambezi River may reverse its flow and flow along the Chobe fault to the west and spreads into the Chobe floodplain. The end point of this reverse flow is Lake Liambezi (Schlettwein *et al.*, 1992). Flood events higher than 8 meters permit to the Zambezi River to overflow its floodplain (in its large wetlands along the Namibia-Zambia border) and to create a several kilometre-wide sea river that reach Lake Liambezi through the Bukalo channel (Schlettwein *et al.*, 1992).

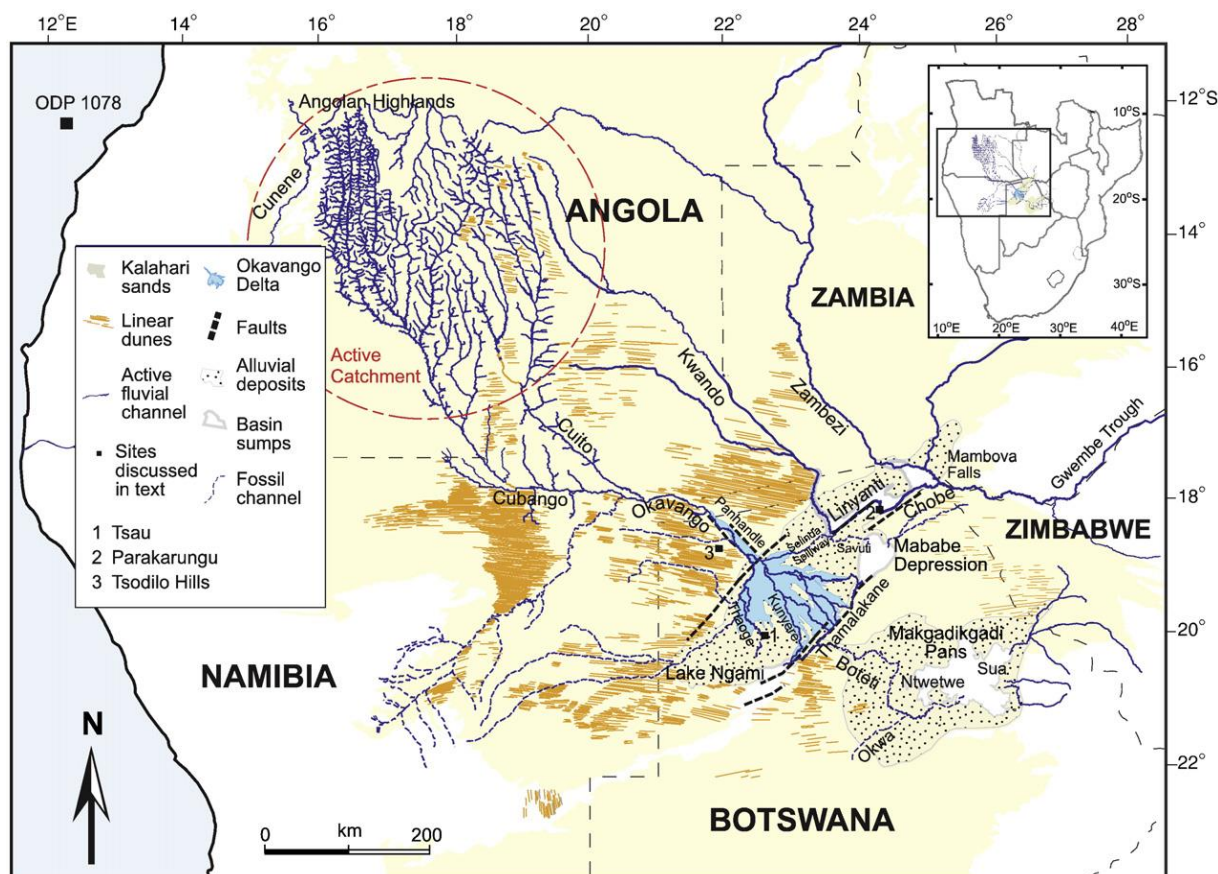


Figure 12 Regional map of the Middle Kalahari and the hydrological systems of the Okavango, Kwando and Zambezi catchments in relation to the sump basins (Lake Ngami, the Mababe Depression and the Makgadikgadi pans) (Burrough *et al.*, 2009).

1.2.5. Climate and flood system

Watershed and sources of Kwando River are in Angola, Zambia and Namibia. Those of the Zambezi River are in Democratic Republic of Congo, Angola and Zambia. Both watersheds are situated in equatorial regions with a humid subtropical climate and a mean annual precipitation of about 1300 mm (Milzow *et al.*, 2009). Hydrologic year for this region is counted from the beginning of the wet season in November. Precipitations are then distributed seasonally depending on the fluctuations of the Intertropical Convergence Zone (ITCZ) and fall mostly between November and March (Pricope *et al.*, 2013; Milzow *et al.*, 2009). Reaching points of Okavango, Kwando and Chobe rivers are located further south in a semi-arid climatic region with mean annual precipitation around 400 mm (Thomas & Shaw, 1991). The Linyanti-Chobe basin receives a mean annual precipitation amount of about 570 mm. Precipitation are mostly under the form of summer thunderstorms occurring almost exclusively during the rainy season from November to March (Ballif, 2018).

Rainwater is relatively dispersed spatially and generally concentrated in the Lake Liambezi region or shallow depressions in the landscape as a result of local and regional precipitation primarily. Nevertheless, the resulting rise in river levels causes annual flood pulses that reach each terminal swamp or water body at a specific time, depending on specific characteristic of each river. Flood pulses of the Kwando reach the Mamili swamps (Figure 2) toward the end of June-July (Pricope *et al.*, 2013). It then takes to the water 3 to 6 months to percolate through Mamili and Linyanti swamps and to pour out in Lake Liambezi (Schlettwein *et al.*, 1990; Burke *et al.*, 2016). The Zambezi River has earlier discharge peaks starting in mid-March and April. It first spreads out across the Zambezi wetlands (Figure 2) but is also being pushed as backflow into the main Chobe channel. The flood pulse reaches thus the floodplain of the Chobe at the end of March. Lake Liambezi and the surrounding lower

floodplain of the Chobe-Linyanti are then reached at the maximum extent of the floods in April and May, when the water recedes from the Zambezi wetlands and the northeastern part of the basin. As Kwando's flood pulse is situated later in the year, the Chobe River might receive water through sporadic connections from Linyanti channel by the middle of the dry season and depending on the hydro-climatological nature of the year (Pricope *et al.*, 2013). During exceptional floods, the Okavango water penetrate in the Linyanti-Chobe basin via the Selinda Spillway. There may have been more exchange in the past, during more humid phases in the Quaternary, even the formation of large paleo-lakes (Burrough & Thomas, 2008), which have left inherited geomorphological features in the landscape. Regarding the nature of the hydro-climatological year, the main channels of the Linyanti-Chobe Basin as well as Lake Liambezi on average contain surface water for more than 8 months of the year. In contrast, all the other annually inundated surfaces of the Linyanti-Chobe Basin are only inundated for three months or less per year (Pricope *et al.*, 2013).

Water table level plays a critical role to the flood extent. Flood's magnitude is diminished or enhanced according to the water table level (Gumbrecht *et al.*, 2004). Flood extent is then also directly determined by groundwater characteristics such as fingering density points and memory effect of previous hydrological years (Gumbrecht *et al.*, 2004; Bauer *et al.*, 2006).

1.2.6. Soils

An important part of the active global carbon budget at the Earth's surface depends of the terrestrial vegetation together with the soil organic matter reservoir (e.g., Killips & Killips, 2005). The complex interplay of factors such as climate, soil texture, vegetation cover, land use, fire frequency and topography determines the inventory of any soil profile in its total organic carbon (TOC) and carbon isotope composition of the organic matter (expressed in $\delta^{13}\text{C}_{\text{TOC}}$) (e.g., Bird *et al.*, 2004). These two measurements are part of the most valuable techniques and direct tracers for the global cycling of carbon between the geological, terrestrial, marine and atmospheric reservoirs, and the many smaller reservoirs of carbon within each of these four broad subdivisions (e.g., Bird *et al.*, 2004). TOC has the characteristic to integrate the isotopic composition of local vegetation over several years. It thus provides a useful tool to measure the representative carbon isotope composition of regional biomass as a function of environmental conditions prevailing (e.g., Bird *et al.*, 2004). In the present study, the spatial distribution of the isotopic composition of carbon within the TOC pool is used to understand the spatial distribution as well as the related environmental controls on it of the C_3 – and C_4 – type vegetation biomass in the actual environment. The related results are presented in Chapter 2. If $\delta^{13}\text{C}$ value is relevant for modern environment, this turn out to be the case for past environments as well (e.g., Bird *et al.*, 2004). TOC content and $\delta^{13}\text{C}$ value are then used to trace the evolution of biomass cover signature in Lake Liambezi's sediment. It does permit reliable reconstructions of the past environment (following chapters).

In the tropics and sub-tropics, TOC and $\delta^{13}\text{C}$ value are largely controlled by precipitation. However, water availability such as groundwater is of major importance as revealed by Chapter 2 of the present work but as revealed in Bird *et al.* (2004) as well. Indeed, water availability has a direct control on the type and the amount of standing biomass that will be then represented as type and amount of organic carbon input to the soils (e.g., Bird *et al.*, 2004). Bird *et al.*, 2004 reveal low carbon inventories with the preference to C_4 plants where precipitation is low. Carbon inventories rise and $\delta^{13}\text{C}$ of TOC decreases where precipitation rise as a result of increasing carbon inputs to the soil from trees and shrubs using the C_3 photosynthetic pathway. However, the heterogeneous distribution of C_3 and C_4 vegetation in the landscape and its implication into the TOC inventories and the $\delta^{13}\text{C}$ value is to be taken into consideration in the discussion (Bird *et al.*, 2004). Groundwater distribution and circulation demonstrates the same implication to be considered (as shown by Chapter 2).

Despite considerable spatial heterogeneity, coherent trends in both TOC inventories and $\delta^{13}\text{C}$ value of TOC are observed in Bird et al. (2004). They further demonstrate the relevance of using the method of ‘bulking’ many individual samples in order to smooth local heterogeneity and obtain a coherent picture of regional trends (Bird et al., 2004). General trends of $\delta^{13}\text{C}$ values along important transects present a decrease of $\delta^{13}\text{C}$ values with increasing mean annual precipitation. It reflects the increasing dominance of C3 over C4 photosynthesis as mean annual precipitation increases. However, regions where plants have a year-round access to groundwater do not accord with the above described trend. Access to groundwater reveals stronger than mean annual precipitation influence and results in higher weighted TOC inventories and lower weighted $\delta^{13}\text{C}$ values than what would be predicted based on regional trends alone (e.g., Bird et al., 2004).

Soil cover in the Linyanti-Chobe Basin is mainly described as completely covered by Arenosols (Figure 13) (Romanens et al., 2019 and references therein). They are acidic and nutrient poor (Wang et al., 2007). However, considering the multiple actors and the complex microtopography of the basin, soils are in fact much more diverse (Romanens et al., 2019). Factors participating in the soil formation in the region such as hydric conditions, topography, nature of the soil parent material (i.e. aeolian or alluvial), impact of biological activity (termites and plants), as well as fires (natural or caused by arson) lead to an important soil heterogeneity and diversity. Five groups of soils are reported: Chernozems-Phaeozems, Arenosols, salty/sodic soils (Solonchak-Solonetz), Kastanozems, and Calcisols (Romanens et al., 2019). Sandvelds, dry floodplains grasslands and *Baikiaea* forests demonstrate a good correlation with Arenosols. A good correlation is also observed between mixed riverine forests and *Combretum hereroense* woodlands with Kastanozems. The dambo grasslands are associated to Chernozems or Chernic Phaeozems and grouped with the wet floodplain grasslands. *Colophospemum mopane* woodlands are associated to salty/sodic soils (Romanens et al., 2019). Calcisols, Fluvisols or Luvisols are also found depending on the connection to water availability in geographic features such as delta, rivers, and marshes (Mendelson et al., 2004).

Majority of the soils are not covered by litter. The litter, if existent, is made of fresh plant debris from the year. A fast decomposition or integration into the soil is helped by termites and/or combustion due to fires (Romanens et al., 2019).

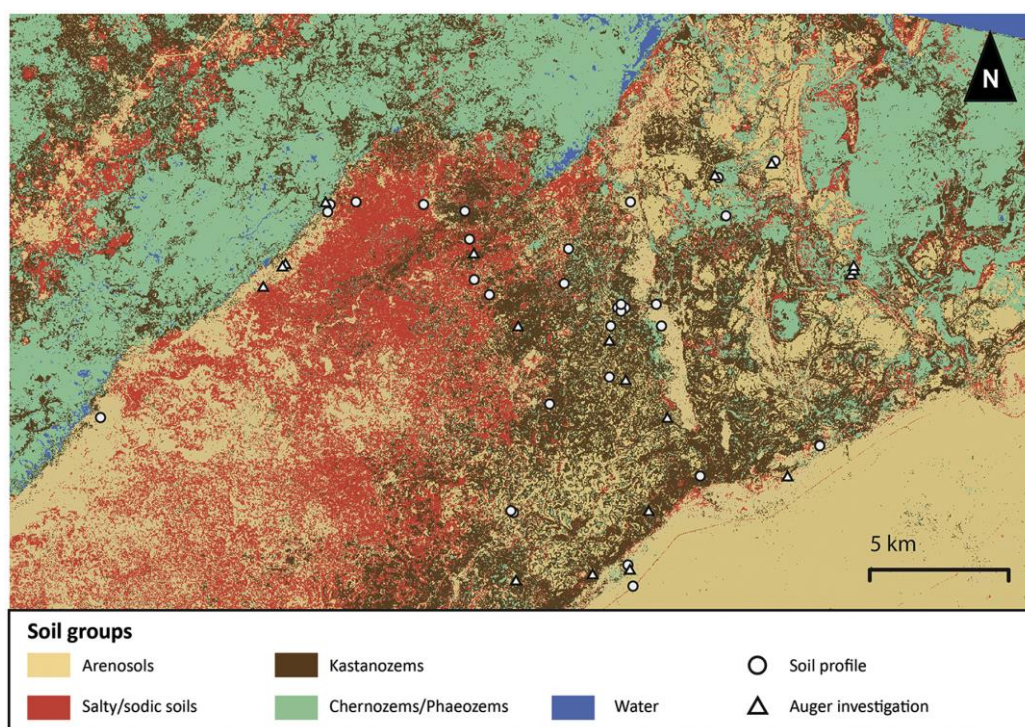


Figure 13 Distribution of the observed and/or sampled soils in the Chobe Enclave (Romanens et al., 2019).

1.2.7. Vegetation

Northern Botswana is covered by a savannah biome. It consist of a cover dominated by grasses and more or less wooded component which is however neither grassland nor forest (Scholes & Archer, 1997, Skarpe & Ringrose, 2014). The region along the Chobe river was classified under five land cover types: floodplain, *Capparis tomentosa* shrubland, *Combretum* shrubland, mixed woodland, and *Baikiaea plurijuga* woodland (Skarpe et al., 2004). Complement studies permitted to enlarge and detail the region into eight groups: Sandveld, *Baikiaea* forest, Dry floodplain grassland, *Colophospermum mopane* woodland, Mixed riverine forest, *Combretum hereroense* woodland, Dambo grassland and Wet floodplain grassland (Figure 14) (Vittoz et al., 2020; Romanens et al., 2019).

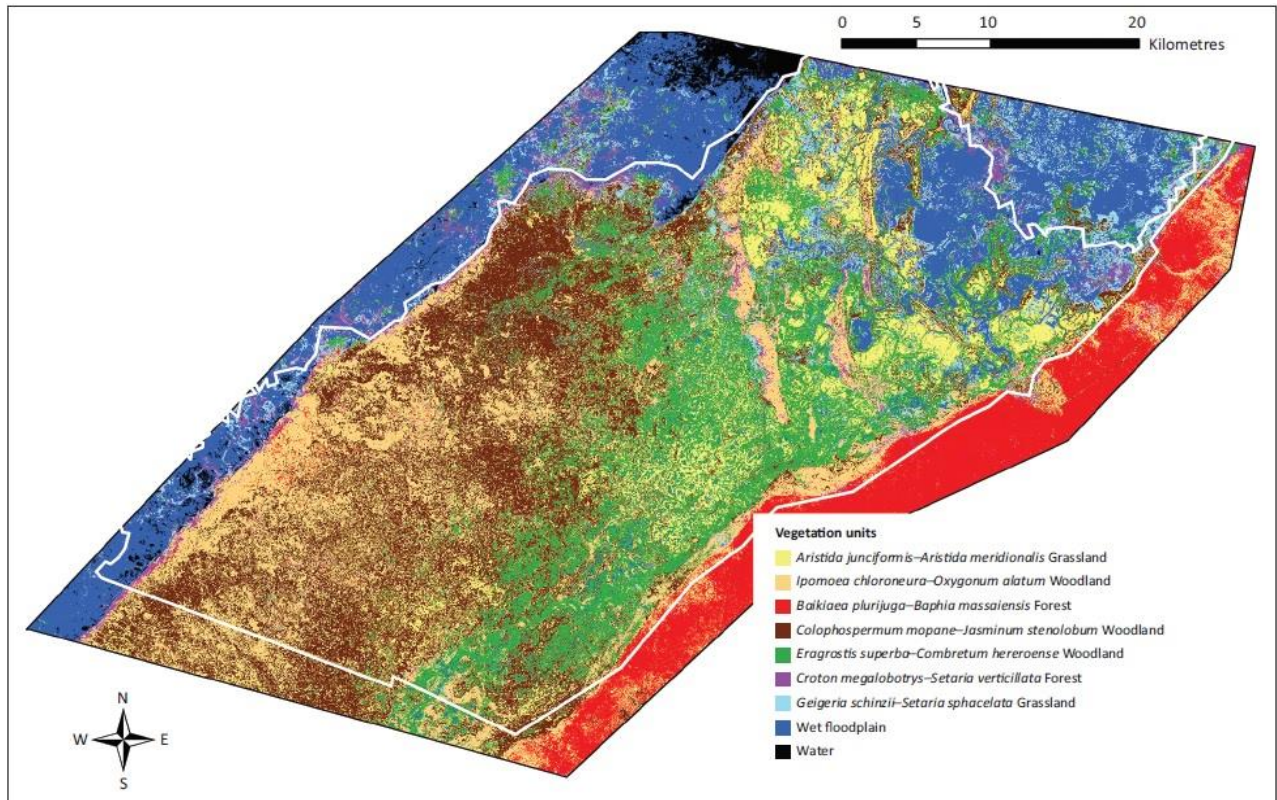


Figure 14 Vegetation map of the Chobe Enclave, delineated by the white line (Vittoz et al., 2020).

Islands are characterized with various tree species such as *Combretum hereroense*, *Terminalia prunioides*, *Acacia nigrescens*, *Acacia tortilis* or *Acacia hebeclada*. Floodplains are dominated by C₄ grasses such as *Aristida spp.* A specific forest dominated by *Colophospermum mopane* is found on the islands of the south-west of the Chobe Enclave. Red sands along the Chobe fault are colonized with *Baikiaea plurijuga* and *Combretum elaeagnoides* woodland (Romanens, 2017).

The present work aimed at the understanding of the geochemical link between vegetation cover and soil organic matter. It is based on the classification made after Romanens et al. (2019). However, this classification is revisited through geochemical results and therefore, describe the northern Botswana region slightly differently. Compared to Romanens et al. (2019), the humid areas along the rivers have been more studied. However, always in a geochemical purpose and therefore it is not to be read as a rigorous vegetation cover study. The purpose of the research presented in Chapter 2 was to obtain methods and tools to better trace past biomes of the region through geochemical values.

1.2.8. Lake Liambezi and its ecology

Lake Liambezi is subject to significant variations in its extent, size and depth. It thus demonstrates periods of complete drying up which can last years (e.g., Peel et al., 2015; Mutelo et al., 2013). Peel et al. (2015) demonstrated the fast recolonization of the lake after several years of total drying by aquatic macrophytes and fishes. Lake vegetation is dominated by emergent aquatic macrophyte *Phragmites australis* that forms dense stands covering large parts of the lake and extensive beds of submerged *Lagarosiphon ilicifolius* and *Najas horrida* occurring in shallower areas (Peel et al., 2015). 46 species of fish in total were reported in the lake where 29 species were recorded in experimental gillnets with a domination by *Brycinus lateralis* and *Schilbe intermedius*, contributing 39.5% and 38.5% by weight of the catches, respectively (Peel et al., 2015). Nutrient input into the lake is mostly via the two Kwando and Zambezi slow-flowing rivers. So, the surrounding reed swamp appears to act as a nutrient sponge which absorbs available nutrients and releases nutrients in detrital form into the open lake (Seaman et al., 1978). The slightly alkaline pH of the lake (values about 7.5-8.5) is not favourable to C₄ Papyrus that prefers slightly acidic waters (Peel et al., 2015; Seaman et al., 1978). C₃ *Phragmites* are then the dominant primary producers of Lake Liambezi (Seaman et al., 1978).

The lake area represents a mosaic of land use and management units (Pricope, 2013). It forms an important part of the local fishery when fulfilled and supports biodiversity, livelihoods and transport systems. When the lake dries up partly or completely, the lakebed is utilised for crop and livestock farming by local communities (Mutelo et al., 2013). It holds subsistence communal lands predominantly utilized for livestock grazing or agricultural lands, differently managed forest reserves in both countries, a national park (Chobe National Park) and several community villages or settlements (Pricope, 2013; Mutelo et al., 2013). Local livelihood of the communities are based on a subsistence economy driven by small-scale rainfed agriculture, fisheries, wild foods and a reliance on natural resources. The natural resources are covered with wood for fuel, tree products for building, grass for thatching, reeds for building courtyards and sleeping mats while Lala palm products are used for weaving baskets (Mutelo et al., 2013). Maize, millet, beans and pumpkins represent the different grown crops where cattle and goat are the common livestock found in lake's area (Mutelo et al., 2013).

Swamp plants such as papyrus and phragmites are renewing seasonally. They represent a large source of organic matter and leads to peat formation in low oxygen conditions. Important amounts of methane gas might be produce through such process. It results in frequent fires, from natural or human origin in the swamps environment of Linyanti-Liambezi area (Pricope et al., 2013). Similar observation is made at the neighbouring system of Okavango ecosystem, where surface fires are a regular and important feature. It clears out accumulated dead plant material and is essential to prevent such accumulation and assist in nutrient recycling. Another typical feature is peat fire that are different from surface fires. They might be ignited by surface fires, but as well by lightning or even spontaneous combustion. The combustion is very slow and is more about smouldering than burning but produces very little smoke. Peat fire may participate to drastically reduce the thickness of peat accumulation with a reduction of up to 90% of the initial volume (McCarthy, 2013). Following similar features, fire outbreaks are frequently reported in Lake Liambezi ecosystem (Mutelo et al., 2013) and are responsive of occasionally deaths of cattle but also of wild animals (Personal communication with guides and local inhabitants).

Water stable isotopes present extremely evaporated values for Lake Liambezi samples (Dyer, 2017). It confirms the endoreic state of the lake for both rainwater and river water of Linyanti and Chobe Rivers. Ionic composition of the lake is similar between dry and wet seasons. However, ion concentration is higher during the dry season, showing the evaporation effect. This important evaporation leads to the ion and calcite saturation of the lake. Dissolved Inorganic Carbon (DIC) isotopic values ($\delta^{13}\text{C}_{\text{DIC}}$) of Lake Liambezi follow the same trends with more positive values during dry season. However, even during the wet season, values are very close to 0‰ VPDB. It confirms the strong

evaporation resulting to the isotopic equilibration towards the atmospheric carbon signature. However, the isotopic $\delta^{13}\text{C}_{\text{DIC}}$ value measured during the dry season might also suggest an influence of the methanogenesis production from the organic rich sediments and peat derived from C_3 Phragmites material (Dyer, 2017).

Significant amount of sepiolite associated with littoral carbonate sediments described by Shaw (2009) are interpreted as indicative of precipitation within a lacustrine/palustrine system of low-energy with fluctuating salinity and pH. They might reflect the unstable characteristics of the local body of water over time, alternating between multiple source feeding and drying phase (Shaw, 2009).

1.3. Objectives of the project

As described above, north Botswana represents a very complex environmental region with multiple factors involved in its environmental cycles and in its landscape. Environmental and landscape features such as rivers, lakes, floodplains, islands and connections in the Linyanti-Chobe Basin evolve a lot. The timing of the evolutions and changes of these features is poorly described. The complexity of such a system makes it difficult to trace and to target the factors of change and evolution. More often in such a complex system, factors of evolution are multiple. In order to understand better the climatic variation and ecosystem evolution in northern Botswana we offer a multidisciplinary approach using traditional and new palaeolimnological tools. This approach required the construction of a structured program where each method represents an additional step with new facets in the interpretation of the environment studied as well as new horizons and perspectives. The present work therefore offers the discovery and understanding of a unique environment through a succession of subjects and methods. Questions and original objectives were proposed at the start of the thesis. They have subsequently greatly evolved, becoming denser, more precise or redirected according to the progress of the results. It is therefore an exploratory work whose goal is to discover an environment, to describe it and to discover its complexity.

However, the origin of the project aims to integrate, develop and validate the use of an innovative method developed in microbiology. The use of endospore-forming Firmicutes was therefore integrated as paleoecological indicators in lake sediments in the multidisciplinary approach of the study. In addition to the exploratory work on the northern Botswana region for a better understanding of its environmental and climatic evolution, the present work also aims to validate the use of the microbiological method in this type of exploratory study.

Within this broad framework, a series of questions can be structured as follows:

- i. Organic matter represents a tool of choice for environmental studies as well as the paleoenvironmental reconstruction of sites such as lakes. Its study is done through geochemistry. The first step of the present study was then to measure and trace the organic matter present in the soils and sediments and to compare it with the vegetation in place. The aim was to highlight the link between the vegetation in place and the surrounding soils or sediments. If this link does exist, the reconstruction of paleolakes is then feasible using the geochemistry of the organic matter present in the sediments. Trends in the distribution of the geochemical composition of organic matter have also been investigated. This in order to observe if one or more trends are emerging in this region.
- ii. Except studies on its limnology and its fish population, Lake Liambezi has never been described. Therefore, a first description of its sedimentology is needed. A multidisciplinary approach has been used. The work is exploratory and the main objectives are to discover the type of sedimentation of the lake with then the objective of determining an environmental history of the lake.
- iii. The next step was therefore the environmental evolution of the lake. To do this, an environmental evolution of each sediment core was carried out using the various tools used (sedimentology,

- geochemistry and microbiology). A dating test was then carried out using the radiocarbon dating method on a selection of samples. This method not showing clear results with a simple interpretation, it was necessary to complete the age model constructed with other methods. Once again, it is thanks to the multidisciplinary approach that we wanted to answer this question.
- iv. The environmental reconstruction of the lake turned out to be complex, including several factors in its evolution, such as the tectonic activity linked to the Okavango Graben, the local geomorphological specificities or even the evolution of the climate. These different factors had to be identified in order to better understand their potential role and above all, to try to measure their impact on the evolution of Lake Liambezi. Each method of the multidisciplinary approach was able to provide information on the influence of each factor. However, we can note that the microbiological approach had a major impact in this understanding. The geochemistry of organic matter as well as the grain-size distribution also played an important role.
 - v. The microbiological approach has proven to be a powerful tool even in purely exploratory work. This method was used at every stage of the present study. It participated in the description of the environmental evolution of each of the three sites. It was then used to complete the age model defined for Lake Liambezi. And its role was crucial in the paleoenvironmental reconstruction of the lake. If the use of this innovative method has been made possible in these different stages, it is because it has brought to the fore phenomena that have gone unnoticed with the more traditional methods. The sulphur cycle in particular as well as the presence of bacteria linked to hydrothermalism. The presence of bacteria linked to hydrothermalism was an important question in this exploratory work. We had to understand their presence, their origin and their meaning.
 - vi. Reconstruction of climate change for southern Africa since the end of the African Humid Period (AHP) is widely debated because little data exists and it is sometimes contradictory. We wanted to compare our climatic deductions against other works dealing with this subject.
 - vii. This exploratory study was conducted with a multidisciplinary approach. What was the integration of the innovative approach using microbiology for the paleoenvironmental reconstruction of a lake, what were its contributions and finally, is it an approach that can be generalized?

The following chapters aim to answer to these questions. Chapter 2 starts with the geochemical description of the soils and vegetation of the Linyanti-Chobe Basin. A few rivers are investigated as well and bring additional information about the geochemistry of sediments coming from the watershed of Lake Liambezi. Following chapters will focus on Lake Liambezi and its sedimentological aspects. Chapter 3 aims at a first characterization of the lake sediments with a precise description of the material found in the sediments and an investigation on the origin of the different material. Chapter 4 introduces the novel approach using microbiology. It is made through a precise description of the evolution of the sediments through depth. In this context, data acquired with more classical methods are added to obtain a direct comparison of the results and to build a global discussion of the evolution of each sampled site. This chapter allows the validation of the use of the microbiology as an environmental tracer in lake sediments; not only in actual sediments, but also in older sediments corresponding to past environmental conditions. Thus, the microbiological approach used in the present work did permit to trace and characterize past environmental conditions. Chapter 5 aims to give an age to the sediments and thus, to the lake. Again, a multidisciplinary approach is used to respond to such a complex environment. The age model is built after a combination of multiple methods. Radiocarbon dating using the ^{14}C -activity of the sediments is completed with diverse relative dating methods using clay mineralogy and microbiology. All obtained results are compiled in the final Chapter 6. The pooling of all the different methods highlights the complementarity of methods coming from various fields and using different material. It did permit to build a precise environmental and climatic history for Lake Liambezi.

1.4. Prior description of the secondary sites sampled

Five additional sediment samples were taken in different tributaries of the lake. For them, sampling has been made with a sanitized shovel and stored into sterilized plastic bags. Samples have been then frozen and transported into a fridge. Two samples have been taken along the Linyanti Swamp at Linyanti Campground. A geological fault forms an area of wetlands composed by a complicated patchwork of swamps and marshes known as Linyanti River. Its distance to Lake Liambezi is about 60 kilometres south-west. Two further samples were taken along the Chobe. A first one in Kavimba, at about 26 kilometres of Lake Liambezi. That sampling site is an oxbow lake of a channel of the Chobe River. It is located along the road from Kasane to Kachikau 2 km northeast side of Legotlhwana. The second site is the large floodplain of the Chobe River at about 26 kilometres southeast before the Chobe River reaches the lake. The area is a wetland composed by a complicated pattern of old channels and oxbow lakes. It is along the road from Kasane to Kachikau, 8.3 km north-eastern side of Kachikau and 4.2 km south-western side of Legotlhwana. The last sampling site is located in the lakeshore at the Linyanti River mouth at the extreme south-west shore of the Lake Liambezi. For these nine first samples, sampling was made with a sanitized shovel and put into sterilized plastic bags. Samples were then frozen. All sampling sites are located in Botswana.

1.4.1. BO01: Thamalakane

The sample was taken on the shore of the Okavango River on the main channel that follows the geological fault that cut the Okavango Delta on its Southeastern part. It is located less than 10 km upstream and at the Northeast of the center of Maun, right upstream of the Okavango River Lodge. Farms, lodges and small villages surround the area.

1.4.2. BO02: Rileys Cresta

Along the same river channel than BO01, that part of the Okavango River plays the role of exit channel for the Okavango Delta because of the geological fault. The river crosses the center of Maun and the sample site is located under a road bridge in the center of the city, front of the Rileys Cresta Hotel. Number of waste pollute the site.

1.4.3. BO03: Khwai River (Kudumane)

The site is a pond that forms an oxbow lake along an old channel of the Khwai River. It is located 3.4 km upstream and Southern part of the little village of Mababe. The Khwai River is a tribute of the Okavango Delta located at the extreme East side of the delta.

1.4.4. BO04: Mababe Bridge

The sampling site is situated along the Khwai River channel, which is a tribute of the Okavango Delta located at the extreme East side of the Delta. The site is at 600 m upstream and West of the village of Mababe.

1.4.5. BO05 and BO06: Linyanti

The site is located along the Linyanti Swamp at Linyanti Campground. A geological fault forms an area of wetlands composed by a complicated patchwork of swamps and marshes known as Linyanti River.

1.4.6. BO07: Chobe

The site is the floodplain of the Chobe River. The area is a wetland composed by a complicated pattern of old channels and oxbow lakes. It is along the road from Kasane to Kachikau, 8.3 km Northeastern side of Kachikau and 4.2 km Southwestern side of Legotlhwana.

1.4.7. BO08: Kavimba

The sampling site is an oxbow lake of a channel of the Chobe River. It is located along the road from Kasane to Kachikau 2 km Northeast side of Legotlhwana.

1.4.8. BO09: Lake Liambezi

The sampling site is located on the extreme South-West shore of the Lake Liambezi.

1.5. Additional projects:

As part of the project of development and validation of this new method in microbiology using spore-forming bacteria, my work also covered side projects conducted by colleagues. The development of the method covered in particular the ecology of spore-formers. This has been published in Paul et al. (2019) and is to be found in the appendix. I also helped for the realisation of the sedimentological and geochemical part of an unpublished Master thesis aiming at the investigation of bacterial communities in high mountain lakes. The work aimed to study the evolution of microbiological communities in a group of lakes testifying to the gradual retreat of a glacier in high mountains (Joeri Lakes in Graubünden) (Fetton-Hayoz, 2018). The Master thesis is to be found in the electronic file related to the present work. Data relative to sedimentology and geochemistry are to be found in the appendix.

As member of the doctoral program in Earth Surface Processes & Paleobiosphere of the Conférence Universitaire de Suisse Orientale (CUSO), I get the opportunity to participate in an ecological survey campaign in the Maldives. This campaign was then fixed with three publications (Beccari et al., 2020; Stainbank et al., 2020; Caragnano et al., 2021). These publications are to be found in the electronic file related to my thesis.

1.6. References

- Ballif, L. 2018. Carbon and nitrogen stable isotope compositions as environmental proxies in savannas of northern Botswana. Unpubl. Master of Science in Biogeosciences, UNIL.
- Bauer, P., Gumbrecht, T., Kinzelbach, W., 2006. A regional coupled surface water/groundwater model of the Okavango Delta, Botswana. *Water Resources Research*, 42.
- Beccari, V., Spezzaferri, S., Stainbank, S., Hallock, P., Basso, D., Caragnano, A., Pisapia, C., Adams, A., Angeloz, A., Del Piero, N., Dietsche, P., Eymard, I., Farley, N., Fau, M., Foubert, A., Lauper, B., Lehmann, A., Maillet, M., Negga, H., Ordonez, L., Peyrotty, G., Rime, V., Rüggeberg, A., Schoelhorn, I., Vimpere, L., 2020. Responses of reef bioindicators to recent temperature anomalies in distinct areas of the North Ari and Rasdhoo atolls (Maldives). *Ecological Indicators*, 112, 1-8.
- Bird, M.I., Veenendaal, E.M., Lloyd, J.J. 2004. Soil carbon inventories and $\delta^{13}C$ along a moisture gradient in Botswana. *Global Change Biology* 10, 342-349.
- Bufford, K.M., Atekwana, E.A., Abdelsalam, M.G., Shemang, E., Atekwana, E.A., Mickus, K., Moidaki, M., Modisi, M.P., Molwalefhe, L., 2012. Geometry and faults tectonic activity of the Okavango Rift Zone, Botswana: Evidence from magnetotelluric and electrical resistivity tomography imaging. *Journal of African Earth Sciences*, 65, 61-71.
- Burke, J.J., Pricope, N.G., Blum, J., 2016. Thermal Imagery-Derived Surface Inundation Modeling to Assess Flood Risk in a Flood-Pulsed Savannah Watershed in Botswana and Namibia. *Remote Sensing*, 8, 676.
- Burrough, S.L., Thomas, D.S.G., 2008. Late Quaternary lake-level fluctuations in the Mababe Depression: Middle Kalahari palaeolakes and the role of Zambezi inflows. *Quaternary Research* 69, 388-403.
- Burrough, S.L., Thomas, D.S.G., Shaw, P.A., Bailey, R.M. 2007. Multiphase Quaternary highstands at Lake Ngami, Kalahari, northern Botswana. *Palaeogeography, Palaeoclimatology, Palaeoecology* 253, 280–299.
- Burrough, S.L., Thomas, Singarayer, J.S., 2009. Late Quaternary hydrological dynamics in the Middle Kalahari: Forcing and feedbacks. *Earth-Science Reviews*, 96, 313–326.
- Caragnano, A., Basso, D., Spezzafari, S., Hallock, P. and Conférence Universitaire de Suisse Occidentale Scientific Party, 2021. A snapshot of reef conditions in North Ari Atoll (Maldives) following the 2016 bleaching event and *Acanthaster planci* outbreak. *Marine and Freshwater Research*, 1-10.
- Cavaillé-Fol, 2020. On a découvert le berceau de l'Humanité. *Science & Vie*, N°1233, juin 2020, 56-71.
- Chevalier, M., Chase, B.M., 2015. Southeast African records reveal a coherent shift from high- to lowlatitude forcing mechanisms along the east African margin across last glacial-interglacial transition. *Quaternary Science Reviews*, 125, 117-130.
- deMenocal, P., Ortiz, J., Guilderson, T., Adkins, J., Sarnthein, M., Baker, L., Yarusinsky, M., 2000. Abrupt onset and termination of the African Humid Period: rapid climate responses to gradual insolation forcing. *Quaternary Science Reviews*, 19, 347-361.
- Dyer, S. 2017. Water cycle in the Northern Kalahari. Unpubl. Master of Science in Biogeosciences, UNIL.
- Fatton-Hayoz, M. 2018. Investigation of bacterial communities in high mountain lakes: Total versus spores' fractions. Unpubl. Master of Science in Biogeosciences, UNINE.
- Gamrod, J.L., 2009. Paleolimnological records of environmental change preserved in Paleo-Lake Mababe, Northwest Botswana. Unpubl. Master of Science, Oklahoma State University.
- Gärtner, A., Linnemann, U., Hofmann, M. 2013. The provenance of northern Kalahari Basin sediments and growth history of the southern Congo Craton reconstructed by U–Pb ages of zircons from recent river sands. *International Journal of Earth Sciences*, 103, 579-595.
- Gumbrecht, T., Wolski, P., Frost, P., McCarthy, T.S., 2004. Forecasting the spatial extent of the annual flood in the Okavango delta, Botswana. *Journal of Hydrology*, 290, 178-191.

- Haddon, I.G., McCarthy, T.S. 2005. The Mesozoic–Cenozoic interior sag basins of Central Africa: The Late-Cretaceous–Cenozoic Kalahari and Okavango basins. *Journal of African Earth Sciences* 43, 316-333.
- Jones, C.R., 1980. The Geology of the Kalahari. *Botswana Notes & Records*, 12, 1-14.
- Killops S.D. and Killops V.J. 2005. Introduction to organic geochemistry (2nd edition). ISBN 0-632-06504-4, Blackwell Publishing, Oxford, UK.
- Kinabo, B.D., Atekwana, E.A., Hogan, J.P., Modisi, M.P., Wheaton, D.D., Kampunzu, A.B. 2007. Early structural development of the Okavango rift zone, NW Botswana. *Journal of African Earth Sciences*, 48, 125-136.
- Kinabo, B.D., Hogan, J.P., Atekwana, E.A., Abdelsalam, M.G., Modisi, M.P., 2008. Fault growth and propagation during incipient continental rifting: Insights from a combined aeromagnetic and Shuttle Radar Topography Mission digital elevation model investigation of the Okavango Rift Zone, northwest Botswana. *Tectonics*, 27, 1-16.
- Kurugundla, C.N., Dikgola, K., Kalaote, K., 2010. Restoration and Rehabilitation of Zibadianja Lagoon in Kwando-Linyanti River System in Botswana. *Botswana Notes and Records*, 42, 79-89.
- McCarthy, T.S., 2013. The Okavango Delta and its place in the geomorphological evolution of southern Africa. *South Africa Journal of Geology*, 116, 1-54.
- Mendelsohn, J., El Obeid, S., 2004. Okavango River: the flow of a lifeline. *Struik*.
- Milzow, C., Kgotlhang, L., Bauer-Gottwein, P., Meier, P., Kinzelbach, W., 2009. Regional review: the hydrology of the Okavango Delta, Botswana - processes, data and modelling. *Hydrogeology Journal*, 17, 1297-1328.
- Moore, A.E., Cotterill, F.P.D., Main, M.P.L., Williams, H.B., 2007. The Zambezi River. *Large Rivers: Geomorphology and Management*, 311-332.
- Mukwati, B.T., Tafesse, N.T., Bagai, Z.B., Laletsang, k. 2018. Hydrogeochemistry of the Kasane Hot Spring, Botswana. *Universal Journal of Geoscience* 6, 131-146.
- Mutelo, M.A. 2013. An understanding of variations in the area extent of Lake Lyambezi: Perspective for water resources management. Unpubl. Master of Science in Integrated Water Resources Management of the University of Zimbabwe.
- Pastier, A.M., Dauteuil, O., Murray-Hudson, M., Moreau, F., Walpersdorf, A., Makati, K. 2017. Is the Okavango Delta the terminus of the East African Rift System? Towards a new geodynamic model: Geodetic study and geophysical review. *Tectonophysics* 712-713, 469-481.
- Pastouret, L., Chamley, H., Delibrias, G., Duplessy, J.C., Thiede, J., 1978. Late Quaternary climatic changes in Western Tropical Africa deduced from deep-sea sedimentation off the Niger delta. *Oceanologica Acta*, 1, 217-232.
- Paul, C., Filippidou, S., Jamil, I., Kooli, W., House, G.L., Estoppey, A., Hayoz, M., Junier, T., Palmieri, F., Wunderlin, T., Lehmann, A., Bindschedler, S., Vennemann, T., Chain, P.S.G., Junier, P., 2019. Bacterial spores, from ecology to biotechnology. *Advances in Applied Microbiology*, 106, 79-111.
- Peel, R.A., Tweddle, D., Simasiku, E.K., Martin, G.D., Lubanda, J., Hay, C.J., Weyl, O.L.F. 2015: Ecology, fish and fishery of Lake Liambezi, a recently refilled floodplain lake in the Zambezi Region, Namibia. *African Journal of Aquatic Science* 40:4, 417-424.
- Pricope, N.G., 2013. Variable-source flood pulsing in a semi-arid transboundary watershed: the Chobe River, Botswana and Namibia. *Environ Monit Assess*, 185, 1883-1906.
- Romanens, R. 2017. Organic matter dynamics and soil diversity in the Chobe Enclave, Botswana. Unpubl. Master of Science in Biogeosciences, UNIL.
- Romanens, R, Pellacani, F., Mainga, A., Fynn, R., Vittoz, P., Verrecchia, E.P., 2019. Soil diversity and major soil processes in the Kalahari basin, Botswana. *Geoderma Regional*, 19.

- Schlettwein, C.H.G., Bethune, S., 1992. Aquatic weeds and their management in southern Africa: biological control of *Salvinia molesta* in the Eastern Caprivi. Wetland conservation conference for southern Africa. IUCN, Gland. 173-187.
- Scholes, R. J., & Archer, S. R., 1997. Tree-grass interactions in savannas. *Annual review of Ecology and Systematics*, 28, 517-544.
- Seaman, M.T., Scott, W.E., Walmsley, R.D., van der Waal, B.C.W., & Toerien, D.F. 1978: A limnological investigation of Lake Liambezi, Caprivi. *Journal of the Limnological Society of Southern Africa* 4:2, 129-144.
- Setti, M., López-Galindo, A., Padoan, M., Garzanti, E. 2014. Clay mineralogy in southern Africa river muds. *Clay Minerals*, 49, 717-733.
- Shaw, A.I., 2009. The characterisation of calcrete based on its environmental settings within selected regions of the Kalahari, Southern Africa. Doctorate Thesis, University of Oxford.
- Shaw, P., 1984. A historical note on the outflows of the Okavango Delta system. *Botswana Notes and Records*, 127-130.
- Singletary, S.J., Hanson, R.E., Martin, M.W., Crowley, J.L., Bowring, S.A., Key, R.M., Ramokate, L.V., Direng, B.B., Krol, M.A., 2003. Geochronology of basement rocks in the Kalahari Desert, Botswana, and implications for regional Proterozoic tectonics. *Precambrian Research*, 121, 47-71.
- Skarpe, C., Arrestad, P.A., Andreassen, H.P., Dhillion, S.S., Dimakatso, T., du Toit, J.T., Halley, D.J., Hytteborn, H., Makhabu, S., Mari, M., Marokane, W., Masunga, G., Modise, D., Moe, S.R., Mojaphoko, R., Mosugelo, D., Motsumi, S., Neo-Mahupeleng, G., Ramotadima, M., Rutina, L., Sechele, L., Sejoe, T.B., Stokke, S., Swenson, J.E., Taolo, C., Vandewalle, M., Wegge, P., 2004. The Return of the Giants: Ecological Effects of an Increasing Elephant Population. *Ambio: A Journal of the Human Environment*, 33, 276-282.
- Skarpe, C., & Ringrose, S., 2014. The Chobe Environment. Elephants and Savanna Woodland Ecosystems: A Study from Chobe National Park, Botswana, 7-29.
- Stainbank, S., Spezzaferri, S., Beccari, V., Hallock, P., Adams, A., Angeloz, A., Basso, D., Caragnano, A., Del Piero, N., Dietsche, P., Eymard, I., Farley, N., Fau, M., Foubert, A., Lauper, B., Lehmann, A., Maillet, M., Negga, H., Ordonez, L., Peyrotty, G., Rime, V., Rüggeberg, A., Schoellhorn, I., Vimpere, L., 2020. Photic stress on coral reefs in the Maldives: The *Amphistegina* bleaching index. *Ecological Indicators*, 113, 1-9.
- Thomas, D.S.G., Burrough, S.L., 2012. Interpreting geoproxies of late Quaternary climate change in African drylands: Implications for understanding environmental change and early human behaviour. *Quaternary International*, 253, 5-17.
- Thomas, D.S.G., Shaw, P.A., 1991. *The Kalahari Environment*. Cambridge University Press, New York.
- Truc, L., Chevalier, M., Favier, C., Cheddadi, R., Meadows, M.E., Scott, L., Carr, A.S., Smith, G.F., Chase, B.M., 2013. Quantification of climate change for the last 20,000 years from Wonderkrater, South Africa: Implications for the long-term dynamics of the Intertropical Convergence Zone. *Palaeogeography, Palaeoclimatology, Palaeoecology*, 386, 575-587.
- Vainer, S., Matmon, A., Erel, Y., Hidy, A.J., Crouvi, O., DeWit, M., Geller, Y., ASTER Team, 2020. Landscape responses to intraplate deformation in the Kalahari constrained by sediment provenance and chronology in the Okavango Basin. *Basin Research*, 00, 1-24.
- Van Der Waal, B.C.W., 1990. Aspects of the fishery of the Eastern Caprivi, Namibia. *MADOQUA*, 17, 1-16.
- Vittoz, P., Pellacani, F., Romanens, R., Mainga, A., Verrecchia, E.P., Fynn, R.W.S., 2020. Plant community diversity in the Chobe Enclave, Botswana: Insights for functional habitat heterogeneity for herbivores. *Koedoe*, 62.
- Walker, M., 2005. *Quaternary Dating Methods*. Wiley, West Sussex, UK.

- Wang, Y., Zheng, S.H.,1989. Paleosol nodules as Pleistocene paleoclimatic indicators, Luochuan, PR China. *Palaeogeography, Palaeoclimatology, Palaeoecology*, 76, 39-44.
- Wiese, R., Hartmann, K., Gummersbach, V.S., Shemang, E.M., Struck, U., Riedel, F., 2020. Lake highstands in the northern Kalahari, Botswana, during MIS 3b and LGM. *Quaternary International*, 558, 10-18.

2. Vegetation and soil carbon and nitrogen contents and stable isotope compositions in savannas of northern Botswana as environmental proxies

Anaël Lehmann¹, Léandre Ballif¹, Pascal Vittoz¹ and Torsten Vennemann^{1&}

¹Institute of Earth Surface Dynamics, Faculty of Geosciences and the Environment, University of Lausanne, CH 1015, Lausanne

[&]Corresponding authors: Torsten Vennemann. Laboratory of Stable Isotope Geochemistry. Institute of Earth Surface Dynamics, University of Lausanne, CH-1015 Lausanne. Mail: Torsten.Vennemann@unil.ch; Phone: +41216924464.

2.1. Abstract

The active global carbon budget at the Earth's surface is in important part represented by the terrestrial vegetation together with the soil organic matter reservoir. The time-integrated isotopic composition of the vegetative cover that existed in the place of study might be reconstruct by the C- and N-isotope composition, in the absence of an important extraneous, aeolian contribution. In tropical and subtropical regions, the isotopic composition is primarily controlled by the climate and follows therefore global trends related notably by the annual average precipitation. However, regional specificities such as regional water availability, topography and physico-chemical properties of the soil, as well as external factors such as land use and fire hazards may influence the type of organic matter, including the presence and abundance of isotopically distinct C₃ and C₄ vegetation, and finally the total amount of organic matter preserved in soils. Studies have confirmed a global trend in Botswana in the distribution of SOM and its isotopic composition. However, north Botswana is crossed by an incipient continental graben basin called Okavango Graben. Structural features formed by the neo-tectonic activity affect the regional hydrological system and create a complex network of rivers and waterbodies. Therefore, the distribution of SOM and its isotopic composition is believed to follow more complicate trends in this region and to correspond more to the water availability and the water table distribution pattern.

The results demonstrate a density and distribution of the vegetation cover and type in the Linyanti-Chobe basin clearly related to the geomorphology as well as the proximity to both ground and surface waters. Isotopic measurements on trees demonstrate a higher water stress for shallow rooted trees compared to deep rooted trees, demonstrating the high dependence of the trees to the water table. Intra-species water stress is also observed depending on the access to water of the location. It allows then a better understanding of the well developed riparian forest along the waterbodies and of the stunted Mopane tree forests away from the main waterbodies. For all the built classes, the $\delta^{13}\text{C}_{\text{SOM}}$ shows a direct relationship with the type of vegetation that covers it. A direct relationship can be therefore established between plant cover and isotopic signal of carbon from soil organic matter. This allow us to believe in a poor organic matter transport and the possibility to use SOM of paleo-soils or sediments to reconstruct the plant cover of the deposit. This exercise is indeed made for the sampled river sediments and is conclusive as results correspond with field observations. Foliar $\delta^{15}\text{N}$ gave again information about the topography and access to water. The distance of the sampled plants to the water source influenced directly the isotopic composition of N. The water table shows also a role regarding the plant types and species with the depth their roots reaches. The compilation of previous observations made possible the proposal of a simplified representation of the distribution of vegetation and soil geochemistry according to a gradient starting from a water surface (river or lake)

and ending its course away from this body of water. This represents a regional specificity which contradicts the idea of a north-south vegetation gradient linked to the mean annual precipitation (MAP).

In a future optic aiming at the comprehension of the Quaternary and Recent ecological evolution of the region, the present work aims at evaluating the utility of the natural abundance of stable carbon and nitrogen isotopes in soils and sediments from lacustrine or swamp environments to trace shifts between C₃ and C₄ dominance as an estimate of local moisture conditions. The use of these measurements has been here proven and is encouraging for future studies.

2.2. Introduction

The terrestrial vegetation together with the soil organic matter reservoir represent an important part of the active global carbon budget at the Earth's surface (e.g., Killops & Killops, 2005). Understanding the natural biogeochemical changes in these reservoirs with time is hence also essential for improving our knowledge on any anthropogenic changes to the global carbon cycle. The stable isotope compositions (¹³C/¹²C and also ¹⁵N/¹⁴N, for example) of organic matter are commonly used as tracers for global carbon cycling between the different terrestrial reservoirs of carbon as represented by the atmosphere, biosphere, hydrosphere and also the geosphere (e.g., Hoefs, 2015). In the case of the soil organic matter (SOM) reservoir, the C- and N-isotope composition, in the absence of an important extraneous, aeolian contribution, normally provides the time-integrated isotopic composition of the vegetative cover that existed in the place of study (e.g., Park and Epstein, 1960; Sweeney and Kaplan, 1980; O'Leary, 1981; Farquhar et al., 1989). The isotopic composition, in turn, is primarily controlled by the prevailing local and global climate, in tropical and subtropical regions most notably by the annual average precipitation. Precipitation and regional humidity, together with other factors including the topography and physico-chemical properties of the soil, as well as external factors such as land use and fire hazards, also control the type of organic matter, including the presence and abundance of isotopically distinct C₃ and C₄ vegetation, and finally the total amount of organic matter preserved in the soil (e.g., Hayes, 1993; 2001; Bird et al., 2001). The inverse of this is that detailed studies of the amount and isotopic composition of SOM in paleosols can be used for paleoecological and paleoclimatic interpretations, given that the effects of degradation of the organic matter in the sediment/soil but also the local versus aeolian origin of the SOM can be adequately characterized (Deines, 1980; Hayes et al., 1983; Freeman et al., 1990).

Paleoenvironmental research in subtropical southern Africa is complicated, however, largely because of both a low bioproductivity in the semi-arid to arid climates prevailing and also because of a poor preservation of organic matter in the sandy soils that allow for a rapid drainage across the soil horizons and a good ventilation with an ease of access for atmospheric oxygen (Schulze et al., 1996; 1998; Feral et al., 2003; Ringrose et al., 2003; Bird et al., 2004; Swap et al., 2004; Krah et al., 2006). The region of the Okavango Delta and adjacent Chobe-Linyanti River transboundary watershed in northern Botswana and northeastern Namibia represents the most important resource of water for Botswana and northern Namibia. These drainage basins also offer the best potential of preserving organic matter within the soils and lake sediments of both the permanently (Okavango) and seasonally flooded (Chobe-Linyanti River System, including Lake Liambezi) drainage basins (Mubyana et al., 2003; Pricope et al., 2015), which if proven correct, opens up the possibility of paleoenvironmental research to be conducted. In view of the importance of this region as an important groundwater resource, but also because of its touristic and agricultural importance to both the Namibian and Botswana economies, an improved understanding of likely ecological changes expected with the predicted changes in climate in this semi-arid region of South-Central Africa will help to determine the measures required for the best possible preservation of this ecologically sensitive area.

Of importance to studies of mixed C3/C4 ecosystems is that the distribution of SOM and its isotopic composition is determined principally by the heterogeneous distribution of C3 and C4 vegetation in the landscape (e.g. Bird & Pousai, 1997; Bird et al., 2000), but also by the local conditions of moisture. Hence, the sampling approach was to divide the areas of interest into parts dominated by C3 or C4 vegetation, and separately sample these areas as a function of distance from the water courses. The samples are then weighted according to the proportion of C3 and C4 vegetation cover present in the area in order to provide the weighted amount and isotopic composition of the SOM (see also Bird et al., 2001 for discussion).

The present work aims at evaluating the utility of the natural abundance of stable carbon and nitrogen isotopes in soils and sediments from lacustrine or swamp environments to trace shifts between C3 and C4 dominance as an estimate of local moisture conditions. Such data could give new insights on the Quaternary and Recent ecological evolution of the region. It focuses on the soil-vegetation interactions, in terms of resource acquisition by plants, and the cycles of carbon and nitrogen, given the particular hydrology of the Okavango-Kwando-Chobe terminal endoreic system. In particular, we aim to improve our understanding the environmental controls on the distribution and productivity of C3 and C4 biomass in the modern environment and subsequently allow for a better reconstruction of the past environment using the carbon isotope composition of paleosols, phytoliths, soil carbonate, and fossil organic matter.

2.3. Material and methods

2.3.1. Regional settings of northern Botswana

Northern Botswana holds the north of the Kalahari Basin formed by an epeirogenic uplift (Haddon & McCarthy, 2005; Singletary et al., 2003; Jones *et al.*, 1980). It is crossed by an incipient continental graben called Okavango Graben found at the terminal of the southwestern branch of the East African Rift System (Bufford et al., 2012; Haddon & McCarthy, 2005; Jones et al., 1980). Structural features formed by the neo-tectonic activity affect the regional hydrological system (Kinabo et al., 2007) and create a complex network of rivers and waterbodies (Haddon & McCarthy, 2005). It results in the creation of endorheic deltas and lakes for the Okavango, Kwando and Chobe Rivers and builds up a series of sub-basins: The Okavango basin and the Ngami basin in the southwestern part, the Mababe basin and the Linyanti the Linyanti-Chobe basin at the northeastern part. The present study compares several short vegetation and soil traverses from all three basins, but focusses principally on those of the Linyanti-Chobe basin (Figure 15).

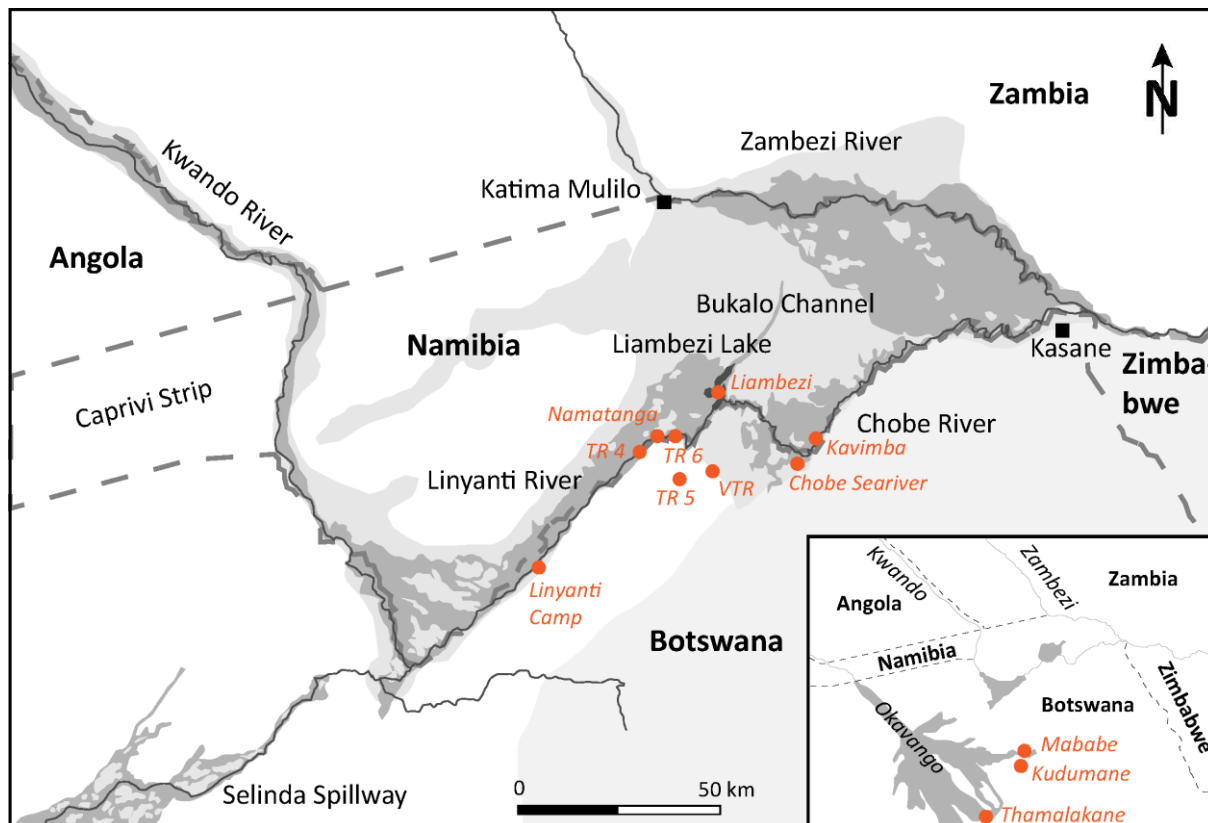


Figure 15 General map of the northern Botswana with the three main river systems: Okavango, Kwando and Zambezi. Enlargement and focus on the Linyanti-Chobe Basin with Lake Liambezi in its middle. Orange dots indicate sampling locations.

2.3.2. Bioclimatic data

The catchments to the Okavango, Kwando, and Zambezi are characterized by a humid, subtropical climate with a mean annual precipitation of 1300 mm. Rainfall occurs seasonally and the intensity depends critically on fluctuations in the positioning of the Intertropical Convergence Zone (ITCZ) but the rainy season is commonly between November and March (Mizlow et al., 2009). The discharge of the three river systems as well as the maximum flooding in the three distal wetlands towards the south is somewhat delayed though, given a slow flow of the groundwater over 100's of km's. The Okavango's and Kwando's maximum floods occur from June to August (Pricope, 2013), while that of the Zambezi has an earlier annual flood pulse that may also spill over into the Linyanti-Chobe wetlands through the Chobe River. The flooding area in the Linyanti-Chobe basin thus peaks between March and May, a few weeks after the Zambezi reaches its maximum discharge (Pricope, 2013). The Okavango waters penetrate in the Linyanti-Chobe basin only during exceptional floods via the Selinda Spillway. The relative exchange from the Zambezi and/or the Okavango/Kwando into the Linyanti-Chobe area may well have been more important during past humid periods, and the existence of a larger paleo-lake during the Quaternary is postulated (Burrough & Thomas, 2008), as supported by inherited geomorphological features in the landscape.

The mean annual precipitation in the Linyanti-Chobe basin is about 570 mm, with the majority of precipitation during the rainy season from November to March (Reference: climate-data.org). It occurs mostly as summer thunderstorm precipitation. The most distal southeastern branches of the Okavango Delta (Thamalakane and Kwai) are located further south of the north-south gradient of regional precipitation and receive a mean annual precipitation of only 450 mm (Reference: climate-data.org). In the Köppen-Geiger classification northern Botswana is classified as a hot semi-arid (steppe) climate (BSh). This classification is characterized by a mean annual temperature above 18 °C, low mean annual precipitation of which 70 % falls between October and March. Arid and semi-arid climates are also

defined by evapo-transpiration exceeding average annual precipitation. The semi-arid climate zones are, however, less extreme than arid climates in that the mean annual precipitation is sufficient to sustain woodland and shrubland communities. Vegetation is typical of southern African dry savannahs and spans from subtropical swamps to shrubland and dry forests, and finally to grasslands. Large-scale zonation of vegetation due to rainfall and temperature parameters determine the distribution of these sub-biomes over the subcontinent. The region covered in this study is unique though as the inland deltas of the Okavango and Kwando rivers, because of geologic, tectonic processes, drain into this arid to semi-arid region, hence establishing a regional-scale and even local-scale zoning of the same large-scale vegetation zones adjacent to the subtropical swamps/flooded areas. The Linyanti-Chobe basin in particular, is at the meeting point between different ecoregions that are all part of the "tropical and subtropical grasslands, savannahs and shrubland" biome (source : www.worldwildlife.org/ecoregions): the Zambebian flooded grasslands, the Zambebian and mopane woodlands, the Kalahari Acacia-Baikiaea woodlands and the Kalahari xeric savannah. The Linyanti-Chobe basin flora thus consists of a mix of species from these contrasting, neighbouring ecosystems.

2.3.3. Sampling

Soil and vegetation samples were collected in August 2016. Seven short transects were chosen from the southeastern part of the Okavango Delta to the Linyanti-Chobe Basin (Fig. 1). In addition, samples were taken from six isolated, including sites at the shores of Lake Liambezi. A total of 31 sites were sampled. The purpose of the transects was to sample along a relative "humidity gradient" with the vegetation adjacent to the present, dry season water bodies having access to the local groundwater (bottom of river or bottom of plain) whereas the vegetation away from such water bodies rapidly changes from a mixed vegetation including larger trees, via a shrub-dominated landscape with occasional trees only, to a typical grassland vegetation or to stunted Mopane tree forests only. Each transect presented a gradual or sometimes abrupt transition in its vegetation, often coinciding with changes in topography. The size of the transects varies according to the sites and ranges from a few tens of meters to several tens of kilometres. In addition, nine samples of sediments from water bodies were taken: four from different arms of the Okavango, two from the Linyanti river, one from the Chobe floodplain, one from within the Chobe river and finally, a sediment bordering the Lake Liambezi.

Systematically, a soil sample as well as samples of a small variety of plants were taken at each site. The soil sample was collected from the topsoil layer. This layer was reached by removing by hand the loose, aeolian sand that covers it until a more compact, cohesive layer was attained. Samples were collected with a small shovel from the first 5-10 cm. We avoided the soil directly below the canopy of trees and selected a point equidistant to surrounding stands. All samples were then put in sterile plastic bags and dried at 50°C for transportation and storage. A total of 28 soils and 44 plants were sampled, and for the plants often several distinct parts (leaves, bark, outer cellulose layers), giving a total of 139 analyses. For the plants, it was a total of 32 species sampled (4 woody perennials, 25 grasses and 3 sedges), in 22 genera within 5 families (order in brackets): Capparaceae (Brassicales), Combretaceae (Myrtales), Cyperaceae (Poales), Fabaceae (Fabales), Poaceae (Poales). Four wooded perennial species were selected to be sampled if present : *Acacia erioloba*, *Colophospermum mopane*, *Combretum mossambicense* and *Boscia albitrunca*. They are not especially dominant species but are readily identifiable and each representative of a different habitat. The bark, mature leaves, young stems and wood of each of these species were sampled on individual trees. The height of each sampled woody individual (m) was estimated visually. Grasses have been selected among the most abundant species. This was done to determine if most grasses follow the C4 pathway, as it is generally assumed for Southern African savannas, and to highlight potential trends in the C and N fractionations for C4 plants. Additionally, the data of grass species helped to build the vegetation classes. All samples were put in

plastic bags and brought back to the VanThuyne-Ridge Research Center for further determination and drying at 50°C.

2.3.4. Geochemical analyses

All vegetation samples were dried in an oven, wrapped in Al foil and transported to the University of Lausanne for analyses. All samples to be analysed for their isotopic composition were taken with a small stainless steel cutting knife, washed in dilute HCl (5 %) and several distilled water cycles. Subsequently, the samples were dried once again at 40 °C prior to their stable isotope analyses. Soil samples were also treated in a similar way, dried in the field at 40 °C and transported to Lausanne. Weighed sample splits were then washed in 10% HCl followed by careful rinse cycles with distilled water and centrifugation, drying at 40 °C and reweighing the samples to note the loss of the carbonate fraction.

Total organic carbon and nitrogen content and isotopic compositions were analysed using a Thermo Finnigan Flash Elemental Analyzer (EA) 1112 linked to a Delta V gas source mass spectrometer. Samples were weighed into Sn-foil capsules and reacted in the EA reactive column with an excess of O₂ heated to 1050 °C. All released gases (H₂O, N₂, CO₂ and SO₂) were transported in a He flow over water traps and passed over a gas chromatographic column into the dual inlet of the mass spectrometer for the carbon and/or nitrogen isotope analyses of the organic matter on CO₂ and N₂, respectively. Each series of about 50 samples was bracketed with six in-house standards (3 different standards, reproduced) at the beginning and end of the sequence for final data normalisation and calculation of the amount of organic carbon/nitrogen within the samples. The analytical error is better than ±0.1 %, based on replicates of the standards and samples. Results are given in the typical δ -notation in permil relative to the isotopic standard VPDB for the $\delta^{13}\text{C}$ and relative to AIR for the $\delta^{15}\text{N}$ values.

2.4. Results

In order to verify how the vegetation structure and composition changes along the selected traverses and sampling locations, the approach described in Tedder (2013) was used. The vegetation classifications proposed by McCarthy et al. (2005) and later also by Tedder et al. (2013) were used to establish the vegetation classes listed in Table 1 below. The goal of such a classification of the vegetation is to simplify the complex change in the composition and structure of the vegetation across the variation in landscape and hence to understand how the species are distributed and what this distribution is principally related to (e.g., precipitation and regional humidity gradients, groundwater levels, topography, physico-chemical properties of the soil, or a combination thereof, etc...), and finally if these changes are compatible with any changes in the stable C- and N-isotopic composition of the dominant plants and SOM for the different sampling sites and traverses.

Amount of samples obtained in field campaign did not statically allowed a classification that correspond to the field observations. However, the aim of the present work is not to argue for a novel vegetation classification for the region. This has been made by various authors (Romanens et al., 2019; Vittoz et al., 2020). On the other hand, the aim of the present study is to classify the region for its geochemical values in soils and plant cover. Therefore, a six-class classification was established, based on the structure of the plant community (presence/absence of woody cover, height of canopy), the type of dominant plants (sedge/grass, tall perennial grass/sparse low tufted grass, tree/shrub), a few diagnostic species based on Roodt (1998; 2015), all as observed and noted in the field. The vegetation classifications proposed by McCarthy et al. (2005) and Tedder et al. (2013) helped to build the classes and to determine the level of precision that was required for our dataset. Geochemical results did permit to confirm the coherence between the chosen classification. The resulting classification is made up out of two classes of wetlands: n°1 - reed bed, which is basically an aquatic grassland, and n°2 - sedgeland; two classes of grasslands: n°3 - floodplain grassland and n°4 - dry grassland; one class of

shrubland: canopy top ≤ 3 m, further divided in two subclasses, one that is dominated by Mopane ($n^{\circ}5a$) or *Combretum* shrubs ($n^{\circ}5b$); and one class of woodland, further divided in two subclasses: $n^{\circ}6a$ - Mopane woodland, and $n^{\circ}6b$ - mixed riverine and marginal floodplain woodlands or *Acacia* woodland. Table 1 summarizes the characteristics and data of each class.

In terms of the C- and N-isotope compositions of the plants, the C_3/C_4 plant separation is well represented. 25 samples of type C_3 plants were identified and 53 samples of type C_4 . For the C_3 plants, the $\delta^{13}C$ values have a range from -29.3 ‰ for an *Acacia* to -25.0 ‰ for *Phragmites australis*. For C_4 type plants, the $\delta^{13}C$ values have a range from -14.5 ‰ for *Cynodon dactylon* to -10.8 ‰ for *Panicum repens*. Nitrogen content in the plants have a range from 0.10 wt% for *Diheteropogon amplexans*, *Heteropogon contortus* and *Hyparrhenia rufa*, up to 2.70 wt% for *Boscia albitrunca*. For the $\delta^{15}N$ values, the range is between -5.6 ‰ for *Hyparrhenia rufa* up to +10.0 ‰ for *Boscia albitrunca*.

The amount of organic carbon in the soils has a range from 0.3 wt% up to 6.0 wt% for 28 of the 30 samples. Only two samples have higher TOC content of 9.6 and 10.1 wt% (samples TR 3.2 and 2.2). For 30 soils analysed, 28 have a range between -23.2 ‰ and -15.2 ‰, but two isolated samples have values of -12.7 ‰ and -12.1 ‰ (samples TR 5.2 and 5.3).

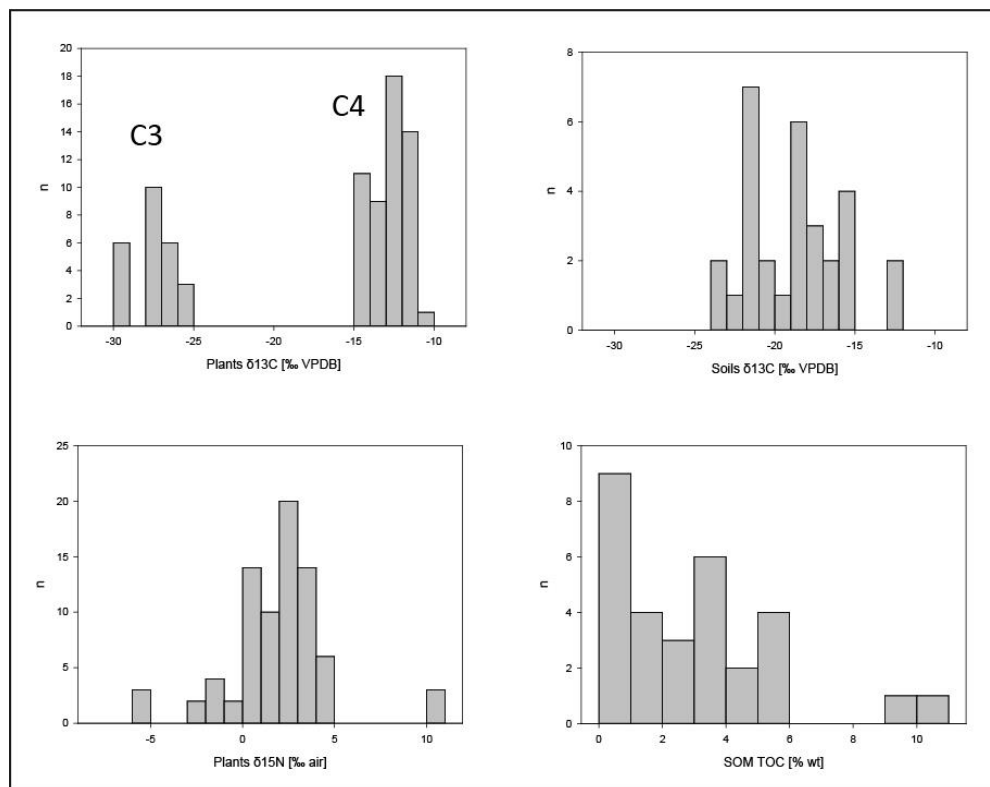


Figure 16 C- and N-isotope compositions of the plants, and C-isotope compositions as well as TOC of the soils. C_{org} isotopic analysis of plants shows the presence of both types of plants: C_3 and C_4 types. C_{org} isotopic analysis of soils shows a mix between the two types.

Table 1: Description of the six classes of vegetation with indication of the average results from the SOM analyses for each class. Diagnostic species and description of each class come from field observations, after Roodt (1998) and Roodt (2015) as well as from the vegetation surveys.

n°	Vegetation class	Diagnostic species	Description	Distribution in the Linyanti-Chobe basin and soil characteristics	$\delta^{13}\text{C}_{\text{SOM}}$ TOC _{SOM}
1.	Reed bed	<i>Phragmites australis</i>	First community along permanent water, forming homogenous stands of reeds up to 5 m high.	Along the Linyanti and Chobe channels and swamps. Shores of Lake Liambezi. Shallow water (not deeper than 1 m).	-22.3 ‰ 2.7 %
2.	Sedgeland	<i>Cyperus</i> spp. <i>Schoenoplectus corymbosus</i> <i>Vossia cuspidata</i> <i>Panicum repens</i> <i>Cynodon dactylon</i>	Sedges and specialised grasses growing in damp, regularly flooded soils. As a pioneer grass, <i>C. dactylon</i> may colonize the drying plains and form homogenous mats. Often heavily grazed.	Outer layer of the Linyanti and Chobe swamps. Damp soil conditions with a high seasonal fluctuation of the water table.	-18.5 ‰ 5.1 %
3.	Floodplain grassland	<i>Cymbopogon excavatus</i> <i>Hyparrhenia rufa</i> <i>Imperata cylindrica</i>	Dense stand of tall perennial grasses (2-3 m) growing on inactive floodable low-lying plains. A particular kind of community occurs in humid depressions with <i>I. cylindrica</i> .	On the bottom of ancient floodplains. Alluvial, dark, compact soil. High impact of human activity.	-15.1 ‰ 3.6 %
4.	Dry grassland	<i>Aristida</i> spp. <i>C. dactylon</i>	Spread tufts of <i>Aristida</i> grass in sandveld, with a high proportion of denuded soil. May be connected to <i>Terminalia sericea</i> sandveld.	Interspersed among the mopane woodland and shrubland, in the drier, more elevated, western part of the Linyanti-Chobe basin.	-18.1 ‰ 0.9 %
5.	a) Shrubland dominated by Mopane	<i>Colophospermum mopane</i>	Small, multi-stemmed Mopane shrubs (≤ 3 m) often showing heavy signs of elephant's grazing.	Occur as a transitional fringe around Mopane woodland on slight dips.	-19.5 ‰ 1.4 %
	b) Shrubland dominated by <i>Combretum</i>	<i>Combretum mossambicense</i> <i>Combretum hereroense</i> <i>Croton megalobotrys</i> <i>Dicrostachys cinerea</i>	Sparse shrubland on elevations, with a well-developed grass layer. Presence of isolated shrubs/trees.	On the top of inherited geomorphological elevations (calcareous platforms, ancient island / beach bank)	-18.0 ‰ 0.9 %
6.	a) Woodland dominated by Mopane	<i>C. mopane</i>	Woodland with tall Mopane trees up to 20 m tall. Grass layer abundant. Numerous termite mounds and pans.	Main woodland in the western part of the Linyanti-Chobe basin. Presence of clay layer and salts.	-21.4 ‰ 3.0 %
	b) riverine or marginal floodplain woodland	<i>Acacia erioloba</i> <i>Combretum imberbe</i> <i>C. mossambicense</i> <i>C. megalobotrys</i> <i>Philenoptera violacea</i>	Highest specific diversity of trees. Complex vertical structure (different height classes). Presence of termite mounds.	Occur on slopes or edges of elevations overhanging floodable lowlands.	-22.0 ‰ 3.0 %

Table 1 Description of the six classes of vegetation with indication of the average results from the SOM analyses for each class. Diagnostic species and description of each class come from field observations, after Roodt (1998) and Roodt (2015) as well as from the vegetation surveys.

Vegetation and soil

The range of the TOC and C-isotopic compositions of the different vegetation classes defined in Table 1 are given in Figure 17, while those for the river sediments are given in Figure 17. The amount of organic carbon contained in the sediments varies from 0.14 wt% for the Okavango at Thamalakane to 9.02 wt% for the sediments on the shores of Lake Liambezi between the mouths of the Linyanti and Chobe rivers. The $\delta^{13}\text{C}$ values of these sediments have values between -23.2 ‰ for sediments from the Linyanti to -18.6 ‰ for sediments near Mababe Bridge, which is an end-of-travel arm of the Okavango Delta.

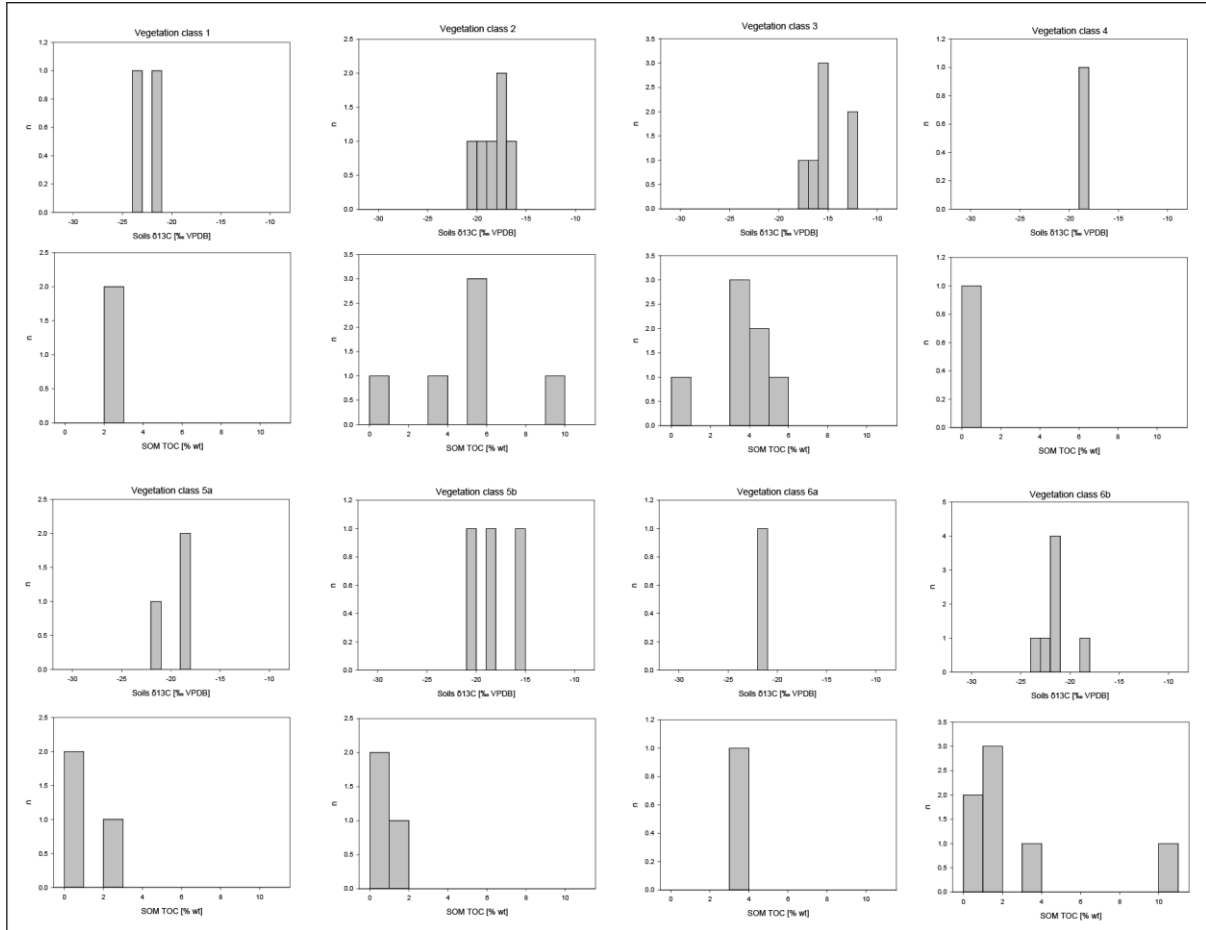


Figure 17 Total organic carbon content and its isotopic composition for the different vegetation classes of this study (Table 1).

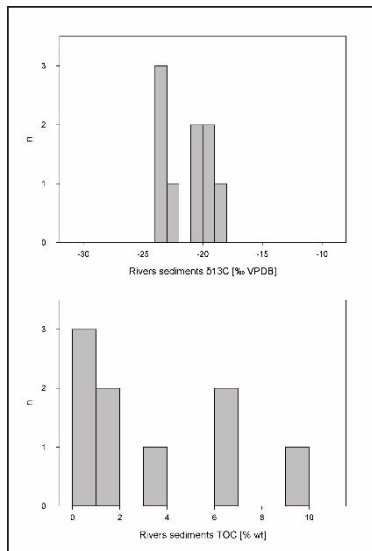


Figure 18 Total organic carbon content and its isotopic composition for the river sediments.

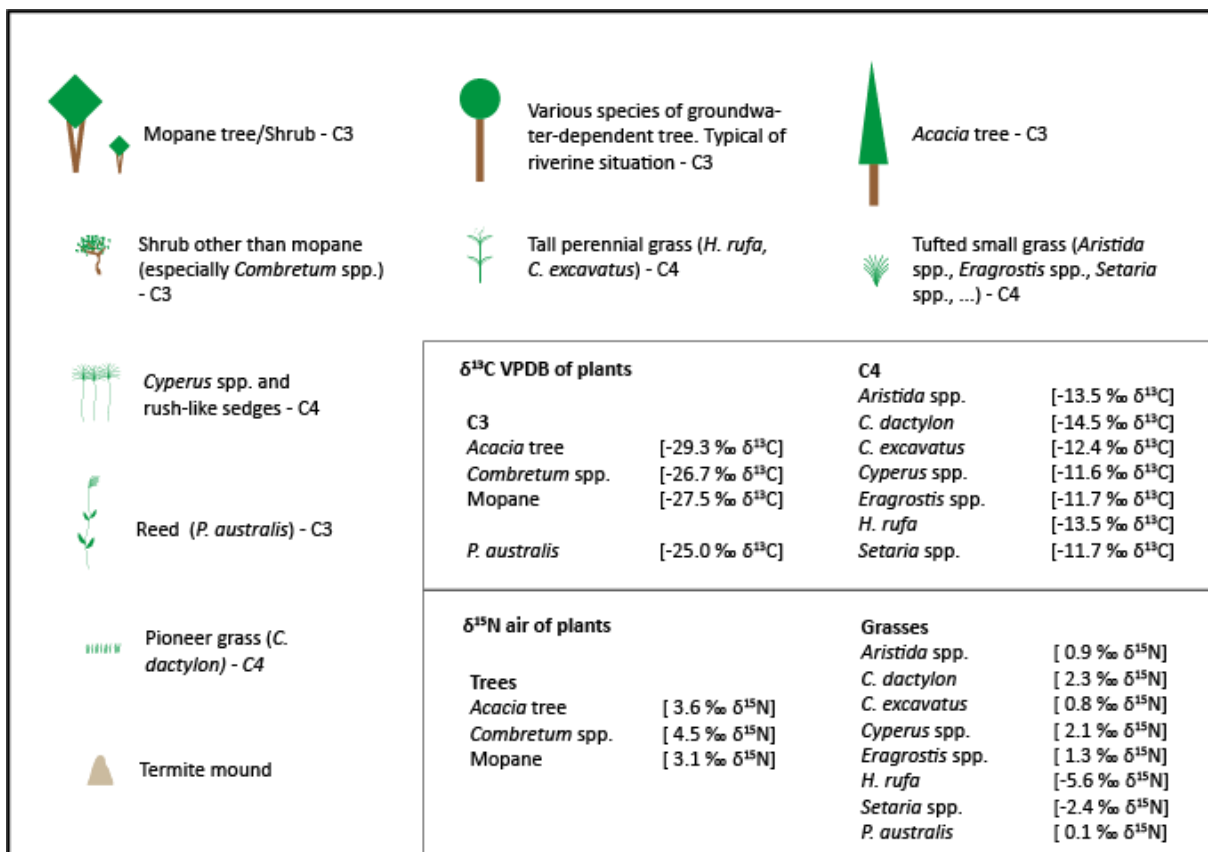


Figure 19 Summary of C- and N-isotope compositions measured for individual plants as well as the symbols used in subsequent diagrams to illustrate the presence/absence of plants as well as their relative abundance in different locations. The isotopic values of the table (as well as of the following ones) are average values of samples of the same species grouping together all the sampled sites as well as the different parts of the plant (for trees). The used isotopic values can be found in the appendix (Chapter 8.3).

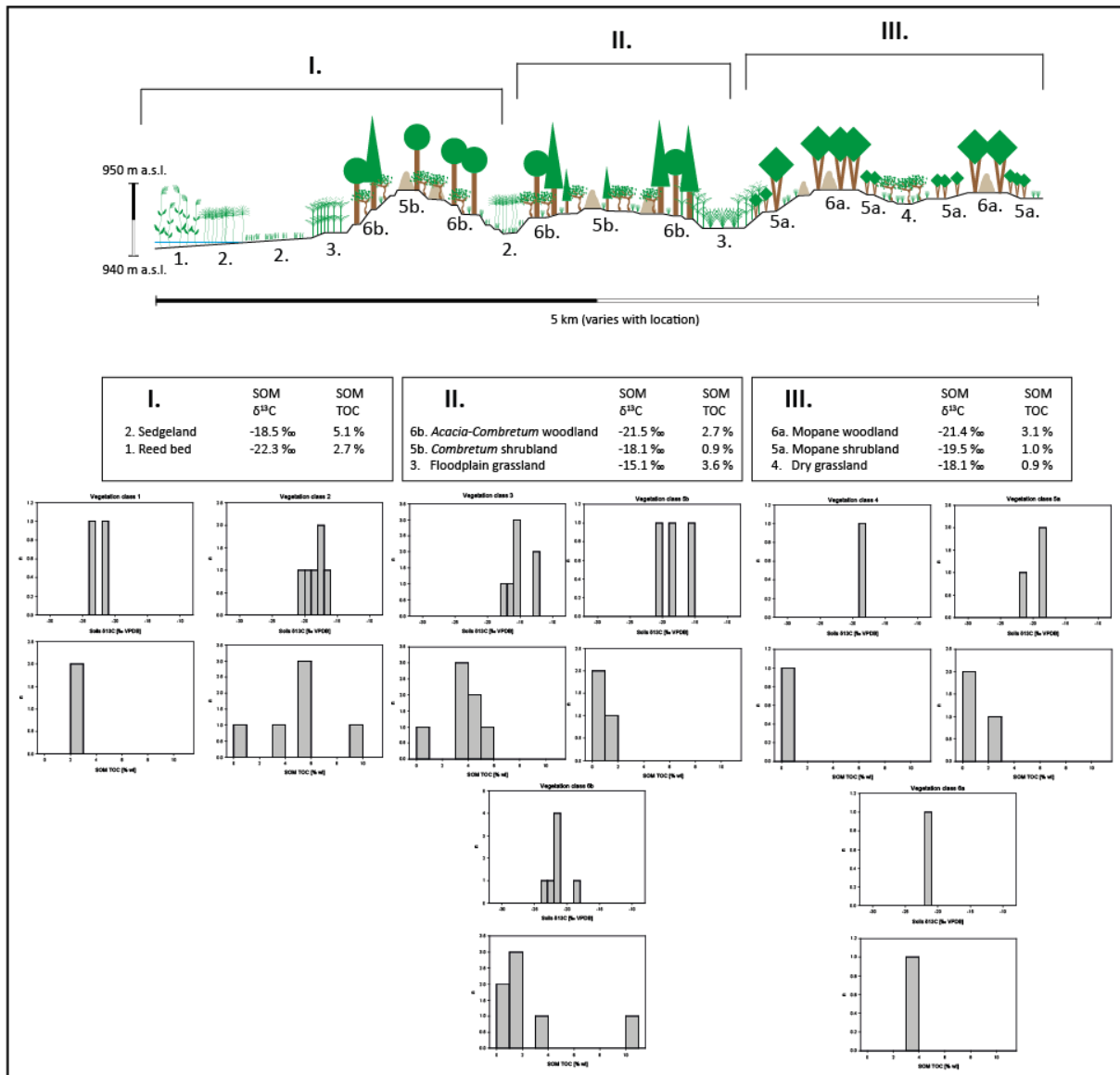


Figure 20 Summary diagram allocating the different transects to the different geomorphic features and the vegetation zones as well as showing the distributions of the TOC contents and C isotopic compositions.

2.5. Discussion

2.5.1. Geographical distribution of vegetation zones in the Linyanti-Chobe basin

The density and distribution of the vegetation cover and type in the Linyanti-Chobe basin is clearly related to the geomorphology as well as the proximity to both ground and surface waters. Areas showing the dominance of a certain plant cover highlight the extent of the influence of major rivers in this area (Linyanti and Chobe). The dominance of shallow-rooted trees such as *C. mopane* in some zones compared to a dominance of deep-rooted bushes and trees such as *Combretum* spp. and *Acacia* spp. throughout the Linyanti-Chobe basin is related to the access to either a shallow seasonal water source or, respectively, good groundwater access. Qualitatively the Linyanti-Chobe basin can thus be divided into three main vegetation zones that are each composed of a mosaic of C₃ wooded elevations and C₄ grass dominated depressions (Figure 20). Zone I covers the Linyanti and Chobe channels and their associated permanent and seasonal swamps with vegetation classes 1 and 2 (Figure 20). It is dominated by sedges (*C. papyrus*, *C. longus*, *S. corymbosus*) and water-loving grasses (*P. australis*, *P. repens*, *V. cuspidate*; Ballif, 2018). It is the most active zone in terms of delta-like dynamics and seasonal flooding with a landscape that resembles that of the adjacent Okavango Delta, including the notable presence of palm-trees (*Hyphaene petersiana*, *Phoenix reclinata*). Floods occur every year and

the soils are inundated for most of the year. This zone is represented by transect locations TR 2.1 (Linyanti Camp), TR 3 (Chobe Seariver), TR 4.1, TR 4.2 (Figure 20). The second zone (II) is dominated by Acacia-Combretum woodlands and Combretum shrubland on elevations adjacent to the grasslands. Zone II is located in the intermediate, central part of the Linyanti-Chobe basin, between the Chobe and Linyanti faults. It also characteristically occurs on emerged carbonate deposits described in particular by Burrough and Thomas (2008). On top of these elevations, dry shrubland dominates with sparse isolated trees. Trees are also present on the margins of elevations where they form mixed woodlands that benefit from the floodplain groundwater but stay well above flood levels. Transects TR 5, TR 6 and TR 7 (VTR), as well as the riverine fringe at TR 2.2 (Linyanti Camp) and TR 4.3, typically represent Zone II and its different communities. Zone III is characterized by Mopane woodlands and shrubland interspersed with sand-dominated communities with *Terminalia spp*, clayey pans and dry saline grasslands. The main source of water for trees comes from stored precipitation in a clayey layer of the soil. Corresponding transect locations include TR 2.3 (Linyanti Camp), TR 4.4, TR 4.5 and TR 4.6.

The sodium-rich clay layer common for Mopane-dominated woodlands may come from the initial inherited delta-like island system, reworked by termites, as the area was isolated from floods due to tectonic tilting of the Linyanti-Chobe basin (Kinabo et al., 2007). Islands in the Okavango Delta have been reported to concentrate dissolved salts at their centre as water is transpired by trees (Wolskip & Savenije, 2006). As this system was disconnected from the flooding dynamics, it was progressively covered by aeolian Kalahari sand. Termite activity may be responsible for the remobilisation of the buried sediments (rich in OM, clay, carbonates and evaporitic salts) inherited from a wetter, delta-like setting. From this point of view, the zonation proposed in Figure 20 and 8 suggests a spatial and temporal succession of communities following tilting of the basin and increased seasonality in flooding events. For the intermediate parts of the basin (Zone II in Figure 20) the seasonal floods provide sufficient alluvium and dissolved nutrients to support the Acacia-Combretum woodlands, Combretum shrubland and with approach to the seasonal river basin the floodplain grasslands of Zone I. In the river basin itself flooding is sufficiently prolonged to support a hydromorphic soil regime ideal for the floodplain grasslands to be maintained.

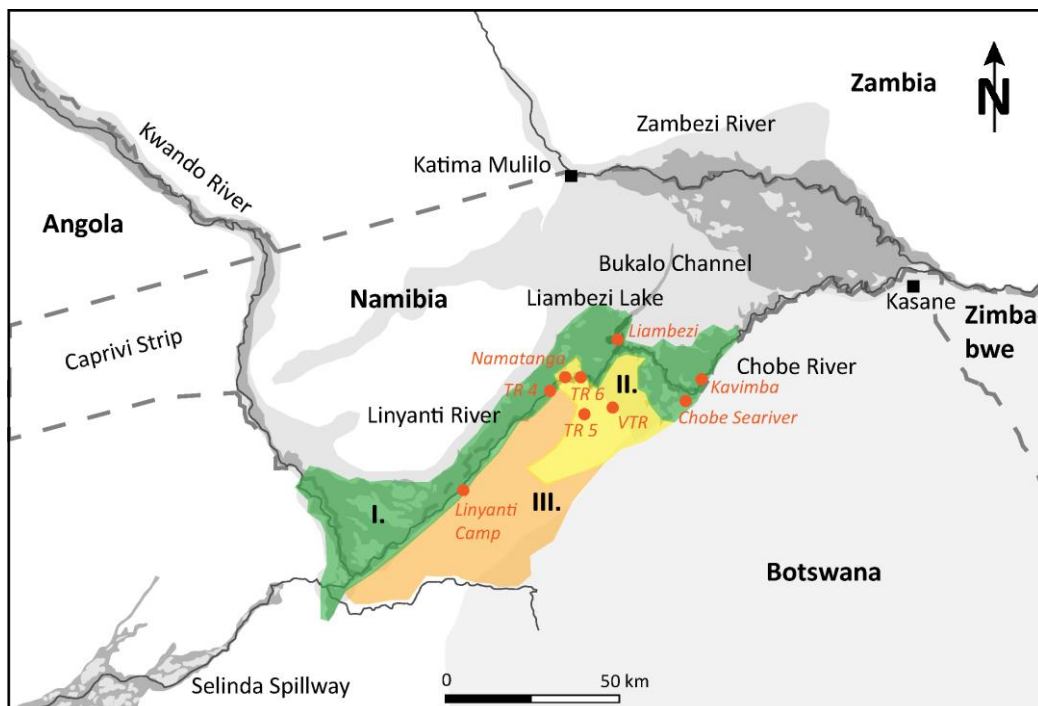


Figure 21 Location of the transects relative to the different vegetation classes defined in Table 1 and supposed extension of each zone. Each zone is related to the local geomorphology as well as the proximity to both ground and surface waters.

2.5.2. Vegetation classes and isotopic compositions

As reviewed in Ehleringer et al. (2000) and Michener and Lajtha (2007) the $\delta^{13}\text{C}$ values of soil organic matter ($\delta^{13}\text{C}_{\text{SOM}}$) integrates the isotopic composition and relative abundance of the different vegetation into the soil. Plants, as primary producers, are by far the most important contributors to the SOM through litterfall and root exudation. In subtropical regions, the SOM may result from a mixture of C_3 and C_4 litter. Below is a qualitative evaluation of the overall abundance and isotopic composition of the SOM in the different vegetation classes defined in Table 1.

2.5.2.1. Reed beds

This class is mainly composed of the dense, tall (4-5 m) homogenous colonies of *P. australis* (typically with $\delta^{13}\text{C}$ values of around -25.0 ‰) growing in inundated areas, along permanent channels or bodies of water. In the Linyanti-Chobe basin, it was mostly found along the Linyanti and Chobe channels and around Lake Liambezi. $\delta^{13}\text{C}_{\text{SOM}}$ has values of -22.3 ‰ typical of a dominance of type C_3 vegetation such as *P. australis*.

2.5.2.2. Sedgeland

This class occurs in continuity with the reed beds, occupying the flood plains of the wetlands. The presence of water is reduced to shorter flood periods compared to the central channels occupied by the reed beds. The dominance of plants from the C_4 -type Cyperaceae family is the main feature of this class: *Cyperus papyrus* (with $\delta^{13}\text{C}$ values of -11.8 ‰), *Cyperus cf. longus* (-11.3 ‰), *Schoenoplectus corymbosus* (-11.2 ‰). Other typical water-loving grasses accompany them: *Panicum repens* (-10.8 ‰), *Vossia cuspidate* (-12.7 ‰); as well as the pioneer grass *Cynodon dactylon* (-14.5 ‰). The $\delta^{13}\text{C}_{\text{SOM}}$ values are somewhat lower though (-18.5 ‰), suggesting significant inputs of detrital organic matter of C_3 type of vegetation derived from the surrounding drainage basin during the seasonal flooding. The soils in this class also have the highest TOC content of the different classes (5.1 wt%). A contribution from inert organic carbon (ashes) resulting from savannah fires is also not excluded considering the importance of slash-and-burn agricultural practices in this area (e.g., Heinl et al., 2007; Pricope et al., 2015).

2.5.2.3. Floodplain grassland

This class includes communities dominated by tall, dense population of grasses such as *Imperata cylindrica* (-13.5 ‰), *Hyparrhenia rufa* (-11.7 ‰), *Cymbopogon excavatus* (-12.4 ‰), *Chrysopogon cf. nigritanus*. Other co-occurring grasses include *C. dactylon* (-14.5 ‰), *Setaria sphacelata* (-11.7 ‰), *Diheteropogon amplexans* (-11.3 ‰), *Sporobolus festivus* (-12.5 ‰). They occur on rather humid low-lying (ancient) floodplains and local depressions that characterize the central part of the Linyanti-Chobe basin. The water balance seems to be a determining factor for the presence of such vegetation. However, the region covered by this class today is rarely flooded by the Linyanti and Chobe rivers. However, if we refer to the annual spatial extent of the floods as described by Pricope (2013), as well as to the presence of alluvial material in the soils, this class represents the external fringe reached by the annual floods. Another point of importance is that these plant communities are found in a small range of altitudes, between 934 and 936 meters above sea level. Mean $\delta^{13}\text{C}_{\text{SOM}}$ value of this class is at -15.1 ‰, approaching values of the present vegetation more closely compared to the sedgeland class, hence giving the rare water-cover, with smaller water borne organic matter contributions from the larger surrounding drainage basin. Some more isolated sites of this class in larger depressions have a vegetation composed entirely of C_4 type of plants and the $\delta^{13}\text{C}_{\text{SOM}}$ value also approaches that of the vegetation in place averaging at -12.1 ‰.

2.5.2.4. *Combretum*/Kalahari shrubland 5b and *Acacia-Combretum*/mixed marginal/riverine woodland 6b

Classes 5b and 6b are mixed plant communities including a set of dominant, deep-rooted wooded perennials and that occur : 1) at the edges of floodable plains, 2) in deep-draining Kalahari sands or 3) on elevations above the flood level. They are grouped because we postulate that they are functionally linked to a groundwater source. The $\delta^{13}\text{C}$ value of *Acacia erioloba* at about -29 ‰ is typically within the range of C_3 vegetation as are the values of the other tree species present: *Boscia albitrunca* (-27.5 ‰), *Colophospermum mopane* (-27.5 ‰), *Combretum mossambicense* (-26.7 ‰). Class 6b includes trees with large simple leaves that may suggest important evapotranspiration and that normally belong to more humid northerner ecoregions such as species from the genus *Ficus*. In this unique region, however, they are found along ephemeral rivers in gallery forests. A hydric stress is found in some *A. erioloba* samples. Indeed, *A. erioloba* samples can be separated in two groups based on their $\delta^{13}\text{C}$ with a 1.5 ‰ gap between the two groups. A first group has $\delta^{13}\text{C}$ values below -30 ‰ and a second group above -28.5 ‰. The SOM of these sites supports a dominance of OM derived from the C_3 plants with $\delta^{13}\text{C}_{\text{SOM}}$ of around -21.5 ‰ and therefore a good relationship with the on-site vegetation.

Class 5b is represented by *Combretum* shrubland that typically occurred on the top of inherited calcareous platforms. The dominance of members of the *Combretaceae* is a characteristic feature of nutrient-poor savannahs as highlighted by Scholes (1990). Indeed it is to be expected that the soils on the platforms are rather poor, as they are not regularly fertilized during flooding. Depending on the proportion of C_4 grasses or C_3 trees in this specific class, $\delta^{13}\text{C}_{\text{SOM}}$ also varies, with a variation of up to 4.2 ‰ but still an average for $\delta^{13}\text{C}_{\text{SOM}}$ of -18.1 ‰, hence a somewhat higher abundance of C_4 grasses compared to Class 6b.

2.5.2.5. Dry grassland

This class is located at higher elevations compared to the flood plains and is typically composed of savannah type of grasses dominated by the genus *Aristida* ($\delta^{13}\text{C}$ values of about -13.5 ‰) and the salt-tolerant *C. dactylon* (-14.5 ‰) that characterize denuded soils. We have also included the Mopane shrub-/woodland area of the western part of the Linyanti-Chobe basin in this class as these areas clearly overlap and generally grade into each other. The SOM values represent well this mixture between plants of type C_4 and C_3 with values averaging at $\delta^{13}\text{C}$ values of -18.1 ‰, but with a low content of SOM. These different characteristics distinguish this class of grasslands from floodplain grasslands of Class 3.

2.5.2.6. Mopane shrubland 5a and Mopane woodland 6a

These two classes are entrenched in areas external to the Linyanti-Chobe system. They do not directly receive floodwaters from the riverine system and hence are largely expected to depend on the seasonal precipitation rather than deep groundwater resources. The soil constitution also plays a role in the distribution and density of the vegetation cover in this class (Roodt, 1998): Mopane shrublands occur where clayey layers with a high water storing capacity occur closer to the surface, while tall Mopane woodlands develop on deeper soils with mixed clay/aeolian sand characteristics (Romanens, 2017). Indeed, *C. mopane* in the Linyanti-Chobe basin favours sodium-rich alkaline soils that distinguish it from *Acacia*, *Boscia*, *Combretum* and *Terminalia* preferences (Stevens et al., 2013; Makhado et al., 2014). The typical presence of pans in Mopane woodlands is a strong indicator of an impermeable layer in the soil. These pans may bear water until late in the dry season. In addition, a high concentration of Na limits the permeability of the soil (Makhado et al., 2014). A similar trend as for classes 5b and 6b is noted for classes 5a and 6a with regards to the $\delta^{13}\text{C}_{\text{SOM}}$ values. A higher proportion of trees gives an average value of -21.4 ‰, while this changes towards values averaging -19.5 ‰ with more abundant C_4 grasses for the Class 5a.

2.5.3. Estimation of water stress using isotope composition

Figure 22 schematized and resumed the distribution of the vegetal cover through the previously described vegetation zones. It schematized and resumed the main trends in the organic carbon isotopic composition of the soil organic matter (SOM) and of four different trees: *Colophospermum mopane* (CM), a shallow rooted tree and three deep-rooted trees: *Acacia erioloba* (AE); *Boscia albitrunca* (BA) and *Combretum mossambicense* (CM). This simplified representation of the landscape of the Linyanti-Chobe Basin did permit to highlight major trends in isotopic composition of soils and trees along general transects. Organic carbon isotopic composition of plants and soils depends on the plant type, vegetal cover and distance (or access) to a source of water. The isotopic composition of organic carbon in soil organic matter reflects first the type of vegetal cover (Figure 22). Thus, the soil organic carbon isotopic composition of the reed beds is largely influenced by the C₃ reed *P. australis*. Sedgeland and floodplain grasslands are dominated by a C₄ plant cover. The soil organic carbon isotopic composition shows therefore higher values. However, the distance and access to a source of water is also reflected through the soil organic carbon isotopic composition. Thus, an increase in the isotopic values of the soil organic carbon occurs from the reed beds to the floodplain grassland (despite the dominant plant type). The restrained access to permanent water (surface water and underground water) is recorded into the isotopic composition of the soil organic carbon. This record is in particular interest for studies aiming at a reconstruction of paleo-climatic and paleo-environmental condition of the region.

The access to a water source depends on the distance to surface water (river and lake) but to underground water as well. Therefore, trees demonstrate a privileged access to groundwater compared to grass. This privileged access to water is reflected in isotopic values of the trees along the transect. Two major information are to be found in the simplified transect (Figure 22). The first information is supported by the shallow rooted species CM and the second is supported by the deep-rooted specie CB. As CM is shallow rooted, its access to groundwater is less favored compared to deep-rooted species. This is explained by a higher water stress when the distance to surface water increases. Isotopic values for CM increase progressively from the sedgeland (-27.8 ‰) to the mopane shrubland (-25.9 ‰). The water stress for deep-rooted species is expressed differently. The access to groundwater is probably more reflecting landscape features than distance from the source of water. Isotopic values for CB increases in both transitions from acacia-combretum woodland to combretum shrubland (-26.1 to -25.2 ‰) and from mopane woodland to mopane shrubland (-26.7 to -25.5 ‰) classes. It demonstrates a privileged access to groundwater for both acacia-combretum woodland and mopane woodland classes. This access is probably related to local morphologic features. The water stress is certainly expressed in the isotopic measurements, however, this stress is to be found in the size of the trees as well. The carbon isotopic measurements of the soil organic matter reflects this stress as well. The increase in the isotopic values from -21.5 to -18.1 ‰ and from -21.4 to -19.5 ‰ from acacia-combretum woodland to combretum shrubland and from mopane woodland to mopane shrubland respectively is certainly to be found with a higher impact of grasses. However, it reflects assuredly the stronger water stress experienced by the trees of these two classes.

The mean isotopic values of CM is 1.8 ‰ higher than of AE. This difference is probably related to the main position along the schematized transect of the two species, AE being mostly located closer to the water source. However, the length of the roots probably plays a role as well, favouring the access to groundwater to AE.

This schematized transect is of major importance to better understand the vegetation distribution and its relation with water availability. Tracing the isotopic composition of the organic carbon of the soils gives information about the vegetal cover, the access to surface and ground- water and the water stress experienced by the site.

The use of nitrogen isotopes in plants is more complex to use for plotting water stress. Depending on the context, however, it can also show this type of stress. This is the case for the comparison of sites 5a and 6a in Figure 20. A 0.4 ‰ higher isotopic signal for plant cover of sites classified in 5a compared to sites classified in 6a results from additional water stress.

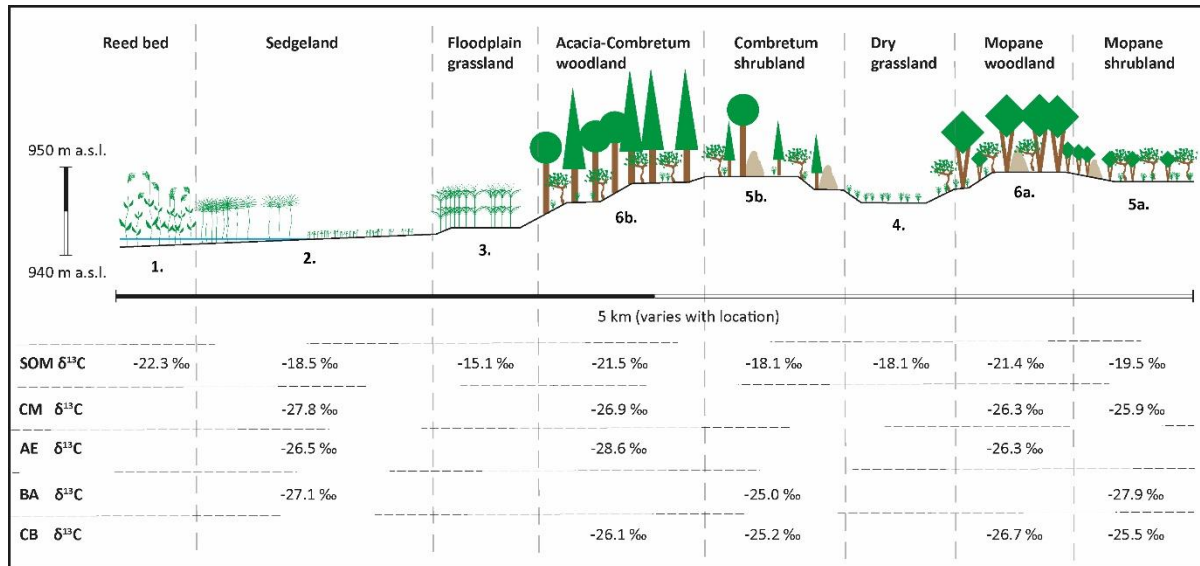


Figure 22 Schematic and simplified drawing of the Linyanti-Chobe Basin landscape and vegetation zone according to the distance from a body of water (Linyanti and Chobe Rivers and Lake Liambezi). The average carbon isotopic values of all sampled sites is given for the soil organic matter (SOM) and four different trees (if present in the site). *Colophospermum mopane* (CM) is a shallow rooted tree, the three other species are deep rooted trees: *Acacia erioloba* (AE); *Boscia albitrunca* (BA) and *Combretum mossambicense* (CB).

The relationship between the weighted $\delta^{13}\text{C}$ and $\delta^{15}\text{N}$ values of stems and leaves of the same tree at different sites along the schematized transect described in Figure 22 tends also to demonstrate an impact due to the distance from the surface water source (river or lake) (Figure 23). It is the case for the shallow rooted tree *Colophospermum mopane* but also for the deep-rooted tree *Acacia erioloba*. The coefficient of determination for these two species follows a similar trend than the 1:1 relationship. This suggests an impact of the distance of the surface water source on the metabolism for these two tree species. This impact is confirmed with Figure 22 where both species present increasing $\delta^{13}\text{C}$ values while increasing the distance from a surface water source (except for AE in class 2 which probably represents a specificity linked to the site itself). The impact of the distance to a surface water source did not seem to affect the deep-rooted tree species *Boscia albitrunca* and *Combretum mossambicense*. Their coefficient of determination is too low to be usable and furthermore, it does not follow the 1:1 relationship. That would suggest that distance to surface water is not decisive for these tree species and that they are able to manage their water needs through different sources. Figure 22 does permit to confirm it, especially with CB. The $\delta^{13}\text{C}$ values of these two species do not show a link to the distance from a surface water source. It rather expresses the possibility for these two tree species to use groundwater as $\delta^{13}\text{C}$ values of classes 6b and 6a tend to demonstrate (Figure 22).

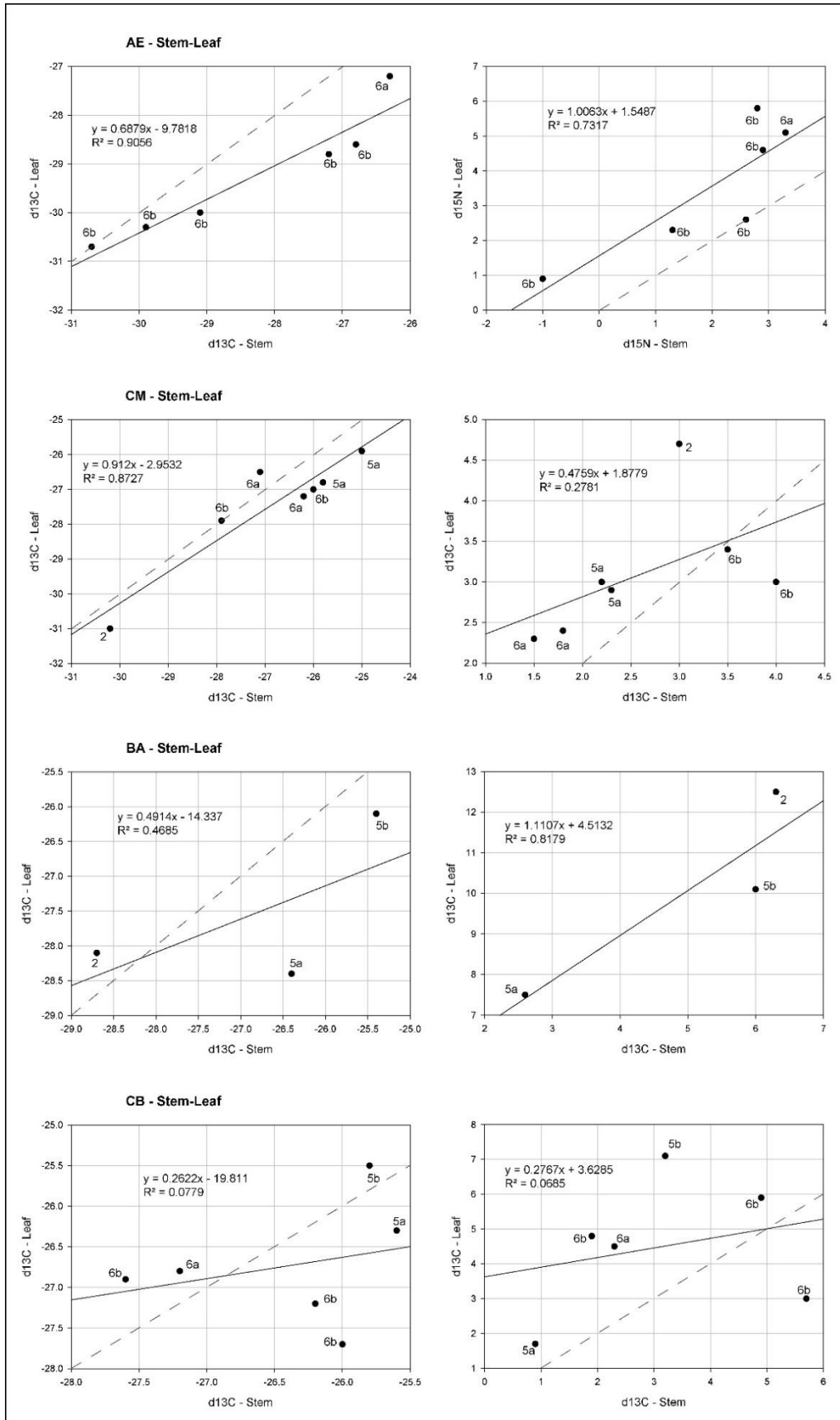


Figure 23 Relationship between the weighted $\delta^{13}\text{C}$ and $\delta^{15}\text{N}$ values of stems and leaves of the same tree at different sites and for the species *Colophospermum mopane* (CM), a shallow rooted tree and three deep rooted tree species: *Acacia erioloba* (AE); *Boscia albitrunca* (BA) and *Combretum mossambicense* (CB). The vegetation class of each sample is specified. The coefficient of determination is given for each species and drawn as a black line. As a comparison to this coefficient, the 1:1 relationship is given by a grey dotted line.

2.5.4. Plant-soil-sediment isotopic relationships

As shown in the description of the classification carried out on the Linyanti-Chobe basin, a direct relationship can be established between plant cover and isotopic signal of carbon from soil organic matter. Indeed, for all the classes observed, the $\delta^{13}\text{C}_{\text{SOM}}$ shows a direct relationship with the type of vegetation that covers it.

We deduce from this a very localized deposit of dead organic matter without obvious transport. This observation corresponds well to the type of environment of the Linyanti-Chobe basin. The low relief of the basin as well as a reduced hydrology reduces the transport of sediments and allows conservation of organic waste in situ. This fact offers in the isotopic composition of organic matter in soils or sediments a powerful environmental tracing tool. Indeed, the $\delta^{13}\text{C}_{\text{SOM}}$ signal can be used to trace a type of plant cover in palaeo-soils or sediments. The signal will not directly testify neither of a specific type of vegetation nor of a precise environment but of a composition making it possible to deduce interpretations according to the conditions.

This work makes it possible to link the production of organic matter in soils with plant activity, its erosion and its transport in the surrounding water points. Figure 18 in comparison to Figure 16 and Figure 17 but also to Figure 20 shows a correlation between the isotopic signal of organic carbon in the soils of the Linyanti-Chobe basin as well as the same isotopic composition but of the sediments of the different bodies of water in the basin. Due to the very poor topography (low relief and low precipitation), the transport of organic matter and its deposition remain localized.

The site for taking the two samples from Linyanti Camp can be classified in class 1 according to the previous description. Both samples show $\delta^{13}\text{C}$ values at -23.0‰ and -23.2‰. Figure 25 also places them close to category C3. Knowing that the $\delta^{13}\text{C}_{\text{SOM}}$ values described for class 1 were -22.3‰, the two samples from Linyanti Camp therefore perfectly represent the local vegetation at the site.

There is however a major factor which is not taken into account in the current study, it is the isotopic composition of the organic carbon of the algae. Indeed, Figure 25 highlights a probable influence of algae in the isotopic composition of the sediment carbon. This influence probably has an effect which is unfortunately not measurable in the present study. Despite everything, the composition of the very local vegetation appears well in the graph.

The Kavimba and Chobe Seariver sites show vegetation that can be classified between classes 1 and 2. The isotopic composition of the organic carbon in the sediment perfectly demonstrates this mixture with values of -20.1‰ and -19.6‰ respectively. Figure 25 also shows this mixture between C3 and C4 type plants. For the Kavimba sample, algae again seem to play a significant role in the composition of organic matter. Field observations also showed a significant number of algae on this site. Even though there is no C/N data concerning the sediment sample at the edge of Lake Liambezi, its classification between classes 1 and 2, the observation of significant algal activity as well as its isotopic composition of the organic carbon at -20.8‰ seem to indicate significant similarity with the Kavimba sample. The correspondence between plant cover (therefore type of environment) and type of organic matter in the sediments again seems to correspond.

Regarding the Thamalakane site, it is not located in the Linyanti-Chobe basin. Nevertheless, it probably follows a similar trend. The geochemical composition of algae seems more important for this site than terrestrial plants. It seems however indicated a mixture C3-C4 which again evokes a mixture of classes 1 and 2.

Like the isotopic composition measured in the $\delta^{13}\text{C}_{\text{SOM}}$, the isotopic composition of organic carbon measured in the sediments of the different bodies of water in the Linyanti-Chobe basin correspond to the isotopic composition of the organic carbon of the plants that surround the different sites. This observation confirms that the correspondence between plant cover and locally deposited organic matter described by Ehleringer et al. (2000) also works for the sediments of the various water plants of the Linyanti-Chobe basin.

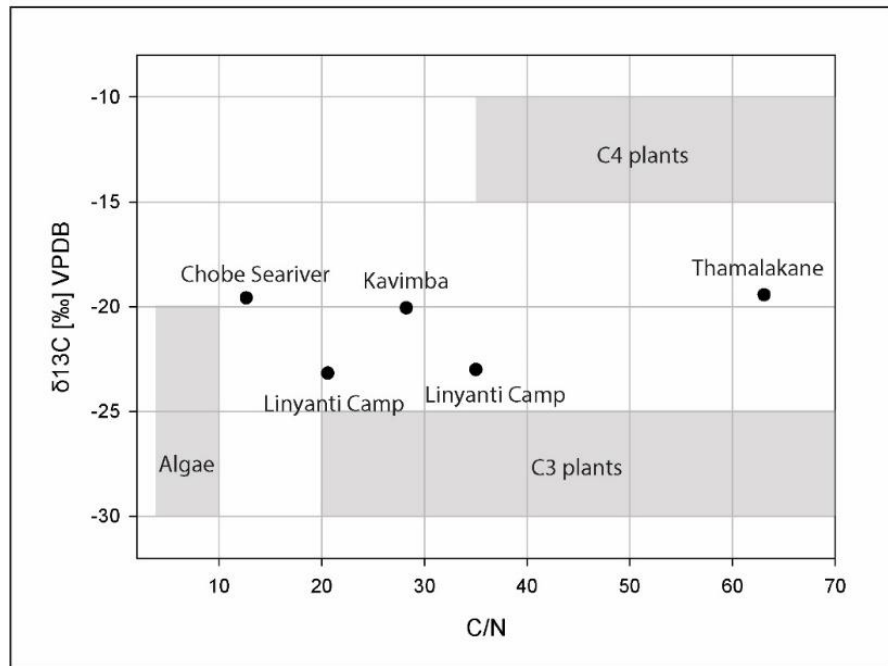


Figure 24 Geochemical values for organic matter sampled in river sediments. Their position on the graph shows a mixture in the composition of their organic matter which varies according to the site between an algal dominance and plant type C_3 or C_4 .

2.5.5. Nitrogen isotopes

Foliar $\delta^{15}\text{N}$ is firstly dependent on the available source of nitrogen in the soil accessible to plant's roots. Nitrogen distribution in the soil as well as its distribution in the local water regime are then important for its availability for the roots. Foliar $\delta^{15}\text{N}$ eventually reflects the mode of N acquisition by plants, local water regime and ecosystemic rates of nutrient recycling (Schulze et al., 1991; Schulze et al., 1996; Schulze et al., 1998; Schulze et al., 1999; Högberg, 1986; Högberg, 1990; Högberg, 1997; Austin & Sala, 1999). Handley et al. (1999) reports negative $\delta^{15}\text{N}$ values for wet and/or cold environments where organic matter accumulates and N pool do not experience as many outputs as drier areas. The observation of the isotopic composition of nitrogen in the different plant species (Figure 16 and Figure 19) as well as the isotopic composition of the plant cover of the different environmental classes (Figure 26) perfectly testifies to these assertions. The two main sources of nitrogen for plants in the Linyanti-Chobe basin will be floodwater or groundwater and soil organic matter. The use of each of these sources will depend on the type of vegetation grass-trees, therefore on the depth of the roots (shallow rooted or deep rooted), the presence or not in significant quantity of organic matter in the soil (TOC) and above all, the presence in quantity of water, of origin of floods or groundwater. The isotopic signal of nitrogen from the plant cover of each site makes it possible to trace from what origin plants draw the nitrogen necessary for their metabolism.

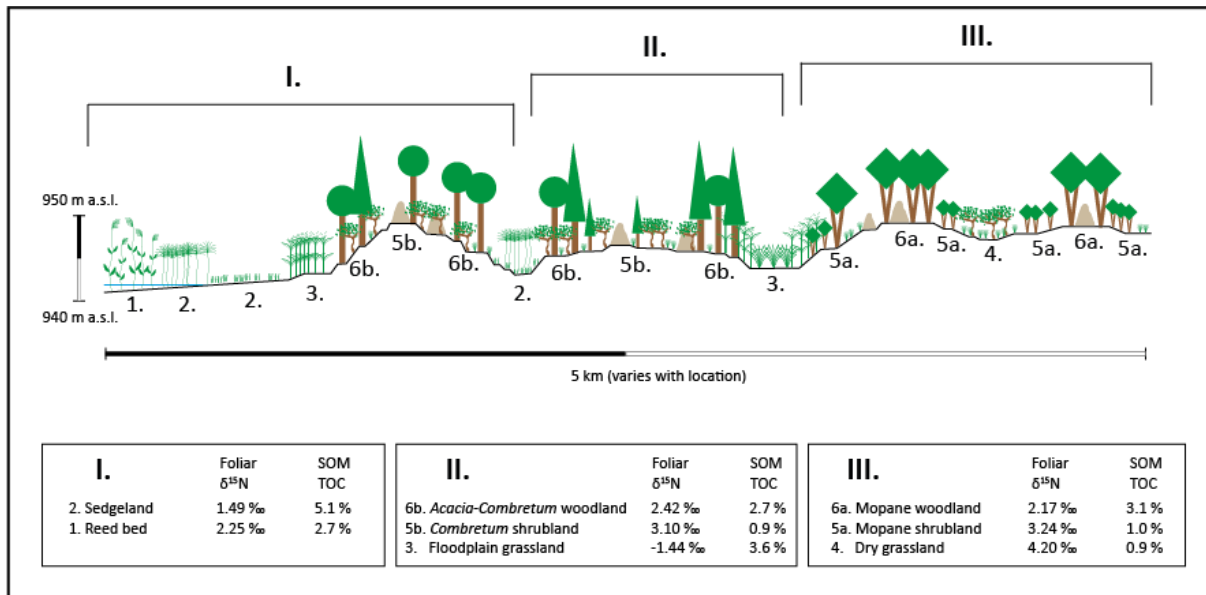


Figure 25 Summary diagram allocating the different transects to the different geomorphic features and the vegetation zones as well as showing the distributions of the TOC contents and N isotopic compositions.

The determination of the different environmental classes described in Table 1 showed a distribution of these classes according to the topography and access to water (rain or floods) of each site. This results in typical vegetation. Classes 1 to 3 (reed bed, sedgeland and floodplain grassland) all show similar characteristics: regularly drowned and composed only of grasses. Regular floods may lead to the potential development of anoxia in the soil. A different set of specialised microflora communities develop in these conditions. The rate of organic matter decomposition decreases because of the switch to alternative, anaerobic respirations. This whole process favours organic matter preservation and storage over degradation. This is the case in those sites with respectively 2.7, 5.1 and 3.6 % TOC. As Handley et al. (1999) reports it, negative $\delta^{15}\text{N}$ values should be found in this type of environment. This is partially the case. Indeed, a slight difference in altitude between the three classes results in a difference in the amount of water that the different sites receive. A transition in the isotopic composition of the plant cover perfectly reflects the availability of water between each of the three classes. Vegetation of class 1 which is more strongly influenced by floods gets its nitrogen from the water of floods with isotopic values $>0\text{‰}$ $\delta^{15}\text{N}$ (average at 2.25 ‰). Class 3 vegetation receives enough water to show soil rich in organic matter, however not enough for vegetation to show an isotopic composition influenced by the nitrogen contained in the flood water. The composition of -1.44‰ $\delta^{15}\text{N}$ shows the use of nitrogen contained in organic matter as a source of nitrogen. Class 2 shows the transition between these two pools of nitrogen with an intermediate composition between the two neighbouring classes: 1.49‰ $\delta^{15}\text{N}$.

As mentioned above, geography in addition to altitude also plays a major role in the distribution of floods and therefore the isotopic composition of nitrogen in plants. Transect of Chobe Seariver is under class 2 with respect to its vegetation. However, it is geographically out of the main Linyanti-Chobe system. Chobe Seariver is a floodplain playing the role of overflow basin of the Chobe. As a result, the flood regime is different from the major system. This reason is probably the explanation for different foliar isotopic composition of nitrogen. The lowest point in altitude of the transect shows a negative value of -1.7‰ $\delta^{15}\text{N}$ that might show similarities with class 3: i.e. edge of the influence of floods in the supply of ions. The following points of the transect all show a positive composition up to the maximum value of 5.7‰ $\delta^{15}\text{N}$. Due to an extended emersion period, plants therefore find another source of nitrogen for points further from the flood limit.

If the vegetation of classes 1 to 3 is composed entirely of grasses, classes 4, 5a/b as well as 6a/b offer mixed vegetation with various species of trees. As shown in Figure 19, the isotopic nitrogen values of different plant species, trees show a systemically higher signal than grasses. Up to a maximum value of 10.00 ‰ $\delta^{15}\text{N}$ for *Boscia albitrunca*. If the isotopic signal of grasses varies between -5.60 to 3.70 ‰ $\delta^{15}\text{N}$ for an average of 0.58‰, that of trees varies between 3.10 and 10.00‰ $\delta^{15}\text{N}$ with an average of 5.30 ‰. As proposed by Evans and Ehleringer (1994) for a desert shrub (*Chrysothamnus nauseosus*) in the arid west of the USA, groundwater may be a stable source of ^{15}N -enriched nitrogen for deep-rooted woody plants. This is probably the case for the sites of the Linyanti-Chobe basin where the deep-rooted vegetation is dependent on underground water (probably recharged by floods).

2.6. Conclusions

The distribution of plant cover and corresponding soil geochemistry has been proposed for the Linyanti-Chobe Basin in the present study. The main variable that governs the distribution of vegetation cover is the availability of water. Preceding studies have demonstrated an evolution of the vegetation relating to a north-south gradient linked to the mean annual precipitation (MAP) (Bird et al., 2004). However, the year-round presence of surface and/or ground- water in the Linyanti-Chobe Basin through the Linyanti and the Chobe Rivers and the Lake Liambezi makes the use of the north-south transect incompatible with the distribution of vegetation and soils in this basin. The distribution of the vegetation and soil geochemistry is proposed following a humidity gradient starting from a surface water source (river or lake) and ending middle of the basin, away from the surface water source. A simplified vision of the vegetation and soil geochemistry is proposed following a schematized transect. The purpose of this schematized transect is a better understanding on the distribution of plant types and plant species along the basin and the related soil geochemistry. It reveals a close relationship between plant cover and soil geochemistry, but furthermore, a strong relationship between river sediment geochemistry and surrounding vegetation. This results in the possible use of soil or sediment geochemistry for the purpose of paleo-climatic and paleo-environmental reconstruction.

First, analyses highlight a large diversity of plants of types C_3 and C_4 throughout the basin. The plant landscape in fact shows significant diversity and heterogeneity in the region. The distribution of plants within the basin is mostly determined by (micro-)topography and the fluctuations of the floods extent. Field observation and laboratory analyses made it possible to delimit three large zones for the Linyanti-Chobe basin according to the plant cover and the soils. The three zones reflect a specific water regime. Access to surface or underground water is major for zone I where trees are absent. Access to water at zone II is moderate and shows deep-rooted trees domination. And zone III shows a limited access to water with shallow-rooted trees domination. Furthermore, each of these zones shows a gradation in its plant cover and makes it possible to divide the three large zones into eight specific classes: Classes 1, 2, 3, 4, 5a-b and 6a-b. A detailed description of the plant cover, its isotopic composition (carbon and nitrogen) as well as the soil (TOC and $\delta^{13}\text{C}_{\text{SOM}}$) makes it possible to describe the ecology of each class. It means the access and influence of water (in quantity and quality), the preservation of organic matter and the link between plant cover and soil. These different analyses made it possible to directly link plant cover and soil (and water action). This is the major postulate of the present work. The second major point of the paper is to be found in the analogy of this first postulate to the sediments of the different water bodies of the Linyanti-Chobe basin. Indeed, the CHN analysis as well as the isotopic values of the organic carbon of the sediments of the different water bodies analysed allow reconstructions of plant cover similar to the type of direct surrounding plant cover.

Previous work has demonstrated the need to take grasses into account in the regional $\delta^{13}\text{C}_{\text{SOM}}$ inventory (Bird et al., 2004). The present work confirm it and demonstrates the distribution of the $\delta^{13}\text{C}_{\text{SOM}}$ along a schematized transect representing the Linyanti-Chobe Basin. The $\delta^{13}\text{C}_{\text{SOM}}$ along the schematized transect reflects directly the site vegetation and is mostly dominated by a mix between grasses and trees and/or C_4 and C_3 vegetation types.

Previous work carried out in this region tended to demonstrate an evolution of the vegetation relating to a north-south gradient linked to the mean annual precipitation (MAP) (Bird et al., 2004). While the MAP decreases from north to south, the grass proportion increases compared to the tree proportion. This change in vegetation is fixed in the soils with an increasing $\delta^{13}\text{C}_{\text{SOM}}$. This statement however does not fit for the Okavango region (Bird et al., 2004). Bird et al. (2004) hypothesizes a year-round access to water for this region as an explanation to this regional difference. The present work fully confirm this hypothesis and proposes a much precise distribution of the vegetation and its corresponding $\delta^{13}\text{C}_{\text{SOM}}$ for the Linyanti-Chobe Basin. Presence of surface and/or groundwater all year-round in this basin results in a distribution of the vegetation following this year-round presence of water and not the MAP. A schematized transect starting at a surface water source (river or lake) and ending in the middle of the basin, at distance of the surface water source is proposed. This transect is built after eight classes proposing each a specific plant cover and a mean $\delta^{13}\text{C}_{\text{SOM}}$. The plant cover is dependent on the distance to the water surface and to the availability of underground water. Its resulting and corresponding $\delta^{13}\text{C}_{\text{SOM}}$ is then dependent to the resulting plant cover and to the water stress lived by the plants. Water stress might be the distance to main source of water (surface or underground), availability of this source of water and the sustainability of this source of water. All these parameters are registered first in plants but then in the soils too.

This link between water availability, water stress, plant cover, plant types and record of these information into the soil organic matter geochemical composition is a precious source of information for paleo-environmental and paleo-climatic reconstruction for the region of the Linyanti-Chobe Basin.

The perspectives made possible by the present work are diverse: The study of the isotopic composition of the soils and the cover of the Linyanti-Chobe basin is new for the region and allows a precise classification of all the types of environments encountered in this area. The classification is easily achievable in the field and possible throughout the year (dry season or wet season). It is also relevant and makes it possible to extend the conclusions obtained on other sites. Indeed, the analysis of the organic matter of the soils allows a description: 1) of the type of vegetal cover of the site, and in fact, to make a deduction of the climate and/or the access to water of the site; 2) the morphology of the site; 3) the water stress suffered by the site, if however the plant cover has been identified.

These observations offer the possibility of studying a body of water (a lake for example) for the purpose of a paleo-environmental reconstruction of the region through the sediments recorded by the body of water.

2.7. References

- Austin, A.T. & Sala, O.E., 1999. Foliar $\delta^{15}\text{N}$ is negatively correlated with rainfall along the IGBP transect in Australia. *Australian Journal of Plant Physiology*, 26, 293-295.
- Ballif, L. 2018. Carbon and nitrogen stable isotope compositions as environmental proxies in savannas of northern Botswana. Unpubl. Master of Science in Biogeosciences, UNIL.
- Bird MI, Lloyd JJ, Santruchkova H et al., 2001. Global soil organic carbon. In: *Global Biogeochemical Cycles in the Climate System* (eds Schulze ED et al.), pp. 185–199. Academic Press, New York.
- Bird MI, Pousai P, 1997. Variation of $\delta^{13}\text{C}$ in the surface soil organic pool. *Global Biogeochemical Cycles*, 11, 313–322.
- Bird, M.I., Veenendaal, E.M., Lloyd, J.J. 2004. Soil carbon inventories and $\delta^{13}\text{C}$ along a moisture gradient in Botswana. *Global Change Biology* 10, 342-349.
- Bird MI, Veenendaal EM, Moyo C et al., 2000. Effect of fire and soil texture on soil carbon dynamics in a sub-humid savannah, Matopos, Zimbabwe. *Geoderma*, 94, 71–90.
- Burrough, S.L., Thomas, D.S.G., 2008. Late Quaternary lake-level fluctuations in the Mababe Depression: Middle Kalahari palaeolakes and the role of Zambezi inflows. *Quaternary Research* 69, 388-403.
- Ehleringer, J.R., Buchmann, N., Flanagan, L.B., 2000. Carbon Isotopes Ratios in belowground Carbon Cycle processes. *Ecological Applications*, 10/2, 412-422.
- Haddon, I.G., McCarthy, T.S. 2005. The Mesozoic–Cenozoic interior sag basins of Central Africa: The Late-Cretaceous–Cenozoic Kalahari and Okavango basins. *Journal of African Earth Sciences* 43, 316-333.
- Handley, L.L., Austin, A.T., Robinson, D., Scrimgeour, C.M., Raven, J.A. et al. 1999. The ^{15}N natural abundance ($\delta^{15}\text{N}$) of ecosystem samples reflects measures of water availability. *Australian Journal of Plant Physiology*, 26, 185-199.
- Heinl, M., Sliva, J., Murray-Hudson, M., Tachebat, B. 2007. Post-fire succession on savannah habitats in the Okavango Delta wetland, Botswana. *Journal of Tropical Ecology*, 23, 705-713.
- Högberg, P. 1986. Soil nutrient availability, root symbioses and tree species composition in tropical Africa: a review. *Journal of Tropical Ecology*, 2, 359-372.
- Högberg, P. 1990. ^{15}N natural abundance as a possible marker of the ectomycorrhizal habit of trees in mixed African woodlands. *New Phytologist*, 115, 483-486.
- Högberg, P. 1997. Tansley Review No. 95. ^{15}N natural abundance in soil-plant systems. *New Phytologist*, 137, 179-203.
- Killops S.D. and Killops V.J. 2005. *Introduction to organic geochemistry* (2nd edition). ISBN 0-632-06504-4, Blackwell Publishing, Oxford, UK.
- Kinabo, B.D., Atekwana, E.A., Hogan, J.P., Modisi, M.P., Wheaton, D.D., Kampunzu, A.B. 2007. Early structural development of the Okavango rift zone, NW Botswana. *Journal of African Earth Sciences*, 48, 125-136.
- Makhado, R.A., Mapaure, I., Potgieter, M.J., Luus-Powell, W.J., Saidi, A.T. 2014. Factors influencing the adaptation and distribution of *Colophospermum mopane* in southern Africa's mopane savannahs – A review. *Bothalia*, 44, 9p.
- McCarthy, J., Gumbricht, T., McCarthy, T.S. 2005. Ecoregion classification in the Okavango Delta, Botswana from multitemporal remote sensing. *International Journal of Remote Sensing*, vol. 26, 19, 4339–4357.
- Michener, R. & Lajtha, K. 2007. *Stable isotopes in Ecology and Environmental Sciences*. Blackwell Publishing, 2nd ed. 566p.
- Pricope, N.G. 2013. Variable-source flood pulsing in a semi-arid transboundary watershed: the Chobe River, Botswana and Namibia. *Environmental Monitoring and Assessment*, 185, 1883-1906.

- Pricope, N.G., Gaughan, A.E., All, J.D., Binford, M.W., Rutina, L.P. 2015. Spatiotemporal analysis of vegetation dynamics in relation to shifting inundation and fire regimes: disentangling environmental variability from land management decision in a southern African transboundary watershed. *Land*, 4, 627-655.
- Romanens, R. 2017. Organic matter dynamics and soil diversity in the Chobe Enclave, Botswana. Unpubl. Master of Science in Biogeosciences, UNIL.
- Romanens, R., Pellacani, F., Mainga, A., Fynn, R., Vittoz, P., Verrecchia, E.P., 2019. Soil diversity and major soil processes in the Kalahari basin, Botswana. *Geoderma Regional*, 19.
- Roodt, V. 1998. The Shell Field Guide Series: part 1. Trees & Shrubs of the Okavango Delta. Medicinal uses and Nutritional value. Shell Oil Botswana, Gaborone, Botswana, 213p.
- Roodt V. 2015. Grasses & Grazers of Botswana and the surrounding savannah. Struik Nature, Cape Town, South Africa, 304p.
- Scholes, R.J. 1990. The influence of soil fertility on the ecology of southern African dry savannahs. *Journal of Biogeography*, vol. 17, 4/5, Savannah Ecology and Management: Australian Perspectives and Intercontinental Comparisons, 415-419.
- Schulze, E.D., Gebauer, G., Ziegler, H., Lange, O.L. 1991. Estimates of nitrogen fixation by trees on an aridity gradient in Namibia. *Oecologia*, 88, 451-455.
- Schulze, E.D., Ellis, R., Schulze, W., Trimborn, P., Ziegler, H. 1996. Diversity, metabolic types and $\delta^{13}\text{C}$ isotope ratios in the grass flora in Namibia in relation to growth form, precipitation and habitat conditions. *Oecologia*, 106, 352-369.
- Schulze, E.D., Williams, R.J., Farquhar, G.D., Schulze, W., Langridge J. et al. 1998. Carbon and nitrogen isotope discrimination and nitrogen nutrition of trees along a rainfall gradient in northern Australia. *Australian Journal of Plant Physiology*, 25, 413-425.
- Schulze, E.D., Farquhar, G.D., Miller, J.M., Schulze, W., Walker, B.H., Williams, R.J. 1999. Interpretation of increased foliar $\delta^{15}\text{N}$ in woody species along a rainfall gradient in northern Australia. *Australian Journal of Plant Physiology*, 26, 296-298.
- Stevens, N., Swemmer, A.M., Ezzy, L., Erasmus, B.F.N. 2013. Investigating potential determinants of the distribution limits of a savannah woody plant: *Colophospermum mopane*. *Journal of Vegetation Science*.
- Tedder, M.J., Kirkman, K.P., Morris, C.D., Trollope, W.S.W., Bonyongo, M.C. 2013. Classification and mapping of the composition and structure of dry woodland and savannah in the eastern Okavango Delta. *Koedoe*, 55, Art. #1100, 8p.
- Vittoz, P., Pellacani, F., Romanens, R., Mainga, A., Verrecchia, E.P., Fynn, R.W.S., 2020. Plant community diversity in the Chobe Enclave, Botswana: Insights for functional habitat heterogeneity for herbivores. *Koedoe*, 62.
- Wolski, p. & Savenike, H.H.G. 2006. Dynamics of floodplain-island groundwater flow in the Okavango Delta, Botswana. *Journal of Hydrology*, 320, 283-301.

3. Sedimentology, mineralogy and geochemistry of sediments from Lake Liambezi, Namibia-Botswana

Anael Lehmann¹, Christophe Paul², Daniel Ariztegui³, Pilar Junier², Torsten Vennemann^{1&}

¹Laboratory of Stable Isotope Geochemistry. Institute of Earth Surface Dynamics, University of Lausanne, Lausanne, Switzerland.

²Laboratory of Microbiology, Institute of Biology, University of Neuchâtel, Neuchâtel, Switzerland.

³Laboratory of Limnogeology and Geomicrobiology, Department of Earth Sciences, University of Geneva, Geneva, Switzerland.

[&]Corresponding authors: Torsten Vennemann. Laboratory of Stable Isotope Geochemistry. Institute of Earth Surface Dynamics, University of Lausanne, CH-1015 Lausanne. Mail: Torsten.Vennemann@unil.ch; Phone: +41216924464.

3.1. Abstract

Wetlands in arid-climates represent a source of life-supporting water in an otherwise inhospitable environment and are therefore unique ecosystems. They often contain a highly specialized flora and fauna and may respond sensitively to any climatic or environmental change. North Botswana having the second largest endorheic delta system in the world, middle of the Kalahari, forms a complex network of rivers and waterbodies controlled by tectonic faults. Lake Liambezi, located at the border with Caprivi Strip, Namibia is part of the Linyanti-Chobe System and remains little described. The aim of the present work is part of a larger multidisciplinary study, which aims at a better understanding of this unique ecosystem. Here, we first expose the characterization of the geochemistry, mineralogy and organic matter content of Lake Liambezi using sedimentary cores. The aim is to highlight the major and trace components of the sediments and to understand their origin and their dynamics.

Organic matter contained in the sediments denotes a dominantly autochthonous origin mostly composed of aquatic plants and algae with a lesser contribution of terrestrial detritus washed into the lake. Terrestrial plant contribution shows a mix between C₃ – and C₄ – type of vegetation with a clear dominance of the C₃ vegetation. It is compatible with the presence of *Phragmites australis* (a C₃ plant) described along the shores of Lake Liambezi. Center Core appears to have a larger proportion of terrestrial vegetation compared to the two other cores, which may be related to a distinct evolution of the three different basins sampled by the cores. This reveals a less commonly flooded site compared to the northern and southern sub-basins. The absence of biogenic or lithogenic calcite or aragonite observed with the SEM contrast with the abundance of biogenic and lithogenic silica. It shows a complete cycle of silica with precipitation, remobilization by dissolution and reprecipitation. The abundance of silica material might be explained by the presence of the Kalahari Desert southwest of the lake and a large riverine catchments composed of crystalline rocks. Mineralogy of the sediment confirms the importance of detrital material coming from the catchment. However, the weathering of primary minerals such as feldspar, plagioclase and micas found in the catchment is climatically-controlled and results in the formation of smectite. Kaolinite is also climatically controlled in the lake vicinity, however, is more complex to interpret. Smectite is therefore used as climate tracer in the lake sediments. Sometimes simultaneous presence of sulphur in its oxidized form as gypsum and in its

reduced form as pyrite demonstrate alternating wet and dry periods during a year. This coexistence is therefore more difficult to use as a climate tracer.

The use of organic matter as a tracer of climatic and environmental change is possible due to its autochthonous origin. The climatically-controlled clay smectite is considered as neo-formed in the region and is therefore of first importance to reconstruct the climatic evolution of the site. In contrast, most of the other variables found in the sediments such as the grain-size, the detrital mineral content and the presence or absence of pyrite and gypsum are controlled by localized features such as the connectivity of the basin to the rivers or the water availability of the site. They do not seem to indicate global trends. They are however of major importance to interpret site specificities and to help correlate other indicators. The understanding of these different characteristics and components origin of Lake Liambezi sediments is important for further interpretations of environmental and climatic evolution of the lake.

3.2. Introduction

Wetlands in arid climates represent unique ecosystems and are of major importance as they represent a source of life-supporting water in an otherwise inhospitable environment. These environments are, however, particularly fragile ecosystems as they often contain a highly specialized flora and fauna that responds sensitively to any climatic or environmental change. The region located in the north of Botswana offers a unique example of this type of environment, being the second largest endorheic delta system in the world. This unique ecosystem is established by two endorheic Okavango and Kwando rivers, but also with changing contributions from the Zambezi River. These three rivers form a complex network controlled by tectonic faults (Haddon & McCarthy, 2005). A minor change in tectonism and faulting can directly influence the morphology and hence the drainage pattern of the entire system. This has been clearly demonstrated by the work of Burrough and Thomas (2008) for the evolution of the paleolakes of the middle of the Kalahari, a region also considered to be the cradle of humanity (e.g., Cavaillé-Fol, 2020).

While the Okavango delta system has been studied for a number of years already (McCarthy, 2013; Milzow et al., 2009; McCarthy et al., 2005 ; Darkoh & Mbalwa, 2014), the adjacent Lake Liambezi drainage system has remained little described. In contrast to the Okavango system, Lake Liambezi is at best only seasonally flooded during the recent past. This system groups together three endorheic deltas: the Kwando delta, a delta seasonally created by overflowing of the Zambezi River, and the Chobe River. However, under different climatic conditions in the past, the Lake Liambezi system may have been similar to the present-day Okavango system. The first limnological description of Lake Liambezi was made in 1978 by Seaman et al.. His study was then taken up by different authors but only with a focus on the fish populations of the lake (Tweddle et al., 2011; Mutelo, Murwira & Kileshye-Onema, 2013; Peel et al., 2015). Their studies highlight the importance of the lake for the surrounding villages and communities of farmers and fishermen as a major resource of freshwater and fish, even under today's conditions of seasonal flooding. A better understanding of the past conditions in this fragile and evolving system is hence not only of local importance but may also serve as an example of what could be the future of the adjacent Okavango system, given expected environmental impact associated with ongoing and future climatic changes.

This work is part of a larger multidisciplinary study, which aims at a better understanding of this fragile ecosystem. It encompasses the first characterization of the geochemistry, mineralogy and organic matter content of Lake Liambezi using sedimentary cores. These results were subsequently examined in the light of past environmental changes that may have led to variations in the geochemical and mineralogical compositions. The microbiological composition of the same sediments as well as their ¹⁴C compositions and hence temporal evolution are discussed in companion papers in order to improve our understanding of the system via a multidisciplinary study.

3.3. Material and methods

3.3.1. Regional and lake settings

Lake Liambezi is located in Namibia, at the eastern side of the Caprivi Strip. The lake is part of a complex drainage system that includes the Kwando and Zambezi rivers. Its Southern shore makes up the border between Namibia and Botswana. It receives water from the Chobe River (a tributary of Zambezi River, deviated due to the Chobe Fault (Haddon and McCarthy, 2005)), Bukalo Channel (a seasonal tributary of Zambezi River), and Linyanti River (or Swamps, natural deviation of Kwando River due to the Linyanti Fault (Haddon and McCarthy, 2005)), as well as rainwater and local runoff water (Figure 26).

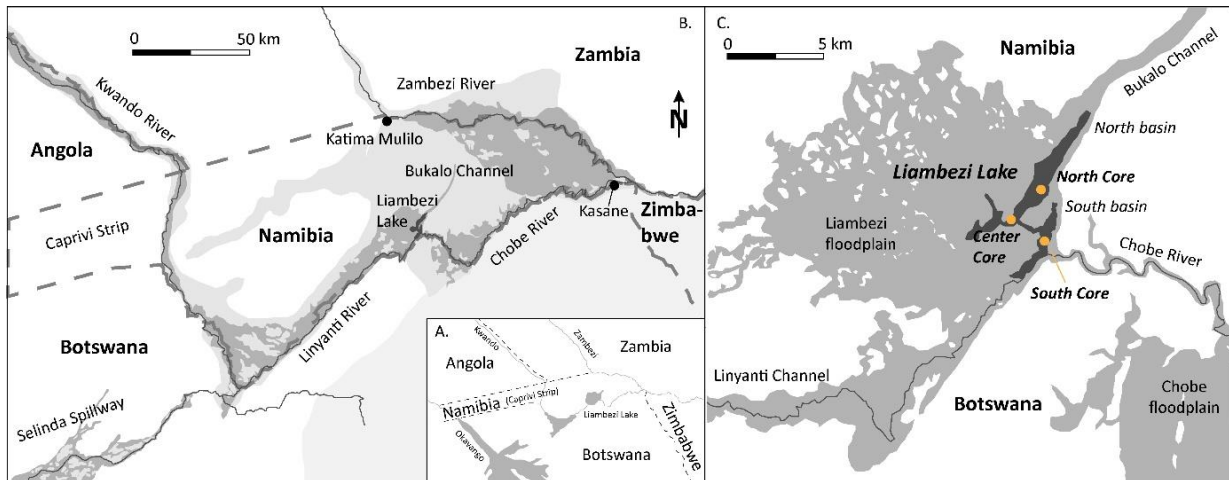


Figure 26 Modified from Peel, 2015. **A.** General map of the region with the three main river systems: Okavango, Kwando and Zambezi; **B.** General map of grouped systems Kwando and Zambezi rivers. Kwando River comes out Angola and turns into Linyanti River after its terrestrial delta joins a tectonic fault along the Namibia and Botswana border. It finishes its course into Lake Liambezi mostly into percolating water in Linyanti swamps. Zambezi River coming down Zambia flows into Lake Liambezi through the Bukalo channel and the Chobe River (Haddon and McCarthy, 2005). The Chobe River reverses its flow depending on water availability and can flow in both directions (Seaman et al., 1978; Peel et al., 2015). The very poor relief generates many flood zones that are formed around the rivers of the system as well as around Lake Liambezi (dark grey); **C.** In dark grey color, map of Lake Liambezi in its full size as described by Seaman et al., 1978. Open-water lake with its two elongated basin is in black. Yellow dots indicate core locations.

Depending on the water level, the Chobe River serves as outflow of the lake (Seaman et al., 1978; Peel et al., 2015). The lake is surrounded by a major flat wetland system characterized by woodlands, wetlands and slow-flowing floodplain rivers (Seaman et al., 1978; Peel et al., 2015). Seaman et al. (1978) reported a system covering some 300 km² of which 100 km² was open water at its full size. The lake changes shape, size and depth between and within years due to the source and the amount of water in the basin (Tweddle et al., 2011). The average depth is approximately 2.5 m (Seaman et al., 1978) but can reach 7 m at the height of the rainy season (Peel et al., 2015). The general shape of the lake varies depending on the water supply. It is separated in two main basins: northern and southern basins, which are connected by a narrow 1.3 km long central channel. The northern basin is approximately 6 km long and 1 km wide at its maximum. It receives water from the Bukalo Channel on the north, from the channel between the two basins on the east and by percolation in its western and southern shores by the Linyanti marsh. The southern basin is 4 km long and 500 m wide. It receives water by the connecting channel to the West, by the Chobe River to the East, the Linyanti marsh all along its South-Western shore and by the Linyanti channel in the South-East (Figure 26). The Linyanti marsh, surrounding the two basins in their western shores is the result of a geological fault that forms an area of wetlands composed of a complicated patchwork of swamps and marshes. The fault is known as the Linyanti Fault (Haddon and McCarthy, 2005). The set of these features forms the Linyanti River. The Chobe River also flows through a fault named the Chobe Fault (Haddon and McCarthy, 2005).

3.3.2. Coring

Three cores were retrieved from the same number of coring locations (Figure 26) using an Uwitec Hammer Action Corer with PVC tubes of 86.0 mm inside diameter. The Center Core (CC) was obtained at the south-eastern side of the northern basin, at about 300 meters from the connecting channel. The South Core (SC) was retrieved in the central part of the southern basin. It is set at about 250 meters close to the mouth of the Chobe River, and at about the same distance of both, Linyanti main channel and the connecting channel. The North Core (NC) was obtained in the central part of the northern basin at ca. 4.2 km from the Bukalo Channel. The three cores were transported to the VanThuyne-Ridge Research Center to be opened, cut, described and sampled under good conditions and using the appropriate equipment. The sampling and grouping of samples was carried out based on visual criteria as reported in Chapter 4.

3.3.3. Mineralogical and geochemical analyses

Scanning electron microscopy (SEM) was done using the Tescan Mira II LMU. Field emission (Shottky-FE) SEM equipped with SE, in-lens SE and BSE detectors. EDX and EBSD analyses used a Penta-FET 3x detector and a Nordlys S camera, respectively, both being monitored by the AZtec 2.4 software package released by Oxford Instruments. This instrument also allows for low-vacuum BSE observations up to 50 Pa. Grain-size analysis were run with a Malvern Mastersizer 2000 grain-sizer that uses the principle of laser diffraction to measure particles between 0.01 μm and 2 mm in size. Two modules of dispersion were used: Hydro 2000S, which allows wet samples to be analysed, and Scirocco 2000, for dry samples. X-Ray diffraction (XRD) analyses of the whole rock were prepared following the procedure of Kübler (1987) and Adatte et al. (1996). The standard deviation recognized for granular minerals (quartz, calcite, K-feldspar, Na-plagioclase, dolomite and gypsum) is 5 %. For other minerals (phyllosilicates, pyrite and goethite), the standard deviation is 10 %. The standard deviation recognized for clay analyses is 5 %. Whole-rock major element contents were determined by X-ray fluorescence (XRF), using a wavelength-dispersive PANalytical AxiosmAX spectrometer fitted with a 4 kW Rh X-ray tube. The analyses were performed on fused-disks prepared from 1.2 g of calcined sample powder mixed with Lithium-tetraborate (1:5 mixture). The XRF calibrations were based on 21 international silicate rock reference materials. The data are reported on a loss of ignition (LOI)-free basis. Standard deviations are as follows: SiO_2 0.08 %, TiO_2 <0.01 %, Al_2O_3 0.02 %, Fe_2O_3 0.01 %, MgO 0.01 %, CaO 0.01 %, K_2O 0.01 %. Trace elements analyses were conducted on disks obtained by pressing 12 g of sample powder on a support of Hoechst-wax-C. Calibration of trace elements was based on synthetic standards and international silicate rock reference materials. Standard deviations are as follows: Cr 0.6 %, Mn 0.3 %, Co 1.4 %, Cu 0.6 %, Zn 0.6 %, Sr 0.5 %, Zr 0.3 %, Ba 2.1 %, Pb N.A., S 0.01 %. The method is based on Potts, 1986. Total organic carbon and nitrogen were determined using the Thermo Finnigan Flash EA 1112 analyzer. Samples were heated up to 500 and then 900 °C in the presence of O_2 , the released gas (H_2O , N_2 , CO_2 and SO_2) transported over a chromatographic column and then measured by a thermal conductivity detector. Stable carbon isotope analyses of bulk organic matter in sediments were done using a Thermo Finnigan Flash EA 1112 linked to a Delta V mass spectrometer. The sediment was combusted in the presence of O_2 and the CO_2 produced was introduced into the mass spectrometer with He as the transporting agent. The analytical error is inferior to 0.1 ‰ and results are given relative to the isotopic standard VPDB. A Rock-Eval 6 pyrolyzer manufactured by Vinci Technologies was used to characterize the organic matter. The standard Rock-Eval parameters provide information on the amount of total organic carbon (TOC) and are further interpreted as proxies for the source (aquatic or terrestrial) of the organic matter (Hydrogen Index vs. Oxygen Index; Sebag et al. (2018)). All analyses have been done at Institutes of Earth Sciences and Earth Surface Dynamics of the University of Lausanne.

3.4. Results

Figure 27 to 14 show the pictures and the results for the three cores with a selection of parameters through depth. The evolution of most of the parameters follows the visual separation represented by different grey coloured surfaces in Figure 27-29. The cores will be described from the bottom to the top. The lowermost sediments of the North Core (Figure 27) display lower TOC, N and S values than the upper part. Major and trace elements decrease from bottom to top to increase again in the uppermost sample. Clay minerals show similar trends except smectite and vermiculite. In general vermiculite content mirror smectite with some exceptions. The mineralogy of the sediments does not show a clear pattern. The Center Core (Figure 28) generally has low concentrations for organic carbon cycle related elements, with somewhat higher concentrations in samples CC17, CC14, and CC12 as well as samples CC06, CC03, and CC02. Major and trace elements increase from bottom to top with a significant peak for most of the elements in sample CC14. SiO_2 compound demonstrate the opposite trend. Clay minerals show similar trends than most of the elements except smectite and vermiculite. The mineralogy of the sediments does not show a clear pattern except for quartz and the phyllosilicates which follow a similar trend than most of the elements. It highlights the major difference in trend between the mineral quartz composed of SiO_2 and the compound SiO_2 . The South Core (Figure 29) has a clear separation between the lower group of samples compared to upper group of samples. The organic carbon associated elements show an increase from the bottom to the top with however a slowdown in the increase for the upper group. Trace elements such as Ba, Zr, Sr, Mn and Cr show a decrease from the bottom to the end of the first group with a consecutive increase in the second group of samples. Other trace elements show more or less the opposite trend. If major compounds such as TiO_2 and SiO_2 show an important decrease in the first group of samples and then a slowdown in the decrease with an almost flattening, and Fe_2O_3 and Al_2O_3 the opposite trend, MgO , CaO and K_2O show a continuous increase with however two accentuations of the increase in the lowest samples and again in the upper samples. Clay minerals show undefined trends except smectite and vermiculite again. Except for quartz, phyllosilicates and gypsum, the pattern of the minerals is not clear.

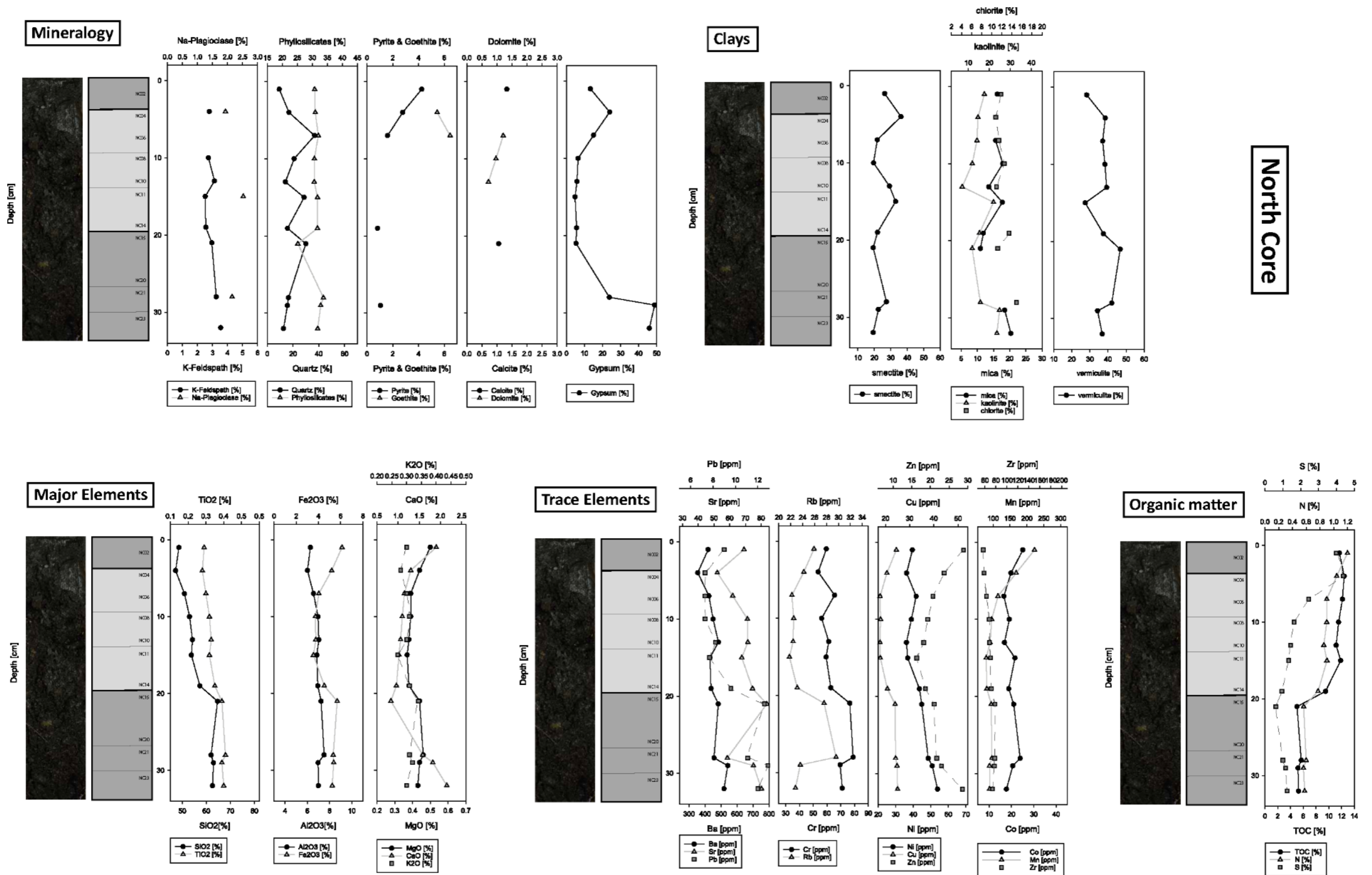


Figure 27 Pictures of the North Core and selected parameters relative to depth: Main minerals and clays along with a selection of major and traces elements as well as elements associated with the organic fraction. The standard deviation or the analytical error of the different analysis are less than or equal to the size of the symbol.

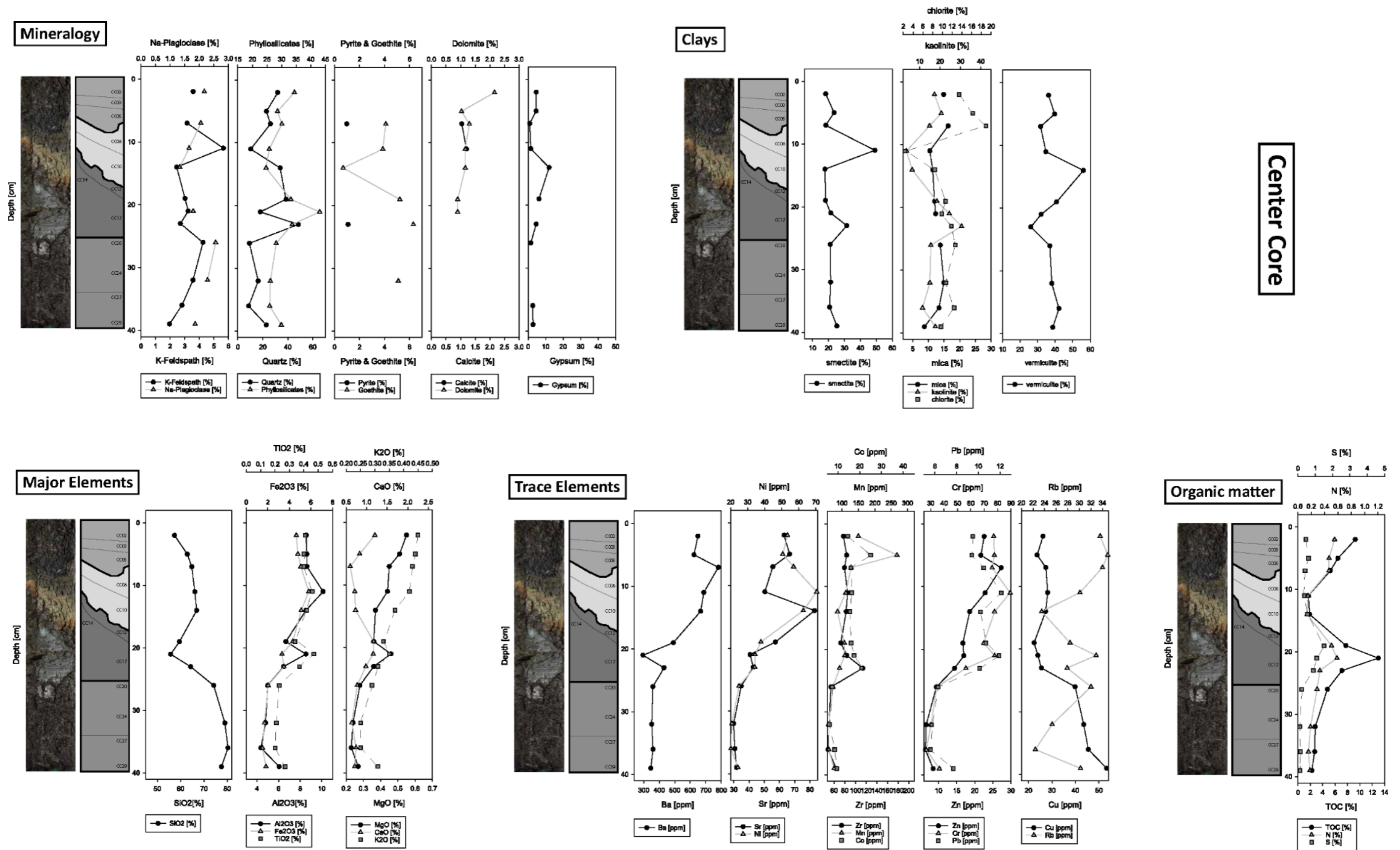


Figure 28 Pictures of the Center Core and selected parameters relative to depth: Main minerals and clays along with a selection of major and traces elements as well as elements associated with the organic fraction. The standard deviation or the analytical error of the different analysis are less than or equal to the size of the symbol.

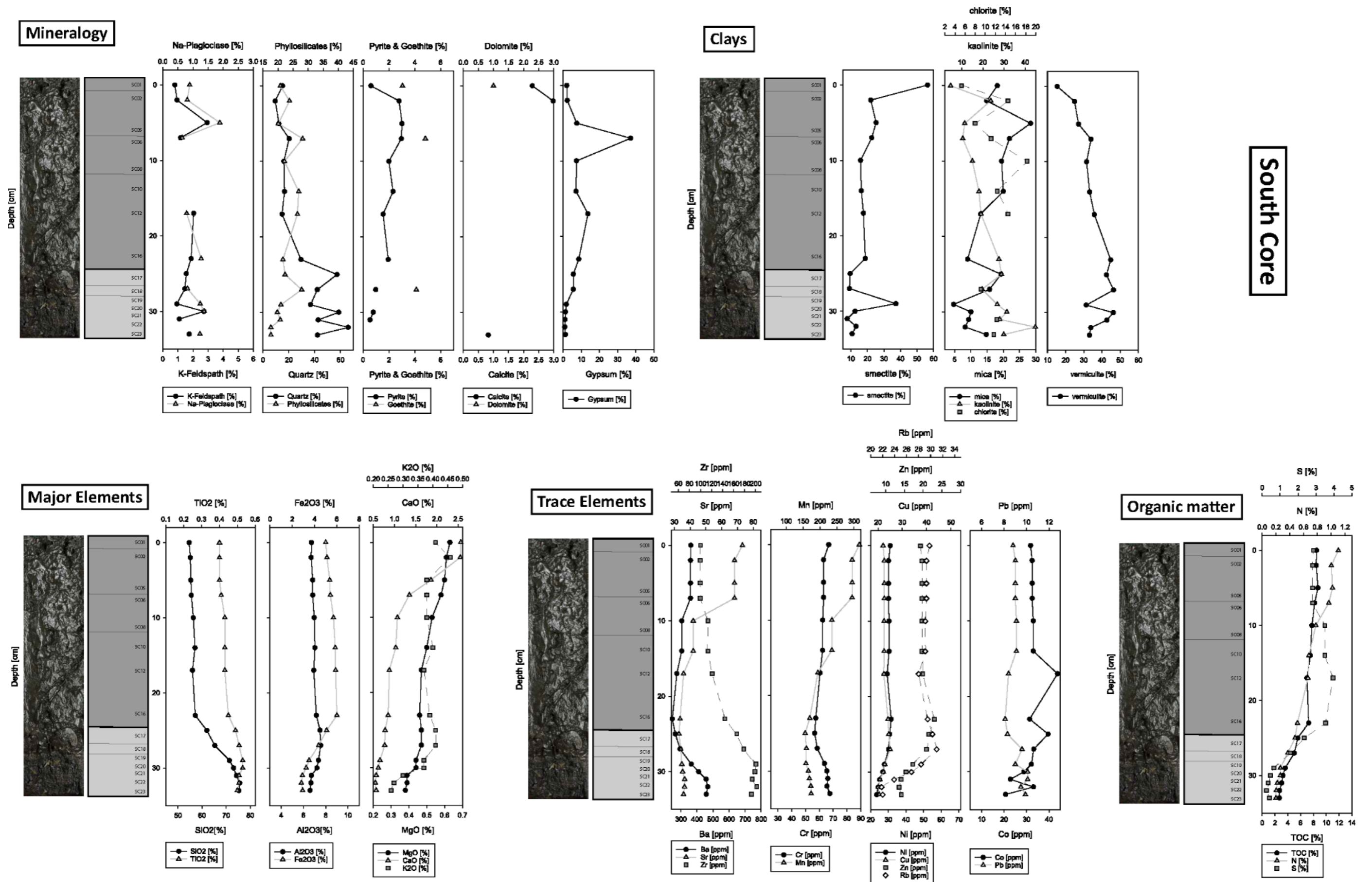
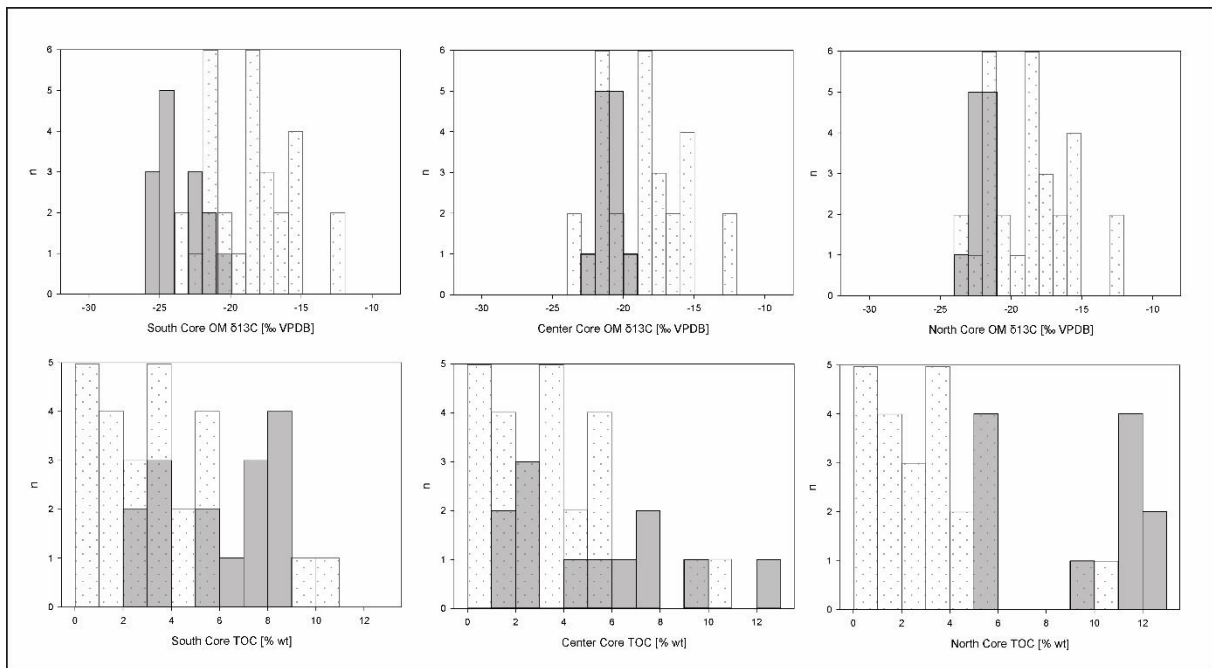


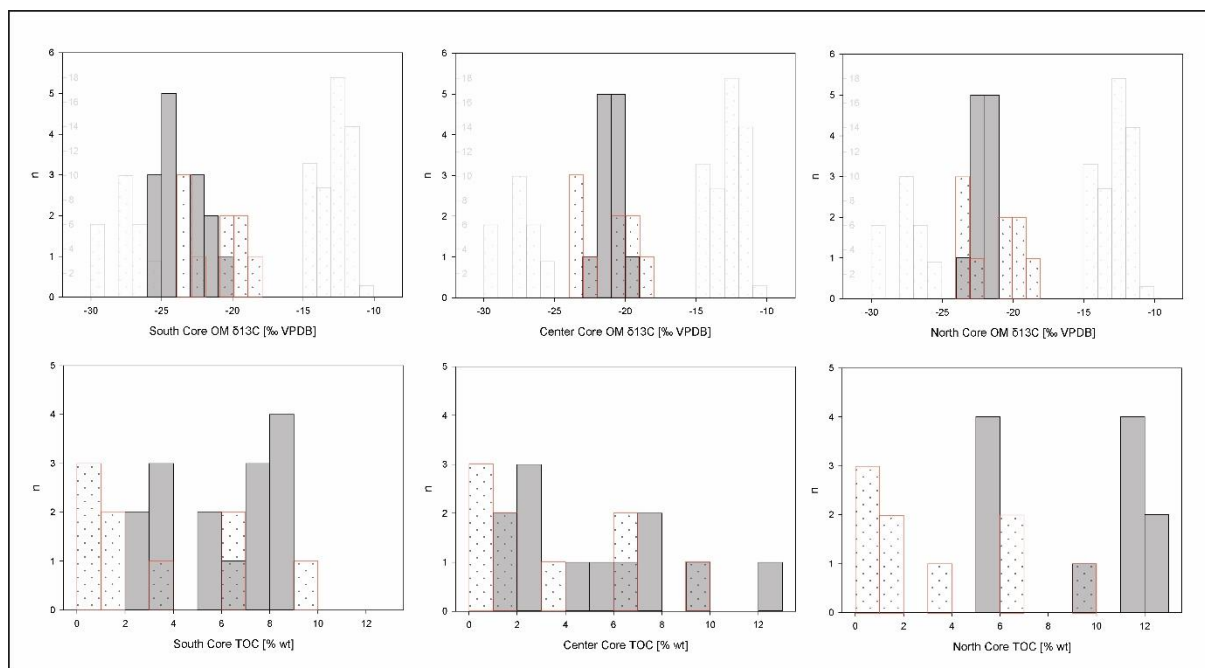
Figure 29 Pictures of the South Core and selected parameters relative to depth: Main minerals and clays along with a selection of major and trace elements as well as elements associated with the organic fraction. The standard deviation or the analytical error of the different analysis are less than or equal to the size of the symbol.

Sedimentology, mineralogy and geochemistry of sediments of Lake Liambezi

Figure 30 shows the range of the amount of organic carbon contained in the sediments of each core as well as the range of isotopic values for organic carbon. The North Core has a variation from 5.0 to 12.4 % of its weight in total organic carbon (TOC) and a variation of $\delta^{13}\text{C}$ values between -21.6 and -23.6 ‰. For the Center Core, TOC varies between 1.7 and 13.0 % and the isotopic values between -19.7 and -22.7 ‰. The core has the least amount of organic matter (for samples CC08 and CC10). The South Core shows a variation in TOC from 2.7 to 8.7 % and isotopic variation from -20.4 to -25.6 ‰. It is the core with the highest isotopic variations between the three. Figure 30 shows also the comparison with results given in Chapter 2. The comparison to the soils of the Linyanti-Chobe Basin shows more negative isotopic values and higher organic carbon content for the lake sediments. Comparison with river sediments of the region (Okavango, Linyanti and Chobe) shows similar statements. The comparison with the sampled vegetation of the Linyanti-Chobe Basin (Chapter 2 reveals an isotopic signal of the organic carbon from the lake's sediment closer to the C_3 – type vegetation.



a)



b)

Figure 30 For figures a) and b), top row: isotopic values of organic carbon in per mil VPDB for each core; bottom row: amount of organic carbon contained in the sediments of each core. For both analysis, Y axis is the number of sample per core in a given range of data relative to the X axis. Fig. a) comparison of lake data with soils analysis made in Chapter 2. Soils results are represented with dotted boxes and come from the Linyanti-Chobe Basin. Fig. b) comparison of same data with river sediments in dotted red boxes and with vegetation in dotted light-grey boxes. Y axis-scale for vegetation data is in light-grey as well. Vegetation comes from the Linyanti-Chobe Basin and river sediments are from the three main rivers: Okavango, Linyanti and Chobe (Chapter 2).

A selection of samples coming from the three cores has been inspected using a Scanning Electron Microscope (SEM) to qualitatively characterize the type of material and its arrangement. Only the organisation, the visual amount, the quality, the position, and the association of the different elements composing the sediment have been evaluated. No quantitative measurement was performed using SEM. SEM images revealed a mud composed of a heterogeneous composition dominated by siliceous features. This heterogeneous mud is composed of rare quartz grains <200 μm (Table 2, Table 4b, Table 9), numerous siliceous organisms (diatoms (Table 3b, Table 4a, Table 7), fragments of diatoms, phytoliths (silicified vegetal cells, Table 3a, Table 5, Table 8a,b), sponge spicules (Table 3a, Table 8d), algal cyst (Table 8c), silicified Cyanobacteria colonies (Gloeocapsae, Chroococcae, Table 8e,f (Sebag and Verrecchia, 1999)), amorphous silica precipitations (Table 9e,f), organic material such as charcoal particles (Table 3b), plant fragments, as well as remains of algae, framboidal pyrite (Table 9d) as well as a large mass of clayey mud. Quartz sand grains show traces of aeolian or riverine transport. Some show V-shaped traces on their surface, thought to demonstrate silica dissolution (Table 9a,b). Silica dissolution is believed to occur on diatoms fragments as well (Table 9c). The variety of forms composed of silica testifies to the silica saturation of the lake system, as well as its mobility. The traces of dissolution, the variety of siliceous organisms, as well as the presence of amorphous silica demonstrate a significant redistribution of this element. The presence of carbonate was not detected using the electron microscope.



a.

200 μm



b.

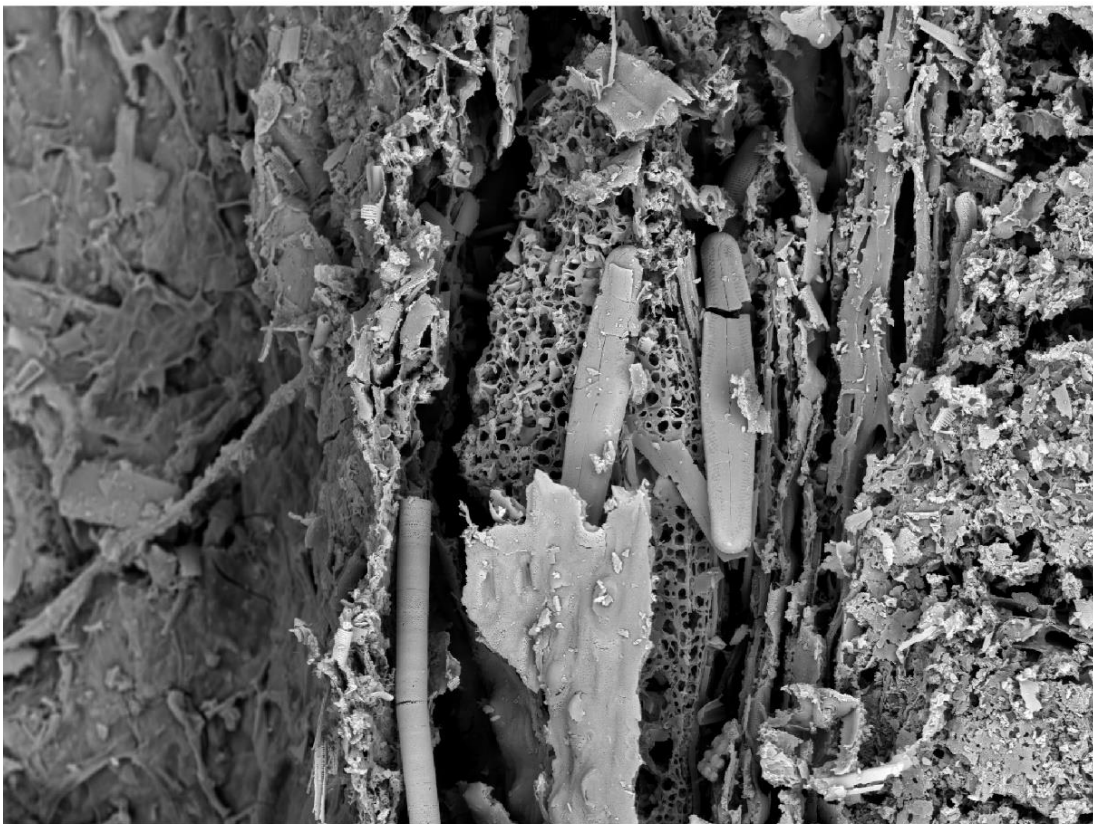
100 μm

Table 2 a. Heterogeneous mud composed of quartz grains, sponge spicules, diatoms and fragments of these organisms partly surrounded and coated by a mass of clayey mud. b. Enlargement of the previous sample.



a.

200 μm



b.

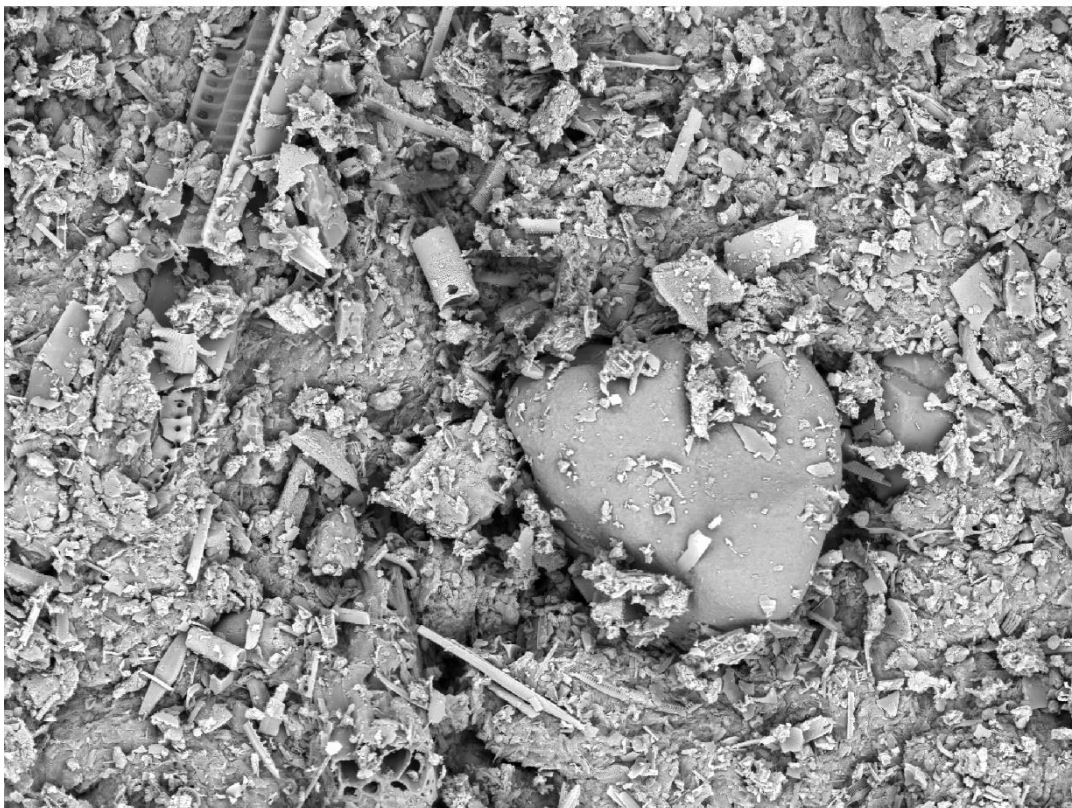
100 μm

Table 3 a. Heterogeneous mud composed of phytoliths, sponge spicules, diatoms and fragments of these organisms partly surrounded and coated by a mass of clayey mud. b. Charcoal remains and well preserved diatoms.



a.

50 μm



b.

100 μm

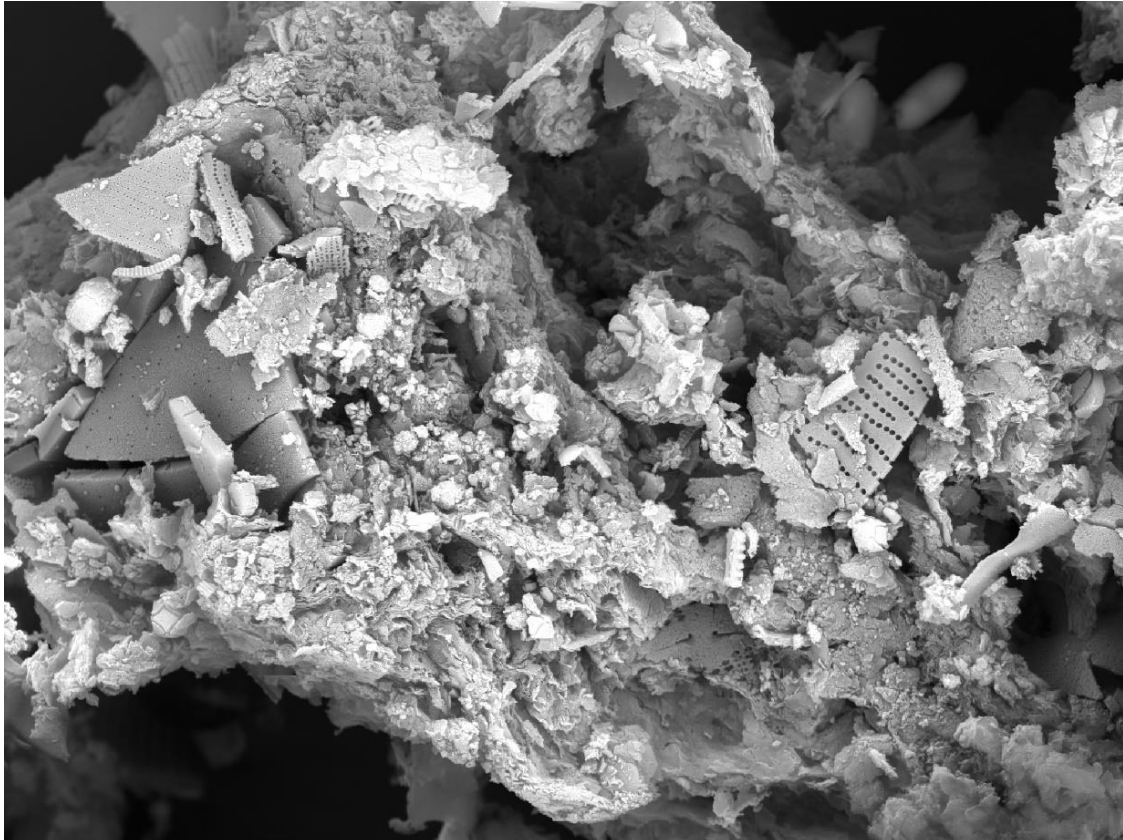
Table 4 a. Mass of clayey mud surrounding fragments of diatoms. b. Mass of clayey mud surrounding fragments of diatoms and quartz grains.



a.

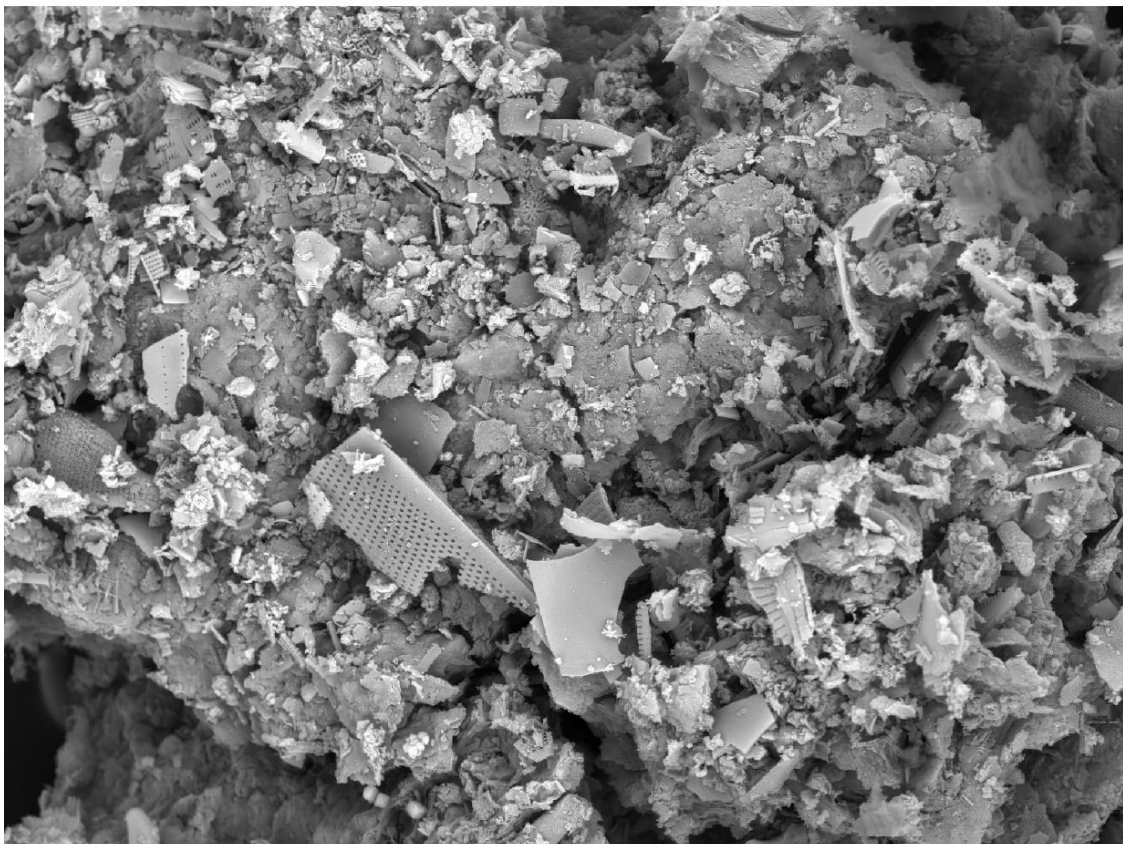
100 μm

Table 5 a. Phylolith and sponge spicule surrounded by a heterogeneous mass of diatoms fragments and clayey mud.



a.

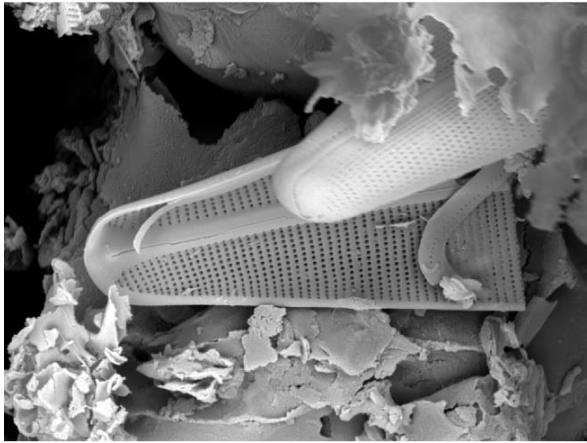
10 µm



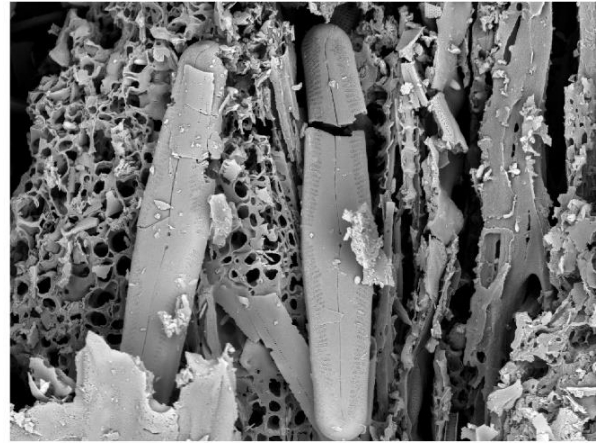
b.

20 µm

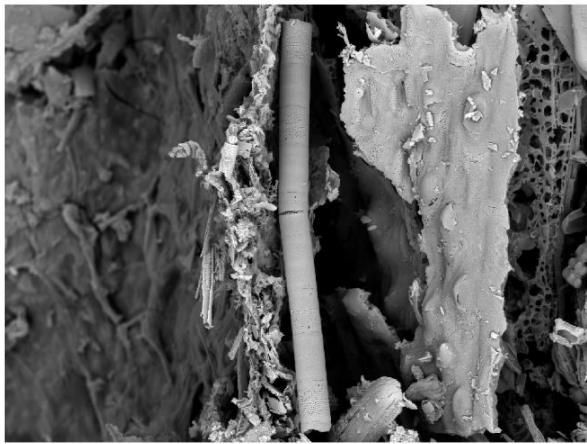
Table 6 Detail of the clayey mud composed of clays and diatom fragments.



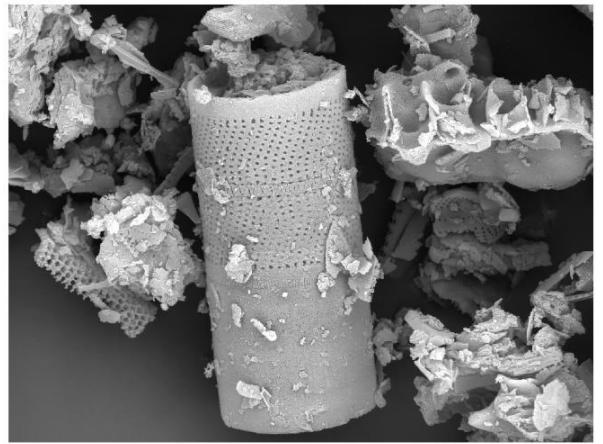
a.  10 μm



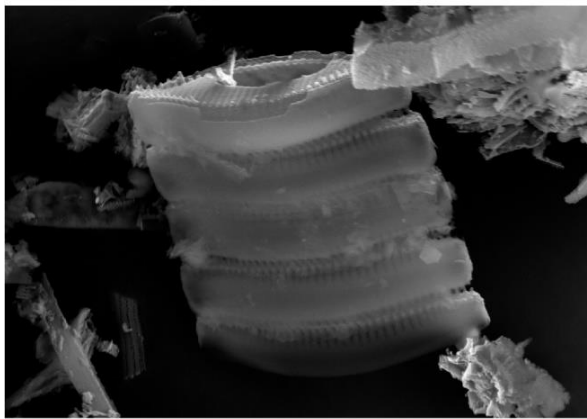
b.  20 μm



c.  50 μm

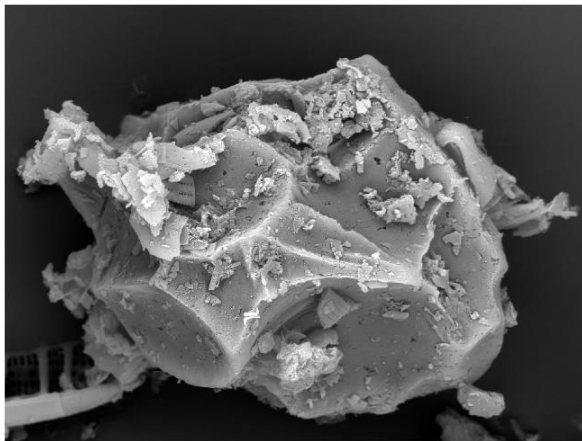


d.  10 μm

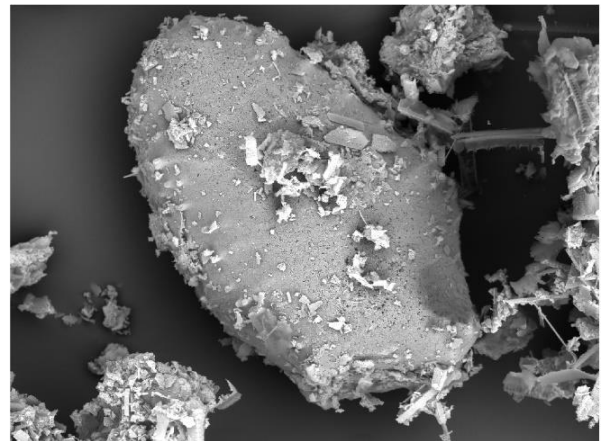


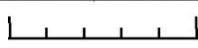
e.  10 μm

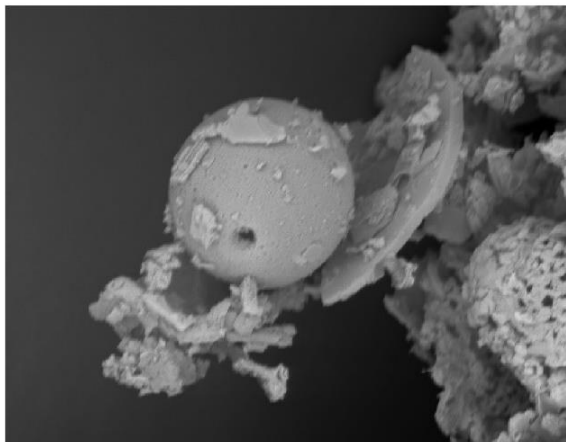
Table 7 Different types of diatom.



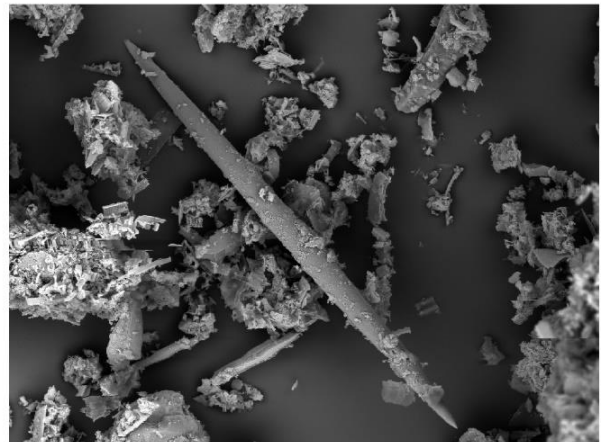
a.  20 μm

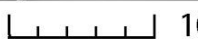


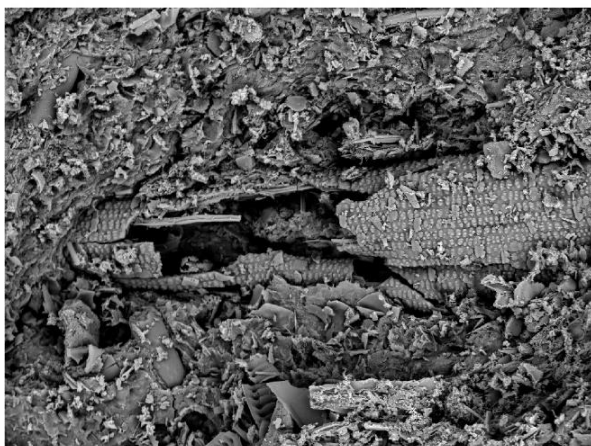
b.  50 μm

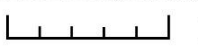


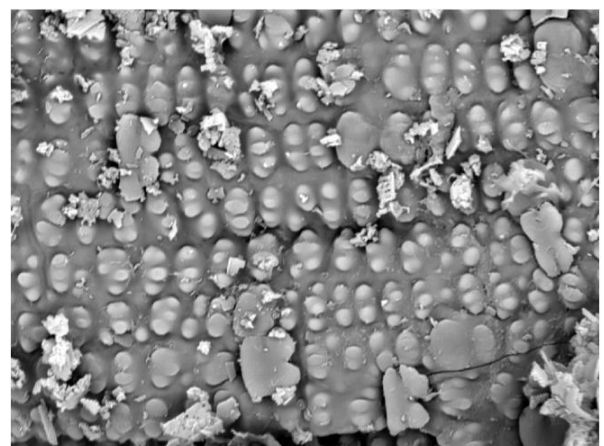
c.  10 μm



d.  100 μm



e.  100 μm



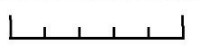
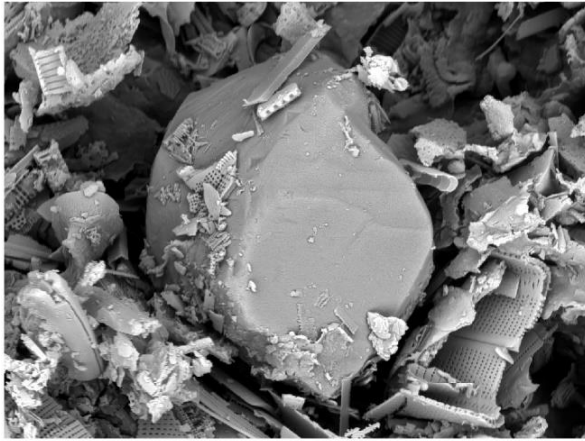

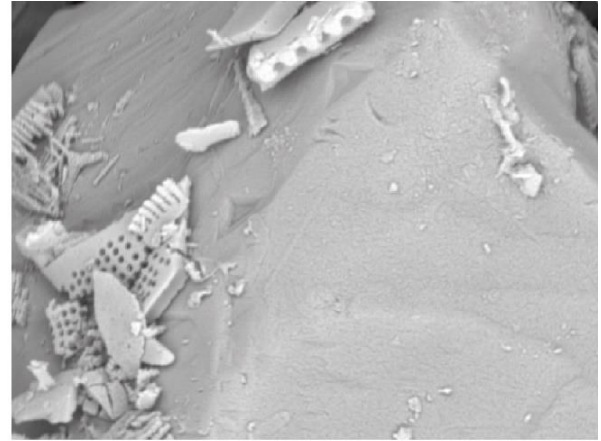
f.  20 μm

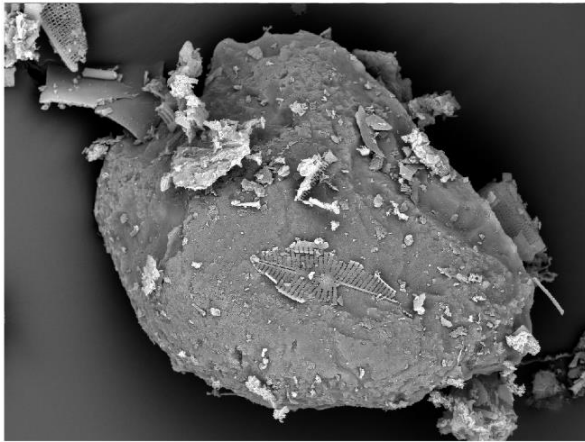
Table 8 a. Phytolith. b. Phytolith. c. Algal cyst. d. Sponge spicule. e. Silicified Cyanobacteria colonies (*Gloeocapsae*, *Chroococcaceae*). f. Detail of the silicified Cyanobacteria colonies.



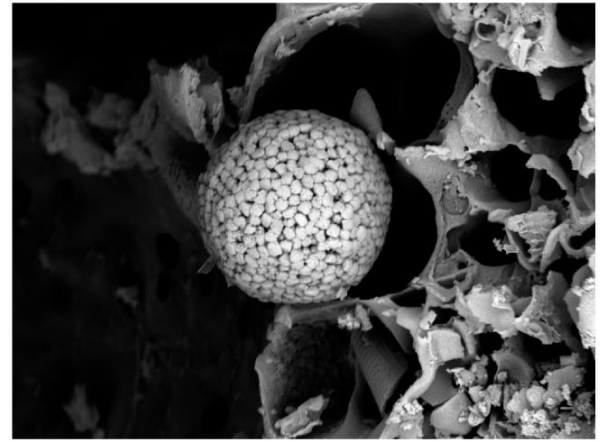
a.  20 μm



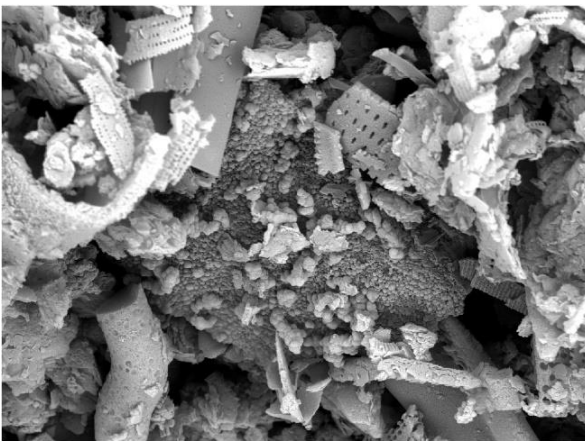
b.  5 μm



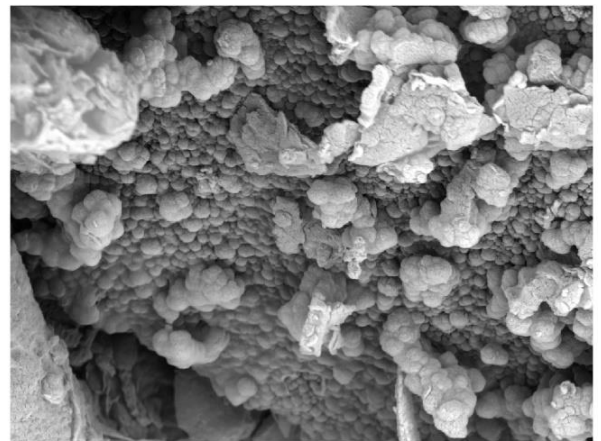
c.  20 μm



d.  10 μm



e.  5 μm



f.  2 μm

Table 9 a. Quartz grain with possible dissolution V-shaped marks. b. Detail of the V-shaped marks. c. Diatom frustule showing supposed dissolution marks (deposited on a quartz grain). d. Framboidal pyrite. e. Precipitation of amorphous silica. f. Detail of the amorphous silica.

Figure 31 shows ternary diagrams with the grain-size distribution for the three cores. For the North Core, the two upper samples are categorised as silty clay loam due to their lower amount of sand. All the other samples are of the silt-loam category. The Center Core has some samples well grouped into the silt loam category with the exception of the two samples representing the light-coloured part of the core. These two samples have a higher sand fraction, moving the CC08 sample to the loam category. The South Core shows homogeneous values with, however, two groups of samples. Separation of the groups is similar than for the other analyses (see Figure 29). Grain-size is distributed in silt loam category with the top section of the core of slightly finer grains.

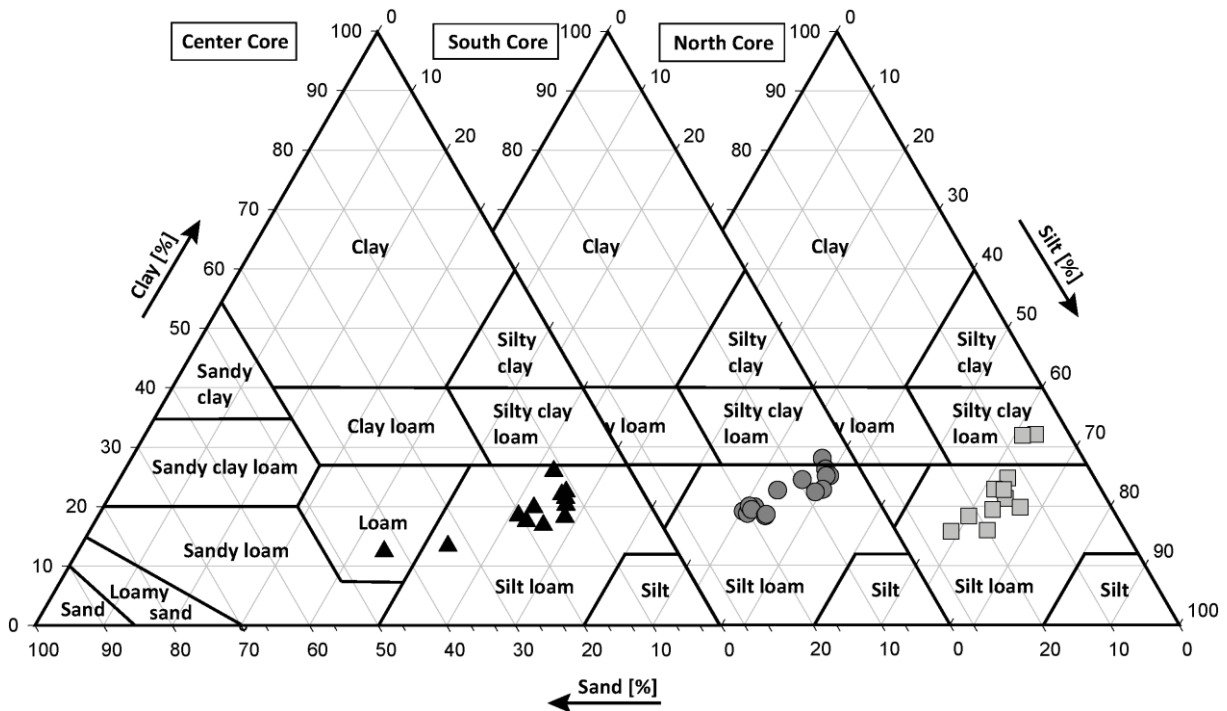


Figure 31 Ternary diagram of the particle size distribution for the three cores. It shows a classification between loam, silt loam and silty clay loam for all the samples.

The mineralogy of the three cores includes Na-plagioclase, K-feldspars, phyllosilicates, quartz, pyrite, and goethite but also depending of the samples, dolomite, calcite, and gypsum (Figure 32). Na-plagioclase and K-feldspar follow a similar trend in the three cores. Quartz and phyllosilicates display a different trend compared to the feldspars, often defining similar tendencies in terms of changes in abundance. Pyrite and goethite are not present in all samples and do not show any particular trend. Same for calcite and dolomite. Gypsum is found in all the samples but has particularly high presence in some samples (SC06, NC04, NC20-23). In terms of quantity, the sediments are dominated by quartz and phyllosilicates. Regarding clays, smectite, mica, kaolinite, chlorite and vermiculite are present in variable proportions (Figure 33). While mica, kaolinite and chlorite change their abundance in concert, smectite and vermiculite make up the balance. The latter two, however, change their abundance at the cost of each other (Figure 33).

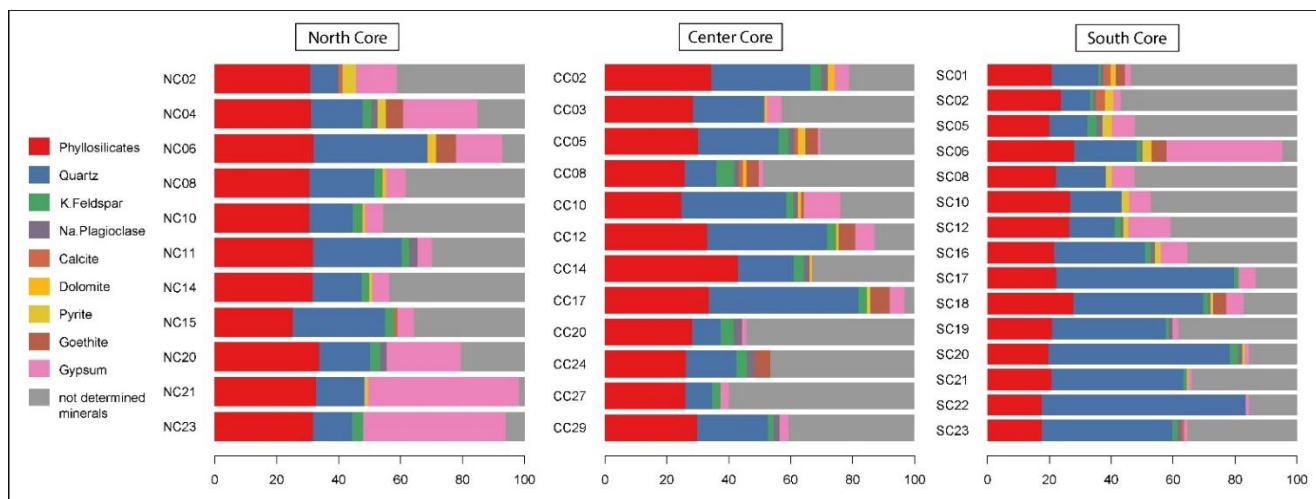


Figure 32 X-Ray diffraction (XRD) analyses of the whole rock for the three cores.

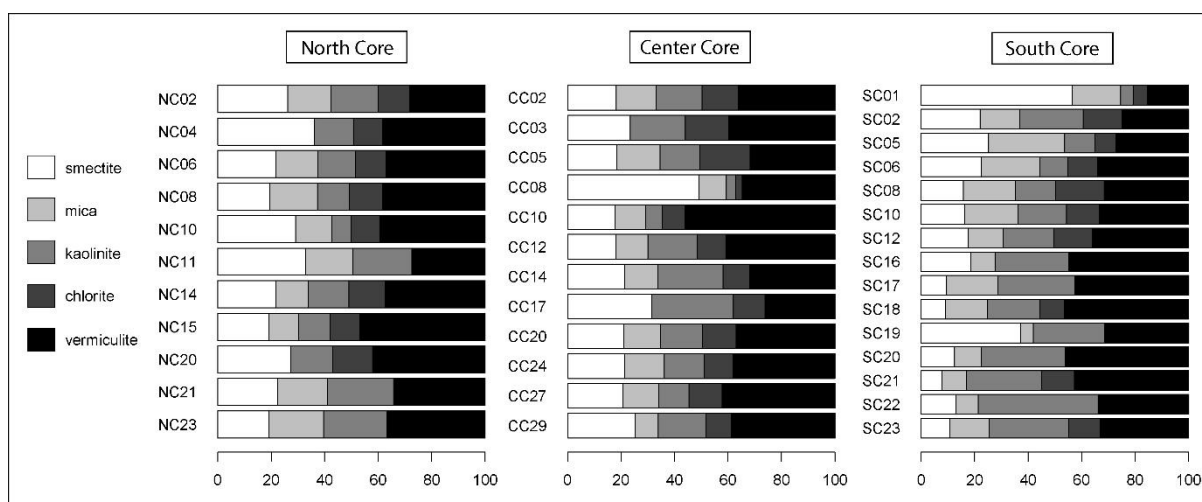


Figure 33 X-Ray diffraction (XRD) analyses of the clays for the three cores.

For the North as well as the South Core, the various major elements decrease towards the top of the profile, with the exception of CaO, which remains low throughout the profile, and Al₂O₃, which remains relatively constant. The trace elements show a similar trend in broad outline (Figure 27). For the Center Core, only the SiO₂ decreases in concentration, while all of the other major elements generally decrease, including the Al₂O₃. For the trace elements, the trends are similar compared to the major elements, with Zr following the decrease in SiO₂, but many metals, notably the heavy metals not changing their concentrations markedly. Ba is an exception notably in the Center Core, as it actually increases towards the top (Figure 29).

3.5. Discussion

3.5.1. Origin of the organic matter

The amount of TOC in the sediments provides useful information about the prevailing environmental conditions during deposition. High TOC values might indicate both a weak oxygenation of the sediments and/or high sedimentation rates leading to preservation of the organic fraction (e.g., Ariztegui et al., 2001 and references herein). TOC fraction coupled with carbon isotope composition of the organic matter (expressed in $\delta^{13}\text{C}_{\text{TOC}}$) is one of the most valuable techniques and direct tracers for the global cycling of carbon between the geological, terrestrial, marine and atmospheric reservoirs, and the many smaller reservoirs of carbon within each of these four broad subdivisions (e.g., Bird et al., 2004). It provides a useful tool to measure and trace the environmental conditions prevailing during

the deposit. It allows in addition to estimate the C_3 – and C_4 – type vegetation contribution to the sediment (e.g., Bird et al., 2004). Figure 34 proposes to characterize the origin of the organic matter according to the isotopic composition of the organic carbon and the C/N ratio of the organic matter. The figure presents also a comparison of the lake sediment with the river sediments of the lake's tributaries. This representation makes it possible to estimate the type of plant of the watershed and of the lake itself. Figure 35 compares the isotopic composition of the organic matter with the quantity of organic carbon contained in the sediment (TOC). This representation makes it possible to complete and refine the characterization of organic matter as well as to better trace its origin. It builds groups of samples that demonstrate a specific environmental history for each of the groups.

The present-day vegetation and soil organic matter geochemistry of the Lake Liambezi region has been summarized in Chapter 2. It showed a mixed C_3 - C_4 type vegetation in relation to the access to surface and/or groundwater. The geochemistry of the organic matter contained in the sediments of Lake Liambezi makes it possible to demonstrate a dominantly autochthonous production dominated by aquatic plants and algae with a lesser contribution of terrestrial detritus washed into the lake (Figure 30, Figure 34 and Figure 35). For the terrestrial plant contribution, both the C_3 – and C_4 – type of vegetation are contributing, but with a clear dominance of the C_3 vegetation. This is compatible with the observation reported in Chapter 2 with the presence of *Phragmites australis* along the shores of Lake Liambezi. *Phragmites australis* is a C_3 plant with a C-isotopic composition of -25.0 ‰ that occupies the buffer zone between flooded and exposed areas around Lake Liambezi (Chapter 2). Hence, a dominantly autochthonous origin of organic matter can be proposed. Furthermore, the Center Core appears to have a larger proportion of terrestrial vegetation compared to the two other cores, which may be related to a distinct evolution of the three different basins sampled by the cores. The Center Core is likely to be less commonly flooded compared to the northern and southern sub-basins.

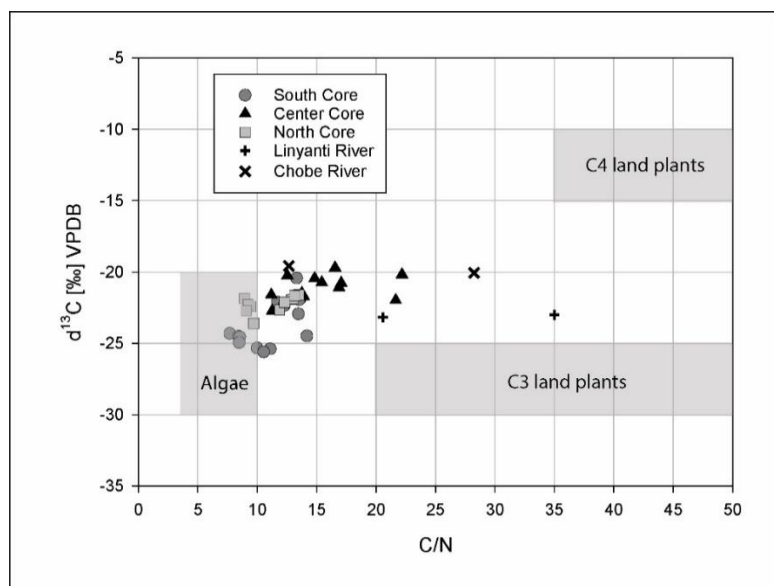


Figure 34 Characterization of the origin of the organic matter according to the isotopic data of carbon and the C/N ratio of the organic matter for the samples of the three cores. Data of rivers Linyanti and Chobe taken from Chapter 2 have been added as comparison. The lake sediments show a more lacustrine organic matter composition compared to river sediments. A difference between the three cores is also marked.

Figure 35 shows a distribution of samples by distinct group. The groups constructed reflect a separation similar to the separation made according to visual criteria when opening the cores. This visual and geochemical difference demonstrates different environmental conditions during deposition for these different groups of samples. This reflects environmental conditions that change overall in a clear manner between the different groups of samples of South and North Cores. For the Center Core, these changes seem to be more gradual.

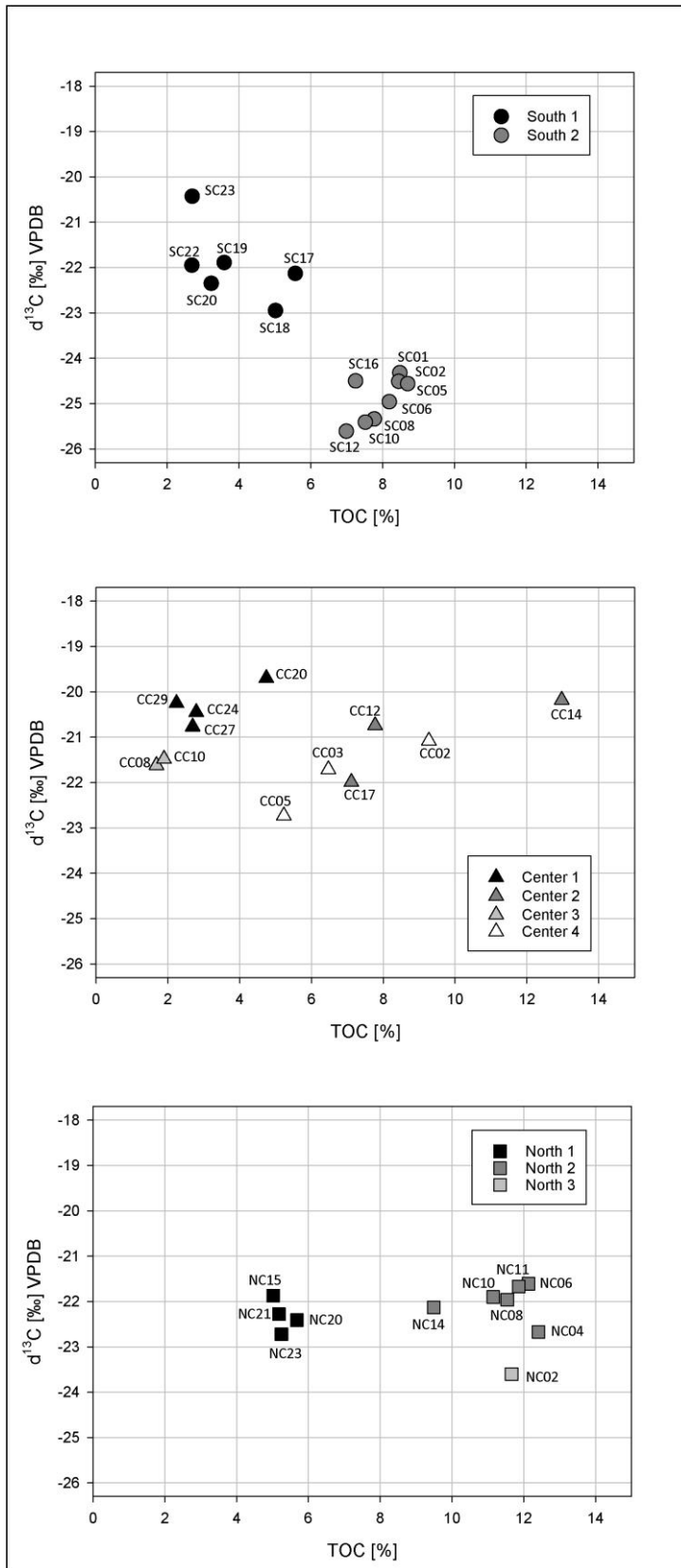


Figure 35 Diagram relating the $\delta^{13}\text{C}$ of the organic matter as well as the quantity of organic matter (TOC) contained in the sediments. The three cores are shown with the South Core at the top, the Center Core in the middle and the North Core at the bottom. The samples are grouped according to the visual criteria described in a chapter above. The dark colour represents the deepest samples (bottom of the cores).

The isotopic analyses linked to the C/N ratio demonstrate a composition of the organic matter coming from a mixture between an algal production and a terrestrial production represented by a mixture of the C₃-C₄ types (Figure 34). For South and North Cores, algal production is dominant. For the Center Core, the mixture is more marked towards the terrestrial. The pseudo van Krevelen diagram also reveals this mixed organic matter source between a terrestrial and algal origin (Figure 36). Center Core also demonstrates a more terrestrial signature in its composition compared to South and North Cores. However, the quality of the organic matter turns out to be immature and rich in oxygen, which brings it closer to peat rather than to lacustrine sediments. This mixed source of organic matter demonstrates the seasonal cycle of the lake but also cycles of wetter or drier periods with variations in the water level which can go from lake environment to totally dry, passing through all the intermediate stages (palustrine, marsh, fens). The environment must however remain sufficiently humid or flooded to show a rate of preservation of organic matter which allows quantities ranging between 1.7 to 13%. Depending on the flooding conditions, the biological activity developing in the direct surroundings of the sampled sites will favor algal or terrestrial activity. The cycle of the seasons allows the development of both types of organisms and results in the recording of a mixture. The variations in the quality of the organic matter on a core make it possible to determine the environmental evolution that the lake has experienced. A detailed description of these changes will be made in Chapter 4.

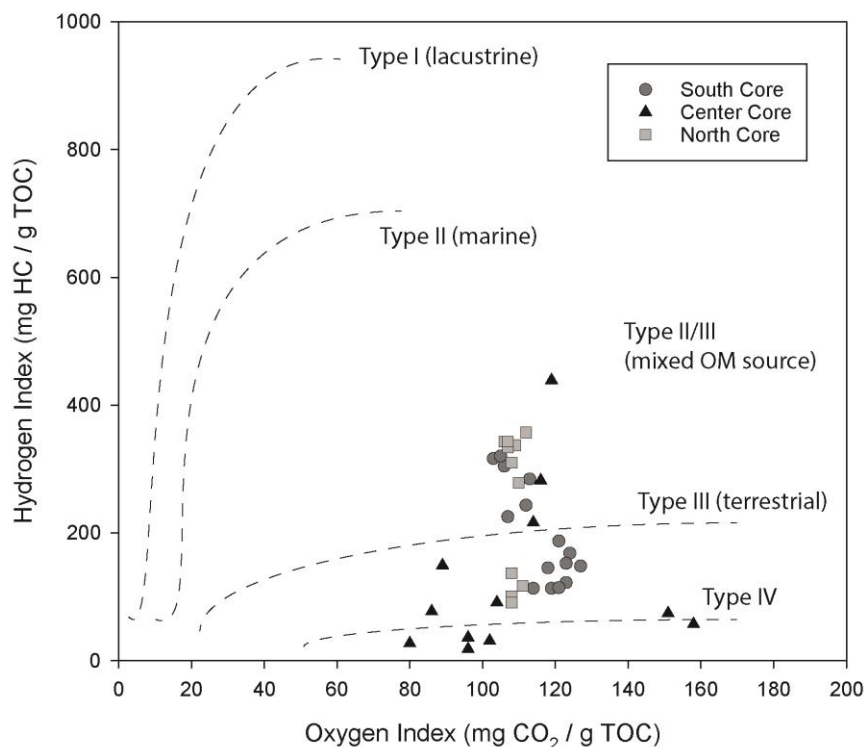


Figure 36 Pseudo van Krevelen diagram of the lake sediments. Quality and origin of the organic matter is estimated after the Hydrogen Index (HI) and the Oxygen Index (OI) made with the Rock Eval analysis.

If the data is taken in order of depth, the geochemical composition of the organic matter of the sediments of the lake presented with Figure 34, Figure 35 and Figure 36 makes it possible to compare and highlight a production of organic matter which changes over time in its quantity and quality, and therefore its origin. These differences are related to environmental conditions that change over time and will be detailed in Chapter 4.

3.5.2. Grain-size: End-member analysis

Grain-size measurements have been processed in order to achieve an End-Member Mixing Analysis (EMMA). 45 samples out of 47 were processed. The data from both CC08 and CC10 samples were of too poor quality to be used for this analysis. The type of material of these samples is probably the cause. Five end-members could be constructed from these 45 samples and are shown in Figure 37. They represent more than 95% of the variance of the data. Each end-member reflects ideal stocks of a specific sedimentary regime, composed itself of a specific sediment composition. Each end-member shows a succession of platykurtic, mesokurtic or leptokurtic curves. Each of these peaks represents a sedimentary stock of a precise composition. The following assertion must be verified with SEM in order to validate them. However, considering the other analyses carried out, as well as the SEM images obtained for several samples, these suggestions are considered accurate and will be used for the rest of the work. The leptokurtic curves found in EM 1, 2 and 5 at a size of about 100-110 μm are probably composed of well-sorted sand grains from the neighbouring Kalahari Desert. The leptokurtic curve of EM 4 at about 120-130 μm probably represents coarser grains of the same desert sand. The difference in size between these two sediment stocks probably lies in the type of transport experienced by the sand grains. The grains of EM 4, being coarser probably demonstrate a fluvial transport versus an aeolian transport for the Kalahari grains found in EM 1, 2 and 5. However, the grains present in the study samples probably experienced fluvial transport for their vast majority. If the leptokurtic curves of EM 1, 2 and 5 seem to demonstrate aeolian sorting for sand grains of this size, these grains of aeolian origin were probably reworked by a fluvial action. What stands out above all between these four end-members is therefore a different energy in transport. EM4 seems to demonstrate the greatest transport energy with coarser grains. EM1 demonstrates a perfectly leptokurtic curve with a greater volume compared to EM2 and 5. The same curve for EM2 is slightly less leptokurtic and of lower volume. EM5 further reduces these two parameters compared to EM1 and 2. This tendency tends to demonstrate a decrease in energy between these three end-members. If the assertion that a majority of these grains has experienced a fluvial reworking (despite their aeolian origin), it is possible to deduce that the end-members EM 1, 2, 4 and 5 demonstrate a decrease in the energy of fluvial transport that goes from EM4 > EM1 > EM2 > EM5.

The little mesokurtic curve for EM 4 and 5 at the size of 30-50 μm is probably composed of desert loess. The platykurtic to mesokurtic curves found in all five EM at the size of about 10-20 μm represents probably a sludge composed of crushed diatoms. The different stocks of EM 1, 2, 4 and 5 mainly represent sedimentary stocks with a fluvial or aeolian transport signature. The end-member 3 (EM3) is composed of a mesokurtic curve that demonstrate poorly sorted material. It does not show a well-defined stock but rather a composition of multiple stocks that are composed of various authigenic lacustrine production. According to the SEM images, this authigenic material is composed of a mixture of diatoms, phytoliths, sponge spicules and other lacustrine biological production. The bumps present beyond 50 μm seem to demonstrate the presence of runoff. The presence of the bumps at different sizes shows a material of varying size and therefore a transport energy of varying strength.

Thanks to the different sedimentary stocks highlighted by the five end-members, each end-member thus allows to categorize a type of environment specific to each. EM4 represents a fluvial sedimentation. EM1, then, reflects also a fluvial sedimentation, of however less energy and with aeolian influence, as suggested by the size of the two different stocks of desert sand grains. EM2 demonstrates a very similar tendency than EM1 with however a different volume of stocks. The curve of sands is less leptokurtic and of lower volume. Contrariwise, the mesokurtic curves of both crushed diatoms (10-20 μm) and desert loess (30-40 μm) is increasing in volume compared to EM1. A similar trend is demonstrated with EM5. It is then considered to observe a decreasing fluvial energy from EM1 to EM5 (EM1 > EM2 > EM5). EM4 might represent a river environment. EM1 also, with however less energy. Similar statement for EM2 and then EM5. This decrease in energy probably results in an

increase in the water level and the change from a river environment to a lake environment from EM4 to EM5. EM5 probably represents a lake environment with a weak current and therefore a contribution of fluvial and aeolian sediments.

The presence of water in the landscape of northern Botswana is mainly through runoff (see Dyer, 2017), which always induces a flow. This process is well reflected in the end-members described above. However, the presence of water can occur by percolation and thus form marsh areas with many ponds with no current. A marsh-type aquatic life develops there. This type of environment is reflected with the EM3. The shape of the grain-size curve in fact demonstrates the presence of a current of low intensity and variable in power as well as an authigenic biological production. EM3 therefore translates a lacustro-palustrine environment of low water level far from runoff areas.

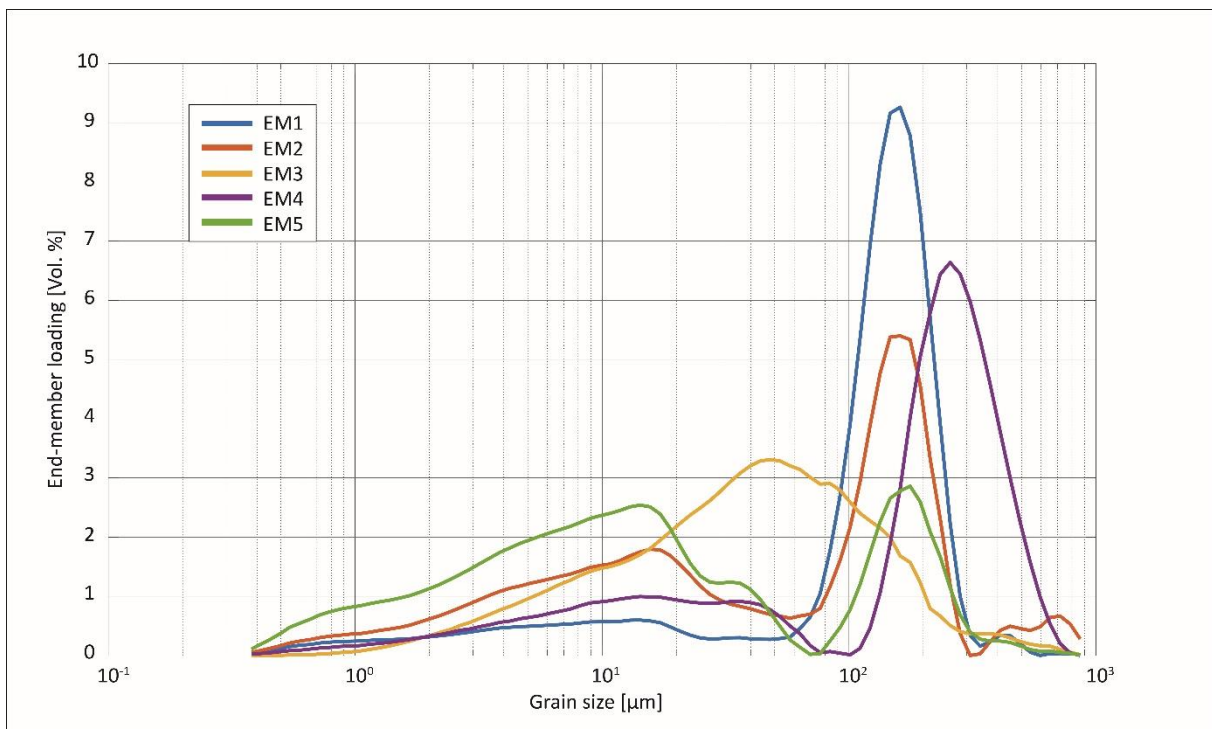


Figure 37 End-member mixing analysis of 45 samples of river or lake sediments coming from rivers Okavango, Linyanti and Chobe, and Lake Liambezi. Each end-member represents a specific sedimentary process with ideal stocks of sediments. EM1, 2, 4 and 5 reflect mainly of river and aeolian sediments. EM3 refers mostly of authigenic lacustrine production.

The five end-members, which define the grain-size assemblage of the 45 samples are presented in Figure 37. Figure 38 shows the composition of each sample according to its proportion of each end-member. This results in a well-defined categorization of the samples. The proportions in different end-members make it possible to better understand what each sample is composed of (in terms of material source and process) and thus, to deduce a geomorphological situation or/and a geomorphological evolution of the site. The tributaries are well demarcated from the sediment of Lake Liambezi. Indeed, in general, they consist of more proportions of EM4 and EM1, which reflect a typical grain-size of rivers with a current that allows the transport of coarser material. Conversely, the sediments of Lake Liambezi are mainly composed of EM3 and EM5. EM3 represents a pond and EM5 represents a low-energy water surface (a lake) with sometimes a low-energy fluvial or aeolian sediment contribution. EM5 therefore has a higher water level than EM3 as well as a connection to tributaries.

The grain-size turns out to be a good mirror of the geomorphology of the different sites. Dominated by end-members EM1 and EM4, the grain-size distributions of BO01 to BO05 reflect a river environment. Samples BO01 to BO04 are all four situated along branches of the Okavango River. These four sites demonstrated an active river during both dry and wet seasons (August 2016 and March

2017). Sample BO08 has been sampled along the Chobe River at Kavimba. The Chobe River also demonstrates an active river at that site. The Linyanti River shows a more complex flow. Sometimes water is transferred by flow and sometimes by percolation. The result is a complex interweaving of ponds, oxbow lakes and branches of rivers with current. The two samples taken from this river reflect this complex construction. Sample BO05 shows a river environment similar to the river samples of the Okavango and Chobe Rivers with EM1 and EM4. Sample BO06 shows a mix between EM1 and EM3. This site shows a pond environment with sometimes its connection to a river current and thus, the fluvial sediment input typical of a river environment. BO07 was taken along the Chobe at a site called Chobe Seariver. This site represents a vast floodplain linked to the floods of the Chobe River. The layout of the site makes it look more like a lake than a river. When the Chobe floods arrive, the site transforms into a vast body of water, transforming the site from a vast grassy plain to a lake (see Ballif, 2018). This type of environment is found in the end-members that make up its grain-size signature. The composition of its end-members is similar to those of samples taken from Lake Liambezi (BO09, NS, CC and SC). The mixture between EM3 and EM5 reflects a lake-like production. Sample BO09 was taken from the shores of Lake Liambezi. It therefore also reflects a similar composition in end-members as the Chobe Seariver site or the three sites NS, CC and SC.

The end-member analysis for the North Core shows three different phases that reflect the separation of groups of samples presented later in Chapter 4.4 but already present in Figure 27 and Figure 40. A first phase combines samples NC23 to NC15 (with the exception of NC20 that does not show EM2). The samples of this first phase are composed of EM2, 3, 4, and 5. This mixture suggests an environment which varies throughout the year with more or less flooded phases probably linked to the seasonal system of rains and floods. The site must represent mainly a fluvial environment with calmer periods, which see the formation of a shallow lake. The fluvial regime demonstrated by this first phase of the North Core, however, shows a different end-member composition from the samples of BO rivers (BO01-BO05 and BO08). The site therefore has different fluvial dynamics. It may be related to the presence of the Bukalo Channel in its direct environment. It is therefore conceivable that the current which is perceived thanks to the EM2 and EM4 reflects the floods of the Zambezi through that channel. The site then shows progressive flooding with the following phase that groups the samples NC14 to NC06. Both EM2 and EM4 have disappeared and only EM3 and EM5 remain. This suggests a decrease in the current present on the site. It is perhaps a question of a higher water level, a more stable geomorphological situation and the remoteness of the Bukalo Channel. The final phase is composed of the two samples NC04 and NC02 where only EM5 remains. This composition offers a calm lake environment and a water level higher than the two previous phases.

The Center Core only demonstrates the presence of EM3 and EM5. The evolution in the proportion of each end-member seems cyclical with periods richer in one or the other. The absence of end-members linked to a more pronounced water current probably indicates the position of the site, which is far from the main tributaries (Linyanti River, Chobe River and Bukalo Channel). This composition of end-members seems to demonstrate an unstable lacustro-palustrine environment, the water level of which varies and shows periods of flooding and emersion.

South Core also demonstrates a composition made only of EM3 and EM5, which testifies of a lacustro-palustrine environment. However, the distribution of the two end-members shows a gradual transition from the dominance of EM3 over EM5 to the reverse situation. This demonstrates the gradual transition from a shallower to deeper lacustro-palustrine environment, so, from a pond environment to a lake environment.

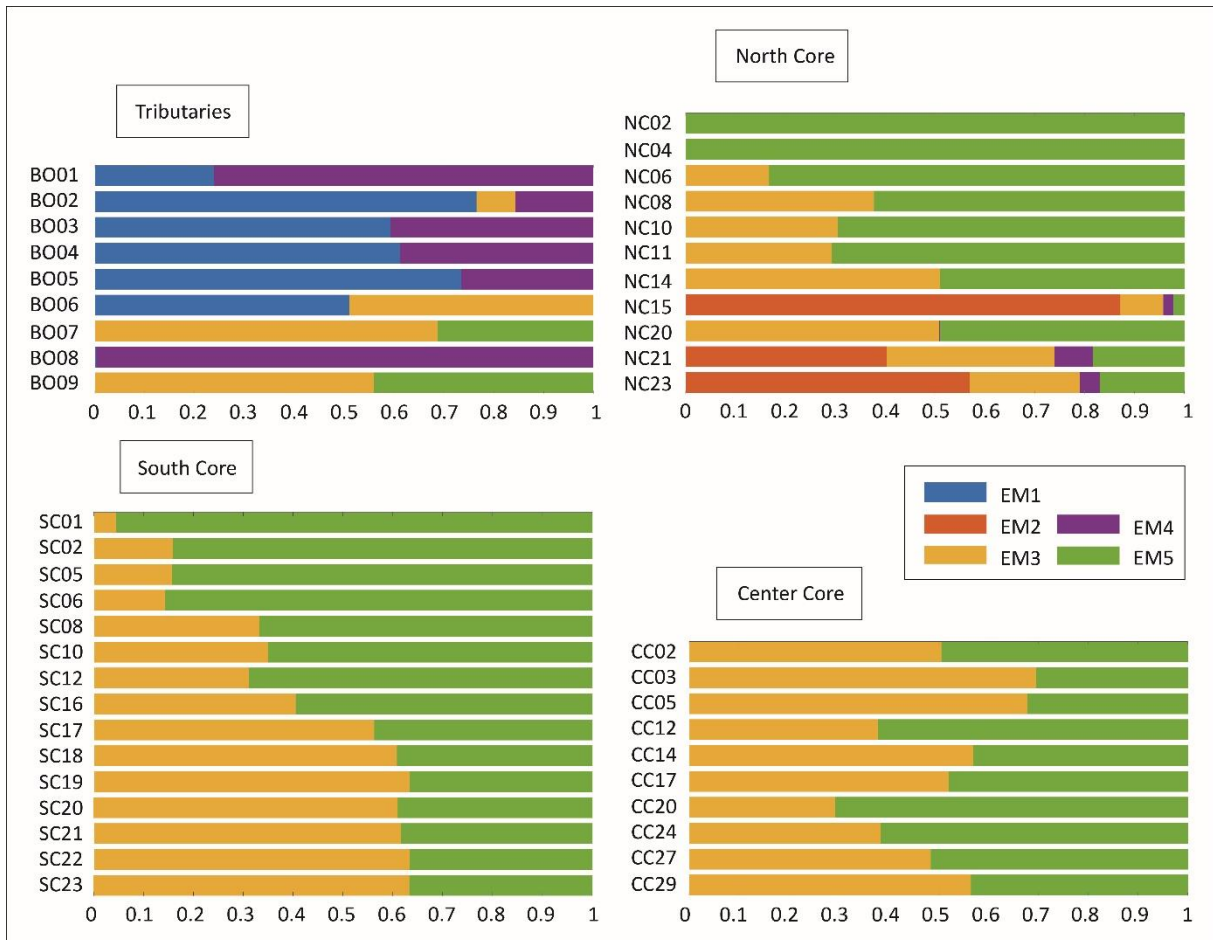


Figure 38 End-member composition (in proportion) for river and lake sediments from rivers Okavango, Linyanti and Chobe and for Lake Liambezi. BO samples come from rivers. Precise location of BO samples can be found on the map in Chapter 2 (Figure 15). BO01 and BO02 come from location called Thamalakane; BO03 comes from Kudumane; BO04 comes from Mababe. All four samples come from the Okavango watershed. BO05 and BO06 come from the Linyanti River at the Linyanti Campsite location. BO07 is the Chobe Seariver site and BO08 the Kavimba site, both are located along the Chobe River. BO09 is located at the southern shore of Lake Liambezi. Other samples respect the denomination followed in this chapter (NC, SC and CC). BO samples demonstrate the predominant sediment regime at the site itself. These sites being for the most part a river, the sediment regime which appears, thanks to the end-member analysis, to be a fluvial regime. The differences observed between the sites lie in the characteristics specific to each site. Lakes samples (NC, SC and CC) demonstrate the evolution of sediment regimes within the three sediment cores. These regimes oscillate between more or less flooded sites.

3.5.3. Silica – abundance and origin

Dyer (2017) reports a saturation index for calcite based on surface water analyses from several tributaries of Lake Liambezi as well as the lake itself. In addition, Lake Liambezi shows alkaline conditions for wet and dry seasons (Dyer, 2017). However, no biogenic neither lithogenic calcite nor aragonite was noted with the SEM. In contrast, SEM studies do indicate a major presence of different genera of biogenic SiO₂, occasionally with dissolution-reprecipitation features, resulting in different forms of silica (Table 2 to Table 9). The remobilization of the silica also taking place in an alkaline environment, the saturation of the environment with silica is such that this precipitation is dominant and therefore not favourable to the precipitation of carbonates. The sporadic and rare presence of calcite detected by the XRD measurements probably corresponds to coarser-grained calcite of detrital origin from the catchment area. Dolomite observed in the same samples as calcite in XRD analyses would also support a detrital origin (e.g. Haddon and McCarthy, 2005; Setti et al., 2014).

The Kalahari Desert southwest of the lake as well as the larger riverine catchments that are composed of crystalline rocks would support that at least some of the silica is of detrital origin (Haddon and McCarthy, 2005; Gärtner et al., 2014; De Carvalho and al., 2000; De Waele et al., 2008). Not

surprisingly quartz grains make up between 10 to 65 % of the sediment, depending on the specific horizons (average of about 26 %). Quartz grains may show Fe-coating, surface features that support either a fluvial or aeolian transport, and also occur in various sizes. Dissolution features are also often to be noted (Table 9a-c). Hence silica was available to the aqueous solutions and hence was readily redistributed, also in biogenic form. The sediments are made up of 47 to -80 wt% of SiO₂ in the different samples with an average of 62 wt%. The siliceous organisms that precipitate silica in its amorphous form (SiO₂ n.H₂O) include several different diatom species, sponge spicules, silicified vegetal cells (phytoliths) and silicified Cyanobacteria colonies (*Gloeocapsa*, Chroococcales). As illustrated in Table 9c the biogenic silica, in this case the diatoms, also often show dissolution features. The abundance of all these different forms of biogenic, amorphous silica is finally also compatible with the high loss of ignition (LOI) from the XRF measurements. Indeed, amorphous silica is composed of about 15 to 30 % of its weight in adsorbed and crystal-bound water in its structure. This water is lost and measured during the ignition at 1050°C in the samples preparation.

3.5.4. Origin of the sediment components and importance of clays

The weathering of primary minerals such as feldspar, plagioclase and micas is climatically-controlled and can result in the formation of clay minerals. The intensity and distribution of rain are the main controlling parameters of weathering. Large amounts of rainfall fosters kaolinite formation. In contrast, seasonal and more sparse precipitation followed by intense evaporation periods favours the formation of smectite (Meunier, 2003). Following the transformation stages, phyllosilicates are often formed in early stages of alteration whereas smectite appears in most weathered stages (Banfield & Eggleton, 1990; Meunier, 2003). Meunier (2003) compiled different studies showing the transformation of micas into smectite through an organic and inorganic acid solution. Observation of the parental minerals (feldspar, plagioclase and micas) as well as newly formed clays (phyllosilicate, kaolinite and smectite) allows climatic trends and the climatic evolution of the studied site (Meunier, 2003).

As indicated by Setti et al. (2014), clays are a major and very effective tool in determining current or past climates. Mineral associations may vary significantly along any one river, depending on the characteristics of the watershed (bedrock, sediment sources and climate). Clay minerals transported by rivers directly reflect the composition of soils in the drainage basin as well as the climatic conditions of formation. It is therefore interesting to first characterize the watersheds of the Kwando River and the Zambezi. Haddon and McCarthy (2005) and Setti et al. (2014) describe a Kwando watershed consisting of the Kalahari units. This implies a composition rich in quartz with additional K-feldspar up to 11 % and a low abundance or absence of plagioclase and calcite. According to Setti et al. (2014) calcite is considered to be detrital, from continental (pedogenic) carbonates found locally in the Kalahari catchment. The sediments have variable phyllosilicate content, up to 30 %. Clay minerals are dominated by smectite (> 40 %), 10-40 % of mica and kaolinite; chlorite is absent (c.f. Setti et al., 2014). Gärtner et al. (2013) and Setti et al. (2014) describe the watershed of the Zambezi to also be made up of the Kalahari units, but also including Karoo basalts and other igneous mafic and Karoo-aged sedimentary units. This brings a composition for the transported sediments dominated by detrital quartz and feldspars (63-85 %), as well as the phyllosilicates (up to 40 %). Calcite is found in small amounts only (<5 %). Concerning clays, smectite is dominant and kaolinite content varies from 4 % to 36 %, while chlorite is minor or absent (c.f. Setti et al., 2014). In tropical areas, where precipitation alternates with dry periods, the intensity of weathering favors illite-smectite as dominant clay minerals, following a sequence of illite-smectite-kaolinite with increasing intensity of weathering (Moore, 1989; Setti et al., 2014). Hence an abundance of kaolinite indicates high rainfall and a warm climate, abundant smectite will indicate a moderate weathering process. The results of this study are taken to confirm the work of Setti.

Trends in different minerals proportions reveal a correlation between mica, chlorite and kaolinite with other minerals such as k-feldspar and quartz. Following literature, these minerals are considered of detrital origin (e.g. Haddon and McCarthy, 2005; Setti et al., 2014; Gärtner et al., 2013). Mica and chlorite probably come from the parent material of the watershed. Kaolinite is probably climatically formed in the watersheds of both Kwando and Zambezi Rivers under warmer and more humid conditions. Therefore, it is found from detrital origin in Lake Liambezi, transported from both watersheds. Smectite presents a specific trend in its proportion (Figure 27-29). In regard to the local dryer and less hot climate and to the specific trends of its amount, smectite is therefore believed to be neo-formed in Lake Liambezi region. Thus, smectite is considered to be of major importance as climate tracer for the climate evolution of the region, and more specifically for Lake Liambezi. Kaolinite shows also specific trends. However, it seems more complicated to use it as a climate tracer as it seems to follow sedimentary pulses and not climatic evolution.

Smectite show variations in relative quantity between 8-56% which are interpreted as changing drier and wetter periods. The wetter periods allow a more efficient weathering process not only in the transformation of minerals (and therefore precipitation of smectite) but also for their transport and further deposition. Therefore, horizons containing higher amounts of smectite are interpreted as formed during wetter periods whereas those containing lower amounts are considered as indicative of drier periods. The origin of vermiculite is more difficult to explain due to its variable characteristics (e.g., Moore and Reynolds, 1989). Vermiculite might be an intermediate clay between the parent minerals and the smectite. This would mean that during drier periods, with therefore fewer physical and chemical weathering, the stage of transformation of certain minerals into smectite does not take place fully remaining at the vermiculite stage. This would result in a higher rate of vermiculite formation in dry periods, lower in wet periods. The analyses of samples from Lake Liambezi indeed show an anticorrelation between smectite and vermiculite contents throughout depth for the three cores (Figure 27-29). The relative amounts of gypsum, another indicator of prevalent dry conditions, correlate well with those of vermiculite (Figure 27-29).

3.5.5. Discussion of the sulphur content and the pyrite occurrence and their implication to the redox conditions: a complementary presence

Sulphur might be found under different forms: sulphate, sulphide, organic sulphur and element sulphur. Sulphate might be present with gypsum (CaSO_4), an evaporitic mineral and barite (BaSO_4), an often hydrothermal mineral. Sulphide might be found as sphalerite (ZnS), pyrite (FeS_2) and (HS^-) (where (HS^-) represents actually (H_2S) and is therefore not visible). The organic form is found as DMS (Dimethyl sulphide): ($(\text{CH}_3)_2\text{S}$). The sum of total sulphur found in the samples is then:

$$\sum[\text{S}] = ([\text{BaSO}_4], [\text{CaSO}_4]) + ([\text{ZnS}], [\text{FeS}_2], [\text{HS}^-]) + ([(\text{CH}_3)_2\text{S}])$$

In Lake Liambezi, sulphur is widely describe in both gypsum and pyrite form. Pyrite appears only sporadically (except for South Core) and gypsum is in greater quantity (average values at 9.5 wt%) (Figure 27-29 and Figure 32). Both minerals can be interpreted in terms of climatic conditions. These two minerals are complementary since gypsum is the oxidized counterpart of pyrite. The sulphide form, framboidal pyrite observed in Lake Liambezi sediments (Table 9d **Erreur ! Source du renvoi introuvable.**), requires reducing and anoxic conditions to precipitate. Condition of formation are believed to be richer in water or humid conditions. The sulphate form, gypsum, might testifies of oxidizing and dry conditions. This complementary conditions of presence for each form containing sulphur might give information about humid or dry periods. However, both pyrite and gypsum are found in the same samples, meaning in the same periods, which is *a priori* contradictory. The high seasonality of the region, showing a humid period rich in precipitation and floods may be humid

enough to create anoxic conditions into the sediment and precipitate framboidal pyrite. Contrariwise, the dry season might be dry enough to dry part of the lake, favours well ventilated soils and oxidizing conditions and precipitate gypsum. This cycle might also not occur in the same year, but in a multi-year cycle. The presence of both oxidizing and reducing forms in same samples is therefore plausible.

Gypsum is a secondary mineral formed in dry environments (like the Makgadikgadi Salt Pan, which is located less than 300 kilometers from the lake) and does not exclude an aeolian transport into Lake Liambezi though. Gypsum minerals have also been described in the study of thin sections from samples taken from termite mounds about fifteen kilometers south of Lake Liambezi (Darini, 2019). The origin of the gypsum minerals present in the sediments of Lake Liambezi has not been further investigated. However, whether the gypsum crystals are neo-formed *in-situ* or carried by the wind, the origin of the sulphur composing them may be multiple and remains unclear.

Other minerals containing sulphur are not describe with the methods used for the present study. However, elements composing the different minerals are measured with the XRF method. It means they might appear in little quantity and not be measured in their mineral form. A detail discussion about them is therefore difficult to build.

3.5.6. Barium origin

The presence of low temperature hydrothermal vents (up to 50°C) is described at less than 100 kilometres away from Lake Liambezi (Mukwati et al., 2018). The tectonic activity linked to the Okavango Graben (e.g. Kinabo et al., 2007) makes sense to a hydrothermal activity in the vicinity of the faults. As often related to hydrothermalism, the presence of barium in the sediments raised the question of its origin. For North and South Cores, barium follows a similar trend to strontium, calcium or lead (Figure 27 and Figure 29). Its trend is also related to other elements considered of detrital origin. It might therefore be considered as detrital too. Deepest portion of Center Core shows similar trends (Figure 28). However, upper part of Center Core (since CC10) shows changes from about 400 ppm to 700 ppm that are not seen in other elements. This different trend compared to other profile and compared to the other elements raised the question of a detrital origin too.

Barium of detrital origin might be in the carbonate form $BaCO_3$ coming from the whiterite which is a detrital mineral derived from feldspar (Na-plagioclase series). Barium of hydrothermal origin is in the form of barite ($BaSO_4$) and is part of the barite group. Barite group is composed of barite and three accompanying minerals: celestine ($SrSO_4$), anglesite ($PbSO_4$) and hashemite ($(Ba,Cr)SO_4$) with possible trace element Ca. These minerals are usually typical of low temperature hydrothermalism. Strontianite ($SrCO_3$) and dolomite ($CaMg(CO_3)_2$) are two carbonates often related with the barite group. Strontianite shows trace of Ca, and might be associated with calcite, harmotome ($(Ba_{0.5},Ca_{0.5},Na,K)_5Al_5Si_{11}O_{32}\cdot 12(H_2O)$) and sulphur. Dolomite shows trace elements of Fe, Mn, Co, Pb and Zn and might be associated with calcite and sulphite. Most of the different elements found in the accompanying minerals are found in the Lake Liambezi's sediments and are described in the XRF analysis. However, the chosen methods did not allow the observation and description of these spoken minerals. Their hypothetical presence can therefore only be a supposition. If the element barium may have a detrital origin and be brought by the two rivers Kwando and Zambezi, the mineral barite can only have a hydrothermal origin. However, this mineral has not been described in the lake's samples. This supposition is therefore to be taken as a guess and ask further investigation. Indeed, these questions could be the subject of future studies as well as questions for future work aimed at a better understanding of the activity of the fault system linked to the Okavango Graben.

Analyses of the composition of surface water versus groundwater after Dyer (2017) reveal an electrical conductivity varying from a factor of two to a factor of five, underground water being two to five times richer in elements. Electrical conductivity for surface water for both humid and dry season are as follows: Linyanti 281-294 $\mu S\ cm^{-1}$, Chobe 128-831 $\mu S\ cm^{-1}$ and Zambezi 69-390 $\mu S\ cm^{-1}$.

Groundwater of two different boreholes in the direct region surrounding the lake shows an electrical conductivity of 1367-1672 $\mu\text{S cm}^{-1}$. Water analysis made after Mukwati et al. (2018) show an electrical conductivity up until 22320 $\mu\text{S cm}^{-1}$ with a mean value of 5173 $\mu\text{S cm}^{-1}$, analysis made close to the hydrothermal spring having higher electrical conductivity values. The waters analysed are enriched in elements, including barium. Regarding these two works, the mineral enrichment of water seems to be done more by underground action than by sediment transport from the watershed. This raises the question of the origin of the minerals transported by water. Are these minerals and elements originating from the watershed, or from the subsoil, including potential hydrothermal activity? The work of Mukwati et al. (2018) demonstrate that an enrichment in elements and minerals linked to hydrothermal activity exists for this region (through hydrothermal vents). A more in-depth study for the Lake Liambezi region therefore seems full of meaning and would undoubtedly provide answers as to the mechanisms linked to the evolution of the landscape in this region.

3.5.7. Characterization of type of deposit

Given that the sediments contain > 2 wt% of organic matter and have a fine-grained nature that may exclude effective oxygenation, these sediments can be characterized as sapropel. They are also very siliceous with a majority of biogenic silica and lesser amounts of detrital quartz grains. The mineralogical analyses summarized above also includes a large fraction of undetermined inorganic material that is often represented by biogenic, amorphous silica but also by a poorly crystallized, fine-grained clay mineral fraction.

3.6. Conclusion

Limnology and fish population have been described for Lake Liambezi (e.g. Seaman et al., 1978; Peel et al., 2015). However, its sedimentology has never been investigated. A first characterization of it and a first understanding in the origin of the sediments components has been made with the present study. Lake Liambezi represents wetlands in an arid climate with a specialized flora and fauna. Due to the very poor landscape of the region, its ecosystem is particularly fragile and sensitive to any climatic or environmental change. In regard to these specific environmental conditions, the choice has been made to manage a multidisciplinary study. Using methods coming from various fields does permit to effectively target the origin of the various components of the sediments and thus target their use for additional studies. The detailed description of the sediments did permit to target four important and useful characteristics of the lake's sediments for further investigations. The organic matter of the sediments is autochthonous and is therefore usable as an inherent characteristic of the sediments. The absence of biogenic or lithogenic calcite nor aragonite does not allow further geochemical investigation that are often classical for lakes environment. On the other side, the climatically linked clay smectite is autochthonous in the region and is therefore usable as a climatic tracer. Finally, some other sediment characteristics such as the grain-size, the detrital mineral content and the presence or absence of pyrite and gypsum seem to be mostly related to the environmental condition of the site itself at a specific time. The propensity of the site to be inundated or dried due to its situation and/or its connection to the rivers, lake's basin or marshes seem to define those parameters. They seem to support more flooding events and seasonality than long-lasting climatic conditions.

The understanding of the characteristics and components of Lake Liambezi sediments allow us to conduct further environmental investigation of the lake with a comprehension of its sedimentology. The mechanisms of sedimentation within Lake Liambezi have been here demonstrated and efficient tools for climatic and environmental comprehension and description have been highlighted.

Acknowledgments

Thank you to Professor Eric Verrecchia for his help regarding the processing of grain-size data, the End-Members Mixing Analysis (EMMA) as well as his help in interpreting these data.

3.7. References

- Adatte, T., Stinnesbeck, W., Keller G. 1996. Lithologic and mineralogic correlations of near K/T boundary clastic sediments in NE Mexico: Implication for origin and nature of deposition. Sp. publications, Soc Geol of America. 307, 211-226.
- Ariztegui, D., Chondrogianni, C., Lami, A., Guilizzoni, P. & Lafargue, E. 2001. Lacustrine organic matter and the Holocene paleoenvironmental record of Lake Albano (central Italy). *Journal of Paleolimnology* 26/3, 283-292.
- Banfield, J.F. & Eggleton, R.A. 1990. Analytical transmission electron microscope studies of plagioclase, muscovite, and K-feldspar weathering. *Clays & Miner.*, 38, 77-89.
- Bird, M.I., Veenendaal, E.M., Lloyd, J.J. 2004. Soil carbon inventories and $\delta^{13}\text{C}$ along a moisture gradient in Botswana. *Global Change Biology* 10, 342-349.
- Burrough, S.L., Thomas, D.S.G., 2008. Late Quaternary lake-level fluctuations in the Mababe Depression: Middle Kalahari palaeolakes and the role of Zambezi inflows. *Quaternary Research* 69, 388-403.
- Cavaillé-Fol, 2020. On a découvert le berceau de l'Humanité. *Science & Vie*, N°1233, juin 2020, 56-71.
- Darini, I. 2019. Micromorphological evolution of termite mound soils in time. Unpubl. Bachelor of Geosciences and Environment, UNIL.
- Darkoh, M.B.K & Mbalwa, J.E., 2014. Okavango Delta – A Kalahari oasis under environmental threats. *Biodiversity & Endangered Species*, 2, 4.
- DeCarvalho, H., Tassinari, C., Alves, P.H. 2000. "Geochronological review of the Precambrian in western Angola: links with Brazil." *Journal of African Earth Sciences*, 31, 383-402.
- DeWaele, B., Johnson, S.P., Pisarevsky, S.A. 2008. "Palaeoproterozoic to Neoproterozoic growth and evolution of the eastern Congo Craton: its role in the Rodinia puzzle." *Precambrian Research*, 160, 127-141.
- Dyer, S. 2017. Water cycle in the Northern Kalahari. Unpubl. Master of Science in Biogeosciences, UNIL.
- Gärtner, A., Linnemann, U., Hofmann, M. 2013. The provenance of northern Kalahari Basin sediments and growth history of the southern Congo Craton reconstructed by U–Pb ages of zircons from recent river sands. *International Journal of Earth Sciences*, 103, 579-595.
- Haddon, I.G., McCarthy, T.S. 2005. The Mesozoic–Cenozoic interior sag basins of Central Africa: The Late-Cretaceous–Cenozoic Kalahari and Okavango basins. *Journal of African Earth Sciences* 43, 316-333.
- Kübler, B, 1987. Cristallinité de l'illite, méthodes normalisées de préparations, méthodes normalisées de mesures. *Cahiers Institut Géologie de Neuchâtel, Suisse, série ADX*.
- McCarthy, T.S., 2013. The Okavango Delta and its place in the geomorphological evolution of southern Africa. *South Africa Journal of Geology*, 116, 1-54.
- McCarthy, J., Gumbricht, T., McCarthy, T.S., 2005. Ecoregion classification in the Okavango Delta, Botswana from multitemporal remote sensing. *International Journal of Remote Sensing*, 26:19, 4339-4357.
- Meunier, A. 2003. *Argiles*. Contemporary Publishing International, GB Science Publisher, Collection Géosciences.
- Milzow, C., Kgotlhang, L., Bauer-Gottwein, P., Meier, P., Kinzelbach, W., 2009. Regional review: the hydrology of the Okavango Delta, Botswana - processes, data and modelling. *Hydrogeology Journal*, 17, 1297-1328.
- Moore, D. and Reynolds, R., 1989. *X-Ray-diffraction and the identification and analysis of clay-minerals*. Oxford University Press, 332 p.
- Mutelo, M.A., Murwira, A. & Kileshye-Onema, J.M., 2013. An understanding of variations in the area extent of Lake Lyambezi: Perspective for water resources management. Unpubl. Master of Science in Integrated Water Resources Management of the University of Zimbabwe.

- Mukwati, B.T., Tafesse, N.T., Bagai, Z.B., Laletsang, k. 2018. Hydrogeochemistry of the Kasane Hot Spring, Botswana. *Universal Journal of Geoscience* 6, 131-146.
- Peel, R.A., Tweddle, D., Simasiku, E.K., Martin, G.D., Lubanda, J., Hay, C.J., Weyl, O.L.F. 2015: Ecology, fish and fishery of Lake Liambezi, a recently refilled floodplain lake in the Zambezi Region, Namibia. *African Journal of Aquatic Science* 40:4, 417-424.
- Potts, P.J., 1986. A handbook of silicate rock analysis.
- Romanens, R, Pellacani, F., Mainga, A., Fynn, R., Vittoz, P., Verrecchia, E.P., 2019. Soil diversity and major soil processes in the Kalahari basin, Botswana. *Geoderma Regional*, 19.
- Seaman, M.T., Scott, W.E., Walmsley, R.D., van der Waal, B.C.W., & Toerien, D.F. 1978: A limnological investigation of Lake Liambezi, Caprivi. *Journal of the Limnological Society of Southern Africa* 4:2, 129-144.
- Sebag, D., Garcin, Y., Adatte, T., Deschamps, P., Ménot, G., Verrecchia, E.P., 2018. Correction for the siderite effect on Rock-Eval parameters: Application to the sediments of Lake Barombi (southwest Cameroon). *Organic Geochemistry* 123, 126-135.
- Sebag, D., Verrecchia, E.P. 1999. Biogeochemical Cycle of Silica in an Apolyhaline Interdunal Holocene Lake (Chad, N'Guigmi Region, Niger). *Naturwissenschaften* 86, 475-478.
- Setti, M., López-Galindo, A., Padoan, M., Garzanti, E. 2014. Clay mineralogy in southern Africa river muds. *Clay Minerals*, 49, 717-733.
- Tweddle, D., Weyl, O.L.F., Hay, C.J., Peel, R.A., Shapumba, N. 2011. Lake Liambezi, Namibia: Fishing community assumes management responsibility. Technical Report no. MFMR/NNF/WWF/Phase II/4.

4. Cross correlation of bacterial communities and geological proxies in paleoecology: a holistic approach for the study of past environmental history

Christophe Paul^{1*}, Anael Lehmann^{2*}, Sevasti Filippidou¹, Mathilda Fatton¹, Thomas Junier³, Daniel Ariztegui⁴, Torsten Vennemann^{2&}, Pilar Junier^{1&}

* These authors contributed equally to this work

¹Laboratory of Microbiology, Institute of Biology, University of Neuchâtel, Neuchâtel, Switzerland.

²Laboratory of Stable Isotope Geochemistry. Institute of Earth Surface Dynamics, University of Lausanne, Lausanne, Switzerland.

³Vital-IT group, Swiss Institute of Bioinformatics, Lausanne, Switzerland.

⁴Laboratory of Limnogeology and Geomicrobiology, Department of Earth Sciences, University of Geneva, Geneva, Switzerland.

[&]Co-Corresponding authors: Pilar Junier. Laboratory of Microbiology. Rue Emile-Argand 11, CH-2000 Neuchatel. Mail: pilar.junier@unine.ch; Phone: +4132718224; Fax: +41327183001. Torsten Vennemann. Laboratory of Stable Isotope Geochemistry. Institute of Earth Surface Dynamics, University of Lausanne, CH-1015 Lausanne. Mail: Torsten.Vennemann@unil.ch; Phone: +41216924464.

4.1. Abstract

To date, no general marker, representative for all bacteria, exists in paleoecology. This is a main gap since bacteria are the most abundant and diverse group of organisms among all domains of life. They colonized all ecosystems, even the most extremes, and are involved in all biochemical cycling of elements. Their community are shaped by the environment, which is shaped by bacterial activity in response. A biological marker targeting bacteria would be undoubtedly of main interest for paleoecological studies. In the past decades, due to advances in the field of metagenomics, the use of DNA have been proposed as a possible bio-indicator. However, DNA and vegetative cells are subjected to degradation, and therefore, their use remains uncertain. Due to their ability to withstand degradation for extended times, spores or other lysis-resistant structures might represent an ideal marker for paleoecology.

The aim of the present work is to evaluate the possible use of bacterial DNA as a marker for paleoecological studies. Both DNA extracted from the total and the lysis-resistant community has been investigated. This project is part of a larger multidisciplinary study, which aims at a better understanding of a unique ecosystem located at the eastern side of the Caprivi Strip, Namibia. The region is a complex network of rivers and waterbodies controlled by tectonic faults. Lake Liambezi, located middle of the Linyanti-Chobe Basin is part of that complex drainage system including the Kwando and Zambezi Rivers in the north of the Kalahari Desert. Except a limnological study and studies about its fish population, it remains poorly studied. The understanding of the environmental history of Lake Liambezi will help to better understand the dynamic of this constantly evolving environment. In addition to the use of bacterial DNA, the present study compiles the geochemical and mineralogical data exposed in a companion paper.

Changes in both the total and the lysis-resistant community reflected changes in the environmental conditions, providing complementarity information. The observed changes correlate with the results obtained in geochemical and mineralogical studies. Precise description of the three sampled sites shows a very characteristic morphological evolution of each site. The northern site shows a sudden deepening from a shallow to a deeper lake environment. The southern site presents a gradual transition from a marsh to lake conditions. The site of the center presents a more complex development. It starts with a marsh environment. There follows a period of progressive drying leading to an emersion of the site. Despite the emersion, the sediments still record an annual flood regime similar to today. The site then registers a gradual re-flooding leading the site to a return of marsh conditions. The alternation between climatic periods (wet and dry periods) is shown in the results. However, the general evolution of the three sites shows more complexity. Morphological evolution of each of the three sites might be correlated to a more global evolution with a potential relation to a regional tectonic activity. The high abundance of sulphur-oxidizing and thermophilic bacteria revealed an active sulphur cycle and likely hydrothermal activity within the lake.

This study applying such a multidisciplinary approach demonstrates the potential of bacterial DNA in paleoecology. It demonstrates the applicability of using bacterial DNA (total and/or lysis-resistant) to identify changes and variability in the environmental conditions. Moreover, it did permit to highlight presence of hydrothermal activity within Lake Liambezi and other processes such as an active Sulphur cycle. Such features were not noticed so clearly with more classical tools. The following stage will be to correlate the three sites together and to give a time scale for the lake history and the inherent environmental changes (or evolution) of each site, but moreover of the lake.

4.2. Introduction

Paleoecological studies using sedimentary records of aquatic ecosystems provide a unique temporal perspective on patterns, causes, and rates of ecological change due to natural hydrologic and climatic variability, and anthropogenic activity over various time scales. Paleoecology is not only relevant to investigate the past history of an ecosystem and its response to change, but also to determine baseline conditions used as targets of restoration policies (Willard & Cronin, 2007). In aquatic ecosystems, various geochemical, biogeochemical, geological, biological and physical proxies are traditionally employed for investigating ecosystem history from the surrounding catchment, the atmosphere, and the aquatic system itself (Gorham et al., 2001). An ever expanding list of proxies is becoming available for paleolimnologist, offering new opportunities for an increased understanding of the impact of environmental change on ecosystems. In particular, the emergence of DNA-based analysis of lake sediments is opening up the possibility of including taxa that could not be used in past, as they did not produce a distinct morphological fossil structure. This is particularly relevant in the case of organisms such as bacteria, for which only a handful of specific biomarkers, such as fossil photosynthetic pigments (Gorham et al., 2001; Dreßler et al., 2007), were available until recently.

The ability of using bacteria in paleolimnology is highly relevant, given the importance of bacteria in aquatic ecosystems. Bacteria have a considerable cumulative mass in most lakes (water column and sediment) (Mrozik, Nowak & Piotrowska-Seget, 2014). Given the phylogenetic and functional diversity of bacterial communities, bacteria are usually able to colonize every available habitat (Nealson, 1997). Moreover, because of their role on the biogeochemical cycling of elements (Madsen, 2011), the response of bacterial communities to environmental change is complex, as they can be simultaneously a response and a driver of environmental change (Chen et al. 2015 and references therein). Therefore, analysing how the structure of bacterial communities change over time might provide valuable information about the evolution of environmental conditions, the resilience of an ecosystem, or the impact of anthropogenic activity.

Technological advances in the field of environmental genomics now allow for studies of microbial communities from sedimentary records. To achieve this, environmental genomics uses “ancient” or “fossil” DNA as a proxy (Coolen & Gibson, 2009; Boere et al., 2011; Fernandez-Carazo et al., 2013; Pansu et al., 2015). However, the use of DNA-dependent methods for the study of bacterial communities in paleoecology raises the question of DNA preservation in sediments. DNA degradation has been shown to be influenced by multiple biotic and abiotic factors, leading to a differential degradation rate across taxa (Boere et al. 2011 and references therein). Moreover, in-situ activity (Nealson, 1997; Haglund et al., 2003) and possible modifications of the community structure during sediment diagenesis could lead to a misinterpretation of the environmental conditions at the time of deposition. Alternatively, extracting DNA from bacterial resting states, and notably endospores and other spore-like structures, might avoid these limitations (Wunderlin et al., 2014a). The use of such structures has been examined and proposed as an alternative to total DNA-based analyses (Renberg & Nilsson, 1992; Wunderlin et al., 2014a; Paul et al., 2019).

The development of molecular tools to specifically enrich lysis-resistant cells has created new venues in this field of research (Wunderlin et al. 2013; Bueche et al. 2013; Wunderlin et al. 2014).

A combination of these methods was successfully used to assess the impact of eutrophication (Wunderlin et al., 2014a) and of the antibiotic era on the bacterial communities in sediments of Lake Geneva (Madueño et al., 2018). The aim of this study is to broaden the application of this approach and to test its complementarity to more traditional paleolimnological proxies. The site selected is the Lake Liambezi, located in the border between Namibia and Botswana.

Lake Liambezi is an ephemeral lake that floods seasonally, depending on the annual precipitation pattern of the region. It is a major resource of freshwater for the surrounding villages and communities of farmers and fishermen (Tweddle et al., 2011; Mutelo, Murwira & Kileshye-Onema, 2013; Peel et al., 2015). To date, except for a brief description made by Seaman et al. (1978), the lake has been poorly studied. In Chapter 3, discuss the geochemical compositions of the sediments of the lake in the light of likely environmental and climatic changes. These characteristics can then be compared to the results of the present work, that concentrates on the use of the characteristic microbiologic tools for a complimentary interpretation of the paleoecologic evolution of the Lake Liambezi sediments.

4.3. Material and methods

4.3.1. Regional settings and lake description

Lake Liambezi is located in Namibia, at the eastern side of the Caprivi Strip. The lake is part of a complex drainage system that includes the Kwando and Zambezi rivers. Its Southern shore makes up the border between Namibia and Botswana. It receives water from the Chobe River (a tribute of Zambezi River, deviated due to the Chobe Fault (Haddon and McCarthy, 2005)), Bukalo Channel (a seasonal tribute of Zambezi River), and Linyanti River (or Swamps, natural deviation of Kwando River due to the Linyanti Fault (Haddon and McCarthy, 2005)), as well as rainwater and local runoff water (Figure 39).

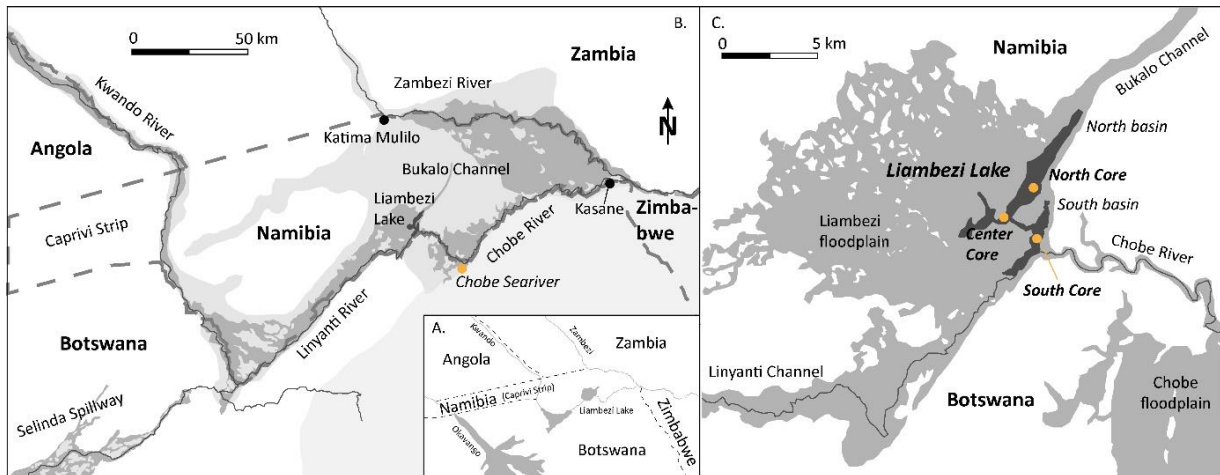


Figure 39 Partially inspired by Peel, 2015. **A.** General map of the region with the three main river systems: Okavango, Kwando and Zambezi; **B.** General map of grouped systems Kwando and Zambezi rivers. Kwando river comes out Angola and turns into Linyanti river after its terrestrial delta joins a tectonic fault along the Namibia and Botswana border. It finishes its course into Liambezi lake mostly into percolating water in Linyanti swamps. Zambezi river coming down Zambia flows into Liambezi lake through the Bukalo channel and the Chobe river (Haddon and McCarthy, 2005). The Chobe river is able to reverse its flow depending the water availability and to flow in both directions (Seaman et al., 1978; Peel et al., 2015). Due to the very poor relief terrain, many flood zones form around the rivers of the system as well as around Lake Liambezi (dark grey); **C.** In dark grey color, map of Liambezi lake in its full size as described by Seaman et al., 1978. Open-water lake with its two elongated basin is in black. Cores locations are represented by a yellow dot.

Depending on the water level, the Chobe River serves as outflow of the lake (Seaman et al., 1978; Peel et al., 2015). The lake is surrounded by a major flat wetland system characterized by woodlands, wetlands and slow-flowing floodplain rivers (Seaman et al., 1978; Peel et al., 2015). Seaman et al. (1978) report a system covering some 300 km² of which 100 km² is open water at its full size. The lake changes shape, size and depth between and within years due to the source and the amount of water in the basin (Tweddle et al., 2011). The average depth is of approximately 2.5 m (Seaman et al., 1978) but can reach 7 m at the height of the rainy season (Peel et al., 2015). The general shape of the lake varies depending on the water supply. It is generally separated in two main basins: Northern and Southern basins, which are connected by a narrow 1.3 km long central channel. The Northern basin is approximately 6 km long and 1 km wide at its maximum. It receives water from the Bukalo Channel on the north, from the channel between the two basins on the east and by percolation in its western and southern shores by the Linyanti marsh. Southern basin is 4 km long and 500 m wide. It receives water by the connecting channel in its west, by the Chobe River in its east, the Linyanti marsh all along its south-western shore and by the Linyanti channel in the south-east (Figure 39). The Linyanti marsh, surrounding the two basins in their western shores is the result of a geological fault that forms an area of wetlands composed by a complicated patchwork of swamps and marshes. The fault is known under the Linyanti Fault (Haddon and McCarthy, 2005). The set of these features forms the Linyanti River. The Chobe is also delimited through a fault named the Chobe Fault (Haddon and McCarthy, 2005).

4.3.2. Sampling

Three cores were obtained from the same number of sampling locations (Figure 39). Sampling was performed with an Uwitec Hammer Action Corer with PVC tubes of 86.0 mm inside diameter. The Center Core (CC) was obtained in the northern basin, at its south-eastern side at about 300 meters close to the connecting channel. The South Core (SC) was sampled at the southern basin in its central part. It is set at about 250 meters close to the Chobe river mouth, and at about the same distance of both, Linyanti main channel and the connecting channel. The North Core (NC) was obtained in the northern basin, in its central part. Its distance to the Bukalo Channel is about 4.2 km. The three cores were transported to the VanThuyne-Ridge Research Center to be opened, cut, described and sampled

under the right conditions and the appropriate equipment. Samples from microbiological studies were obtained under a controlled atmosphere using a Bunsen burner to sterilize all the equipment used. Samples were stored and transported in sterile plastic bags and kept refrigerated. Separation of the samples as well as their distribution into groups of samples was carried out on the basis of visual criteria reported in the appendices. Sedimentological, mineralogical and geochemical analyses have been done at Institutes of Earth Sciences and Earth Surface Dynamics of the University of Lausanne and are described and discussed in Chapter 3. Components and origin of the sediments are discussed in the same paper.

4.3.3. Use of data obtained by the RockEval method as environmental tracer

Quality of organic matter is measured using the HI and OI indices measured with the RockEval method. These indices provide information on the oxidation of organic matter. They can however be used in this context as indices concerning the origin of organic matter (Sebag et al., 2018). Figure 40-42 and Figure 45 show the different movements of the HI and OI indices according to the samples.

4.3.4. DNA extraction

DNA from both the lysis-resistant cell fraction and the total community were obtained using an indirect DNA extraction method previously described by Wunderlin et al. (2013). This method consists of a pre-extraction of cells from the sediment prior to DNA extraction. For the lysis-resistant fraction, a spore separation step was applied prior to DNA extraction (Wunderlin et al., 2014b, 2016). Briefly, the pre-extraction of cells from the sediment was done using 3 g of wet sediment added to 15 mL of Na-Hexa-meta-phosphate. The sediment slurry was homogenized using an Ultra-Thurrax® Tube Drive control (IKA, Stauffen, Germany) for 2x1 min at 15'500 rpm, followed by 10 min of sedimentation. The supernatant was retrieved and reserved for following steps, and the remaining pellet was re-extracted using the same amount of Na-Hexa-meta-phosphate (15 mL), followed by homogenization and sedimentation. The two supernatant solutions were pooled and slowly centrifuged at 20 g for 10 min to remove the remaining mineral particles, and finally filtered onto a sterile 0.2 µm pore-size nitrocellulose filters (Merck Millipore, Darmstadt, Germany).

Half of the filter was used for the DNA extraction of the total bacterial community. The FastDNA®SPIN kit for soil (MP Biomedicals, USA) was used following the manufacturer procedure, with a modification consisting in three successive bead-beating steps applied in order to retrieve DNA from the hard-to-break bacterial cells (Wunderlin et al., 2013). The supernatant obtained from these three successive bead-beating steps was treated separately and pooled by ethanol precipitation at the end of the extraction. DNA extracts were resuspended in PCR-grade water. The second half of the filter was used for the DNA extraction of the lysis-resistant cell fraction, using a method for the physical separation of spores (or spore-like structures) from the vegetative cells (Wunderlin et al., 2014b, 2016). After addition of physiological water and homogenization with vortex, the resuspended samples were heated at 65°C for 20 min, followed by two successive chemical treatments first with lysozyme (10 mg/mL) for 60 min, and then with a mix of NaOH 0.5 N and SDS 1% also for 60 min. DNase digestion was performed at this stage in order to avoid any contamination by traces of free DNA from vegetative cells. Finally, the lysis-resistant cells were retrieved on a 0.2 µm pore-size filter. DNA extraction was performed using the FastDNA®SPIN kit for soil (MP Biomedicals, USA) as described above, following the same modified protocol with three successive bead-beating steps. DNA quantifications were performed using the Qubit® dsDNA HS Assay Kit, on a Qubit® 2.0 Fluorometer (Invitrogen, Carlsbad, CA, USA).

4.3.5. Sequencing and data analysis

DNA extracts were sent for sequencing to Fasteris (Geneva, Switzerland), using the Illumina MiSeq platform (Illumina, San Diego, USA). The hypervariable V3-V4 regions of the 16S rRNA gene were targeted using the universal primers Bakt_341F (5'-CCTACGGGNGGCWGCAG-3') and Bakt_805R (5'-GACTACHVGGGTATCTAATCC-3') (Herlemann et al., 2011). The Mothur toolsuite (Schloss et al., 2009) was used to analyse the sequence data, following the standard procedure of MiSeq SOP (Kozich et al., 2013), with the exception of an additional step of singleton removal applied prior to the clustering in OTUs. The alignment of amplicons and the taxonomic assignment of representative OTUs was performed using the SILVA NR v123 reference database (Quast et al., 2013). After quality filtering and removal of chimeras, a total of 7'022'420 amplicons were retained (1'565'908 unique sequences). Singletons (1'364'141 sequences) as well as unclassifiable sequences and sequences belonging to undesirable lineages (chloroplast, mitochondria, archaea, and eukaryote; corresponding to 196'256 total and 4'460 unique sequences, respectively) were also removed. Clustering of the 5'462'023 remaining sequences (197'307 unique sequences) into OTUs using average neighbor clustering and a 97% identity threshold led to the identification of 34'159 OTUs. Sequences are available in GenBank under the BioProject accession numbers PRJNA 396429.

4.3.6. Statistical and multivariate analysis

Statistical and multivariate analysis on the community and environmental data were performed using R version 3.5.1 (R Core Team, 2014), and the package *vegan* (Oksanen et al., 2017) and *phyloseq* (McMurdie & Holmes, 2013). Community structure was analysed using principal coordinate analysis (PCoA), based on Bray-Curtis dissimilarity and Hellinger transformation of the OTU table. OTUs accounting for less than 100 sequences in the whole dataset were removed prior to the analysis, to limit the random effect of the detection of rare OTUs and, in the case of the lysis-resistant community, to reduce the potential background of OTUs representing contamination by members of the non-lysis-resistant community. The procedure was repeated for each subset of data, when analysing single cores or community fraction. Grouping of samples was tested using hierarchical cluster analysis using the Ward algorithm based on Bray-Curtis dissimilarity, and the best number of clusters was defined using the silhouette width measure with the function *silhouette* from the *cluster* package (Maechler et al., 2019). Constrained hierarchical clustering was performed using the *chclust* function from the *rioja* package (Juggins, 2019). Data were transformed as described above. Environmental data were analysed by principal component analysis (PCA) after standardization of the variables (zero mean and unit variance). Difference between groups, based on community composition, geochemical data or visual criteria, was tested using Permutational Multivariate Analysis of Variance (PERMANOVA) using the *Adonis* function from the *vegan* package, based on the same dissimilarity matrix as described above, with 1000 permutations. Post hoc analyses for pairwise comparisons were performed using the function *pairwise.adonis* from the package *pairwiseAdonis* (Martinez Arbizu, 2017), with 1000 permutations and Holm correction. The contribution of OTUs to the variance between groups was tested using SIMPER analysis (*vegan*).

Non-exhaustive selection of sulfur-oxidizing and sulfate-reducing bacteria was performed by selecting OTUs assigned to the Family Chlorobiaceae, Chromatiaceae and Ectothiorhodospiraceae. In addition, all OTUs assigned to a genus containing the prefixes "Desulf" and "Sulf", or the expression "thio" were also selected. The genera *Rheinheimera* and *Nitrosococcus* were removed since they are not known to oxidize sulfur (Brenner, Krieg & Staley, 2005; Hayashi et al., 2018). Non-exhaustive selection of thermophilic bacteria was performed by selecting OTUs assigned to a genus containing the expression "therm". In addition, the genus *Alicyclobacillus*, whose known representatives are thermophilic or moderately thermophilic (Schleifer, 2009), and the genera *Desulfurispora* and *Desulfotomaculum*, both including thermophilic representatives (Kaksonen et al., 2007; Schleifer,

2009), were included to the selection since they were found in high relative abundance in many of the samples.

4.4. Results

Each core was sub-sampled, based on its visual characteristics when opened (Figure 40-42). Samples were then grouped in sections, due to similar characteristics of sediments (Chapter 3 and appendices of present chapter). The grouping of samples was verified and refined by comparison with other methods including sedimentological, mineralogical, geochemical and microbiological analyses.

In each layer, the total community and the lysis-resistant community were investigated. However, in several cases the analysis failed for one or the other and therefore, a direct comparison was not always possible and this was the case for the three sediment cores (data indicated by a shade of grey in Figure 40-42). Constrained and unconstrained cluster analyses were performed to define groups of communities with similar composition within each core and the best number of clusters was determined using silhouette width measure. Globally, the grouping of samples was coherent with the visual, sedimentological, mineralogical and geochemical characterization of the sediments for both the total and the lysis-resistant communities.

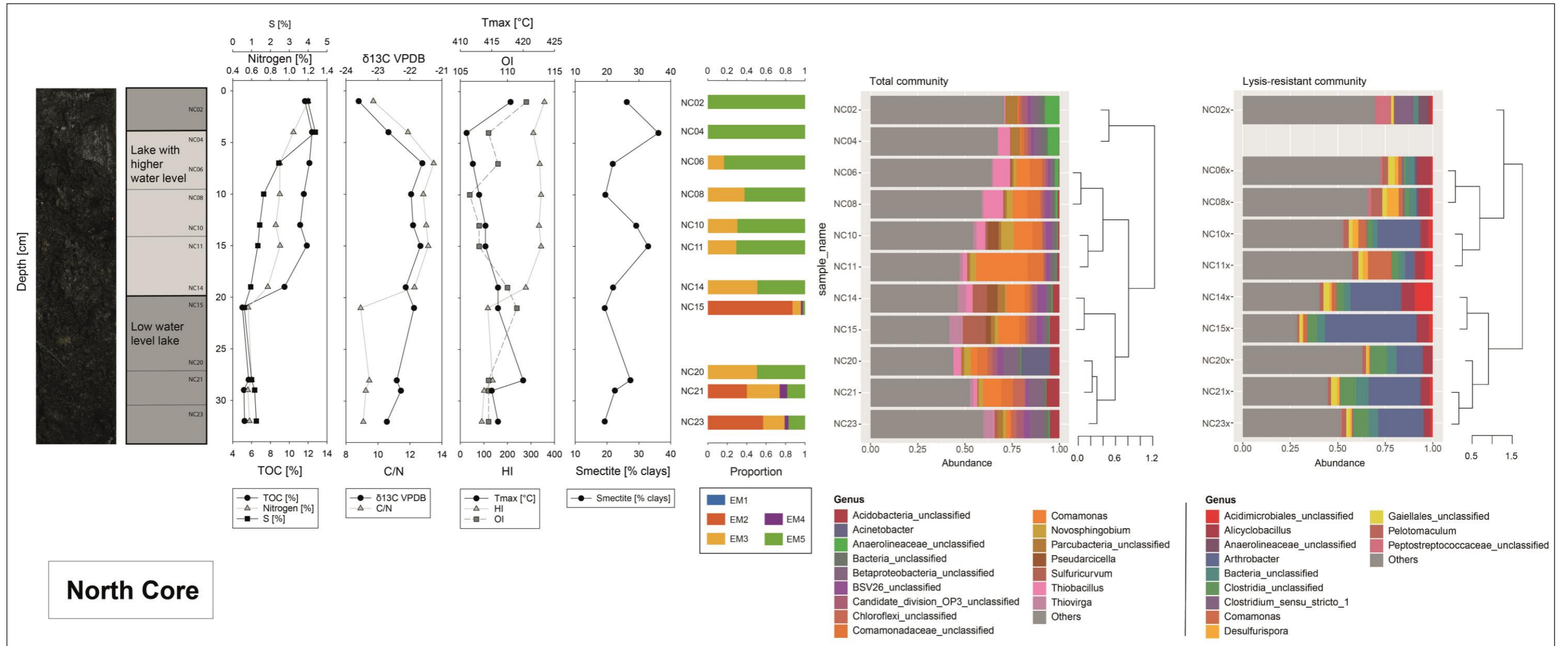


Figure 40 Picture of North Core, opened facing a selection of characteristic parameters through depth including total organic carbon (TOC), nitrogen (N_{org}), sulphur, C/N ratio, $\delta^{13}\text{C}$, HI-OI indices, T_{max} , smectite proportion in percentage of clay minerals, grain-size end-member analysis and the characterization of the total and lysis-resistant bacterial communities, based on 16S rRNA gene amplicon sequencing. Only the most abundant genera (>2% of the community in average or >5% in one sample) are shown. Constrained hierarchical clustering was performed using the *chclust* function based on Bray-Curtis dissimilarity and the Hellinger-transformed community table. For each community, only the OTUs with at least 100 sequences among all samples were kept. The standard deviation or the analytical error of the different analysis are less than or equal to the size of the symbol.

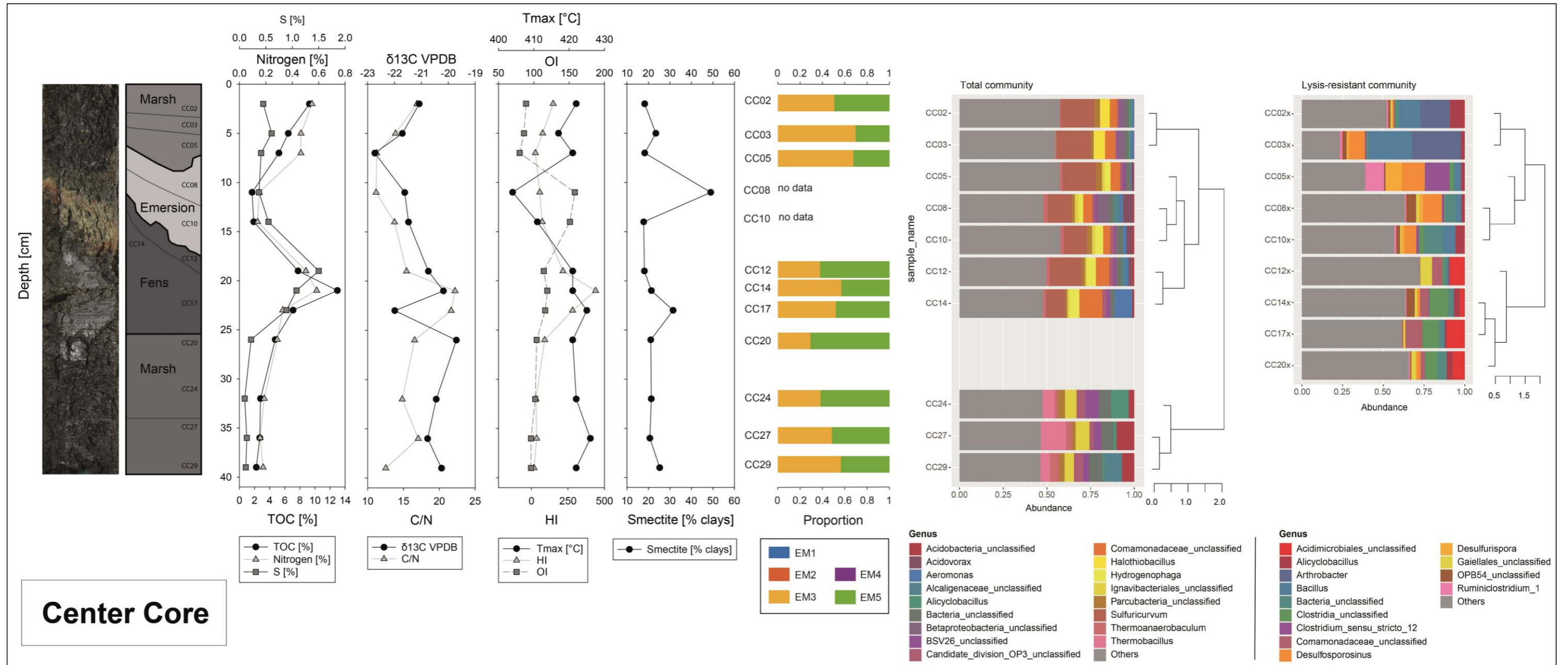


Figure 41 Picture of Center Core, opened facing a selection of characteristic parameters through depth including total organic carbon (TOC), nitrogen (N_{org}), sulphur, C/N ratio, $\delta^{13}C$, HI-OI indices, T_{max} , smectite proportion in percentage of clay minerals, grain-size end-member analysis and the characterization of the total and lysis-resistant bacterial communities, based on 16S rRNA gene amplicon sequencing. Only the most abundant genera (>2% of the community in average or >5% in one sample) are shown. Constrained hierarchical clustering was performed using the *chclust* function based on Bray-Curtis dissimilarity and the Hellinger-transformed community table. For each community, only the OTUs with at least 100 sequences among all samples were kept. The standard deviation or the analytical error of the different analysis are less than or equal to the size of the symbol.

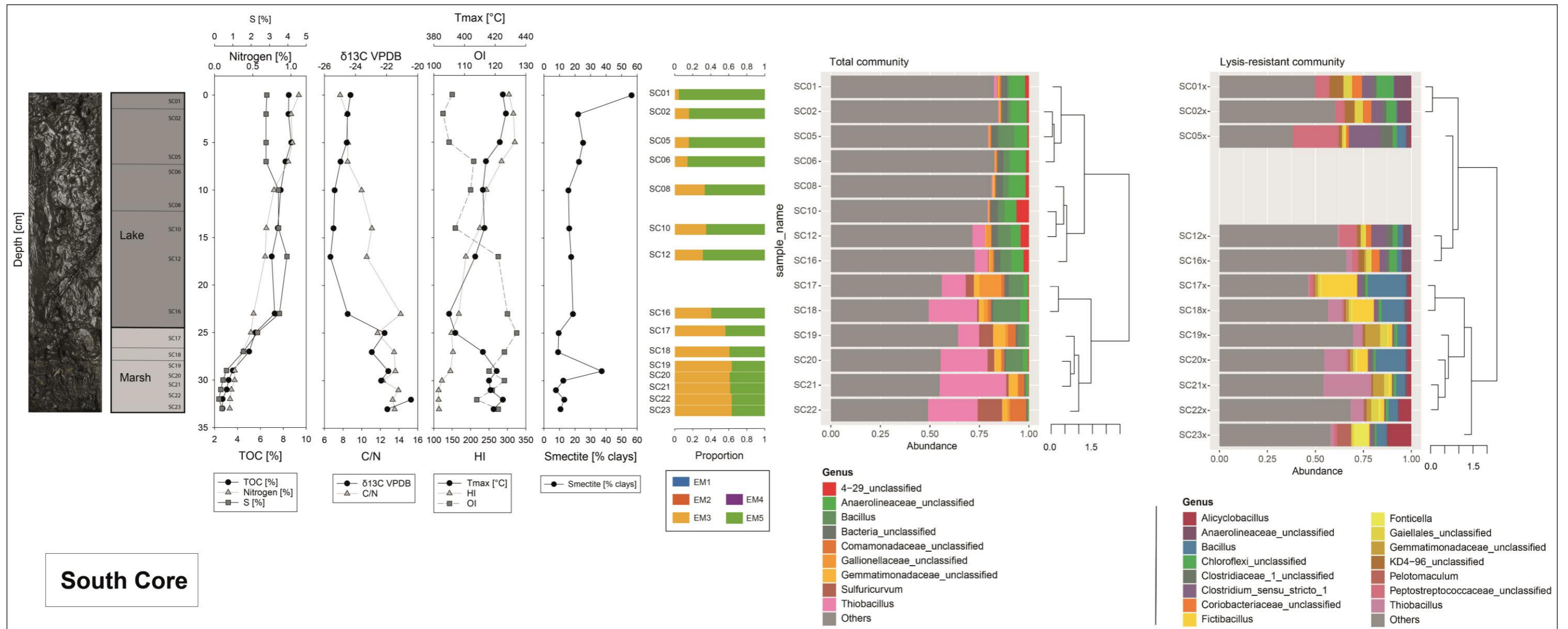


Figure 42 Picture of South Core, opened facing a selection of characteristic parameters through depth including total organic carbon (TOC), nitrogen (N_{org}), sulphur, C/N ratio, $\delta^{13}C$, HI-OI indices, T_{max} , smectite proportion in percentage of clay minerals, grain-size end-member analysis and the characterization of the total and lysis-resistant bacterial communities, based on 16S rRNA gene amplicon sequencing. Only the most abundant genera (>2% of the community in average or >5% in one sample) are shown. Constrained hierarchical clustering was performed using the chclust function based on Bray-Curtis dissimilarity and the Hellinger-transformed community table. For each community, only the OTUs with at least 100 sequences among all samples were kept. The standard deviation or the analytical error of the different analysis are less than or equal to the size of the symbol.

4.4.1. North Core

The north core (NC) was retrieved in the middle of the northern basin in the estimated deepest part of that basin, and was 35.5 cm long. The core was sub-sampled in 11 samples and grouped in three sections (NC15 to NC23 from 21-32 cm; NC04 to NC14 from 4-19 cm; and NC02 at 1 cm).

Slight differences raised from the different clustering analyses applied to the bacterial community composition (BCC). While both samples NC14 and NC04 were assigned to the 2nd group based on the visual characteristics, analysis of the BBC placed them in the 1st group (lower section) and the 3rd (upper section) respectively, for both communities (sample NC04x was missing; Figure 43).

4.4.2. Center Core

The center core (CC) was obtained near the mouth of the connecting channel, on the edge of the north basin, where water depth is lower. The core had a total length of 41 cm and was the longest of the cores obtained. 12 different sub-sampling were made, that were further grouped into four sections. The first section included samples CC20 to CC29 (26-39 cm). The second section included samples CC12 to CC17 (19-23 cm). The third section included samples CC08 to CC10 (11-14 cm), which showed numerous marmorisation traces in sample CC10. The fourth section included samples CC02 to CC05 (2-7 cm).

Although the constrained clustering of the BCC was generally coherent with the visual and geochemical characterization of the sediments, some minor differences appeared. For both communities, sample CC05, assigned to the upper section based on visual characteristics, grouped with samples CC08 and CC10 (Figure 43). As well, sample CC20x clustered in the 2nd group (with CC12x to CC17x) based on the lysis-resistant community (no data for the total community), while it was assigned to the 1st group based on the visual characteristics. But this is probably due to the lack of data for the lower samples (CC29x to CC24x). A difference was also observed when comparing the cluster analyses of the total and lysis-resistant communities. For the lysis-resistant community, the main split in the clusters occurred between samples CC10x and CC12x. Although a change was also observed in the total community at this stage, it did not define two separate clusters between samples CC05 to CC14.

4.4.3. South Core

The south core (SC) was retrieved in the middle of the southern basin, close to the Chobe mouth and the Linyanti main channel (about 250 m), and was 34.3 cm. The core was subsampled in 15 samples that were further grouped in 2 sections. The first section includes samples SC17 to SC23 (25-33 cm). The second section includes samples SC01 to SC16 (0-23 cm).

Constrained clustering of the BCC was coherent with the visual and geochemical characterization of the sediments, for both the total and lysis-resistant community.

4.5. Discussion

4.5.1. Applicability of using bacterial DNA for sediments: Bacterial Community Composition (BCC) changes as environmental tracer

The results of the different sediment analysis methods used in the present study were compared to each other. The separation into different groups of samples according to the different methods is found to be similar for all the methods except three samples (NC04, NC14 and CC05). This is not an error for these three samples. These are transition samples that show a delay of one or another parameter relative to the others for reasons inherent to the site. The good concordance between changes in bacterial communities with regard to visual, sedimentary, mineralogical and geochemical parameters confirms the use of bacteria as an environmental tracer in sedimentary records.

This demonstrates the applicability of using bacterial DNA (total and/or lysis-resistant) to identify changes and variability in the environmental conditions.

4.5.2. Hydrothermalism and Sulphur oxidation

The clustering and PCoA analyses supported the fact that the main changes in the environmental conditions in Lake Liambezi were reflected in the bacterial community. However, to infer the specific drivers of this differentiation based on the analysis of the total BCC is not only difficult, but it can be highly speculative. Bacterial communities in the sediments appeared to be extremely diverse and complex (977-4766 OTUs and 214-633 genera per sample), making the interpretation of the results difficult (Wunderlin et al., 2014a). In most layers, taxa associated to various types of metabolisms (aerobic respiration, anaerobic respiration, fermentation) and environments (soil, freshwater, marsh, hot springs) were found. In addition, the taxonomic assignment of OTUs is limited at the best to the genus level, and some OTUs could only be classified to higher taxonomic level, which hinders the prediction of metabolic potential. Therefore, an alternative approach that consisted on the selection of specific metabolisms for the inference of environmental change was tested. The analysis of the BCC pointed towards two interesting phenomena, notably a very active sulphur cycle and potential hydrothermal activity in the area.

A high relative abundance of sulphur-oxidizing bacteria was observed in most sediment layers (Figure 43A). *Sulfuricurvum*, *Thiobacillus*, *Thiovirga* were the most abundant genera, their proportions varying over time and across cores. In contrast, the relative abundance of sulphate reducers was much lower and a community of sulphate reducers was mainly seen in the lysis-resistant fraction (Figure 43B). The higher relative abundance of sulphur oxidizers compared to sulphate reducers can be explained by the usual low content of sulphate in lacustrine environments compared to marine ones (Jin et al., 2017). Sulphate reduction is often considered to be a minor metabolism in lacustrine sediments, due to low availability of sulphate and organic matter. However, in eutrophic lakes the higher productivity and the rapid consumption of oxygen might favour this metabolism (Holmer & Storkholm, 2001). High abundance of *Sulfuricurvum* and *Thiobacillus* have already been reported in eutrophic lakes (Chen et al., 2015), and thus, similar conditions might have occurred in Lake Liambezi, at least periodically, due to an increase in ecosystem productivity.

While sulphate-reducing bacteria showed a relatively constant abundance in the total community, their abundance pattern was highly variable in the lysis-resistant community. Notably, a sharp increase in sulphate reducers was observed in the section CC10x-CC03x of the Center Core. Similar increase are observable in the North Core in sample NC08x. This was characterized by a high abundance of *Desulfosporosinus*, *Desulfurispora* and *Desulfotomaculum* (*Desulfurispora* in the north core). The last two genera include thermophilic species (Kaksonen et al., 2007; Schleifer, 2009). Interestingly, this increase might be related to samples showing a potential intensive hydrothermal activity (see below). This might suggest a link between the supposed hydrothermal activity and the sulphur cycle. Detection of thermophilic sulphate-reducing bacteria has already been reported in hot sediments from a hydrothermal vent in a Lake Tanganyika, with the availability of sulphate being attributed to hydrothermal fluids (Elsgaard et al., 1994). However, an increase of sulphate-reducing organisms was not observed in the total community, which suggests that these organisms were deposited in an inactive state. The deposition of exogenous spores, originating from distant hydrothermal sources, could also partly explained the abundance patterns. However, such exogenous inputs could be expected to be more important in the proximity of an inflow, which is not the case here.

The presence of a high proportion of thermophilic and moderately thermophilic bacteria (Figure 43C) could be interpreted as a clue of hydrothermal activity. *Alicyclobacillus*, *Thermoanaerobaculum*, *Thermobacillus*, *Acidothermus* and *Desulfurispora* were among the most abundant taxa. The optimum growth temperatures for these groups ranged between 55 °C to 60 °C (Mohagheghi, Grohmann & Himmel, 1986; Kaksonen et al., 2007; Schleifer, 2009; Losey et al., 2013), except for *Alicyclobacillus* (35-65°C) (Schleifer, 2009). Interestingly, a previous study reported low temperature hydrothermal

Cross correlation of bacterial communities and geological proxies

activity in Kasane (about 100 km from the sampling site), with temperatures ranging from 25°C to 50°C (Mukwati et al., 2018). While the abundance of thermophilic bacteria in the lysis-resistant fraction could be attributed to hydrothermal activity occurring in the region and the transport and deposition of spores or lysis-resistant structures, the presence and high relative abundance of organisms with optimum temperature growth of 55-60 °C in the total fraction suggests hydrothermal activity as a relevant process happening in the lake.

In summary, the availability of organic matter/hydrothermal activity could change over time and be a driver of community selection. Therefore, abundance patterns of sulphur-oxidizing, sulphate reducing, and thermophilic bacteria could be used as a proxy to strengthen the interpretation of ecosystem history.

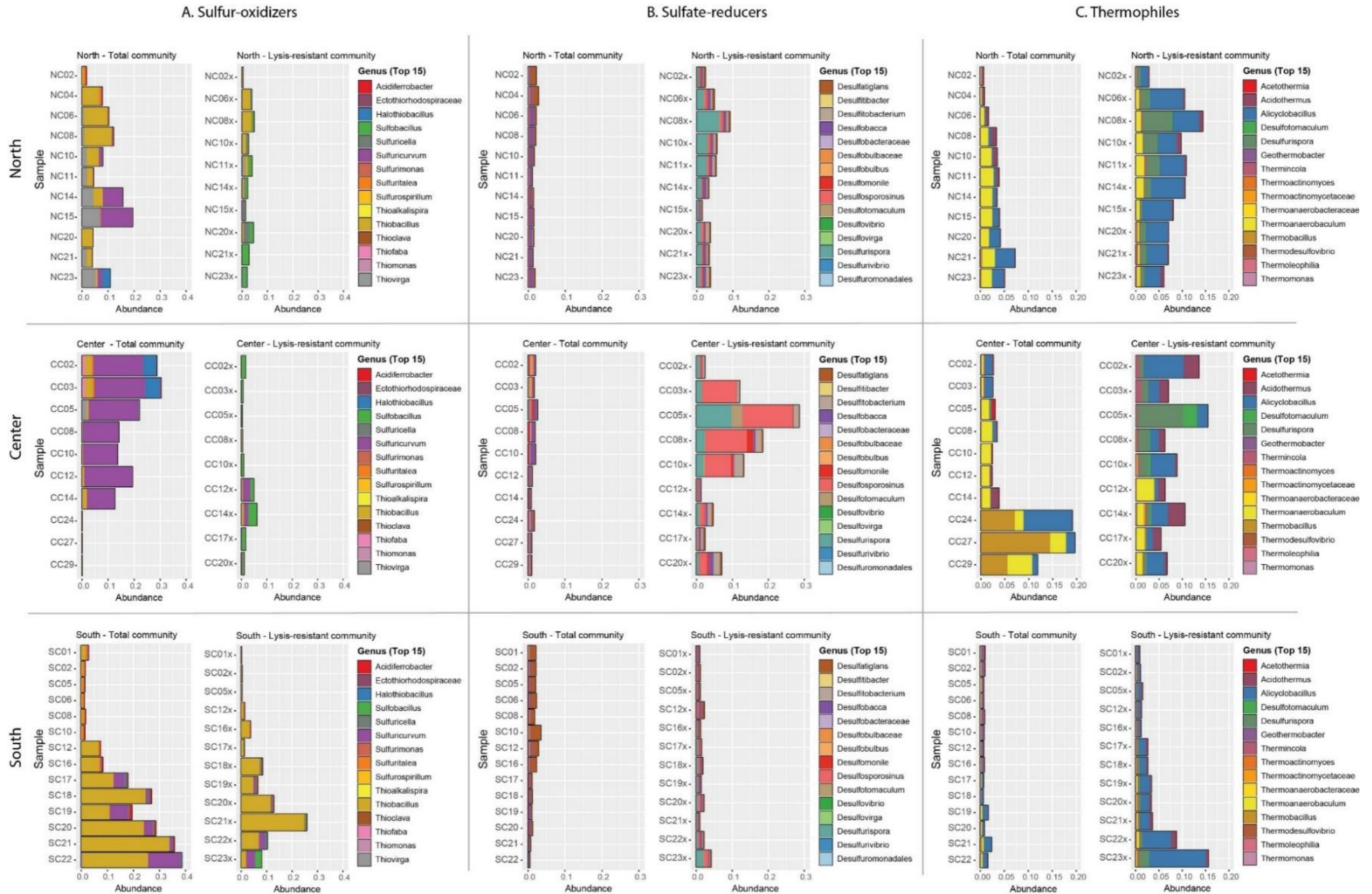


Figure 43 Characterization of the (A) sulphur-oxidizing, (B) sulphate-reducing and (C) thermophilic populations from the total and lysis-resistant community in sediments from Lake Liambezi, based on 16S rRNA gene amplicon sequencing. Relative abundance of the 15 most abundant genera (mean) is represented.

4.5.3. Importance of the climate facing the sites

As Burrough (2007) highlights, due to complex channel-avulsing alluvial fan system, high stages cannot automatically be attributed to climatic variations within the catchment, as channel-switching may play a role in directing flow towards different sumps at different times. Thus, in order not to confuse climatic variation and sedimentary response, the location of the site, its connection with the system as well as its geomorphology will be decisive in order to interpret the sedimentary deposits. As described in Chapter 3, smectite appears to be climate related for the Linyanti-Chobe region. So, results show no correlation or anti-correlation between smectite and quantity of minerals typically linked to detritism in this system (Na-plagioclase, quartz, phyllosilicates, mica, chlorite and kaolinite (Chapter 3). This difference in the location and in the morphology of the site is also observed in the amplitude of certain signals. This is the case with smectite for the Center and North Cores. With a more marked response to climatic variations for the Center Core due to its location, the smectite variations shows a greater amplitude than for the North Core which shows a more stable environment in its drowning. The grain-size of a sample seems to be the result of several parameters linked to the geomorphology of the site as well as to the water availability of the site (Chapter 3). The water availability will depend on the altitude of the site and its position, on the connection to the tributaries but also on the climate. In fact, the use of grain-size in the reconstruction of the climatic evolution of a site is not simple. Such a reconstruction must be considered within the framework of a global paleo-environmental reconstruction in a global and integrated approach which integrates a reconstruction as much morphological as climatic. Such an approach will make it possible not to over interpret the influence of one parameter or the other and above all, to understand all the challenges of a site. This work will be done in Chapter 6. Sediment show a total organic carbon measured at 1.7-13 % of the weight considered as mostly autochthonous. Organic carbon isotopic composition and organic matter quality (RockEval method) have been measured on bulk material; no picking has been made. Results showed a mixed origin dominated by aquatic plants and algae with a lesser contribution of terrestrial detritus. For the terrestrial plant contribution, both the C₃ – and C₄ – type of vegetation are contributing, but with a clear dominance of the C₃ vegetation (Chapter 3). The contribution of C₃ – type correspond with the presence of *Phragmites australis* described along the shores of Lake Liambezi (Seaman et al., 1978; Chapter 2).

The geochemical composition gives tendencies of the dominant vegetation cover. The vegetal cover is considered as changing and adapting to environmental and climatic variations. Organic matter geochemical composition provides therefore a tool of major importance to interpret environmental and climatic evolutions. Figure 44 and Figure 45 demonstrated the changing composition of the organic matter reflecting environmental and climatic changes. According to the data, the impact of the environment type to the vegetation is however stronger than the impact of the climate to the vegetation. Changes in the type of environment observed in the data (Figure 44 and Figure 45) are recorded with a greater amplitude compared to climatic changes. The poor correspondence between smectite peaks and a major change in the type of environment reinforces this interpretation. Therefore, smectite trends only correlates with the minor changes in the organic matter geochemical composition.

The relationship between the deposit environment and the climate is therefore not obvious. The type of environment (fens, marsh, open lake or dried up) is related to the water availability. This latter is linked to the climate, but even more to the connectivity of the site to the watershed. Vegetation type follows a similar trend with well developed Riparian forest (Chapter 2; Romanens et al., 2019; Vittoz et al., 2020). The organic matter amount and its geochemical values confirm the strong link between vegetation type and water availability in the direct vicinity (Chapter 2). Because of this link between morphology and vegetation, the link between climate and vegetation is not obvious. Major changes in organic matter geochemistry are following major environmental changes in the three

different sites (see following chapters). However, minor changes towards higher or lower isotopic values or C/N ratio (and in fact towards more C₃ – or C₄ – type or even algae if plotted like in Figure 45) occur in exact same samples than changes in smectite content (Figure 44). This link confirm the impact of the climate change on the vegetation geochemical values.

SEM images have demonstrated framboidal pyrite (Chapter 3). Chapter 3 has assumed that its presence testifies of anoxic condition. The presence of framboidal pyrite is rather found in the horizons with good preservation of organic matter (NC04-02; CC17 and CC05; SC16-02). However, this is not an absolute truth. Other parameters are taken into account. The same is true for climate change. If the presence of framboidal pyrite can correspond to the wettest periods (NC04-02; CC17; SC16-01), it can also correspond to the establishment of the wetter climate (NC21, NC14 and NC06; SC21-20) or even show a delay in the wet period (CC05; SC18). Local differences explain this and will be described in the chapter devoted to the description of each core.

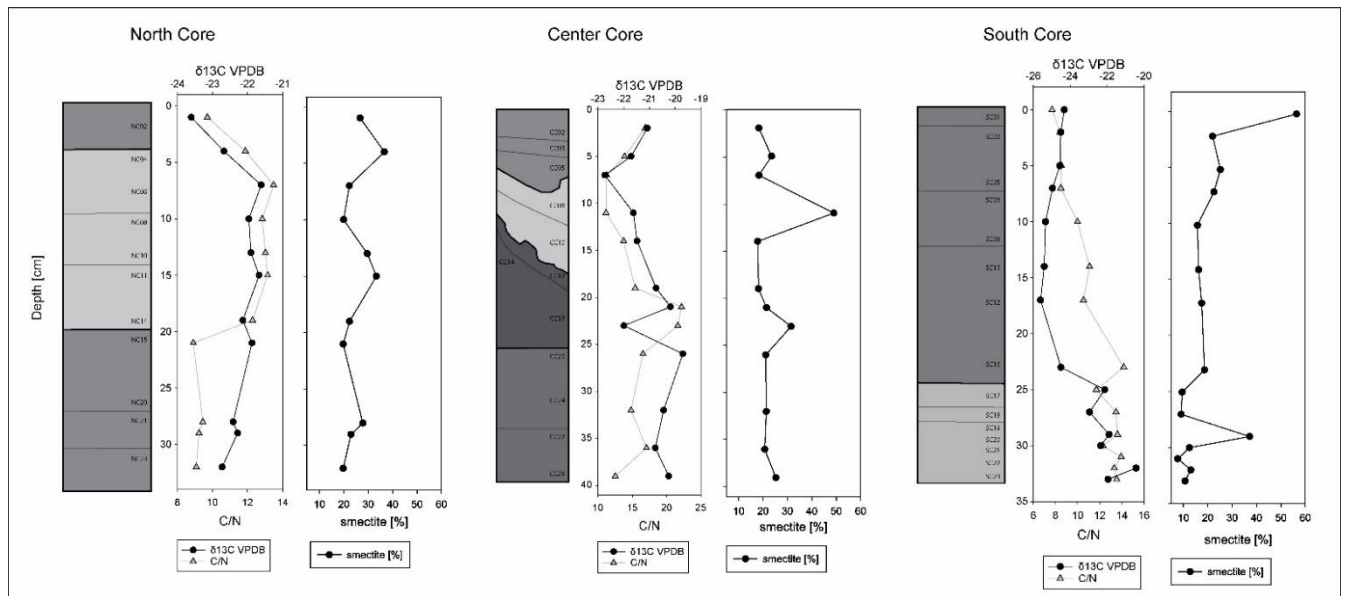


Figure 44 Comparison of $\delta^{13}\text{C}$ and C/N ratio of the organic matter with smectite content of each core. The standard deviation or the analytical error of the different analysis are less than or equal to the size of the symbol.

4.5.4. Cores interpretation

4.5.4.1. North Core

The geomorphologic location of North Core allows to show a very stable origin and evolution in organic matter geochemistry and quality with only slight changes. The location of the core, in the middle of the northern basin at its estimated deepest part, offers a protected deposit area to minor climatic changes. The sediment show a lake environment all along the core, with water level variability. The stability of the area is shown with the oxygen index in Figure 45 that stays stable all along the core. However, the two distinct groups of samples formed by the hydrogen index highlight a slight change between the lower samples (NC23 to NC15) and the upper part of the core (NC14 to NC02). A decrease of the hydrogen index with time is normal due to progressive degradation of organic matter. However, the two groups are very well spotted. It suggest a slight change in the preservation and origin of the deposited sediment. Drier condition in lower core part would bring a more pronounced seasonality and lower lake level, favouring the degradation of the organic matter. This might also decrease the terrestrial input due to lower productivity.

4.5.4.1.1. Lower section (NC23-NC15)

In the lower section of the North Core (NC23-NC15), the low accumulation of well degraded organic matter with an algal/lacustrine origin suggests lacustrine conditions, but with a low water level, favouring the degradation of organic matter. Due to a low water level, the Bukalo channel might have arrived closer to the coring site (compared to a more humid period) as shown by a higher proportion of sand in the grain-size. The end-member analyses demonstrate also an input of coarser grain compared to upper samples suggesting a low water level and an input from a river such the Bukalo Channel. The proportion of smectite in samples NC23 and NC15 supports a dry period interrupted by a more humid period (NC21-NC20). This short wet episode is also supported by the T_{max} values of the NC20 sample. The move to a higher T_{max} in this sample might reflect the higher resistance of siliceous algae to degradation (diatoms) and indicates higher lacustrine productivity. However, this humid episode does not seem to have a major impact on the origin/quality of organic matter nor the lake water level. Low accumulation of organic matter along the whole section of the core might also be the reflect of a low terrestrial productivity associated to the dry climate.

Cluster analysis on the bacterial community placed sample NC14 in this section (for both the total and the lysis-resistant communities), while it belongs to the overlying section based on the visual characterization of the sediment and other analyses. The slow increase of the lake level and the progressive change of the physico-chemical conditions at the sediment-water interface might explain the delay in the response of the bacterial community to the climate change. While a change in the climate could rapidly impact the terrestrial productivity and subsequent accumulation of organic matter, the change in the water level and the physico-chemical conditions at the sediment-water interface might take a longer time to establish.

In these samples, sulfur oxidizers were detected in high abundance (representing up to 20% in the total community), highlighting the important of the sulfur cycle. By contrast, sulfate-reducing bacteria were detected at low abundance, suggesting that the sulfide does not originate from sulfate reduction, but rather from the degradation of organic matter. The additional input of sulfide from hydrothermal sources is also plausible. Oxidic conditions at the water-sediment interface associated to a dry period and low water column levels were supported by the presence of numerous aerobes, including: *Sulfuricurvum*, *Comamonas*/Comamonadaceae and Acidobacteria, *Thiobacillus* and *Thiovirga*.

Despite the relative low impact in the total community of the wet period identified in NC21-NC20 a change in the BCC, as illustrated by the clusterings and the shift in the population of sulfur oxidizers. While the samples NC23, NC15 and NC14 (corresponding to the driest periods) were dominated by *Sulfuricurvum* and *Thiovirga*, samples NC21 and NC20 (wetter period) were dominated by *Thiobacillus*.

The large diversity of bacterial communities reflects good water stratification. This in fact reflects a sufficient height of water to develop the different types of bacteria and brings an additional element for the classification of a lake environment. The same statement is similar for the three sections of the core.

4.5.4.1.2. Mid-section (NC14-NC04)

The period covered by the samples NC14-NC04 saw the establishment of a more humid climate leading to the increase of the lake level, as suggested by the origin and quality of the organic matter. The accumulation of organic matter with a higher input of terrestrial material and better preservation is consistent with an increase in the terrestrial vegetation productivity and a decrease in the oxygen availability. The smaller grain-size compared to the preceding section also supports low energy conditions typical for a higher water stand. End-member analysis of grain-size suggests a progressive flooding from NC14 to NC04. The gradual change towards dominance of EM5 suggests an increasing water level. The smectite abundance shows more variability, with significant peaks in NC11 and NC04

interspersed by lower values in NC08 and NC06, indicating an alternation of humid and dry periods. However, this latter appears to have a lower incidence, since no major impact on the characteristics (origin and quality) of the organic matter was observed.

During this period, thermophiles remain abundant, with abundances comparable to what was observed in the preceding period. The decrease of *Alicyclobacillus* (aerobic) in favor of *Thermoanaerobaculum* (anaerobic) notably (Schleifer, 2009; Losey et al., 2013), is one change pointing at a trend towards a more humid period. Similarly to the preceding section, bacteria from the sulfur cycle remain important in this section. Sulfur oxidation subsist a prevalent biological process for this section. Interestingly, *Sulfuricurvum* and *Thiovirga* disappear almost completely in favor of *Thiobacillus*. This supports the association of *Sulfuricurvum* to dry (and oxygen-rich) environments, and *Thiobacillus* to wet (oxygen-poor) environments. In addition, sulfate reducers increased in the lysis-resistant fraction. This was characterized by increasing abundance of mainly *Desulfurispora*, a genus including the thermophilic species *Desulfurispora thermophila* (Kaksonen et al., 2007), possibly indicating hydrothermal activity as described above.

4.5.4.1.3. Upper section (NC02)

The upper section of the core, only represented by the sample NC02, corresponds to a period of dry climate. This can be seen with the decrease in smectite and the algal origin of organic matter suggesting a decrease of organic productivity. However the dry period does not have an impact on the lake level which remain high. Organic matter is well preserved (with high C_{org} and HI), suggesting anoxic conditions to prevail. The grain-size, which continue to decrease, also support the persistence of a high water level. The end-member analysis confirms it with an upper section (which starts already with sample NC04 for the end-member analysis) where only EM5 subsists.

Bacterial community also support the establishment of persisting anoxic conditions, illustrated by the decrease of sulfur-oxidizing bacteria and the increase of Anaerolineaceae (in both fractions). Sulfate-reduction appeared to be slightly higher in this section of the core, supporting this interpretation. Thermophilic bacteria also decrease in the upper sediment, suggesting their abundance in the sediment is not the fact of the climate and high associated temperature, but might be the reflect of decreasing hydrothermal activity. These trends were already seen in sample NC04, which groups with sample NC02 in the cluster analysis, confirming that the bacterial community composition is the reflect of high lake level and perennial anoxic conditions, rather than induced by the dryer climate.

4.5.4.2. Center Core

Center Core is nowadays located on the edge of the north basin. The site offers a lower water depth than the other two sites. As a result, the site is more strongly subject to variations in water level and/or hydrological regime changes. This is reflected by a high variability in the stability of the organic matter in the core, compared to the other sampling sites (South and North Cores). The organic matter shows in particular a greater terrigenous origin than the two other cores, with a more marked C_3 - C_4 mixture towards the C_4 type. So perhaps an influence of the more marked herbaceous compared to *Phragmites australis* (Chapter 2). Figure 45 presents the evolution through depth of the quality of organic matter and other parameters from which the climatic evolution is taken for this site. Four groups of samples emerge of this analysis. The site starts with the registration of marsh conditions for the lower section. A gradual and continuous drying leads the site to a fens environment for the second section, before total drying for section of samples CC10-CC08. CC08 provides a return to richer water conditions for the site and leads to the characterization of the last section of samples as marsh environment.

An increase in barium content is observed from the CC12 sample. This increase was discussed in companion paper Chapter 3) and its origin is still discussed.

4.5.4.2.1. Lower section (CC29-CC20)

The first section demonstrates a marsh nature with both terrestrial and lacustrine organic matter composition and a low organic matter preservation. It attests of a typical marsh environment with a seasonal flooding and maybe emersion but always under water saturated condition. Following the smectite profile, the deepest sample depicts the end of a humid period. All the upper samples of the section are considered as a dry period. It causes the site to gradually dry up. The end-member analysis for the grain-size suggests also a lacustro-palustrine environment varying in its richness in water, but without drastic change of environment.

The biological interpretation of this section is only based on the total bacterial community (sequencing of the lysis-resistant community did not work). In this section the presence of a high proportion of thermophilic and moderately thermophilic bacteria (including *Thermobacillus*, *Thermoanaerobaculum*, *Alicyclobacillus*) could be interpreted as evidence of hydrothermal activity in the lake during the sedimentation period of this section. Contrary to most other layers with such observation, this hydrothermal event was not associated to the presence of sulfur-oxidizing bacteria. The latter were almost entirely absent in this section, suggesting that sulfide is not available for sulfur oxidation during this period. This can be the result of either low productivity and/or a rapid turnover of organic matter, favored by oxic conditions during this mostly dry, albeit water-logged period, thus favoring aerobic conditions in the water column and at the sediment-water interface. In addition, chemical oxidation of sulfide (Whitcomb, Delaune & Patrick, 1989; Luther et al., 2011) might limit its availability for biological sulfur-oxidation.

4.5.4.2.2. Mid-section (CC17-CC12)

The second group of samples shows a water level decrease with a water table that comes very close to the surface and a more marked seasonality. However, the immaturity of the organic matter composition (in RockEval analysis) is typical for anoxic environment and suggests a water-logged environment. The type of environment formed are fens with a higher organic carbon content and a better hydrogen index preservation. A similar current landscape is probably to be sought on the site of Chobe Seariver (Figure 39), described in Chapter 2. The following decrease in organic carbon content as well as a strong decrease in hydrogen index for the last sample of the group testifies of a rarefaction of the flowing water year around and a progression of the situation to a complete emersion. However, sample CC12 still receive enough of water to keep saturated water condition as the oxygen index shows. Indeed, oxygen index of the present sample does not show any change compared with the previous samples and proposes an environment saturated enough with water to keep its partly anoxic condition. This section corresponds to a dry climatic period, interrupted by a humid episode in sample CC17, as indicated by the smectite profile. This wetter episode is also found through the composition of organic matter which shows a greater proportion in the contribution of plants of terrestrial origin. However, that short humid period is not strong enough to slow down the drying up of the site.

Oxic conditions at the water-sediment interface associated to a dry period and low water column levels were suggested by the presence of numerous aerobes and microaerophiles in the bacterial community, including: *Sulfuricurvum*, Comamonadaceae, Acidobacteria, *Aeromonas*, *Acidovorax* and *Hydrogenophaga*. Moreover, the decrease in strictly anaerobic organisms (*Thermoanaerobaculum*, Ignavibacteriales and Acidobacteria) suggests increasing oxygen availability.

By contrast with the preceding section, sulfur oxidation appeared as a main biological process, with a sharp increase of sulfur-oxidizing bacteria (up to 20% in the total community). Similarly to what have been observed in the north core, the sulfide is supposed to originate from the degradation of organic matter and/or hydrothermalism, given the low abundance of sulfate-reducing bacteria. Despite a decrease, thermophilic bacteria remained abundant (3-4% of the total community).

The large dominance of *Sulfuricurvum* in the center core compared to the north core highlights the difference in the hydrological regime in both core locations, with lower lake level in the center area, as shown by the geochemical data as well. This supports the association of *Sulfuricurvum* to dry (and oxygen-rich) environments, and *Thiobacillus* to wet (oxygen-poor) environments.

4.5.4.2.3. CC10-CC08

The horizon CC10 reveals the apogee of the drying out in progress in the preceding sections. It shows a total emersion of the site with marmorisation traces, important oxidation of the organic matter, bad preservation of organic carbon and a fall in the C/N ratio. Despite the radical change in the preservation of organic matter, the nature of the sediments does not change (same components as the other sections) and reveals a probable seasonal flooding of the site. The wet period which covers the CC08 sample allows a gradual re-flooding of the site and a return to better preservation of organic matter. The brutal shift in the grain-size to an important sand proportion during the setting up of that humid period demonstrates also a return to a greater impact of the seasonal floods for the site. The site is however sufficiently emerged to show significant similarities with the CC10 sample. The end-member analysis is missing for these two samples. The quality of the data is the cause. However, this poor quality confirms that a major environmental event is taking place at this location and time.

During this period, bacteria from the sulfur cycle remain important, but in contrast to the previous section, sulfate-reducing organisms were slightly more abundant in the total community. Thermophiles also remained abundant in this section, with abundances comparable to what was observed in the preceding period, (and suggesting continuity of the hydrothermal activity). Maximum Ba level was reached in CC05, corresponding to an equally sharp increase in sulfate-reducing bacteria in the lysis-resistant fraction. This was characterized by increasing abundance of *Desulfosporosinus*, and the potentially thermophilic genera *Desulfurispora* and *Desulfotomaculum* (Kaksonen et al., 2007; Schleifer, 2009). The high abundance of thermophilic sulfate-reducing bacteria might be seen as a clue of intensive hydrothermal activity at that time.

Surprisingly, no evidence for the development of a soil (or at least the emersion of the sediment) in sample CC10 was reflected in the BCC, while we could expect a major change in the BCC due to the drastic change in the environmental conditions. BCC from samples CC10, CC08 and CC05 is similar to the community identify in the preceding section, in that sense that neither cluster analysis, PCoA, nor Permanova detected a significant change in the community. Likewise, the transition to a more humid period and a return to dry conditions was not reflected, samples CC05 to CC10 being grouped together. This could be due to both the slow flooding of the lake and the colonization of the sediment after flooding. Although a transition to a humid period was recorded in CC08, the system has been flooded gradually and it is likely that the sediments were periodically re-emerged and the lake level remained low even during wet season. In addition, the flooding of the sediment probably induced a change in the community within the sediment, overlaying the signal of the community hosting the sediment during the emersion period. Sediment in situ activity may impact layers representing extended period. This could explain that, neither the hydrological variations, nor a main change in the community in sample CC10, were reflected in the BCC.

4.5.4.2.4. Upper section (CC05-CC02)

The upper part of the central core shows a return to marsh conditions similar to the first section. There is a return to richer water conditions for the site and a more constant flooding. In fact, better preservation of organic matter with characteristics similar to the samples of the first section. The end-member analysis of grain-size confirms this return to condition richer in water as well. A last shift to dryer conditions is seen with the last sample of the core (CC02). The smectite profile presents a dry period cut by a humid period for sample CC03.

Similarly to the preceding sections, the predominance of sulfur-oxidizing bacteria indicated an active sulfur cycle. As observed in the previous sections, sulfate-reducing bacteria were detected at low abundance, suggesting that sulfide originates from the degradation of organic matter and/or hydrothermal activity. The high abundance of *Sulfuricurvum* testimonies of a non-entirely lacustrine (but marsh) environment, which is in accordance with the geochemical analyses. However, presence of other sulfur-oxidizers, such as *Thiobacillus*, suggests more humid conditions compared to the preceding period. (In addition, the presence of *Halothiobacillus* and *Thiofaba*, both halotolerant, suggest an increase input of salt, although this was not measured.) The combined presence of numerous thermophilic and sulfur-oxidizing bacteria suggest hydrothermal events.

4.5.4.3. South Core

South Core show a progressive change from marsh conditions to a lake environment. The transition appears between samples SC18 to sample SC12 with the sample SC16 as transition sample. It is shown in the Figure 45 with the geochemistry of the organic matter. In the organic matter geochemistry and in the quality of it, it is transcribed with a higher C_4 composition in lower samples that suggest a stronger input of terrestrial organic matter and its better preservation. The lower amount in organic carbon content (TOC) supports this description. More humid condition allow then in upper samples to preserve more organic carbon due to less oxygenation of the sediment and to show a stronger lacustrine geochemistry composition. The good preservation of terrestrial organic matter in lower horizons is due to the proximity of the shore and of the Linyanti mouth to the present site.

The quality of organic matter in Figure 45 shows the change with a delay comparing to the geochemistry with the change occurring only in SC10. Similarly to what was observed in the north core, this could be explained by the time needed to increase the lake level following the beginning of the humid period. The vegetation might react more rapidly.

4.5.4.3.1. Lower section (SC23-SC17)

Horizons SC23 to SC17 show a mix in the origin of the organic matter, with terrestrial input and a local algae production (see Chapter 3 to get an explanation about the interpretation of a local organic matter production). The high T_{max} might reflect the contribution of siliceous algae. Grain-size, with high proportion of sand, indicates a high energy aquatic system that might correspond to a marsh environment with running water (low water level with a river mouth that get always closer to the core site or river with more and more energy). The end-member composition confirms this status of marsh environment with the presence of ponds. It confirms the evolution to an environment richer in water and with an increasing level of water towards the upper samples of this section. However, this transition is progressive and not strong. The low accumulation of the organic matter and high oxidation compared to the overlying samples also support a low water level, favouring the degradation of organic matter. This section of the core corresponds to a dry period, as indicated by the smectite profile. The brief humid episode recorded in sample SC19 appears to be not strong or long enough to affect the type of environment (and sediment deposit) recorded in the core. However, it appears that it marks the transition to a lake regime, as indicated by the increasing C_{org} . The following samples show then a transition from marsh to lake environment (SC18-SC12). The transition sample is SC16.

The predominance of sulfur-oxidizing bacteria indicated an active sulfur cycle. Sulfate-reducing bacteria were detected at low abundance, suggesting that sulfide originates from the degradation of organic matter and/or hydrothermal activity. The presence of *Sulfuricurvum* testimonies of a non-entirely lacustrine environment, which is in accordance with the geochemical analyses. This is contradictory with the most relevant sulfur oxidizer, *Thiobacillus*, which elsewhere is linked to wetter

conditions. This conflict is an additional demonstration of the importance of the morphology of the site as well as the climate cycles with high seasonality variations.

4.5.4.3.2. Upper section (SC16-SC01)

In the upper section of the core, the shift to lacustrine condition is reflected by the accumulation of organic matter and lower oxidation, due to the increasing water level. A decreasing proportion of terrestrial material and a T_{\max} reflecting a higher contribution of siliceous algae propose a higher autochthonous production of organic matter. Thus, a slight change in the organic matter composition and a decrease of the water energy complement the explanation of a change in the type of deposits. The smectite also shows a general increase from sample SC16, indicating a humid period. The end-member analysis for grain-size shows two separate periods. A first change in the proportion of the two end-members present in this core takes place after sample SC17. SC16 marks a decrease in EM3 and an increase in EM5. This proportion remains fairly stable despite a weak trend towards always more EM5 towards SC08. A second sharper transition takes place between SC08 and SC06 with the same tendency. This evolution towards a domination of EM5 for the upper part of the South Core suggests a progressive flooding with however two more marked phases which take place at the transitions highlighted with the end-members of the grain-size distribution.

Sulfur-oxidizing bacteria disappeared almost completely during this period, indicating that the sulfur cycle might be extremely limited. The disappearance of sulfur and iron-oxidizing bacteria in favor of fermentative bacteria (Anaerolinaceae) and the slight increase of sulfate-reducing bacteria in the total community suggests the establishment of persistent anoxic conditions, which is consistent with the description based on geochemical measurements. This is confirmed by the increase in pyrite (Chapter 3). Interestingly, sulfate-reducing bacteria slightly increased in the upper section of the south core, while they decrease in the lysis-resistant fraction. The hypothesis in this case is that persistent anoxic conditions and the availability of substrates for sulfate reduction might prevail when the water level is high (Holmer 2001). On the contrary, when lake water levels are low, the upper sediment is regularly oxygenated and sulfate reduction is sporadic, leading to sporulation/germination in response to the change in oxygen and substrate availability. In this case, sulfate-reducing bacteria might be better detected in the lysis-resistant fraction. That was illustrated in the center core during the period of emersion/reflooding, which showed the abundance of sulfate-reducing bacteria increase drastically.

Cross correlation of bacterial communities and geological proxies

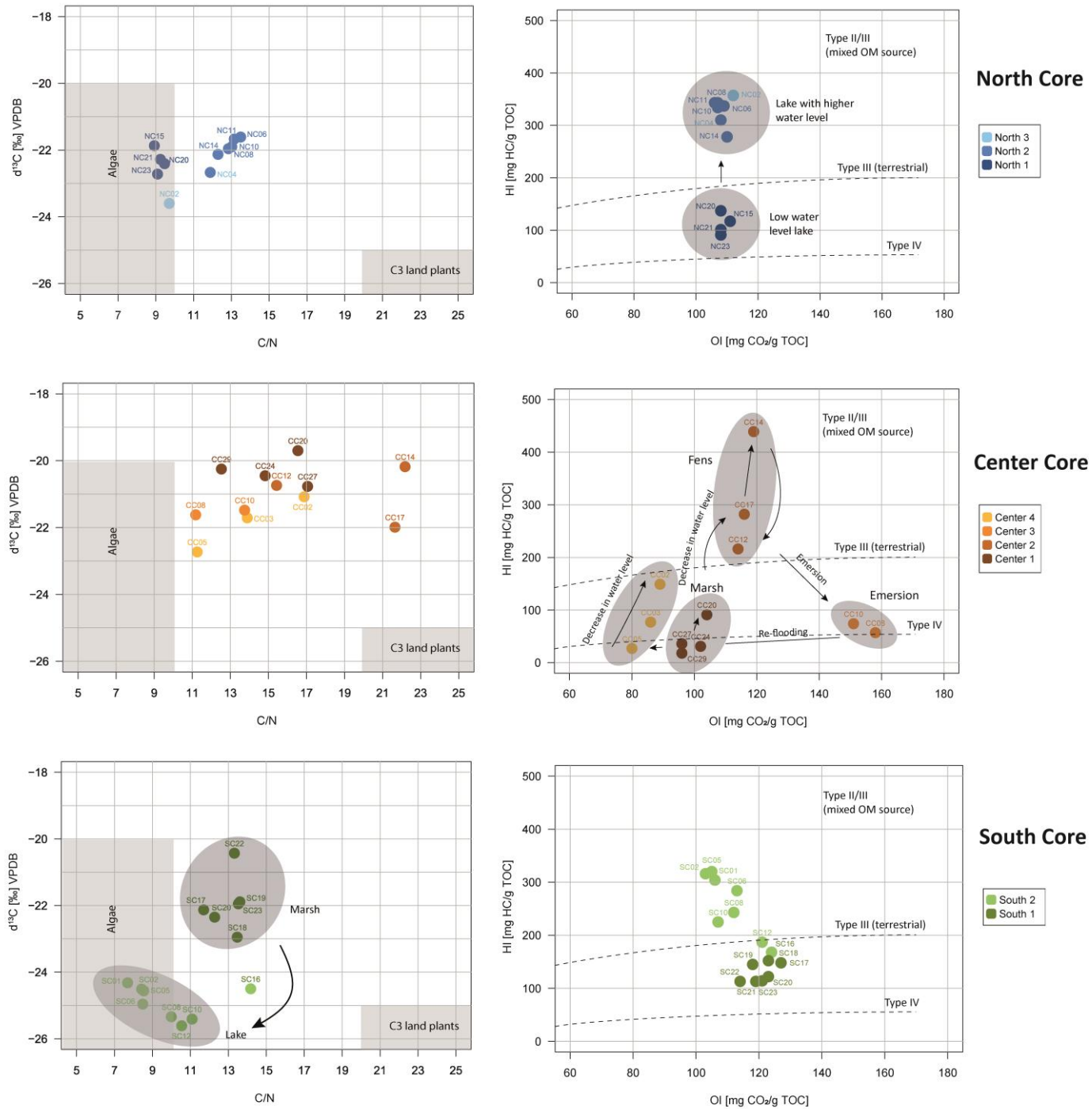


Figure 45 Characterization of the organic matter. On the left, graphics defining the origin of the organic matter, based on $\delta^{13}\text{C}$ and C/N ratio for samples from the north core, center core, and south core. On the right, graphics describing the quality of the organic matter, based on the Hydrogen Index (HI) and the Oxygen Index (OI) from the Rock Eval analysis for samples from the North Core, Center Core, and South Core. The HI-OI graphs integrate the variables of the pseudo-van Krevelen diagram presented in Chapter 3.

4.6. Conclusion

Regarding the importance of bacteria in aquatic ecosystems, its use in paleolimnology is highly relevant. The accumulative mass of bacteria in most of lakes (in water column and sediment) is considerable (Mroziak, Nowak & Piotrowska-Seget, 2014). Bacteria are usually able to colonize every available habitat (Nealson, 1997) and to show a response to environmental changes (Chen et al. 2015 and references therein). Therefore, studies on the bacterial communities change over time might provide valuable information about the evolution of environmental conditions and about the resilience of the ecosystem. Results of the present study are very encouraging in this sense. The applicability of using bacterial DNA (total and/or lysis-resistant) to identify changes and variability in the environmental conditions of Lake Liambezi was successful. The method showed coherent changes in the total and lysis-resistant bacterial communities with other geological proxies. Moreover, it highlighted specific biological processes such as biological-mediated sulphur cycling and potential hydrothermal activity. This demonstrates the relevance of the use of this method as well as its applicability in multidisciplinary approach.

The pooling of the results obtained with each method of this multidisciplinary study (Chapter 3 and present chapter) did permit to give a specific story and evolution for each of the three sites. The evolution of each site is strongly related to the location of the site with its geomorphology and its response to the climatic evolution. The climatic evolution is definitely reflected in the organic matter record and reflect a vegetation response and evolution to it. It is also reflected in the bacteria communities. However, the major evolution observed in both, bacterial communities and mineralogy-geochemistry of the sediments, demonstrate rather the complex association between the morphology of the site (its location) and the climate evolution.

4.7. References

- Boere AC., Sinninghe Damsté JS., Rijpstra WIC., Volkman JK., Coolen MJL. 2011. Source-specific variability in post-depositional DNA preservation with potential implications for DNA based paleoecological records. *Organic Geochemistry* 42:1216–1225. DOI: 10.1016/j.orggeochem.2011.08.005.
- Brenner D., Krieg N., Staley J. 2005. *Bergey's Manual of Systematic Bacteriology - Vol 2 Proteobacteria Part B*. Springer-Verlag, Berlin, Germany. DOI: 10.1245/s10434-010-1229-3.
- Bueche M., Wunderlin T., Roussel-Delif L., Junier T., Sauvain L., Jeanneret N., Junier P. 2013. Quantification of endospore-forming firmicutes by quantitative PCR with the functional gene *spo0A*. *Applied and Environmental Microbiology* 79:5302–5312. DOI: 10.1128/AEM.01376-13.
- Burrough, S.L., Thomas, D.S.G., Shaw, P.A., Bailey, R.M. 2007. Multiphase Quaternary highstands at Lake Ngami, Kalahari, northern Botswana. *Palaeogeography, Palaeoclimatology, Palaeoecology* 253, 280–299.
- Chen N., Yang JS., Qu JH., Li HF., Liu WJ., Li BZ., Wang ET., Yuan HL. 2015. Sediment prokaryote communities in different sites of eutrophic Lake Taihu and their interactions with environmental factors. *World Journal of Microbiology and Biotechnology* 31:883–896. DOI: 10.1007/s11274-015-1842-1.
- Coolen MJL., Gibson JAE. 2009. Ancient DNA in lake sediment records. *PAGES news* 17:104–106.
- Dreßler M., Hübener T., Görs S., Werner P., Selig U. 2007. Multi-proxy reconstruction of trophic state, hypolimnetic anoxia and phototrophic sulphur bacteria abundance in a dimictic lake in Northern Germany over the past 80 years. *Journal of Paleolimnology* 37:205–219. DOI: 10.1007/s10933-006-9013-x.
- Elsgaard L., Prieur D., Mukwaya GM., Jorgensen BB. 1994. Thermophilic sulfate reduction in hydrothermal sediment of Lake Tanganyika, East Africa. *Applied and Environmental Microbiology* 60:1473–1480.
- Fernandez-Carazo R., Verleyen E., Hodgson DA., Roberts SJ., Waleron K., Vyverman W., Willemotte A. 2013. Late Holocene changes in cyanobacterial community structure in maritime Antarctic lakes. *Journal of Paleolimnology* 50:15–31. DOI: 10.1007/s10933-013-9700-3.
- Gorham E., Brush GS., Graumlich LJ., Rosenzweig ML., Johnson AH. 2001. The value of paleoecology as an aid to monitoring ecosystems and landscapes, chiefly with reference to North America. *Environmental Reviews* 9:99–126. DOI: 10.1139/er-9-2-99.
- Haddon, I.G., McCarthy, T.S. 2005. The Mesozoic–Cenozoic interior sag basins of Central Africa: The Late-Cretaceous–Cenozoic Kalahari and Okavango basins. *Journal of African Earth Sciences* 43, 316–333.
- Haglund AL., Lantz P., Törnblom E., Tranvik L. 2003. Depth distribution of active bacteria and bacterial activity in lake sediment. *FEMS Microbiology Ecology* 46:31–38. DOI: 10.1016/S0168-6496(03)00190-9.
- Hayashi K., Busse HJ., Golke J., Anderson J., Wan X., Hou S., Chain PSG., Prescott RD., Donachie SP. 2018. *Rheinheimeria Salexigens* sp. nov., isolated from a fishing hook, and emended description of the genus *Rheinheimeria*. *International Journal of Systematic and Evolutionary Microbiology* 68:35–41. DOI: 10.1099/ijsem.0.002412.
- Herlemann DP., Labrenz M., Jürgens K., Bertilsson S., Waniek JJ., Andersson AF. 2011. Transitions in bacterial communities along the 2000 km salinity gradient of the Baltic Sea. *The ISME Journal* 5:1571–1579. DOI: 10.1038/ismej.2011.41.
- Holmer M., Storkholm P. 2001. Sulphate reduction and sulphur cycling in lake sediments: A review. *Freshwater Biology* 46:431–451. DOI: 10.1046/j.1365-2427.2001.00687.x.

- Jin L., Lee CS., Ahn CY., Lee HG., Lee S., Shin HH., Lim D., Oh HM. 2017. Abundant iron and sulphur oxidizers in the stratified sediment of a eutrophic freshwater reservoir with annual cyanobacterial blooms. *Scientific Reports* 7:1–10. DOI: 10.1038/srep43814.
- Juggins S. 2019. rioja: Analysis of Quaternary Science Data.
- Kaksonen AH., Spring S., Schumann P., Kroppenstedt RM., Puhakka JA. 2007. *Desulfurispora thermophila* gen. nov., sp. nov., a thermophilic, spore-forming sulfate-reducer isolated from a sulfidogenic fluidized-bed reactor. *International Journal of Systematic and Evolutionary Microbiology* 57:1089–1094. DOI: 10.1099/ijs.0.64593-0.
- Kozich JJ., Westcott SL., Baxter NT., Highlander SK., Schloss PD. 2013. Development of a dual-index sequencing strategy and curation pipeline for analyzing amplicon sequence data on the miseq illumina sequencing platform. *Applied and Environmental Microbiology* 79:5112–5120. DOI: 10.1128/AEM.01043-13.
- Losey NA., Stevenson BS., Busse HJ., Damsté JSS., Rijpstra WIC., Rudd S., Lawson PA. 2013. *Thermoanaerobaculum aquaticum* gen. nov., sp. nov., the first cultivated member of acidobacteria subdivision 23, isolated from a hot spring. *International Journal of Systematic and Evolutionary Microbiology* 63:4149–4157. DOI: 10.1099/ijs.0.051425-0.
- Luther GW., Findlay AJ., MacDonald DJ., Owings SM., Hanson TE., Beinart RA., Girguis PR. 2011. Thermodynamics and kinetics of sulfide oxidation by oxygen: A look at inorganically controlled reactions and biologically mediated processes in the environment. *Frontiers in Microbiology* 2:1–9. DOI: 10.3389/fmicb.2011.00062.
- Madsen EL. 2011. Microorganisms and their roles in fundamental biogeochemical cycles. *Current Opinion in Biotechnology* 22:456–464. DOI: 10.1016/j.copbio.2011.01.008.
- Madueño L., Paul C., Junier T., Bayrychenko Z., Filippidou S., Beck K., Greub G., Bürgmann H., Junier P. 2018. A historical legacy of antibiotic utilization on bacterial seed banks in sediments. *PeerJ* 6:e4197. DOI: 10.7717/peerj.4197.
- Maechler M., Rousseeuw P., Struyf A., Hubert M., Hornik K. 2019. cluster: Cluster Analysis Basics and Extensions.
- Martinez Arbizu P. 2017. PairwiseAdonis: Pairwise Multilevel Comparison Using Adonis. R Package Version 0.3.
- McMurdie PJ., Holmes S. 2013. Phyloseq: An R Package for Reproducible Interactive Analysis and Graphics of Microbiome Census Data. *PLoS ONE* 8. DOI: 10.1371/journal.pone.0061217.
- Meunier, A. 2003. *Argiles*. Contemporary Publishing International, GB Science Publisher, Collection Géosciences.
- Mohagheghi A., Grohmann K., Himmel M. 1986. Isolation and characterization of *Acidothermus cellulolyticus* gen. nov., sp. nov., a new genus of thermophilic, acidophilic, cellulolytic bacteria. *International Journal of Systematic Bacteriology* 36:435–443. DOI: 10.1099/00207713-36-3-435.
- Mrozik A., Nowak A., Piotrowska-Seget Z. 2014. Microbial diversity in waters, sediments and microbial mats evaluated using fatty acid-based methods. *International Journal of Environmental Science and Technology* 11:1487–1496. DOI: 10.1007/s13762-013-0449-z.
- Mukwati, B.T., Tafesse, N.T., Bagai, Z.B., Laletsang, k. 2018. Hydrogeochemistry of the Kasane Hot Spring, Botswana. *Universal Journal of Geoscience* 6, 131-146.
- Mutelo, M.A., Murwira, A. & Kileshye-Onema, J.M., 2013. An understanding of variations in the area extent of Lake Lyambezi: Perspective for water resources management. Unpubl. Master of Science in Integrated Water Resources Management of the University of Zimbabwe.
- Nealson KH. 1997. SEDIMENT BACTERIA: Who's There, What Are They Doing, and What's New? *Annual Review of Earth and Planetary Sciences* 25:403–34. DOI: 10.1146/annurev.earth.25.1.403.

- Oksanen J., Blanchet FG., Friendly M., Kindt R., Legendre P., McGlenn D., Minchin PR., O'Hara RB., Simpson GL., Solymos P., Stevens MHH., Szoecs E., Wagner H. 2017. *vegan: Community Ecology Package*.
- Pansu J., Giguët-Covex C., Ficetola GF., Gielly L., Boyer F., Zinger L., Arnaud F., Poulenard J., Taberlet P., Choler P. 2015. Reconstructing long-term human impacts on plant communities: An ecological approach based on lake sediment DNA. *Molecular Ecology* 24:1485–1498. DOI: 10.1111/mec.13136.
- Paul C., Filippidou S., Jamil I., Kooli W., House GL., Estoppey A., Hayoz M., Junier T., Palmieri F., Wunderlin T., Lehmann A., Bindschedler S., Vennemann T., Chain PSG., Junier P. 2019. *Bacterial spores, from ecology to biotechnology*. Elsevier Inc. DOI: 10.1016/bs.aams.2018.10.002.
- Peel, R.A., Tweddle, D., Simasiku, E.K., Martin, G.D., Lubanda, J., Hay, C.J., Weyl, O.L.F. 2015: Ecology, fish and fishery of Lake Liambezi, a recently refilled floodplain lake in the Zambezi Region, Namibia. *African Journal of Aquatic Science* 40:4, 417-424.
- Quast C., Pruesse E., Yilmaz P., Gerken J., Schweer T., Yarza P., Peplies J., Glöckner FO. 2013. The SILVA ribosomal RNA gene database project: Improved data processing and web-based tools. *Nucleic Acids Research* 41:590–596. DOI: 10.1093/nar/gks1219.
- Renberg I., Nilsson M. 1992. Dormant bacteria in lake sediments as paleoecological indicators. *Journal of Paleolimnology* 7:127–135. DOI: 10.1007/BF00196867.
- Romanens, R, Pellacani, F., Mainga, A., Fynn, R., Vittoz, P., Verrecchia, E.P., 2019. Soil diversity and major soil processes in the Kalahari basin, Botswana. *Geoderma Regional*, 19.
- Schleifer KH. 2009. Phylum XIII. Firmicutes Gibbons and Murray 1978, 5 (Firmacutes [sic] Gibbons and Murray 1978, 5). In: De Vos P, Garrity GM, Jones D, Krieg N, Ludwig W, Rainey F, Schleifer K-H, Whitman W eds. *Bergey's Manual of Systematic Bacteriology Volume 3*. Dordrecht Heidelberg London New York: Springer, 19–1317.
- Schloss PD., Westcott SL., Ryabin T., Hall JR., Hartmann M., Hollister EB., Lesniewski RA., Oakley BB., Parks DH., Robinson CJ., Sahl JW., Stres B., Thallinger GG., Van Horn DJ., Weber CF. 2009. Introducing mothur: Open-source, platform-independent, community-supported software for describing and comparing microbial communities. *Applied and Environmental Microbiology* 75:7537–7541. DOI: 10.1128/AEM.01541-09.
- Seaman, M.T., Scott, W.E., Walmsley, R.D., van der Waal, B.C.W., & Toerien, D.F. 1978: A limnological investigation of Lake Liambezi, Caprivi. *Journal of the Limnological Society of Southern Africa* 4:2, 129-144.
- Sebag, D., Garcin, Y., Adatte, T., Deschamps, P., Ménot, G., Verrecchia, E.P., 2018. Correction for the siderite effect on Rock-Eval parameters: Application to the sediments of Lake Barombi (southwest Cameroon). *Organic Geochemistry* 123, 126-135.
- Tweddle, D., Weyl, O.L.F., Hay, C.J., Peel, R.A., Shapumba, N. 2011. Lake Liambezi, Namibia: Fishing community assumes management responsibility. Technical Report no. MFMR/NNF/WWF/Phase II/4.
- Vittoz, P., Pellacani, F., Romanens, R., Mainga, A., Verrecchia, E.P., Fynn, R.W.S., 2020. Plant community diversity in the Chobe Enclave, Botswana: Insights for functional habitat heterogeneity for herbivores. *Koedoe*, 62.
- Whitcomb JH., Delaune RD., Patrick WH. 1989. Chemical oxidation of sulfide to elemental sulfur: its possible role in marsh energy flow. *Marine Chemistry* 26:205–214. DOI: 10.1016/0304-4203(89)90003-0.
- Willard DA., Cronin TM. 2007. Paleoecology and ecosystem restoration: case studies from Chesapeake Bay and the Florida Everglades. *Frontiers in Ecology and the Environment* 5:491–498.

- Wunderlin T., Corella JP., Junier T., Bueche M., Loizeau J-L., Girardclos S., Junier P. 2014a. Endospore-forming bacteria as new proxies to assess impact of eutrophication in Lake Geneva (Switzerland-France). *Aquatic Sciences* 76:103–116. DOI: 10.1007/s00027-013-0329-0.
- Wunderlin T., Junier T., Paul C., Jeanneret N., Junier P. 2016. Physical Isolation of Endospores from Environmental Samples by Targeted Lysis of Vegetative Cells. *JOVE-Journal of Visualized Experiments*. DOI: 10.3791/53411.
- Wunderlin T., Junier T., Roussel-Delif L., Jeanneret N., Junier P. 2013. Stage 0 sporulation gene A as a molecular marker to study diversity of endospore-forming Firmicutes. *Environmental Microbiology Reports* 5:911–924. DOI: 10.1111/1758-2229.12094.
- Wunderlin T., Junier T., Roussel-Delif L., Jeanneret N., Junier P. 2014b. Endospore-enriched sequencing approach reveals unprecedented diversity of Firmicutes in sediments. *Environmental Microbiology Reports* 6:631–639. DOI: 10.1111/1758-2229.12179.

4.8. Supplementary material

4.8.1. Detailed description of the cores

4.8.1.1. North Core

4.8.1.1.1. Sedimentology and texture

The first group included samples NC15 to NC23 (21-32 cm). Sediments showed a diffuse shiny black lamination, with a clayey texture in very compact aggregates. The structure was compact, with plasticity, sticky and poorly friable. The sediment had a strong smell of organic matter and plant macro-debris were absent (which was also the case in the other sections). The second group included samples NC04 to NC14 (4-19 cm). Like the preceding group, sediments showed a diffuse shiny black lamination and a clayey texture in very compact aggregates. In contrast to the preceding group, the structure is different. It showed a loose structure with no plasticity, was not sticky but friable. The smell of organic matter was less marked. The third group included only sample NC02 (1 cm). This horizon showed a diffuse shiny black lamination as well. Texture was fine clayey. Its structure is loose with a high plasticity, was sticky and friable.

4.8.1.1.2. Geochemistry

In the lower section of the core (NC23-NC15), sediments were characterized by low organic carbon (C_{org}) and nitrogen (N_{org}), high C/N ratio, mid $\delta^{13}C$, mid OI, low HI, and higher proportion of sand in the grain-size. The end-member analysis also demonstrates an important part of EM2 as well as the presence of EM4 in this first section, which is not the case for other sections of the three cores. These two end-members show a coarse fraction in upper quantity compared to other end-members found in the three cores. The characterization of the organic matter based on C/N ratio and $\delta^{13}C$ indicates a lacustrine origin of the organic matter. The quality of the organic matter, based on the HI-OI indices from the Rock Eval analysis, suggests better oxidation of the organic matter compared to the overlying sections. In addition, the low C_{org} also suggest higher degradation of the organic matter. The following section of the core (NC14-NC04) brings a change in the deposits. The sharp increase in organic carbon and the shift in the quality of the organic matter suggests an accumulation and a better preservation of the organic matter. The grain-size decreases in size supposing lower energy conditions. The change in end-member analysis is also going to a gradual change to higher rate of EM5. The shift to the following section was already observed in sample NC04, which exhibits intermediate characteristics, illustrating a gradual rather than an abrupt change in the environmental conditions. In the upper section (sample NC02), C_{org} remains relatively constant, while C/N ratio and $\delta^{13}C$ sharply decrease, and N_{org} , OI, HI and T_{max} slightly increase. This indicates low oxidation of the organic matter and a decrease of the terrestrial organic matter input. Concerning the end-member analysis, only EM5 remains.

4.8.1.1.3. Microbiology

In the lower section (NC23-NC14), the total community was mainly composed of *Comamonas*/Comamonadaceae, BSV26 (Ignavibacteriales), Acidobacteria, Betaproteobacteria, Chloroflexi, *Thiovirga* and *Sulfuricurvum*. The five last taxa were also identified as representatives of this section by the SIMPER analysis. The 2nd section (NC11-NC06) saw an Increase in *Acidovorax*, *Thiobacillus*, *Comamonas*, *Hydrogenophaga*, *Pseudarcicella*, as indicated by Simper analysis. Other abundant taxa were *Novosphingobium*, Comamonadaceae, BSV26 (Ignavibacteriales). The section was also marked by the almost disappearance of *Sulfuricurvum*, *Thiovirga*, and *Alicyclobacillus*. The total community of the upper most section of the core (NC04 and NC02) was characterized by an increase in organisms associated to the superphylum Parcubacteria, and the orders Burkholderiales and Xanthomonadales. Most abundant taxa also included representatives of Anaerolinaceae, Ignavibacteriales (BSV26), Betaproteobacteria, Chloroflexi, and Bacteroidetes. A sharp decrease in *Thiobacillus* was also noted (disappearing in sample NC02).

In the lower section of the core (NC23x-NC14x), the lysis-resistant community appeared to be dominated by *Arthrobacter*, which could represent almost 50% of the community. Other abundant taxa were Clostridia, and *Alicyclobacillus*, while SIMPER analysis identified Acidimicrobiales as an indicator of this core section. The middle section (NC1x1-NC06x) saw the decrease of *Arthrobacter* compared to the preceding dry period, notably in samples NC06x and NC08x. The section was also characterized by *Comamonas*, *Hydrogenophaga* and other Comamonadaceae, *Acidovorax*, *Novosphingobium*, DA111 (Rhodospirillales), *Thiobacillus*, *Desulfurispora* and *Alicyclobacillus*, as indicated by their relative abundance and the SIMPER analysis. In the upper section (represented only by NC02x since NC04x was missing), an increase in *Clostridium*/Clostridiaceae, Peptostreptococcaceae and Anaerolinaceae, and a decrease in *Alicyclobacillus* was observed. *Bacillus* and Chloroflexi were also among the most abundant taxa.

4.8.1.2. Center Core

4.8.1.2.1. Sedimentology and texture

The first group includes samples CC20 to CC29 (26-39 cm). The sediments were very fine-laminated, with a diffuse horizontal orientation, and a matte black colour. Texture was clayey in fine lamination and the structure was very compact, with no plasticity. Sediments were not sticky and cohesive. Organic matter smell was light. No macro-debris of plants were observed. The second group includes samples CC12 to CC17 (19-23 cm). Except a change in colour from matte black to matte brown, observations were similar to the preceding section. Only sample CC12 showed a more complex orientation of the lamination. The third group includes samples CC08 to CC10 (11-14 cm). These horizons showed a heterogeneous sloping lamination, clearly marked with the overlaying horizons. Their colour was grey to beige with numerous marmorisation traces in sample CC10. The texture was clayey. The structure was compact, and showed plasticity. Sediments were sticky and friable. No smell and macro-debris of plants were noted. The fourth group includes samples CC02 to CC05 (2-7 cm). These horizons showed a clear horizontal lamination, with matte black colour. The texture was clayey, in aggregates. The sediments had a loose structure, very friable, and were slightly plastic and sticky. Organic matter smell was strong and macro-debris of plants were absent.

4.8.1.2.2. Geochemistry

Sediments from the lower section of the core (CC20-CC29) were characterized by low C_{org} and N_{org} content, variable C/N ratio, high $\delta^{13}C$, and low HI and OI and a high T_{max} . Characterization of the organic matter indicates a mixed origin (terrestrial and lacustrine). The quality of the organic matter, with low OI and HI, might testify of this mixed origin, and relative low oxidation. The high T_{max} testifies of an important part of diatoms (Siliceous skeleton difficult to “crack” to extract the composition of the organic matter composing the diatom. And in fact, the operation requires a higher temperature.). However, low C_{org} accumulation and low HI suggest a high degradation of organic matter. The end-member analysis of the grain-size shows variations between proportion of EM3 and EM5 for the entire core, with an exception for CC10 and CC08 where no results have been obtained due to the quality of the data. Samples from the 2nd section of the core (CC17-CC12) showed high variability in their geochemical and sedimentological characteristics, although they were grouped together based on their visual characteristics. In samples CC17 and CC14, increasing C_{org} attests the accumulation of organic matter, reaching its maximum in CC14. The characterization of the organic matter demonstrated a higher contribution of terrestrial organic matter and its better preservation (increasing HI and C_{org}). Grain-size showed an increase in sand proportion, reflecting a higher water energy. The trend was inverted in the following sample CC12, suggesting a return to the preceding environmental settings. In the 3rd section (CC08 and CC10), the trend already observed in sample CC12 continued, with a decrease in C_{org} and N_{org} , C/N ratio, $\delta^{13}C$ and HI, and an increase of OI. Important oxidation of

the organic matter, as illustrated by the HI and OI, and low accumulation of C_{org} supports the periodic emersion suggested by marmorisation traces in sample CC10. The origin of the organic matter indicates a diminution of terrestrial contribution. Increase in the grain-size attested high energy in water flow, reflecting the seasonal flooding. Sadly, the end-member analysis is not able to confirm it or to bring additional information as no measurements were made due to the quality of the data. The absence of marmorisation traces in sample CC08 suggests a water-logged environment, indicating a gradual re-flooding of the sediment. C/N ratio shows a terrestrial organic matter input again but organic matter is less and less oxidized as well as its preservation is better again. The smectite quantity shows a strong increase. A brutal shift in the grain-size to an important sand proportion during the setting up of that humid period demonstrates a return to a greater impact of seasonal floods for the site. In the upper section of the core (CC02-CC05), a sharp increase in C_{org} and N_{org} , C/N ratio and $\delta^{13}C$, combined to a slight increase of HI and a sharp decrease of OI was observed. Characterization of the organic matter indicated its mixed origin, with an increasing contribution of terrestrial material, and low oxidation. Progressive accumulation of C_{org} indicated a better preservation and/or higher productivity. This suggests higher water inputs compared to the preceding section. The decrease in sand proportion also support an increasing lake level, leading to decreasing energy of water flow.

4.8.1.2.3. Microbiology

In the first section of the core (CC29-CC24), sediments exhibited high relative abundance of OTUs associated to thermophilic organisms including *Thermobacillus*, *Thermoanaerobaculum*, *Alicyclobacillus*. All these organisms have been previously isolated from hot springs or geothermal areas (Schleifer, 2009; Losey et al., 2013; Kim et al., 2014; Sahay et al., 2017). Ignavibacteriales and Acidobacteria appeared to be characteristic of this core section, as indicated by SIMPER analysis, and a genus belonging to the class Dehalococcoidia was among the most abundant genera. The second section (represented only by CC14 and CC12) was dominated by *Sulfuricurvum*. We also observed a decrease in thermophilic and strictly anaerobic organisms compared to the preceding period (*Thermobacillus*, *Thermoanaerobaculum*, *Alicyclobacillus*, Ignavibacteriales) and an increase in aerobic (Comamonadaceae), microaerobic (*Sulfuricurvum*, *Hydrogenophaga*) and facultative aerobic organisms (*Aeromonas*). In the third section, (CC10-CC05), the total community was similar to the preceding section, as indicated by the clustering analysis. However, a slight increase of *Acidovorax* and decrease of Comamonadaceae was observed. In the upper section (CC03 and CC02), similarly to the previous period, the total community was characterized by a high relative abundance of *Sulfuricurvum*, but also by the presence of other sulfur-oxidizers (*Halothiobacillus*, *Thiobacillus*, *Thiofaba*, *Alicyclobacillus*). Representatives from the Comamonadaceae, Anaerolineaceae, and Nitrospiraceae/Nitrospirales, microaerophilic, fermentative, and nitrifying (aerobic) bacteria respectively, were also among the most abundant taxa.

No data were obtained for lysis-resistant community for CC29 to CC24 (first section). In the second section (CC20x-CC12x), Acidimicrobiales, Clostridia, Comamonadaceae, *Hydrogenophaga*, *Aeromonas*, and JG37-AG-4 (Chloroflexi) were the main components of the community as indicated by their high relative abundance and SIMPER analysis. The following section (CC10x-CC05x) was characterized by an increase in *Bacillus*, Gallionellaceae, Peptococcaceae, and an unclassified Firmicutes (class OPB54), according to SIMPER analysis. The upper section was characterized by a wide domination of *Arthrobacter* and *Bacillus*, commonly found in soils, as well as the presence of several thermo-acidophilic bacteria, including *Alicyclobacillus*, *Sulfobacillus*, *Acidothermus* and *Pullulanibacillus*, previously found in hot springs and/or acid mine drainage (Mohagheghi, Grohmann & Himmel, 1986; Schleifer, 2009; Pereira et al., 2013; Méndez-García et al., 2015). The sulfur oxidizer *Desulfosporosinus* was also present in high abundance in sample CC03x.

4.8.1.3. South Core

4.8.1.3.1. Sedimentology and texture

The first group includes samples SC17 to SC23 (25-33 cm). These horizons showed a diffuse, dark brown, shiny horizontal lamination. The texture was clayey. The sediments were very compact and showed great plasticity. There were non-sticky but cohesive. Strong smell of organic matter and presence of macro-debris of plants were noted. The second group includes samples SC01 to SC16 (0-23 cm). These horizons showed a clear horizontal lamination, of shiny black colour. The texture was clayey in fine lamination. The sediments were very compact and showed great plasticity. They were sticky, slightly friable, and emitted a strong smell of organic matter. No macro-debris of plants were observed.

4.8.1.3.2. Geochemistry

In the lower section of the core (SC23-SC17), sediments showed relative constant characteristics from sample SC23 to SC19, followed by a progressive change in samples SC18 and SC17. Samples SC23 to SC19 showed low C_{org} and N_{org} , and high C/N ratio and $\delta^{13}C$. Characterization of the organic matter based on C/N ratio and $\delta^{13}C$ demonstrated a mix between a terrestrial input and a local algae production. Quality of the organic matter, as shown by the RockEval analysis, revealed high OI and T_{max} , and low HI, and testified of a higher oxidation compared to the overlying samples. The higher proportion of sand in these samples suggests a higher water energy. The end-member analysis is suggesting a similar trend, showing an environment changing progressively from pond to lake. An increase in both C_{org} and HI in samples SC17 and SC18 indicated accumulation and preservation of organic matter. The origin and quality of the organic matter did not show a significant change, except a decrease of T_{max} . In upper section of the core (SC16-SC01), the trends observed in the previous samples SC18 and SC17 were more pronounced. C_{org} , N_{org} and $\delta^{13}C$ fixed to high and low values respectively, while C/N ratio decreased progressively. RockEval analysis showed irregular decrease of OI and increase of HI and T_{max} . High C_{org} indicated a higher accumulation of organic matter. Its characterization revealed a shift in its origin and quality. Mainly from lacustrine origin, as indicated by the relation between C/N ratio and $\delta^{13}C$, as well as the increasing T_{max} , the organic matter showed a low degree of degradation (high HI and low OI), which is consistent with the increasing C_{org} accumulation. In addition, the decreasing grain-size indicates decreasing water energy. The end-member analyses confirms it as well with an environment evolving up to a well-developed lacustrine environment.

4.8.1.3.3. Microbiology

Total community in the lower section of the core (SC17-SC22) was highly dominated by *Thiobacillus* and to a lesser extent *Sulfuricurvum* (sulfur-oxidizing bacteria; Kodama and Watanabe 2004; Sievers and Swings 2005), which can represent almost 40% of the community in lower samples. Other abundant and representatives genera were *Bacillus* (aerobe or facultative anaerobe) (Schleifer, 2009), and genera belonging to the family Anaerolinaceae (fermenter) (Yamada et al., 2006), Gallionellaceae (iron-oxidizer) (Sievers & Swings, 2005), Gemmatimonadaceae and Comamomonadaceae (both aerobes) (Sievers & Swings, 2005; Krieg et al., 2010). In the upper section of the core (SC01-SC16), an unclassified Anaerolinaceae was the most abundant genus. *Bacillus* was also among the most abundant taxa, although its relative abundance decreased compared to the preceding period. The total community was also characterized by an increase in Xanthomonadales, Burkholderiales and Nitrospiraceae/Nitrospirales (4-29_unclassified) abundance. Sulfur- and iron-oxidizing bacteria (*Thiobacillus*, *Sulfuricurvum* Gallionellaceae) were well detected in the first two samples of the section (SC16 and SC12) and decreased in the top of the core. Community appeared to

be extremely diverse, with ~75% of the community being composed of genera accounting for less than 2% of the whole community in average, or 5% in maximum.

Regarding the lysis-resistant community, the lower section of the core was characterized by a high relative abundance of *Thiobacillus*, *Bacillus* and *Fictibacillus*, with high variations between samples. Gaiellales, *Gemmatimonas*/Gemmatimonadaceae and *Alicyclobacillus* were also among the most abundant taxa, although the latter decrease along the section. Although sample SC23x belong to the same cluster, it exhibited a particular community, composed of *Alicyclobacillus*, *Pelotomaculum* (anaerobic, termite guts and anaerobic sludge), *Fonticella* (hot springs) and *Bacillus* as main representatives. In the upper section (SC01x-SC16x), the lysis-resistant community was characterized by a sharp increase in *Clostridium*/Clostridiaceae, Peptostreptococcaceae, Coriobacteriaceae, all associated to mammal microbiome (Lozupone et al., 2012; Clavel, Lepage & Charrier, 2014; Browne et al., 2016). Likewise, Comamonadaceae and an unidentified Chloroflexi (KD4-96_unclassified) showed to increase. Gaiellales and Anaerolinaceae were also identified among the most abundant taxa. We also observed the decrease *Alicyclobacillus*.

5. Dating the sediments of Lake Liambezi, Namibia-Botswana

Anael Lehmann¹, Christophe Paul², Daniel Ariztegui³, Pilar Junier^{2&}, Torsten Vennemann^{1&}

¹Laboratory of Stable Isotope Geochemistry. Institute of Earth Surface Dynamics, University of Lausanne, Lausanne, Switzerland.

²Laboratory of Microbiology, Institute of Biology, University of Neuchâtel, Neuchâtel, Switzerland.

³Laboratory of Limnogeology and Geomicrobiology, Department of Earth Sciences, University of Geneva, Geneva, Switzerland.

&Co-Corresponding authors: Torsten Vennemann. Laboratory of Stable Isotope Geochemistry. Institute of Earth Surface Dynamics, University of Lausanne, CH-1015 Lausanne. Mail: Torsten.Vennemann@unil.ch; Phone: +41216924464. Pilar Junier. Laboratory of Microbiology. Rue Emile-Argand 11, CH-2000 Neuchatel. Mail: pilar.junier@unine.ch; Phone: +4132718224; Fax: +41327183001.

5.1. Abstract

The north Botswana region is composed of a complex network of rivers and waterbodies controlled by tectonic faults. If the endorheic drainage system of the Okavango Delta has been well studied and described, the neighbouring endorheic drainage system of Lake Liambezi remains poorly investigated. As part of a multidisciplinary study, the paleoenvironmental and -ecological evolution of Lake Liambezi has been studied through a number of sediment cores. These cores have been sampled and examined for their overall geochemical, mineralogical and microbiological composition. Results and interpretations are to be found in companion papers.

In order to provide the environmental evolution for each sedimentary core it is critical to develop a chronological model. Thus, the aim of the present work is to date the cores and to get a time frame for the environmental history of the lake reconstructed throughout different proxies. In regards to the sediments, we have examined the ¹⁴C-compositions of a number of samples. However, dating with radiometric methods on sedimentary components is challenging at least. Sixteen samples were measured for their ¹⁴C-activity and only nine were considered plausible and were retained. Additional methods had to be used to complete the gaps. Mineralogical and the geochemical data indicate that the sediments are not heavily bioturbated and thus allowing to use other correlation dating methods. Companion papers have presented smectite as a climate related neo-formed clay. Smectite content has thus been used to correlate the three cores together. Analogously, the novel analysis of the bacterial community composition (BCC) revealed the possibility of using it to reinforce and validate the correlation between the three cores. This exercise has been repeated using different approach. The age determined following this multidisciplinary approach give an age of 1618 to 51 years BP for the North Core, 5424 to 420 years BP for the Central Core, and from 950 to 0 years BP for the South Core. The average vertical accretion rate deduced from the obtained age runs from 1 cm/30 years for the South Core to 1 cm/115 years for the Center Core.

The time periods covered by each core are slightly staggered and covering sometimes slightly different periods of sedimentation. This is most probably the result of tectonic movements along the faults within this region. The obtained age will allow thus paleo-environmental interpretations for the

lakes evolution and therefore to give the possibility to date potential tectonic movements affecting the lake.

5.2. Introduction

As part of a multidisciplinary study on the paleoenvironmental and -ecological evolution of the Lake Liambezi drainage system, a number of sediment cores have been sampled and examined for their overall geochemical and also microbiological composition. This drainage system is similar to that of the more well-known Okavango Delta system that it is also an endorheic drainage system although at present it is only seasonally flooded. Under different climatic conditions in the past, however, the Lake Liambezi system may have been similar to the present-day Okavango system. A better understanding of the past conditions in this fragile and evolving system hence not only is of local importance but may also serve as an example of what could be the future of the adjacent Okavango System, given further climatic and environmental changes.

Compared to the Okavango Delta, Lake Liambezi has been less studied. The first limnological description of Lake Liambezi was published in 1978 by Seaman. His study was subsequently taken up by different authors but with a focus on the populations of fish within the lake (e.g., Tweddle et al., 2011; Mutelo, Murwira & Kileshye-Onema, 2013; Peel et al., 2015). Their studies highlight the importance of the lake for the surrounding villages and communities of farmers and fishermen as a major resource of freshwater and fish, even under today's conditions of seasonal flooding only.

As outlined in Haddon & McCarthy (2005) northern Botswana represents a complex drainage system, whose evolution has been controlled by tectonism and faulting. Given the overall flat topography of the region, minor changes in tectonism and faulting may result in substantial changes in the morphology and hence the drainage pattern of the system as demonstrated by Burrough and Thomas (2008). In order to place the ongoing paleoecological studies into a time frame that can be used for paleo-environmental interpretations, we have radiocarbon dated three different short sediment cores from Lake Liambezi. As expected in a sedimentary system with low sedimentation rates dating with radiometric methods on sedimentary components is challenging at least. This is because such sediments are prone to post-depositional bioturbation related to the seasonal flooding, as well as variable past and present lake level stands due to tectonic/faulting activity in the drainage basin. Here, the results obtained from ^{14}C dating are combined with the correlation of datasets described in two companion papers focusing on sedimentological and microbiological approaches to help characterize relative changes in environmental conditions over the past several thousands of years. This is important in order to bring a temporal aspect to the paleoenvironmental evaluations in this ecologically very fragile region and is necessary for estimates of both future and past impacts on these systems in central- northern Botswana, a region also considered as the cradle of mankind (Cavaillé-Fol, 2020).

5.3. Material and methods

5.3.1. Regional settings and lake description

Lake Liambezi is located in Namibia, at the eastern side of the Caprivi Strip. The lake is part of a complex drainage system that includes the Kwando and Zambezi rivers. Its Southern shore makes up the border between Namibia and Botswana. It receives water from the Chobe River (a tributary of Zambezi River, deviated due to the Chobe Fault (Haddon and McCarthy, 2005)), Bukalo Channel (a seasonal tributary of Zambezi River), and Linyanti River (or Swamps, natural deviation of Kwando River due to the Linyanti Fault (Haddon and McCarthy, 2005)), as well as rain and local runoff waters (Figure 46).

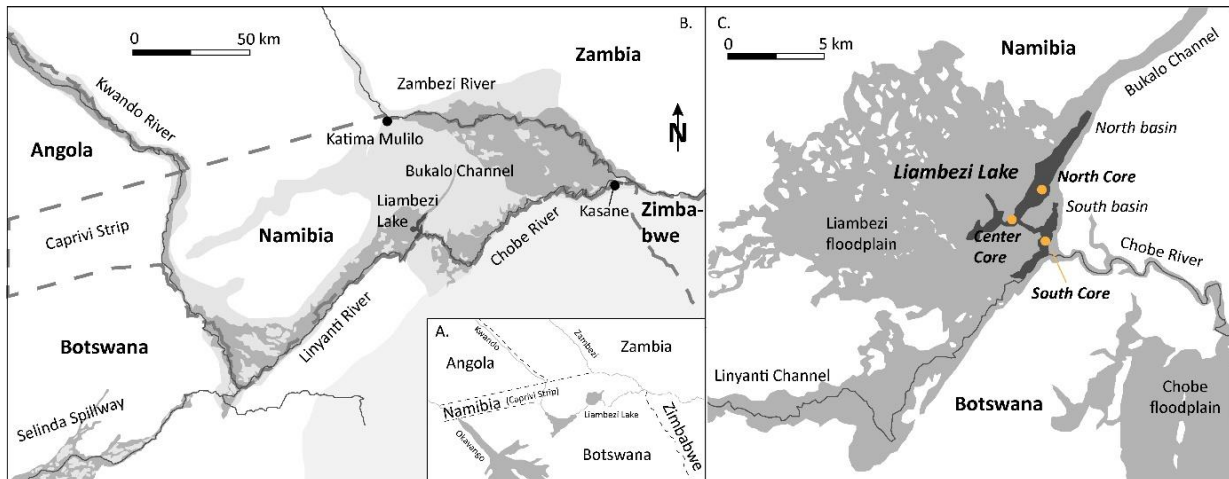


Figure 46 Modified from Peel, 2015. **A.** General map of the region with the three main river systems: Okavango, Kwando and Zambezi; **B.** General map of grouped systems Kwando and Zambezi rivers. Kwando River comes out Angola and turns into Linyanti River after its terrestrial delta joins a tectonic fault along the Namibia and Botswana border. It finishes its course into Lake Liambezi mostly into percolating water in Linyanti swamps. Zambezi River coming down Zambia flows into Lake Liambezi through the Bukalo channel and the Chobe River (Haddon and McCarthy, 2005). The Chobe River reverses its flow depending on water availability and can flow in both directions (Seaman et al., 1978; Peel et al., 2015). The very poor relief generates many flood zones that are formed around the rivers of the system as well as around Lake Liambezi (dark grey); **C.** In dark grey color, map of Lake Liambezi in its full size as described by Seaman et al., 1978. Open-water lake with its two elongated basin is in black. Yellow dots indicate core locations.

Depending on the water level, the Chobe River serves as outflow of the lake (Seaman et al., 1978; Peel et al., 2015). The lake is surrounded by a major flat wetland system characterized by woodlands, wetlands and slow-flowing floodplain rivers (Seaman et al., 1978; Peel et al., 2015). Seaman et al. (1978) reported a system covering some 300 km² of which 100 km² was open water at its full size. The lake changes shape, size and depth between and within years due to the source and the amount of water in the basin (Tweddle et al., 2011). The average depth is approximately 2.5 m (Seaman et al., 1978) but can reach 7 m at the height of the rainy season (Peel et al., 2015). The general shape of the lake varies depending on the water supply. It is generally separated into two main basins: Northern and Southern basins, which are connected by a narrow 1.3 km long central channel. The Northern basin is approximately 6 km long and 1 km wide at its maximum. It receives water from the Bukalo Channel to the north, from the channel between the two basins to the east and by percolation in its western and southern shores via the Linyanti marsh. The Southern basin is 4 km long and about 500 m wide. The western shore receives water from the connecting channel, the Chobe River to the East, the Linyanti marsh along its south-western shore and the Linyanti channel to the south-east (Figure 46). The Linyanti marsh, surrounding the two basins on their western shores is also the result of a fault that dissects the wetlands into a complicated patchwork of swamps and marshes. The fault is known as the Linyanti Fault (Haddon and McCarthy, 2005). The set of these features forms the Lake Liambezi drainage system and the Linyanti River. The Chobe River is also diverted through a fault named the Chobe Fault (Haddon and McCarthy, 2005).

5.3.2. Sampling

Three cores were obtained from the same number of sampling locations (Figure 46) (Chapter 3; Chapter 4). The three cores were opened, split into halves, described and sampled under laboratory conditions at the VanThuyne-Ridge Research Centre in Botswana. A higher resolution sampling of the material intended for radiocarbon dating was done in the laboratories of the University of Lausanne. Between four and seven samples per core were chosen for radiocarbon dating. In both Center and North Cores, small pieces of charcoal and macro rests were handpicked when present, whereas bulk sediment material was sampled when charcoal was lacking. Due to the absence of any macro rests in

the South Core, only bulk sediment samples were taken. Analogously, the lack of organisms with carbonate shells in all the retrieved sedimentary cores reduced the choice of material to be dated. The selected samples were measured for their ^{14}C -activity at the Laboratory of Ion Beam Physics of the ETH Zürich. Samples were prepared according to the methodology described in Hajdas (2008) and Hajdas et al. (2007) and the calculated age followed the convention of Stuiver and Polach (1977), using the program OxCal 4.3 (Ramsey, 2009) with the IntCal 13 calibration curve (Reimer et al., 2013).

Complementary sedimentological, mineralogical and geochemical analyses have been done at the Institutes of Earth Sciences and Earth Surface Dynamics of the University of Lausanne and are detailed in Chapters 3 and 4. Complementary methods using a microbiological approach have been prepared and analysed at the Laboratory of Microbiology of the Institute of Biology of the University of Neuchâtel following methods described in Chapter 4. All related results are to be found in those companion papers. Methods, results and interpretations used in further chapters are detailed in those companion papers.

5.4. Results

5.4.1. Radiocarbon dating

Sixteen samples were measured for their ^{14}C -activity as summarised in Table 10. Seven samples of charcoal and bulk sediment were analysed from the North Core, giving ages ranging between 1082 and 1740 years BP. Five samples of charcoal and bulk sediment from the Center Core delivered ages between 1882 and 4697 years BP. The youngest ages with dates ranging from 219 to 898 years BP were obtained for the South Core where only bulk sediment was dated.

sample	depth [cm]	material	^{14}C age [yrs BP] $\pm 1\sigma$
SC05	5	sediment	259 \pm 21
SC12	17	sediment	424 \pm 21
SC17	25	sediment	219 \pm 21*
SC22	32	sediment	898 \pm 21
CC02	2	sediment	1882 \pm 24*
CC03	5	charcoal	2710 \pm 22*
CC10	14	charcoal	2006 \pm 23
CC20	26	charcoal	3243 \pm 24
CC27	36	charcoal	4697 \pm 25
NC04	4	sediment	1089 \pm 22*
NC04	4	charcoal	1673 \pm 23*
NC11	15	charcoal	1740 \pm 23*
NC11	15	sediment	1682 \pm 23*
NC15	21	sediment	1082 \pm 25
NC21	29	sediment	1512 \pm 26
NC23	32	charcoal	1618 \pm 23

Table 10 ^{14}C ages obtained on charcoal or bulk sediment samples from three cores of Lake Liambezi. Samples identified with an asterisk (*) were discarded as outlined in the discussion.

5.5. Discussion

5.5.1. Sources of the organic matter

Chemical and isotopic analyses of a selection of samples of soils and river sediments taken from the Linyanti-Chobe Basin (Chapter 2) have demonstrated a poor transport and therefore an autochthonous origin. A similar statement is made for the organic matter of the Lake Liambezi's sediments (Chapter 3). These lacustrine sediments contain organic matter that is compatible with a dominantly aquatic (algae) origin, with lesser amounts of terrestrial plant material from the lake shores. The isotopic composition of organic carbon coupled with the C/N composition of the North and South Cores showed organic matter dominated by algae (Chapter 3 and Figure 47). However,

allochthonous organic matter, notably an aeolian input, can never be completely excluded. Partial reworking of the sediment is not excluded either and, thus, contamination of the isotopic composition of the organic carbon cannot be completely ruled out. These results should therefore be taken with caution. However, $\delta^{13}\text{C}$ values and C/N ratio do not show flattened and homogenized values (Figure 47). It is then assumed that the sediments are not much bioturbated and that the observed values can be considered as rather “primary” peaks. Their correlation with changes in smectite contents strengthen this previous statement as these changes correlate with those observed in the geochemical composition of the organic matter (Figure 47 and chapter 4). Therefore, the combined correlation of the organic carbon isotopic composition, the C/N ratio and smectite content, sedimentary sequence is considered as non-heavily bioturbated and thus usable for both dating and environmental reconstructions.

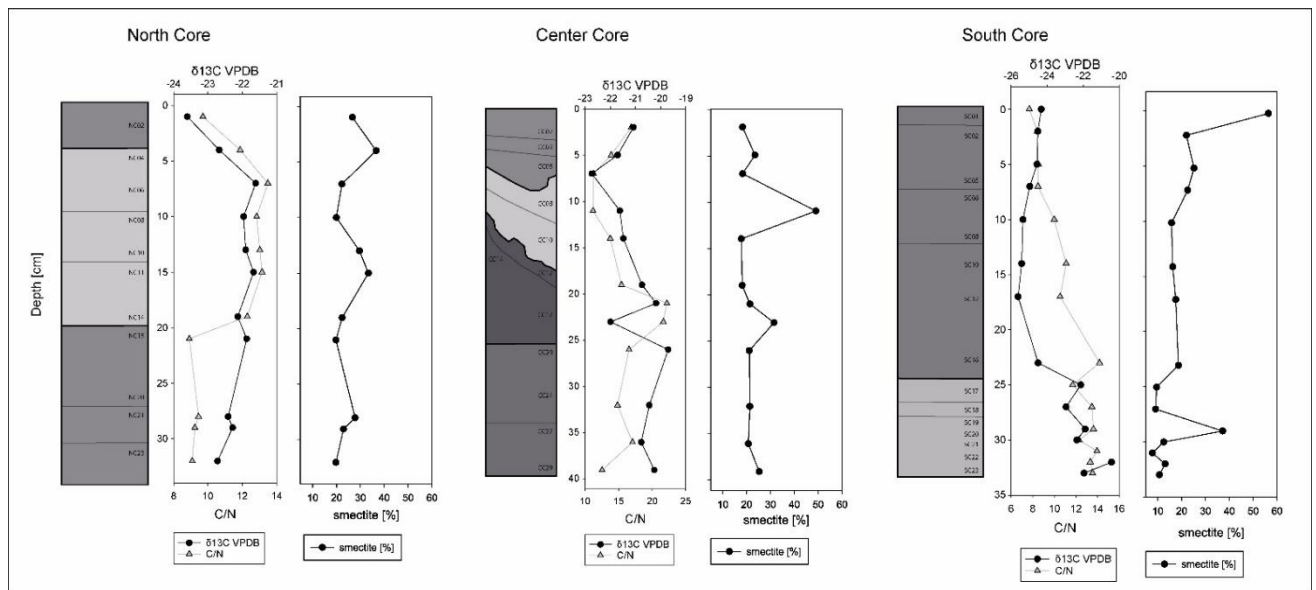


Figure 47 Comparison of $\delta^{13}\text{C}$ and C/N ratio of the organic matter with smectite content of each core. The standard deviation or the analytical error of the different analysis are less than or equal to the size of the symbol.

5.5.2. Dating

Samples for which the ages are deviating from other results from the same core were duplicated and/or measured from a level as close as possible to the first sample, if not enough material was left for a second run. The sample NC04 was measured in a plant macro-rest as well as on bulk material (see Table 10). They delivered ages that differs by almost 600 years. This demonstrates the potential biases of the method and only results showing a general correlation were retained avoiding age reversals (Figure 48). Multiple reasons might be responsible of this difference such as a mixture of organic matter from different sources and ages as well as sediment focusing and/or reworking, for example.

To fill the gap of the absolute dating and refine the age model, two complementary approaches were used. As shown in Figure 47 the sediments of the three cores are considered to be non-heavily bioturbated and thus usable and robust enough to be dated with relative dating methods as the two used in the present paper. The first approach was to compare the radiocarbon ages to the presence and relative abundance of minerals that can be linked to variations in climate. As discussed in Chapter 3, smectite is a neo-formed mineral that in the Linyanti-Chobe region can be related to climate variations. Its relative presence in the sediments is considered as relevant to correlate the three different sites (chapter 5.5.1 and Figure 47). Figure 48 shows the age model after combining the radiocarbon ages with the correlated peaks of smectites and Figure 49 shows the estimated ages for each sample after combining the two methods. A second innovative approach to improve the age

model uses microbiological data as an environmental proxy (Chapter 4). A correlation of the profiles of the three cores using variations in the total and the lysis-resistant communities as well as the thermophile and sulphur-oxidizers bacteria confirms the age model primarily constructed with the ^{14}C dates. The combined dataset is summarized in Figure 51-54 showing the correlation of the microbiological communities and the proposed new age model.

5.5.2.1. Limitations of ^{14}C dating in this lake

The shallow water levels of this lacustrine system along with the seasonal flooding of this region may lead to an almost total desiccation of the basin (Chapter 4) during extended periods. As a result the sediments can be reworked or even fully removed, hence perturbing the original ^{14}C composition. The development of vegetation from various sources (lacustrine, shore plants, etc.) as well as an equally varied biological activity (roots, termites, bioturbation in general) may possibly perturbate the ^{14}C composition. The low presence of the ^{14}C isotope in proportion to other carbon isotopes makes it more sensitive to reworking events. A reworking of the sediment will therefore have a more marked impact on the resulting isotopic signal for this isotope compared to stable isotopes. The resulting biases in its measurement are therefore better marked than in the measurements of stable isotopes and make its use more sensitive. This is the reason why we choose in this work to be wary of the radiocarbon results while taking the stable isotope results with more confidence. This problem of representativeness compared to abundance can also be done in relation to other analyses (as clays, microbial communities,...).

5.5.3. Correlation using clay minerals

By analogy to the studies by Setti et al. (2014), the abundance and type of clay minerals allow for an interpretation of the past weathering conditions and hence indirectly of past or present changes in climate. In Chapter 3 have noted several distinct levels with higher relative amounts of smectite in the soils of the Linyanti-Chobe basin. A total of six horizons with higher relative abundances of smectite were identified in the three cores over the last 5,424 years (Figure 50). Each peak of smectite may correspond to a wetter period compared to the intervals between these peaks. Four peaks were identified in the Center Core that, according to the radiocarbon ages, covers the last 5,424-420 yrs. Based on these ages the four peaks can be dated at about 5424, 2933, 1500, and 770 years BP. The North Core (1618-51 years BP) encompasses three peaks that are tentatively correlated with the Center Core: 1416, 773, and about 206 years BP. The most recent peak would not be present in the Center Core. For the South Core (covering 950-0 years BP), three peaks are indicated and these could be interpreted to correspond to the North and Center Cores peaks at: 780, 259, and finally a last peak at about 0 years BP. This correlation is, however, only valid if there was no substantial sediment reworking or that there are no erosional gaps in the three studied cores. The latter appears to agree with the organic matter content and isotopic composition of the sediment that do not attest of an important reworking (chapter 5.5.1 and Figure 47). Furthermore, the very flat area with the very even topography make difficult to support a high erosive system able to drastically erode the deposits. Because this is difficult to corroborate using only this approach we have used a second, independent approach to help correlate the relative ages between the three cores as discussed below.

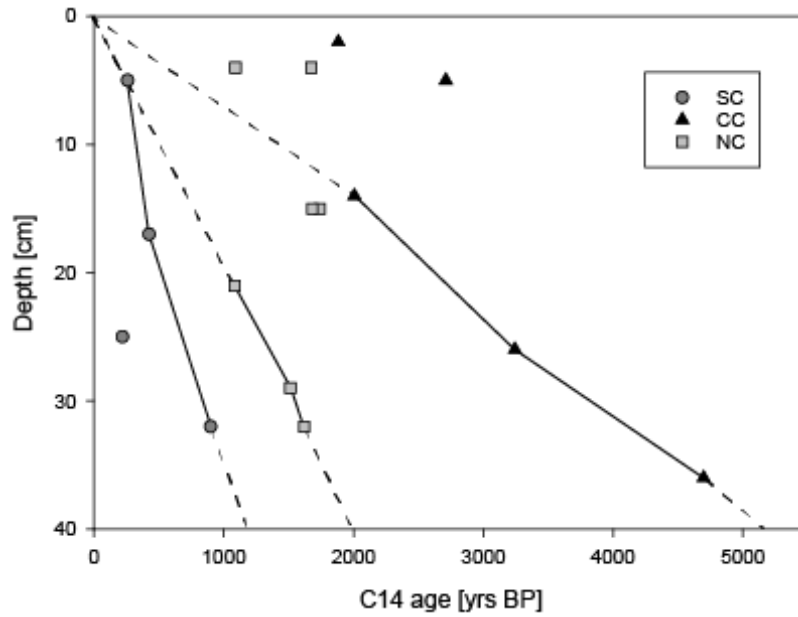


Figure 48 Projection of the ^{14}C ages obtained according to the depth of the samples. The link between certain samples presents a straight line connecting age 0. These samples were kept in the age model constructed in the present study. The other samples were estimated to be biased and in fact not kept for the age model.

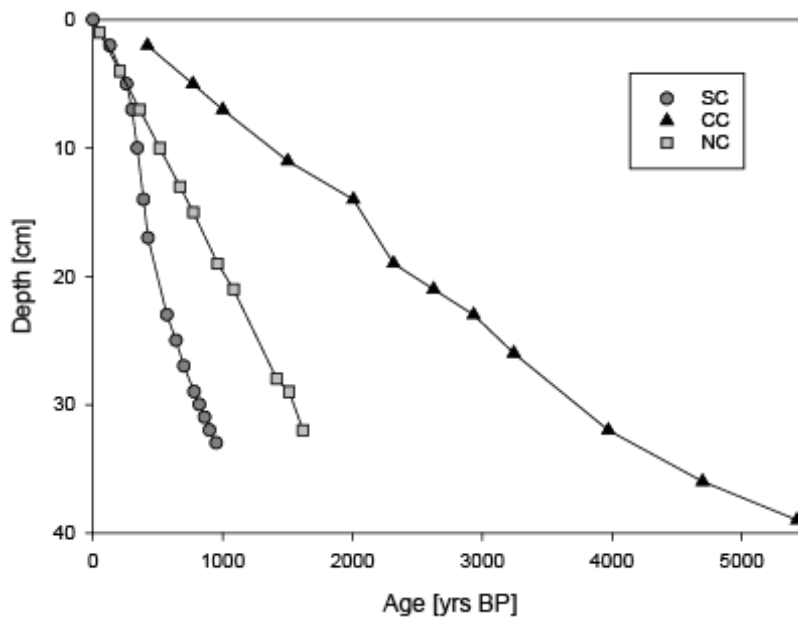


Figure 49 Age model obtained by combining the ^{14}C ages and the correlation of the peaks of smectites (Figure 50) and the microbial communities (Figure 51-54) between the three cores. They do not modify drastically the projections obtained in Figure 48.

Dating the sediments of Lake Liambezi

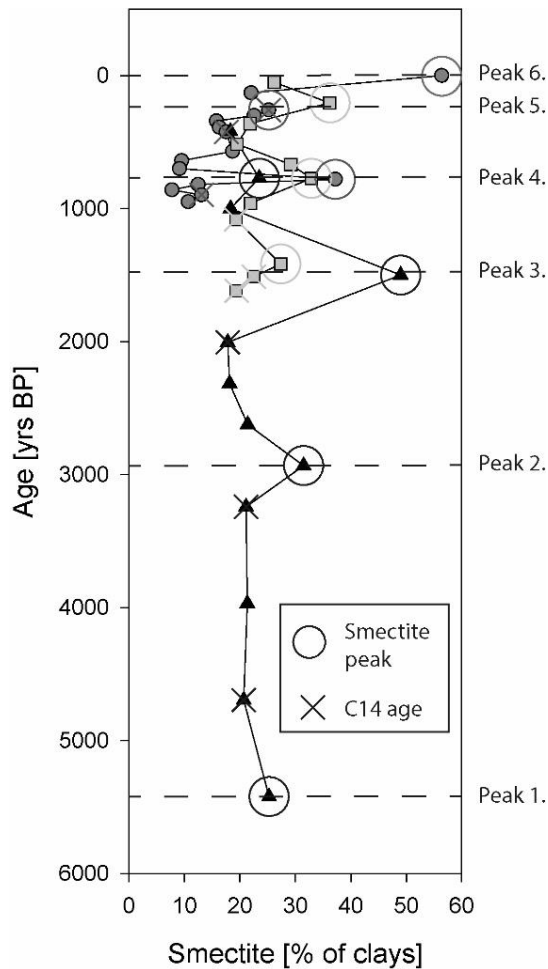


Figure 50 Projection of the ages preserved with the smectite composition of the samples. Smectite peaks represent wet periods when a greater amount of smectite is formed. A correction of the age projection obtained with Figure 48 was performed so that the smectite peaks correspond from one core to another. Six peaks are represented in all for the period of the last 5424 years BP. The ^{14}C ages which were selected are marked with a cross.

5.5.4. Correlation using microbiological communities

Analysis of the bacterial community composition (BCC) of the three cores indicates a variability that depends first and foremost on the site itself and its own unique environmental characteristics, but with trends that are similar for both the total and the lysis-resistant communities (Chapter 4; Figure 51 and Figure 52). A cluster analysis for their entire population supports a site dependent grouping of the samples exposing substantial similarities between them (except the upper samples from the North and Centre Cores) (Figure 51 and Figure 52). The specific environmental conditions of each site such as local morphology, water depth and/or their relative vicinity to the tributaries are the main drivers of the BCC. While site-specific environmental conditions primarily govern the BCC, larger changes at a lake scale influence the observed variations into each group of samples (Figure 51 and Figure 52). Changes imposed on a global scale, such as extended periods of dry and wet conditions (at climate-relevant scales of centuries or more), changes in the hydrological regimes, and global ecological changes (Chapter 4) are the cause of these internal changes into each group of samples. These changes are sufficiently pronounced so as to allow them to be correlated between the three sites and hence offer an additional correlation tool for relative dating.

Although the bacterial communities appears to be site dependent, main changes in their composition occur at the same time in all cores (better seen with North and South Cores due to close time covering; Figure 54). This indicates that changing environmental conditions drove a change in the BCC at all sites. Climatic changes are supposed to affect the whole system, independently of the

sampling location. The heterogeneity of the sampling sites explain the differences in the BCC at each site, although the changes appear to occur simultaneously. The observed correspondence between the cores, with simultaneous changes in the BCC, highlight the consistency of the constructed age model.

The selection of specific metabolisms (sulphur-oxidizing and thermophilic bacteria) has been proposed as an alternative approach for the inference of environmental drivers based on the analysis of the BCC, which is limited by the complexity of the bacterial community (Chapter 4). Their abundance and distribution across cores make them ideal candidates for that purpose as they present a very active sulphur cycle and potential hydrothermal activity in Lake Liambezi. The correlation of the abundance patterns of sulphur-oxidizers and thermophiles in the three cores (total community) illustrates the effect of the corrections made in the age model contributed by the analysis of the BCC and geochemical proxies (smectite, $\delta^{13}\text{C}$ and C/N) (or illustrates the coherence of the elaborated age model). When the relative abundances of sulphur-oxidizers and thermophiles are displayed across a common time line for the three cores (Figure 53), the similarity of the patterns of abundance and community composition are striking. Thermophilic bacteria are highly abundant in the lowest section of the Centre Core (5424-3970 years BP). The next peak in thermophilic bacteria occurs in the lower section of the North Core for the period covering 1618-1416 years BP. This peak is found in the Centre Core at sample CC08 as well. The next two peaks are also noteworthy. They are found at the lowest section of the South Core with samples SC22-21 (898-860 years BP) and SC19 (780 years BP) and correlate with samples NC11-10 (773-670 years BP). The correlation between the three cores based on sulphur-oxidizing bacteria focuses on the presence or absence of a bacterial set more than on their absolute quantity (peaks). As abundance peaks are more difficult to link, given slightly different conditions in each site, the set seems to be more relevant and permits similarities across the three sites to be correlated. This is the case for samples NC15-14 showing a similar set than samples CC06 and SC12 (period running from 1082-898 years BP). The period covering samples NC11-10, CC03 and SC17-19 (780-640 years BP) also show similarities; The upper part of the three cores includes a similar set of bacteria as well (NC08-02, CC02 and SC16-01; 570-0 years BP). The correlations in the presence/absence of bacterial sets can be assumed to be the result of environmental modifications that have an impact on all the three micro-ecosystems simultaneously. The environmental implications will be discussed in Chapter 6.

Dating the sediments of Lake Liambezi

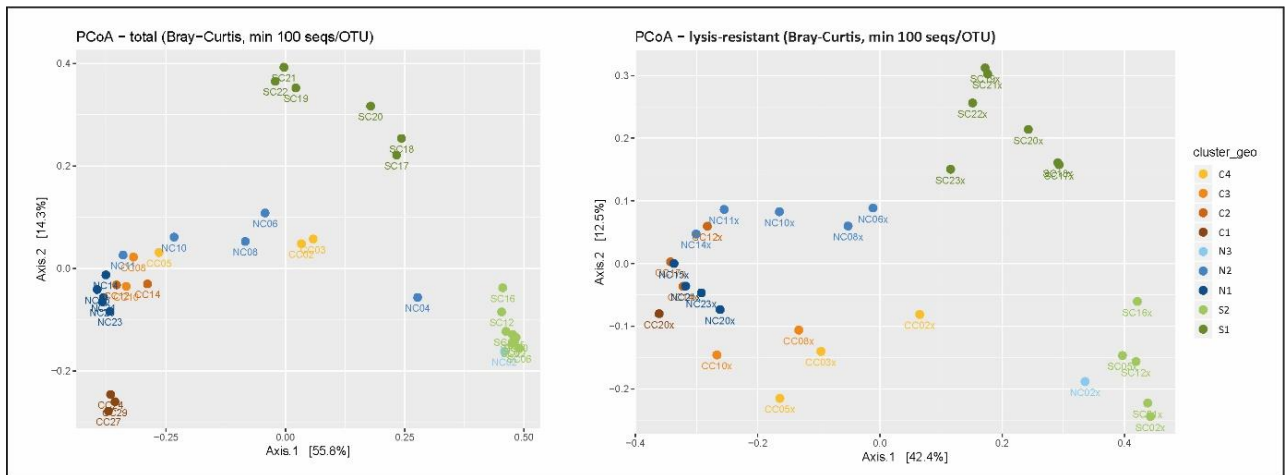


Figure 51 Principal coordinates analysis (PCoA) triplot of the total and the lysis-resistant communities based on Bray-Curtis dissimilarity and Hellinger transformation of the OTU table. OTUs represented by less than 100 sequences in the whole dataset were removed from the analysis. Colours correspond to the main grouping of samples defined for each core, identified from the visual characterization of the sediments.

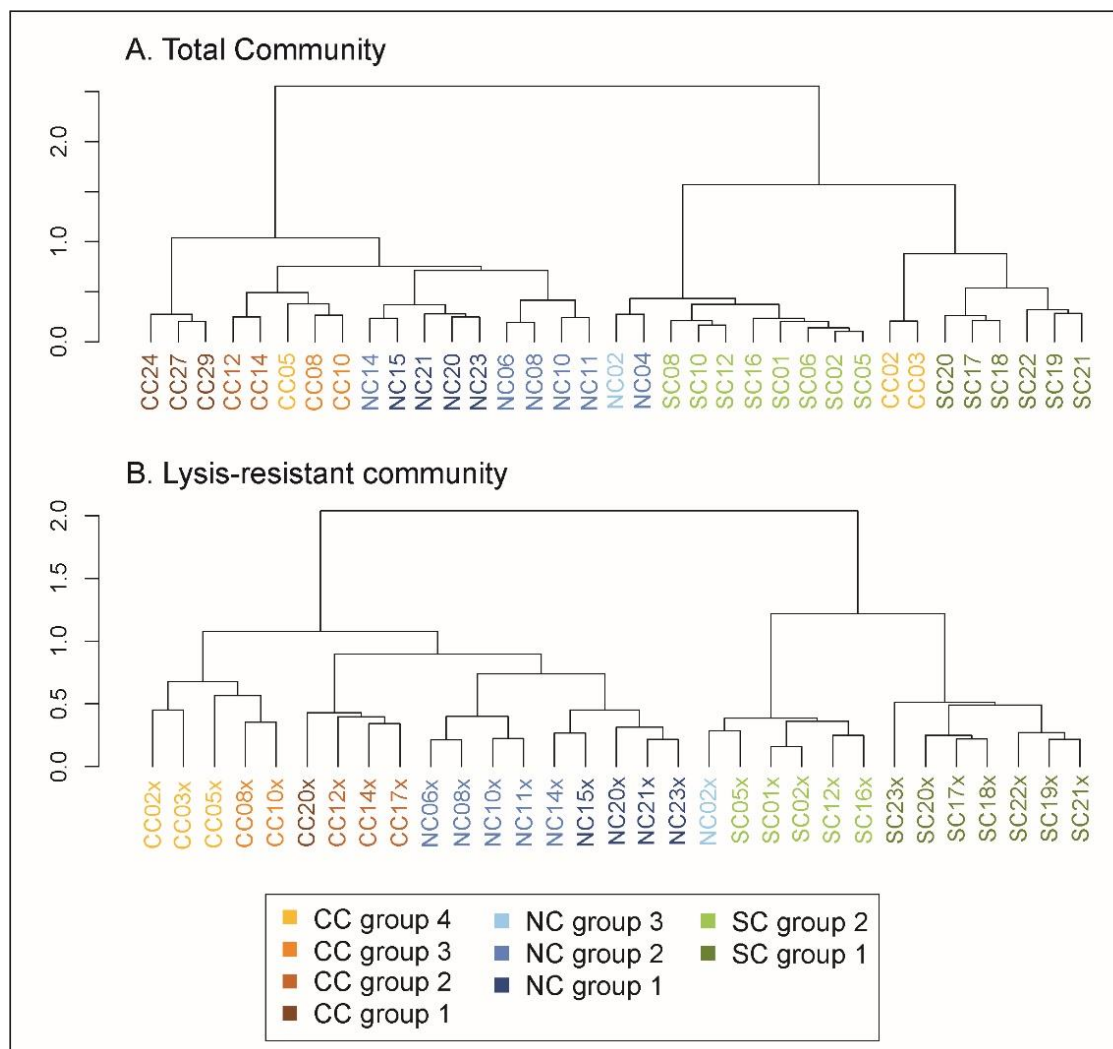


Figure 52 Clustering analysis using Ward algorithm of the (A) total community and (B) the lysis-resistant community. Distance between samples were calculated using Bray-Curtis dissimilarity based on the Hellinger-transformed community table. For each community, only the OTUs with at least 100 sequences among all samples were kept.

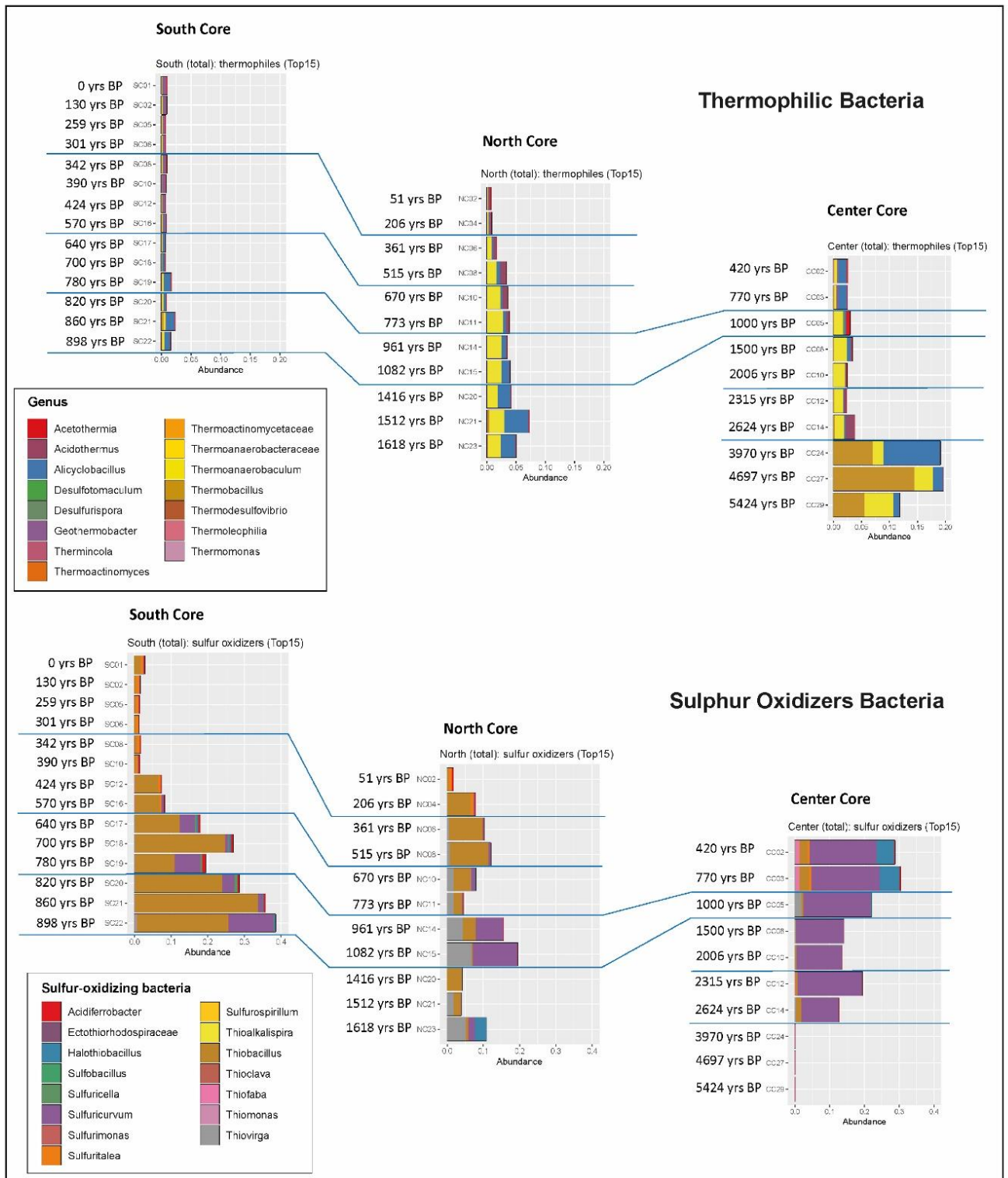


Figure 53 Estimated ages added to the different samples with the rapprochement through similarities in the grouping of genus in the communities of thermophilic bacteria contained in sediments for the upper figure and sulphur oxidizers bacteria for the bottom figure. The rapprochement are shown with blue lines.

Dating the sediments of Lake Liambezi

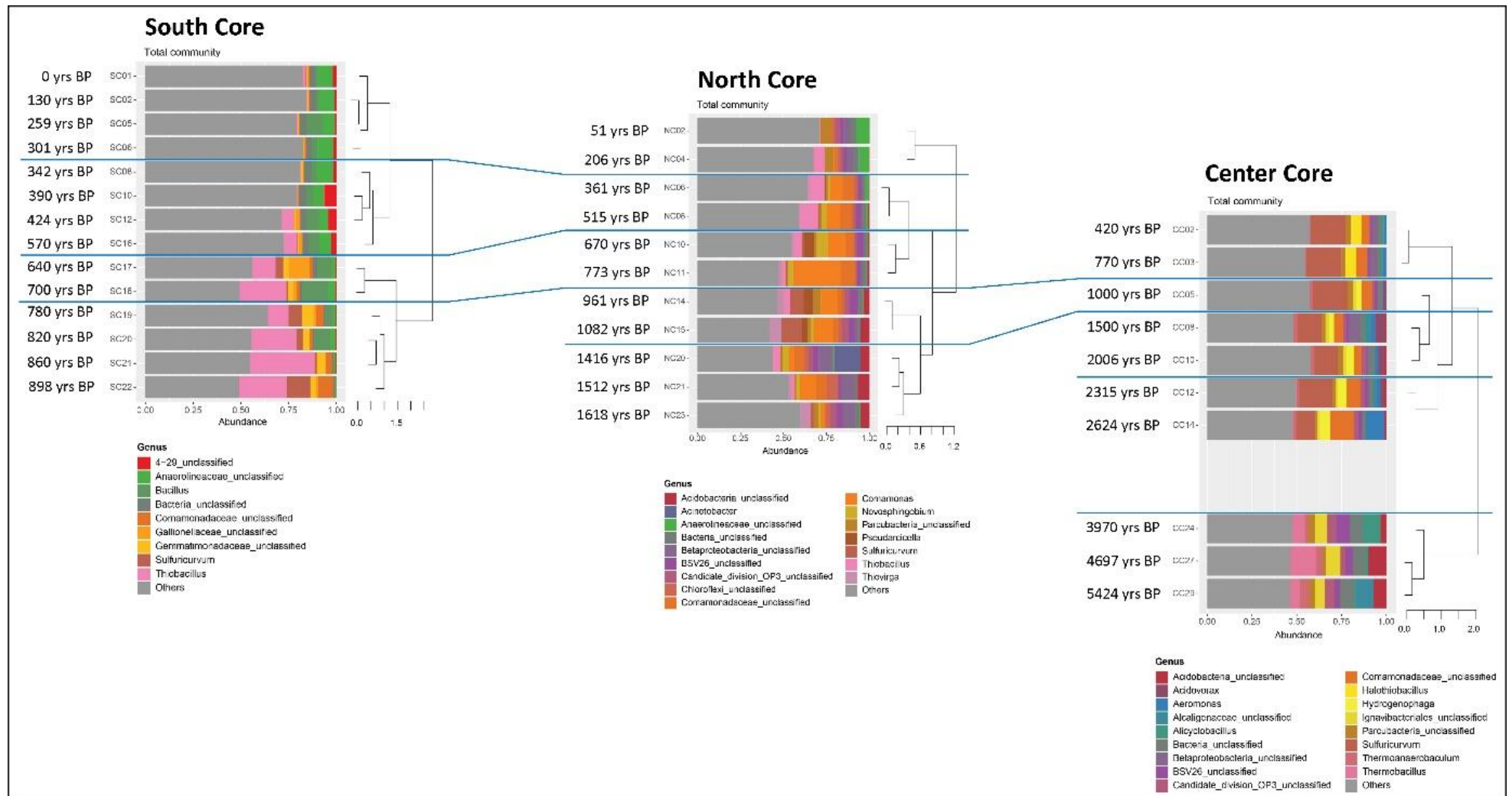


Figure 54 Characterization of the total bacterial communities, based on 16S rRNA gene amplicon sequencing. Only the most abundant genera (>2% of the community in average or >5% in one sample) are shown. Constrained hierarchical clustering was performed using the *chclust* function based on Bray-Curtis dissimilarity and the Hellinger-transformed community table. For each community, only the OTUs with at least 100 sequences among all samples were kept. The age model was built regarding the link made between the three cores relating to the clustering model. The link are connected with blue lines.

5.5.5. Average vertical accretion rate

As explained in Frouin et al., 2007, the term accretion rate (expressed in cm/year) is preferred to the term sedimentation rate due to its dependence to the topography. A slight change in the topography (aka geomorphology) of the site and the vertical accretion rate is changed (Frouin et al., 2007, Bennett & Buck, 2016). If the topography of the site does indeed seem to play an important role for the three sampled sites, their geographical location must also be taken into account. The South Core has the highest vertical accretion rate (1 cm/30 years). Its location in the middle of the narrowest basin (between the northern and central basins; Fig. 1) as well as its location close to the mouth of the Chobe River and not far from that of the Linyanti River may explain this. In fact this basin may have been independently created by recent tectonic movements along the Chobe fault. The North Core presents a rather similar situation, however in a slightly larger basin and to a greater distance from a river mouth (Bukalo channel). This explains a lower vertical accretion rate (1 cm/51 years). The Central Core presents a much more flared topographic situation as well as much more diffuse sources of sediment (the site is in a more external position compared to the two main basins). This results in a lower vertical accretion rate (1 cm/115 years) and it may even be affected by several stages of erosion because of a spillage of water into the southern basin. The given values are average values extrapolated over the entire depth of the core. With changes in climate, topography, and hence related geomorphology, all basins may have experienced periods of preferential deposition versus periods dominated by erosion with a renewed steepening of the gradient through tectonic block-faulting.

5.6. Conclusion

As part of a multidisciplinary study on the paleoenvironmental and -ecological evolution of Lake Liambezi, three sedimentary cores have been radiocarbon dated. The cores have been retrieved in three different sites along Lake Liambezi. In order to correlate the three sites and to place the two preceding studies into a time frame, a series of samples have been radiocarbon dated using the organic matter present in the sediments. However, features such as seasonal flooding and associated, climatically and tectonically driven changes in past and present lake levels complicate the establishment of a simple age model. This complexity provides a potential bias for the ^{14}C data and the true relative chronology requires independent estimates of relative ages based on the mineralogy and also the microbiological communities preserved in the three cores. These data were compared to the ^{14}C data that is more sensitive to local bioturbation, deep root penetration of present-day vegetation, and/or localised sedimentary reworking by, for example, termite communities. The shallow depth of the lake, the low accretion rate as well as a substantial biological activity may explain this situation. Nevertheless, a general trend in relative ages can be established for each of the three sites correcting and extrapolating some of the key radiocarbon results for the three cores as absolute markers. The first approach uses the bulk mineralogical changes as an estimate of relative, climate-driven changes (cf Chapter 3). The second approach is based on an innovative, new microbiological community interpretation (cf Chapter 4). Total bacterial communities but sulphur-oxidizers and thermophilic bacteria as well change uniquely throughout the three sediment cores and their presence/absence may be used to correlate the three cores and validate the proposed age model based on a reduced number of key ^{14}C results to establish a quite robust chronology.

Our results indicate that the North Core covers the time interval between 1618 and 51 years BP, whereas the Central Core between 5424 and 420 years BP, and from 950 years BP to present for the South Core. Hence the three cores are to be used in a staggered fashion, covering different, only slightly overlapping periods of sedimentation within the larger Lake Liambezi hydrological system, likely because of tectonic movements along the faults within this region.

5.7. References

- Bennett, K.D. & Buck, C.E., 2016. Interpretation of lake sediment accumulation rates. The Holocene I-II.
- Burrough, S.L., Thomas, D.S.G., 2008. Late Quaternary lake-level fluctuations in the Mababe Depression: Middle Kalahari palaeolakes and the role of Zambezi inflows. *Quaternary Research* 69, 388-403.
- Cavaillé-Fol, 2020. On a découvert le berceau de l'Humanité. *Science & Vie*, N°1233, juin 2020, 56-71.
- Frouin, M., Sebag, D., Durand, A., Laignel, B., Saliege, J.F., Mahler, B.J., Fauchard, C., 2007. Influence of paleotopography, base level and sedimentation rate on estuarine system response to the Holocene sea-level rise: The example of the Marais Vernier, Seine estuary, France. *Sedimentary Geology*, 200, 15-29.
- Haddon, I.G., McCarthy, T.S. 2005. The Mesozoic–Cenozoic interior sag basins of Central Africa: The Late-Cretaceous–Cenozoic Kalahari and Okavango basins. *Journal of African Earth Sciences* 43, 316-333.
- Hajdas I. 2008. Radiocarbon dating and its applications in Quaternary studies. *E&G Quaternary Science Journal* 57.
- Hajdas I., Bonani G., Furrer H., Mäder A., Schoch W. 2007. Radiocarbon chronology of the mammoth site at Niederweningen, Switzerland: Results from dating bones, teeth, wood, and peat. *Quaternary International* 164–165:98–105.
- Mutelo, M.A., Murwira, A. & Kileshye-Onema, J.M., 2013. An understanding of variations in the area extent of Lake Lyambezi: Perspective for water resources management. Unpubl. Master of Science in Integrated Water Resources Management of the University of Zimbabwe.
- Peel, R.A., Tweddle, D., Simasiku, E.K., Martin, G.D., Lubanda, J., Hay, C.J., Weyl, O.L.F. 2015: Ecology, fish and fishery of Lake Liambezi, a recently refilled floodplain lake in the Zambezi Region, Namibia. *African Journal of Aquatic Science* 40:4, 417-424.
- Ramsey CB. 2009. Bayesian Analysis of Radiocarbon Dates. *Radio* 51:337–360.
- Reimer PJ., Bard E., Bayliss A., Beck JW., Blackwell PG., Ramsey CB., Buck CE., Cheng H., Edwards RL., Friedrich M., Grootes PM., Guilderson TP., Hafliadason H., Hajdas I., Hatté C., Heaton TJ., Hoffmann DL., Hogg AG., Hughen K., Kaiser KF., Kromer B., Manning SW., Niu M., Reimer RW., Richards DA., Scott EM., Southon JR., Staff RA., Turney CSM., van der Plicht J. 2013. IntCal13 and Marine13 Radiocarbon Age Calibration Curves 0–50,000 Years cal BP. *Radiocarbon* 55:1869–18874.
- Seaman, M.T., Scott, W.E., Walmsley, R.D., van der Waal, B.C.W., & Toerien, D.F. 1978: A limnological investigation of Lake Liambezi, Caprivi. *Journal of the Limnological Society of Southern Africa* 4:2, 129-144.
- Setti, M., López-Galindo, A., Padoan, M., Garzanti, E. 2014. Clay mineralogy in southern Africa river muds. *Clay Minerals*, 49, 717-733.
- Stuiver M., Polach HA. 1977. Discussion Reporting of 14C Data. *Radiocarbon* 19:355–363.
- Tweddle, D., Weyl, O.L.F., Hay, C.J., Peel, R.A., Shapumba, N. 2011. Lake Liambezi, Namibia: Fishing community assumes management responsibility. Technical Report no. MFMR/NNF/WWF/Phase II/4.

6. Lake Liambezi: a climatic and environmental record for the last 5500 years BP through a multidisciplinary study

Anael Lehmann^{1*}, Christophe Paul^{2*}, Daniel Ariztegui³, Pilar Junier^{2&}, Torsten Vennemann^{1&}

* These authors contributed equally to this work

¹Laboratory of Stable Isotope Geochemistry. Institute of Earth Surface Dynamics, University of Lausanne, Lausanne, Switzerland.

²Laboratory of Microbiology, Institute of Biology, University of Neuchâtel, Neuchâtel, Switzerland.

³Laboratory of Limnogeology and Geomicrobiology, Department of Earth Sciences, University of Geneva, Geneva, Switzerland.

[&]Co-Corresponding authors: Torsten Vennemann. Laboratory of Stable Isotope Geochemistry. Institute of Earth Surface Dynamics, University of Lausanne, CH-1015 Lausanne. Mail: Torsten.Vennemann@unil.ch; Phone: +41216924464. Pilar Junier. Laboratory of Microbiology. Rue Emile-Argand 11, CH-2000 Neuchatel. Mail: pilar.junier@unine.ch; Phone: +4132718224; Fax: +41327183001.

6.1. Abstract

Wetlands in arid climates are unique ecosystems which represent a source of life-supporting water in an otherwise inhospitable environment. They are of major importance for an often specialized flora and fauna. These environments are, however, particularly fragile ecosystems as they respond sensitively to any climatic or environmental change. North Botswana holds the second largest endorheic delta system in the world in the north part of the Kalahari Desert. Structural features formed by the neo-tectonic activity affect the regional hydrological system and create a complex network of rivers, deltas and waterbodies. It leads to the creation of multiple basins with sedimentary records of the climatic conditions and the environmental evolution of the region. However, the records are sparse, scarce and short due to the constant evolution of the waterbodies. Lake Liambezi, located middle of the Linyanti-Chobe Basin, offers thus a unique sediment record of this central region. The complexity of studying continental sediments brought the project to a multidisciplinary study. It regroups the work of three companion papers using classical tools in sedimentology, mineralogy and geochemistry but also an innovative approach using sedimentology. It encompasses the nature of the sediments, their origin and their deposition processes, the evolution of the sediments and finally the dating of the three sampled sediment cores.

The aim of the present work is to correlate and coordinate all the results previously obtained and get a global reconstruction of the environmental and climatic evolution of Lake Liambezi for the last 5500 years BP.

In response to previous studies aiming to give a climatic evolution for the region, we propose a much precise and detailed climatic reconstruction for the recent past (last 5420 years BP). Formation and evolution of Lake Liambezi in two elongated basins seem related to the tectonic activity linked to the Okavango Graben. The north basin has probably been formed at about 5420 years BP in a tectonic opening. A supposed extension towards the northeast of this first basin is believed to occur around 1650 years BP. At about 1000 years BP, a second basin is believed to open in the south of the first basin following the last recorded tectonic event affecting the lake. Presence of thermophilic bacteria seems

to support a tectonic action in the different evolution of the lake's shape. Successively, the resulting depressions are filled with lacustrine and fluvio-deltaic sediments. Sediment type and content are driven by the environmental conditions resulting of the watershed, the climate and the morphology of the site.

The formation and evolution of the lake seem to be closely related to the regional tectonic activity and tend to demonstrate a recent activity of the Okavango Graben system. We see in the present study one more example of the importance of the tectonic activity in the evolution of the different rivers, deltas and waterbodies of the region. The evolution of the different ecosystems related to water availability must therefore be thought through a probable tectonic activity, at least for part of their evolution.

6.2. Introduction

Wetlands in arid climates represent unique ecosystems and are of major importance for an often specialized flora and fauna. They represent a source of life-supporting water in an otherwise inhospitable environment. These environments are, however, particularly fragile ecosystems as they respond sensitively to any climatic or environmental change. North Botswana region is made of an epeirogenic uplift that formed the Kalahari Basin (Haddon & McCarthy, 2005; Singletary et al., 2003; Jones *et al.*, 1980). North part of this basin is crossed by an incipient continental graben found at the terminal of the southwestern branch of the East African Rift System (Bufford et al., 2012; Haddon & McCarthy, 2005; Jones et al., 1980). It forms a topographic depression filled with Quaternary lacustrine and fluvio-deltaic sediments and is bounded by northeast-trending normal faults called the Okavango Graben. These faults affect the course of the rivers Okavango, Kwando and Zambezi and forms the second largest endorheic delta system of the world with the two rivers Okavango and Kwando and the partial deviation of the Zambezi named Chobe (Bufford et al., 2012). Structural features formed by the neo-tectonic activity affect the regional hydrological system (Kinabo et al., 2007) and create a complex network of rivers and waterbodies (Haddon & McCarthy, 2005). Burrough and Thomas (2008) present an example of this phenomenon with the evolution of the paleolakes of the middle Kalahari, also considered to be the cradle of humanity (Cavaillé-Fol, 2020).

The basin formation of North Botswana does permit the sedimentary records of the climatic conditions and the environmental evolution of the region. However, the constantly evolution and move of the few lakes of the region renders the continental sediment record sparse, scarce and short (e.g. Burrough et al., 2007). Lake Liambezi situated in the middle of the Linyanti-Chobe Basin system offers a unique sediment record of this central region. Because of the complexity of continental sediment, the choice has been made to direct the project in a multidisciplinary way regrouping classical tools in sedimentology, mineralogy, geochemistry and dating as well. An innovative tool using microbiology has been added to enrich the study with invisible information for the more classical tools. The multidisciplinary approach did permit to enlarge the understanding of the sediment record presented in companion papers treating of the sedimentology-geochemistry-mineralogy (Chapter 3), the microbiology (Chapter 4) and the dating of the sediments (relative and absolute dating by ^{14}C) (Chapter 5). The pooling of these different works allows a global vision of the evolution of Lake Liambezi from its formation to its evolution until its current form. This brings together a history of more than 5500 years. Understanding the different forces present in the North Botswana region allows a better approach for the future evolutions of this system, which are essential for the various surrounding populations.

6.3. Material and methods

6.3.1. Regional settings and lake description

Lake Liambezi is located in Namibia, at the eastern side of the Caprivi Strip. The lake is part of a complex drainage system that includes the Kwando and Zambezi rivers. Its Southern shore makes up the border between Namibia and Botswana. It receives water from the Chobe River (a tributary of Zambezi River, deviated due to the Chobe Fault (Haddon and McCarthy, 2005)), Bukalo Channel (a seasonal tributary of Zambezi River), and Linyanti River (or Swamps, natural deviation of Kwando River due to the Linyanti Fault (Haddon and McCarthy, 2005)), as well as rainwater and local runoff water (Figure 55). Depending on the water level, the Chobe River serves as outflow of the lake (Seaman et al., 1978; Peel et al., 2015). The lake is surrounded by a major flat wetland system characterized by woodlands, wetlands and slow-flowing floodplain rivers (Seaman et al., 1978; Peel et al., 2015). Seaman et al. (1978) reported a system covering some 300 km² of which 100 km² was open water at its full size. The lake changes shape, size and depth between and within years due to the source and the amount of water in the basin (Tweddle et al., 2011). The average depth is of approximately 2.5 m (Seaman et al., 1978) but can reach 7 m at the height of the rainy season (Peel et al., 2015). The general shape of the lake varies depending on the water supply. It is generally separated in two main basins: Northern and Southern basins, which are connected by a narrow 1.3 km long central channel. The Northern basin is approximately 6 km long and 1 km wide at its maximum. It receives water from the Bukalo Channel on the north, from the channel between the two basins on the east and by percolation in its western and southern shores by the Linyanti marsh. The Southern basin is 4 km long and 500 m wide. The West shore receives water by the connecting channel, the Chobe River in the East shore, the Linyanti marsh all along its south-western shore and by the Linyanti channel in the south-east (Figure 55). The Linyanti marsh, surrounding the two basins in their western shores is the result of a geological fault that forms an area of wetlands composed by a complicated patchwork of swamps and marshes. The fault is known as the Linyanti Fault (Haddon and McCarthy, 2005). The set of these features forms the Linyanti River. The Chobe River also flows through a fault named the Chobe Fault (Haddon and McCarthy, 2005).

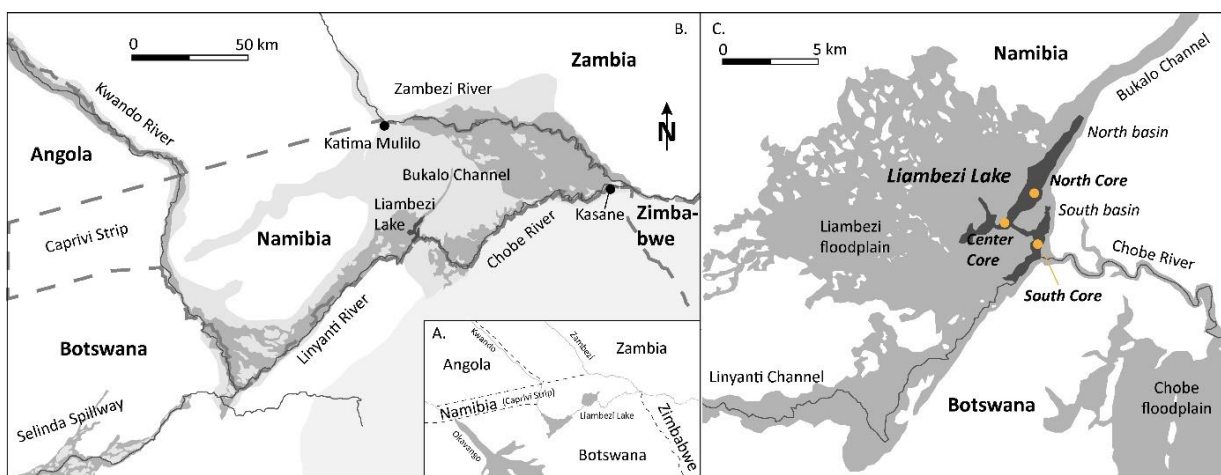


Figure 55 Modified from Peel, 2015. A. General map of the region with the three main river systems: Okavango, Kwando and Zambezi; B. General map of grouped systems Kwando and Zambezi rivers. Kwando River comes out Angola and turns into Linyanti River after its terrestrial delta joins a tectonic fault along the Namibia and Botswana border. It finishes its course into Lake Liambezi mostly into percolating water in Linyanti swamps. Zambezi River coming down Zambia flows into Lake Liambezi through the Bukalo channel and the Chobe River (Haddon and McCarthy, 2005). The Chobe River reverses its flow depending on water availability and can flow in both directions (Seaman et al., 1978; Peel et al., 2015). The very poor relief generates many flood zones that are formed around the rivers of the system as well as around Lake Liambezi (dark grey); C. In dark grey color, map of Lake Liambezi in its full size as described by Seaman et al., 1978. Open-water lake with its two elongated basin is in black. Yellow dots indicate core locations.

6.3.2. Sampling

Three cores were obtained from the same number of sampling locations (Figure 55). Sampling was performed with an Uwitec Hammer Action Corer with PVC tubes of 86.0 mm inside diameter. The center core (CC) was obtained in the northern basin, at its south-eastern side at about 300 meters close to the connecting channel. The south core (SC) was sampled at the southern basin in its central part. It is set at about 250 meters close to the Chobe river mouth, and at about the same distance of both, Linyanti main channel and the connecting channel. The north core (NC) was obtained in the northern basin, in its central part. Its distance to the Bukalo Channel is about 4.2 km. The three cores were transported to the VanThuyne-Ridge Research Center to be opened, cut, described and sampled under the right conditions and the appropriate equipment. Samples from microbiological studies were obtained under a controlled atmosphere using a Bunsen burner to sterilize all the equipment used. Samples were stored and transported in sterile plastic bags and kept refrigerated. Separation of the samples as well as their distribution into groups of samples was carried out on the basis of visual criteria reported in Chapter 4. Sedimentological, mineralogical and geochemical analyses have been done at Institutes of Earth Sciences and Earth Surface Dynamics of the University of Lausanne. A precise description of the different methods is to be found in Chapter 3. The ^{14}C -activity of a selection of samples has been prepared in the laboratories of the Earth Surface Dynamics Institute of the University of Lausanne and measured at the Laboratory of Ion Beam Physics of the ETH Zürich. Precise method is to be found in Chapter 5. Microbiology analyses have been prepared and analysed following methods described in Chapter 4 at the Laboratory of Microbiology at the Institute of Biology of the University of Neuchâtel.

6.4. Results

The results of the present work are a compilation of three companion papers. For the sake of repetition, a precise description of the results will not be made in the present work. All the results and the accompanying discussion used for the present compilation are to be found in the three companion papers. Sedimentology, mineralogy and geochemistry results are to be found in Chapters 4 and 5. Chapter 4 presents also a precise description of the bacterial communities composition. An age model based on a multidisciplinary approach is performed and a precise description of the construction of this age model is made in Chapter 5.

6.5. Discussion

6.5.1. General remarks on sediment characteristics

Sediments are close to condensed series due to a low vertical accretion rate and an important organic matter content. Vertical accretion rate was measured at about 1cm/30yrs and 1cm/115yrs according to the core (Chapter 5 and organic matter amount at about 1.7 to 13.0 % with a mean value at 6.7% (Chapter 3. Vertical accretion rate is preferred to "sedimentation rate" as it is expressed in cm/year and depends partly of the topography (Frouin et al., 2007). With such a low vertical accretion rate, the choice has been made to conduct a multidisciplinary study. A multidisciplinary approach will give the opportunity to crosscheck the observations and measurements between various fields. Major evolutions are thus confirmed through different methods and strengthens the results.

Due to the local climate showing well-marked dry and wet periods, environmental changes might take a certain period of time before to appear in some sediments characteristics. Therefore, a crosschecking of various methods is needed to fix in time a climate or environmental evolution. Some characteristics might indeed present a delay compared to others to fix some changes because of an important resilience.

Based on companion papers, Figure 56 groups together the environmental descriptions and evolutions of each site (Chapter 4, the defined age model (Chapter 5), and the climate assumptions

made after the smectite profile (Chapter 3). Figure 56 presents the delayed record of Center Core which start at about 5500 years BP, North Core at about 1620 years BP and South Core at about 950 years BP. Figure 56 and Figure 59 expose the changes through time of each site. The figures liken the three sites in their environmental evolution in comparison to the climate evolution. These comparisons give a general view of the lake evolution.

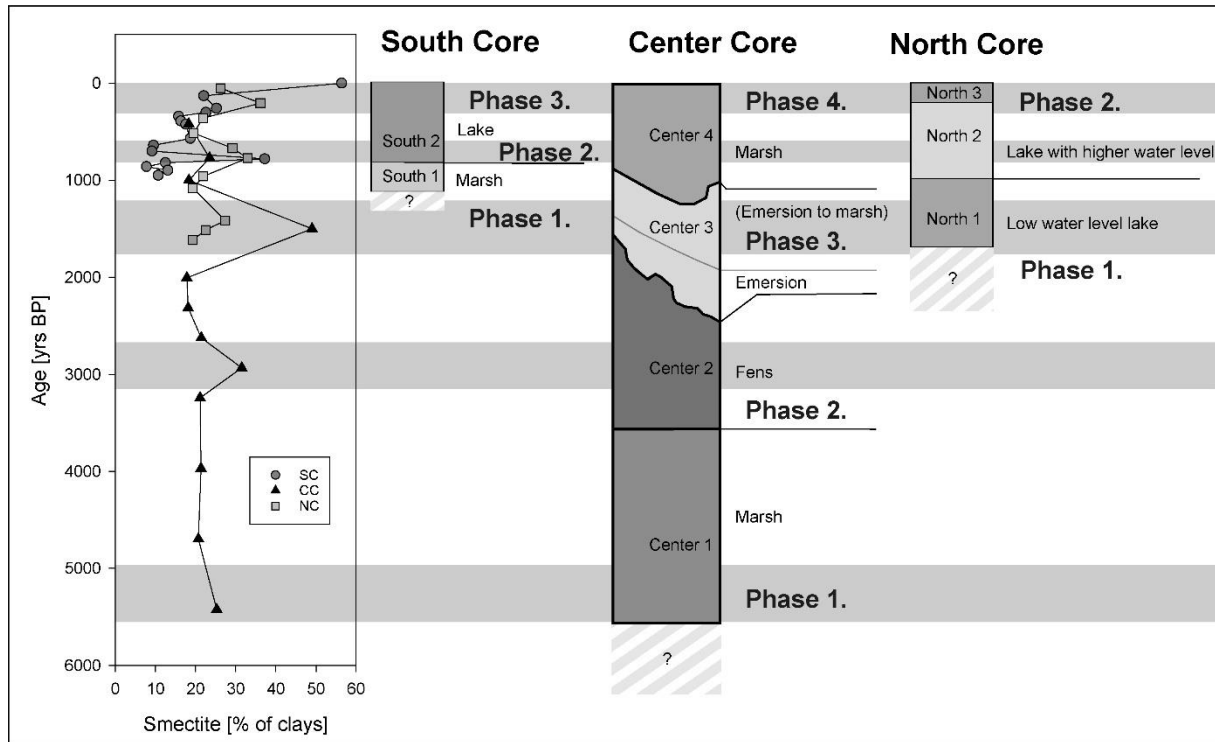


Figure 56 Climatic and environmental reconstruction as well as tectonic assumptions for Lake Liambezi. Climatic reconstruction based on the evolution of the smectite content of the sediments with white-coloured dry periods and grey-coloured wet periods. Integration of the characterization of the sediment deposition environment of the three cores into the climate model while respecting the correlation model of the estimated ages. Addition of tectonic speculations based on various observations following **phase** description of Figure 59.

6.5.2. General climatic reconstruction and comparison to other studies

Paleoclimate records are often scarce, discontinuous and/or loosely dated regarding the interior of southern Africa (Sletten et al., 2012). Furthermore, syntheses of paleoclimate data in this subcontinent have shown that paleoclimate patterns can vary at regional scale. This results in correlation problems between records from different sites with inadequate or even false matches (Sletten et al., 2012 and references herein; Burrough et al., 2007; Thomas et al., 2012). However, all studies seem to agree on a climate event at the scale of the African continent from 14.5 to 5 ka BP called the African Humid Period (AHP). This humid period is attributed to a non-linear response to Northern Hemisphere summer insolation forcing that first strengthened, then weakened the African Monsoon system, amplified by atmosphere-vegetation feedbacks (Berke et al., 2012). Berke et al. (2012) shows that the climate signal linked to AHP is spatially and temporally variable across Africa. The exact dating varies with region. Above all, studies do not agree on the end of this period. Some studies apply for an abrupt end while others for a gradual end (Berke et al., 2012; deMenocal et al., 2000 (Quaternary Science Reviews); deMenocal et al., 2000 (Science); McGee et al., 2013; Pausata et al., 2020; Sletten et al., 2013). Again, the question of variability due to regional characteristics seems to prevail. While these considerations seem to apply for AHP, they can probably concern all the other observed climatic periods. Comparison of the data from this study with similar studies does indeed seem to emphasize this question (Burrough et al., 2007; Thomas et al., 2012; Sletten et al., 2013).

The current study uses clay mineralogy as the main tool for determining climate change for the northern region of Botswana. A detailed and comparative study of the sediment mineralogy of Lake Liambezi has shown that smectite has a different cycle from all the other minerals and clays. It could be shown that smectite was directly related to climate change (Chapter 3). The evolution of the quantity of smectite within a sediment core for Lake Liambezi reflects the alternation between wetter and drier periods. The comparison of the conclusions drawn from this mineral against other proxies can provide indications on the evolution of the climate (such as the quality of the organic matter), with no obvious contradiction. On the contrary, the data complement each other well (Chapter 4 and current Chapter). This approach made it possible to highlight five wet periods for the last 5.5 ka BP. A first period runs from 5400 to 4700 years BP, a second from 3100 to 2650 years BP, a third from 1900 to 1150 years BP, a fourth from 820 to 575 years BP and finally a last one from 301 years BP to today (Table 11).

Comparison with studies of recent climate change in southern Africa shows good match, especially with Sletten et al. (2013) and is detailed in Figure 57 (Burrough et al., 2007; Thomas et al., 2012; Sletten et al., 2013). Sletten et al. (2013) focused on a petrographic and geochemical record of climate change over the last 4600 years taken from a stalagmite in the Dante Cave in north-eastern Namibia. It shows a record of a gradual transition from wet to dry conditions from 4.6 to 3.3 ka BP, a variable but pronounced dry period from 3.3 to 1.8 ka, and a wet but variable period from 1.8 ka to the present with at least three wet/dry cycles. Sletten et al. (2013) showed an evolution similar to the one based on the sediments of Lake Liambezi, except for some dating details.

The beginning of the studied records from Lake Liambezi demonstrate the presence of a wet period running up to 4700 years BP. Sletten et al. (2013) also proposed a gradual transition from a wet period to a dry period. This transition probably corresponds to the recording of the end of the AHP for the regions of northern Botswana and northern Namibia. The end of AHP is also reported in studies by Burrough et al. (2007) and Thomas et al. (2012) within the sites of Drotsky's Cave, Lake Ngami, Panhandle Pollen Record, Molopo Drainage, Linear and Lunette Dunes (SW) and Lake Paleo-Makgadikgadi. The next humid period is recorded from 3100 to 2650 years BP in Lake Liambezi's sediments. Sletten et al. (2013) reported it earlier, from 3340 to 3315 years BP and described it as a brief wet interval. In the other studies, this wet event is also reported for the site of Drotsky's Cave, Lake Ngami, Molopo Drainage, Gaap Escarpment, and Lake Paleo-Makgadikgadi, however with variable dates (Burrough et al., 2007; Thomas et al., 2012; Sletten et al., 2013). Then, Sletten et al. (2013) reported a very dry period which lasted until and 1800 years BP and 1900 years BP for the present study. Then, Sletten et al. (2013) described the start of a wet period at 1800 BP and continuing until today. The onset at 1800 years BP coincides with the beginning of the Iron Age in southern Africa for Sletten et al. (2013), suggesting that wetter conditions facilitated migrations and/or changes in food production that may have contributed to a transition in human technologies and lifestyles. During this last wet period, Sletten et al. (2013) described three wetter peaks at 1300-1100 years BP, 800-680 years BP and 350-50 years BP. Those correspond almost perfectly with the present study which also shows a wet period for the last 1900 years. However, the present study emphasized a slight difference regarding the first wet peak, from 1900 to 1150 years BP. This period corresponds with the records of the sites of Dante Cave, Drotsky's Cave, Lake Ngami, Panhandle Pollen Record, Molopo Drainage, Wonderwerk Cave and Kathu Vlei, Linear and Lunette Dunes (SW) and Lake Paleo-Makgadikgadi (Burrough et al., 2007; Thomas et al., 2012; Sletten et al., 2013). The following wet peak is recorded from 820 to 575 years BP in Lake Liambezi and reported from 800 to 680 years BP in Dante Cave (Sletten et al., 2013). It also shows correspondences with the sites of Lake Ngami and Gaap Escarpment (Burrough et al., 2007; Thomas et al., 2012). The other studies are not detailed enough for the upper part of the records and there is no precise description of more recent times. The last wet period is recorded from 301 years BP to today in the present study and from 350 to 50 years BP in Sletten et al.

(2013). Sletten et al. (2013) referred to particularly humid conditions for the period 230 to 100 years BP and correlated it with the Little Ice Age (LIA). Conversely, the period from 700 to 350 years BP would correspond to the Medieval Warm Period (Sletten et al., 2013).

Roughly, the conclusions of the current work as well as Sletten et al. (2013)'s, well match with the work of Berke et al. (2012). Berke et al. (2012) studied sediments of Lakes Tanganyika, Malawi, and Turkana in tropical East Africa and also observed a progressive end of the AHP, emphasizing wetter and warmer conditions than preceding conditions. Their studies showed drier and colder situations recorded from 5 to 3 ka BP. They then highlighted the presence of LIA with decreasing temperatures for the period from 700 to 150 years BP. Decreasing temperatures could also correspond to the increasing humidity recorded in Dante Cave (Sletten et al., 2013) and Lake Liambezi. Berke et al. (2012) indicated increasing temperatures from about 50 years BP. These increasing temperatures could correspond to the recent lesser wet conditions observed in both Dante Cave (Sletten et al., 2013) and Lake Liambezi. The climatic cooling episodes seem to correlate with deMenocal et al. (2000, in Science)'s study and the present work. Indeed, deMenocal et al. (2000, in Science) postponed a succession of cooling events that occurred at the following periods: 6.0, 4.6, 3.0, 1.9, 0.8 and 0.35 ka BP. All these cooling events reported by deMenocal et al. (2000, in Science) correspond precisely to the wetter period reported in the present study.

Even if some heterogeneity exists according to the sites, and thus displaying some spatial and temporal variations across Africa, the present study establishes an excellent correspondence with the above-mentioned studies.

Works of Thomas et al. (2012) and Burrough et al. (2007) have built reconstructions for the last ~150 ka interpreted in terms of changes in hydrological balance from conditions more humid or more arid than today. Even if today's studies are more spatially detailed with a stronger chronometric underspinning, the results are still controversial (Thomas et al., 2012). The reason is to be found in the sources of paleo-data, which are not based on highly resolved organic or isotope records but rather on interpretation of spatially extensive geomorphological proxies of past environments. Geo-proxies such as landforms associated with lacustrine and aeolian activity, are often used as source of data for reconstructing climate evolution (Thomas et al., 2012; Burrough et al., 2007). When interpretations are compared with other studies, they sometimes show conflict and are sometimes removed from regional climate change syntheses (Thomas et al., 2012). Thomas et al. (2012) warns against a forced interpretation to correlate regional records with more global records taken from ice and ocean cores, that may ignore the complexity within a specific environmental system.

The present study perfectly reflect the danger of regarding spatial geomorphological proxies as proof of a precise climate regime. The discrimination between climate evolution and environmental evolution is perfectly reflected in the Lake Liambezi's sediment. Environmental conditions are firstly related to water availability of the site through its geomorphology and its connectivity to the water network. Climate is second factor only. Therefore, environmental condition of a specific site should not be taken as a climate trend proof. Moreover, Thomas et al. (2012) highlights the importance of local complexity of regional sites. Once again, the water availability through the geomorphology of the site as well as its connection to the water network are to be taken into account. Such water availability, middle of an arid climate might generate a localized climate regime slightly different than climate at a more regional scale. These reasons do permit to better understand such disparities between our climate model and those from the two compared studies. The morphology of Lake Liambezi has been taken into account and a specific climatically mineral has been preferred to reconstruct climate variations for the last 5500 years BP.

Periods of time	Type of climate	Involved samples
5424-4700 years BP	Humid	CC29
4700-3100 years BP	Dry	CC20, CC24, CC27
3100-2650 years BP	Humid	CC17
2650-1900 years BP	Dry	CC10, CC12, CC14
1900-1150 years BP	Humid	CC08, NC20, NC21, NC23
1150-820 years BP	Dry	CC05, NC14, NC15, SC20, SC21, SC22, SC23
820-575 years BP	Humid	CC03, NC10, NC11, SC17, SC18, SC19
575-301 years BP	Dry	CC02, NC06, NC08, SC08, SC10, SC12, SC16
301-0 years BP	Humid	NC02, NC04, SC01, SC02, SC05, SC06

Table 11 Distribution of the climatic evolution of the Liambezi region for the last 5500 years

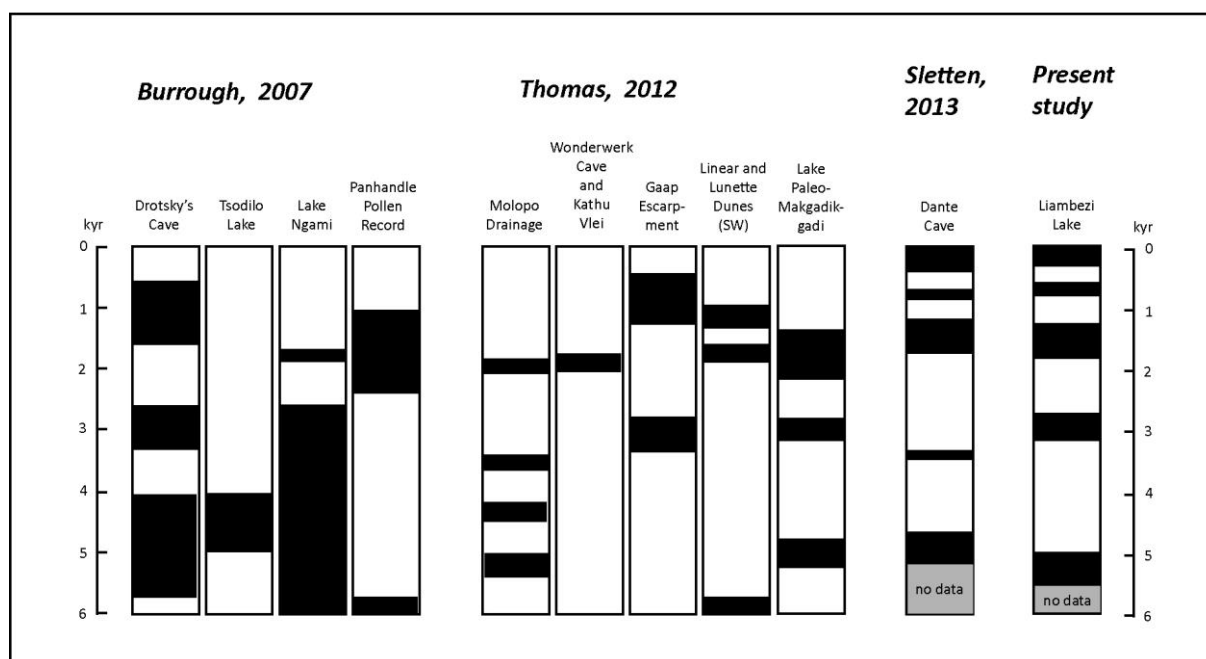


Figure 57 Comparison between the summary works of Burrough et al. (2007) and Thomas et al. (2012), the work on the Dante Cave in northeastern Namibia from Sletten et al. (2013) and the present data. Presentation of the distribution of wet (black) and dry (white) periods for the last 6000 years.

6.5.3. Understanding the environmental evolution of Lake Liambezi

Present regional hydrological systems such as water bodies and rivers in the Okavango Graben are strongly affected by structural features such as sub-basins, depressions and ridges, formed by the neo-tectonic activity of the region (Kinabo et al., 2007). The result is a complex network of rivers and waterbodies (Haddon & McCarthy, 2005). As part of the Okavango Graben, the similar statement is true for the Linyanti-Chobe Basin. The resulting topographic depression are filled with Quaternary lacustrine and fluvio-deltaic sediments (Bufford et al., 2012). Sedimentary records of Lake Liambezi seems to express a similar trend. Its formation and the evolution in shape of its two basins seem to demonstrate a close link with the tectonic activity of the Okavango Graben. We support in the present paper that the three sampled records are the result of the tectonic opening of two distinct basins. A tectonic event might have permitted to open firstly the north basin at about 5420 years BP. The resulting depression was then filled with lacustrine and fluvio-deltaic sediments. The watershed, the climate, the shape of the lake and the resulting environmental conditions for the lake govern then the sediment type, content and quality (Chapters 3-5). The lake and its environmental condition seem to evolve later on with the extension of the north basin and the beginning of the North Core record to accommodate the new environmental context. The record of the South Core seems to demonstrate a

last important tectonic event with the supposed opening of the south basin. These tectonic events theory might be supported with the important presence of thermophilic bacteria and partly with the sulphur-oxidizers bacteria (Figure 64). The mineralogy did not permit to support an active tectonic activity except eventually with a slight increase in the barium quantity top of the Center Core discussed in Chapter 6.5.7. A recent tectonic activity able to influence the formation and shape of Lake Liambezi would help understanding the sediment recording of the three cores.

6.5.4. General history of Lake Liambezi: from its supposed tectonic origin to its filling with lacustrine sediments according to climatic and environmental evolutions

The record of the Center Core, dated at about 5500 years BP might demonstrate the tectonic opening of the northern basin of the actual Lake Liambezi (Figure 58). The opening occurred probably in the southwest part of the current basin and was probably accompanied by hydrothermal features, as the thermophilic bacteria seem to testify (Figure 64). The site recorded a marsh environment. A dry period lasted then from 5000-3100 years BP and causes the drying out of the site. It resulted in the transition from marsh to fens around 3500 years BP. The humid period recorded from 3100 to 2650 years BP did not permit to reverse the progressive drying out of the site. It resulted in the emersion of the site of Center Core. Even if the total emersion of the site was only seasonal or ephemeral, the lacustrine sediments show an important oxidation of the organic matter beyond 2200 years BP (until ~1900 years BP). This emersion is probably the result of the long lasting dry period of about 3100 years (less the 450 years of the brief humid period). However, the Center Core site might also be located at the edge of the active lake basin and thus be more affected by the water level variations.

The record of the North Core since 1620 years BP represent probably a re-activation of tectonic activity in the region with the believed extension of the north basin towards the northeast (Figure 58). It is again supported by a higher presence of thermophilic bacteria in both Center and North Core (Figure 64). A slight difference between the Center Core and the North Core mineralogy might also support the activation of the Bukalo Channel with this extension towards the northeast (Chapter 3). North Core registered a low water level, which is believed to demonstrate the youth of the extension. A humid periods is recorded from 1900-1100 years BP. The extension of the north basin as well as the humid period probably permit to the Center Core site to get re-flooded and to show marsh conditions in its sediments (Figure 56). The North Core site recorded an evolution from low water to higher water level in its sediment with a transition around 1000 years BP. The record of South Core dated around 1000 years BP seems to show a last tectonic event affecting the lake site. This tectonic event is believed to open the south basin (Figure 58). This tectonic activity might be supported with the slight increase of thermophilic bacteria shown in the three cores (Figure 64). South Core recorded a marsh environment, which seems to demonstrate its new formation. The most recent periods (from 800 years BP) show a wetter climate and allow the three sites to be maintained in richer water conditions. South core showed the passage from marsh to lake around 600 years BP. Top part of the Center Core is missing or only partially shown. Its location offset from the two current basins is the reason. The site shows a lower sediment accumulation.

Lake Liambezi : a climatic and environmental record

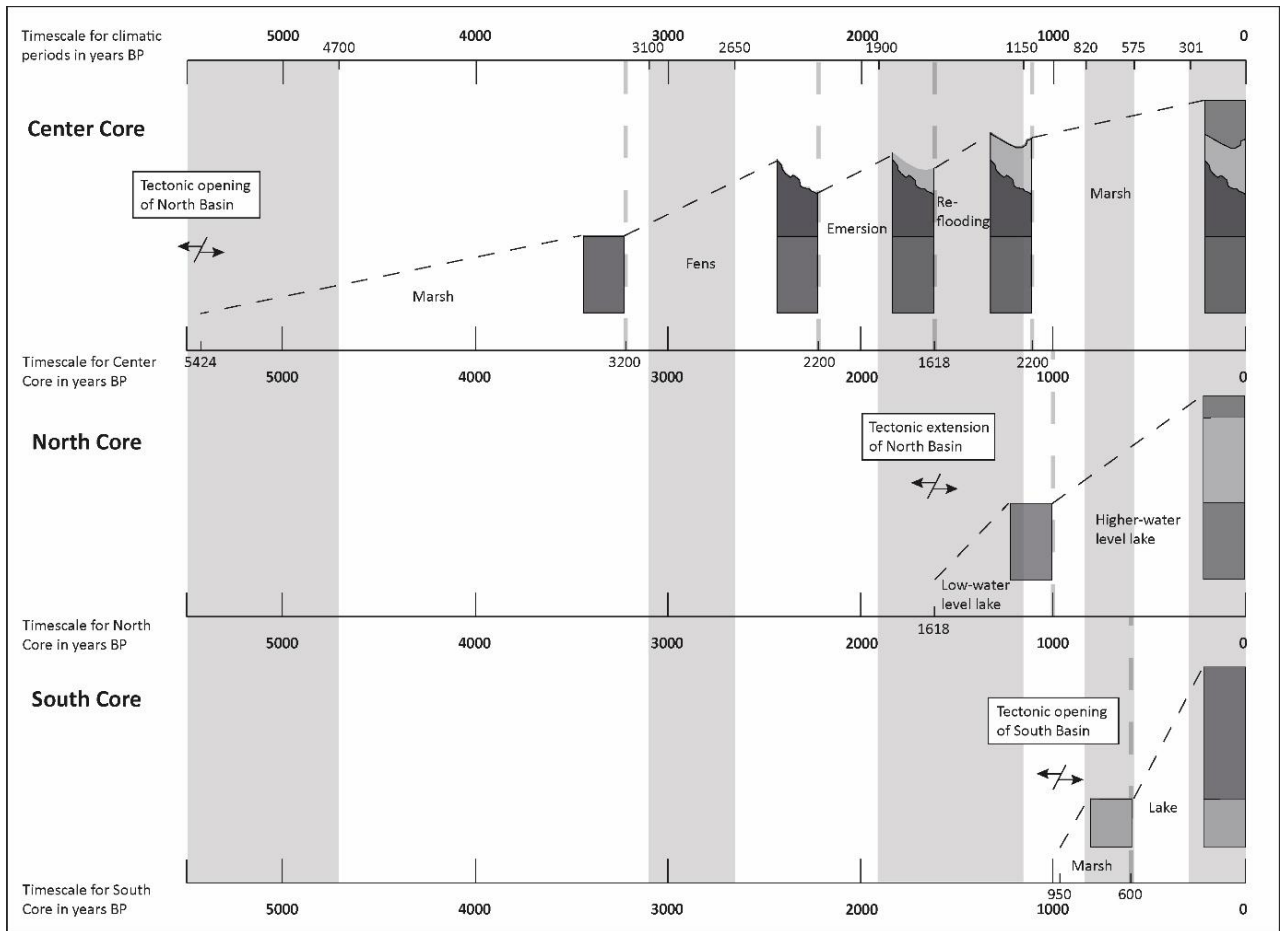


Figure 58 Compilations of various considerations about the climatic evolution of the studied region, the environmental evolution of the three sampled sites, the sedimentological evolution of each core and some tectonic assumptions for the lake. Climatic reconstruction represents wet periods in light grey and dry periods in white. Environmental considerations are separated with light grey dotted lines. Tectonic activity is believed to shape new basins and/or to redistribute rivers course. The new built basins might be then studied thanks to their sediment filling driven by the rivers, the environmental conditions and the climate. Sedimentology does permit to highlight the origin of the sediments, the environmental condition of the site and the climate evolution. However, sedimentology might also suggest through certain signs the presence of a probable tectonic activity.

Lake Liambezi : a climatic and environmental record

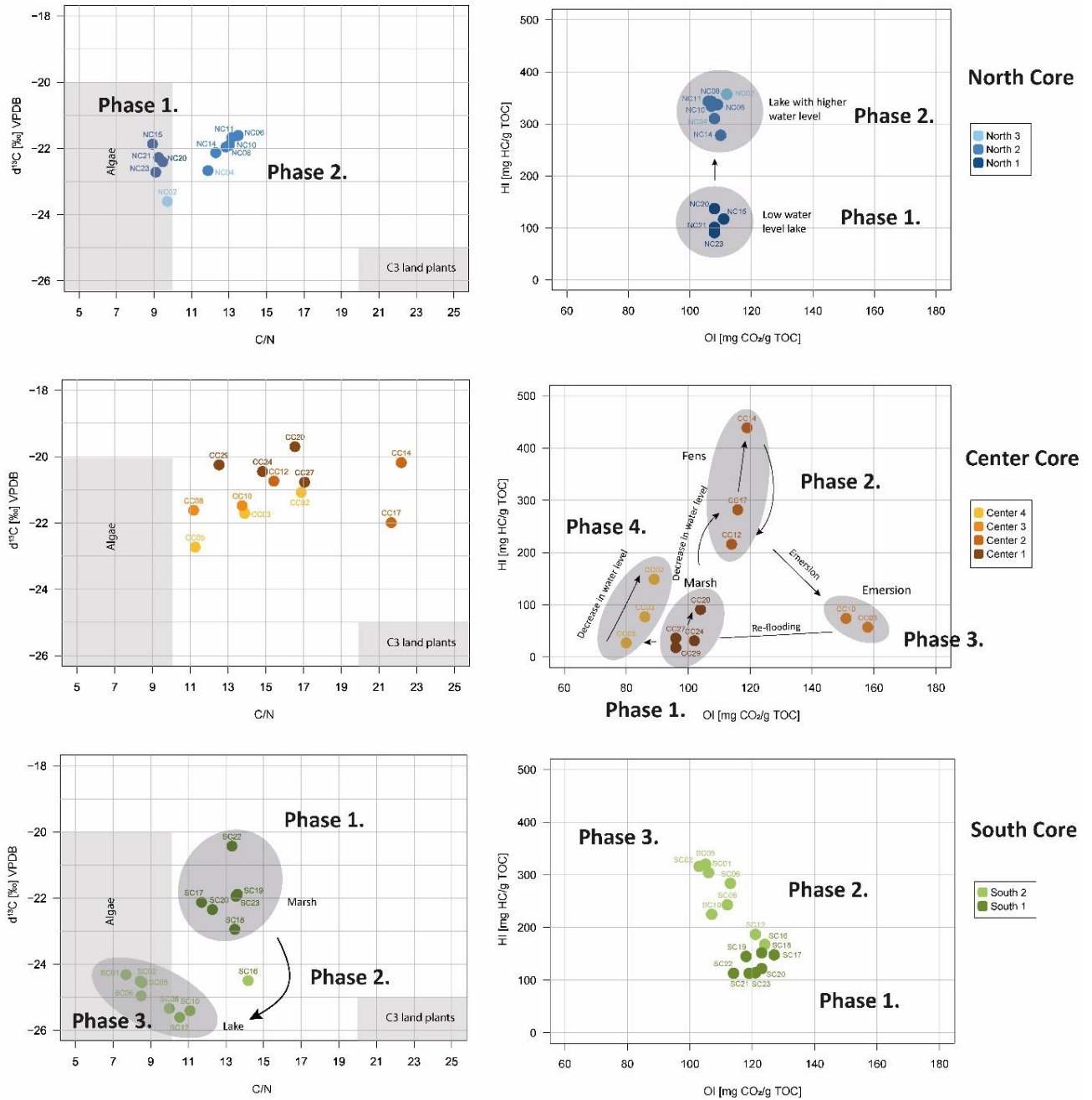


Figure 59 Evolution of the environmental status of the three different sites through the organic matter quality (see further explanation in Chapters 2 and 3). **North core:** **Phase 1.** Extension of the north basin towards the northeast ≥ 1620 years BP; **Phase 2.** Change of environmental conditions and probable connection to the new southern basin ≥ 1000 years BP; **Center core:** **Phase 1.** Opening of the north basin > 5500 yrs BP; **Phase 2.** Extension of the north basin towards the northeast ≥ 1620 years BP; **Phase 3.** The site is located on the outskirts of the main basin (~ 2200 - 1500 yrs BP); **Phase 4.** Re-flooding of the site, environmental evolution and probable connection with the new southern basin ≥ 1000 years BP; **South core:** **Phase 1.** Opening of the southern basin ≥ 1000 yrs BP; **Phase 2.** Transition (samples SC16 and SC12); **Phase 3.** Environmental evolution of the site ≥ 570 years BP.

6.5.5. Grain-sizes: geomorphological evolution in relationship with the evolution of the end-member analysis

The geomorphological conditions of each site are the primary driver of the site's grain-size characteristics. Thus, each phase described for the three sampling sites has a unique end-member signature (Figure 60). The transition to new geomorphological conditions results in the evolution of the proportions of end-members present in the grain-size analysis. This observation increases the argument in favour of a Lake Liambezi evolving mainly according to the tectonic evolution of the faults on which it was formed. For the Center Core, a first major change occurred between samples CC20 and CC17 (between 3200-2900 years BP). The absence of grain-size results for samples CC10 and CC08 does not allow us to observe the evolution of end-members for this level of major importance in the interpretation of the Center Core. However, this lack of results is probably indicative that something affecting the grain-size distribution took place at this time on this site. The end-member analysis for the grain-size distribution of the Center Core shows a site that is not stable and does not show a linear evolution from one situation to another. This shows a site that is constantly changing between a more or less flooded situation, moving from periods of higher water levels where the site ends up in the form of a lake to drier periods where the site ends up in the form of a pond/marsh. These complex transitions seem to correspond with the eccentric situation of the sampling site in relationship to the two main basins.

The geomorphological transition of the North Core site between samples NC15 and NC14 (between 1080-960 years BP) also marks an important transition in the end-member composition for grain-size distributions. Although the transition to the upper samples NC04 and NC02 is not specified by an explicit line in Figure 60, the end-member analysis shows a last major transition under the environmental conditions of the site. These two major transitions mark the North Core site's shift from a low-water lake situation (or seasonal ponds) under the influence of a tributary (probably the Bukalo Channel (Chapter 3)) to a higher water-level lake. This two-step transition is made by a progressive flooding for the middle part of the core (NC14-NC06) with a progressive and reversed evolution of the two end-members EM3 and EM5. The climatic evolution between dry and wet periods also shows an influence on the grain-size distribution and therefore on the end-member composition. The end of the wet period present during the deposit of the NC23-NC20 samples seems to affect the site with the NC20 sample, which shows a slightly different end-member composition with the absence of EM2 and therefore testifies to an environment with more abundant water. Similar observation for the wet period, which sees the deposits of samples NC11 and NC10. The end-member composition is more influenced by EM5, which tends to show an environment with more abundant water (Chapter 3).

The South Core site shows a gradual transition from a shallow flooded site to a lake situation. However, this gradual development takes place through two well-defined transitions. The first transition corresponds to the phase change between marsh to lacustrine in samples SC17 and SC16 (640-570 years BP). This transition corresponds in fact to a geomorphological change of the site which results in a deeper water environment. The second transition is between samples SC08 and SC06 (340-300 years BP). This evolution of end-members seems to correspond to the establishment of a more humid climate. A greater flooding of the site therefore results in the evolution of the grain-size distribution recorded in the sediments.

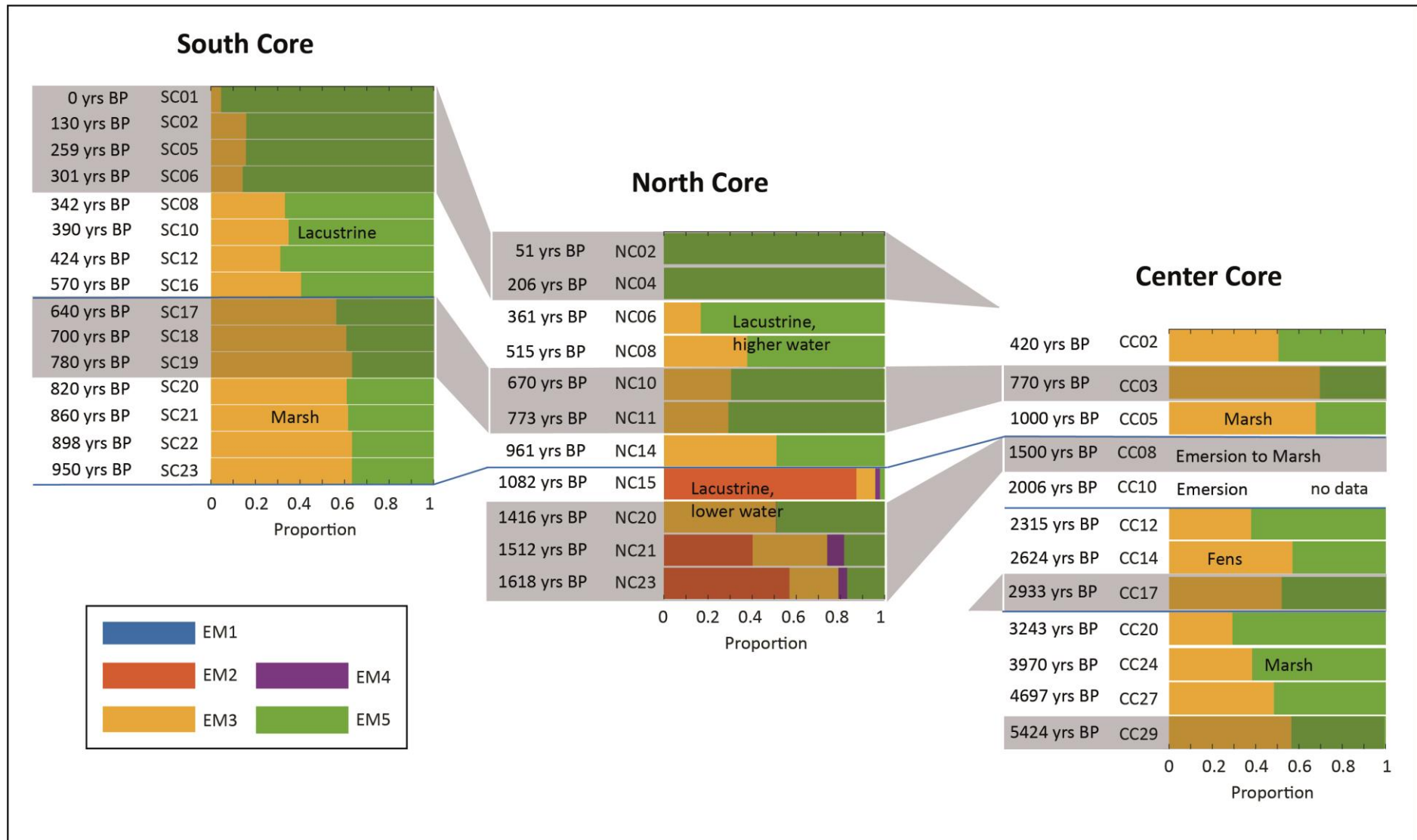


Figure 60 Comparison of the evolution of the different phases for each site with the end-member analysis of the grain-size (Chapter 3). The grain-size changes according to the geomorphological evolutions of the different sites. However, the influence of climate change also seems to exert an influence on the grain-size distribution. Wet periods are highlighted in light grey.

6.5.6. Bacterial Community Composition (BCC) evolution and characteristics

It has been shown in Chapter 4 that changes in the community reflect the changes in hydrological regime at regional scale, due to climatic and geomorphologic factors. In addition, a high dependency to sampling site has been highlighted. Each core tells a different story, reflecting local environmental conditions in addition to the regional environment. Although the regional change drives the BCC changes, local environment is the main factor shaping the BCC.

The regrouping of samples made with the analysis of the total and lysis-resistant bacterial community using clustering and PCoA (Figure 61 and 44; and Chapter 5 is similar to the regrouping of samples made with more classical analysis in sedimentology, mineralogy and geochemistry. The first given signal of the clustering analysis is the per-core grouping of the samples (Chapter 5). However, when clusterings of each individual cores are confronted, the temporal similarity in the changes of the bacterial community highlights the close relationship to the climate and environmental changes along the history of the lake (Figure 63; Chapter 5). It strengthens largely the use of the microbiological methods in comparison to the more classical used tools, and provides valuable information for the reconstruction of the lake history summarized in chapter 6.5.4.

Due to the wide diversity and complexity of the bacterial community, the use of a selection of specific metabolisms has been proposed as an alternative approach for the inference of environmental drivers based on the analysis of the BCC (Chapter 4). Sulphur-oxidizing bacteria and other metabolisms linked to the sulphur cycle have shown to be dominant in the sediment of Lake Liambezi, as well as thermophilic bacteria. These organisms have been selected to strengthen our interpretation of the ecosystem and the environmental changes. Changes in the abundance of these specific communities can be assumed to be the result of environmental modification impacting the whole ecosystem simultaneously. The particularities of the evolution of these two types of bacteria made it possible to help the temporal correlation between the three cores (Chapter 5). They also provided a better understanding of the environmental evolution of each site. However, thermophilic bacteria were more specifically used to highlight the supposed tectonic activity at the origin of the opening of the two basins forming the Lake Liambezi (Figure 64). Due to the presence of these specific communities, tectonic activity of the region linked to the Okavango Grabensystem is thought to be accompanied by hydrothermal activity. The base of each core start with a higher rate of thermophilic bacteria compared to the rest of the core. The samples of Center Core, age related to the supposed tectonic extension of north basin and to the supposed opening of the south basin present a slight change in thermophilic bacteria communities. A similar statement is true for the sample of North Core age related with the supposed opening of south basin (Figure 64). The supposed tectonic events related to the formation and evolution of Lake Liambezi are then thought to be closely related with a low temperature hydrothermal activity (Chapter 4. Marked presence of *Alicyclobacillus*, *Thermoanaerobaculum*, *Thermobacillus* and *Acidothermus*, helped more specifically to give these correlations, as all of them are moderately thermophilic with optimum growth temperatures ranging between 55°C to 60°C (Mohagheghi, Grohmann & Himmel, 1986; Kaksonen et al., 2007; Schleifer, 2009; Losey et al., 2013).

Sulphur-oxidizer communities in Lake Liambezi depend mainly on the water level and the oxygen availability. The lake being shallow, the variation in depth linked to the dry and wet seasons can demonstrate a significant alternation of redox conditions, as demonstrated by the physicochemical parameters of the sediments, but also the bacterial communities. In the case of Lake Liambezi, the water level mainly depends on the morphology of the lake. This morphology seems to be closely linked to the regional tectonic activity. In fact, by analogy, sulphur-oxidizer communities seem to correlate with tectonic event. However, it should be understood that this is related to the water level and not to the tectonic activity itself. Climatic variations (cycles of greater amplitude) also play a major role in the quantity of water in the lake, and therefore its depth. In fact, sulphur-oxidizer communities also seem to show an influence of climatic variations. By contrast, in same horizons, sulphate-reducing

bacteria are detected at low abundance, suggesting that the sulphide does not originate from sulphate reduction, but rather from the degradation of organic matter.

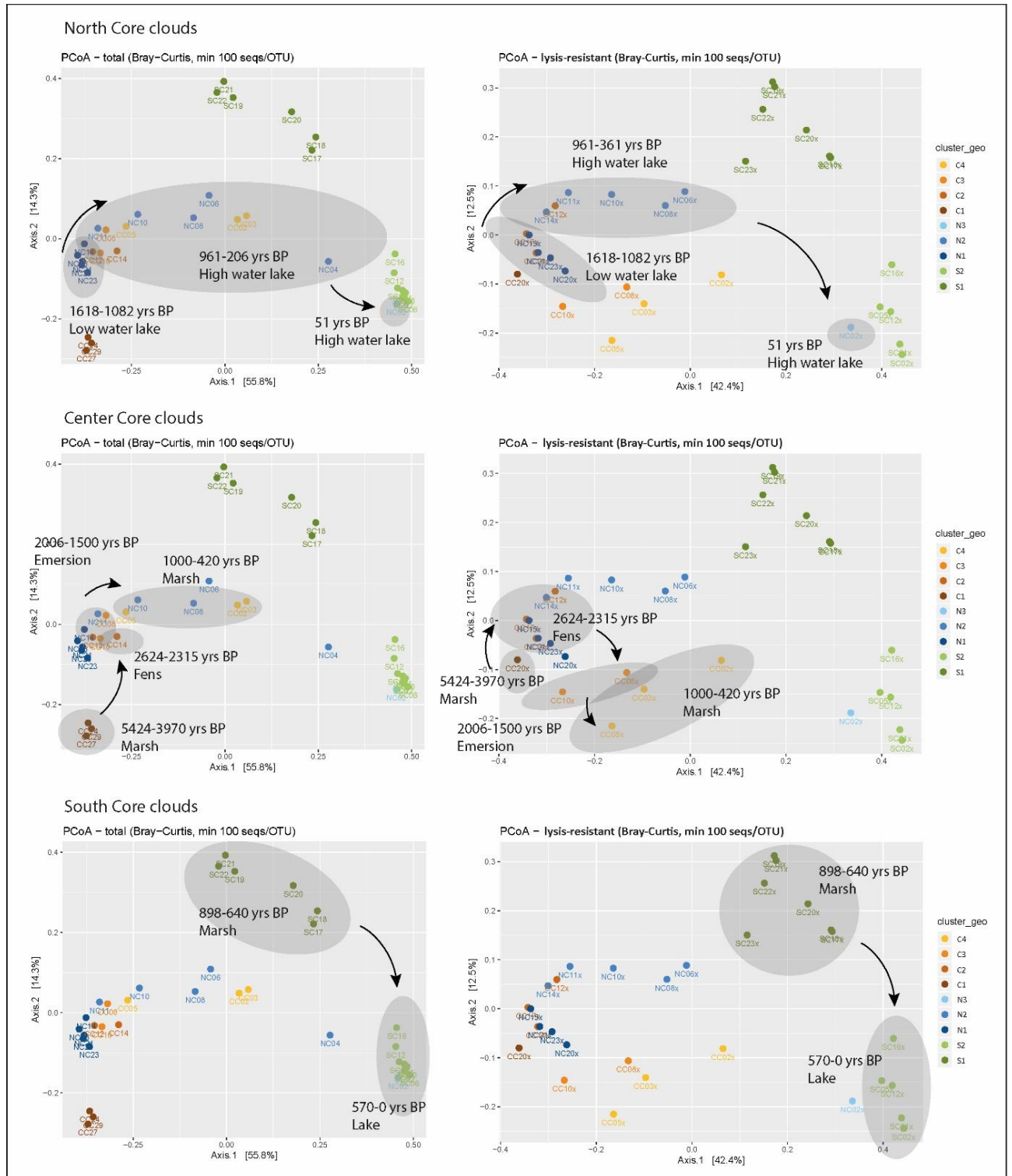


Figure 61 Principal coordinates analysis (PCoA) triplot of the total and the lysis-resistant communities based on Bray-Curtis dissimilarity and Hellinger transformation of the OTU table. OTUs represented by less than 100 sequences in the whole dataset were removed from the analysis. Colours correspond to the main grouping of samples defined for each core, identified from the visual characterization of the sediments. Ages and environmental status of the different groups of samples are added in clouds to better present the environmental separation revealed by the PCoA. The resulting grouping of samples confirm and strengthen the grouping made with the other methods and reassert the environmental evolution of each site made in chapter 6.5.4, Figure 59, Figure 62 and Figure 63.

Lake Liambezi : a climatic and environmental record

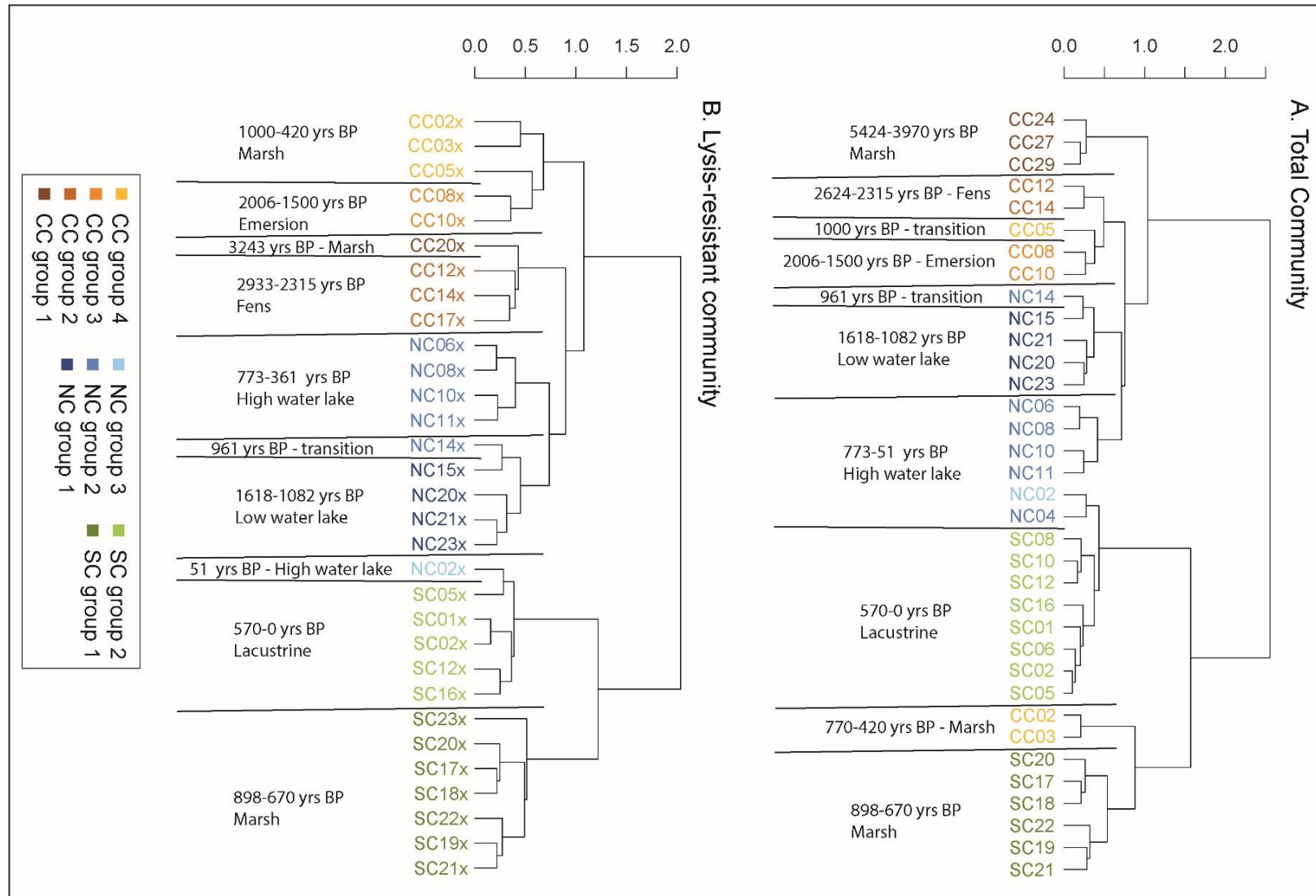


Figure 62 Clustering analysis using Ward algorithm of the (A) total community and (B) the lysis-resistant community. Distance between samples were calculated using Bray-Curtis dissimilarity based on the Hellinger-transformed community table. For each community, only the OTUs with at least 100 sequences among all samples were kept. Ages and environmental status of the different groups of samples are added to better present the environmental separation revealed by the clustering analysis.

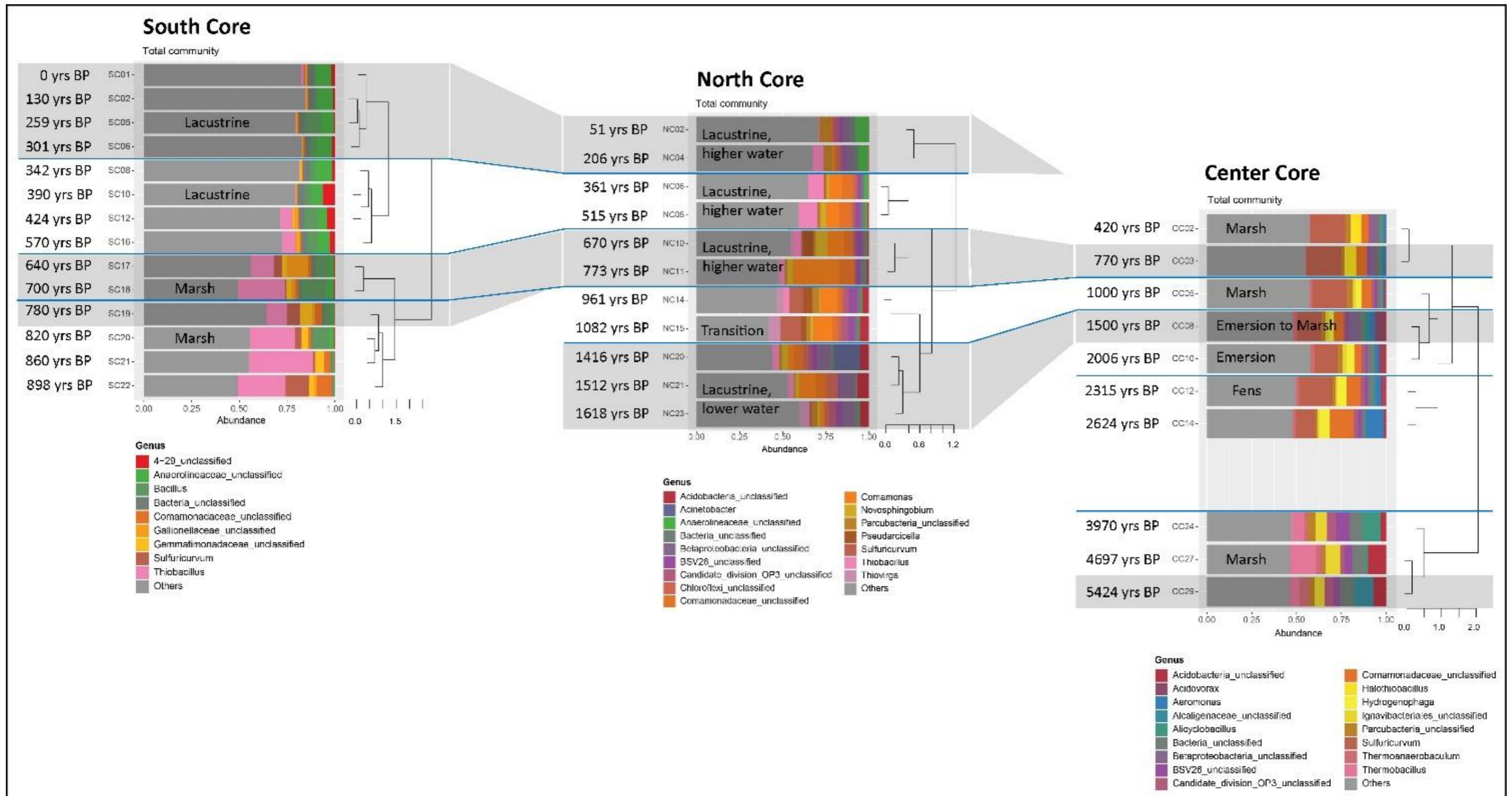


Figure 63 Characterization of the total bacterial communities, based on 16S rRNA gene amplicon sequencing. Only the most abundant genera (>2% of the community in average or >5% in one sample) are shown. Constrained hierarchical clustering was performed using the *chclust* function based on Bray-Curtis dissimilarity and the Hellinger-transformed community table. For each community, only the OTUs with at least 100 sequences among all samples were kept. The age model built in Chapter 5 with the link realised after the clustering (blue lines) are added. The climatic period are represented with dry period in white and wet period in grey-shade colour. Environmental state are also added. An important relation is highlighted between the climate evolution between wet and dry periods and with the environmental statuses of the different group of samples built with the clustering method. It correlates well with the more classical used methods as well.

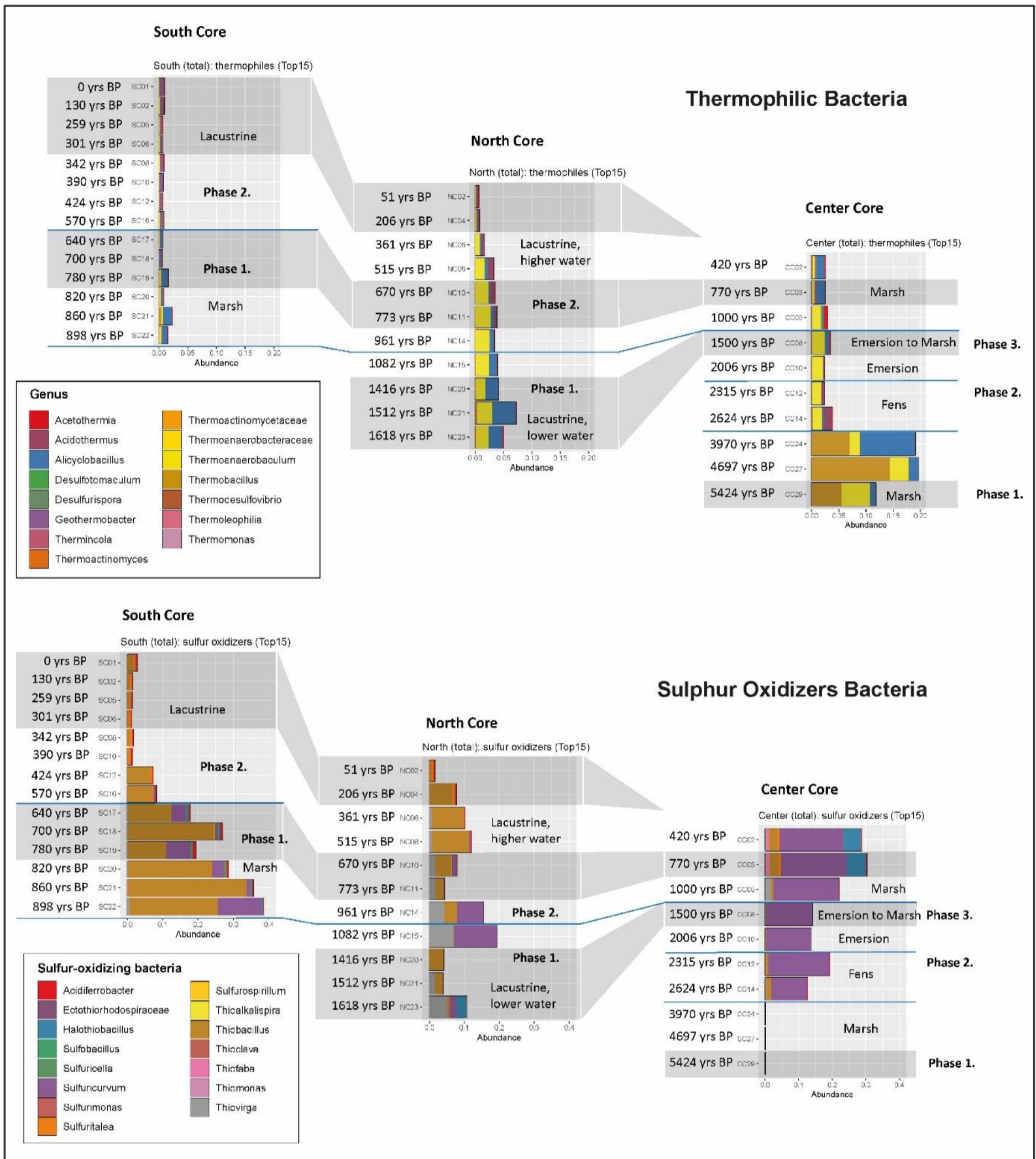


Figure 64 Communities of thermophilic bacteria contained in sediments for the upper figure and sulphur-oxidizers bacteria for the bottom figure. Shaded areas represent wet periods. Based on the constructed age model, there is a good relation between the samples attributed to identical climatic periods. This is particularly obvious when comparing the north and center cores, which showed high similarity in their BCC over time, as illustrated by the PCoA (Figure 61). **North core: Phase 1.** Extension of the north basin towards the northeast ≥ 1620 years BP; **Phase 2.** Change of environmental conditions and probable connection to the new southern basin ≥ 1000 years BP; **Center core: Phase 1.** Opening of the north basin > 5500 years BP; **Phase 2.** Extension of the north basin towards the northeast ≥ 1620 years BP; **Phase 3.** Environmental evolution of the site and probable connection with the new southern basin ≥ 1000 years BP; **South core: Phase 1.** Opening of the southern basin ≥ 1000 years BP; **Phase 2.** Environmental evolution of the site ≥ 570 years BP.

6.5.7. Mineralogy and hydrothermalism

As presented in the previous chapters, the supposed tectonic opening of the northern basin around 5500 years BP, its extension at around 1650 years BP and the opening of the southern basin at around 1000 years BP are accompanied by the marked presence of thermophilic bacteria. The regional tectonic activity seems thenceforth to be accompanied and characterized by an hydrothermal activity. Mineralogy did not demonstrate it, neither confirm it clearly (Chapter 3). Presence of barium, an element often related to hydrothermalism was describe in the three cores. However, it was mostly thought to be related to detritism (Chapter 3). However, question of its origin was asked for the upper part of the Center Core where barium content changed from 400 ppm to 700 ppm around 2000 years BP (sample CC10). This change was not followed by the other detrital elements described in the core. The timing of this change occurred a few hundreds years before the supposed opening of the north-eastern extension of the north basin (around 1650 years BP). Nonetheless, there is no clear relation between these two supposed events. Barium content origin remains not clear for the upper part of Center Core and there is still no clear proof of hydrothermal activity demonstrated by the mineralogy to attest what is shown with the bacteria communities.

6.5.8. Reviews and discussion of a potential reworking of top part for North and Center Cores

The lake was estimated to show relatively stable sedimentation throughout the recording of each of the three cores. However, this is an estimate made using the evolution of all measured parameters and correlated together. This method has probably attenuated different local developments and hid potential reworking. It is therefore probable that the evolution of the sedimentation of each site is in reality more complex. Thus, the contact surface between samples CC12 and CC10 or even CC08 and CC06 probably represent an erosion surface, as visual observation tends to suggest. However, it is difficult to estimate from geochemical measurements the extent of this erosion surface. The estimated age model do not show contradiction. Therefore, the erosion surface must be limited in time and not be sufficiently reflected in the sedimentological, geochemical and microbiological results to be demonstrated.

Since the radiocarbon measurements for the samples NC11, NC04 and CC03 did not show a satisfactory result during a first analysis (i.e. which allowed the construction of a simple age model based on the correspondence between the samples), they have been doubled. The second analysis still failed to confirm the age pattern suggested by all the other analyses (Figure 48 in Chapter 5). The other measurements having been considered as usable in the construction of a coherent age model, it was deduced that these samples had to show contamination in their organic carbon. This contamination may actually reveal a reworking of the sediment due to erosion. The presence of organic matter with an older radiocarbon age than assumed in these horizons is probably due to the erosion and the reworking of older sediments in the vicinity and then, their sedimentation at the NC and CC sites. It may also be a partial reworking of the sediments of these horizons for the North and Center Cores. The results obtained from the top parts of these two cores must therefore be carefully considered and verified with multiple methods. The lack of radiocarbon data for the top part of the NC and CC cores and the potential reworking of this top part makes the interpretation of the environmental evolution more complex and less certain.

However, no data shows a homogenization of the top part of the NC or CC cores (neither the mineralogical or elemental data, nor the geochemistry, nor the grain-size, nor the microbiology). This reworking should therefore not be sufficiently important to erase the characteristics that each method demonstrated. As a result, assertions about the environmental evolution of each site, but above all, of Lake Liambezi can be considered highly probable.

A remark can however be made in favour of the reworking of part of the sediments. The isotopic analyses of the organic carbon of the sediments show slightly different values (on average) for all the samples from the South Core compared to the two other cores. The isotopic analyses show values suggesting a more humid climate with values inclining for a vegetation richer in C3 (Figure 34, Chapter 3). This would suggest that the South Core was sedimented during a period that is not recorded, or not recorded in the same way for the North and Center Cores. Either the upper part (and therefore the most recent) is missing for the North and Center Cores, or it is, at least in part, reworked. A possible interpretation for this remark would be as follows. First, the northern basin is formed and filled with sediment. A sediment recording is made at the central site, then at the north site. When the southern basin opens, a reworking of the sediments in the northern basin takes place. This opening appears around 1000 years BP. It corresponds to the loss of the radiocarbon coherence for the North Core as well as to the re-flooding of the central site and the erosion surface assumed between CC08 and CC06. It can then be imagined that the sediment filling of the southern basin is partly done with the erosion and the reworking of the sediments of the northern basin. This would explain an isotopic signal from the South Core slightly different from the North and Center Cores as well as a top part more difficult to interpret for these last two cores. The result would therefore be Center and North Cores with a full core bottom in place; a top part (above 1000 years BP) partly reworked and a top layer maybe totally missing. And on the other hand, a complete South Core which then makes it possible to complete the missing data for the most recent part of the last thousand years.

6.6. Conclusion

Lake Liambezi is located middle of wetlands in an arid climate with a specialized flora and fauna (e.g. Seaman et al., 1978; Peel et al., 2015). It has then a highly sensitive response to any climatic or environmental change. The structural features formed by the neo-tectonic activity affect the regional hydrological system and lead to a complex network of rivers and waterbodies which are evolving constantly through time (Kinabo et al., 2007; Haddon & McCarthy, 2005; Burrough et al., 2007; Burrough et al., 2009). The choice of a multidisciplinary study including classical tools in sedimentology, mineralogy and geochemistry and the innovative method using the bacterial community composition (BCC) and the bacterial lysis-resistant community met the initial expectations. Each chosen method brought specific information able to better trace and expose each parameter in detail (Chapters 3-5). The pooling of all the parameters in the present paper did permit to define a general understanding of the lake ecology and evolution through time. A climatic evolution for the last 5500 years has been proposed and compared to previous studies and seems to offer a much-detailed story for the close past. The higher precision comes especially with having taken into account the discrimination between climate evolution and environmental evolution and not having based our climate reconstruction after spatial geomorphological proxies as proof of a precise climate regime.

The global history of the actual Lake Liambezi for the last 5500 years BP seemed to be closely related to the regional tectonic activity related itself to the Okavango Grabensystem. This activity seems to be responsible of Lake Liambezi formation with the opening of its northern basin in a first time, its north-eastern extension in a second time and the opening of a second basin in its south as last tectonic feature for Lake Liambezi. This tectonic opening formed topographic depressions consequently filled with lacustrine sediments. Those sediments offered records of the climatic conditions and the environmental evolution of the site. If the tectonic activity seemed of major importance to the formation of topographic depressions, the morphologic shape of the basin and the climatic conditions then permitted the record of the environmental evolution of Lake Liambezi.

6.7. References

- Berke, M.A., Johnson, T.C., Werne, J.P., Schouten, S., Sinninghe Damsté, J.S. 2012. A mid-Holocene thermal maximum at the end of the African Humid Period. *Earth and Planetary Science Letters* 351-352, 95-104.
- Bufford, K.M., Atekwana, E.A., Abdelsalam, M.G., Shemang, E., Atekwana, E.A., Mickus, K., Moidaki, M., Modisi, M.P., Molwalefhe, L., 2012. Geometry and faults tectonic activity of the Okavango Rift Zone, Botswana: Evidence from magnetotelluric and electrical resistivity tomography imaging. *Journal of African Earth Sciences*, 65, 61-71.
- Burrough, S.L., Thomas, D.S.G., 2008. Late Quaternary lake-level fluctuations in the Mababe Depression: Middle Kalahari palaeolakes and the role of Zambezi inflows. *Quaternary Research* 69, 388-403.
- Burrough, S.L., Thomas, D.S.G., Shaw, P.A., Bailey, R.M. 2007. Multiphase Quaternary highstands at Lake Ngami, Kalahari, northern Botswana. *Palaeogeography, Palaeoclimatology, Palaeoecology* 253, 280–299.
- Burrough, S.L., Thomas, Singarayer, J.S., 2009. Late Quaternary hydrological dynamics in the Middle Kalahari: Forcing and feedbacks. *Earth-Science Reviews*, 96, 313–326.
- Cavaillé-Fol, 2020. On a découvert le berceau de l'Humanité. *Science & Vie*, N°1233, juin 2020, 56-71.
- deMenocal, P., Ortiz, J., Guilderson, T., Adkins, J., Sarnthein, M., Baker, L., Yarusinsky, M. 2000. Abrupt onset and termination of the African Humid Period: rapid climate responses to gradual insolation forcing. *Quaternary Science Reviews* 19, 347-361.
- deMenocal, P., Ortiz, J., Guilderson, T., Sarnthein, M. 2000. Coherent High- and Low-Latitude Climate Variability During the Holocene Warm Period. *Science* 288 (5474), 2198-2202.
- Frouin, M., Sebag, D., Durand, A., Laignel, B., Saliege, J.F., Mahler, B.J., Fauchard, C., 2007. Influence of paleotopography, base level and sedimentation rate on estuarine system response to the Holocene sea-level rise: The example of the Marais Vernier, Seine estuary, France. *Sedimentary Geology*, 200, 15-29.
- Haddon, I.G., McCarthy, T.S. 2005. The Mesozoic–Cenozoic interior sag basins of Central Africa: The Late-Cretaceous–Cenozoic Kalahari and Okavango basins. *Journal of African Earth Sciences* 43, 316-333.
- Jones, C.R., 1980. The Geology of the Kalahari. *Botswana Notes & Records*, 12, 1-14.
- Kaksonen AH., Spring S., Schumann P., Kroppenstedt RM., Puhakka JA. 2007. *Desulfurispora thermophila* gen. nov., sp. nov., a thermophilic, spore-forming sulfate-reducer isolated from a sulfidogenic fluidized-bed reactor. *International Journal of Systematic and Evolutionary Microbiology* 57:1089–1094. DOI: 10.1099/ijs.0.64593-0.
- Kinabo, B.D., Atekwana, E.A., Hogan, J.P., Modisi, M.P., Wheaton, D.D., Kampunzu, A.B. 2007. Early structural development of the Okavango rift zone, NW Botswana. *Journal of African Earth Sciences*, 48, 125-136.
- Losey NA., Stevenson BS., Busse HJ., Damsté JSS., Rijpstra WIC., Rudd S., Lawson PA. 2013. *Thermoanaerobaculum aquaticum* gen. nov., sp. nov., the first cultivated member of acidobacteria subdivision 23, isolated from a hot spring. *International Journal of Systematic and Evolutionary Microbiology* 63:4149–4157. DOI: 10.1099/ijs.0.051425-0.
- McGee, D., deMenocal, P.B., Winckler, G., Stuut, J.B.W., Bradtmiller, L.I. 2013. The magnitude, timing and abruptness of changes in North African dust deposition over the last 20,000 yr. *Earth and Planetary Science Letters* 371-372, 163-176.
- Mohagheghi A., Grohmann K., Himmel M. 1986. Isolation and characterization of *Acidothermus cellulolyticus* gen. nov., sp. nov., a new genus of thermophilic, acidophilic, cellulolytic bacteria. *International Journal of Systematic Bacteriology* 36:435–443. DOI: 10.1099/00207713-36-3-435.

- Mukwati, B.T., Tafesse, N.T., Bagai, Z.B., Laletsang, k. 2018. Hydrogeochemistry of the Kasane Hot Spring, Botswana. *Universal Journal of Geoscience* 6, 131-146.
- Pausata, F.S.R., Gaetani, M., Messori, G., Berg, A., Maia sw Souza, D., Sage, R.F., deMenocal, P. 2020. The Greening of the Sahara: Past Changes and Future Implications. *One Earth* 2, 235-250.
- Peel, R.A., Tweddle, D., Simasiku, E.K., Martin, G.D., Lubanda, J., Hay, C.J., Weyl, O.L.F. 2015: Ecology, fish and fishery of Lake Liambezi, a recently refilled floodplain lake in the Zambezi Region, Namibia. *African Journal of Aquatic Science* 40:4, 417-424.
- Schleifer KH. 2009. Phylum XIII. Firmicutes Gibbons and Murray 1978, 5 (Firmacutes [sic] Gibbons and Murray 1978, 5). In: De Vos P, Garrity GM, Jones D, Krieg N, Ludwig W, Rainey F, Schleifer K-H, Whitman W eds. *Bergey's Manual of Systematic Bacteriology Volume 3*. Dordrecht Heidelberg London New York: Springer, 19–1317.
- Seaman, M.T., Scott, W.E., Walmsley, R.D., van der Waal, B.C.W., & Toerien, D.F. 1978: A limnological investigation of Lake Liambezi, Caprivi. *Journal of the Limnological Society of Southern Africa* 4:2, 129-144.
- Singletary, S.J., Hanson, R.E., Martin, M.W., Crowley, J.L., Bowring, S.A., Key, R.M., Ramokate, L.V., Direng, B.B., Krol, M.A., 2003. Geochronology of basement rocks in the Kalahari Desert, Botswana, and implications for regional Proterozoic tectonics. *Precambrian Research*, 121, 47-71.
- Sletten, H.R., Railsback, L.B., Liang, F., Brook, G.A., Marais, E., Hardt, B.F., Cheng, H., Edwards, R.L. 2013. A petrographic and geochemical record of climate change over the last 4600 years from a northern Namibia stalagmite, with evidence of abruptly wetter climate at the beginning of southern Africa's Iron Age. *Palaeogeography, Palaeoclimatology, Palaeoecology* 376, 149–162.
- Thomas, D.S.G. & Burrough, S.L, 2012. Interpreting geoproxies of late Quaternary climate change in African drylands: Implications for understanding environmental change and early human behaviour. *Quaternary International*, 253, 5-17.
- Tweddle, D., Weyl, O.L.F., Hay, C.J., Peel, R.A., Shapumba, N. 2011. Lake Liambezi, Namibia: Fishing community assumes management responsibility. Technical Report no. MFMR/NNF/WWF/Phase II/4.

7. General conclusion

The north Botswana region has been described as uniquely representing wetlands in an arid climate. It holds a specialized flora and fauna and is a source of life-supporting water in the middle of an arid region. This region, is however, particularly fragile as it responds sensitively to any climatic or environmental change. It holds the second largest endorheic delta system in the world organised with the two endorheic Okavango and Kwando rivers, and the changing contributions from the Zambezi River. These three rivers form a complex network controlled by tectonic faults (Haddon & McCarthy, 2005). A minor change in tectonism and faulting can significantly influence the morphology and hence the drainage pattern of the entire system. This has been clearly demonstrated by the work of Burrough & Thomas, 2008 for the evolution of the paleolakes of the middle Kalahari, also considered to be the cradle of humanity (Cavaillé-Fol, 2020).

Okavango Delta and Ngami lakes have been studied and described through numerous studies (e.g. Burrough *et al.*, 2007; Huntsman-Mapila *et al.*, 2006; McCarthy, 2013; Milzow *et al.*, 2009). In comparison, the Linyanti-Chobe Basin has been poorly documented and remains poorly understood. Multiple factors are involved in the environmental cycles involved in the landscape formation and form therefore a complex system. Environmental and landscape features such as rivers, lakes, floodplains, islands and connections in the Linyanti-Chobe Basin evolve a lot. The timing of the evolutions and changes of these features is poorly described. The complexity of such a system makes it difficult to trace and to target the factors of change and evolution. More often in such a complex system, factors of evolution are multiple. Furthermore, climate variations during the Quaternary in northern Namibia and Botswana are poorly documented and understood as well (Thomas *et al.*, 2012; Burrough *et al.*, 2007; Chevalier *et al.*, 2015). Paleo-environmental archives with well-dated proxies are difficult to find or target and results might show inconsistencies and even contradictions (Thomas *et al.*, 2012; Burrough *et al.*, 2007). Interpretations of late Quaternary climate variation in the Kalahari are therefore controversial (Wiese *et al.*, 2020).

The main and overarching goal of the present work was therefore to understand better the climatic variation and ecosystem evolution in northern Botswana using traditional and new palaeolimnological tools. From this perspective, it was necessary to evolve step by step in order to carry out this exploratory work. Each step carried out made it possible to evolve towards the next to finally obtain an exploratory work with very vast methods and very dense in data. This exploratory work made it possible to target the relevant characteristics of this terrain as well as the methods allowing them to be traced. It also made it possible to highlight new questions relating to the functioning of certain characteristics and to make proposals for their possible resolution in future work.

The first step was to understand the geochemical relationship between vegetation and soils. It could be shown that the organic matter of the soils as well as the sediments directly reflects the vegetation of the site. This observation was then very useful in the paleoenvironmental reconstruction of the three sites sampled at Lake Liambezi. It was also demonstrated in this first step that the geochemical composition of organic matter is more dependent on the geomorphological characteristics of the northern Botswana region than the generally accepted north-south climate transect for southern Africa.

In order to understand climatic variations and the evolution of the different ecosystems of this region, the next step focused on Lake Liambezi. It was first necessary to clear the composition of the sediments of Lake Liambezi in order to understand its characteristics. Using many methods in different disciplines (sedimentology, geochemistry and microbiology), the sediments of Lake Liambezi could be described in detail and its characteristics discussed. The study demonstrated a sediment rich in organic matter of autochthonous production with a dominance of aquatic plants and algae and a lesser contribution of terrestrial detritus washed into the lake. Mineralogical, elemental and grain-size

General conclusion

studies have also shown a large proportion of detrital elements in the sediments. However, two minerals seem to demonstrate a different cycle, largely linked to the environmental and climatic conditions of the environment. The sediments of the lake show an important cycle of silica with a redistribution of this silica through dissolution and reprecipitation. The presence of many siliceous organisms has been widely documented. The clay cycle has also been studied especially with smectite which seems to demonstrate a different cycle from other clays. Variations in smectite content are probably related to variations in climate between wetter and drier periods. This mineral therefore turns out to be of major importance for the paleo-climatic reconstruction of the region.

The multidisciplinary approach introduced an innovative method coming from microbiology. Firstly, this work permitted to confirm the applicability of using bacterial DNA (total and/or lysis-resistant) to identify changes and variability in the environmental conditions. In addition to confirming the correct functioning of this new approach, the method has above all shown the relevance of its use for such an environment. It made it possible to supplement the observations carried out with the more traditional methods, but above all, it made it possible to highlight the characteristics of the sediments which escaped the more traditional methods.

Microbiology has made it possible to refine the environmental descriptions produced with sedimentological and geochemical methods. But above all, it has put forward cycles or phenomena that other methods have not made it possible to demonstrate. Microbiology has highlighted an important sulfur cycle in the sediments of Lake Liambezi. It also highlighted the presence of hydrothermal activity in the direct surroundings of the lake, or even within the lake. These different characteristics of the sediments of Lake Liambezi will be especially useful in the various paleoenvironmental and paleoclimatic reconstructions carried out for the lake and its region.

The next step was the attempt to build an age model for the lake. The composition of the sediments led to the choice of radiocarbon dating. The ^{14}C -activity for a selection of samples (charcoal pieces or bulk material) demonstrated a possible reconstruction for some of the cores. However, this dating attempt also showed that a reworking, or even total erosion of the top of the CC and NC cores was possible. Even so, the other methods (sedimentology, geochemistry and microbiology) demonstrated that the cores remained exploitable and that even by accommodating a partial reworking for the top of these two cores, the environmental and climatic deductions remained relevant. In fact, a sediment age model has been proposed. This age model is based on radiocarbon dates. It has been largely completed using microbiology and the use of total communities as well as a selection of specific communities showing characteristics of interest and usable for the purpose of site correlation.

The final step in the paleoenvironmental and paleoclimatic reconstruction of the Lake Liambezi site was to gather all the data useful for this purpose. The pooling of the age model and the environmental and climatic deductions for each site made it possible to propose a model of climatic and environmental change that is unique for the region. Even though this environmental and climatic model will probably evolve in future studies (or even be partially questioned), it makes it possible to lay an interesting basis for the region. On the one hand, it proposes a climatic and environmental reconstruction for the last 5500 years, but above all, it demonstrates what are the characteristics of the lacustro-palustrine environments of this region and what are the relevant tools for the study of these environments. One of the major points of the final stage of this exploratory study was to demonstrate that climate change and environmental change are two distinct things and partially independent of each other. The environmental evolution of a specific site depends on its geomorphological characteristics as well as its links with regional tributaries. The influence of climate on the environmental characteristics of a site is only secondary. This characteristic makes it possible to raise the difficulty of studies aiming at the environmental reconstruction of lakes located in northern Botswana such as Lake Ngami or paleo-Lake Makgadikgadi (e.g. Burrough et al., 2007).

The deduced environmental evolution of Lake Liambezi proposed a close relation with the regional tectonic activity and tends to demonstrate a recent activity of the Okavango Graben. Presence of thermophilic bacteria seems to support a tectonic action in the different evolution of the lake's shape. The regional hydrological system is affected by the structural features formed by the neo-tectonic activity (Kinabo et al., 2007). It results in the creation of a complex network of rivers and waterbodies (Haddon & McCarthy, 2005). The exact same statement is confirmed for the Lake Liambezi environmental history. Its formation and part of its evolution are probably the results of a tectonic activity linked to the Okavango Graben. The resulting depressions are then filled with lacustrine and fluvio-deltaic sediments and reflect the environmental conditions set with the location and the connectivity to the watershed.

7.1. Initial questions

The uniqueness of north Botswana has been demonstrated, holding a complex network of rivers, marshes, wetlands and lakes controlled by tectonic faults (Haddon & McCarthy, 2005). This complex system is in constant evolution and reflect the tectonic, climatic and environmental evolutions. If such evolutions have been demonstrated for the neighbouring Okavango Delta, it has never been shown for the Linyanti-Chobe Basin. This region remains poorly covered, studied or understood. Therefore, the choice was established to focus on this extraordinary basin, showing a high complexity of connection between the different rivers and waterbodies. The present work, focusing on Lake Liambezi, situated middle of the Linyanti-Chobe Basin aimed at demonstrating similar dependence to tectonic, climatic and environmental evolutions for its history compared to the Okavango Delta. A better understanding of Lake Liambezi evolution might help to understand the possible evolution of the neighbouring Okavango Delta. The following section aims to answer questions that arose during the development of the project:

- i. The link between vegetation and soil organic matter geochemistry has been demonstrated for the Linyanti-Chobe Basin. The organic matter geochemical composition of the soils reflects the vegetation cover. A similar link has been shown for the sediments of the tributaries of Lake Liambezi as well as the lake's sediment. The sediments reflect the direct neighbouring vegetation. It is thus thought that the organic matter of soils and sediments might be considered as autochthonous with only a poor transport. It results in the possibility of using the organic matter conserved in paleo-soils and in waterbodies sediments to reconstruct past vegetation cover.
- ii. Lake Liambezi has been investigated through a number of sediment cores. A precise description of its sediment has been made with a precise description on the origin of the different sediments components. Organic matter contained in the sediments denotes a dominantly autochthonous origin mostly composed of aquatic plants and algae with a lesser contribution of terrestrial detritus washed into the lake. Terrestrial plant contribution shows a mix between C₃ – and C₄ – type of vegetation with a clear dominance of the C₃ vegetation. It is compatible with the presence of *Phragmites australis* (a C₃ plant) described along the shores of Lake Liambezi. The lacustrine and terrestrial contributions are changing according to the site and/or the depth. The absence of biogenic calcite has been noticed and thus demonstrates the absence of a biogenic carbonate cycle for Lake Liambezi. Contrariwise, a very rich biogenic silica cycle has been observed with various forms of biogenic silica. Mineralogy of the sediment confirms the importance of detrital material coming from the catchment. However, the weathering of primary minerals such as feldspar, plagioclase and micas found in the catchment is climatically-controlled and results in the formation of smectite. Smectite might therefore be used as climate tracer

in the lakes sediments. The other parameters of the sedimentology such as the grain-size, the detrital mineral content and the presence or absence of pyrite and gypsum are controlled by localized features such as the connectivity of the basin to the rivers or the water availability of the site (and thus water level). A novel method using bacterial DNA (total and/or lysis-resistant) developed by the Laboratory of Microbiology at the Institute of Biology of the University of Neuchâtel has been used to identify changes and variability in the environmental conditions of the lake. Similarly to other methods used in the present study, the bacterial communities changed in regard to the site and the depth in accordance with the observed changes related to the other methods. The pooling of the results obtained with each method of this multidisciplinary study did permit to give a specific story and evolution for each of the three sites.

- iii. In order to get a time frame in the described evolution of the three sampled sites, and thus, to give an environmental history to the lake, an age model was built following multiple methods. With regards to the sediments, the ^{14}C -compositions of a number of samples has been examined. However, dating with radiometric methods on sedimentary components is challenging at least and complementary methods have been used. Thanks to the mineralogy and the geochemistry, the cores have been considered as non-heavily bioturbated and thus usable and robust enough to be dated with relative dating methods. Smectite content has been used as well as bacterial community composition and a selection of bacterial communities. Following this multidisciplinary approach, gave estimated ages of 1618 to 51 years BP for the North Core, 5424 to 420 years BP for the Central Core, and from 950 to 0 years BP for the South Core. The average vertical accretion rate deduced from the obtained age runs from 1 cm/30 years for South Core to 1 cm/115 years for Center Core. The time periods covered by each core are slightly staggered and covering sometimes slightly different periods of sedimentation. It is thought to be the result of local environmental differences. These environmental differences are related to the climatic evolution but moreover to the morphology of the site.
- iv. Precise description of the three sampled sites showed a very characteristic morphological evolution for each site. The northern site shows a sudden deepening from a shallow to a deeper lake environment. The southern site presents a gradual transition from a marsh to lake conditions. The site of the center presents a more complex development. It starts with a marsh environment. There follows a period of progressive drying leading to an emersion of the site. Despite the emersion, the sediments still record an annual flood regime similar to today. The site then registers a gradual re-flooding leading the site to a return of marsh conditions. The evolution of each site is strongly related to the location of the site with its geomorphology and its response to the climatic evolution. The climatic evolution is definitely reflected in the organic matter record and reflects a vegetation response and evolution to it. It is also reflected in the bacteria communities. However, the major evolution observed in both, bacterial communities and mineralogy-geochemistry of the sediments, demonstrate rather the complex association between the morphology of the site (its location) and the climate evolution
- v. However, the microbiology has revealed a high proportion of thermophilic and moderately thermophilic bacteria. this has been interpreted to suggest hydrothermal activity within the lake. A complex network in the regional hydrological system evolving constantly due to the structural features formed by the neo-tectonic activity of the Okavango Graben has been demonstrated (e.g. Kinabo et al., 2007; Haddon & McCarthy, 2005; Burrough et al., 2007; Burrough et al., 2009). A link between the presence of

thermophilic bacteria and a potential tectonic activity affecting the lake has thus been made. Structural features formed by the neo-tectonic activity is thus believed to affect the lake and help to its environmental evolution. Formation and evolution of Lake Liambezi in two elongated basins seems to follow a tectonic opening linked to the Okavango Graben and its fault system. The north basin has probably been formed at about 5420 years BP following a tectonic opening. A supposed extension towards the northeast of this first basin is believed to occur around 1650 years BP. At about 1000 years BP, a second basin is believed to open in the south of the first basin following the last recorded tectonic event affecting the lake. Presence of thermophilic bacteria seems to support this tectonic action in the different evolution of the lake's shape. Successively, the resulting depressions are then filled with lacustrine and fluvio-deltaic sediments. Sediment type and content are driven by the environmental conditions resulting of the watershed, the climate and the morphology of the site. Since then, the formation and evolution of the lake seem to be closely related to the regional tectonic activity and tend to demonstrate a recent activity of the Okavango Graben system.

- vi. Previous work aiming at a climatic reconstruction of the region compiled a variety of data and studies all covering the northern Botswana and northern Namibia region (Burrough et al., 2007; Thomas et al., 2012). Their work covered a period of 250,000 years. The present work is interested in only the last 5500 years. Therefore, the present work proposed a higher resolution for this period of time compared to the two other studies. Methods and material used are different for each described site. Therefore, important differences are found between each site. However, correlations are encouraging and similarities are more or less good (especially between the present work and Thomas et al. (2012)). Results are showing an alternation between wet and dry periods of variable duration. The present work used the climatically linked clay named smectite as main climatic tracer. Refinements and slight corrections can be made using other tools such as the geochemistry.
- vii. The results of this study demonstrate the applicability of using bacterial DNA (total and/or lysis-resistant) to identify changes and variability in the environmental conditions. Changes in the total and lysis-resistant bacterial communities were consistent with other geological proxies and demonstrated their relevance as a paleoecological proxy. Moreover, it did permit to highlight specific biological processes such as biological-mediated sulphur cycling and potential hydrothermal activity through a high abundance of sulphur-oxidizing and thermophilic bacteria. Furthermore, in this particular case, the method demonstrated another advantage. The good correlation between the changes in the total and lysis-resistant bacterial communities with other geological proxies and a particular cycle of thermophilic bacteria did permit to use the method as a relative dating method, as correlation between the three cores were feasible.

Following this multidisciplinary approach, the sedimentology of Lake Liambezi turns out to be rich in information. The obtained information are listed hereafter in order to get a summary of it. The tools used to obtain such information are also indicated.

- Vegetation type: organic matter geochemistry
- Bacterial Communities Composition (BCC): DNA extraction
- Water level: BCC, organic matter geochemistry, grain-size and mineralogy
- Basin connectivity to the watershed: grain-size and mineralogy
- Climatic evolution: smectite and organic matter geochemistry
- Hydrothermal activity: thermophilic bacteria

General conclusion

The recorded environmental conditions of the lake into the sediments reflects firstly the geomorphology of the site and secondly the climate. Environmental conditions are the complex combination of the set of information exposed here above.

Geomorphology of the site is dependent of multiple variables, such as local specificities or climate. However, according to our studies, it seems above all to be dependent of the tectonic activity of the region. Tectonic activity is believed to shape most of the depressions of the region. The resulting depressions are then filled with water and form waterbodies or lakes which are then filled with lacustrine and fluvio-deltaic sediments. These sediments record then the neo-formed environmental situation.

The nicest example of this situation is recorded in the organic matter and in the clay content of the Lake Liambezi's sediment. Evolution of the geochemical record of the organic matter ($\delta^{13}\text{C}$ and C/N) correlates with the main morphological evolution of the lake (Figure 65): transition from low water level lake to higher water level lake for North Core; transition from marsh to fens to a total drying up and back to marsh conditions after a re-flooding for Center Core; transition from marsh to lake conditions for South Core. However, the climate evolution shown by the smectite content variations tends to demonstrate correlations with the minor changes in the organic matter composition. Thus, it is a demonstration of the previous assessment. The site is first, dependent to its geomorphological shape and secondly, dependent to the climate variations.

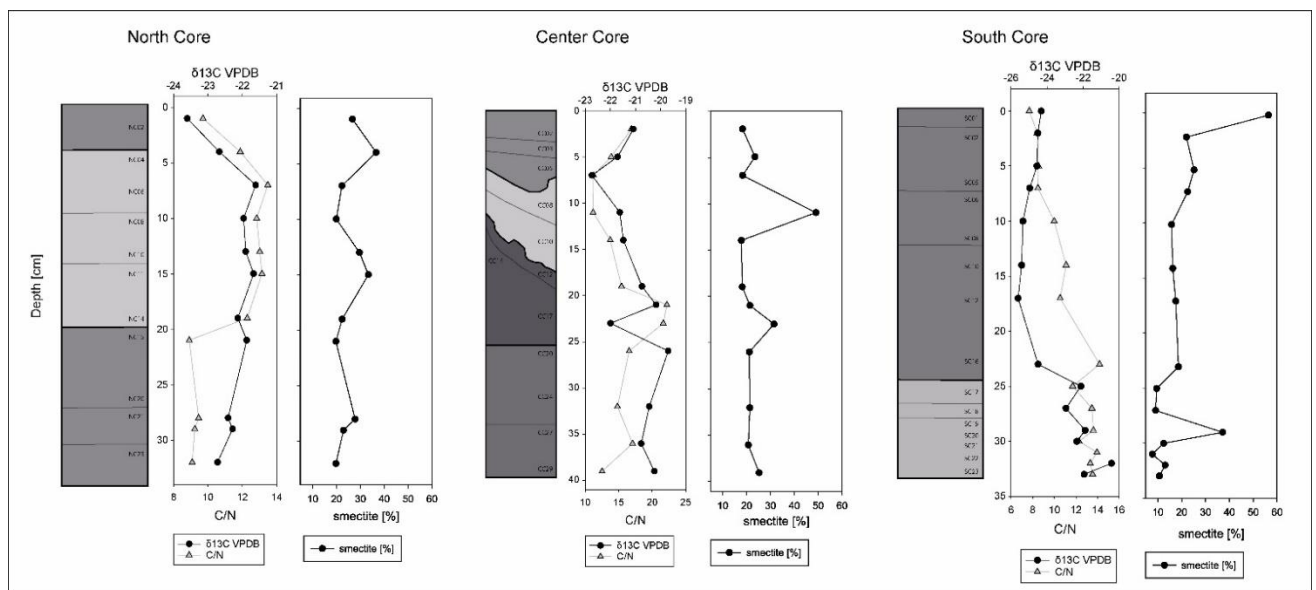


Figure 65 Comparison of $\delta^{13}\text{C}$ and C/N ratio of the organic matter with smectite content of each core. The standard deviation or the analytical error of the different analysis are less than or equal to the size of the symbol.

Each method did permit to progress in specific fields. However, only the pooling of the data allowed to enlarge our vision and allowed us to draw conclusions on the paleo-environmental evolution of the region. Moreover, the complexity of the site sometimes renders it difficult to have a clear definition of some variables of the sediments. The broader vision obtained through this multidisciplinary approach has allowed us to overcome this problem. It results a coherent environmental evolution of the region when compared to similar studies (e.g. Sletten et al., 2013; Burrough et al., 2007; Thomas et al., 2012).

7.2. Weaknesses of present work

As explained in the preface, the present thesis work has undergone many adaptations following changes and redirections beyond the control of the authors (my supervisors and myself). Even if the project submitted by the SNF was built as an exploratory project to test the used methods in various environments and environmentally different systems, an initial work had been done on the initial field. It means that the initial project was to be carried out on a site already well described and cleared. Regarding Lake Liambezi, the very nature of the sediments had never been described. It means, it was necessary to carry out a description of the sediment in order to describe its components. An important work of description therefore had to be undertaken before being able to get to the heart of the project, which was the environmental reconstruction of the lake for the past. The work therefore represented a double difficulty: a first description of the sedimentology of Lake Liambezi; as well as an environmental reconstruction. The project being ambitious and very vast, it is very likely that future studies will bring clarifications or corrections to this first exploratory work.

Nevertheless, the present work lays the foundations for future work not only on Lake Liambezi, but on understanding the establishment of the landscape of northern Botswana in relation to tectonism. Indeed, it has been shown with the present work that if the evolution of the landscape of this region depends partly on the climate, the tectonic evolution makes it possible to redefine the distribution of rivers and bodies of water and thus modify the landscape in an important way. This is therefore additional work for the region which demonstrates the importance of taking regional tectonics into account if we want to study and understand the evolution of the landscape of northern Botswana and thus better understand possible future evolutions.

The problems encountered during the preparation of the field campaign as well as during the field resulted in the sampling of only three cores between 30 to 40 cm. In addition, the three cores collected each represent a different period and their pooling is not obvious. It may even be subject to discussion. This therefore results in a problem of representativeness which makes the discussions and conclusions of the present work subject to discussion. These are the hazards of exploratory work. However, as indicated in the previous paragraph, the results are encouraging and provide a database for planning future work in this region. In order to increase the representativeness of the work as well as complete the information obtained, it would be necessary to obtain a larger number of sediment cores and to extend the sampling to the entire lake. A comparison of the sites and a pooling of data would thus make it possible to better understand the overall dynamics of the lake. The comparison of the data would also allow a description of the environmental evolution more solid because check on multiple sites. In addition, the current work has made it possible to highlight which methods are indicative of environmental conditions. Thus, thanks to a more restricted choice of methods, and to a larger sampling, the additional work in order to complete the present work would be achievable.

7.3. Evolution of the region

Lake Liambezi evolution for the coming years will definitely be closely related to the climate evolution of the region. However, the present work has demonstrated a close link between origin, formation and evolution of Lake Liambezi and the activity of the Okavango Graben fault system. The evolution of the fault system will largely condition the future shape of the lake and its evolution or its disappearance (its transformation to another type of environmental feature). The present study confirmed that a tectonic change could radically modify the shape of the lake and thus its environmental adaptation to it. Quaternary unconsolidated sediments of the Okavango Graben are mainly composed and underlain by lacustrine and fluvio-deltaic sediments of varying thickness (Bufford *et al.*, 2012). This demonstrates a permanent evolution of the landscape as well as a permanent redistribution of figures linked to the course of the water in which Lake Liambezi fits perfectly. The nature of the landscape as well as the active tectonic activity allows a constantly

changing and constantly evolving landscape. This dynamic creates an entanglement of channels typical of anastomosed river observable with the naked eye on any aerial photograph taken in the region. The study of water bodies in this type of ecology becomes even more stimulating and challenging (e.g., Burrough *et al.*, 2007; Burrough *et al.*, 2008; Burrough *et al.*, 2009; Huntsman-Mapila *et al.*, 2006; Shaw *et al.*, 2003; Grove *et al.*, 1969). A similar statement is true as well for the other systems of the region such as the Okavango Delta for example.

7.4. Perspectives

The multidisciplinary approach integrating sedimentology, geochemistry as well as microbiology has made it possible to obtain a very broad and complete vision of the sediments of the northern Botswana region. This multidisciplinary approach is original and full of potential. This procedure made it possible to highlight the characteristics specific to the sediments in this region. Thus, the presence of numerous siliceous organisms could be demonstrated, as well as an evolution of the quantity of smectite probably linked to changes in the climate. These points deserve additional studies in order to derive additional information and on the one hand to refine our results, but above all, to demonstrate significant potential for other environmental studies in this region. Thus, it would be interesting to deepen the cycle of silica. A first step would be to measure the proportion of silica of detrital origin (wind and fluvial quartz grains) versus silica of biogenic origin. In a next step, it would be possible to carry out an isotopic study on the biogenic silica. These two analyses would undoubtedly make it possible to better perceive changes in climate and its impacts on biologic activity and thus to strengthen or correct the built climate model. Another approach aimed at verifying the constructed climate model would be to better investigate the mineralogy. A study on the precise origin of smectite would probably provide crucial information. For this, more precise work on the diffractograms of XRD analyses could be used. A mineralogical reconstruction from data in elements (XRF measurements) could also be carried out in order to better target the detrital, climatic, hydrothermal or even biological origin of the various minerals. In this same perspective, isotopic analyses of the clay minerals would also be considered.

The presence of hydrothermal vents in the region has been demonstrated (Mukwati *et al.*, 2018). The presence of such sources within Lake Liambezi or in its direct surroundings is suggested by the analysis of microbiological communities. Some measurements in the water analyses of Dyer (2017) could also suggest the presence of hydrothermal vents in the vicinity of some sites. A more in-depth study of this type of source could be undertaken in order to measure what type of hydrothermalism it is and what is its link with the presence of faults linked to the Okavango Graben in the region.

The presence of carbonate was not observed in the SEM analyses. In addition, the presence of calcite and dolomite reported in the mineralogical analyses is sporadic and attributed to a detrital origin coming from the watershed. However, the pH conditions of Lake Liambezi as well as the calcite saturation index is reached for the waters of the lake. In addition, the presence of carbonate sediments is widely documented for the northern Botswana region (e.g. Burrough *et al.*, 2008). How is it that despite a current situation which could allow the precipitation of carbonates in the lacustro-palustrine environments of northern Botswana, no trace is reported and that the silica cycle is largely dominant? This question is all the more relevant as the precipitation conditions of carbonate deposits in the region are not understood. Their origin, their formation as well as their meaning remain controversial. The study of the sediments of Lake Liambezi offers a new database of current conditions and the recent past. These data will probably make it possible to better target the conditions required to better understand the alternations between carbonate or siliceous deposits of the past in this region.

Further work on the precise geomorphological description of the region and a better understanding of the faults arrangement in the region will provide an important clues to reconstruct the environmental development of the Linyanti-Chobe Basin. In such a perspective, a geophysical

survey might be an option. Geophysical methods (e.g. reflection seismology) might bring some interesting help for further investigation in the field of landscape evolution and timing in the formation and evolution of the different water bodies of northern Botswana. However, it should be borne in mind that these sedimentary basins are never deep (probably less than 10 meters for the most part) and can show significant lateral variations. The separation between climate influence and environmental change must also always be kept in mind. The paleoenvironmental and paleoclimatic reconstruction of the region therefore always remains complex and a simple approach is difficult to envisage.

7.5. References

- Bufford, K.M., Atekwana, E.A., Abdelsalam, M.G., Shemang, E., Atekwana, E.A., Mickus, K., Moidaki, M., Modisi, M.P., Molwalefhe, L., 2012. Geometry and faults tectonic activity of the Okavango Rift Zone, Botswana: Evidence from magnetotelluric and electrical resistivity tomography imaging. *Journal of African Earth Sciences*, 65, 61-71.
- Burrough, S.L., Thomas, D.S.G., 2008. Late Quaternary lake-level fluctuations in the Mababe Depression: Middle Kalahari palaeolakes and the role of Zambezi inflows. *Quaternary Research* 69, 388-403.
- Burrough, S.L., Thomas, D.S.G., Shaw, P.A., Bailey, R.M. 2007. Multiphase Quaternary highstands at Lake Ngami, Kalahari, northern Botswana. *Palaeogeography, Palaeoclimatology, Palaeoecology* 253, 280–299.
- Burrough, S.L., Thomas, D.S.G., Singarayer, J.S., 2009. Late Quaternary hydrological dynamics in the Middle Kalahari: Forcing and feedbacks. *Earth-Science Reviews*, 96, 313-326.
- Cavallé-Fol, 2020. On a découvert le berceau de l'Humanité. *Science & Vie*, N°1233, juin 2020, 56-71.
- Chevalier, M., Chase, B.M., 2015. Southeast African records reveal a coherent shift from high- to lowlatitude forcing mechanisms along the east African margin across last glacialinterglacial transition. *Quaternary Science Reviews*, 125, 117-130.
- Grove, A.T., 1969. Landforms and Climatic Change in the Kalahari and Ngamiland. *The Geographical Journal*, 135, 191-212.
- Haddon, I.G., McCarthy, T.S. 2005. The Mesozoic–Cenozoic interior sag basins of Central Africa: The Late-Cretaceous–Cenozoic Kalahari and Okavango basins. *Journal of African Earth Sciences* 43, 316-333.
- Huntsman-Mapila, P., Ringrose, S, Mackay, A.W., Downey, W.S., Modisi, M., Coetzee, S.H., Tiercelin, J.J., Kampunzu, A.B., Vanderpost, C., 2006. Use of the geochemical and biological sedimentary record in establishing palaeo-environments and climate change in the Lake Ngami basin, NW Botswana. *Quaternary International*, 148, 51-64.
- Kinabo, B.D., Atekwana, E.A., Hogan, J.P., Modisi, M.P., Wheaton, D.D., Kampunzu, A.B. 2007. Early structural development of the Okavango rift zone, NW Botswana. *Journal of African Earth Sciences*, 48, 125-136.
- McCarthy, T.S., 2013. The Okavango Delta and its place in the geomorphological evolution of southern Africa. *South Africa Journal of Geology*, 116, 1-54.
- Milzow, C., Kgotlhang, L., Bauer-Gottwein, P., Meier, P., Kinzelbach, W., 2009. Regional review: the hydrology of the Okavango Delta, Botswana - processes, data and modelling. *Hydrogeology Journal*, 17, 1297-1328.
- Mukwati, B.T., Tafesse, N.T., Bagai, Z.B., Laletsang, k. 2018. Hydrogeochemistry of the Kasane Hot Spring, Botswana. *Universal Journal of Geoscience* 6, 131-146.
- Peel, R.A., Tweddle, D., Simasiku, E.K., Martin, G.D., Lubanda, J., Hay, C.J., Weyl, O.L.F. 2015: Ecology, fish and fishery of Lake Liambezi, a recently refilled floodplain lake in the Zambezi Region, Namibia. *African Journal of Aquatic Science* 40:4, 417-424.
- Seaman, M.T., Scott, W.E., Walmsley, R.D., van der Waal, B.C.W., & Toerien, D.F. 1978: A limnological investigation of Lake Liambezi, Caprivi. *Journal of the Limnological Society of Southern Africa* 4:2, 129-144.
- Shaw, P.A., Bateman, M.D., Thomas, D.S.G., Davies, F., 2003. Holocene fluctuations of Lake Ngami, Middle Kalahari: chronology and responses to climatic change. *Quaternary International*, 111, 23-35.
- Sletten, H.R., Railsback, L.B., Liang, F., Brook, G.A., Marais, E., Hardt, B.F., Cheng, H., Edwards, R.L. 2013. A petrographic and geochemical record of climate change over the last 4600 years from a

- northern Namibia stalagmite, with evidence of abruptly wetter climate at the beginning of southern Africa's Iron Age. *Palaeogeography, Palaeoclimatology, Palaeoecology* 376, 149–162.
- Thomas, D.S.G., Burrough, S.L., 2012. Interpreting geoproxies of late Quaternary climate change in African drylands: Implications for understanding environmental change and early human behaviour. *Quaternary International*, 253, 5-17.
- Wiese, R., Hartmann, K., Gummersbach, V.S., Shemang, E.M., Struck, U., Riedel, F., 2020. Lake highstands in the northern Kalahari, Botswana, during MIS 3b and LGM. *Quaternary International*, 558, 10-18.

8. Appendix: Poster presentations, data and collaborations

8.1. Poster presentations

Poster presentation at the 16th Swiss Geoscience Meeting in Bern, Switzerland, 1st December 2018.

16th Swiss Geoscience Meeting, Bern 2018

Reconstruction of ecological evolution of lakes based on multidisciplinary proxies: the case of Lake Liambezi, Botswana.

Anaël Lehmann*, Christophe Paul**, Sevasti Filippidou**, Léandre Ballif*, Shannon Dyer*, Pilar Junier**, Torsten Vennemann*.

*Institute of Earth Surface Dynamics, University of Lausanne, CH-1015 Lausanne (anael.lehmann@unil.ch, torsten.vennemann@unil.ch)

**Laboratory of Microbiology, Institute of biology, Rue Émile-Argand 11, CH-2000 Neuchâtel

Lake Liambezi is an ephemeral lake that is seasonally replenished from several distinct sources of water. It is located at the Eastern side of Caprivi Strip, straddling the border between Namibia and Botswana. The drainage basin of the lake is a large, flat wetland, including some woodlands, which contains a typically slow-flowing floodplain river (Seaman et al., 1978; Peel et al., 2015). Seaman et al. (1978) estimated a drainage basin of some 300 km², of which 100 km² is open water at its full size. The Lake changes its shape, size, and depth seasonally and over the years due to fluctuating contributions of water from its distinct source regions. Its depth averages about 2.5 m (Seaman et al. 1978) but can reach 7 m at its peak (Peel et al. 2015). The lake forms two elongated basins with a South-West to North-West direction joined by a main channel.

The main source of water for Lake Liambezi is the Zambezi River with two different entries during years of flooding. A first entry is through the Chobe River, which can reverse its flow direction and enter the lake from the east of the southern basin. A second entry is via the Bukalo Channel from the Caprivi floodplain of the Zambezi River and it enters the lake from the northeast of the northern basin. Another source of water is the Kwando River that percolates through the wetlands out via the Linyanti Channels. Its waters flow eastward along the Namibia-Botswana border into the lake from the west of the two basins. Rainfall and runoff from the area north of the lake also contributes to the water inputs. Depending on the lake level, an outflow from the lake is permit via the Chobe River (Seaman et al. 1978, and Peel et al. 2015).

The present study is based on two field campaigns: one, a reconnaissance study during the dry season (September 2016), while a second one was conducted at the end of the rainy season during March 2017. Water from multiple sources of ground and surface waters were collected to better understand the drainage and hydrodynamics in this relatively flat area (Dyer, 2017). It was also established that the present climate supports a vegetation representing both the C3 and C4 photosynthetic cycles (Ballif, 2018). While the former is favored in wet/cold environments, the latter is pronounced in dry/warm settings. These two functional types differ profoundly in their physiology, metabolism, water-use efficiency, resource acquisition and growth form. They also discriminate very differently against ¹³C during photosynthesis, such that the C-isotope composition of organic matter accumulated in soils or sediments may provide valuable information on the local ecosystem. In parallel to these geochemical studies the endospore forming communities have been analysed together with physical (grain size) analyses. During the second field campaign three cores of 40 cm each were sampled. One in the Northern basin a second

in the Southern basin and the last one in the northern part of the channel between the two basins. Sediments of the cores were first characterized by scanning electron microscopy that indicated a large fraction of diatoms in the sediments. Subsequent isotope analysis of carbon ($^{13}\text{C}/^{12}\text{C}$ and ^{14}C), nitrogen, hydrogen and oxygen of the organic matter and also RockEval measurements will evaluate the composition and quality of the organic matter as it is expected to be largely of autochthonous origin within the sediments of the lake. The lithogenic fraction is analysed via X-ray diffraction and fluorescence for the mineralogy and bulk chemical composition. Collectively, these analyses should allow for good estimates of the sedimentation rates, age of the sediment and a paleoecological interpretation that will then be compared to information obtained from endospore forming communities, a novel biological marker proposed in paleoecological reconstructions.



Figure 1. Southern Basin of Lake Liambezi during the dry season (September 2016). The water level is low during this season. Lehmann A.

Figure 2. SEM image of a core sample showing coal and diatoms. The core samples show diatoms and organic matter as major content.

REFERENCES

- Ballif, L. 2018: Carbon and nitrogen stable isotope compositions as environmental proxies in savannas of northern Botswana. Unpubl. Master of Science in Biogeosciences, UNIL.
- Dyer, S. 2017: Water cycle in the Northern Kalahari. Unpubl. Master of Science in Biogeosciences, UNIL.
- Peel, RA., Tweddle, D., Simasiku, EK., Martin, GD., Lubanda, J., Hay, CJ., Weyl, OLF. 2015: Ecology, fish and fishery of Lake Liambezi, a recently refilled floodplain lake in the Zambezi Region, Namibia. *African Journal of Aquatic Science* 40:4, 417-424.
- Seaman, M.T., Scott, W.E., Walmsley, R.D., van der Waal, B.C.W., & Toerien, D.F. 1978: A limnological investigation of Lake Liambezi, Caprivi. *Journal of the Limnological Society of Southern Africa* 4:2, 129-144.

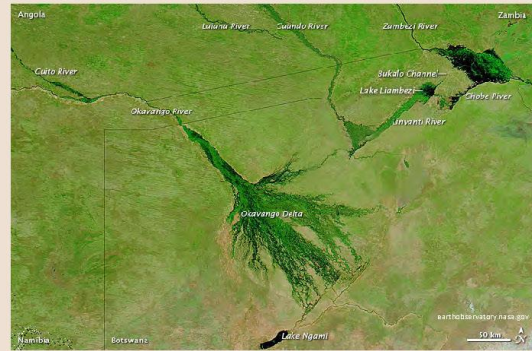
Lake Liambezi, Botswana

Reconstruction of ecological evolution of lakes based on multidisciplinary proxies

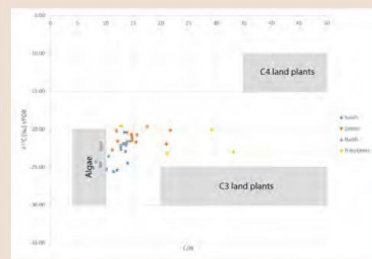
Anaël Lehmann*, Christophe Paul**, Sevasti Filippidou**, Shannon Dyer*, Pilar Junier**, Torsten Vennemann*.

*Institute of Earth Surface Dynamics, University of Lausanne, CH-1015 Lausanne (anael.lehmann@unil.ch, torsten.vennemann@unil.ch)

**Laboratory of Microbiology, Institute of biology, Rue Émile-Argand 11, CH-2000 Neuchâtel

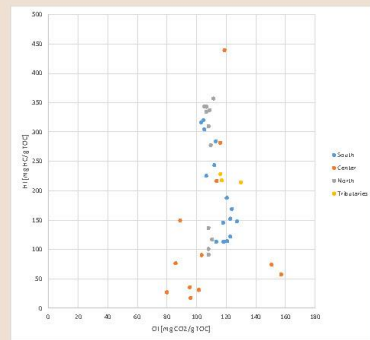


Lake Liambezi is an ephemeral lake seasonally replenished from several distinct sources of water. It is located at the Eastern side of Caprivi Strip, straddling the border between Namibia and Botswana. The drainage basin of the lake is a large, flat wetland, including some woodlands, which contains a typically slow-flowing floodplain river (Seaman et al., 1978; Peel et al., 2015). Seaman et al. (1978) estimated a drainage basin of some 300 km², of which 100 km² is open water at its full size. The Lake changes its shape, size, and depth seasonally and over the years due to fluctuating contributions of water from its distinct source regions.



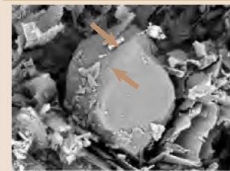
Three cores were taken on three different sectors of the lake.

$\delta^{13}\text{C}$ [%o] VPDB over C/N ratio shows a mix in the origin of organic matter in the sediments between algae and plants. The ratio varies between the different cores but also within the same core throughout its history. It shows an evolution of water regime and origin of water all along time.

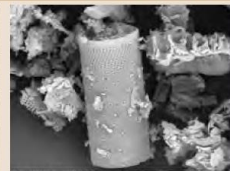


[Fig 1]

The X-ray fluorescence spectrometry reveals the mineral SiO₂ to be the most abundant mineral present in the sediments of the lake. The Scanning Electron Microscopy (SEM) confirms the major place of SiO₂ and shows a preponderant silica cycle into the sediments.



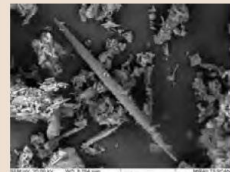
[Fig 1]



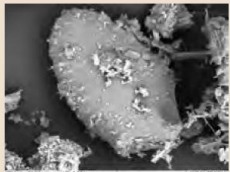
[Fig 2]



[Fig 3]



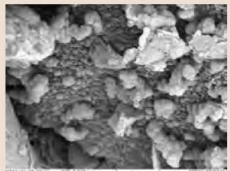
[Fig 4]



[Fig 5]



[Fig 6]

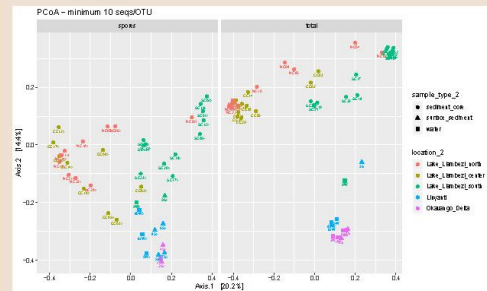


[Fig 7]

Exhibit of the silica cycle present into the lake with:

Dissolution:
[Fig 1] dissolution marks on quartz grain

Precipitation:
[Fig 2 and 3] diatoms;
[Fig 4] sponge spicule;
[Fig 5] silicified vegetal cells (phytolite);
[Fig 6] silicified Cyanobacteria colonies (*Gloeocapsa*, *Chroococcales*);
[Fig 7] silica precipitation under amorphous form.



[Fig 2]

RockEval data [Fig 1] as well as endospore-forming Firmicutes (endospores) communities and total bacterial communities [Fig 2] show differences in the three cores as well as within the same core. It shows an evolution of water regime, origin of water and ecology all along the time with variations in correlations between the different sectors of the lake.

Perspectives:
Paleoecological and paleoenvironmental interpretations will be refined according to the results to come. Coming ¹⁴C dating results will permit to give an idea of the correlation between the different deposits with in addition a sedimentation rate.



Geophysical Research Abstracts
 Vol. 21, EGU2019-9888, 2019
 EGU General Assembly 2019
 © Author(s) 2019. CC Attribution 4.0 license.



Paleoecological reconstruction of Lake Liambezi, Botswana using multidisciplinary proxies

Anaël Lehmann (1), Christophe Paul (2), Sevasti Filippidou (2), Léandre Ballif (1), Shannon Dyer (1), Pilar Junier (2), and Torsten Vennemann (1)

(1) Institute of Earth Surface Dynamics, Geosciences and Environment, Lausanne, Switzerland, (2) Laboratory of Microbiology, Institute of Biology, Faculty of Science, Neuchâtel, Switzerland

Lake Liambezi is located at the Eastern side of Caprivi Strip, straddling the border between Namibia and Botswana. The drainage basin of the lake is a large, flat wetland, including some woodlands, which contains a typically slow-flowing floodplain river (Seaman et al., 1978; Peel et al., 2015). The Lake changes its shape, size, and depth seasonally and over the years due to fluctuating contributions of water from its distinct source regions. The lake forms two elongated basins with a South-West to North-West direction joined by a main channel. The present study is based on multiple methods conducted on the watershed as well as on the lake. The aim is to give a paleoecological interpretation of the lake with isotopic and multi-proxy records. During the two field campaigns conducted during the dry season (September 2016) as well as at the end of the rainy season during March 2017, water from multiple sources of ground and surface waters were collected to better understand the drainage and hydrodynamics (Dyer, 2017). It was also established that the present climate supports a vegetation representing both the C3 and C4 photosynthetic cycles (Ballif, 2018). As they discriminate very differently against ^{13}C during photosynthesis, such that the C-isotope composition of organic matter accumulated in soils or sediments may provide valuable information on the local ecosystem. In parallel to these geochemical studies three cores of 40 cm each were sampled in the lake. Sediments of the cores were first characterized by scanning electron microscopy that indicated a large fraction of diatoms in the sediments. Subsequent isotope analysis of carbon ($^{13}\text{C}/^{12}\text{C}$ and ^{14}C), nitrogen, hydrogen and oxygen of the organic matter and also RockEval measurements will evaluate the composition and quality of the organic matter. The lithogenic fraction is analysed via X-ray diffraction and fluorescence for the mineralogy and bulk chemical composition. Collectively, these analyses should allow for good estimates of the sedimentation rates, age of the sediment and a paleoecological interpretation that will then be compared to information obtained from endospore forming communities, a novel biological marker proposed in paleoecological reconstructions.

REFERENCES

- Ballif, L. 2018: Carbon and nitrogen stable isotope compositions as environmental proxies in savannas of northern Botswana. Unpubl. Master of Science in Biogeosciences, UNIL.
- Dyer, S. 2017: Water cycle in the Northern Kalahari. Unpubl. Master of Science in Biogeosciences, UNIL.
- Peel, R.A., Tweddle, D., Simasiku, E.K., Martin, G.D., Lubanda, J., Hay, C.J., Weyl, O.L.F. 2015: Ecology, fish and fishery of Lake Liambezi, a recently refilled floodplain lake in the Zambezi Region, Namibia. *African Journal of Aquatic Science* 40:4, 417-424.
- Seaman, M.T., Scott, W.E., Walmsley, R.D., van der Waal, B.C.W., & Toerien, D.F. 1978: A limnological investigation of Lake Liambezi, Caprivi. *Journal of the Limnological Society of Southern Africa* 4:2, 129-144.

Paleoecological reconstruction of Lake Liambezi, Botswana using multidisciplinary proxies

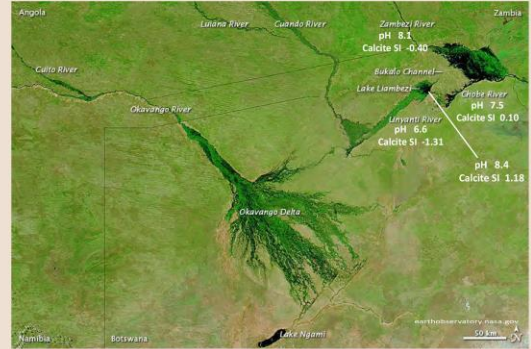


Anaël Lehmann*, Christophe Paul**, Sevasti Filippidou**, Léandre Ballif*, Shannon Dyer*, Pilar Junier**, Torsten Vennemann*.

*Institute of Earth Surface Dynamics, University of Lausanne, CH-1015 Lausanne (anael.lehmann@unil.ch, torsten.vennemann@unil.ch)
 **Laboratory of Microbiology, Institute of biology, Rue Émile-Argand 11, CH-2000 Neuchâtel

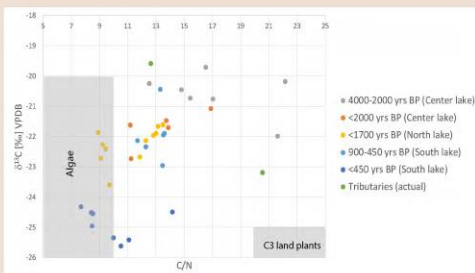


Lake Liambezi is an ephemeral lake seasonally replenished from several distinct sources of water. It is located at the eastern side of the Caprivi Strip, straddling the border between Namibia and Botswana. Its drainage basin is a large, flat wetland, including some woodlands, that includes a typically slow-flowing floodplain river (Seaman et al., 1978; Peel et al., 2015). Seaman et al. (1978) estimated a drainage basin of some 300 km², of which 100 km² is open water at its full size. The Lake changes its shape, size, and depth seasonally and over the years due to fluctuating contributions of water from its distinct source regions.

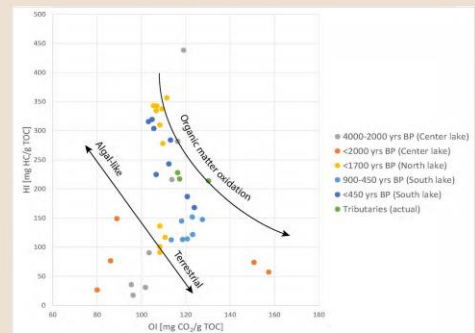


Three cores have been taken on three different sectors of the lake: northern and southern basins and in the central area between the two basins. Isotope analysis of carbon (¹³C/¹²C and ¹⁴C), nitrogen, hydrogen and oxygen of the organic matter and also RockEval measurements have been made on the core sediments. A novel biological marker for paleoecological reconstructions using **endospore forming communities** is proposed to help refine the interpretations. The results show distinct assemblages in space and time and present changes from dryer to wetter conditions with soils and peat-like sediments to more lacustrine sediments.

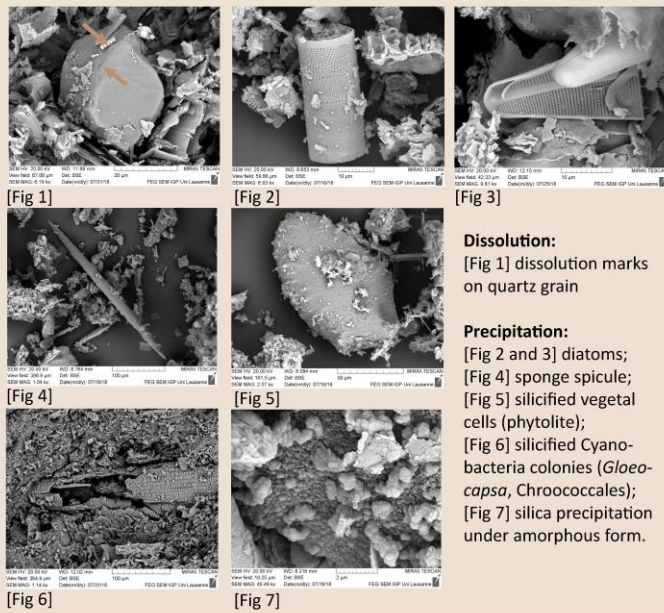
Origin of organic matter through $\delta^{13}C$ [‰] VPDB over C/N ratio



Organic matter quality with RockEval method



X-ray fluorescence spectrometry, X-ray diffraction as well as Scanning Electron Microscopy (SEM) reveal **SiO₂** to be the most abundant phase present in the sediments of the lake (Fig 1 to 7). Even though there may be a distinct Ca source (with hydrothermal sources along the Chobe River – Mukwati et al., 2018) carbonate saturation and precipitation remains rare and the silica cycle is clearly more important.

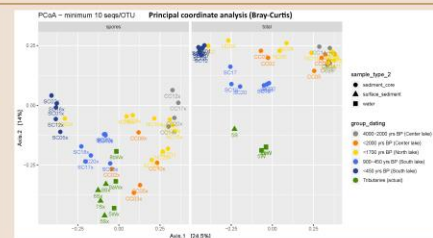


Dissolution:
 [Fig 1] dissolution marks on quartz grain

Precipitation:
 [Fig 2 and 3] diatoms;
 [Fig 4] sponge spicule;
 [Fig 5] silicified vegetal cells (phytolite);
 [Fig 6] silicified Cyanobacteria colonies (*Glaeocapsa*, Chroococcales);
 [Fig 7] silica precipitation under amorphous form.

Bacterial community analysis

Both total bacterial communities and spore communities show variability and distinct assemblages in space and time. Spore communities have a higher dispersion in the PCoA than the total bacterial community (related to the evolution of the environment).



Conclusion

1. Chemical and isotopic composition is different as a function of age (stratigraphy).
2. Bacterial communities also change as a function of age.
3. Hence, chemical and biological preservation is suggested and this clearly improves our environmental interpretations.



References: [1] Ballif, L. 2018: Carbon and nitrogen stable isotope compositions as environmental proxies in savannas of northern Botswana. Unpubl. Master of Science in Biogeochemistry, UNIL. [2] Dyer, S. 2017: Water cycle in the Northern Kalahari. Unpubl. Master of Science in Biogeochemistry, UNIL. [3] Mukwati, B.T., Tafesse, N.T., Bagai, Z.B., Laletsang, K. 2018: Hydrogeochemistry of the Kasane Hot Spring, Botswana. *Universal Journal of Geoscience* 6(S): 131-146. [4] Peel, R.A., Tweddle, D., Simasiku, E.K., Martin, G.D., Lubanda, J., Hay, C.I., Weyl, O.F. 2015: Ecology, fish and fishery of Lake Liambezi, a recently refilled floodplain lake in the Zambezi Region, Namibia. *African Journal of Aquatic Science* 40:4, 417-424. [5] Seaman, M.T., Scott, W.E., Walmsley, R.D., van der Waal, B.C.W., & Toerien, D.F. 1978: A limnological investigation of Lake Liambezi, Caprivi. *Journal of the Limnological Society of Southern Africa* 4:2, 129-144.



Appendix

8.2. Water data

8.2.1. Samples name, location and other details

sample	sample_name	general_status	status_dry_season	status_wet_season	watershed	location_feature	location_name	coordinates	elevation	sample_type	sample_type_2	depth	sampling_date_1	sampling_date_2	dna_treatment_spores	dna_treatment_total
Liambezi Lake																
Liambezi_Lake	SD-17	south_lake	south_lake	south_lake	linyanti_chobe_zambezi	liambezi_lake	south_basin_south	17.961056 S 24.360778 E	930	water	lake_water	0	August_2016	March_2017	spores	total
pt_233	SD-36	south_lake		lake	linyanti_chobe_zambezi	liambezi_lake	south_basin_south	17.959778 S 24.354806 E	931	water	lake_water	0		March_2017		
pt_232	SD-35	south_lake		lake	linyanti_chobe_zambezi	liambezi_lake	south_basin_center	17.946806 S 24.372861 E	931	water	lake_water	0		March_2017		
pt_229	SD-34	north_lake		lake	linyanti_chobe_zambezi	liambezi_lake	north_basin_north	17.898140 S 24.382667 E	931	water	lake_water	0		March_2017		
Linyanti watershed																
Linyanti_River	SD-09	tributaries	tributaries	tributaries	linyanti	linyanti_marsh	linyanti_campground	18.294861 S 23.907444 E	942	water	river_water	0	August_2016	March_2017	spores	total
Linyanti_Campground	SD-10	tributaries	borehole	borehole	linyanti	linyanti_marsh	linyanti_campground	18.295750 S 23.907667 E	947	water	underground_water	0	August_2016	March_2017		
Namatanga	SD-11	tributaries	borehole	dry	linyanti	linyanti_marsh	namatanga	18.024556 S 24.204500 E	935	water	underground_water	0	August_2016			
Chobe watershed																
Kasane_Chobe	SD-19	tributaries	tributaries	tributaries	chobe	chobe_river	kasane	17.794528 S 25.152250 E	926	water	river_water	0	August_2016	March_2017		
Chobe_National_Park	SD-37	tributaries		tributaries	chobe	chobe_river	chobe_national_park	17.839222 S 25.008306 E	934	water	river_water	0		March_2017		
Kavimba	SD-15	tributaries	tributaries	tributaries	chobe	oxbow_lake_of_chobe_river	north_legotlhwana	18.060083 S 24.590972 E	934	water	river_water	0	August_2016	March_2017	spores	total
Kavimba_center	SD-16	tributaries	tributaries	tributaries	chobe	oxbow_lake_of_chobe_river	north_legotlhwana	18.060083 S 24.590972 E	934	water	river_water	0	August_2016			
Chobe_Seariver	SD-14	tributaries	tributaries	tributaries	chobe	chobe_marsh	south_legotlhwana	18.106194 S 24.549944 E	930	water	lake_water	0	August_2016	March_2017		
Satau	SD-18	tributaries	tributaries	tributaries	chobe	chobe_marsh	satau	18.018194 S 24.411000 E	931	water	river_water	0	August_2016	March_2017		
Kachikabwe	SD-13	tributaries	borehole	dry	chobe	chobe_marsh	kachikabwe	18.181111 S 24.432472 E	936	water	underground_water	0	August_2016			
Chobe watershed, eventually Linyanti watershed, but out of the Liambezi Lake system																
VTR	SD-12	tributaries	borehole	borehole	chobe	chobe_marsh	VTR	18.111556 S 24.315639 E	936	water	underground_water	0	August_2016	March_2017		
Zambezi watershed																
Katima_Mulilo	SD-29	tributaries		tributaries	zambezi	zambezi_river	katima_mulilo	17.491083 S 24.316333 E	937	water	river_water	0		March_2017		
Mwande	SD-30	tributaries		tributaries	zambezi	zambezi_river	mwande	17.518528 S 24.822306 E	937	water	river_water	0		March_2017		
Bukalo	SD-28	tributaries		tributaries	zambezi	bukalo_channel	bukalo	17.721306 S 24.520444 E	935	water	river_water	0		March_2017		
pt_219	SD-27	tributaries		oxbow_lake	zambezi	zambezi_flood_plain	kabbe	17.721556 S 24.648556 E	937	water	lake_water	0		March_2017		
pt_218	SD-26	tributaries		oxbow_lake	zambezi	zambezi_flood_plain	east_kabula	17.818556 S 24.732833 E	935	water	lake_water	0		March_2017		
Kazungula	SD-31	tributaries		tributaries	zambezi	zambezi_river	kazungula	17.791653 S 25.265200 E	924	water	river_water	0		March_2017		
Zambezi watershed but out of Liambezi Lake system																
Devil's_Pool	SD-20	tributaries	tributaries	tributaries	zambezi	zambezi_river	victorias_fall	17.923608 S 25.852281 E	885	water	river_water	0	August_2016	March_2017		
Okavango watershed																
Ntwetwe	SD-32	tributaries		pan	okavango	makgadikgadi_pan	east_zoroga	20.145417 S 25.723306 E	911	water	lake_water	0		March_2017		
Mopipi	SD-21	tributaries	borehole	tributaries	okavango	makgadikgadi_pan	mopipi	21.213833 S 24.900250 E	914	water	underground_water	0	August_2016	March_2017		
Mopipi_Dam	SD-33	tributaries		pan	okavango	makgadikgadi_pan	mopipi	21.212194 S 24.884861 E	911	water	lake_water	0		March_2017		
Motopi	SD-22	tributaries	tributaries	tributaries	okavango	boteti_river	motopi	20.212056 S 24.127250 E	925	water	river_water	0	August_2016	March_2017		
Ryleys_Cresta	SD-03	tributaries	tributaries	tributaries	okavango	okavango_delta	ryleys_cresta	19.990056 S 23.429944 E	936	water	river_water	0	August_2016	March_2017		total
Airport_Maun	SD-23	tributaries	tap_water	tap_water	okavango	okavango_delta	airport_maun	19.975711 S 23.428242 E	947	water	tap_water	0	August_2016	March_2017		
Thamalakane	SD-01	tributaries	tributaries	tributaries	okavango	okavango_delta	thamalakane	19.927556 S 23.512139 E	937	water	river_water	0	August_2016	March_2017		total
Okavango_River_Lodge	SD-02	tributaries	tributaries	tributaries	okavango	okavango_delta	okavango_river_lodge	19.928972 S 23.512667 E	937	water	river_water	0	August_2016	March_2017		
Boro	SD-25	tributaries	tributaries	tributaries	okavango	okavango_delta	boro	19.846000 S 23.402444 E	941	water	river_water	0	August_2016	March_2017		
Tshwaaga	SD-24	tributaries	tributaries	tributaries	okavango	okavango_delta	tshwaaga_island	19.827917 S 23.380333 E	942	water	river_water	0	August_2016			
Kudumane	SD-04	tributaries	tributaries	tributaries	okavango	khwai_river	kudumane	19.212694 S 23.991306 E	929	water	river_water	0	August_2016	March_2017		total
Mababe_Bridge	SD-05	tributaries	tributaries	tributaries	okavango	khwai_river	mababe_bridge	19.178583 S 23.991111 E	930	water	river_water	0	August_2016	March_2017		
Mababe_South_Gate	SD-06	tributaries	borehole	borehole	okavango	khwai_river	mababe_south_gate	19.102889 S 23.985250 E	929	water	underground_water	0	August_2016	March_2017		
Okavango + Linyanti watersheds but out of Liambezi Lake system																
Savuti	SD-07	tributaries	borehole	borehole	okavango_linyanti	savuti_channel	savuti	18.567083 S 24.065028 E	936	water	underground_water	0	August_2016	March_2017		
Gcotha_Gate	SD-08	tributaries	borehole	borehole	okavango_linyanti	gcotha_hills	gcotha_gate	18.387917 S 24.237222 E	961	water	underground_water	0	August_2016	March_2017		

8.2.3. Data for the wet season

sample	T_wet	EC_wet	pH_wet	O2_mg_l_wet	O2_sat_wet	CaCO3_wet	N_wet	PO4_wet	Fluorure_wet	Chlorure_wet	Nitrite_wet	Bromure_wet	Nitrate_wet	Sulfate_wet	Phosphate_wet	Lithium_wet	Sodium_wet	Ammonium_wet	Potassium_wet	Magnesium_wet	Calcium_wet	HCO3_wet	CO3_wet	TOC_wet	IC_wet	TC_wet	d13C_VPDB_wet	DIC_wet	d18O_VSMOW_wet	dD_VSMOW_wet	Calcite_Si_wet	
Liambezi Lake																																
Liambezi_Lake	28.40	693.00	7.27	2.38	34.20	180	2.50	0.25	0.16	26.95	3.52	0.07	0.64	147.02	0.00	0.01	47.67	1.45	26.27	18.23	88.00	183.05	0.19	72.64	205.04	113.00	-0.73	183.00	-1.95	-23.67	-0.01	
pt_233	28.00	691.00	8.07	5.11	73.30	220			0.22	20.71	0.02	0.15	0.10	176.61	0.00	0.01	51.92	0.48	24.68	19.03	90.23	164.75	1.07	52.86	179.43	88.18	-0.18	167.00	-1.77	-23.59	0.72	
pt_232	27.80	252.00	7.64	4.39	61.60	140			0.07	1.71	0.00	0.01	0.05	35.56	0.00	0.00	11.57	0.05	7.86	5.42	30.85	73.22	0.16	13.33	79.91	29.06	-1.37	73.00	-4.41	-36.98	-0.76	
pt_229	28.60	349.00	8.21	4.58	66.40	160			0.10	2.98	0.01	0.02	0.01	59.23	0.00	0.00	20.37	0.08	11.23	8.59	39.58	108.00	0.94	19.13	90.38	36.92	-2.72	110.00	-5.20	-39.46	0.42	
Linyanti watershed																																
Linyanti_River	23.80	281.00	7.42	4.55	59.90	160	2.40	0.34	0.08	54.05	0.02	0.12	0.37	8.93	0.00	0.00	13.99	0.39	18.61	7.31	43.37	86.64	0.11	38.86	113.39	61.18	-4.77	87.00	-2.30	-23.13	-0.43	
Linyanti_Campground	24.30	294.00	6.33	1.11	15.10	130	2.70	0.74	0.08	10.56	0.04	0.04	0.03	0.13	0.00	0.01	15.31	2.74	11.84	5.65	33.48	209.90	0.02	20.52	156.57	51.32	6.37	210.00	1.72	-0.49	-1.25	
Namatanga																																
Chobe watershed																																
Kasane_Chobe	26.70	253.00	7.22	3.31	47.10	70	0.50	0.15	0.03	16.09	0.02	0.10	0.10	15.78	0.00	0.00	15.13	0.03	1.51	3.06	12.72	37.83	0.03	7.81	48.55	17.36	-5.58	38.00	-4.89	-35.41	-1.43	
Chobe_National_Park	20.90	127.90	7.25	4.03	50.20				0.02	4.87	0.01	0.01	0.02	6.22	0.00	0.00	8.90	0.15	1.64	2.88	12.70	36.43	0.03	9.50	41.24	17.62	-4.86	30.00	-5.72	-44.96	-1.50	
Kavimba	28.80	791.00	7.33	2.77	39.70	200	1.60	0.25	0.05	29.24	0.02	0.05	0.07	199.03	0.00	0.01	35.43	0.59	16.90	22.28	122.06	184.27	0.22	27.66	205.80	68.16	-2.98	185.00	-3.50	-29.52	0.19	
Kavimba_center																																
Chobe_Seariver	29.30	831.00	7.93	6.01	89.20	130	1.60	0.25	0.07	13.80	0.03	0.04	0.25	316.20	0.01	0.01	39.30	0.33	17.99	24.36	134.08	116.54	0.55	38.10	239.73	85.29	1.12	118.00	-3.40	-26.10	0.58	
Satau	30.10	679.00	8.64	5.47	81.10	190	1.90	0.28	0.12	5.21	0.05	0.01	0.05	209.98	0.00	0.00	37.53	0.20	16.00	14.32	92.19	111.05	2.74	13.00	129.04	38.40	-2.86	117.00	-3.43	-28.24	1.10	
Kachikabwe																																
Chobe watershed, eventually Linyanti watershed, but out of the Liambezi Lake system																																
VTR	27.60	1377.00	6.84	3.28	45.90	420	0.80	0.40	0.10	67.85	0.03	0.14	0.44	228.22	0.01	0.05	270.62	2.46	39.56	23.36	53.41	453.96	0.18	9.21	409.21	89.80	-5.33	454.00	-0.24	-14.00	-0.36	
Zambezi watershed																																
Katima_Mulilo	25.10	68.90	8.07	4.80	65.50	35	<0.5	0.14	0.02	2.44	0.04	0.01	0.05	1.25	0.00	0.00	3.00	0.14	1.04	2.73	9.39	32.22	0.16	5.40	33.10	11.91	-6.58	7.00	-4.19	-27.44	-0.76	
Mwande	29.80	81.80	7.60	4.06	60.00	40	0.70	0.12	0.02	13.64	0.02	0.04	0.05	1.31	0.00	0.00	3.57	0.08	1.61	2.32	7.88	12.87	0.03	5.63	35.30	12.58	-9.03	13.00	-4.20	-27.53	-1.65	
Bukalo	28.00	390.00	8.23	3.95	55.50	210	1.70	0.37	0.12	18.07	0.01	0.01	0.01	7.42	0.04	0.00	20.98	0.18	7.19	10.88	57.45	208.68	1.94	18.41	214.69	60.67	-4.29	213.00	-5.38	-43.69	0.87	
pt_219	26.70	213.00	9.02	6.48	89.60	150	1.70	0.28	0.06	60.79	0.01	0.01	0.04	3.70	0.00	0.00	9.57	0.16	3.98	4.17	39.78	81.15	4.38	4.68	112.42	26.80	-5.11	91.00	-4.79	-35.95	1.03	
pt_218	28.80	124.80	8.21	6.12	88.00	70	1.30	0.28	0.03	4.81	0.01	0.05	0.01	0.87	0.00	0.00	16.40	0.14	2.09	2.11	9.34	61.63	0.52	7.13	63.05	19.53	-3.78	36.00	-3.82	-32.04	-0.33	
Kazungula	27.60	77.00	7.36	3.95	55.50	50	1.30	0.12	0.04	5.45	0.00	0.01	0.01	0.86	0.00	0.00	3.69	0.04	1.37	2.40	7.66	32.09	0.04	5.01	35.13	11.93	-7.19	12.00	-4.94	-33.58	-1.54	
Zambezi watershed but out of Liambezi Lake system																																
Devil's_Pool	22.10	86.70	7.66	5.07	66.10	38	0.50	0.37	0.04	7.58	0.02	0.03	0.04	1.46	0.00	0.00	3.60	0.03	1.20	2.56	8.45	35.76	0.07	5.20	37.70	12.62	-7.40	9.00	-4.63	-30.75	-1.24	
Okavango watershed																																
Ntwetwe	27.80	2950.00	9.60	5.68	77.60	440	0.4<0.5	0.28	0.44	784.10	0.06	1.82	1.03	56.31	0.01	0.01	771.96	0.82	53.68	1.28	14.03	243.46	57.61	16.37	434.31	101.90	-5.47	364.00	-2.30	-21.20	1.28	
Mopipi	29.80	160.10	9.70	5.80	85.00	80	2.30	0.18	0.02	17.84	0.01	0.01	0.09	0.59	0.00	0.04	10.88	0.18	5.51	1.58	17.48	33.56	9.24	10.51	43.06	18.99	-16.58	14.00	-2.60	-19.46	0.81	
Mopipi_Dam	31.80	3550.00	9.85	5.03	76.50	100	1.40	0.49	0.46	1116.31	0.00	1.99	0.69	60.32	1.00	0.01	1033.01	0.63	20.08	0.47	11.60	104.34	44.41	9.07	16.44	12.30	-11.96	202.00	1.77	1.79	1.05	
Motopi	29.00	162.20	7.84	3.87	56.40	110	1.00	0.18	0.12	24.35	0.00	0.05	0.00	1.37	0.00	0.00	10.33	0.09	6.24	4.07	15.51	30.69	0.11	14.96	67.87	28.32	-5.96	31.00	2.13	-0.80	-0.78	
Ryleys_Cresta	32.50	98.50	6.75	2.45	37.80	70	1.70	0.25	0.06	3.88	0.01	0.05	0.02	1.40	0.00	0.00	4.75	0.07	4.16	2.60	9.44	32.40	0.01	13.94	44.21	22.65	-7.65	12.00	-3.77	-31.87	-2.00	
Airport_Maun	31.00	670.00	7.23	3.83	57.70	360	1.80	0.86	0.25	21.05	0.02	0.05	0.86	11.85	0.20	0.01	39.90	0.29	17.37	13.09	101.84	358.17	0.37	8.23	377.66	82.56	-8.43	359.00	3.11	4.83	0.38	
Thamalakane	31.90	95.70	6.94	3.78	57.30	70	1.80	0.14	0.06	5.43	0.01	0.01	0.01	1.40	0.00	0.00	5.40	0.15	4.66	2.76	9.74	40.09	0.02	17.49	49.57	27.24	-9.41	17.00	-3.39	-30.21	-1.69	
Okavango_River_Lodge	32.70	315.00	6.90	3.31	50.90	170	0.80	0.55	0.22	3.63	0.05	0.02	0.05	4.70	0.10	0.01	10.42	0.08	5.26	5.49	45.27	138.51	0.07	5.76	173.95	40.00	-9.14	117.00	2.57	2.47	-0.56	
Boro	24.30	91.90	6.78	4.50	62.00	55	1.70	0.18	0.05	13.88	0.00	0.01	0.13	0.15	0.00	0.00	4.63	0.08	3.68	3.17	10.85	34.54	0.01	15.22	47.36	24.54	-8.76	21.00	-3.89	-32.01	-1.99	
Tshwaaga																																
Kudumane	28.40	155.70	7.25	4.07	58.80	90	<0.5	0.52	0.08	11.26	0.01	0.05	0.01	0.19	0.28	0.00	10.59	0.14	14.98	3.54	11.33	60.41	0.06	16.99	67.67	30.31	-6.34	41.00	-2.69	-24.99	-0.32	
Mababe_Bridge	28.10	158.10	7.54	2.95	42.20	120	2.00	0.18	0.09	16.47	0.01	0.05	0.03	1.76	0.00	0.00	16.00	0.04	7.48	3.37	11.78	79.93	0.15	13.79	84.94	30.51	-6.10	36.00	-4.03	-33.51	-0.80	
Mababe_South_Gate	21.80	352.00	8.35	5.23	68.10	170	1.20	0.43	0.27	34.43	0.01	0.06	3.39	50.05	0.00	0.01	52.86	0.25	5.97	4.57	21.35	129.97	1.40	4.49	169.17	37.78	-8.19	133.00	1.00	-5.78	0.29	
Okavango + Linyanti watersheds but out of Liambezi Lake system																																
Savuti	21.60	565.00	8.02	4.68	61.80	320	1.20	0.37	0.36	15.82	0.11	0.05	3.33	48.51	0.00	0.01	33.17	0.21	19.36	12.61	53.96	244.07	1.26	3.68	313.25	65.34	-10.86	247.00	1.52	-3.42	0.61	
Gcotha_Gate	22.30	549.00	8.27	5.45	71.40	340	2.60	0.34	0.35	14.87	0.01	0.05																				

8.3. Vegetation data:

8.3.1. Species and mean geochemical values

family	code	sample_type	sampling_date	woody_species	graminoid_species	type_C3_C4	rooting	drought_strategy	N2_fixation	n	TOC	d13C_VPDB	TN	d15N_air	C_N
Mimosoideae	AE	plant	August_2016	Acacia_erioloba		C3	deep_rooted	semi_deciduous	yes	6	48.20	-29.30	2.00	3.60	24.10
Capparaceae	BA	plant	August_2016	Boscia_albitrunca		C3	deep_rooted	semi_deciduous	no	3	42.50	-27.50	2.70	10.00	15.74
Caesalpinioideae	CM	plant	August_2016	Colophospermum_mopane		C3	shallow_rooted	deciduous	yes	7	51.00	-27.50	1.60	3.10	31.88
Combretaceae	CB	plant	August_2016	Combretum_mossambicense		C3	deep_rooted	deciduous	no	6	44.10	-26.70	2.10	4.50	21.00
Poaceae	AR	plant	August_2016		Aristida_rhinochloa	C4				1	42.40	-13.50	0.30	0.90	141.33
Poaceae	BD	plant	August_2016		Brachiaria_deflexa	C4				1	43.40	-13.60	0.20	0.80	217.00
Poaceae	CC	plant	August_2016		Cenchrus_ciliaris	C4				2	44.00	-13.00	0.40	1.00	110.00
Poaceae	CD	plant	August_2016		Cynodon_dactylon	C4				10	40.30	-14.50	1.40	2.30	28.79
Poaceae	CE	plant	August_2016		Cymbopogon_excavatus	C4				5	45.70	-12.40	0.20	0.80	228.50
Poaceae	DA	plant	August_2016		Diheteropogon_ampectens	C4				1	43.20	-11.30	0.10	-1.20	432.00
Poaceae	DE	plant	August_2016		Digitaria_eriantha	C4				2	45.00	-12.90	0.40	1.40	112.50
Poaceae	EA	plant	August_2016		Eragrostis_aspera	C4				4	44.70	-12.80	0.40	2.20	111.75
Poaceae	EB	plant	August_2016		Eragrostis_biflora	C4				1	44.40	-14.10	0.40	-0.10	111.00
Poaceae	EC	plant	August_2016		Enneapogon_cenchroides	C4				1	43.60	-12.70	0.30	0.30	145.33
Poaceae	EI	plant	August_2016		Eragrostis_inamoena	C4				1	43.90	-13.60	0.40	0.60	109.75
Poaceae	EL	plant	August_2016		Eragrostis_lehmanniana_var_lehmanniana	C4				1	45.10	-13.70	0.50	3.70	90.20
Poaceae	EM	plant	August_2016		Enteropogon_macrostachyus	C4				1	43.40	-11.70	0.30	-0.70	144.67
Poaceae	EP	plant	August_2016		Eragrostis_lappula	C4				1	45.20	-12.80	0.20	0.20	226.00
Poaceae	ES	plant	August_2016		Eragrostis_superba	C4				1	44.00	-13.60	0.20	1.40	220.00
Poaceae	HC	plant	August_2016		Heteropogon_contortus	C4				1	43.10	-11.80	0.10	0.50	431.00
Poaceae	HR	plant	August_2016		Hyparrhenia_rufa	C4				3	41.50	-11.70	0.10	-5.60	415.00
Poaceae	IC	plant	August_2016		Imperata_cylindrica	C4				1	43.30	-13.50	0.20	-1.90	216.50
Poaceae	PR	plant	August_2016		Panicum_repens	C4				1	45.40	-10.80	2.40	1.80	18.92
Poaceae	PS	plant	August_2016		Pogonarthria_squarrosa	C4				1	43.10	-13.80	0.60	1.60	71.83
Poaceae	SF	plant	August_2016		Sporobolus_festivus	C4				2	44.80	-12.50	0.50	1.00	89.60
Poaceae	SP	plant	August_2016		Schmidtia_pappophoroides	C4				2	44.50	-12.90	0.40	2.10	111.25
Poaceae	SS	plant	August_2016		Setaria_sphacelata_var_sericea	C4				2	38.80	-11.70	0.40	-2.40	97.00
Poaceae	VC	plant	August_2016		Vossia_cuspidata	C4				1	39.40	-12.70	0.60	2.40	65.67
Cyperaceae	CL	plant	August_2016		Cyperus_longus	C4				1	41.30	-11.30	1.00	1.30	41.30
Cyperaceae	CP	plant	August_2016		Cyperus_papyrus	C4				3	44.50	-11.80	1.90	2.90	23.42
Cyperaceae	SC	plant	August_2016		Schoenoplectus_corymbosus	C4				2	44.30	-11.20	2.30	-1.10	19.26
Poaceae	PA	plant	August_2016		Phragmites_australis	C3				3	39.10	-25.00	2.50	0.10	15.64

8.4. Soils data

sample	sample_name	general_status	watershed	location_feature	location_name	coordinates	elevation [m]	sample_type	sample_type_2	depth	sampling_date
Liambezi Lake											
Liambezi_Lake	LL_1	lake_bank	linyanti_chobe_zambezi	liambezi_lake	south_basin_south	17.961056 S 24.360778 E	930	sediment	soil	0	August_2016
Linyanti watershed											
Linyanti_River	TR_2.1	floodplain	linyanti	linyanti_marsh	linyanti_campground	18.294861 S 23.907444 E	942	sediment	soil	0	August_2016
Linyanti_River	TR_2.2	river_bank	linyanti	linyanti_marsh	linyanti_campground	18.295750 S 23.907667 E	947	sediment	soil	0	August_2016
Linyanti_River	TR_2.3	plateau	linyanti	linyanti_marsh	linyanti_campground	18.300944 S 23.913833 E	947	sediment	soil	0	August_2016
Transect_4	TR_4.1	floodplain	linyanti	linyanti_marsh	south_west_namatanga	18.062528 S 24.163889 E	937	sediment	soil	0	August_2016
Transect_4	TR_4.2	floodplain	linyanti	linyanti_marsh	south_west_namatanga	18.062778 S 24.164347 E	938	sediment	soil	0	August_2016
Transect_4	TR_4.4	ridge	linyanti	linyanti_marsh	south_west_namatanga	18.064639 S 24.165694 E	941	sediment	soil	0	August_2016
Transect_4	TR_4.5	plateau_bank	linyanti	linyanti_marsh	south_west_namatanga	18.069000 S 24.165694 E	940	sediment	soil	0	August_2016
Transect_4	TR_4.6	plateau	linyanti	linyanti_marsh	south_west_namatanga	18.069806 S 24.170583 E	939	sediment	soil	0	August_2016
Transect_4	TR_4.3a	river_bank	linyanti	linyanti_marsh	south_west_namatanga	18.062861 S 24.164556 E	938	sediment	soil	0	August_2016
Transect_4	TR_4.3b	river_bank	linyanti	linyanti_marsh	south_west_namatanga	18.063139 S 24.164944 E	939	sediment	soil	0	August_2016
Transect_6	TR_6.1	river_bank	linyanti	linyanti_marsh	east_Namatanga	18.031778 S 24.236750 E	937	sediment	soil	0	August_2016
Transect_6	TR_6.2	floodplain	linyanti	linyanti_marsh	east_Namatanga	18.030611 S 24.236056 E	936	sediment	soil	0	August_2016
Linyanti watershed but out of Liambezi Lake system											
Transect_5	TR_5.1	ridge	linyanti	local_lowlands	south_paranatungu	18.106806 S 24.249528 E	936	sediment	soil	0	August_2016
Transect_5	TR_5.2	river_bank	linyanti	local_lowlands	south_paranatungu	18.107194 S 24.249806 E	936	sediment	soil	0	August_2016
Transect_5	TR_5.3	floodplain	linyanti	local_lowlands	south_paranatungu	18.107583 S 24.250028 E	936	sediment	soil	0	August_2016
Elephant_Pan	EP	pan	linyanti	local_lowlands	south_paranatungu	18.120472 S 24.266833 E	935	sediment	soil	0	August_2016
Chobe watershed											
Chobe_Seariver	TR_3.1	marsh	chobe	chobe_marsh	south_legotlhwana	18.106194 S 24.549944 E	930	sediment	soil	0	August_2016
Chobe_Seariver	TR_3.2	marsh	chobe	chobe_marsh	south_legotlhwana	18.106236 S 24.549900 E	930	sediment	soil	0	August_2016
Chobe_Seariver	TR_3.3	marsh_bank	chobe	chobe_marsh	south_legotlhwana	18.106306 S 24.549833 E	930	sediment	soil	0	August_2016
Chobe watershed, eventually Linyanti watershed, but out of the Liambezi Lake system											
Transect_7	TR_7.1	plateau	chobe	chobe_marsh	east_VTR	18.115750 S 24.332083 E	937	sediment	soil	0	August_2016
Transect_7	TR_7.2	river_bank	chobe	chobe_marsh	east_VTR	18.115458 S 24.332000 E	936	sediment	soil	0	August_2016
Transect_7	TR_7.3	floodplain	chobe	chobe_marsh	east_VTR	18.115194 S 24.331861 E	934	sediment	soil	0	August_2016
Bungallow_Island	BI_VTR_BI1	island	chobe	chobe_marsh	VTR	18.112556 S 24.317194 E	936	sediment	soil	0	August_2016
Bungallow_Island	BI_VTR_BI2	island	chobe	chobe_marsh	VTR	18.112556 S 24.317194 E	936	sediment	soil	50	August_2016
Lab_Plain	LP_VTR_LP1	floodplain	chobe	chobe_marsh	VTR	18.112222 S 24.316806 E	935	sediment	soil	0	August_2016
Lab_Plain	LP_VTR_LP2	floodplain	chobe	chobe_marsh	VTR	18.112222 S 24.316806 E	935	sediment	soil	50	August_2016
Okavango watershed											
Kudumane	TR_1.4	delta_bank	okavango	khwai_river_bank	kudumane	19.212694 S 23.991306 E	929	sediment	soil	0	August_2016
Kudumane_Road	TR_1.1	delta_bank	okavango	okavango_delta_bank	south_sankuyo	19.493250 S 23.866278 E	944	sediment	soil	0	August_2016
Kudumane_Road	TR_1.2	delta_bank	okavango	okavango_delta_bank	north_sankuyo	19.316500 S 23.922667 E	946	sediment	soil	0	August_2016
Kudumane_Road	TR_1.3	delta_bank	okavango	khwai_river_bank	south_kudumane	19.243444 S 23.969139 E	941	sediment	soil	0	August_2016

Appendix

sample	sample_name	sampling_status_2	sampling_status_3	vegetation_type	vegetation_class	vegetation_class	vegetation_subclass	woody_cover	canopy_height	TOC	d13C_VPDB	av_tree_foliage_d15N	av_herb_d15N	CaCO3_content
Liambezi Lake														
Liambezi_Lake	LL_1	floodplain	sedgeland	swamp_sedgeland	2	sedgeland		0		3.43	-19.74		1.85	6.30
Linyanti watershed														
Linyanti_River	TR_2.1	river	reed_area	reed_bed	1	reed_bed		0		2.57	-23.17		0.47	11.70
Linyanti_River	TR_2.2	bank	woodland	riverine_forest	6b	woodland	riverine	80	25	10.07	-21.50	5.04	3.11	2.00
Linyanti_River	TR_2.3	plain	open_woodland	mopane_shrubland	5a	shrubland	mopane_dominated	50	3	2.28	-21.40	3.04		1.30
Transect_4	TR_4.1	river	reed_area	reed_bed	1	reed_bed		0		2.73	-21.40		4.03	7.60
Transect_4	TR_4.2	river	grassland	sedgeland	2	sedgeland		0		5.63	-20.87		1.22	8.20
Transect_4	TR_4.4	plain	woodland	mopane_woodland	6a	woodland	mopane_dominated	60	20	3.07	-21.43	2.29	2.04	1.60
Transect_4	TR_4.5	plain	low_woodland	mopane_shrubland	5a	shrubland	mopane_dominated	40	3	0.52	-18.99	3.04	1.58	1.00
Transect_4	TR_4.6	plain	open_woodland	dry_grassland	4	grassland		0		0.90	-18.11		4.20	0.40
Transect_4	TR_4.3a	bank	woodland	riverine_forest	6b	woodland	riverine	60	15	1.24	-21.84	3.73	1.90	2.50
Transect_4	TR_4.3b	bank	woodland	riverine_forest	6b	woodland	riverine	60	15	3.20	-23.18	3.81	2.75	1.10
Transect_6	TR_6.1	bank	woodland	acacia_marginal_woodland	6b	woodland	riverine	80	25	1.73	-22.49	0.86	-0.12	2.40
Transect_6	TR_6.2	floodplain	grassland	floodplain_grassland	3	grassland		0		5.96	-15.86		-2.63	4.70
Linyanti watershed but out of Liambezi Lake system														
Transect_5	TR_5.1	plain	open_woodland	combretum_shrubland	5b	shrubland	combretum_dominated	35	5	1.86	-15.84		0.13	1.90
Transect_5	TR_5.2	floodplain	grassland	floodplain_grassland	3	grassland		0		3.10	-12.69		-3.83	3.40
Transect_5	TR_5.3	floodplain	grassland	floodplain_grassland	3	grassland		0		4.84	-12.07		-1.92	4.80
Elephant_Pan	EP	floodplain	pan	floodplain_pan	3	grassland		0		4.21	-15.56			5.00
Chobe watershed														
Chobe_Seariver	TR_3.1	floodplain	reed_area	sedgeland	2	sedgeland		0		5.99	-18.88		-1.71	6.20
Chobe_Seariver	TR_3.2	floodplain	grassland	c_dactylon_mat	2	sedgeland		0		9.55	-17.66		0.40	12.30
Chobe_Seariver	TR_3.3	floodplain	grassland	c_dactylon_mat	2	sedgeland		0		5.78	-17.47		5.69	9.30
Chobe watershed, eventually Linyanti watershed, but out of the Liambezi Lake system														
Transect_7	TR_7.1	plain	open_woodland	combretum_shrubland	5b	shrubland	combretum_dominated	45	3	0.36	-18.30	1.68	1.99	4.10
Transect_7	TR_7.2	bank	low_woodland	mixed_marginal_woodland	6b	woodland	riverine	60	15	0.92	-21.08	4.51	0.74	11.70
Transect_7	TR_7.3	river	grassland	floodplain_grassland	3	grassland		0		3.15	-17.07		0.02	2.60
Bungallow_Island	BI_VTR_BI1	island	woodland	mixed_marginal_woodland	6b	woodland	riverine	70	15	1.16	-21.83		0.33	10.00
Bungallow_Island	BI_VTR_BI2	island	woodland	mixed_marginal_woodland	6b	woodland	riverine	70	15	0.30	-18.40			15.10
Lab_Plain	LP_VTR_LP1	river	grassland	floodplain_grassland	3	grassland		0		3.32	-15.21		1.17	4.40
Lab_Plain	LP_VTR_LP2	river	grassland	floodplain_grassland	3	grassland		0		0.80	-16.90			3.80
Okavango watershed														
Kudumane	TR_1.4	floodplain	open_woodland	c_dactylon_mat	2	sedgeland		10	12	0.31	-16.14	8.64	5.30	0.30
Kudumane_Road	TR_1.1	plain	woodland	acacia_mopane_woodland	6a	woodland	mopane_dominated	50	6					
Kudumane_Road	TR_1.2	plain	low_woodland	mopane_shrubland	5a	shrubland	mopane_dominated	40	3	0.31	-18.19	5.23	3.30	1.00
Kudumane_Road	TR_1.3	plain	open_woodland	kalahari_shrubland	5b	shrubland	combretum_dominated	20	3	0.49	-20.03	8.59		0.70

8.5. Tributaries data

8.5.1. Samples name, location and other details

sample	sample_name	coordinates	elevation [m]	depth [cm]	general_status	status_dry_season	watershed	location_feature	location_name	sample_type	sample_type_2	sampling_date_1	dna_treatment_spores	dna_treatment_total
Thamalakane	BO01	19.927556 S 23.512139 E	937	0	tributaries	tributaries	okavango	okavango_delta	thamalakane	sediment	river_sediment	August_2016	no data	total
Ryleys_Cresta	BO02	19.990056 S 23.429944 E	936	0	tributaries	tributaries	okavango	okavango_delta	ryleys_cresta	sediment	river_sediment	August_2016	spores	total
Kudumane	BO03	19.212694 S 23.991306 E	929	0	tributaries	tributaries	okavango	khwai_river	kudumane	sediment	river_sediment	August_2016	spores	total
Mababe_Bridge	BO04	19.178583 S 23.991111 E	930	0	tributaries	tributaries	okavango	khwai_river	mababe_bridge	sediment	river_sediment	August_2016	spores	no data
Linyanti_River	BO05	18.294861 S 23.907444 E	942	0	tributaries	tributaries	linyanti	linyanti_marsh	linyanti_campground	sediment	river_sediment	August_2016	spores	total
Linyanti_River	BO06	18.294861 S 23.907444 E	942	0	tributaries	tributaries	linyanti	linyanti_marsh	linyanti_campground	sediment	river_sediment	August_2016	spores	no data
Chobe_Seariver	BO07	18.106194 S 24.549944 E	930	0	tributaries	tributaries	chobe	chobe_marsh	south_legotlhwana	sediment	river_sediment	August_2016	spores	no data
Kavimba	BO08	18.060083 S 24.590972 E	934	0	tributaries	tributaries	chobe	oxbow_lake_of_chobe_river	north_legotlhwana	sediment	river_sediment	August_2016	spores	no data
Liambezi_Lake	BO09	17.961056 S 24.360778 E	930	0	tributaries	south_lake	linyanti_chobe_zambezi	liambezi_lake	south_basin_south	sediment	lake_sediment	August_2016	spores	no data

8.5.2. Mineralogy data

sample	depth [cm]	Phyllosilicates	Quartz	Feldspath-	Plagioclase	Calcite	Dolomite	Pyrite	Goethite	Gypse	Indosée	sum		smectite	mica	kaolinite	chlorite	vermiculite	sum
Thamalakane	0	12.81	71.06	1.52	no data	no data	0.49	no data	no data	no data	14.13	100		8.00	17.76	61.36	no data	12.88	100
Ryleys_Cresta	0	13.50	76.19	0.72	no data	no data	no data	no data	no data	no data	9.58	100		9.45	11.11	65.53	no data	13.91	100
Kudumane	0	7.91	80.22	7.82	no data	no data	no data	no data	no data	no data	4.05	100		6.91	18.51	64.54	no data	10.04	100
Mababe_Bridge	0	20.45	62.34	0.65	no data	no data	no data	no data	no data	no data	16.56	100		6.57	14.64	69.90	no data	8.89	100
Linyanti_River	0	10.96	83.69	0.67	no data	no data	no data	no data	no data	no data	4.68	100		20.08	no data	53.56	no data	26.36	100
Linyanti_River	0	14.55	67.33	0.81	no data	no data	no data	no data	no data	no data	17.31	100		17.30	15.22	22.39	20.17	24.91	100
Chobe_Seariver	0	24.88	32.56	2.15	no data	no data	no data	no data	no data	1.22	39.19	100		23.02	15.87	10.86	11.36	38.89	100
Kavimba	0	7.84	75.10	3.57	0.84	no data	no data	no data	no data	no data	12.66	100		36.62	no data	12.10	12.10	39.17	100
Liambezi_Lake	0	20.56	40.78	3.19	no data	no data	no data	3.47	no data	1.50	30.50	100		16.16	10.37	15.37	29.45	28.66	100

8.5.3. Major elements data

sample	depth [cm]	SiO2	TiO2	Al2O3	Fe2O3	MnO	MgO	CaO	Na2O	K2O	P2O5	LOI	Cr2O3	NiO	not_meas	new_sum	in % wt	LOI at 1050°C	S
Thamalakane	0	97.50	0.06	0.69	0.12	0.00	0.05	0.00	0.01	0.13	0.01	0.54	0.00	0.00	0.89	100			no data
Ryleys_Cresta	0	92.56	0.17	1.68	0.37	0.01	0.11	0.11	0.04	0.35	0.02	3.70	0.00	0.00	0.87	100			no data
Kudumane	0	95.47	0.15	1.24	0.26	0.00	0.07	0.03	0.03	0.28	0.01	1.69	0.00	0.00	0.77	100			no data
Mababe_Bridge	0	94.72	0.12	1.71	0.36	0.00	0.09	0.06	0.02	0.25	0.01	1.81	0.00	0.00	0.83	100			no data
Linyanti_River	0	89.42	0.10	0.90	0.24	0.00	0.07	0.22	0.00	0.06	0.02	8.23	0.00	no data	0.75	100			0.49
Linyanti_River	0	80.68	0.22	2.35	0.69	0.01	0.15	0.41	0.02	0.14	0.03	14.53	0.00	no data	0.77	100			0.38
Chobe_Seariver	0	75.85	0.15	2.18	0.92	0.02	0.21	0.89	0.07	0.28	0.07	18.54	0.00	no data	0.83	100			0.53
Kavimba	0	90.17	0.14	2.00	0.94	0.01	0.24	0.43	0.16	0.27	0.02	4.94	0.00	no data	0.67	100			0.15
Liambezi_Lake	0	59.94	0.42	5.71	4.74	0.04	0.43	1.00	0.07	0.31	0.10	26.76	0.01	0.01	0.45	100			2.74

8.5.4. Trace elements data

sample	depth [cm]	Sc	V	Cr	Mn	Co	Ni	Cu	Zn	Ga	Ge	As	Se	Br	Rb	Sr	Y	Zr	Nb	Mo	Ag	Cd
Thamalakane	0	no data	no data	no data	no data	no data	no data	no data	no data	no data	no data	no data	no data	no data	no data	no data	no data	no data	no data	no data	no data	no data
Ryleys_Cresta	0	no data	no data	no data	no data	no data	no data	no data	no data	no data	no data	no data	no data	no data	no data	no data	no data	no data	no data	no data	no data	no data
Kudumane	0	no data	no data	no data	no data	no data	no data	no data	no data	no data	no data	no data	no data	no data	no data	no data	no data	no data	no data	no data	no data	no data
Mababe_Bridge	0	no data	no data	no data	no data	no data	no data	no data	no data	no data	no data	no data	no data	no data	no data	no data	no data	no data	no data	no data	no data	no data
Linyanti_River	0	2.00	21.90	14.10	29.60	20.40	4.40	7.20	1.80	1.00	1.10	4.20	no data	1.90	2.80	8.70	3.00	71.30	1.30	no data	no data	no data
Linyanti_River	0	3.00	55.70	26.10	61.90	30.70	10.90	12.10	4.80	2.90	1.30	3.50	no data	4.60	8.40	17.10	6.20	123.60	3.10	1.40	4.10	no data
Chobe_Seariver	0	3.40	37.40	18.30	154.00	17.10	13.60	25.50	16.10	2.40	no data	4.50	no data	10.50	16.20	36.60	7.30	63.70	2.10	3.30	no data	no data
Kavimba	0	5.20	24.70	30.00	60.90	31.00	8.00	10.90	7.60	2.20	1.40	4.60	no data	1.50	16.60	19.30	4.20	90.20	1.40	no data	3.20	no data
Liambezi_Lake	0	6.60	125.10	59.20	318.90	25.30	28.60	18.40	17.00	6.70	1.00	4.50	no data	20.90	24.40	43.70	13.80	141.80	6.30	1.90	5.20	no data
		Sn	Sb	Te	I	Cs	Ba	La	Ce	Nd	Sm	Yb	Hf	Ta	W	Hg	Tl	Pb	Bi	Th	U	
Thamalakane	0	no data	no data	no data	no data	no data	no data	no data	no data	no data	no data	no data	no data	no data	no data	no data	no data	no data	no data	no data	no data	no data
Ryleys_Cresta	0	no data	no data	no data	no data	no data	no data	no data	no data	no data	no data	no data	no data	no data	no data	no data	no data	no data	no data	no data	no data	no data
Kudumane	0	no data	no data	no data	no data	no data	no data	no data	no data	no data	no data	no data	no data	no data	no data	no data	no data	no data	no data	no data	no data	no data
Mababe_Bridge	0	no data	no data	no data	no data	no data	no data	no data	no data	no data	no data	no data	no data	no data	no data	no data	no data	no data	no data	no data	no data	no data
Linyanti_River	0	4.90	no data	no data	no data	2.60	130.60	no data	8.60	4.30	no data	no data	no data	no data	378.80	no data	no data	no data	no data	no data	no data	no data
Linyanti_River	0	4.90	no data	no data	no data	2.90	205.90	8.30	15.60	4.70	4.80	no data	2.20	no data	501.30	no data	no data	1.50	no data	1.40	1.00	
Chobe_Seariver	0	4.60	no data	3.10	no data	no data	240.20	9.90	16.20	6.40	no data	no data	no data	no data	237.30	no data	no data	1.80	no data	1.70	7.90	
Kavimba	0	4.20	no data	no data	no data	no data	139.30	no data	no data	5.30	no data	no data	2.10	no data	547.10	no data	no data	no data	no data	no data	no data	no data
Liambezi_Lake	0	4.70	no data	no data	7.70	no data	328.80	13.20	33.20	13.10	no data	no data	no data	no data	124.30	no data	no data	8.30	no data	4.50	1.60	

8.5.5. Organic matter data

sample	depth [cm]	vegetation_class	d13C_VPDB	Nitrogen [% wt]	Hydrogen [% wt]	TOC [% wt]	C_N															
Thamalakane	0		-22.58	0.000	0.045	0.14	no data															
Ryleys_Cresta	0		-19.43	0.020	0.270	1.28	63.09															
Kudumane	0		-23.09	0.000	0.121	0.57	no data															
Mababe_Bridge	0		-18.55	0.000	0.156	0.43	no data															
Linyanti_River	0	1	-23.01	0.111	0.466	3.87	35.01															
Linyanti_River	0	1	-23.18	0.294	1.031	6.05	20.58															
Chobe_Seariver	0	2	-19.58	0.530	1.465	6.70	12.65															
Kavimba	0	1, 2	-20.06	0.061	0.358	1.72	28.24															
Liambezi_Lake	0	1, 2	-20.82	no data	no data	9.02	no data															
		HI [mg HC/g TOC]	OI [mg CO2/g TOC]	PC [%]	RC [%]	MINC [%]	Tmax [°C]	S1 [mg HC/g]	S2a [mg HC/g]	S2b [mg HC/g]	S3	Contrib.A1	Contrib.A2	Contrib.A3	Contrib.A4	Contrib.A5	I_index	R_index	A0			
Thamalakane	0	196	219	0.03	0.11	0.02	412	0.00	0.27	0.00	0.31	21.37	22.06	23.88	19.14	13.53	0.26	0.57	0.24			
Ryleys_Cresta	0	227	159	0.30	0.98	0.08	330	0.01	2.90	0.00	2.03	20.14	27.22	25.72	18.99	7.92	0.27	0.53	0.03			
Kudumane	0	238	183	0.14	0.43	0.04	410	0.01	1.36	0.00	1.05	18.31	25.43	27.95	19.80	8.50	0.19	0.56	0.07			
Mababe_Bridge	0	117	145	0.06	0.37	0.04	405	0.01	0.50	0.00	0.63	17.33	21.89	26.41	19.68	14.67	0.17	0.61	0.17			
Linyanti_River	0	214	130	0.83	3.04	0.13	326	0.02	8.28	0.00	5.04	24.61	33.80	23.18	12.61	5.79	0.40	0.42	0.01			
Linyanti_River	0	228	116	1.34	4.71	0.17	328	0.02	13.80	0.00	7.04	23.70	30.47	24.46	15.26	6.10	0.35	0.46	0.00			
Chobe_Seariver	0	217	117	1.42	5.27	0.27	420	0.03	14.56	0.00	7.85	18.66	26.93	27.31	21.01	6.09	0.22	0.54	0.01			
Kavimba	0	164	138	0.30	1.42	0.11	420	0.01	2.82	0.00	2.37	no data	no data	no data	no data	no data	no data	no data	no data	no data	no data	
Liambezi_Lake	0	215	126	1.92	7.10	0.30	327	0.04	19.41	0.00	11.36	no data	no data	no data	no data	no data	no data	no data	no data	no data	no data	

8.5.1. Grain-size data

	BO01	BO02	BO03	BO04	BO05	BO06	BO07	BO08	BO09				BO01	BO02	BO03	BO04	BO05	BO06	BO07	BO08	BO09
Channel Diameter (Lower)	Diff.	Diff.	Diff.	Diff.	Diff.	Diff.	Diff.	Diff.	Diff.		Channel Diameter (Lower)	Diff.	Diff.	Diff.	Diff.	Diff.	Diff.	Diff.	Diff.	Diff.	Diff.
um	Volume	Volume	Volume	Volume	Volume	Volume	Volume	Volume	Volume		um	Volume	Volume	Volume	Volume	Volume	Volume	Volume	Volume	Volume	Volume
	%	%	%	%	%	%	%	%	%			%	%	%	%	%	%	%	%	%	%
0.38	0.01	0.01	0.01	0.01	0.01	0.03	0.05	0.02	0.09		69.62	0.66	1.86	1.68	0.83	1.02	1.98	1.94	0.79	1.87	
0.41	0.01	0.03	0.02	0.03	0.03	0.06	0.09	0.03	0.16		76.43	0.92	2.41	2.19	1.10	1.38	2.30	1.81	0.90	1.73	
0.45	0.02	0.04	0.03	0.04	0.05	0.09	0.14	0.04	0.23		83.90	1.31	3.24	2.85	1.53	1.92	2.76	1.68	1.05	1.58	
0.50	0.03	0.06	0.05	0.06	0.06	0.12	0.20	0.06	0.33		92.10	1.92	4.43	3.69	2.25	2.72	3.37	1.53	1.28	1.39	
0.54	0.04	0.08	0.06	0.07	0.08	0.15	0.25	0.07	0.41		101.10	2.81	5.95	4.73	3.37	3.85	4.09	1.40	1.58	1.20	
0.60	0.04	0.09	0.07	0.09	0.09	0.18	0.29	0.08	0.48		110.99	4.02	7.57	5.92	4.91	5.31	4.86	1.30	1.97	1.01	
0.66	0.05	0.10	0.07	0.10	0.10	0.20	0.33	0.10	0.54		121.84	5.48	8.91	7.15	6.71	6.97	5.58	1.26	2.45	0.87	
0.72	0.05	0.11	0.08	0.10	0.11	0.23	0.37	0.11	0.61		133.75	7.03	9.62	8.23	8.49	8.55	6.10	1.27	3.01	0.77	
0.79	0.06	0.11	0.09	0.11	0.12	0.25	0.41	0.12	0.66		146.82	8.42	9.49	8.95	9.88	9.72	6.29	1.30	3.63	0.69	
0.87	0.06	0.12	0.09	0.11	0.12	0.26	0.44	0.13	0.71		161.18	9.37	8.59	9.15	10.54	10.18	6.04	1.31	4.29	0.61	
0.95	0.06	0.12	0.09	0.12	0.12	0.28	0.46	0.14	0.74		176.94	9.67	7.15	8.70	10.30	9.76	5.33	1.25	4.92	0.50	
1.05	0.06	0.12	0.09	0.12	0.12	0.29	0.49	0.14	0.77		194.23	9.26	5.46	7.64	9.17	8.51	4.25	1.10	5.50	0.36	
1.15	0.06	0.12	0.09	0.11	0.12	0.30	0.51	0.15	0.80		213.22	8.23	3.78	6.13	7.39	6.66	2.98	0.88	5.95	0.21	
1.26	0.06	0.11	0.08	0.11	0.12	0.31	0.53	0.15	0.82		234.07	6.79	2.32	4.44	5.33	4.59	1.75	0.63	6.23	0.09	
1.38	0.05	0.11	0.08	0.11	0.12	0.32	0.56	0.16	0.84		256.95	5.24	1.25	2.89	3.40	2.72	0.78	0.44	6.32	0.02	
1.52	0.05	0.10	0.08	0.10	0.11	0.33	0.59	0.16	0.86		282.07	3.86	0.66	1.74	1.94	1.38	0.23	0.33	6.18	0.00	
1.67	0.04	0.10	0.07	0.10	0.11	0.34	0.62	0.17	0.88		309.64	2.83	0.50	1.09	1.10	0.69	0.03	0.30	5.84	0.00	
1.83	0.04	0.10	0.07	0.09	0.11	0.36	0.66	0.17	0.91		339.92	2.17	0.60	0.85	0.77	0.51	0.00	0.30	5.30	0.00	
2.01	0.04	0.09	0.06	0.09	0.11	0.38	0.71	0.18	0.95		373.15	1.79	0.77	0.86	0.74	0.59	0.00	0.31	4.61	0.00	
2.21	0.03	0.09	0.06	0.09	0.11	0.40	0.76	0.18	0.98		409.63	1.54	0.81	0.90	0.76	0.69	0.00	0.29	3.82	0.00	
2.42	0.03	0.09	0.06	0.09	0.11	0.42	0.83	0.19	1.03		449.67	1.28	0.64	0.82	0.67	0.62	0.00	0.21	3.00	0.00	
2.66	0.03	0.09	0.05	0.09	0.12	0.45	0.90	0.20	1.08		493.63	0.96	0.36	0.61	0.43	0.38	0.00	0.11	2.21	0.00	
2.92	0.03	0.10	0.05	0.10	0.12	0.48	0.97	0.20	1.14		541.89	0.61	0.13	0.34	0.16	0.12	0.00	0.04	1.51	0.00	
3.21	0.03	0.10	0.05	0.10	0.13	0.52	1.06	0.21	1.20		594.87	0.32	0.04	0.11	0.02	0.01	0.00	0.01	0.92	0.00	
3.52	0.03	0.11	0.05	0.11	0.14	0.56	1.15	0.22	1.27		653.03	0.11	0.04	0.02	0.00	0.00	0.00	0.00	0.47	0.00	
3.86	0.03	0.11	0.05	0.11	0.15	0.59	1.24	0.23	1.35		716.87	0.01	0.02	0.00	0.00	0.00	0.00	0.00	0.18	0.00	
4.24	0.03	0.12	0.06	0.12	0.16	0.63	1.33	0.24	1.42		786.95	0.00	0.00	0.00	0.00	0.00	0.00	0.00	0.04	0.00	
4.66	0.03	0.13	0.06	0.12	0.17	0.67	1.43	0.26	1.50		863.88	0.00	0.00	0.00	0.00	0.00	0.00	0.00	0.01	0.00	
5.11	0.03	0.13	0.06	0.13	0.18	0.71	1.53	0.27	1.58		948.34	0.00	0.00	0.00	0.00	0.00	0.00	0.00	0.00	0.00	
5.61	0.03	0.14	0.06	0.13	0.19	0.75	1.63	0.28	1.66		1041.05	0.00	0.00	0.00	0.00	0.00	0.00	0.00	0.00	0.00	
6.16	0.03	0.14	0.06	0.13	0.19	0.78	1.72	0.29	1.74		1142.83	0.00	0.00	0.00	0.00	0.00	0.00	0.00	0.00	0.00	
6.76	0.03	0.15	0.06	0.13	0.20	0.82	1.81	0.30	1.82		1254.55	0.00	0.00	0.00	0.00	0.00	0.00	0.00	0.00	0.00	
7.42	0.03	0.15	0.06	0.13	0.20	0.85	1.90	0.31	1.90		1377.20	0.00	0.00	0.00	0.00	0.00	0.00	0.00	0.00	0.00	
8.15	0.03	0.15	0.06	0.12	0.21	0.89	2.00	0.33	1.99		1511.84	0.00	0.00	0.00	0.00	0.00	0.00	0.00	0.00	0.00	
8.94	0.03	0.16	0.05	0.12	0.21	0.92	2.08	0.34	2.08		1659.64	0.00	0.00	0.00	0.00	0.00	0.00	0.00	0.00	0.00	
9.82	0.03	0.16	0.06	0.12	0.21	0.95	2.17	0.34	2.18		1821.89	0.00	0.00	0.00	0.00	0.00	0.00	0.00	0.00	0.00	
10.78	0.03	0.17	0.06	0.12	0.22	0.98	2.24	0.35	2.28		2000.00										
11.83	0.03	0.17	0.06	0.12	0.22	1.01	2.30	0.36	2.38												
12.99	0.03	0.19	0.06	0.12	0.23	1.04	2.36	0.36	2.48		Very coarse sand	0.00	0.00	0.00	0.00	0.00	0.00	0.00	0.00	0.00	
14.26	0.03	0.20	0.07	0.13	0.24	1.07	2.41	0.37	2.59		coarse sand	1.05	0.23	0.47	0.18	0.12	0.00	0.05	3.13	0.00	
15.65	0.03	0.21	0.08	0.14	0.25	1.10	2.43	0.37	2.68		medium sand	19.66	5.60	9.76	9.82	7.58	1.04	2.30	37.28	0.03	
17.18	0.04	0.23	0.09	0.14	0.25	1.11	2.41	0.37	2.70		fine sand	58.76	46.41	53.23	61.11	57.97	32.75	7.74	33.53	3.24	
18.86	0.04	0.23	0.09	0.14	0.25	1.11	2.34	0.37	2.65		very fine sand	17.10	34.35	28.20	20.71	23.16	24.94	10.93	10.01	9.64	
20.71	0.04	0.24	0.10	0.13	0.23	1.09	2.23	0.37	2.53		silt	0.98	5.81	2.57	3.55	5.76	25.17	52.65	9.11	55.65	
22.73	0.04	0.24	0.10	0.12	0.22	1.08	2.14	0.37	2.41		clay	0.60	1.55	1.00	1.53	1.80	6.05	11.58	2.72	14.89	
24.95	0.04	0.26	0.11	0.12	0.21	1.08	2.10	0.38	2.34		colloid	0.43	0.87	0.65	0.84	0.89	1.84	3.04	0.88	4.95	
27.39	0.04	0.31	0.14	0.13	0.23	1.13	2.16	0.41	2.35		tot sum	98.59	94.82	95.88	97.73	97.28	91.80	88.28	96.67	88.40	
30.07	0.05	0.37	0.17	0.16	0.26	1.20	2.28	0.44	2.44												
33.01	0.07	0.45	0.22	0.20	0.30	1.30	2.44	0.49	2.57												
36.24	0.09	0.52	0.29	0.24	0.34	1.41	2.57	0.54	2.68		After C. K. Wentworth classification:										
39.78	0.11	0.59	0.37	0.27	0.37	1.49	2.63	0.58	2.70												
43.67	0.14	0.69	0.47	0.31	0.40	1.55	2.60	0.62	2.64		Sand: 2mm-1/16mm	96.57	86.58	91.65	91.82	88.83	58.74	21.01	83.95	12.91	
47.94	0.19	0.82	0.60	0.36	0.44	1.58	2.49	0.64	2.50		Silt: 1/16mm-1/256mm	0.98	5.81	2.57	3.55	5.76	25.17	52.65	9.11	55.65	
52.63	0.25	0.99	0.77	0.43	0.50	1.62	2.35	0.66	2.32		Clay: <1/256mm	1.03	2.42	1.65	2.37	2.69	7.89	14.61	3.61	19.84	
57.77	0.35	1.21	0.99	0.52	0.60	1.67	2.21	0.69	2.15		tot sum	98.59	94.82	95.88	97.73	97.28	91.80	88.28	96.67	88.40	
63.42	0.48	1.48	1.29	0.65	0.77	1.78	2.07	0.73	2.00												

8.6. Lake Liambezi sediments data

8.6.1. Samples name, location and other details

sample	sample_name	coordinates	elevation [m]	depth [cm]	sample	sample_name	coordinates	elevation [m]	depth [cm]	sample	sample_name	coordinates	elevation [m]	depth [cm]
SC01	SC01	17.944778 S 24.372028 E	931	0	CC02	CC02	17.933806 S 24.354139 E	931	2	NC02+03	NC02	17.922833 S 24.368861 E	931	1
SC02+03	SC02	17.944778 S 24.372028 E	931	2	CC03+04	CC03	17.933806 S 24.354139 E	931	5	NC04+05	NC04	17.922833 S 24.368861 E	931	4
SC05	SC05	17.944778 S 24.372028 E	931	5	CC05+06+07	CC05	17.933806 S 24.354139 E	931	7	NC06+07	NC06	17.922833 S 24.368861 E	931	7
SC06	SC06	17.944778 S 24.372028 E	931	7	CC08+09	CC08	17.933806 S 24.354139 E	931	11	NC08	NC08	17.922833 S 24.368861 E	931	10
SC08	SC08	17.944778 S 24.372028 E	931	10	CC10+11	CC10	17.933806 S 24.354139 E	931	14	NC10	NC10	17.922833 S 24.368861 E	931	13
SC10	SC10	17.944778 S 24.372028 E	931	14	CC12+13	CC12	17.933806 S 24.354139 E	931	19	NC11	NC11	17.922833 S 24.368861 E	931	15
SC12+13	SC12	17.944778 S 24.372028 E	931	17	CC14+15+16	CC14	17.933806 S 24.354139 E	931	21	NC14	NC14	17.922833 S 24.368861 E	931	19
SC16	SC16	17.944778 S 24.372028 E	931	23	CC17+18+19	CC17	17.933806 S 24.354139 E	931	23	NC15	NC15	17.922833 S 24.368861 E	931	21
SC17	SC17	17.944778 S 24.372028 E	931	25	CC20+21+22	CC20	17.933806 S 24.354139 E	931	26	NC20	NC20	17.922833 S 24.368861 E	931	28
SC18	SC18	17.944778 S 24.372028 E	931	27	CC24+25	CC24	17.933806 S 24.354139 E	931	32	NC21+22	NC21	17.922833 S 24.368861 E	931	29
SC19	SC19	17.944778 S 24.372028 E	931	29	CC27	CC27	17.933806 S 24.354139 E	931	36	NC23+24	NC23	17.922833 S 24.368861 E	931	32
SC20	SC20	17.944778 S 24.372028 E	931	30	CC29	CC29	17.933806 S 24.354139 E	931	39					
SC21	SC21	17.944778 S 24.372028 E	931	31										
SC22	SC22	17.944778 S 24.372028 E	931	32										
SC23	SC23	17.944778 S 24.372028 E	931	33										

8.6.2. Radiocarbon data and estimated climatic and environmental data for estimated age model

Results of AMS 14C analysis of sample material submitted to AMS laboratory, ETH Zürich

Sample Code	depth [cm]	Material	C14 age BP	±1σ	F14C	±1σ	δC13 ‰	±1σ	mg C	C/N
SC05	5	sediment	259	21	0.9683	0.0026	-25.9	1	0.99	9.99
SC12+13	17	sediment	424	21	0.9486	0.0025	-27.6	1	0.99	11.36
SC17	25	sediment	219	21	0.9732	0.0026	-23.4	1	0.98	12.32
SC22	32	sediment	898	21	0.8943	0.0024	-22.3	1	1.00	10.44
CC02	2	sediment	1882	24	0.7910	0.0024	-23.2	1	0.42	
CC03+04	5	charcoal	2710	22	0.7136	0.0020	-26.3	1	0.99	17.93
CC10+11	14	charcoal	2006	23	0.7790	0.0023	-22.8	1	0.98	
CC20+21+22	26	charcoal	3243	24	0.6679	0.0020	-22.0	1	0.99	
CC27	36	charcoal	4697	25	0.5572	0.0017	-20.7	1	0.98	
NC04	4	sediment	1089	22	0.8730	0.0024	-22.6	1	0.69	
NC04+05	4	charcoal	1673	23	0.8120	0.0023	-22.4	1	0.99	
NC11	15	charcoal	1740	23	0.8052	0.0023	-23.2	1	0.99	
NC11	15	sediment	1682	23	0.8110	0.0023	-21.2	1	0.62	
NC15	21	sediment	1082	25	0.8740	0.0027	-23.9	1	0.26	
NC21	29	sediment	1512	26	0.8280	0.0026	-24.4	1	0.27	
NC23+24	32	charcoal	1618	23	0.8176	0.0024	-20.0	1	0.61	

sample	sample_name	age [yrs BP]	climate	details	environment	sample	sample_name	age [yrs BP]	climate	details	environment
NC02+03	NC02	51	humid	intermediate	High water lake	SC01	SC01	0	humid		lacustrine
NC04+05	NC04	206	humid		High water lake	SC02+03	SC02	130	humid	intermediate	lacustrine
NC06+07	NC06	361	dry		High water lake	SC05	SC05	259	humid		lacustrine
NC08	NC08	515	dry		High water lake	SC06	SC06	301	humid		lacustrine
NC10	NC10	670	humid		High water lake	SC08	SC08	342	dry		lacustrine
NC11	NC11	773	humid		High water lake	SC10	SC10	390	dry		lacustrine
NC14	NC14	961	dry		High water lake	SC12+13	SC12	424	dry		lacustrine
NC15	NC15	1082	dry		Low water lake	SC16	SC16	570	dry		lacustrine
NC20	NC20	1416	humid		Low water lake	SC17	SC17	640	humid	intermediate	marsh
NC21+22	NC21	1512	humid		Low water lake	SC18	SC18	700	humid	intermediate	marsh
NC23+24	NC23	1618	humid	intermediate	Low water lake	SC19	SC19	780	humid		marsh
						SC20	SC20	820	dry	intermediate	marsh
CC02	CC02	420	dry		marsh	SC21	SC21	860	dry		marsh
CC03+04	CC03	770	humid		marsh	SC22	SC22	898	dry		marsh
CC05+06+07	CC05	1000	dry		marsh	SC23	SC23	950	dry		marsh
CC08+09	CC08	1500	humid		emersion to marsh						
CC10+11	CC10	2006	dry		emersion						
CC12+13	CC12	2315	dry		fens						
CC14+15+16	CC14	2624	dry		fens						
CC17+18+19	CC17	2933	humid		fens						
CC20+21+22	CC20	3243	dry		marsh						
CC24+25	CC24	3970	dry		marsh						
CC27	CC27	4697	dry		marsh						
CC29	CC29	5424	humid		marsh						

8.6.3. Mineralogy data

sample	depth [cm]	Phyllosilicates	Quartz	Feldspath-K	Plagioclase-Na	Calcite	Dolomite	Pyrite	Goethite	Gypse	Indosée	sum		smectite	mica	kaolinite	chlorite	vermiculite	sum
SC01	0	20.75	15.09	0.80	0.89	2.29	1.00	0.61	3.05	1.92	53.59	100		56.40	18.14	4.71	5.30	15.44	100
SC02+03	2	23.78	9.50	0.94	0.81	2.98	no data	2.79	no data	2.22	56.97	100		22.01	14.89	23.67	14.52	24.92	100
SC05	5	20.08	12.32	2.94	1.89	no data	no data	3.02	no data	7.46	52.30	100		25.19	28.41	11.35	7.97	27.08	100
SC06	7	28.13	20.20	1.18	0.64	no data	no data	2.96	4.82	37.27	4.80	100		22.54	21.90	10.45	11.14	33.97	100
SC08	10	22.11	16.14	no data	no data	no data	no data	2.00	no data	7.30	52.45	100		15.76	19.48	14.98	18.26	31.52	100
SC10	14	26.84	16.62	no data	no data	no data	no data	2.32	no data	7.07	47.15	100		16.27	20.00	18.12	12.39	33.22	100
SC12+13	17	26.41	14.73	2.04	0.79	no data	no data	1.55	no data	13.65	40.84	100		17.54	13.03	19.07	14.52	35.84	100
SC16	23	21.61	29.34	1.88	1.27	no data	no data	1.95	no data	8.59	35.35	100		18.67	8.99	27.56	no data	44.78	100
SC17	25	22.31	57.32	1.56	no data	no data	no data	no data	no data	5.58	13.24	100		9.50	19.27	28.77	no data	42.47	100
SC18	27	27.82	41.95	1.46	0.82	no data	no data	0.99	4.12	5.58	17.25	100		9.10	15.76	19.63	9.11	46.39	100
SC19	29	20.92	36.80	0.93	1.24	no data	no data	no data	no data	1.69	38.44	100		37.20	4.72	26.75	no data	31.34	100
SC20	30	19.74	58.60	2.72	1.37	no data	no data	0.79	no data	1.27	15.50	100		12.46	10.01	31.31	no data	46.22	100
SC21	31	20.71	42.67	1.10	no data	no data	no data	0.54	no data	1.06	33.91	100		7.73	9.33	27.97	12.29	42.67	100
SC22	32	17.60	65.94	no data	no data	no data	no data	no data	no data	0.85	15.62	100		13.08	8.27	44.81	no data	33.85	100
SC23	33	17.62	42.14	1.75	1.23	0.83	n.d.	no data	no data	1.21	35.22	100		10.66	14.74	29.83	11.66	33.11	100
CC02	2	34.40	31.92	3.58	2.17	no data	2.16	no data	no data	4.68	21.10	100		18.27	14.86	17.21	13.44	36.22	100
CC03+04	5	28.58	22.92	no data	no data	no data	1.03	no data	no data	4.61	42.86	100		23.48	no data	20.59	16.25	39.68	100
CC05+06+07	7	30.10	26.07	3.16	2.05	1.04	1.30	0.98	4.10	0.90	30.30	100		18.29	16.29	14.82	18.90	31.71	100
CC08+09	11	25.78	10.34	5.65	1.65	1.20	1.16	no data	3.86	1.54	48.82	100		49.01	10.43	3.54	2.33	34.70	100
CC10+11	14	24.69	33.83	2.45	1.33	no data	1.16	no data	0.69	11.96	23.89	100		17.80	11.36	6.35	8.43	56.06	100
CC12+13	19	33.18	38.50	3.02	no data	no data	0.90	no data	5.22	6.20	12.98	100		18.13	11.95	18.44	10.64	40.84	100
CC14+15+16	21	43.08	17.92	3.24	1.79	no data	0.90	no data	no data	no data	33.07	100		21.38	12.29	24.48	9.86	31.99	100
CC17+18+19	23	33.61	48.37	2.71	no data	no data	no data	1.08	6.30	4.67	3.26	100		31.49	no data	30.50	11.83	26.18	100
CC20+21+22	26	28.16	9.30	4.25	2.56	no data	no data	no data	no data	1.50	54.22	100		21.09	13.80	15.48	12.65	36.98	100
CC24+25	32	26.18	16.34	3.57	2.28	no data	no data	no data	5.10	no data	46.53	100		21.33	14.91	14.98	10.70	38.07	100
CC27	36	25.94	8.70	2.81	no data	no data	no data	no data	no data	2.65	59.90	100		20.68	13.35	11.43	12.39	42.15	100
CC29	39	29.90	22.76	1.96	1.86	no data	no data	no data	no data	2.81	40.71	100		25.26	8.72	17.65	9.72	38.65	100
NC02+03	1	30.75	9.28	no data	no data	1.33	no data	4.25	no data	13.27	41.12	100		26.21	16.13	17.61	11.83	28.23	100
NC04+05	4	30.96	16.88	2.78	1.93	no data	no data	2.77	5.45	23.97	15.26	100		36.15	no data	14.58	10.81	38.46	100
NC06+07	7	31.98	36.72	no data	no data	no data	1.21	1.60	6.45	15.05	6.98	100		21.81	15.64	14.11	11.41	37.04	100
NC08	10	30.66	20.87	2.73	no data	no data	0.97	no data	no data	6.44	38.33	100		19.48	17.86	11.87	12.48	38.31	100
NC10	13	30.63	14.06	3.13	no data	no data	0.72	no data	no data	5.84	45.62	100		29.17	13.54	7.09	10.96	39.24	100
NC11	15	31.72	28.65	2.51	2.52	no data	no data	no data	no data	4.76	29.85	100		32.91	17.72	21.94	no data	27.43	100
NC14	19	31.70	15.77	2.55	no data	no data	no data	0.83	no data	5.63	43.53	100		21.90	11.87	15.32	13.44	37.47	100
NC15	21	25.17	29.89	2.95	no data	1.06	no data	no data	no data	5.29	35.64	100		19.30	10.93	11.82	11.20	46.74	100
NC20	28	33.68	16.53	3.25	2.15	no data	no data	no data	no data	23.78	20.61	100		27.35	no data	15.70	14.91	42.04	100
NC21+22	29	32.78	15.64	no data	no data	no data	no data	1.05	no data	48.88	1.66	100		22.48	18.46	24.83	no data	34.23	100
NC23+24	32	31.77	12.62	3.54	no data	no data	no data	no data	no data	45.93	6.15	100		19.29	20.36	23.57	no data	36.79	100

8.6.4. Major elements data

sample	depth [cm]	SiO2	TiO2	Al2O3	Fe2O3	MgO	CaO	Na2O	K2O	P2O5	LOI	Cr2O3	NiO	not_measured	new_sum	in % wt	LOI at 1050°C	S
SC01	0	54.66	0.40	6.72	5.00	0.63	2.56	0.11	0.41	0.14	28.62	0.01	0.01	0.69	100			2.85
SC02+03	2	55.12	0.40	6.70	5.11	0.61	2.55	0.13	0.46	0.14	28.49	0.01	0.01	0.23	100			2.81
SC05	5	55.33	0.40	6.83	5.36	0.60	1.86	0.12	0.38	0.14	28.28	0.01	0.01	0.65	100			2.81
SC06	7	55.56	0.41	6.84	5.42	0.58	1.35	0.11	0.38	0.14	28.21	0.01	0.01	0.95	100			2.81
SC08	10	56.38	0.43	6.97	5.70	0.53	1.07	0.09	0.38	0.12	27.51	0.01	0.01	0.76	100			3.49
SC10	14	57.06	0.43	7.03	5.86	0.50	1.03	0.10	0.40	0.10	26.60	0.01	0.01	0.83	100			3.49
SC12+13	17	56.03	0.43	6.93	5.89	0.47	0.88	0.09	0.37	0.09	27.94	0.01	0.01	0.83	100			3.95
SC16	23	57.19	0.45	7.16	6.01	0.46	0.85	0.09	0.39	0.08	26.33	0.01	0.01	0.95	100			3.54
SC17	25	61.99	0.49	7.49	5.08	0.47	0.78	0.09	0.41	0.07	22.24	0.01	no data	0.87	100			2.34
SC18	27	65.26	0.51	7.55	4.37	0.47	0.77	0.08	0.41	0.06	19.79	0.01	no data	0.69	100			1.58
SC19	29	71.37	0.53	7.35	3.51	0.44	0.66	0.08	0.37	0.08	15.00	0.01	no data	0.60	100			0.65
SC20	30	73.08	0.53	7.21	3.25	0.44	0.62	0.07	0.37	0.08	13.85	0.01	no data	0.48	100			0.46
SC21	31	74.25	0.51	6.72	2.91	0.39	0.57	0.05	0.30	0.07	13.23	0.01	no data	0.95	100			0.34
SC22	32	75.60	0.51	6.68	2.82	0.39	0.55	0.05	0.27	0.07	12.09	0.01	no data	0.93	100			0.24
SC23	33	75.29	0.50	6.60	2.93	0.38	0.57	0.05	0.26	0.07	12.42	0.01	no data	0.88	100			0.41
CC02	2	57.35	0.41	8.57	4.64	0.55	1.20	0.07	0.45	0.10	25.90	0.01	0.01	0.69	100			0.45
CC03+04	5	62.85	0.40	8.62	4.79	0.51	0.83	0.08	0.44	0.11	21.12	0.01	0.01	0.21	100			0.61
CC05+06+07	7	64.74	0.40	8.63	5.06	0.45	0.60	0.09	0.43	0.11	18.82	0.01	0.01	0.64	100			0.41
CC08+09	11	66.08	0.46	10.13	5.80	0.44	0.71	0.13	0.42	0.12	15.45	0.02	0.01	0.22	100			0.37
CC10+11	14	66.86	0.42	8.54	5.10	0.37	0.73	0.12	0.37	0.11	16.71	0.01	0.01	0.64	100			0.55
CC12+13	19	59.48	0.34	6.67	4.31	0.36	1.17	0.10	0.33	0.10	26.48	0.01	0.01	0.64	100			1.50
CC14+15+16	21	55.72	0.47	8.53	3.31	0.46	1.16	0.06	0.35	0.04	29.37	0.01	0.01	0.51	100			1.08
CC17+18+19	23	64.29	0.37	6.46	3.49	0.36	0.98	0.08	0.31	0.05	23.02	0.01	0.01	0.55	100			0.89
CC20+21+22	26	74.18	0.23	4.99	2.03	0.28	0.77	0.05	0.29	0.03	16.29	0.01	no data	0.85	100			0.22
CC24+25	32	78.97	0.21	4.79	1.69	0.24	0.64	0.05	0.25	0.02	12.44	0.00	no data	0.68	100			0.10
CC27	36	80.30	0.20	4.36	1.50	0.23	0.74	0.05	0.25	0.02	11.80	0.00	no data	0.54	100			0.14
CC29	39	77.49	0.27	6.05	1.83	0.27	0.71	0.07	0.31	0.02	12.24	0.01	no data	0.72	100			0.12
NC02+03	1	48.58	0.29	6.27	6.12	0.50	1.90	0.07	0.30	0.14	35.03	0.01	0.01	0.76	100			3.98
NC04+05	4	47.17	0.28	6.01	5.19	0.44	1.30	0.07	0.28	0.09	38.31	0.01	0.01	0.82	100			4.38
NC06+07	7	50.89	0.30	6.55	4.03	0.39	1.15	0.07	0.30	0.08	35.66	0.01	0.01	0.56	100			2.44
NC08	10	53.03	0.32	6.96	3.72	0.39	1.10	0.08	0.31	0.07	33.43	0.01	0.01	0.56	100			1.64
NC10	13	54.22	0.33	7.03	3.76	0.38	1.06	0.07	0.30	0.07	32.42	0.01	0.01	0.32	100			1.43
NC11	15	53.75	0.32	6.85	3.55	0.37	1.02	0.07	0.27	0.06	32.98	0.01	0.01	0.74	100			1.33
NC14	19	57.31	0.35	6.94	4.52	0.38	0.96	0.08	0.31	0.09	28.17	0.01	0.01	0.85	100			0.95
NC15	21	64.65	0.39	7.24	5.69	0.44	0.83	0.09	0.34	0.12	19.67	0.01	0.01	0.50	100			0.61
NC20	28	61.96	0.41	7.51	5.33	0.46	1.58	0.08	0.31	0.09	21.34	0.02	0.01	0.88	100			1.00
NC21+22	29	62.97	0.39	6.97	5.37	0.44	1.82	0.08	0.32	0.10	20.71	0.01	0.01	0.82	100			1.16
NC23+24	32	62.55	0.40	6.99	5.24	0.43	2.15	0.08	0.30	0.10	20.94	0.01	0.01	0.79	100			1.25

8.6.5. Trace elements data

sample	depth [cm]	Sc	V	Cr	Mn	Co	Ni	Cu	Zn	Ga	Ge	As	Se	Br	Rb	Sr	Y	Zr	Nb	Mo	Ag	Cd
SC01	0	7.70	131.30	66.80	315.80	31.80	31.10	22.10	19.30	8.00	no data	4.10	no data	21.90	29.80	73.10	13.00	100.00	6.10	4.00	5.20	no data
SC02+03	2	7.50	131.20	63.10	294.50	32.50	30.10	22.60	19.70	8.00	1.00	4.00	no data	23.70	29.30	68.10	12.70	99.40	6.00	3.30	5.00	no data
SC05	5	7.50	131.20	63.10	294.50	32.50	30.10	22.60	19.70	8.00	1.00	4.00	no data	23.70	29.30	68.10	12.70	99.40	6.00	3.30	5.00	no data
SC06	7	7.50	131.20	63.10	294.50	32.50	30.10	22.60	19.70	8.00	1.00	4.00	no data	23.70	29.30	68.10	12.70	99.40	6.00	3.30	5.00	no data
SC08	10	8.50	131.60	62.40	234.60	33.00	30.40	22.50	19.70	8.20	1.30	4.60	no data	20.90	29.10	41.90	13.40	113.30	6.30	2.50	no data	no data
SC10	14	8.50	131.60	62.40	234.60	33.00	30.40	22.50	19.70	8.20	1.30	4.60	no data	20.90	29.10	41.90	13.40	113.30	6.30	2.50	no data	no data
SC12+13	17	9.60	126.30	60.50	193.20	43.80	29.30	22.40	19.90	8.50	no data	no data	no data	18.50	28.00	35.80	13.30	121.00	6.60	2.10	no data	no data
SC16	23	9.40	129.40	57.40	169.50	31.40	31.60	24.10	23.00	8.50	1.10	4.50	no data	13.50	29.50	33.60	15.30	144.30	6.80	2.70	no data	no data
SC17	25	10.10	127.80	56.60	155.90	39.60	30.80	24.40	21.50	9.50	1.40	6.50	no data	10.10	30.30	32.90	17.00	166.00	7.40	2.50	5.90	no data
SC18	27	10.20	131.30	58.50	159.50	33.20	30.10	25.00	20.90	9.30	1.50	4.70	no data	9.30	31.00	34.00	17.00	178.60	7.80	2.20	5.00	no data
SC19	29	10.20	133.30	63.70	158.10	32.20	27.80	22.80	17.20	9.00	1.30	4.50	no data	7.30	28.40	34.70	15.90	200.70	8.20	1.90	4.10	no data
SC20	30	8.70	138.40	65.50	165.30	28.80	26.90	22.20	15.40	8.50	1.40	5.50	no data	7.10	26.80	35.20	15.90	198.80	7.80	2.20	6.00	no data
SC21	31	10.00	147.10	66.10	168.40	22.80	25.10	20.80	14.10	8.00	1.50	4.60	no data	6.10	23.90	36.50	15.90	193.80	7.60	1.90	3.10	no data
SC22	32	8.40	145.30	65.50	172.60	33.10	24.20	20.10	13.60	7.70	1.70	7.60	no data	5.80	21.80	36.40	14.90	201.70	7.60	1.70	4.70	no data
SC23	33	8.70	146.30	67.60	173.50	20.70	23.40	20.50	14.20	7.50	1.70	3.00	no data	5.90	22.00	35.80	13.70	192.40	7.20	1.20	3.00	no data
CC02	2	10.20	145.30	77.10	149.90	14.50	53.30	26.20	22.60	9.70	1.10	10.20	no data	16.00	33.60	63.00	10.50	77.50	6.40	4.80	5.90	no data
CC03+04	5	8.50	145.40	77.60	267.80	25.00	50.50	23.70	21.70	9.90	1.40	9.50	no data	16.70	34.90	66.60	10.60	83.60	6.40	2.50	5.70	no data
CC05+06+07	7	11.30	149.30	75.90	127.90	15.90	56.90	27.40	27.30	10.10	1.30	9.70	no data	21.50	34.00	55.60	10.70	79.50	6.50	5.50	5.00	no data
CC08+09	11	11.90	170.30	89.40	111.60	16.30	70.50	28.20	22.90	11.40	1.40	12.40	no data	10.30	30.10	50.40	7.40	85.20	7.30	4.80	5.60	no data
CC10+11	14	11.30	148.50	77.70	86.40	15.50	62.60	27.30	18.60	10.40	1.10	14.20	no data	5.20	23.50	83.00	6.90	82.50	6.90	8.50	5.00	no data
CC12+13	19	9.80	134.50	69.70	107.30	16.00	37.70	22.40	16.70	9.10	1.10	11.50	no data	14.20	28.40	57.30	10.00	72.50	5.40	5.10	4.50	no data
CC14+15+16	21	8.60	145.10	77.80	108.40	17.40	34.30	24.00	17.00	10.20	1.40	9.40	no data	12.80	32.90	40.70	10.50	83.90	6.30	2.50	4.40	no data
CC17+18+19	23	8.90	113.70	56.30	92.80	20.90	34.10	25.50	14.40	8.00	1.40	12.10	no data	11.60	27.90	42.80	10.20	113.80	5.60	3.60	4.00	no data
CC20+21+22	26	6.20	66.40	34.50	72.60	7.30	24.90	39.90	9.40	6.20	no data	7.10	no data	4.70	32.00	34.90	10.30	53.90	3.60	1.10	5.10	no data
CC24+25	32	6.50	59.50	30.20	59.20	6.00	20.70	43.50	6.60	5.80	no data	5.80	no data	1.60	25.30	29.90	9.60	50.30	3.30	no data	5.90	no data
CC27	36	7.00	51.70	26.70	59.90	8.40	20.10	45.50	6.40	5.50	no data	6.80	1.00	2.00	22.40	30.70	11.40	48.70	2.90	no data	4.50	no data
CC29	39	9.00	78.10	36.50	76.00	9.40	24.20	53.30	8.50	7.50	no data	5.00	no data	1.70	30.20	31.80	15.90	64.00	4.10	no data	5.60	no data
NC02+03	1	7.90	107.20	59.60	222.60	25.10	39.50	24.50	28.90	7.40	no data	6.00	no data	33.60	25.90	69.10	10.80	57.00	4.50	4.10	3.10	no data
NC04+05	4	6.00	101.20	53.60	168.30	19.80	36.20	20.60	23.70	6.70	no data	4.80	no data	26.30	24.20	52.10	10.00	58.00	4.30	3.10	no data	no data
NC06+07	7	7.00	102.50	65.50	114.70	16.60	41.60	17.80	20.70	7.20	no data	6.00	no data	16.10	22.20	61.90	10.20	62.70	4.60	3.00	4.50	no data
NC08	10	7.20	108.90	56.10	96.00	19.10	38.90	18.00	19.30	7.70	no data	4.30	no data	15.00	22.50	71.30	9.50	67.90	4.80	2.90	5.20	no data
NC10	13	7.70	113.40	61.30	91.40	16.90	36.10	17.80	18.20	7.80	no data	6.10	no data	14.50	22.40	71.50	9.40	68.20	5.10	3.30	5.80	3.40
NC11	15	6.90	111.50	59.40	79.90	21.60	36.80	17.90	16.30	7.90	1.00	6.50	no data	13.70	21.80	67.70	9.10	70.00	4.90	3.00	4.90	no data
NC14	19	9.10	126.00	62.80	81.60	18.80	43.50	20.80	18.70	8.80	1.10	8.10	no data	14.70	23.10	74.50	9.40	71.30	5.60	4.00	4.20	no data
NC15	21	11.30	154.00	76.60	94.80	21.00	44.80	24.00	21.00	10.00	1.30	8.80	no data	15.30	27.60	83.60	10.10	78.10	6.60	3.90	5.10	3.20
NC20	28	10.50	160.70	79.00	96.50	23.90	48.50	24.20	21.70	10.90	1.20	8.10	no data	14.60	29.60	58.50	12.70	77.60	6.50	3.50	5.60	no data
NC21+22	29	9.00	139.40	69.50	89.50	20.60	50.80	24.80	23.00	9.40	1.20	9.80	no data	14.60	23.60	75.10	11.70	76.80	6.40	4.20	6.60	no data
NC23+24	32	9.80	143.70	71.10	89.70	17.80	53.80	25.00	28.60	9.40	no data	9.60	no data	15.60	22.80	80.20	12.70	73.80	6.30	4.10	4.60	no data
sample	depth [cm]	Sn	Sb	Te	I	Cs	Ba	La	Ce	Nd	Sm	Yb	Hf	Ta	W	Hg	Tl	Pb	Bi	Th	U	
SC01	0	14.70	no data	no data	5.90	no data	361.50	17.80	33.90	14.50	no data	no data	3.00	no data	79.80	no data	no data	8.80	no data	5.70	1.70	
SC02+03	2	13.10	no data	no data	7.80	5.20	360.10	16.70	32.00	14.60	no data	no data	no data	no data	80.80	no data	no data	9.00	no data	5.50	2.30	
SC05	5	13.10	no data	no data	7.80	5.20	360.10	16.70	32.00	14.60	no data	no data	no data	no data	80.80	no data	no data	9.00	no data	5.50	2.30	
SC06	7	13.10	no data	no data	7.80	5.20	360.10	16.70	32.00	14.60	no data	no data	no data	no data	80.80	no data	no data	9.00	no data	5.50	2.30	
SC08	10	14.50	no data	no data	5.30	4.00	305.00	15.20	30.40	13.80	no data	no data	4.00	no data	92.80	no data	no data	9.10	no data	5.10	1.50	
SC10	14	14.50	no data	no data	5.30	4.00	305.00	15.20	30.40	13.80	no data	no data	4.00	no data	92.80	no data	no data	9.10	no data	5.10	1.50	
SC12+13	17	19.00	no data	no data	5.00	2.50	274.60	17.20	33.60	16.70	6.70	no data	2.90	no data	131.40	no data	no data	8.40	no data	5.90	1.10	
SC16	23	9.90	no data	no data	6.30		246.50	16.00	36.80	17.80	3.60	no data	2.50	no data	117.30	no data	no data	8.10	no data	5.80	1.30	
SC17	25	13.90	no data	no data	3.70	2.30	265.10	21.40	39.70	17.50	4.90	no data	2.70	no data	277.30	no data	no data	8.30	no data	6.10	1.90	
SC18	27	11.40	no data	no data	no data	3.80	295.20	22.80	40.70	18.80	5.90	no data	2.90	no data	163.80	no data	no data	9.60	no data	6.30	2.40	
SC19	29	9.10	no data	no data	no data	2.60	364.40	17.60	38.60	17.70	5.30	no data	4.00	no data	237.10	no data	no data	9.00	no data	6.10	1.10	
SC20	30	7.40	no data	no data	no data	3.80	410.00	21.90	38.80	16.30	5.00	no data	3.40	no data	219.00	no data	no data	10.10	no data	6.20	2.70	
SC21	31	8.40	no data	no data	no data	2.20	456.60	18.90	37.70	17.70	no data	no data	2.70	no data	143.70	no data	no data	10.10	no data	5.70	2.60	
SC22	32	10.60	no data	no data	no data	no data	467.20	16.10	33.60	14.20	5.20	no data	2.70	no data	286.40	no data	no data	9.50	no data	5.60	2.00	
SC23	33	6.90	no data	no data	no data	no data	458.50	19.80	39.00	18.00	no data	no data	2.70	no data	186.20	no data	no data	9.90	no data	5.00	1.40	
CC02	2	9.10	no data	no data	no data	no data	649.70	18.10	23.90	9.50	no data	2.00	no data	no data	25.90	no data	no data	9.50	no data	4.80	2.10	
CC03+04	5	7.20	no data	no data	no data	no data	624.40	15.40	25.20	12.50	no data	no data	no data	no data	87.00	no data	no data	9.40	no data	4.70	1.90	
CC05+06+07	7	8.30	no data	no data	no data	2.10	780.70	17.40	30.50	14.70	no data	no data	no data	no data	35.40	no data	no data	10.50	no data	5.40	2.30	
CC08+09	11	6.80	no data	no data	no data	no data	687.40	7.20	20.90	8.90	no data	no data	no									

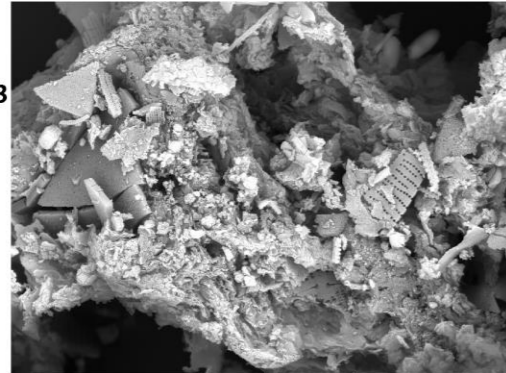
8.6.6. Organic matter data

sample	depth [cm]	d13C_VPDB	Nitrogen [% wt]	Hydrogen [% wt]	TOC [% wt]	C_N	HI [mg HC/g TOC]	OI [mg CO2/g TOC]	PC [%]	RC [%]	MINC [%]	Tmax [°C]	S1 [mg HC/g]	S2a [mg HC/g]	S2b [mg HC/g]	S3	Contrib.A1	Contrib.A2	Contrib.A3	Contrib.A4	Contrib.A5	I_index	R_index	A0
SC01	0	-24.32	1.103	1.886	8.48	7.69	304	106	2.39	6.09	0.46	425	0.11	25.77	0.00	8.95	17.56	22.47	29.57	25.22	5.17	0.13	0.60	0.00
SC02+03	2	-24.51	1.002	1.948	8.45	8.43	316	103	2.46	5.99	0.45	427	0.09	26.66	0.00	8.72	17.57	24.19	29.08	24.57	4.59	0.16	0.58	0.01
SC05	5	-24.56	1.019	2.022	8.70	8.54	320	105	2.57	6.13	0.36	423	0.13	27.82	0.00	9.12	22.20	23.83	28.45	21.71	3.81	0.21	0.54	0.01
SC06	7	-24.96	0.965	2.005	8.19	8.49	284	113	2.20	5.99	0.34	414	0.17	23.25	0.00	9.27	23.70	25.67	29.61	18.47	2.55	0.22	0.51	0.01
SC08	10	-25.34	0.778	1.793	7.77	9.99	243	112	1.82	5.95	0.31	412	0.18	18.87	0.00	8.73	23.34	25.03	31.22	17.88	2.53	0.19	0.52	0.02
SC10	14	-25.41	0.678	1.793	7.52	11.09	225	107	1.64	5.88	0.29	413	0.18	16.90	0.00	8.02	20.33	24.33	32.03	20.34	2.98	0.14	0.55	0.02
SC12+13	17	-25.61	0.663	1.761	6.99	10.54	187	121	1.34	5.65	0.33	407	0.27	13.08	0.00	8.43	25.79	26.08	32.03	13.85	2.23	0.21	0.48	0.03
SC16	23	-24.50	0.511	1.766	7.25	14.18	168	124	1.27	5.98	0.30	390	0.12	12.21	0.00	8.98	24.34	27.07	30.35	14.70	3.54	0.23	0.49	0.02
SC17	25	-22.13	0.476	1.519	5.57	11.70	148	127	0.88	4.69	0.25	394	0.09	8.23	0.00	7.10	24.01	26.04	30.14	15.22	4.58	0.22	0.50	0.02
SC18	27	-22.95	0.373	1.362	5.02	13.47	152	123	0.81	4.21	0.20	412	0.06	7.63	0.00	6.17	18.62	23.38	30.49	20.74	6.77	0.14	0.58	0.02
SC19	29	-21.89	0.264	1.125	3.59	13.61	145	118	0.55	3.04	0.16	421	0.04	5.22	0.00	4.24	14.74	21.24	30.34	24.56	9.12	0.07	0.64	0.03
SC20	30	-22.35	0.263	1.053	3.23	12.28	122	123	0.44	2.79	0.16	416	0.03	3.93	0.00	3.97	13.73	21.63	31.38	23.78	9.46	0.05	0.65	0.02
SC21	31	no data	0.220	0.988	3.06	13.94	113	119	0.39	2.67	0.18	417	0.02	3.48	0.00	3.63	13.14	21.54	31.21	24.40	9.71	0.05	0.65	0.02
SC22	32	-20.43	0.203	0.918	2.70	13.32	113	114	0.34	2.37	0.15	425	0.02	3.05	0.00	3.07	10.64	19.50	30.65	27.87	11.33	-0.01	0.70	0.04
SC23	33	-21.95	0.199	0.939	2.69	13.53	114	121	0.35	2.34	0.16	419	0.02	3.07	0.00	3.25	13.30	20.84	31.33	24.93	9.59	0.04	0.66	0.04
CC02	2	-21.08	0.549	1.744	9.27	16.88	149	89	1.38	7.90	0.38	422	0.02	13.85	0.00	8.25	11.55	20.89	31.67	27.30	8.59	0.01	0.68	0.01
CC03+04	5	-21.71	0.466	1.409	6.47	13.89	77	86	0.56	5.90	0.28	417	0.02	4.95	0.00	5.57	9.93	20.05	32.76	26.64	10.62	-0.04	0.70	0.03
CC05+06+07	7	-22.73	0.465	1.235	5.23	11.26	27	80	0.23	5.00	0.27	421	0.03	1.40	0.00	4.19	12.32	19.16	26.28	23.96	18.27	0.08	0.69	0.10
CC08+09	11	-21.62	0.150	1.335	1.68	11.18	57	158	0.15	1.53	0.16	404	0.02	0.96	0.00	2.64	14.19	20.05	26.68	21.13	17.94	0.11	0.66	0.13
CC10+11	14	-21.48	0.137	1.337	1.89	13.75	74	151	0.20	1.69	0.17	411	0.02	1.40	0.00	2.85	14.76	20.99	29.92	21.62	12.69	0.08	0.64	0.09
CC12+13	19	-20.74	0.503	1.762	7.77	15.43	216	114	1.64	6.13	0.27	421	0.04	16.81	0.00	8.84	18.26	19.32	31.05	24.79	6.58	0.08	0.62	0.01
CC14+15+16	21	-20.18	0.585	2.814	12.97	22.18	439	119	5.15	7.82	0.42	421	0.05	56.89	0.00	15.45	21.93	19.43	28.67	24.30	5.68	0.16	0.59	0.00
CC17+18+19	23	-21.99	0.328	1.616	7.11	21.65	282	116	1.89	5.22	0.27	425	0.03	20.03	0.00	8.28	17.88	19.73	30.78	25.96	5.64	0.09	0.62	0.01
CC20+21+22	26	-19.70	0.287	1.077	4.74	16.55	91	104	0.49	4.25	0.27	421	0.02	4.30	0.00	4.91	12.15	18.32	33.62	27.90	8.02	-0.04	0.70	0.02
CC24+25	32	-20.45	0.188	0.875	2.79	14.83	31	102	0.15	2.64	0.21	422	0.01	0.87	0.00	2.84	13.56	19.47	27.56	24.35	15.04	0.08	0.67	0.13
CC27	36	-20.77	0.157	0.834	2.69	17.06	36	96	0.15	2.54	0.18	426	0.01	0.97	0.00	2.57	14.70	16.85	25.94	27.31	15.20	0.09	0.68	0.12
CC29	39	-20.25	0.179	1.115	2.24	12.53	18	96	0.09	2.15	0.18	422	0.01	0.40	0.00	2.16	18.98	19.13	22.08	20.18	19.59	0.24	0.62	0.24
NC02+03	1	-23.60	1.200	3.194	11.66	9.71	357	112	3.81	7.84	0.36	418	0.11	41.56	0.00	13.00	20.01	23.53	30.07	22.80	3.59	0.16	0.56	0.01
NC04+05	4	-22.67	1.044	3.244	12.41	11.88	310	108	3.59	8.81	0.34	411	0.45	38.42	0.00	13.43	25.39	21.45	31.55	18.56	3.04	0.17	0.53	0.00
NC06+07	7	-21.61	0.899	3.021	12.13	13.49	337	109	3.77	8.36	0.33	412	0.11	40.92	0.00	13.25	22.91	21.16	30.72	20.97	4.23	0.16	0.56	0.01
NC08	10	-21.96	0.899	2.921	11.54	12.84	343	106	3.63	7.92	0.32	413	0.05	39.63	0.00	12.18	22.29	21.18	30.51	21.44	4.57	0.15	0.57	0.00
NC10	13	-21.90	0.856	2.832	11.15	13.02	334	107	3.42	7.73	0.35	414	0.05	37.26	0.00	11.89	21.67	21.47	30.39	21.76	4.70	0.15	0.57	0.00
NC11	15	-21.67	0.902	2.964	11.86	13.15	343	107	3.72	8.14	0.34	414	0.04	40.62	0.00	12.68	21.20	21.52	30.52	21.95	4.81	0.15	0.57	0.00
NC14	19	-22.13	0.772	2.446	9.49	12.29	278	110	2.47	7.01	0.33	416	0.03	26.35	0.00	10.40	17.23	22.42	31.85	23.40	5.10	0.10	0.60	0.01
NC15	21	-21.87	0.563	1.708	5.02	8.92	117	111	0.64	4.38	0.24	416	0.02	5.89	0.00	5.57	11.02	20.32	33.92	25.88	8.86	-0.03	0.69	0.02
NC20	28	-22.41	0.600	1.890	5.68	9.46	137	108	0.81	4.86	0.25	420	0.02	7.76	0.00	6.15	12.54	18.88	32.48	27.32	8.79	-0.01	0.69	0.02
NC21+22	29	-22.28	0.560	1.809	5.18	9.24	101	108	0.59	4.59	0.24	415	0.02	5.21	0.00	5.60	11.67	19.48	32.94	26.19	9.71	-0.02	0.69	0.03
NC23+24	32	-22.72	0.577	1.836	5.25	9.09	91	108	0.55	4.69	0.24	416	0.02	4.80	0.00	5.68	10.76	19.43	33.51	26.07	10.23	-0.05	0.70	0.01

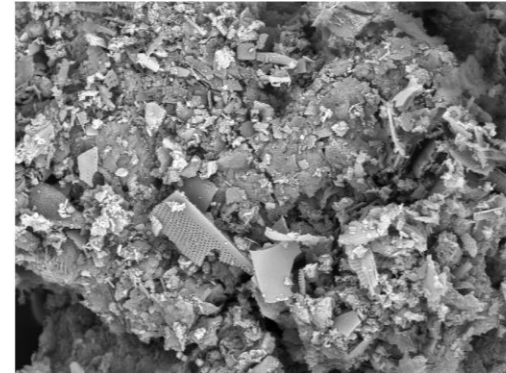
Channel Diameter (Lower)	NC02-03 NC04-05 NC06-07 NC08 NC10 NC11 NC14 NC15 NC20 NC21-22 NC23-24												Channel Diameter (Lower)	NC02-03 NC04-05 NC06-07 NC08 NC10 NC11 NC14 NC15 NC20 NC21-22 NC23-24											
	Diff.		Diff.		Diff.		Diff.		Diff.		Diff.			Diff.		Diff.		Diff.		Diff.		Diff.			
	Volume %	Volume %	Volume %	Volume %	Volume %	Volume %	Volume %	Volume %	Volume %	Volume %	Volume %	Volume %		Volume %	Volume %	Volume %	Volume %	Volume %	Volume %	Volume %	Volume %	Volume %	Volume %		
0.38	0.13	0.13	0.11	0.09	0.10	0.10	0.08	0.06	0.07	0.05	0.07	69.62	0.52	0.72	1.03	1.29	1.26	1.16	1.62	1.75	1.55	1.66	1.65		
0.41	0.23	0.23	0.19	0.16	0.17	0.18	0.14	0.10	0.13	0.08	0.12	76.43	0.53	0.72	1.02	1.24	1.26	1.14	1.48	1.70	1.45	1.55	1.58		
0.45	0.34	0.34	0.28	0.23	0.25	0.26	0.20	0.15	0.19	0.12	0.17	83.90	0.53	0.70	1.02	1.19	1.26	1.12	1.32	1.61	1.33	1.42	1.48		
0.50	0.48	0.49	0.40	0.33	0.36	0.37	0.28	0.21	0.27	0.18	0.25	92.10	0.51	0.65	0.99	1.13	1.23	1.08	1.15	1.49	1.19	1.27	1.35		
0.54	0.60	0.61	0.49	0.41	0.44	0.46	0.35	0.26	0.33	0.22	0.31	101.10	0.47	0.58	0.96	1.06	1.18	1.02	1.00	1.36	1.06	1.12	1.23		
0.60	0.70	0.72	0.57	0.48	0.52	0.53	0.41	0.31	0.39	0.26	0.36	110.99	0.43	0.51	0.93	1.00	1.12	0.97	0.87	1.25	0.95	1.00	1.12		
0.66	0.79	0.82	0.65	0.54	0.59	0.60	0.47	0.35	0.45	0.30	0.41	121.84	0.38	0.46	0.91	0.95	1.06	0.92	0.78	1.18	0.90	0.93	1.06		
0.72	0.88	0.92	0.72	0.60	0.65	0.67	0.52	0.39	0.50	0.34	0.46	133.75	0.34	0.44	0.89	0.91	1.01	0.88	0.73	1.15	0.89	0.90	1.04		
0.79	0.96	1.01	0.78	0.65	0.71	0.72	0.57	0.43	0.55	0.37	0.50	146.82	0.28	0.42	0.88	0.86	0.96	0.84	0.69	1.15	0.90	0.90	1.05		
0.87	1.02	1.08	0.82	0.69	0.75	0.76	0.61	0.46	0.58	0.40	0.53	161.18	0.20	0.38	0.83	0.80	0.90	0.79	0.63	1.13	0.89	0.90	1.04		
0.95	1.07	1.14	0.86	0.72	0.79	0.80	0.64	0.49	0.62	0.44	0.56	176.94	0.11	0.30	0.74	0.72	0.82	0.71	0.53	1.07	0.83	0.84	0.98		
1.05	1.12	1.20	0.89	0.75	0.82	0.82	0.67	0.51	0.65	0.47	0.59	194.23	0.04	0.19	0.60	0.61	0.71	0.62	0.39	0.93	0.69	0.72	0.84		
1.15	1.17	1.26	0.92	0.77	0.85	0.85	0.70	0.54	0.69	0.50	0.62	213.22	0.01	0.08	0.42	0.50	0.57	0.52	0.22	0.75	0.49	0.56	0.65		
1.26	1.23	1.31	0.95	0.80	0.88	0.88	0.73	0.57	0.72	0.54	0.66	234.07	0.00	0.02	0.24	0.39	0.42	0.43	0.09	0.58	0.29	0.40	0.45		
1.38	1.28	1.36	0.98	0.83	0.91	0.90	0.76	0.60	0.76	0.59	0.69	256.95	0.00	0.00	0.10	0.29	0.27	0.33	0.02	0.45	0.16	0.29	0.31		
1.52	1.34	1.41	1.01	0.86	0.94	0.93	0.80	0.63	0.80	0.63	0.73	282.07	0.00	0.00	0.03	0.20	0.14	0.23	0.00	0.41	0.11	0.24	0.25		
1.67	1.41	1.46	1.05	0.90	0.98	0.97	0.85	0.67	0.84	0.69	0.78	309.64	0.00	0.00	0.00	0.12	0.06	0.13	0.00	0.43	0.13	0.25	0.27		
1.83	1.49	1.52	1.10	0.95	1.03	1.02	0.90	0.72	0.90	0.75	0.84	339.92	0.00	0.00	0.00	0.05	0.02	0.06	0.00	0.49	0.21	0.31	0.34		
2.01	1.59	1.59	1.17	1.02	1.09	1.08	0.97	0.78	0.96	0.82	0.91	373.15	0.00	0.00	0.00	0.01	0.00	0.01	0.00	0.55	0.32	0.37	0.42		
2.21	1.69	1.66	1.24	1.09	1.16	1.15	1.04	0.84	1.04	0.90	0.98	409.63	0.00	0.00	0.00	0.00	0.00	0.00	0.00	0.56	0.39	0.41	0.46		
2.42	1.81	1.74	1.33	1.17	1.24	1.23	1.12	0.91	1.11	0.98	1.07	449.67	0.00	0.00	0.00	0.00	0.00	0.00	0.00	0.52	0.40	0.41	0.45		
2.66	1.92	1.82	1.43	1.26	1.33	1.31	1.21	0.99	1.20	1.08	1.16	493.63	0.00	0.00	0.00	0.00	0.00	0.00	0.00	0.46	0.34	0.38	0.39		
2.92	2.05	1.91	1.53	1.36	1.43	1.41	1.31	1.07	1.29	1.17	1.26	541.89	0.00	0.00	0.00	0.00	0.00	0.00	0.00	0.42	0.23	0.35	0.33		
3.21	2.17	1.99	1.65	1.47	1.53	1.51	1.41	1.16	1.39	1.27	1.36	594.87	0.00	0.00	0.00	0.00	0.00	0.00	0.00	0.43	0.11	0.33	0.28		
3.52	2.28	2.08	1.76	1.57	1.64	1.62	1.51	1.25	1.48	1.37	1.46	653.03	0.00	0.00	0.00	0.00	0.00	0.00	0.00	0.49	0.04	0.33	0.26		
3.86	2.39	2.16	1.88	1.68	1.74	1.72	1.62	1.34	1.58	1.47	1.55	716.87	0.00	0.00	0.00	0.00	0.00	0.00	0.00	0.53	0.01	0.26	0.24		
4.24	2.47	2.23	1.98	1.79	1.84	1.82	1.72	1.43	1.67	1.57	1.65	786.95	0.00	0.00	0.00	0.00	0.00	0.00	0.00	0.44	0.00	0.14	0.18		
4.66	2.55	2.30	2.09	1.88	1.93	1.91	1.82	1.51	1.76	1.66	1.73	863.88	0.00	0.00	0.00	0.00	0.00	0.00	0.00	0.25	0.00	0.04	0.09		
5.11	2.60	2.36	2.19	1.98	2.01	2.00	1.91	1.60	1.84	1.76	1.81	948.34	0.00	0.00	0.00	0.00	0.00	0.00	0.00	0.06	0.00	0.00	0.02		
5.61	2.64	2.42	2.27	2.06	2.09	2.08	1.99	1.68	1.91	1.84	1.88	1041.05	0.00	0.00	0.00	0.00	0.00	0.00	0.00	0.01	0.00	0.00	0.00		
6.16	2.67	2.46	2.35	2.14	2.15	2.15	2.07	1.75	1.98	1.92	1.94	1142.83	0.00	0.00	0.00	0.00	0.00	0.00	0.00	0.00	0.00	0.00	0.00		
6.76	2.69	2.50	2.41	2.21	2.21	2.21	2.15	1.82	2.04	2.00	1.99	1254.55	0.00	0.00	0.00	0.00	0.00	0.00	0.00	0.00	0.00	0.00	0.00		
7.42	2.71	2.55	2.47	2.27	2.26	2.27	2.21	1.89	2.10	2.07	2.03	1377.20	0.00	0.00	0.00	0.00	0.00	0.00	0.00	0.00	0.00	0.00	0.00		
8.15	2.74	2.60	2.53	2.33	2.32	2.32	2.28	1.96	2.16	2.14	2.08	1511.84	0.00	0.00	0.00	0.00	0.00	0.00	0.00	0.00	0.00	0.00	0.00		
8.94	2.78	2.66	2.59	2.39	2.36	2.38	2.35	2.03	2.22	2.22	2.12	1659.64	0.00	0.00	0.00	0.00	0.00	0.00	0.00	0.00	0.00	0.00	0.00		
9.82	2.82	2.72	2.63	2.45	2.41	2.43	2.42	2.10	2.28	2.29	2.16	1821.89	0.00	0.00	0.00	0.00	0.00	0.00	0.00	0.00	0.00	0.00	0.00		
10.78	2.87	2.78	2.66	2.50	2.45	2.48	2.48	2.17	2.34	2.37	2.19	2000.00													
11.83	2.94	2.84	2.70	2.55	2.50	2.54	2.55	2.25	2.40	2.45	2.24														
12.99	3.02	2.92	2.75	2.62	2.56	2.62	2.64	2.34	2.49	2.54	2.31	Very coarse sand	0.00	0.00	0.00	0.00	0.00	0.00	0.00	0.01	0.00	0.00	0.00		
14.26	3.09	2.97	2.80	2.69	2.64	2.70	2.73	2.44	2.59	2.65	2.39	coarse sand	0.00	0.00	0.00	0.00	0.00	0.00	0.00	2.63	0.38	1.45	1.40		
15.65	3.09	2.96	2.81	2.75	2.69	2.76	2.81	2.53	2.67	2.73	2.47	medium sand	0.00	0.00	0.13	0.67	0.49	0.77	0.02	3.86	2.05	2.66	2.89		
17.18	2.94	2.82	2.73	2.73	2.67	2.76	2.82	2.55	2.69	2.77	2.49	fine sand	0.99	1.84	4.60	4.79	5.39	4.79	3.28	6.76	4.99	5.23	6.04		
18.86	2.62	2.52	2.56	2.63	2.56	2.65	2.75	2.50	2.62	2.73	2.43	very fine sand	0.54	0.73	1.06	1.36	1.28	1.20	1.75	1.78	1.64	1.76	1.71		
20.71	2.19	2.13	2.31	2.45	2.36	2.46	2.60	2.36	2.46	2.61	2.29	silt	62.98	61.13	62.60	63.94	61.59	62.96	66.88	58.83	63.03	63.97	60.10		
22.73	1.76	1.74	2.05	2.25	2.13	2.25	2.42	2.20	2.28	2.44	2.12	clay	24.94	24.47	18.89	16.49	17.57	17.41	15.60	12.60	15.41	13.24	14.67		
24.95	1.44	1.47	1.84	2.09	1.96	2.09	2.28	2.05	2.13	2.29	1.99	colloid	7.19	7.49	5.87	4.88	5.33	5.44	4.26	3.20	4.08	2.75	3.73		
27.39	1.30	1.35	1.73	2.02	1.86	2.00	2.22	1.97	2.06	2.19	1.93	tot sum	96.63	95.66	93.14	92.13	91.65	92.58	91.78	89.66	91.58	91.06	90.54		
30.07	1.30	1.36	1.71	2.03	1.85	1.99	2.24	1.96	2.08	2.16	1.95														
33.01	1.37	1.43	1.73	2.08	1.88	2.01	2.30	1.99	2.14	2.17	2.02														
36.24	1.42	1.48	1.73	2.11	1.90	2.01	2.36	2.03	2.19	2.20	2.09	After C. K. Wentworth classification:													
39.78	1.37	1.44	1.67	2.08	1.86	1.94	2.36	2.04	2.19	2.19	2.11														
43.67	1.21	1.30	1.55	1.96	1.75	1.80	2.29	2.01	2.13	2.15	2.06	Sand: 2mm-1/16mm	0.54	0.73	1.06	1.36	1.28	1.20	1.75	1.78	1.64	1.76	1.71		
47.94	0.99	1.10	1.39	1.80	1.60	1.61	2.17	1.95	2.01	2.06	1.97	Silt: 1/16mm-1/256mm	62.98	61.13	62.60	63.94	61.59	62.96	66.88	58.83	63.03	63.97	60.10		
52.63	0.77	0.92	1.24	1.62	1.45	1.43	2.03	1.88	1.88	1.95	1.87	Clay: <1/256mm	32.12	31.96	24.76	21.37	22.90	22.85	19.86	15.79	19.49	16.00	18.40		
57.77	0.62	0.79	1.12	1.47	1.34	1.29	1.88	1.82	1.75	1.85	1.78	tot sum	95.64	93.82											

8.6.8. SEM images

CC03



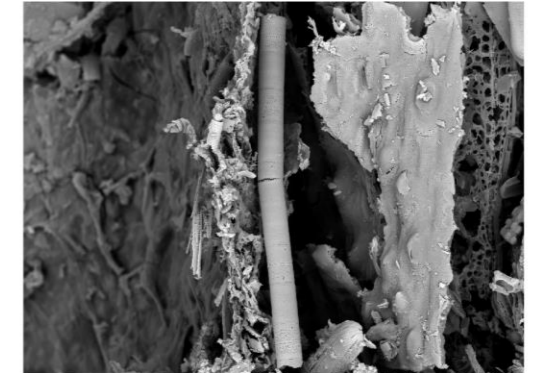
SEM HV: 20.00 kV WD: 8.497 mm
View field: 51.65 µm Det: BSE
SEM MAG: 8.04 kx Date(m/d/y): 07/16/18
MIRAI TESCAN
FEG SEM IGP Uni Lausanne



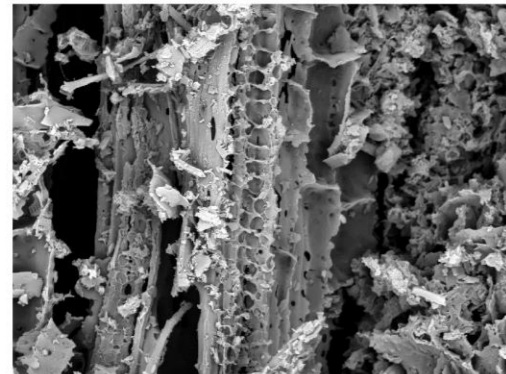
SEM HV: 20.00 kV WD: 8.472 mm
View field: 140.1 µm Det: BSE
SEM MAG: 2.96 kx Date(m/d/y): 07/16/18
MIRAI TESCAN
FEG SEM IGP Uni Lausanne



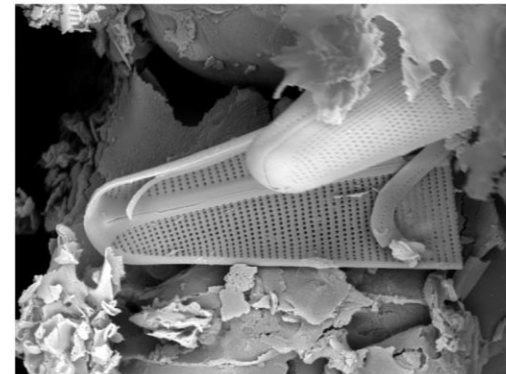
SEM HV: 20.00 kV WD: 11.95 mm
View field: 1.17 mm Det: BSE
SEM MAG: 356 x Date(m/d/y): 07/25/18
MIRAI TESCAN
FEG SEM IGP Uni Lausanne



SEM HV: 20.00 kV WD: 12.14 mm
View field: 186.3 µm Det: BSE
SEM MAG: 2.23 kx Date(m/d/y): 07/25/18
MIRAI TESCAN
FEG SEM IGP Uni Lausanne



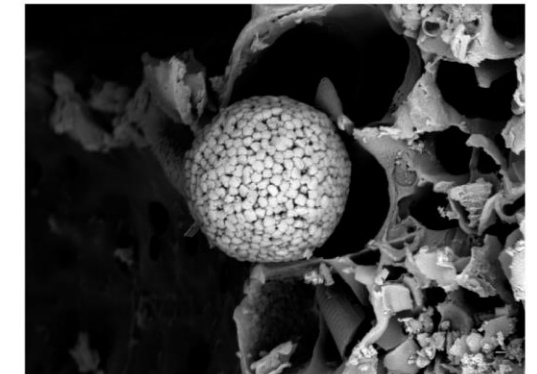
SEM HV: 20.00 kV WD: 12.13 mm
View field: 156.3 µm Det: BSE
SEM MAG: 2.66 kx Date(m/d/y): 07/25/18
MIRAI TESCAN
FEG SEM IGP Uni Lausanne



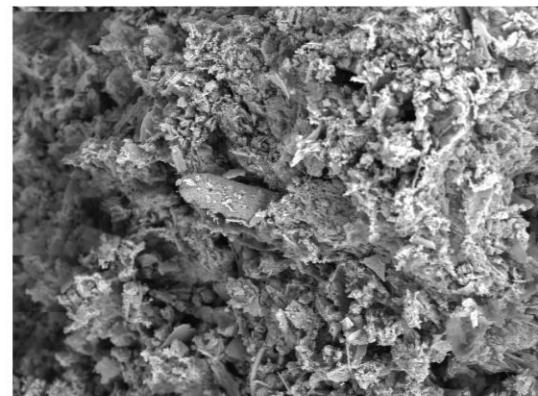
SEM HV: 20.00 kV WD: 12.15 mm
View field: 42.33 µm Det: BSE
SEM MAG: 9.81 kx Date(m/d/y): 07/25/18
MIRAI TESCAN
FEG SEM IGP Uni Lausanne



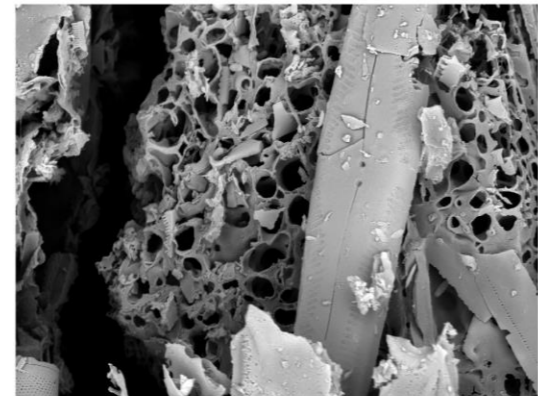
SEM HV: 20.00 kV WD: 11.95 mm
View field: 378.4 µm Det: BSE
SEM MAG: 1.10 kx Date(m/d/y): 07/25/18
MIRAI TESCAN
FEG SEM IGP Uni Lausanne



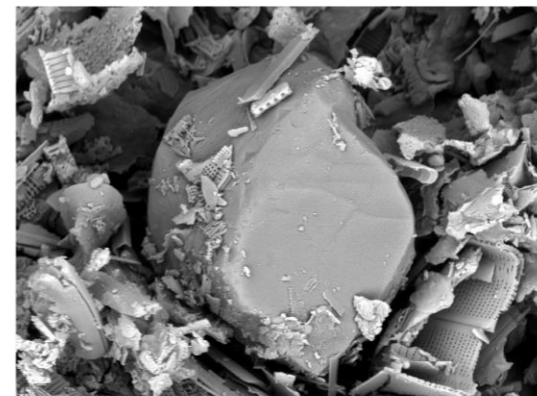
SEM HV: 20.00 kV WD: 12.01 mm
View field: 39.91 µm Det: BSE
SEM MAG: 10.40 kx Date(m/d/y): 07/25/18
MIRAI TESCAN
FEG SEM IGP Uni Lausanne



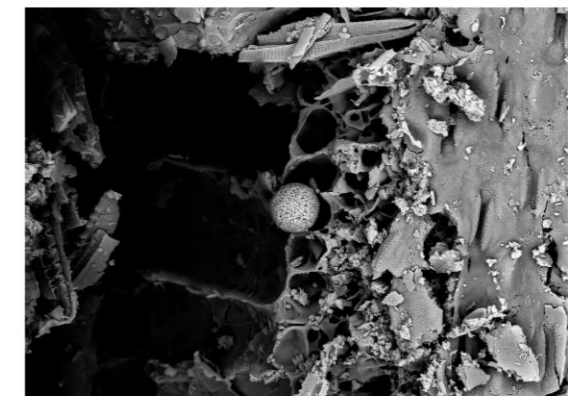
SEM HV: 20.00 kV WD: 8.061 mm
View field: 298.5 µm Det: BSE
SEM MAG: 1.39 kx Date(m/d/y): 07/16/18
MIRAI TESCAN
FEG SEM IGP Uni Lausanne



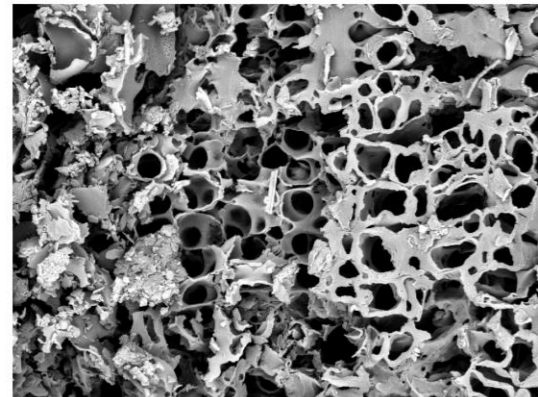
SEM HV: 20.00 kV WD: 12.16 mm
View field: 85.83 µm Det: BSE
SEM MAG: 4.84 kx Date(m/d/y): 07/25/18
MIRAI TESCAN
FEG SEM IGP Uni Lausanne



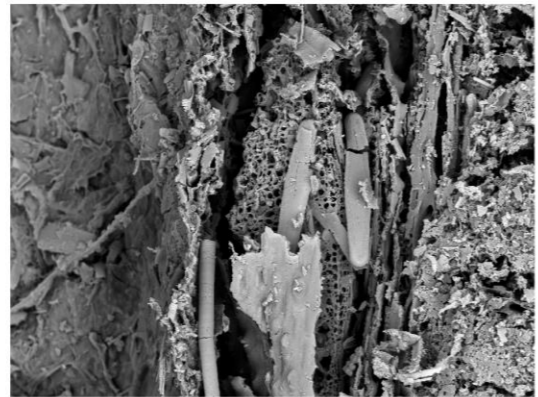
SEM HV: 20.00 kV WD: 11.99 mm
View field: 67.06 µm Det: BSE
SEM MAG: 6.19 kx Date(m/d/y): 07/31/18
MIRAI TESCAN
FEG SEM IGP Uni Lausanne



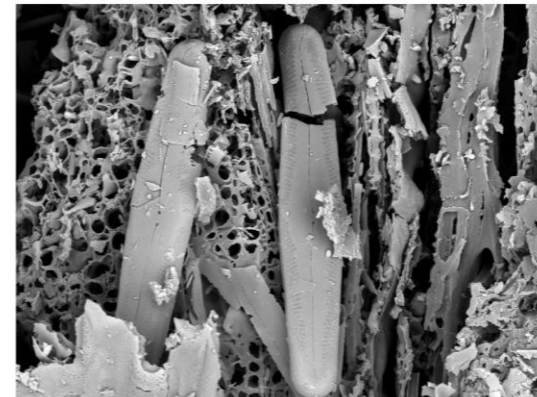
SEM HV: 20.00 kV WD: 12.01 mm
View field: 145.0 µm Det: BSE
SEM MAG: 2.86 kx Date(m/d/y): 07/25/18
MIRAI TESCAN
FEG SEM IGP Uni Lausanne



SEM HV: 20.00 kV WD: 11.88 mm
View field: 89.19 µm Det: BSE
SEM MAG: 4.65 kx Date(m/d/y): 07/25/18
MIRAI TESCAN
FEG SEM IGP Uni Lausanne



SEM HV: 20.00 kV WD: 12.16 mm
View field: 328.5 µm Det: BSE
SEM MAG: 1.26 kx Date(m/d/y): 07/25/18
MIRAI TESCAN
FEG SEM IGP Uni Lausanne

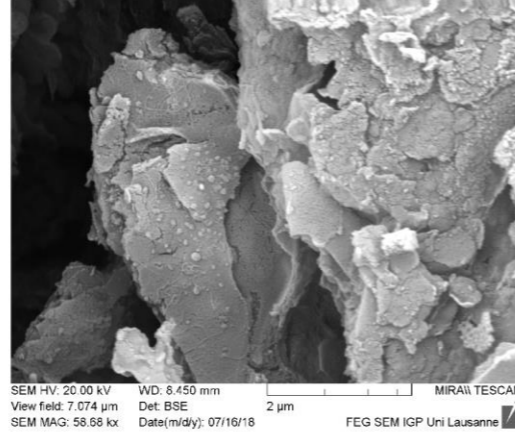
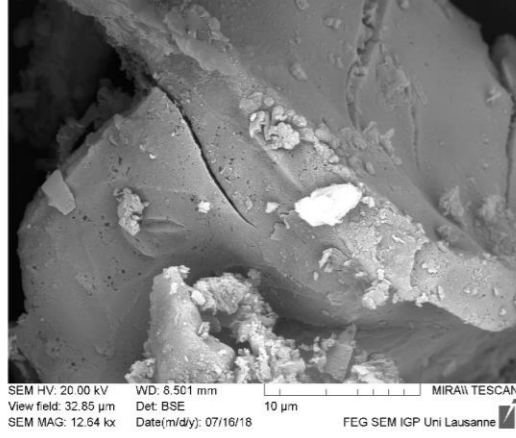
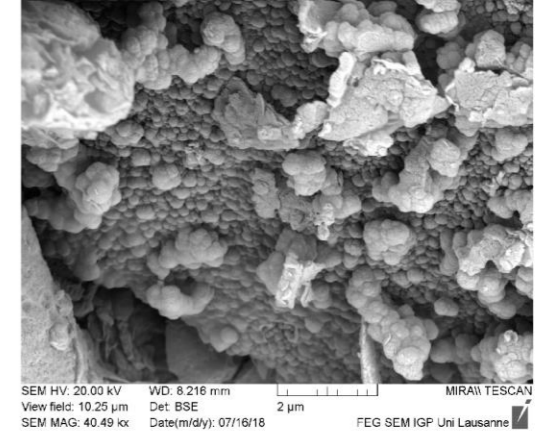
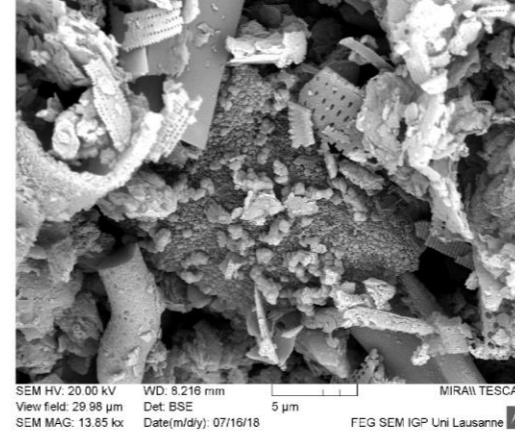
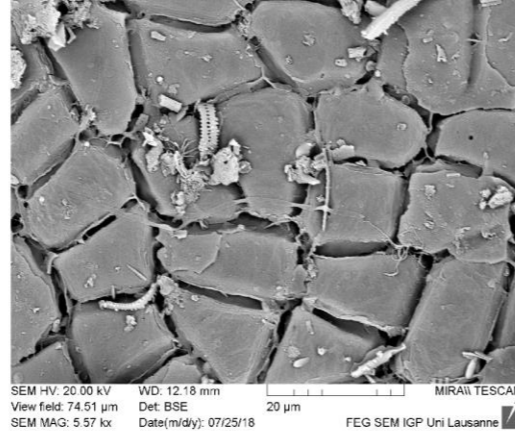
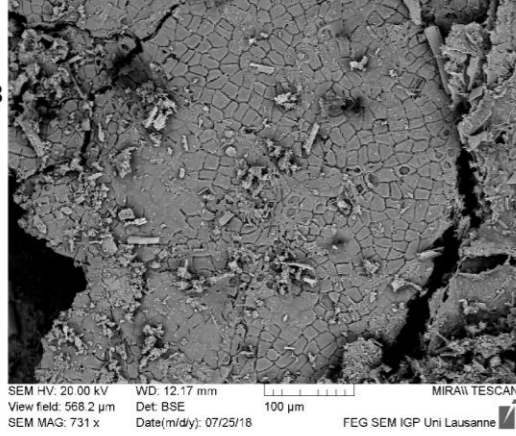


SEM HV: 20.00 kV WD: 12.16 mm
View field: 136.4 µm Det: BSE
SEM MAG: 3.04 kx Date(m/d/y): 07/25/18
MIRAI TESCAN
FEG SEM IGP Uni Lausanne

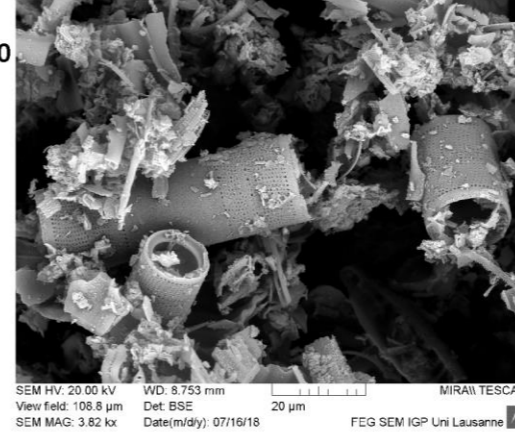


SEM HV: 20.00 kV WD: 12.09 mm
View field: 672.9 µm Det: BSE
SEM MAG: 617 x Date(m/d/y): 07/25/18
MIRAI TESCAN
FEG SEM IGP Uni Lausanne

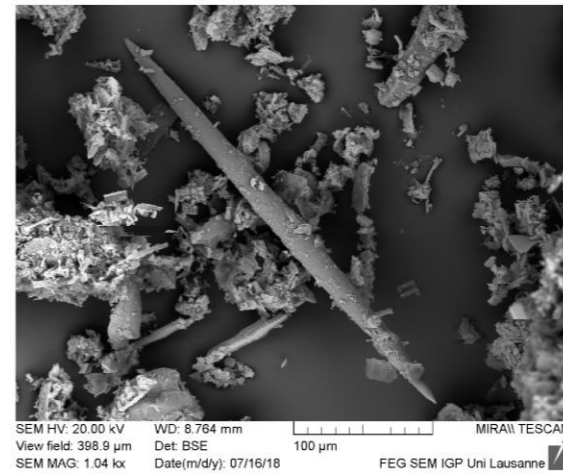
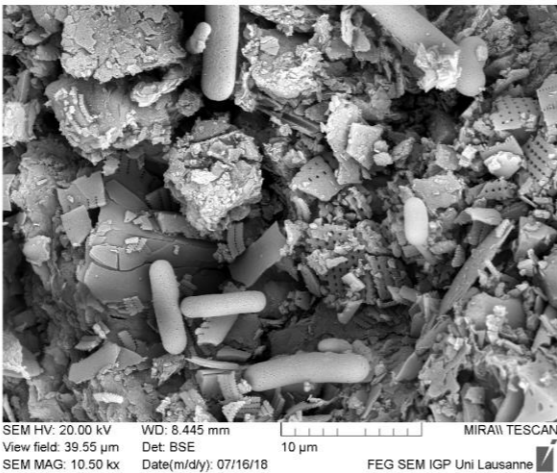
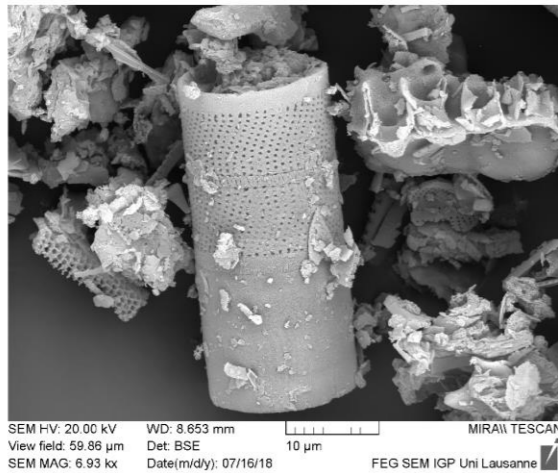
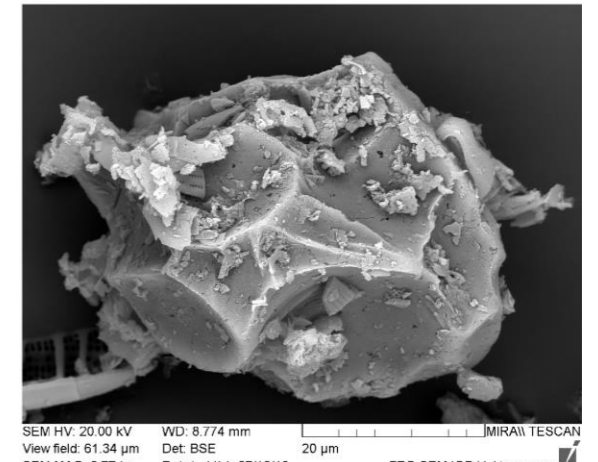
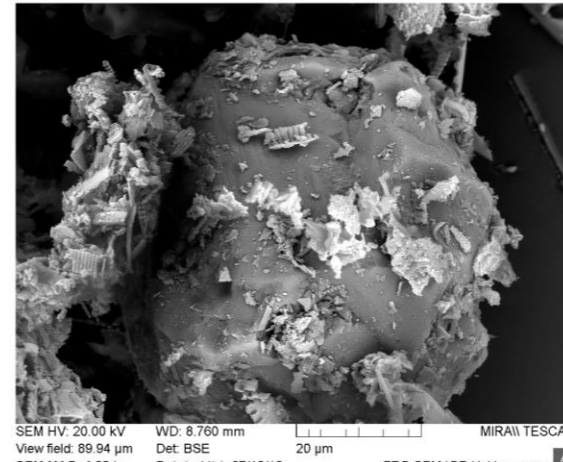
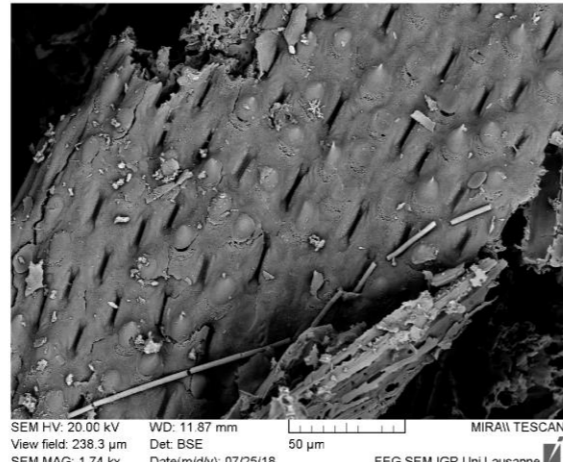
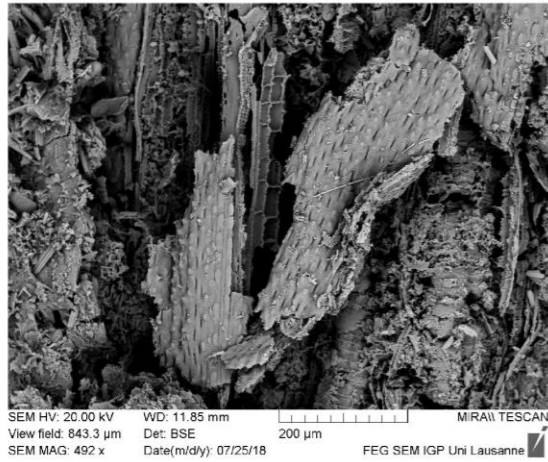
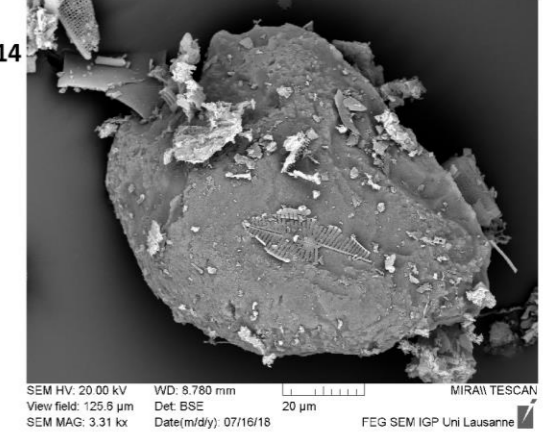
CC03



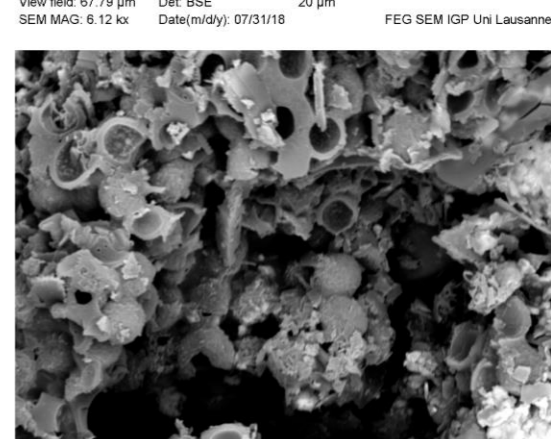
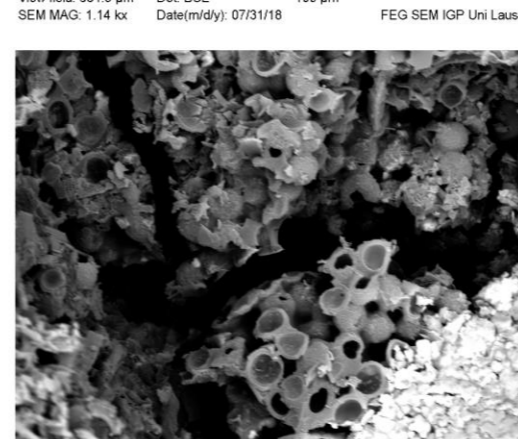
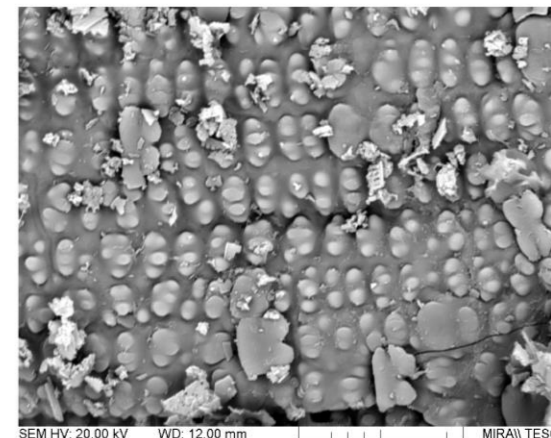
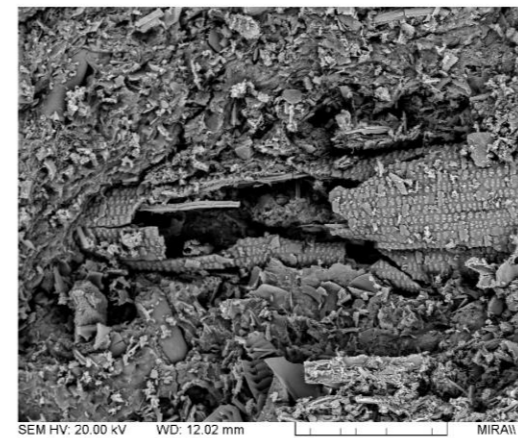
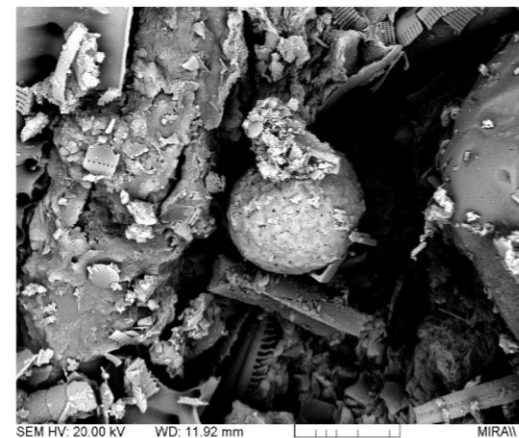
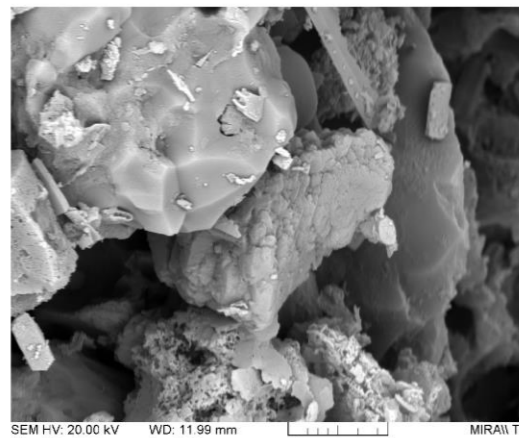
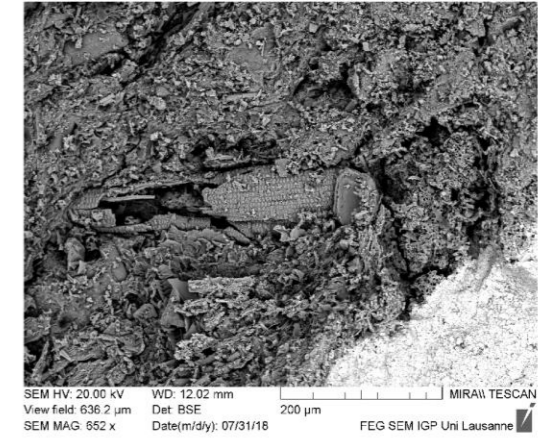
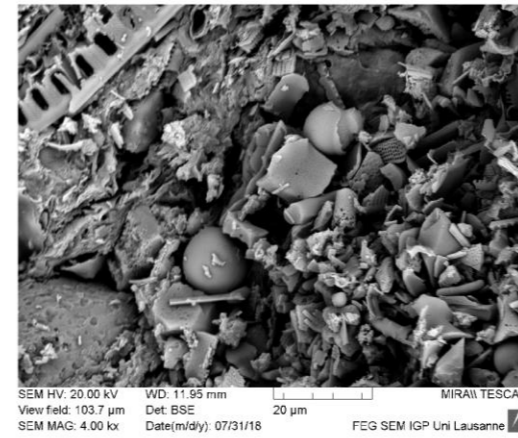
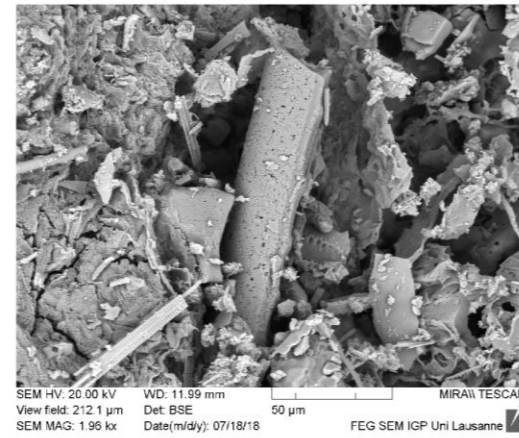
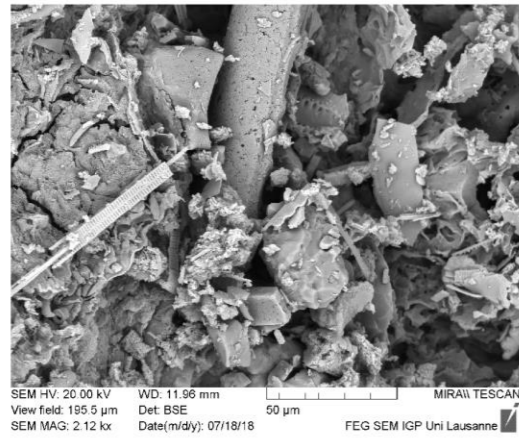
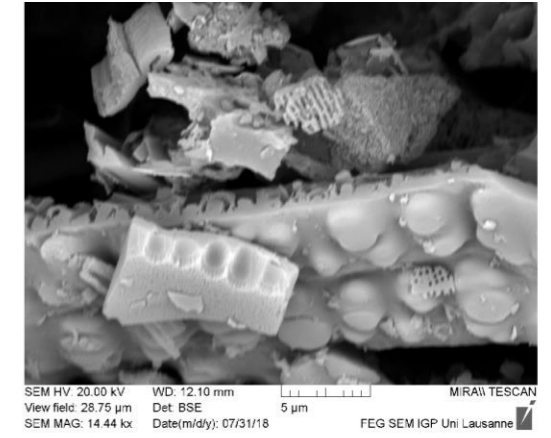
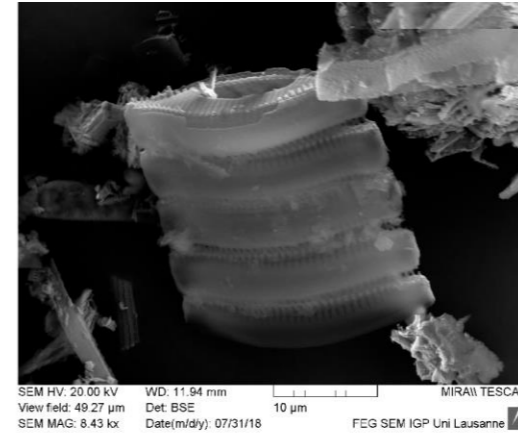
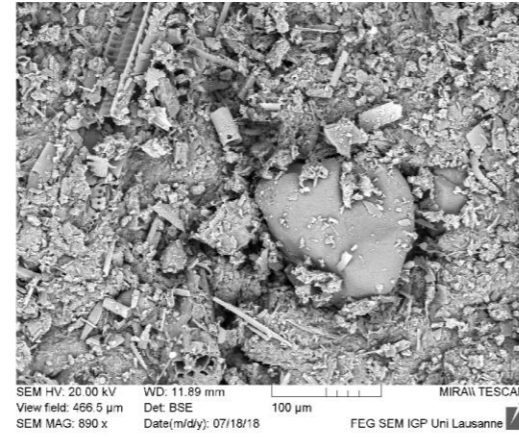
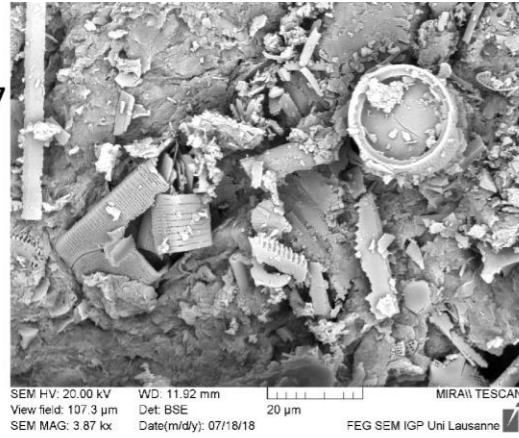
CC10



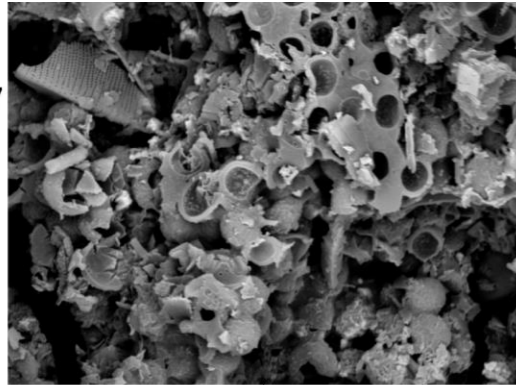
CC14



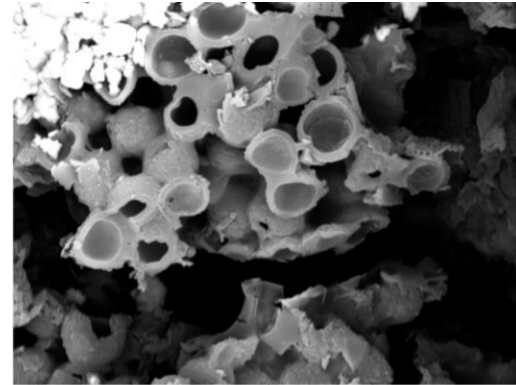
CC17



CC17

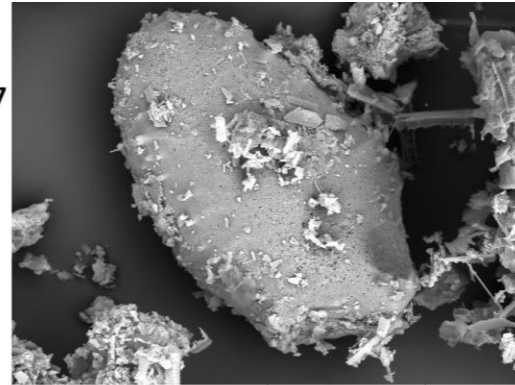


SEM HV: 20.00 kV WD: 11.97 mm
View field: 64.13 µm Det: BSE
SEM MAG: 6.47 kx Date(m/d/y): 07/31/18
MIRAII TESCAN
FEG SEM IGP Uni Lausanne



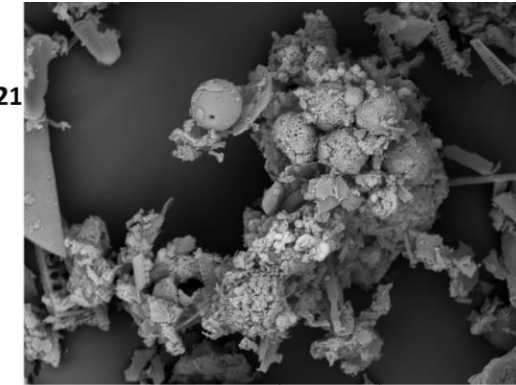
SEM HV: 20.00 kV WD: 12.06 mm
View field: 49.42 µm Det: BSE
SEM MAG: 8.40 kx Date(m/d/y): 07/18/18
MIRAII TESCAN
FEG SEM IGP Uni Lausanne

CC17

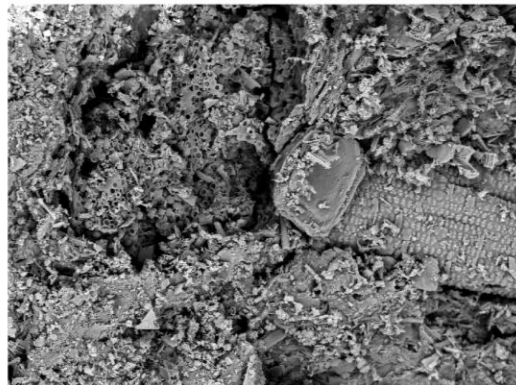


SEM HV: 20.00 kV WD: 8.584 mm
View field: 161.5 µm Det: BSE
SEM MAG: 2.57 kx Date(m/d/y): 07/16/18
MIRAII TESCAN
FEG SEM IGP Uni Lausanne

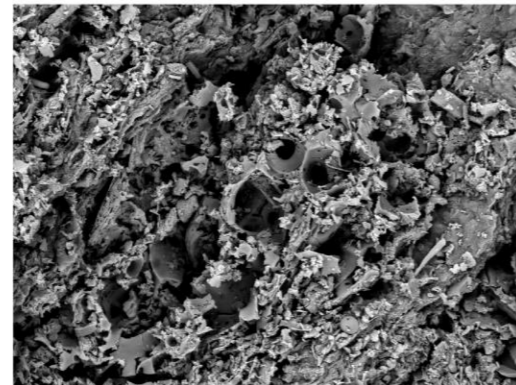
NC21



SEM HV: 20.00 kV WD: 12.03 mm
View field: 102.2 µm Det: BSE
SEM MAG: 4.06 kx Date(m/d/y): 07/30/18
MIRAII TESCAN
FEG SEM IGP Uni Lausanne

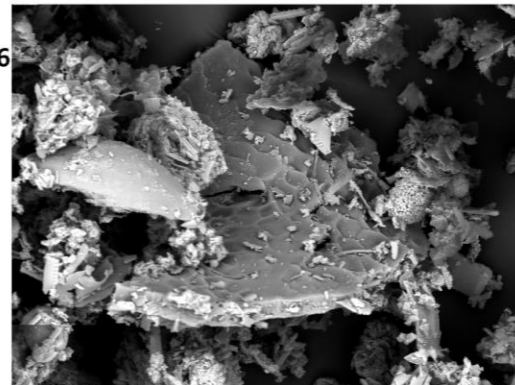


SEM HV: 20.00 kV WD: 12.06 mm
View field: 348.2 µm Det: BSE
SEM MAG: 1.19 kx Date(m/d/y): 07/18/18
MIRAII TESCAN
FEG SEM IGP Uni Lausanne

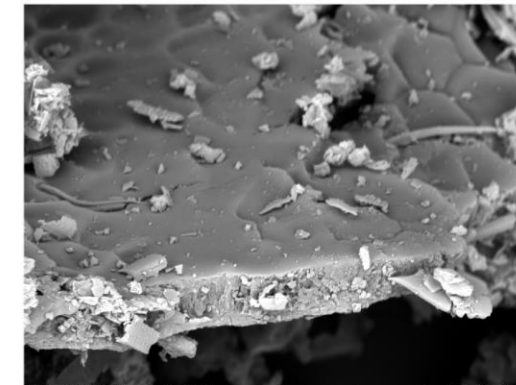


SEM HV: 20.00 kV WD: 11.99 mm
View field: 234.3 µm Det: BSE
SEM MAG: 1.77 kx Date(m/d/y): 07/31/18
MIRAII TESCAN
FEG SEM IGP Uni Lausanne

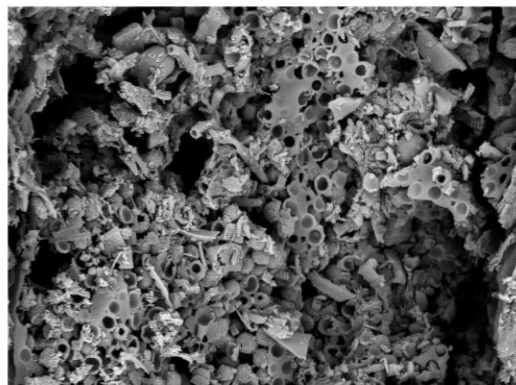
NC06



SEM HV: 20.00 kV WD: 12.33 mm
View field: 204.0 µm Det: BSE
SEM MAG: 2.04 kx Date(m/d/y): 07/30/18
MIRAII TESCAN
FEG SEM IGP Uni Lausanne



SEM HV: 20.00 kV WD: 12.24 mm
View field: 68.50 µm Det: BSE
SEM MAG: 6.06 kx Date(m/d/y): 07/30/18
MIRAII TESCAN
FEG SEM IGP Uni Lausanne

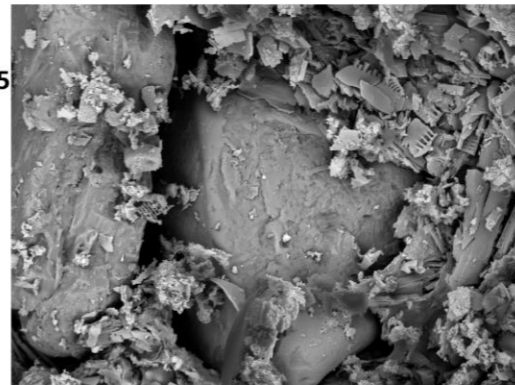


SEM HV: 20.00 kV WD: 12.06 mm
View field: 156.5 µm Det: BSE
SEM MAG: 2.65 kx Date(m/d/y): 07/18/18
MIRAII TESCAN
FEG SEM IGP Uni Lausanne

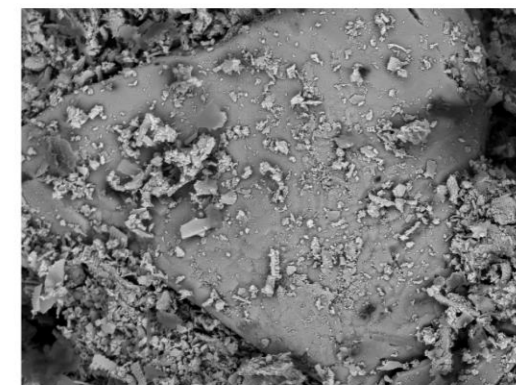


SEM HV: 20.00 kV WD: 12.03 mm
View field: 98.41 µm Det: BSE
SEM MAG: 4.22 kx Date(m/d/y): 07/31/18
MIRAII TESCAN
FEG SEM IGP Uni Lausanne

NC15



SEM HV: 20.00 kV WD: 11.95 mm
View field: 162.8 µm Det: BSE
SEM MAG: 2.55 kx Date(m/d/y): 07/31/18
MIRAII TESCAN
FEG SEM IGP Uni Lausanne



SEM HV: 20.00 kV WD: 11.93 mm
View field: 190.1 µm Det: BSE
SEM MAG: 2.18 kx Date(m/d/y): 07/31/18
MIRAII TESCAN
FEG SEM IGP Uni Lausanne

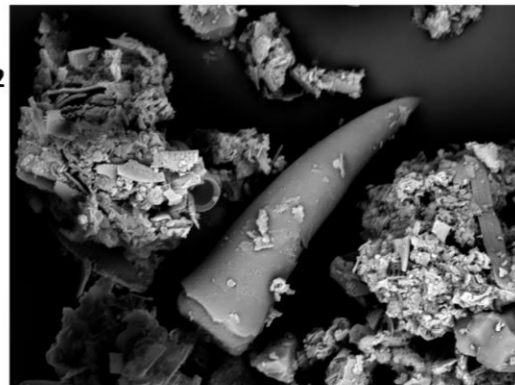


SEM HV: 20.00 kV WD: 12.00 mm
View field: 317.4 µm Det: BSE
SEM MAG: 1.31 kx Date(m/d/y): 07/18/18
MIRAII TESCAN
FEG SEM IGP Uni Lausanne



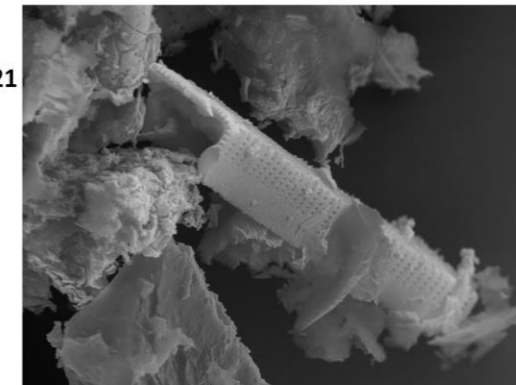
SEM HV: 20.00 kV WD: 12.02 mm
View field: 553.8 µm Det: BSE
SEM MAG: 750 x Date(m/d/y): 07/18/18
MIRAII TESCAN
FEG SEM IGP Uni Lausanne

SC12



SEM HV: 20.00 kV WD: 12.73 mm
View field: 104.0 µm Det: BSE
SEM MAG: 3.99 kx Date(m/d/y): 07/31/18
MIRAII TESCAN
FEG SEM IGP Uni Lausanne

SC21



SEM HV: 20.00 kV WD: 8.523 mm
View field: 33.76 µm Det: BSE
SEM MAG: 12.30 kx Date(m/d/y): 07/16/18
MIRAII TESCAN
FEG SEM IGP Uni Lausanne

8.6.9. Selection of photos of Lake Liambezi and its tributaries as well as sampling and laboratory work



Lake Liambezi, southern basin
August 2016
Close the mouth of the Linyanti River.
Large floodplain forming the shores of Lake
Liambezi.



Lake Liambezi, southern basin
August 2016
Fishermen on their mokoro.



Lake Liambezi, southern basin
August 2016



Lake Liambezi, southern basin
August 2016
Fishermen on their mokoro.



Lake Liambezi, southern basin
August 2016
Fishermen on their mokoro (traditional boat
carved out of a tree trunk).



Lake Liambezi, southern basin
August 2016
Close to the mouth of the Linyanti River.
Water and sediment sampling on the shores of
the lake. From left to right: Ali Mainga,
Shannon Dyer, Torsten Vennemann and
Léandre Ballif.



Lake Liambezi, southern basin
August 2016

Channel mouth of the Linyanti River.

Group of fishermen and their mokoro. Our guide Ali Mainga borrowed one to sample the lake water further in the center of the basin and further away from the mouth of the Linyanti River.



Lake Liambezi, southern basin
March 2017

Close to the mouth of the Chobe River.



Lake Liambezi, southern basin
August 2016

Channel mouth of the Linyanti River.



Lake Liambezi, southern basin
March 2017

Close to the mouth of the Chobe River.



Lake Liambezi, northern basin
March 2017

Fishermen on their mokoro, near the exit of the channel which connects the two basins, not far from the site where the Center Core was taken.



Lake Liambezi, northern basin
March 2017

Close to the mouth of the Chobe River.



Lake Liambezi, southern basin
March 2017
Close to the mouth of the Chobe River.



Lake Liambezi, southern basin
March 2017
Close to the mouth of the Chobe River.



VanThuyne-Ridge Research Center
March 2017
Work table for opening and segmenting cores from Lake Liambezi in a controlled atmosphere and sterilized equipment for samples dedicated to microbiological and sedimentary analyses.



Linyanti River, Linyanti Campsite
August 2016
Water and sediment sampling on the shores of the main channel of the river. From left to right: Léandre Ballif, Torsten Vennemann and Ali Mainga.



Linyanti River, Linyanti Campsite
August 2016
Vegetation and soil sampling of the embankment which delimits the south-eastern extent of the river. From left to right: Shannon Dyer, Léandre Ballif, John VanThuyne, Ali Mainga and Torsten Vennemann.



Chobe River, Chobe Seariver
August 2016
Water and sediment sampling of the vast floodplains of the Chobe River. From left to right: Shannon Dyer, Léandre Ballif and Ali Mainga.

8.7. Joeri Lakes data

8.7.1. Water data

sample	Anions_mg/L	Fluorure	Chlorure	Nitrite	Bromure	Nitrate	Sulfate	Phosphate	Cations_mg/L	Lithium	Sodium	Ammonium	Potassium	Magnesium	Calcium	d18O VSMOW	dD VSMOW	d13C ‰PDB	µmol CO2	mmol/L CID	mg/L CID	‰ol cor.
Glacier		0.0049	0.0261	0.0131	no data	0.0105	no data	no data		no data	0.0649	0.0049	0.0582	0.0734	0.4409	-14.01	-100.88	-10.94	0.07	0.03		1.30
L1_WiC1		0.3242	0.0525	0.0069	0.0011	0.1535	0.8331	no data		no data	0.4677	0.0015	0.1594	0.1631	2.6608	-13.29	-95.82	-8.29	0.21	0.05		1.85
L1_WiP1		0.2897	0.0725	0.0073	0.0013	0.1590	3.1361	no data		0.0006	0.6194	no data	0.3833	0.5929	5.6219	-13.22	-95.98	-8.64	0.43	0.10		4.23
L1_WiP2a		0.2760	0.1875	0.0034	0.0013	0.2121	4.1317	no data		0.0006	0.6285	0.0022	0.6159	0.6626	6.1227	-13.40	-96.50	-6.74	0.42	0.10		4.01
L1_WiP2b		0.2859	0.0598	0.0038	0.0012	0.1645	4.2985	no data		no data	0.6587	0.0020	0.4362	0.6870	6.1242	-13.48	-97.12	-7.60	0.54	0.13		5.35
L1_WP2_Inlet		0.3163	0.0458	0.0054	0.0012	0.1389	8.1649	0.0016		no data	0.8143	0.0016	0.4967	1.0216	6.8346	-13.01	-92.76	-4.96	0.53	0.11		3.85
L1_WiP3		0.3577	0.0562	0.0053	0.0014	0.3572	4.7801	no data		0.0008	0.7287	0.0017	0.5448	0.8450	7.7297	-13.50	-97.08	-6.48	0.65	0.15		6.08
L13_WiC1		0.1317	0.1100	0.0028	0.0015	0.0045	1.6592	no data		no data	0.3027	no data	0.1782	0.2156	2.2138	-13.54	-98.42	-9.70	0.21	0.05		1.93
L13_WiP1		0.1212	0.0534	0.0030	0.0015	0.0041	0.7402	no data		no data	0.2761	0.0012	0.1425	0.1817	1.7171	-13.36	-97.22	-7.12	0.22	0.04		1.50
L13_WiP2		0.1741	0.0720	no data	no data	0.2976	0.9859	0.0030		no data	0.3552	no data	0.1916	0.2020	1.9661	-13.29	-95.44	-9.10	0.21	0.04		1.36
L13_WiP3		0.1215	0.0853	0.0063	no data	0.0077	0.4148	no data		no data	0.2837	0.0019	0.1399	0.1766	1.6708	-13.38	-97.31	-7.77	0.20	0.04		1.65
L21_Wi_Outlet		0.0763	0.0440	0.0059	0.0013	0.0321	2.2381	no data		no data	0.4654	no data	0.2213	0.6421	3.5011	-12.68	-90.97	-11.72	0.30	0.07		2.63

8.7.2. Radiocarbon data

Results of AMS 14C analysis of sample material submitted to AMS laboratory, ETH Zürich										
Sample Code	depth [cm]	Material	C14 age BP	±1σ	F14C	±1σ	δC13 ‰	±1σ	mg C	C/N
LC2-10	10	sediment	7126	25	0.4118	0.0013	-27.0	1	0.99	13.84
LC2-16	16	sediment	6936	25	0.4217	0.0013	-26.6	1	0.98	13.55
LC2-20	20	sediment	5676	24	0.4933	0.0015	-26.7	1	0.68	10.07

8.7.3. Grain-size data

	LC1-07	LC2-07	LC2-08	LC2-09	LC2-10	LC2-11	LC2-12	LC2-13	LC2-14	LC2-15	LC2-16	LC2-17	LC2-18	LC2-19	LC2-20		LC1-07	LC2-07	LC2-08	LC2-09	LC2-10	LC2-11	LC2-12	LC2-13	LC2-14	LC2-15	LC2-16	LC2-17	LC2-18	LC2-19	LC2-20
Channel Diameter (Lower) um	Diff. Volume %	Diff. Volume %	Diff. Volume %	Diff. Volume %	Diff. Volume %	Diff. Volume %	Diff. Volume %	Diff. Volume %	Diff. Volume %	Diff. Volume %	Diff. Volume %	Diff. Volume %	Diff. Volume %	Diff. Volume %	Diff. Volume %	Channel Diameter (Lower) um	Diff. Volume %	Diff. Volume %	Diff. Volume %	Diff. Volume %	Diff. Volume %	Diff. Volume %	Diff. Volume %	Diff. Volume %	Diff. Volume %	Diff. Volume %	Diff. Volume %	Diff. Volume %	Diff. Volume %	Diff. Volume %	Diff. Volume %
0.38	0.17	0.03	0.03	0.03	0.02	0.02	0.02	0.02	0.03	0.03	0.02	0.04	0.05	0.06	0.07	69.62	0.39	2.99	3.15	2.88	2.91	2.75	2.46	2.94	3.11	2.55	3.22	2.17	1.45	1.37	
0.41	0.30	0.05	0.05	0.05	0.04	0.04	0.03	0.04	0.04	0.05	0.04	0.06	0.06	0.09	0.10	76.43	0.41	3.22	3.31	3.01	3.08	2.98	2.71	3.02	3.26	2.75	3.28	2.15	1.51	1.41	
0.45	0.44	0.07	0.07	0.07	0.07	0.07	0.05	0.04	0.07	0.07	0.06	0.09	0.13	0.15	0.19	83.90	0.41	3.45	3.45	3.14	3.24	3.19	2.97	3.08	3.41	2.94	3.31	2.11	1.57	1.42	
0.50	0.62	0.10	0.10	0.10	0.09	0.07	0.06	0.09	0.10	0.08	0.13	0.18	0.21	0.27	0.27	92.10	0.35	3.64	3.57	3.26	3.40	3.39	3.27	3.11	3.53	3.13	3.30	2.04	1.59	1.40	
0.54	0.76	0.13	0.12	0.12	0.12	0.09	0.08	0.12	0.12	0.10	0.16	0.23	0.26	0.34	0.34	101.10	0.27	3.81	3.65	3.36	3.55	3.59	3.60	3.13	3.61	3.32	3.28	1.94	1.58	1.33	
0.60	0.88	0.15	0.14	0.14	0.14	0.11	0.09	0.14	0.14	0.14	0.12	0.19	0.27	0.39	0.39	110.99	0.19	3.94	3.71	3.46	3.71	3.79	3.96	3.16	3.65	3.53	3.26	1.82	1.55	1.24	
0.66	0.98	0.17	0.16	0.16	0.15	0.12	0.10	0.15	0.16	0.13	0.21	0.30	0.35	0.45	0.45	121.84	0.15	4.04	3.74	3.55	3.87	4.00	4.33	3.21	3.65	3.77	3.24	1.70	1.51	1.16	
0.72	1.07	0.19	0.18	0.18	0.17	0.14	0.11	0.17	0.18	0.15	0.24	0.33	0.39	0.49	0.49	133.75	0.13	4.10	3.72	3.62	4.01	4.19	4.66	3.27	3.62	4.00	3.17	1.58	1.48	1.09	
0.79	1.14	0.20	0.19	0.20	0.18	0.15	0.12	0.18	0.19	0.16	0.26	0.36	0.42	0.53	0.53	146.82	0.14	4.07	3.63	3.63	4.07	4.30	4.89	3.30	3.53	4.18	3.01	1.48	1.44	1.04	
0.87	1.18	0.21	0.20	0.21	0.19	0.16	0.13	0.19	0.21	0.17	0.27	0.38	0.44	0.56	0.56	161.18	0.15	3.92	3.43	3.53	3.99	4.23	4.92	3.22	3.39	4.20	2.74	1.35	1.38	1.00	
0.95	1.20	0.22	0.21	0.22	0.20	0.16	0.14	0.20	0.21	0.18	0.28	0.40	0.46	0.59	0.59	176.94	0.15	3.60	3.10	3.27	3.71	3.94	4.68	2.95	3.15	4.00	2.39	1.18	1.27	0.94	
1.05	1.21	0.22	0.22	0.23	0.21	0.17	0.14	0.21	0.22	0.19	0.29	0.41	0.48	0.61	0.61	194.23	0.10	3.11	2.63	2.85	3.23	3.41	4.17	2.50	2.84	3.56	2.04	0.94	1.10	0.84	
1.15	1.22	0.23	0.22	0.23	0.21	0.17	0.15	0.21	0.23	0.19	0.30	0.42	0.49	0.63	0.63	213.22	0.05	2.51	2.09	2.32	2.63	2.73	3.47	1.94	2.47	2.97	1.76	0.67	0.89	0.72	
1.26	1.23	0.23	0.23	0.24	0.22	0.18	0.15	0.22	0.23	0.20	0.30	0.42	0.51	0.65	0.65	234.07	0.01	1.91	1.58	1.79	2.02	2.05	2.74	1.41	2.10	2.38	1.53	0.41	0.67	0.59	
1.38	1.25	0.23	0.23	0.24	0.22	0.18	0.15	0.22	0.24	0.20	0.31	0.44	0.52	0.67	0.67	256.95	0.00	1.42	1.17	1.36	1.53	1.50	2.11	1.04	1.79	1.91	1.32	0.23	0.49	0.49	
1.52	1.27	0.24	0.24	0.25	0.23	0.18	0.15	0.22	0.24	0.20	0.32	0.45	0.54	0.69	0.69	282.07	0.00	1.08	0.91	1.06	1.20	1.15	1.68	0.88	1.57	1.64	1.06	0.14	0.38	0.43	
1.67	1.31	0.24	0.24	0.26	0.23	0.19	0.15	0.23	0.25	0.21	0.33	0.47	0.56	0.72	0.72	309.64	0.00	0.90	0.78	0.89	1.02	0.98	1.43	0.91	1.43	1.57	0.72	0.13	0.34	0.43	
1.83	1.38	0.25	0.25	0.27	0.24	0.19	0.16	0.23	0.25	0.22	0.34	0.49	0.59	0.77	0.77	339.92	0.00	0.82	0.73	0.80	0.93	0.92	1.31	1.06	1.34	1.64	0.77	0.16	0.34	0.46	
2.01	1.48	0.26	0.26	0.28	0.25	0.20	0.16	0.24	0.26	0.23	0.35	0.52	0.63	0.82	0.82	373.15	0.00	0.78	0.69	0.71	0.85	0.89	1.23	1.24	1.25	1.77	0.12	0.20	0.36	0.49	
2.21	1.60	0.27	0.27	0.29	0.26	0.21	0.17	0.25	0.27	0.24	0.37	0.55	0.68	0.88	0.88	409.63	0.00	0.70	0.62	0.59	0.74	0.82	1.12	1.37	1.12	1.87	0.02	0.21	0.35	0.48	
2.42	1.74	0.29	0.29	0.31	0.27	0.22	0.17	0.27	0.29	0.25	0.40	0.59	0.74	0.96	0.96	449.67	0.00	0.55	0.50	0.42	0.58	0.71	0.98	1.41	0.93	1.89	0.00	0.18	0.30	0.43	
2.66	1.90	0.31	0.31	0.33	0.29	0.23	0.18	0.28	0.30	0.26	0.43	0.64	0.81	1.05	1.05	493.63	0.00	0.36	0.36	0.26	0.41	0.59	0.83	1.40	0.69	1.80	0.00	0.10	0.23	0.34	
2.92	2.09	0.34	0.33	0.35	0.31	0.24	0.19	0.30	0.32	0.28	0.46	0.70	0.89	1.15	1.15	541.89	0.00	0.19	0.24	0.14	0.29	0.51	0.73	1.37	0.44	1.55	0.00	0.04	0.15	0.22	
3.21	2.28	0.37	0.36	0.38	0.33	0.26	0.20	0.33	0.35	0.30	0.49	0.76	0.98	1.26	1.26	594.87	0.00	0.08	0.18	0.09	0.22	0.50	0.71	1.35	0.23	1.23	0.00	0.01	0.10	0.12	
3.52	2.48	0.40	0.38	0.41	0.36	0.27	0.21	0.35	0.37	0.32	0.53	0.84	1.08	1.38	1.38	653.03	0.00	0.05	0.16	0.08	0.21	0.56	0.77	1.06	0.08	1.28	0.00	0.00	0.07	0.06	
3.86	2.66	0.43	0.41	0.44	0.38	0.29	0.22	0.38	0.39	0.34	0.57	0.91	1.19	1.51	1.51	716.87	0.00	0.05	0.18	0.10	0.23	0.70	0.87	0.59	0.02	0.38	0.00	0.00	0.07	0.02	
4.24	2.84	0.46	0.45	0.48	0.41	0.31	0.24	0.41	0.42	0.36	0.61	1.00	1.31	1.64	1.64	786.95	0.00	0.09	0.21	0.13	0.28	0.91	0.96	0.15	0.00	0.09	0.00	0.00	0.08	0.02	
4.66	2.99	0.50	0.48	0.51	0.44	0.33	0.25	0.44	0.45	0.39	0.66	1.09	1.43	1.76	1.76	863.88	0.00	0.14	0.25	0.14	0.34	1.18	1.06	0.02	0.00	0.01	0.00	0.00	0.09	0.03	
5.11	3.11	0.53	0.52	0.55	0.47	0.36	0.27	0.47	0.47	0.41	0.70	1.18	1.55	1.89	1.89	948.34	0.00	0.18	0.29	0.14	0.42	1.49	1.20	0.00	0.00	0.00	0.00	0.00	0.08	0.07	
5.61	3.19	0.57	0.56	0.60	0.50	0.38	0.28	0.50	0.50	0.43	0.75	1.28	1.68	2.01	2.01	1041.05	0.00	0.21	0.30	0.14	0.48	1.69	1.21	0.00	0.00	0.00	0.00	0.00	0.07	0.11	
6.16	3.24	0.60	0.60	0.64	0.54	0.40	0.30	0.54	0.53	0.46	0.79	1.38	1.80	2.12	2.12	1142.83	0.00	0.22	0.24	0.10	0.40	1.41	0.91	0.00	0.00	0.00	0.00	0.00	0.04	0.12	
6.76	3.25	0.64	0.64	0.69	0.57	0.43	0.32	0.58	0.56	0.48	0.84	1.48	1.93	2.23	2.23	1254.55	0.00	0.22	0.13	0.05	0.23	0.80	0.44	0.00	0.00	0.00	0.00	0.00	0.01	0.07	
7.42	3.25	0.68	0.68	0.74	0.61	0.45	0.34	0.62	0.59	0.51	0.88	1.59	2.06	2.33	2.33	1377.20	0.00	0.17	0.03	0.01	0.06	0.20	0.10	0.00	0.00	0.00	0.00	0.00	0.00	0.02	
8.15	3.22	0.72	0.73	0.79	0.64	0.48	0.36	0.66	0.62	0.54	0.94	1.71	2.19	2.42	2.42	1511.84	0.00	0.09	0.00	0.00	0.01	0.02	0.01	0.00	0.00	0.00	0.00	0.00	0.00	0.00	0.00
8.94	3.16	0.76	0.78	0.85	0.69	0.51	0.38	0.71	0.66	0.56	1.00	1.84	2.32	2.51	2.51	1659.64	0.00	0.02	0.00	0.00	0.00	0.00	0.00	0.00	0.00	0.00	0.00	0.00	0.00	0.00	0.00
9.82	3.08	0.81	0.83	0.91	0.73	0.54	0.41	0.77	0.70	0.60	1.06	1.97	2.45	2.58	2.58	1821.89	0.00	0.00	0.00	0.00	0.00	0.00	0.00	0.00	0.00	0.00	0.00	0.00	0.00	0.00	0.00
10.78	2.98	0.86	0.89	0.98	0.78	0.58	0.44	0.83	0.74	0.63	1.13	2.10	2.57	2.64	2.64	2000.00															
11.83	2.91	0.92	0.96	1.06	0.84	0.62	0.47	0.90	0.80	0.67	1.21	2.25	2.69	2.70	2.70																
12.99	2.89	0.98	1.03	1.15	0.90	0.66	0.50	0.99	0.86	0.72	1.30	2.40	2.80	2.74	2.74	Very coarse sand	0.00	0.94	0.71	0.30	1.17	4.12	2.66	0.00	0.00	0.00	0.00	0.00	0.12	0.33	
14.26	2.89	1.05	1.12	1.24	0.97	0.71	0.54	1.08	0.93	0.76	1.41	2.56	2.90	2.78	2.78	coarse sand	0.00	0.77	1.52	0.83	1.99	5.85	6.30	4.53	0.78	4.04	0.00	0.05	0.64	0.55	
15.65	2.85	1.12	1.20	1.33	1.05	0.77	0.58	1.17	1.01	0.81	1.51	2.69	2.96	2.78	2.78	medium sand	0.00	6.62	5.76	6.09	7.24	7.59	10.69	9.31	10.11	14.09	3.60	1.35	2.78	3.55	
17.18	2.67</																														

Channel Diameter (Lower)														Channel Diameter (Lower)													
LC3-03	LC3-04	LC3-05	LC3-06	LC3-07	LC3-08	LC3-10	LC12-01	LC12-02	LC12-03	LC12-04	LC12-05	LC12-06		LC3-03	LC3-04	LC3-05	LC3-06	LC3-07	LC3-08	LC3-10	LC12-01	LC12-02	LC12-03	LC12-04	LC12-05	LC12-06	
Diff.	Diff.	Diff.	Diff.	Diff.	Diff.	Diff.	Diff.	Diff.	Diff.	Diff.	Diff.	Diff.		Diff.	Diff.	Diff.	Diff.	Diff.	Diff.	Diff.	Diff.	Diff.	Diff.	Diff.	Diff.	Diff.	
Volume	Volume	Volume	Volume	Volume	Volume	Volume	Volume	Volume	Volume	Volume	Volume	Volume		Volume	Volume	Volume	Volume	Volume	Volume	Volume	Volume	Volume	Volume	Volume	Volume	Volume	
%	%	%	%	%	%	%	%	%	%	%	%	%		%	%	%	%	%	%	%	%	%	%	%	%	%	
0.38	0.05	0.03	0.02	0.02	0.01	0.01	0.01	0.03	0.04	0.04	0.04	0.04		69.62	1.47	1.22	1.20	1.17	0.81	1.51	1.20	2.66	2.67	2.69	2.54	2.62	2.68
0.41	0.08	0.05	0.04	0.03	0.02	0.03	0.02	0.05	0.07	0.07	0.06	0.07	0.07	76.43	1.53	1.28	1.28	1.25	0.87	1.63	1.25	2.66	2.72	2.82	2.71	2.80	2.85
0.45	0.12	0.07	0.06	0.05	0.03	0.04	0.03	0.08	0.10	0.10	0.09	0.10	0.10	83.90	1.57	1.34	1.37	1.33	0.93	1.76	1.28	2.65	2.74	2.93	2.87	2.96	3.02
0.50	0.17	0.10	0.09	0.07	0.04	0.06	0.04	0.11	0.14	0.15	0.13	0.14	0.14	92.10	1.60	1.38	1.45	1.42	0.99	1.89	1.30	2.61	2.74	3.00	3.02	3.10	3.15
0.54	0.22	0.12	0.11	0.09	0.05	0.07	0.04	0.14	0.17	0.18	0.16	0.18	0.17	101.10	1.61	1.42	1.52	1.50	1.05	2.02	1.31	2.56	2.71	3.05	3.15	3.21	3.26
0.60	0.25	0.14	0.12	0.10	0.06	0.08	0.05	0.16	0.20	0.21	0.19	0.21	0.20	110.99	1.60	1.46	1.60	1.58	1.11	2.15	1.31	2.50	2.68	3.09	3.27	3.29	3.36
0.66	0.28	0.16	0.14	0.12	0.07	0.09	0.06	0.18	0.22	0.24	0.21	0.23	0.22	121.84	1.60	1.53	1.68	1.68	1.19	2.29	1.31	2.46	2.65	3.12	3.39	3.37	3.44
0.72	0.31	0.18	0.16	0.13	0.07	0.10	0.07	0.20	0.25	0.26	0.24	0.26	0.25	133.75	1.62	1.62	1.78	1.78	1.28	2.42	1.31	2.43	2.63	3.15	3.50	3.43	3.50
0.79	0.34	0.19	0.17	0.14	0.08	0.11	0.07	0.22	0.27	0.28	0.25	0.28	0.27	146.82	1.66	1.74	1.88	1.90	1.38	2.52	1.31	2.39	2.60	3.15	3.58	3.45	3.51
0.87	0.36	0.20	0.18	0.15	0.09	0.12	0.08	0.23	0.28	0.30	0.27	0.29	0.28	161.18	1.72	1.88	1.98	2.02	1.47	2.59	1.30	2.33	2.53	3.08	3.58	3.39	3.43
0.95	0.37	0.21	0.18	0.16	0.09	0.13	0.08	0.24	0.29	0.31	0.28	0.30	0.29	176.94	1.77	2.01	2.06	2.12	1.55	2.60	1.28	2.21	2.38	2.90	3.43	3.20	3.20
1.05	0.38	0.21	0.19	0.16	0.09	0.13	0.08	0.25	0.30	0.32	0.29	0.31	0.30	194.23	1.79	2.12	2.10	2.20	1.61	2.54	1.23	2.00	2.14	2.59	3.12	2.86	2.83
1.15	0.39	0.22	0.19	0.17	0.10	0.14	0.08	0.26	0.31	0.33	0.29	0.32	0.31	213.22	1.77	2.19	2.09	2.22	1.64	2.42	1.18	1.75	1.83	2.18	2.69	2.43	2.37
1.26	0.40	0.22	0.19	0.17	0.10	0.14	0.08	0.26	0.32	0.33	0.30	0.32	0.32	234.07	1.71	2.22	2.05	2.20	1.67	2.28	1.16	1.50	1.51	1.75	2.20	1.98	1.90
1.38	0.41	0.22	0.20	0.18	0.10	0.15	0.09	0.27	0.33	0.34	0.31	0.33	0.33	256.95	1.63	2.20	2.00	2.15	1.71	2.15	1.20	1.30	1.25	1.39	1.76	1.59	1.50
1.52	0.43	0.23	0.20	0.18	0.11	0.15	0.09	0.28	0.33	0.35	0.31	0.34	0.33	282.07	1.55	2.16	1.98	2.11	1.80	2.06	1.31	1.20	1.08	1.14	1.44	1.32	1.22
1.67	0.45	0.24	0.21	0.19	0.11	0.15	0.09	0.29	0.34	0.36	0.32	0.35	0.34	309.64	1.48	2.10	1.98	2.10	1.92	2.02	1.51	1.18	1.00	1.00	1.23	1.16	1.05
1.83	0.47	0.25	0.21	0.20	0.11	0.16	0.09	0.30	0.36	0.37	0.34	0.36	0.36	339.92	1.42	2.04	2.01	2.13	2.08	2.00	1.80	1.23	0.98	0.94	1.11	1.06	0.95
2.01	0.51	0.26	0.22	0.21	0.12	0.17	0.09	0.31	0.37	0.39	0.35	0.38	0.38	373.15	1.34	1.96	2.04	2.19	2.23	1.98	2.15	1.28	0.97	0.88	1.02	0.96	0.86
2.21	0.55	0.28	0.24	0.22	0.13	0.18	0.10	0.33	0.39	0.41	0.38	0.40	0.40	409.63	1.23	1.87	2.04	2.25	2.37	1.93	2.54	1.30	0.94	0.79	0.90	0.81	0.74
2.42	0.60	0.30	0.25	0.24	0.14	0.19	0.10	0.35	0.42	0.44	0.40	0.43	0.43	449.67	1.08	1.77	1.98	2.28	2.45	1.84	2.94	1.25	0.85	0.65	0.74	0.60	0.57
2.66	0.65	0.33	0.27	0.25	0.14	0.20	0.11	0.38	0.45	0.47	0.43	0.46	0.46	493.63	0.90	1.66	1.86	2.26	2.47	1.73	3.32	1.14	0.72	0.46	0.54	0.37	0.37
2.92	0.72	0.36	0.29	0.27	0.15	0.21	0.12	0.40	0.48	0.51	0.46	0.50	0.49	541.89	0.72	1.58	1.72	2.19	2.45	1.62	3.66	1.01	0.57	0.28	0.35	0.17	0.20
3.21	0.80	0.39	0.32	0.29	0.17	0.22	0.12	0.44	0.52	0.54	0.50	0.54	0.53	594.87	0.58	1.54	1.61	2.10	2.41	1.55	3.94	0.88	0.43	0.14	0.18	0.06	0.08
3.52	0.88	0.43	0.34	0.32	0.18	0.24	0.13	0.47	0.56	0.59	0.54	0.58	0.57	653.03	0.49	1.58	1.57	2.02	2.41	1.54	4.14	0.77	0.32	0.07	0.08	0.02	0.02
3.86	0.96	0.46	0.37	0.34	0.19	0.25	0.14	0.51	0.61	0.63	0.58	0.63	0.62	716.87	0.45	1.67	1.61	1.98	2.45	1.60	4.22	0.67	0.23	0.03	0.03	0.01	0.01
4.24	1.05	0.50	0.39	0.36	0.20	0.27	0.16	0.54	0.65	0.68	0.63	0.67	0.66	786.95	0.46	1.82	1.76	2.00	2.58	1.71	4.18	0.59	0.16	0.02	0.01	0.00	0.00
4.66	1.14	0.53	0.42	0.38	0.21	0.29	0.17	0.58	0.70	0.72	0.67	0.72	0.70	863.88	0.51	2.00	1.98	2.08	2.82	1.87	4.04	0.51	0.13	0.03	0.01	0.00	0.00
5.11	1.23	0.57	0.44	0.41	0.22	0.30	0.18	0.63	0.75	0.77	0.71	0.76	0.75	948.34	0.58	2.20	2.25	2.22	3.18	2.08	3.81	0.44	0.12	0.03	0.00	0.00	0.01
5.61	1.32	0.60	0.46	0.43	0.24	0.32	0.19	0.67	0.80	0.82	0.75	0.81	0.79	1041.05	0.66	2.38	2.53	2.38	3.60	2.28	3.54	0.39	0.13	0.03	0.00	0.00	0.01
6.16	1.41	0.63	0.48	0.45	0.25	0.34	0.21	0.71	0.85	0.86	0.79	0.85	0.83	1142.83	0.74	2.54	2.83	2.57	4.09	2.51	3.28	0.35	0.14	0.02	0.00	0.00	0.00
6.76	1.49	0.66	0.50	0.46	0.26	0.35	0.22	0.76	0.89	0.90	0.83	0.89	0.87	1254.55	0.82	2.66	3.09	2.76	4.58	2.71	3.04	0.31	0.16	0.01	0.00	0.00	0.00
7.42	1.57	0.68	0.52	0.48	0.27	0.37	0.24	0.80	0.94	0.95	0.87	0.93	0.92	1377.20	0.69	2.71	3.31	2.92	5.00	2.88	2.80	0.23	0.13	0.00	0.00	0.00	0.00
8.15	1.64	0.71	0.54	0.50	0.28	0.39	0.26	0.85	1.00	0.99	0.91	0.97	0.96	1511.84	0.40	2.61	3.37	2.95	5.18	2.94	2.52	0.12	0.08	0.00	0.00	0.00	0.00
8.94	1.72	0.74	0.56	0.52	0.29	0.40	0.28	0.91	1.05	1.04	0.96	1.02	1.00	1659.64	0.10	2.47	3.35	2.91	5.21	2.94	2.29	0.03	0.02	0.00	0.00	0.00	0.00
9.82	1.78	0.76	0.58	0.54	0.30	0.42	0.30	0.97	1.11	1.09	1.00	1.06	1.05	1821.89	0.01	2.26	3.25	2.78	5.14	2.91	2.09	0.00	0.00	0.00	0.00	0.00	0.00
10.78	1.84	0.78	0.60	0.56	0.31	0.44	0.32	1.03	1.18	1.15	1.05	1.11	1.10	2000.00													
11.83	1.89	0.81	0.62	0.58	0.32	0.47	0.35	1.10	1.25	1.21	1.10	1.16	1.16														
12.99	1.94	0.84	0.65	0.61	0.34	0.49	0.38	1.18	1.33	1.28	1.17	1.23	1.22	Very coarse sand	3.42	17.61	21.72	19.27	32.79	19.18	19.57	1.43	0.66	0.07	0.00	0.00	0.01
14.26	1.99	0.88	0.68	0.64	0.35	0.52	0.41	1.27	1.42	1.36	1.23	1.30	1.30	coarse sand	3.79	12.40	12.49	14.59	18.30	11.97	28.00	4.87	1.95	0.60	0.66	0.27	0.33
15.65	2.01	0.91	0.71	0.66	0.37	0.55	0.45	1.36	1.51	1.43	1.30	1.36	1.36	medium sand	10.64	15.76	15.89	17.48	17.03	15.71	16.76	9.88	7.77	7.26	8.74	7.88	7.27
17.18	1.99	0.92	0.73	0.68	0.38	0.57	0.48	1.44	1.59	1.49	1.35	1.41	1.41	fine sand	12.03	13.80	13.94	14.44	10.61	17.36	8.78	14.61	15.63	18.81	22.11	20.74	20.75
18.86	1.91	0.91	0.73	0.69	0.38	0.59	0.51	1.50	1.64	1.52	1.37	1.42	1.43	very fine sand	1.44	1.16	1.13	1.10	0.75	1.39	1.15	2.64	2.63	2.56	2.38	2.45	2.50
20.71	1.79	0.87	0.71	0.68	0.38	0.60	0.54	1.55	1.67	1.52	1.37	1.41	1.42	silt	46.55	23.81	19.77	18.75	11.02	17.62	14.74	41.75	44.31	41.49	37.44	38.97	39.20
22.73	1.66	0.83	0.69	0.67	0.38	0.61	0.56	1.60	1.69	1.52	1.36	1.40	1.41	clay	8.60	4.40	3.69	3.38	1.94	2.67	1.52	5.09	6				

Channel Diameter (Lower) um	LC18-01	LC18-02	LC18-03	LC18-04	LC18-05	LC18-06	LC18-07	LC18-08	LC19-01	LC19-02	LC19-03	LC19-04	LC19-05	LC19-06	LC19-07	Channel Diameter (Lower) um	LC18-01	LC18-02	LC18-03	LC18-04	LC18-05	LC18-06	LC18-07	LC18-08	LC19-01	LC19-02	LC19-03	LC19-04	LC19-05	LC19-06	LC19-07
	Diff. Volume %	Diff. Volume %	Diff. Volume %	Diff. Volume %	Diff. Volume %	Diff. Volume %	Diff. Volume %	Diff. Volume %	Diff. Volume %	Diff. Volume %	Diff. Volume %	Diff. Volume %	Diff. Volume %	Diff. Volume %	Diff. Volume %		Diff. Volume %	Diff. Volume %	Diff. Volume %	Diff. Volume %	Diff. Volume %	Diff. Volume %	Diff. Volume %	Diff. Volume %	Diff. Volume %	Diff. Volume %	Diff. Volume %	Diff. Volume %	Diff. Volume %	Diff. Volume %	Diff. Volume %
0.38	0.01	0.01	0.01	0.01	0.01	0.01	0.02	0.02	0.01	0.01	0.04	0.02	0.03	0.02	0.01	69.62	1.85	1.71	2.39	1.98	1.49	2.40	3.21	3.06	0.96	0.73	1.32	2.40	2.96	2.25	1.57
0.41	0.01	0.01	0.02	0.01	0.01	0.02	0.04	0.03	0.02	0.01	0.07	0.04	0.05	0.03	0.02	76.43	2.04	1.87	2.61	2.17	1.75	2.68	3.30	3.24	1.05	0.81	1.41	2.53	3.09	2.44	1.76
0.45	0.02	0.02	0.03	0.02	0.01	0.02	0.06	0.05	0.03	0.02	0.10	0.06	0.08	0.05	0.03	83.90	2.23	2.02	2.84	2.36	2.05	2.99	3.36	3.42	1.15	0.90	1.50	2.66	3.20	2.64	1.98
0.50	0.03	0.03	0.04	0.03	0.02	0.03	0.08	0.07	0.04	0.02	0.14	0.09	0.11	0.07	0.04	92.10	2.43	2.18	3.06	2.56	2.41	3.32	3.39	3.57	1.25	1.00	1.58	2.77	3.28	2.84	2.24
0.54	0.03	0.03	0.05	0.04	0.02	0.04	0.10	0.08	0.05	0.03	0.18	0.11	0.14	0.09	0.05	101.10	2.61	2.33	3.28	2.76	2.81	3.67	3.40	3.72	1.38	1.12	1.67	2.87	3.33	3.04	2.53
0.60	0.04	0.04	0.06	0.05	0.03	0.05	0.12	0.10	0.06	0.04	0.20	0.13	0.16	0.10	0.06	110.99	2.77	2.47	3.47	2.96	3.24	4.03	3.40	3.85	1.52	1.25	1.78	2.97	3.36	3.25	2.86
0.66	0.05	0.05	0.07	0.05	0.03	0.06	0.13	0.11	0.06	0.04	0.23	0.14	0.18	0.12	0.07	121.84	2.91	2.59	3.63	3.16	3.67	4.37	3.39	3.97	1.68	1.40	1.92	3.06	3.37	3.48	3.23
0.72	0.05	0.05	0.08	0.06	0.04	0.06	0.15	0.13	0.07	0.05	0.25	0.16	0.20	0.13	0.08	133.75	3.00	2.69	3.75	3.33	4.08	4.67	3.36	4.06	1.85	1.56	2.10	3.15	3.38	3.70	3.62
0.79	0.06	0.06	0.09	0.07	0.04	0.07	0.16	0.14	0.08	0.05	0.27	0.17	0.22	0.14	0.09	146.82	3.04	2.75	3.79	3.48	4.44	4.89	3.28	4.09	2.03	1.72	2.28	3.23	3.35	3.91	4.00
0.87	0.06	0.06	0.10	0.07	0.05	0.08	0.18	0.15	0.08	0.06	0.28	0.18	0.23	0.15	0.09	161.18	3.02	2.75	3.72	3.56	4.71	4.98	3.12	4.03	2.20	1.88	2.43	3.25	3.25	4.05	4.36
0.95	0.06	0.07	0.10	0.08	0.05	0.08	0.19	0.16	0.09	0.06	0.30	0.19	0.24	0.16	0.10	176.94	2.92	2.69	3.53	3.57	4.87	4.90	2.84	3.82	2.34	2.02	2.51	3.20	3.06	4.11	4.64
1.05	0.07	0.07	0.11	0.08	0.05	0.09	0.19	0.16	0.09	0.06	0.30	0.20	0.25	0.17	0.11	194.23	2.76	2.57	3.23	3.49	4.89	4.66	2.45	3.45	2.43	2.14	2.50	3.05	2.75	4.04	4.82
1.15	0.07	0.07	0.11	0.08	0.06	0.09	0.20	0.17	0.10	0.07	0.31	0.21	0.26	0.18	0.11	213.22	2.56	2.40	2.84	3.33	4.79	4.26	1.99	2.97	2.49	2.25	2.42	2.82	2.36	3.86	4.89
1.26	0.08	0.08	0.12	0.09	0.06	0.09	0.21	0.18	0.10	0.07	0.32	0.21	0.26	0.18	0.12	234.07	2.36	2.22	2.42	3.13	4.59	3.75	1.52	2.44	2.53	2.36	2.31	2.55	1.95	3.60	4.86
1.38	0.08	0.08	0.12	0.09	0.06	0.10	0.22	0.19	0.11	0.07	0.34	0.22	0.27	0.19	0.12	256.95	2.19	2.06	2.04	2.92	4.31	3.21	1.14	1.93	2.57	2.49	2.23	2.29	1.58	3.30	4.73
1.52	0.08	0.08	0.13	0.10	0.06	0.10	0.23	0.19	0.11	0.08	0.35	0.23	0.28	0.20	0.13	282.07	2.08	1.94	1.73	2.72	3.98	2.70	0.87	1.51	2.63	2.66	2.21	2.08	1.29	2.99	4.52
1.67	0.09	0.09	0.14	0.10	0.07	0.11	0.24	0.20	0.12	0.08	0.37	0.24	0.29	0.20	0.13	309.64	2.03	1.89	1.51	2.55	3.62	2.23	0.72	1.20	2.72	2.85	2.23	1.92	1.11	2.70	4.24
1.83	0.09	0.09	0.14	0.11	0.07	0.11	0.25	0.21	0.12	0.09	0.40	0.25	0.30	0.21	0.14	339.92	2.04	1.87	1.36	2.40	3.26	1.84	0.63	0.98	2.81	3.06	2.26	1.80	0.99	2.41	3.88
2.01	0.09	0.09	0.15	0.11	0.07	0.12	0.27	0.22	0.13	0.09	0.43	0.27	0.32	0.22	0.15	373.15	2.07	1.89	1.25	2.25	2.90	1.50	0.56	0.81	2.88	3.25	2.26	1.69	0.89	2.11	3.45
2.21	0.10	0.10	0.16	0.12	0.08	0.13	0.29	0.24	0.14	0.10	0.47	0.29	0.34	0.24	0.15	409.63	2.10	1.92	1.14	2.09	2.55	1.21	0.47	0.66	2.92	3.41	2.20	1.56	0.77	1.77	2.96
2.42	0.11	0.11	0.17	0.12	0.08	0.13	0.31	0.25	0.15	0.11	0.52	0.31	0.36	0.25	0.16	449.67	2.12	1.96	1.03	1.92	2.21	0.96	0.36	0.51	2.93	3.52	2.07	1.40	0.62	1.41	2.42
2.66	0.11	0.11	0.18	0.13	0.08	0.14	0.33	0.27	0.16	0.11	0.57	0.33	0.39	0.27	0.17	493.63	2.11	1.98	0.92	1.74	1.89	0.75	0.24	0.35	2.90	3.58	1.89	1.22	0.44	1.05	1.88
2.92	0.12	0.12	0.20	0.14	0.09	0.15	0.36	0.29	0.17	0.12	0.62	0.36	0.42	0.29	0.19	541.89	2.10	2.02	0.83	1.58	1.61	0.59	0.13	0.22	2.86	3.60	1.70	1.05	0.29	0.73	1.37
3.21	0.13	0.13	0.21	0.15	0.09	0.16	0.39	0.31	0.18	0.13	0.68	0.39	0.45	0.31	0.20	594.87	2.08	2.06	0.78	1.44	1.37	0.47	0.07	0.11	2.83	3.58	1.52	0.89	0.17	0.47	0.92
3.52	0.14	0.14	0.23	0.16	0.10	0.17	0.42	0.34	0.20	0.14	0.75	0.42	0.49	0.33	0.21	653.03	2.07	2.13	0.78	1.33	1.16	0.40	0.03	0.04	2.81	3.55	1.35	0.75	0.09	0.28	0.56
3.86	0.15	0.15	0.25	0.18	0.11	0.18	0.46	0.36	0.21	0.15	0.81	0.45	0.52	0.36	0.23	716.87	2.07	2.20	0.82	1.24	1.00	0.36	0.02	0.01	2.80	3.49	1.19	0.62	0.06	0.15	0.27
4.24	0.16	0.16	0.27	0.19	0.11	0.20	0.49	0.39	0.22	0.16	0.86	0.49	0.56	0.38	0.24	786.95	2.07	2.29	0.90	1.18	0.88	0.34	0.01	0.00	2.79	3.40	1.03	0.49	0.04	0.08	0.10
4.66	0.17	0.17	0.28	0.21	0.12	0.21	0.53	0.42	0.23	0.17	0.92	0.52	0.60	0.41	0.26	863.88	2.06	2.37	0.99	1.14	0.79	0.33	0.01	0.00	2.77	3.29	0.88	0.38	0.02	0.03	0.02
5.11	0.18	0.18	0.31	0.22	0.13	0.23	0.58	0.45	0.25	0.18	0.97	0.56	0.64	0.44	0.28	948.34	2.05	2.44	1.10	1.12	0.73	0.34	0.01	0.00	2.74	3.16	0.75	0.28	0.01	0.01	0.00
5.61	0.19	0.19	0.33	0.24	0.14	0.24	0.62	0.48	0.26	0.19	1.02	0.59	0.68	0.46	0.30	1041.05	2.01	2.47	1.19	1.11	0.69	0.36	0.01	0.00	2.68	3.00	0.65	0.21	0.00	0.01	0.00
6.16	0.21	0.20	0.35	0.25	0.15	0.26	0.67	0.51	0.27	0.20	1.06	0.62	0.72	0.49	0.31	1142.83	1.98	2.50	1.28	1.12	0.67	0.38	0.01	0.00	2.63	2.87	0.59	0.17	0.00	0.00	0.00
6.76	0.22	0.22	0.37	0.27	0.15	0.28	0.72	0.55	0.28	0.20	1.09	0.66	0.76	0.52	0.33	1254.55	1.93	2.51	1.36	1.14	0.66	0.40	0.01	0.00	2.57	2.74	0.56	0.15	0.00	0.00	0.00
7.42	0.24	0.23	0.40	0.29	0.16	0.30	0.77	0.59	0.29	0.21	1.12	0.69	0.80	0.55	0.35	1377.20	1.88	2.50	1.43	1.16	0.65	0.42	0.00	0.00	2.52	2.64	0.44	0.11	0.00	0.00	0.00
8.15	0.25	0.25	0.43	0.31	0.17	0.32	0.82	0.62	0.31	0.22	1.15	0.73	0.84	0.58	0.38	1511.84	1.79	2.41	1.46	1.15	0.64	0.43	0.00	0.00	2.42	2.49	0.24	0.06	0.00	0.00	0.00
8.94	0.27	0.27	0.46	0.33	0.19	0.34	0.89	0.67	0.32	0.23	1.18	0.77	0.89	0.61	0.40	1659.64	1.71	2.31	1.46	1.14	0.63	0.44	0.00	0.00	2.32	2.37	0.06	0.01	0.00	0.00	0.00
9.82	0.29	0.29	0.49	0.36	0.20	0.37	0.95	0.71	0.33	0.24	1.20	0.81	0.94	0.65	0.42	1821.89	1.62	2.21	1.46	1.13	0.63	0.45	0.00	0.00	2.24	2.27	0.01	0.00	0.00	0.00	0.00
10.78	0.31	0.31	0.52	0.39	0.21	0.39	1.03	0.77	0.34	0.25	1.23	0.86	1.00	0.68	0.44	2000.00															
11.83	0.33	0.33	0.56	0.41	0.22	0.42	1.11	0.82	0.36	0.26	1.25	0.90	1.06	0.72	0.47																
12.99	0.36	0.36	0.60	0.45	0.24	0.46	1.20	0.89	0.37	0.28	1.30	0.96	1.12	0.76	0.49	Very coarse sand	12.93	16.91	9.64	7.95	4.56	2.87	0.02	0.00	17.39	18.38	2.56	0.71	0.00	0.01	0.00
14.26	0.39	0.39	0.64	0.48	0.26	0.49	1.30	0.96	0.39	0.29	1.34	1.02	1.20	0.81	0.52	coarse sand	14.50	15.49	6.18	9.04	7.53	2.84	0.28	0.38	19.60	24.06	8.43	4.46	0.67	1.75	3.

Appendix

		LC20-01	LC20-02	LC20-03	LC20-04	LC20-05	LC20-06	LC20-07	LC20-08	LC20-09	LC20-10	LC20-11	LC20-12	LC20-13	LC20-14	LC20-15			LC20-01	LC20-02	LC20-03	LC20-04	LC20-05	LC20-06	LC20-07	LC20-08	LC20-09	LC20-10	LC20-11	LC20-12	LC20-13	LC20-14	LC20-15
Channel Diameter (Lower) um	Diff.	Diff.	Diff.	Diff.	Diff.	Diff.	Diff.	Diff.	Diff.	Diff.	Diff.	Diff.	Diff.	Diff.	Diff.	Diff.	Channel Diameter (Lower) um	Diff.	Diff.	Diff.	Diff.	Diff.	Diff.	Diff.	Diff.	Diff.	Diff.	Diff.	Diff.	Diff.	Diff.	Diff.	
	Volume	Volume	Volume	Volume	Volume	Volume	Volume	Volume	Volume	Volume	Volume	Volume	Volume	Volume	Volume	Volume		Volume	Volume	Volume	Volume	Volume	Volume	Volume	Volume	Volume	Volume	Volume	Volume	Volume	Volume	Volume	
	%	%	%	%	%	%	%	%	%	%	%	%	%	%	%	%		%	%	%	%	%	%	%	%	%	%	%	%	%	%	%	
0.38	0.02	0.02	0.01	0.02	0.03	0.03	0.02	0.03	0.04	0.03	0.03	0.03	0.02	0.03	0.03	0.03	69.62	3.15	3.05	1.81	2.19	2.69	2.88	2.65	2.51	2.19	2.66	2.11	2.84	2.92	3.63	3.68	
0.41	0.03	0.04	0.03	0.03	0.05	0.05	0.04	0.06	0.07	0.06	0.06	0.04	0.05	0.05	0.05	0.05	76.43	3.42	3.17	1.94	2.36	2.91	2.99	2.76	2.60	2.23	2.57	2.03	3.04	3.06	3.73	3.85	
0.45	0.05	0.06	0.04	0.05	0.07	0.08	0.06	0.08	0.11	0.09	0.09	0.06	0.07	0.07	0.08	0.08	83.90	3.68	3.27	2.08	2.52	3.12	3.07	2.85	2.68	2.26	2.47	1.93	3.21	3.16	3.78	3.99	
0.50	0.07	0.09	0.06	0.07	0.10	0.11	0.08	0.12	0.15	0.13	0.12	0.09	0.10	0.10	0.11	0.11	92.10	3.93	3.34	2.21	2.68	3.32	3.12	2.89	2.73	2.27	2.33	1.82	3.32	3.22	3.78	4.06	
0.54	0.09	0.11	0.07	0.09	0.13	0.14	0.10	0.15	0.19	0.16	0.15	0.11	0.12	0.12	0.14	0.14	101.10	4.13	3.38	2.35	2.83	3.49	3.11	2.90	2.77	2.26	2.16	1.69	3.39	3.22	3.76	4.07	
0.60	0.11	0.13	0.08	0.10	0.15	0.16	0.12	0.17	0.22	0.19	0.18	0.13	0.14	0.14	0.17	0.17	110.99	4.27	3.40	2.47	2.96	3.62	3.08	2.88	2.80	2.23	1.99	1.57	3.43	3.19	3.73	4.02	
0.66	0.12	0.15	0.09	0.12	0.17	0.18	0.13	0.20	0.25	0.22	0.20	0.15	0.16	0.16	0.19	0.19	121.84	4.35	3.39	2.60	3.07	3.70	3.02	2.85	2.82	2.19	1.82	1.46	3.44	3.13	3.67	3.91	
0.72	0.14	0.17	0.10	0.13	0.19	0.20	0.15	0.22	0.27	0.24	0.22	0.17	0.18	0.18	0.21	0.21	133.75	4.34	3.36	2.72	3.17	3.74	2.94	2.81	2.82	2.13	1.65	1.37	3.43	3.05	3.55	3.75	
0.79	0.15	0.18	0.11	0.14	0.20	0.22	0.16	0.23	0.30	0.26	0.24	0.18	0.19	0.19	0.23	0.23	146.82	4.22	3.28	2.81	3.21	3.71	2.83	2.75	2.78	2.03	1.46	1.28	3.34	2.93	3.32	3.50	
0.87	0.16	0.19	0.12	0.15	0.22	0.23	0.17	0.24	0.31	0.28	0.26	0.19	0.20	0.20	0.24	0.24	161.18	3.97	3.12	2.84	3.16	3.59	2.66	2.64	2.65	1.87	1.24	1.14	3.12	2.72	2.93	3.15	
0.95	0.17	0.20	0.12	0.16	0.23	0.24	0.17	0.25	0.32	0.30	0.27	0.20	0.21	0.21	0.25	0.25	176.94	3.58	2.85	2.79	3.01	3.34	2.38	2.45	2.42	1.61	0.97	0.94	2.74	2.39	2.45	2.70	
1.05	0.17	0.21	0.13	0.16	0.23	0.24	0.18	0.26	0.34	0.31	0.28	0.20	0.22	0.22	0.26	0.26	194.23	3.07	2.47	2.65	2.74	2.98	2.01	2.19	2.07	1.25	0.67	0.67	2.18	1.94	2.00	2.15	
1.15	0.18	0.22	0.13	0.17	0.24	0.25	0.18	0.27	0.35	0.32	0.29	0.21	0.22	0.22	0.27	0.27	213.22	2.50	2.00	2.45	2.39	2.52	1.57	1.88	1.66	0.85	0.36	0.37	1.55	1.42	1.66	1.56	
1.26	0.19	0.23	0.14	0.17	0.25	0.25	0.18	0.27	0.36	0.34	0.30	0.21	0.23	0.23	0.27	0.27	234.07	1.93	1.54	2.21	2.02	2.04	1.15	1.60	1.27	0.49	0.14	0.14	0.98	0.94	1.47	1.02	
1.38	0.19	0.24	0.14	0.18	0.26	0.26	0.19	0.28	0.37	0.35	0.31	0.21	0.23	0.23	0.28	0.28	256.95	1.45	1.16	2.01	1.69	1.62	0.83	1.39	0.96	0.26	0.03	0.04	0.62	0.59	1.39	0.62	
1.52	0.20	0.24	0.15	0.18	0.26	0.26	0.19	0.29	0.38	0.36	0.33	0.22	0.24	0.24	0.29	0.29	282.07	1.10	0.90	1.85	1.45	1.30	0.66	1.30	0.78	0.16	0.00	0.03	0.48	0.43	1.29	0.38	
1.67	0.21	0.25	0.15	0.19	0.27	0.27	0.20	0.30	0.40	0.38	0.34	0.22	0.24	0.25	0.30	0.30	309.64	0.88	0.76	1.75	1.31	1.09	0.61	1.30	0.71	0.16	0.00	0.07	0.52	0.46	1.08	0.29	
1.83	0.21	0.27	0.16	0.20	0.29	0.29	0.21	0.31	0.43	0.40	0.36	0.23	0.26	0.26	0.31	0.31	339.92	0.75	0.71	1.69	1.23	0.97	0.64	1.34	0.71	0.22	0.00	0.18	0.66	0.68	0.75	0.28	
2.01	0.23	0.28	0.17	0.21	0.30	0.30	0.22	0.33	0.46	0.43	0.39	0.25	0.27	0.27	0.32	0.32	373.15	0.66	0.70	1.64	1.19	0.89	0.69	1.37	0.71	0.29	0.00	0.31	0.83	1.09	0.39	0.30	
2.21	0.24	0.30	0.18	0.22	0.32	0.32	0.24	0.35	0.50	0.46	0.42	0.26	0.29	0.28	0.33	0.33	409.63	0.59	0.68	1.57	1.14	0.79	0.70	1.34	0.67	0.31	0.00	0.38	0.95	1.61	0.14	0.31	
2.42	0.26	0.32	0.19	0.24	0.34	0.35	0.25	0.38	0.55	0.50	0.45	0.28	0.31	0.30	0.35	0.35	449.67	0.49	0.61	1.48	1.06	0.67	0.64	1.24	0.59	0.27	0.00	0.41	1.02	2.09	0.02	0.27	
2.66	0.27	0.35	0.20	0.26	0.37	0.38	0.27	0.42	0.60	0.54	0.50	0.30	0.33	0.33	0.37	0.37	493.63	0.39	0.51	1.38	0.96	0.52	0.54	1.09	0.48	0.19	0.00	0.41	1.13	2.36	0.00	0.19	
2.92	0.30	0.38	0.22	0.28	0.40	0.41	0.30	0.46	0.67	0.59	0.55	0.32	0.36	0.35	0.40	0.40	541.89	0.29	0.40	1.28	0.87	0.38	0.45	0.94	0.40	0.14	0.00	0.43	1.39	2.10	0.00	0.10	
3.21	0.32	0.41	0.23	0.30	0.43	0.45	0.33	0.50	0.74	0.65	0.60	0.35	0.39	0.38	0.43	0.43	594.87	0.22	0.30	1.21	0.80	0.26	0.39	0.84	0.36	0.11	0.00	0.48	1.83	1.52	0.00	0.03	
3.52	0.34	0.44	0.25	0.32	0.46	0.49	0.36	0.55	0.82	0.71	0.66	0.38	0.43	0.41	0.45	0.45	653.03	0.17	0.22	1.18	0.78	0.18	0.40	0.79	0.36	0.13	0.00	0.59	2.40	0.82	0.00	0.01	
3.86	0.37	0.48	0.27	0.35	0.50	0.54	0.39	0.60	0.91	0.78	0.73	0.41	0.47	0.45	0.49	0.49	716.87	0.14	0.16	1.19	0.79	0.14	0.46	0.78	0.40	0.17	0.00	0.75	2.78	0.38	0.00	0.00	
4.24	0.40	0.52	0.29	0.37	0.54	0.58	0.42	0.66	1.00	0.86	0.81	0.45	0.50	0.48	0.52	0.52	786.95	0.12	0.11	1.25	0.84	0.15	0.54	0.80	0.45	0.22	0.00	0.98	2.34	0.09	0.00	0.00	
4.66	0.44	0.56	0.31	0.40	0.57	0.63	0.46	0.71	1.09	0.94	0.89	0.48	0.55	0.52	0.55	0.55	863.88	0.10	0.07	1.36	0.92	0.18	0.60	0.84	0.50	0.25	0.00	1.26	1.31	0.01	0.00	0.00	
5.11	0.47	0.60	0.33	0.43	0.61	0.67	0.49	0.77	1.19	1.03	0.97	0.51	0.57	0.55	0.59	0.59	948.34	0.10	0.04	1.53	1.04	0.23	0.62	0.90	0.53	0.23	0.00	1.48	0.33	0.00	0.00	0.00	
5.61	0.50	0.65	0.36	0.45	0.65	0.72	0.53	0.84	1.29	1.12	1.06	0.55	0.63	0.59	0.62	0.62	1041.05	0.10	0.01	1.73	1.19	0.30	0.56	0.95	0.52	0.18	0.00	1.53	0.04	0.00	0.00	0.00	
6.16	0.54	0.69	0.38	0.48	0.68	0.77	0.57	0.90	1.40	1.22	1.15	0.58	0.68	0.63	0.66	0.66	1142.83	0.10	0.00	1.97	1.38	0.37	0.45	1.01	0.39	0.10	0.00	1.18	0.00	0.00	0.00	0.00	
6.76	0.58	0.74	0.40	0.51	0.72	0.82	0.61	0.96	1.50	1.32	1.25	0.62	0.72	0.67	0.70	0.70	1254.55	0.09	0.00	2.22	1.59	0.42	0.31	1.06	0.21	0.05	0.00	0.65	0.00	0.00	0.00	0.00	
7.42	0.62	0.79	0.43	0.54	0.76	0.87	0.65	1.03	1.60	1.43	1.36	0.66	0.77	0.72	0.73	0.73	1377.20	0.06	0.00	2.45	1.81	0.35	0.17	0.87	0.05	0.01	0.00	0.16	0.00	0.00	0.00	0.00	
8.15	0.66	0.85	0.45	0.57	0.80	0.92	0.70	1.10	1.71	1.55	1.47	0.70	0.82	0.76	0.78	0.78	1511.84	0.03	0.00	2.57	1.97	0.20	0.06	0.50	0.01	0.00	0.00	0.02	0.00	0.00	0.00	0.00	
8.94	0.70	0.91	0.48	0.61	0.84	0.98	0.75	1.18	1.82	1.68	1.59	0.74	0.88	0.81	0.82	0.82	1659.64	0.01	0.00	2.61	2.07	0.05	0.01	0.13	0.00	0.00	0.00	0.00	0.00	0.00	0.00	0.00	
9.82	0.75	0.97	0.51	0.65	0.89	1.05	0.80	1.26	1.93	1.81	1.71	0.79	0.94	0.87	0.87	0.87	1821.89	0.00	0.00	2.59	2.15	0.01	0.00	0.01	0.00	0.00	0.00	0.00	0.00	0.00	0.00	0.00	
10.78	0.80	1.04	0.54	0.69	0.94	1.12	0.86	1.34	2.05	1.96	1.85	0.83	1.01	0.93	0.93	0.93	2000.00																
11.83	0.86	1.12	0.58	0.73	0.99	1.20	0.93	1.43	2.16	2.11	1.99	0.89	1.09	1.00	0.99	0.99																	

Channel Diameter (Lower) um	LC21-01	LC21-02	LC21-03	LC21-04	LC21-05	LC21-06	LC21-07	LC21-08	LC21-09	LC21-10	LC21-11	LC21-12	LC21-13	LC21-14	LC21-15	Channel Diameter (Lower) um	LC21-01	LC21-02	LC21-03	LC21-04	LC21-05	LC21-06	LC21-07	LC21-08	LC21-09	LC21-10	LC21-11	LC21-12	LC21-13	LC21-14	LC21-15
	Diff.	Diff.	Diff.	Diff.	Diff.	Diff.	Diff.	Diff.	Diff.	Diff.	Diff.	Diff.	Diff.	Diff.	Diff.		Diff.	Diff.	Diff.	Diff.	Diff.	Diff.	Diff.	Diff.	Diff.	Diff.	Diff.	Diff.	Diff.	Diff.	
	Volume	Volume	Volume	Volume	Volume	Volume	Volume	Volume	Volume	Volume	Volume	Volume	Volume	Volume	Volume		Volume	Volume	Volume	Volume	Volume	Volume	Volume	Volume	Volume	Volume	Volume	Volume	Volume	Volume	Volume
%	%	%	%	%	%	%	%	%	%	%	%	%	%	%	%	%	%	%	%	%	%	%	%	%	%	%	%	%	%	%	
0.38	0.02	0.02	0.03	0.04	0.04	0.05	0.04	0.04	0.03	0.01	0.03	0.04	0.04	0.04	0.04	69.62	2.04	2.75	1.98	2.32	2.22	2.07	2.17	2.24	2.20	0.89	1.74	2.09	2.31	2.31	2.27
0.41	0.04	0.04	0.04	0.07	0.07	0.09	0.07	0.07	0.05	0.03	0.06	0.07	0.06	0.07	0.06	76.43	2.31	3.26	2.26	2.45	2.35	2.07	2.34	2.45	2.44	0.99	1.97	2.30	2.51	2.50	2.48
0.45	0.06	0.06	0.07	0.10	0.10	0.13	0.11	0.10	0.08	0.04	0.09	0.10	0.09	0.10	0.09	83.90	2.61	3.79	2.58	2.57	2.48	2.06	2.51	2.67	2.69	1.06	2.16	2.56	2.74	2.71	2.73
0.50	0.09	0.08	0.09	0.14	0.14	0.18	0.15	0.14	0.11	0.05	0.12	0.13	0.13	0.15	0.13	92.10	2.93	4.33	2.93	2.67	2.61	2.03	2.68	2.89	2.94	1.17	2.30	2.87	3.03	2.94	3.00
0.54	0.11	0.10	0.12	0.17	0.18	0.22	0.19	0.17	0.14	0.07	0.14	0.17	0.16	0.18	0.16	101.10	3.28	4.82	3.31	2.77	2.74	1.98	2.83	3.12	3.18	1.31	2.46	3.23	3.35	3.19	3.29
0.60	0.13	0.12	0.14	0.20	0.21	0.26	0.22	0.20	0.16	0.08	0.16	0.19	0.19	0.21	0.19	110.99	3.63	5.23	3.70	2.86	2.87	1.93	2.97	3.36	3.41	1.44	2.67	3.61	3.66	3.41	3.52
0.66	0.15	0.13	0.16	0.23	0.23	0.29	0.24	0.22	0.18	0.08	0.18	0.21	0.21	0.23	0.21	121.84	3.98	5.52	4.09	2.97	3.02	1.90	3.10	3.59	3.61	1.53	2.91	3.91	3.89	3.56	3.68
0.72	0.17	0.15	0.17	0.25	0.26	0.32	0.27	0.24	0.20	0.09	0.19	0.23	0.23	0.25	0.23	133.75	4.31	5.66	4.46	3.08	3.18	1.90	3.24	3.81	3.78	1.60	3.12	4.04	3.98	3.60	3.78
0.79	0.18	0.16	0.19	0.27	0.28	0.35	0.28	0.26	0.21	0.09	0.20	0.25	0.24	0.26	0.24	146.82	4.59	5.64	4.78	3.18	3.31	1.92	3.35	3.98	3.90	1.68	3.25	4.01	3.99	3.62	3.94
0.87	0.20	0.17	0.20	0.29	0.29	0.37	0.29	0.27	0.22	0.09	0.20	0.25	0.25	0.27	0.25	161.18	4.77	5.44	4.98	3.22	3.38	1.92	3.42	4.07	3.91	1.73	3.35	3.97	4.06	3.77	4.27
0.95	0.21	0.18	0.21	0.30	0.31	0.38	0.30	0.28	0.23	0.09	0.20	0.26	0.25	0.27	0.26	176.94	4.81	5.06	5.03	3.15	3.31	1.86	3.40	4.02	3.79	1.71	3.41	4.10	4.31	4.15	4.78
1.05	0.21	0.19	0.22	0.31	0.31	0.39	0.30	0.28	0.23	0.09	0.20	0.26	0.25	0.27	0.26	194.23	4.67	4.54	4.89	2.94	3.09	1.72	3.24	3.81	3.51	1.64	3.37	4.50	4.73	4.72	5.33
1.15	0.22	0.20	0.23	0.32	0.32	0.40	0.31	0.28	0.24	0.09	0.19	0.26	0.25	0.27	0.26	213.22	4.36	3.91	4.57	2.61	2.72	1.49	2.94	3.47	3.10	1.49	3.17	5.02	5.11	5.21	5.56
1.26	0.23	0.21	0.24	0.32	0.33	0.41	0.31	0.29	0.24	0.09	0.19	0.26	0.25	0.27	0.26	234.07	3.93	3.23	4.09	2.22	2.28	1.22	2.55	3.04	2.62	1.26	2.78	5.35	5.12	5.25	5.19
1.38	0.24	0.21	0.24	0.33	0.34	0.41	0.31	0.29	0.24	0.09	0.19	0.26	0.25	0.27	0.26	256.95	3.43	2.59	3.54	1.85	1.86	0.98	2.15	2.61	2.16	1.01	2.29	5.11	4.50	4.58	4.13
1.52	0.24	0.22	0.25	0.34	0.35	0.42	0.31	0.29	0.24	0.09	0.20	0.26	0.26	0.27	0.26	282.07	2.93	2.05	2.98	1.56	1.52	0.81	1.78	2.21	1.79	0.82	1.93	4.16	3.30	3.29	2.63
1.67	0.25	0.22	0.26	0.35	0.36	0.44	0.32	0.29	0.25	0.09	0.21	0.27	0.26	0.28	0.26	309.64	2.47	1.61	2.46	1.36	1.27	0.72	1.50	1.88	1.52	0.74	1.84	2.70	1.86	1.75	1.23
1.83	0.26	0.23	0.27	0.37	0.37	0.46	0.33	0.30	0.26	0.10	0.22	0.28	0.27	0.29	0.27	339.92	2.08	1.29	2.02	1.24	1.11	0.68	1.29	1.61	1.33	0.75	2.02	1.28	0.73	0.62	0.37
2.01	0.27	0.24	0.28	0.39	0.40	0.49	0.35	0.32	0.27	0.10	0.23	0.29	0.28	0.30	0.29	373.15	1.74	1.05	1.63	1.13	0.97	0.65	1.11	1.36	1.18	0.80	2.45	0.39	0.17	0.11	0.06
2.21	0.29	0.25	0.30	0.41	0.42	0.52	0.37	0.33	0.28	0.11	0.24	0.31	0.30	0.32	0.31	409.63	1.43	0.85	1.29	0.99	0.81	0.58	0.92	1.10	1.03	0.80	3.02	0.06	0.02	0.01	0.00
2.42	0.30	0.26	0.31	0.45	0.45	0.56	0.39	0.36	0.29	0.12	0.26	0.33	0.32	0.35	0.33	449.67	1.13	0.66	0.98	0.82	0.62	0.46	0.72	0.83	0.85	0.68	3.53	0.00	0.00	0.00	0.00
2.66	0.32	0.27	0.33	0.48	0.49	0.61	0.43	0.38	0.31	0.13	0.28	0.36	0.35	0.38	0.35	493.63	0.84	0.48	0.71	0.62	0.42	0.29	0.50	0.59	0.65	0.56	3.97	0.00	0.00	0.00	0.00
2.92	0.34	0.28	0.35	0.52	0.53	0.67	0.46	0.41	0.34	0.13	0.30	0.38	0.38	0.41	0.38	541.89	0.59	0.32	0.47	0.42	0.22	0.14	0.31	0.42	0.49	0.58	4.39	0.00	0.00	0.00	0.00
3.21	0.36	0.29	0.37	0.57	0.57	0.73	0.50	0.44	0.36	0.15	0.32	0.42	0.41	0.44	0.42	594.87	0.38	0.18	0.27	0.26	0.09	0.05	0.20	0.31	0.39	0.75	4.17	0.00	0.00	0.00	0.00
3.52	0.38	0.31	0.39	0.61	0.62	0.79	0.55	0.48	0.38	0.16	0.34	0.45	0.44	0.48	0.45	653.03	0.22	0.09	0.14	0.15	0.03	0.02	0.15	0.28	0.39	0.78	2.71	0.00	0.00	0.00	0.00
3.86	0.41	0.32	0.41	0.66	0.67	0.86	0.59	0.51	0.41	0.17	0.37	0.48	0.47	0.51	0.48	716.87	0.12	0.04	0.06	0.08	0.01	0.01	0.16	0.27	0.45	0.82	1.19	0.00	0.00	0.00	0.00
4.24	0.43	0.33	0.44	0.71	0.72	0.94	0.63	0.55	0.44	0.18	0.39	0.51	0.50	0.54	0.51	786.95	0.06	0.02	0.02	0.04	0.01	0.02	0.21	0.27	0.58	1.29	0.22	0.00	0.00	0.00	0.00
4.66	0.45	0.35	0.46	0.76	0.77	1.01	0.68	0.58	0.46	0.19	0.42	0.54	0.53	0.57	0.54	863.88	0.04	0.01	0.00	0.02	0.01	0.03	0.27	0.24	0.77	2.23	0.02	0.00	0.00	0.00	0.00
5.11	0.47	0.36	0.48	0.81	0.82	1.09	0.72	0.61	0.49	0.20	0.43	0.56	0.55	0.60	0.57	948.34	0.03	0.01	0.00	0.01	0.01	0.04	0.32	0.18	1.03	3.03	0.00	0.00	0.00	0.00	0.00
5.61	0.50	0.37	0.50	0.85	0.87	1.17	0.76	0.64	0.51	0.20	0.45	0.58	0.57	0.62	0.59	1041.05	0.02	0.01	0.00	0.00	0.01	0.05	0.35	0.11	1.33	3.62	0.00	0.00	0.00	0.00	0.00
6.16	0.52	0.38	0.52	0.90	0.92	1.25	0.79	0.66	0.53	0.21	0.46	0.60	0.59	0.64	0.61	1142.83	0.02	0.00	0.00	0.00	0.00	0.05	0.34	0.05	1.62	3.99	0.00	0.00	0.00	0.00	0.00
6.76	0.54	0.39	0.54	0.94	0.97	1.33	0.83	0.69	0.55	0.21	0.47	0.61	0.61	0.66	0.62	1254.55	0.02	0.00	0.00	0.00	0.00	0.05	0.32	0.02	1.91	4.23	0.00	0.00	0.00	0.00	0.00
7.42	0.56	0.40	0.56	0.99	1.02	1.41	0.86	0.71	0.56	0.22	0.49	0.63	0.62	0.67	0.64	1377.20	0.02	0.00	0.00	0.00	0.00	0.04	0.24	0.00	1.72	4.69	0.00	0.00	0.00	0.00	0.00
8.15	0.58	0.41	0.58	1.03	1.07	1.50	0.90	0.74	0.58	0.23	0.50	0.65	0.64	0.69	0.66	1511.84	0.01	0.00	0.00	0.00	0.00	0.02	0.13	0.00	1.07	7.61	0.00	0.00	0.00	0.00	0.00
8.94	0.60	0.42	0.60	1.08	1.12	1.59	0.94	0.76	0.60	0.23	0.52	0.66	0.66	0.71	0.69	1659.64	0.00	0.00	0.00	0.00	0.00	0.00	0.03	0.00	0.28	12.73	0.00	0.00	0.00	0.00	0.00
9.82	0.62	0.43	0.62	1.13	1.18	1.69	0.99	0.79	0.62	0.24	0.54	0.68	0.69	0.73	0.71	1821.89	0.00	0.00	0.00	0.00	0.00	0.00	0.00	0.00	0.03	15.66	0.00	0.00	0.00	0.00	0.00
10.78	0.64	0.44	0.64	1.18	1.23	1.79	1.03	0.82	0.64	0.24	0.55	0.70	0.71	0.76	0.74	2000.00															
11.83	0.66	0.45	0.66	1.24	1.30	1.91	1.09	0.86	0.67	0.25	0.56	0.74	0.76	0.81	0.78																
12.99	0.68	0.46	0.68	1.31	1.37	2.04	1.17	0.91	0.70	0.25	0.58	0.79	0.81	0.87	0.84		Very coarse sand	0.09	0.01	0.00	0.00	0.01	0.21	1.42	0.18	7.97	52.53	0.00	0.00	0.00	0.00
14.26	0.71	0.47	0.70</																												

Appendix

Channel Diameter (Lower) um	LC22-01	LC22-02	LC22-03	LC22-04	LC22-05	LC22-06	LC22-07	LC22-08	LC22-09	LC22-10	LC23-01	LC23-02	LC23-03	LC23-04	LC23-05	Channel Diameter (Lower) um	LC22-01	LC22-02	LC22-03	LC22-04	LC22-05	LC22-06	LC22-07	LC22-08	LC22-09	LC22-10	LC23-01	LC23-02	LC23-03	LC23-04	LC23-05	
	Diff. Volume %	Diff. Volume %	Diff. Volume %	Diff. Volume %	Diff. Volume %	Diff. Volume %	Diff. Volume %	Diff. Volume %	Diff. Volume %	Diff. Volume %	Diff. Volume %	Diff. Volume %	Diff. Volume %	Diff. Volume %	Diff. Volume %		Diff. Volume %	Diff. Volume %	Diff. Volume %	Diff. Volume %	Diff. Volume %	Diff. Volume %	Diff. Volume %	Diff. Volume %	Diff. Volume %	Diff. Volume %	Diff. Volume %	Diff. Volume %	Diff. Volume %	Diff. Volume %	Diff. Volume %	
	%	%	%	%	%	%	%	%	%	%	%	%	%	%	%		%	%	%	%	%	%	%	%	%	%	%	%	%	%	%	%
0.38	0.03	0.06	0.04	0.04	0.03	0.03	0.03	0.03	0.03	0.03	0.04	0.05	0.05	0.03	0.02	69.62	2.25	1.91	2.52	2.21	2.40	2.71	2.83	3.11	2.84	2.84	1.72	1.79	1.76	2.71	2.55	
0.41	0.06	0.10	0.06	0.07	0.06	0.05	0.05	0.05	0.06	0.07	0.09	0.09	0.09	0.06	0.03	76.43	2.36	1.91	2.46	2.06	2.37	2.78	2.84	3.13	2.74	2.76	1.57	1.63	1.59	2.65	2.68	
0.45	0.08	0.15	0.09	0.10	0.08	0.07	0.07	0.07	0.07	0.08	0.10	0.13	0.13	0.08	0.05	83.90	2.49	1.90	2.40	1.91	2.34	2.83	2.83	3.13	2.63	2.65	1.41	1.47	1.42	2.56	2.82	
0.50	0.12	0.21	0.13	0.14	0.12	0.10	0.10	0.10	0.10	0.12	0.14	0.19	0.19	0.12	0.07	92.10	2.64	1.89	2.32	1.74	2.30	2.88	2.79	3.10	2.49	2.52	1.25	1.29	1.24	2.45	2.95	
0.54	0.14	0.26	0.16	0.17	0.15	0.12	0.13	0.13	0.15	0.17	0.23	0.24	0.23	0.14	0.08	101.10	2.81	1.89	2.23	1.58	2.25	2.91	2.73	3.04	2.33	2.36	1.09	1.13	1.07	2.32	3.09	
0.60	0.17	0.30	0.19	0.20	0.17	0.14	0.15	0.15	0.17	0.20	0.27	0.28	0.27	0.17	0.10	110.99	2.98	1.88	2.16	1.42	2.21	2.93	2.66	2.96	2.18	2.21	0.95	0.98	0.91	2.18	3.23	
0.66	0.19	0.33	0.22	0.23	0.19	0.16	0.17	0.17	0.19	0.22	0.31	0.31	0.31	0.19	0.11	121.84	3.13	1.89	2.10	1.30	2.19	2.96	2.58	2.87	2.04	2.06	0.84	0.87	0.79	2.05	3.37	
0.72	0.21	0.36	0.24	0.25	0.22	0.18	0.19	0.19	0.22	0.25	0.35	0.35	0.34	0.22	0.12	133.75	3.24	1.89	2.05	1.21	2.18	2.98	2.51	2.77	1.91	1.93	0.76	0.79	0.70	1.93	3.51	
0.79	0.22	0.39	0.26	0.28	0.23	0.19	0.21	0.20	0.23	0.27	0.38	0.38	0.37	0.24	0.14	146.82	3.34	1.90	1.99	1.14	2.17	2.98	2.41	2.63	1.79	1.79	0.70	0.72	0.62	1.80	3.63	
0.87	0.23	0.40	0.27	0.29	0.25	0.20	0.22	0.21	0.25	0.28	0.40	0.40	0.39	0.25	0.15	161.18	3.48	1.94	1.91	1.05	2.12	2.91	2.25	2.43	1.63	1.62	0.62	0.64	0.53	1.64	3.68	
0.95	0.24	0.41	0.28	0.30	0.26	0.21	0.23	0.22	0.26	0.29	0.42	0.42	0.41	0.26	0.15	176.94	3.67	2.01	1.75	0.92	2.00	2.75	2.01	2.14	1.40	1.38	0.51	0.52	0.41	1.42	3.65	
1.05	0.24	0.41	0.29	0.31	0.26	0.22	0.24	0.23	0.27	0.30	0.44	0.44	0.43	0.28	0.16	194.23	3.86	2.09	1.51	0.73	1.78	2.48	1.69	1.76	1.11	1.07	0.37	0.36	0.27	1.15	3.50	
1.15	0.24	0.41	0.30	0.32	0.27	0.23	0.24	0.24	0.27	0.31	0.46	0.46	0.45	0.29	0.17	213.22	3.89	2.10	1.22	0.51	1.50	2.12	1.32	1.33	0.79	0.73	0.20	0.19	0.14	0.85	3.24	
1.26	0.25	0.42	0.30	0.33	0.28	0.23	0.25	0.24	0.28	0.32	0.48	0.48	0.47	0.30	0.17	234.07	3.60	1.94	0.92	0.30	1.20	1.75	0.96	0.93	0.48	0.43	0.07	0.07	0.04	0.57	2.91	
1.38	0.25	0.42	0.31	0.33	0.28	0.24	0.25	0.25	0.29	0.32	0.50	0.50	0.49	0.31	0.18	256.95	2.91	1.58	0.67	0.16	0.94	1.41	0.68	0.63	0.27	0.23	0.01	0.01	0.01	0.37	2.55	
1.52	0.25	0.42	0.31	0.34	0.29	0.24	0.26	0.26	0.29	0.33	0.52	0.52	0.51	0.33	0.19	282.07	1.93	1.04	0.50	0.10	0.76	1.16	0.51	0.44	0.17	0.15	0.00	0.00	0.00	0.26	2.20	
1.67	0.26	0.43	0.32	0.35	0.30	0.25	0.27	0.26	0.30	0.34	0.55	0.55	0.54	0.35	0.20	309.64	0.95	0.51	0.42	0.10	0.66	1.00	0.43	0.37	0.15	0.15	0.00	0.00	0.00	0.22	1.89	
1.83	0.27	0.45	0.33	0.37	0.31	0.26	0.28	0.28	0.32	0.35	0.59	0.58	0.58	0.37	0.21	339.92	0.31	0.17	0.40	0.15	0.61	0.90	0.42	0.35	0.18	0.20	0.00	0.00	0.00	0.24	1.60	
2.01	0.29	0.48	0.35	0.39	0.33	0.28	0.30	0.29	0.33	0.37	0.63	0.62	0.62	0.39	0.22	373.15	0.05	0.03	0.39	0.20	0.56	0.81	0.41	0.35	0.23	0.26	0.00	0.00	0.00	0.27	1.32	
2.21	0.31	0.51	0.37	0.41	0.35	0.30	0.32	0.31	0.35	0.40	0.68	0.67	0.67	0.42	0.24	409.63	0.00	0.00	0.37	0.22	0.50	0.71	0.39	0.32	0.24	0.28	0.00	0.00	0.00	0.27	1.05	
2.42	0.33	0.56	0.40	0.45	0.38	0.32	0.34	0.33	0.38	0.43	0.74	0.73	0.73	0.46	0.25	449.67	0.00	0.00	0.31	0.19	0.40	0.57	0.32	0.25	0.20	0.24	0.00	0.00	0.00	0.23	0.79	
2.66	0.36	0.61	0.43	0.49	0.42	0.34	0.37	0.36	0.41	0.46	0.80	0.80	0.80	0.50	0.27	493.63	0.00	0.00	0.23	0.13	0.28	0.41	0.23	0.15	0.13	0.17	0.00	0.00	0.00	0.17	0.55	
2.92	0.40	0.67	0.47	0.53	0.46	0.37	0.41	0.39	0.45	0.51	0.88	0.88	0.87	0.55	0.30	541.89	0.00	0.00	0.15	0.07	0.16	0.26	0.14	0.07	0.06	0.09	0.00	0.00	0.00	0.10	0.36	
3.21	0.44	0.75	0.52	0.59	0.50	0.41	0.45	0.43	0.50	0.52	0.96	0.96	0.96	0.60	0.32	594.87	0.00	0.00	0.09	0.04	0.08	0.16	0.07	0.02	0.03	0.04	0.00	0.00	0.00	0.05	0.22	
3.52	0.48	0.82	0.58	0.66	0.56	0.45	0.50	0.47	0.55	0.61	1.06	1.05	1.05	0.66	0.35	653.03	0.00	0.00	0.06	0.02	0.04	0.09	0.04	0.01	0.01	0.02	0.00	0.00	0.00	0.03	0.13	
3.86	0.53	0.91	0.64	0.73	0.61	0.49	0.55	0.52	0.61	0.67	1.16	1.14	1.15	0.72	0.38	716.87	0.00	0.00	0.05	0.02	0.03	0.06	0.02	0.00	0.01	0.02	0.00	0.00	0.00	0.02	0.08	
4.24	0.58	0.99	0.70	0.81	0.68	0.54	0.61	0.57	0.68	0.74	1.26	1.24	1.26	0.79	0.41	786.95	0.00	0.00	0.04	0.03	0.03	0.05	0.02	0.00	0.01	0.02	0.00	0.00	0.00	0.03	0.04	
4.66	0.63	1.08	0.77	0.90	0.75	0.59	0.67	0.62	0.75	0.81	1.37	1.35	1.37	0.86	0.45	863.88	0.00	0.00	0.03	0.03	0.03	0.05	0.02	0.00	0.01	0.02	0.00	0.00	0.00	0.03	0.02	
5.11	0.69	1.17	0.85	1.00	0.82	0.64	0.74	0.69	0.82	0.89	1.48	1.45	1.48	0.93	0.48	948.34	0.00	0.00	0.02	0.03	0.03	0.05	0.03	0.00	0.01	0.02	0.00	0.00	0.00	0.04	0.01	
5.61	0.74	1.26	0.93	1.10	0.90	0.70	0.82	0.75	0.91	0.97	1.59	1.56	1.60	1.02	0.52	1041.05	0.00	0.00	0.01	0.03	0.03	0.05	0.04	0.00	0.01	0.03	0.00	0.00	0.00	0.03	0.01	
6.16	0.80	1.35	1.02	1.22	0.99	0.76	0.89	0.82	1.00	1.05	1.71	1.67	1.71	1.10	0.56	1142.83	0.00	0.00	0.01	0.02	0.02	0.05	0.04	0.00	0.01	0.02	0.00	0.00	0.00	0.02	0.01	
6.76	0.86	1.44	1.11	1.34	1.08	0.82	0.98	0.89	1.09	1.14	1.83	1.78	1.83	1.19	0.60	1254.55	0.00	0.00	0.00	0.01	0.01	0.04	0.02	0.00	0.00	0.02	0.00	0.00	0.00	0.01	0.01	
7.42	0.92	1.53	1.20	1.47	1.18	0.89	1.07	0.97	1.19	1.24	1.95	1.90	1.96	1.28	0.65	1377.20	0.00	0.00	0.00	0.00	0.00	0.02	0.01	0.00	0.00	0.00	0.00	0.00	0.00	0.00	0.01	
8.15	0.98	1.63	1.31	1.61	1.28	0.96	1.17	1.06	1.30	1.34	2.08	2.02	2.09	1.38	0.69	1511.84	0.00	0.00	0.00	0.00	0.00	0.01	0.00	0.00	0.00	0.00	0.00	0.00	0.00	0.00	0.00	0.00
8.94	1.06	1.73	1.42	1.76	1.40	1.04	1.27	1.15	1.42	1.45	2.22	2.15	2.23	1.49	0.75	1659.64	0.00	0.00	0.00	0.00	0.00	0.00	0.00	0.00	0.00	0.00	0.00	0.00	0.00	0.00	0.00	0.00
9.82	1.13	1.83	1.55	1.93	1.52	1.13	1.39	1.25	1.55	1.57	2.36	2.29	2.37	1.61	0.80	1821.89	0.00	0.00	0.00	0.00	0.00	0.00	0.00	0.00	0.00	0.00	0.00	0.00	0.00	0.00	0.00	0.00
10.78	1.21	1.94	1.68	2.11	1.65	1.22	1.51	1.36	1.69	1.69	2.51	2.44	2.52	1.73	0.87	2000.00																
11.83	1.30	2.05	1.82	2.30	1.79	1.32	1.64	1.48	1.84	1.83	2.67	2.59	2.68	1.86	0.94																	
12.99	1.40	2.18	1.97	2.50	1.93	1.42	1.78	1.60	2.00	1.97	2.83	2.76	2.85	2.01	1.01	Very coarse sand	0.00	0.00	0.02	0.07	0.06	0.18	0.11	0.00	0.02	0.00	0.00	0.00	0.07	0.00	0.05	
14.26	1.50	2.31	2.13	2.70	2.08	1.53	1.92	1.73	2.16	2																						

	LC24-01	LC24-02	LC24-03	LC24-04	LC24-05	LC24-06	LC24-07	LC24-08			LC24-01	LC24-02	LC24-03	LC24-04	LC24-05	LC24-06	LC24-07	LC24-08
Channel Diameter (Lower) um	Diff. Volume %	Diff. Volume %	Diff. Volume %	Diff. Volume %	Diff. Volume %	Diff. Volume %	Diff. Volume %	Diff. Volume %		Channel Diameter (Lower) um	Diff. Volume %	Diff. Volume %	Diff. Volume %	Diff. Volume %	Diff. Volume %	Diff. Volume %	Diff. Volume %	Diff. Volume %
0.38	0.01	0.01	0.02	0.01	0.02	0.02	0.02	0.02		69.62	2.50	2.19	3.28	3.16	3.36	3.50	3.63	3.28
0.41	0.02	0.02	0.03	0.03	0.03	0.03	0.03	0.03		76.43	2.72	2.44	3.37	3.21	3.37	3.53	3.73	3.33
0.45	0.03	0.03	0.04	0.04	0.04	0.05	0.05	0.04		83.90	2.93	2.71	3.43	3.23	3.34	3.51	3.80	3.35
0.50	0.04	0.04	0.06	0.06	0.07	0.07	0.06	0.07		92.10	3.12	2.98	3.47	3.23	3.29	3.46	3.83	3.34
0.54	0.05	0.05	0.07	0.07	0.08	0.08	0.08	0.09		101.10	3.29	3.27	3.48	3.21	3.21	3.39	3.82	3.29
0.60	0.06	0.05	0.08	0.08	0.10	0.10	0.09	0.11		110.99	3.45	3.56	3.48	3.18	3.11	3.29	3.78	3.23
0.66	0.07	0.06	0.10	0.09	0.11	0.11	0.10	0.12		121.84	3.59	3.84	3.47	3.14	2.99	3.17	3.71	3.14
0.72	0.08	0.07	0.11	0.11	0.12	0.13	0.12	0.13		133.75	3.71	4.10	3.44	3.10	2.86	3.05	3.60	3.05
0.79	0.09	0.08	0.12	0.12	0.14	0.14	0.13	0.15		146.82	3.80	4.32	3.37	3.03	2.71	2.89	3.44	2.92
0.87	0.09	0.08	0.13	0.12	0.15	0.15	0.14	0.16		161.18	3.85	4.47	3.25	2.92	2.52	2.68	3.21	2.75
0.95	0.10	0.09	0.13	0.13	0.16	0.16	0.15	0.17		176.94	3.82	4.52	3.05	2.75	2.27	2.41	2.89	2.51
1.05	0.10	0.09	0.14	0.14	0.16	0.17	0.15	0.18		194.23	3.72	4.47	2.77	2.50	1.98	2.08	2.49	2.21
1.15	0.11	0.10	0.15	0.14	0.17	0.17	0.16	0.19		213.22	3.56	4.33	2.43	2.21	1.65	1.71	2.04	1.86
1.26	0.11	0.10	0.15	0.15	0.18	0.18	0.17	0.20		234.07	3.36	4.10	2.09	1.92	1.35	1.36	1.60	1.52
1.38	0.12	0.11	0.16	0.15	0.18	0.19	0.17	0.21		256.95	3.15	3.83	1.78	1.66	1.10	1.09	1.24	1.23
1.52	0.12	0.11	0.16	0.16	0.19	0.19	0.18	0.22		282.07	2.94	3.54	1.55	1.47	0.95	0.90	0.98	1.03
1.67	0.12	0.11	0.17	0.16	0.20	0.20	0.19	0.23		309.64	2.75	3.24	1.39	1.34	0.87	0.81	0.82	0.91
1.83	0.13	0.12	0.17	0.17	0.21	0.21	0.19	0.24		339.92	2.56	2.93	1.27	1.25	0.85	0.76	0.74	0.84
2.01	0.13	0.13	0.18	0.18	0.22	0.22	0.20	0.25		373.15	2.36	2.60	1.16	1.17	0.84	0.73	0.68	0.79
2.21	0.14	0.13	0.19	0.19	0.23	0.23	0.21	0.27		409.63	2.12	2.25	1.02	1.08	0.81	0.68	0.61	0.72
2.42	0.15	0.14	0.20	0.20	0.24	0.24	0.23	0.29		449.67	1.85	1.88	0.84	0.95	0.74	0.59	0.51	0.61
2.66	0.15	0.15	0.22	0.21	0.26	0.26	0.24	0.31		493.63	1.56	1.51	0.65	0.81	0.65	0.48	0.40	0.48
2.92	0.16	0.15	0.23	0.23	0.28	0.28	0.26	0.33		541.89	1.28	1.16	0.45	0.66	0.54	0.36	0.28	0.35
3.21	0.18	0.16	0.25	0.24	0.30	0.30	0.27	0.36		594.87	1.01	0.86	0.29	0.53	0.44	0.25	0.18	0.25
3.52	0.19	0.18	0.27	0.26	0.32	0.32	0.29	0.39		653.03	0.78	0.61	0.16	0.43	0.36	0.18	0.11	0.17
3.86	0.20	0.19	0.29	0.29	0.34	0.34	0.32	0.42		716.87	0.57	0.42	0.08	0.36	0.29	0.13	0.06	0.13
4.24	0.22	0.20	0.31	0.31	0.37	0.37	0.34	0.45		786.95	0.39	0.27	0.03	0.31	0.25	0.10	0.03	0.11
4.66	0.24	0.21	0.34	0.34	0.40	0.40	0.37	0.49		863.88	0.25	0.16	0.01	0.28	0.21	0.08	0.01	0.09
5.11	0.26	0.23	0.37	0.37	0.44	0.43	0.39	0.52		948.34	0.14	0.09	0.00	0.26	0.19	0.08	0.01	0.08
5.61	0.28	0.25	0.40	0.40	0.47	0.47	0.42	0.56		1041.05	0.06	0.05	0.00	0.25	0.18	0.08	0.01	0.07
6.16	0.30	0.26	0.43	0.43	0.51	0.51	0.46	0.61		1142.83	0.02	0.03	0.00	0.25	0.17	0.09	0.01	0.06
6.76	0.32	0.28	0.47	0.47	0.56	0.55	0.49	0.65		1254.55	0.00	0.01	0.00	0.24	0.16	0.10	0.01	0.04
7.42	0.35	0.30	0.51	0.52	0.61	0.60	0.53	0.70		1377.20	0.00	0.01	0.00	0.18	0.12	0.08	0.01	0.03
8.15	0.38	0.32	0.55	0.56	0.66	0.65	0.58	0.75		1511.84	0.00	0.01	0.00	0.10	0.07	0.05	0.01	0.01
8.94	0.41	0.34	0.60	0.62	0.72	0.71	0.63	0.81		1659.64	0.00	0.01	0.00	0.02	0.02	0.01	0.00	0.00
9.82	0.44	0.37	0.66	0.68	0.79	0.78	0.68	0.88		1821.89	0.00	0.01	0.00	0.00	0.00	0.00	0.00	0.00
10.78	0.48	0.39	0.72	0.74	0.87	0.86	0.75	0.95		2000.00								
11.83	0.53	0.42	0.79	0.82	0.96	0.94	0.82	1.03										
12.99	0.57	0.45	0.88	0.91	1.07	1.04	0.90	1.12		Very coarse sand	0.08	0.13	0.00	1.05	0.73	0.41	0.04	0.22
14.26	0.63	0.48	0.97	1.00	1.18	1.16	0.99	1.23		coarse sand	4.41	3.57	1.03	2.84	2.29	1.17	0.68	1.18
15.65	0.68	0.52	1.07	1.11	1.30	1.28	1.10	1.34		medium sand	19.30	21.76	9.67	9.73	6.81	6.04	5.98	6.61
17.18	0.74	0.55	1.17	1.22	1.43	1.41	1.20	1.44		fine sand	25.83	30.32	20.41	18.44	15.34	16.18	19.26	16.81
18.86	0.79	0.59	1.27	1.33	1.56	1.54	1.31	1.55		very fine sand	2.29	1.96	3.18	3.10	3.32	3.45	3.50	3.21
20.71	0.84	0.62	1.38	1.44	1.69	1.66	1.42	1.64		silt	23.74	18.74	37.95	38.74	44.34	44.37	40.06	43.85
22.73	0.90	0.66	1.49	1.55	1.81	1.79	1.53	1.74		clay	2.11	1.97	2.92	2.88	3.48	3.49	3.24	4.07
24.95	0.96	0.70	1.61	1.68	1.95	1.94	1.66	1.85		colloid	0.64	0.57	0.87	0.86	1.01	1.03	0.95	1.10
27.39	1.03	0.76	1.75	1.82	2.11	2.10	1.82	1.99		tot sum	78.40	79.01	76.03	77.63	77.33	76.14	73.71	77.05
30.07	1.11	0.82	1.92	1.99	2.29	2.29	2.00	2.15										
33.01	1.21	0.91	2.10	2.17	2.48	2.48	2.21	2.32										
36.24	1.33	1.01	2.29	2.35	2.67	2.68	2.42	2.50		After C. K. Wentworth classification:								
39.78	1.45	1.13	2.47	2.52	2.84	2.87	2.63	2.67										
43.67	1.58	1.25	2.64	2.67	2.99	3.03	2.84	2.81		Sand: 2mm-1/16mm	73.51	78.73	58.25	57.52	51.17	51.11	55.75	50.97
47.94	1.73	1.40	2.80	2.81	3.11	3.17	3.02	2.93		Silt: 1/16mm-1/256mm	23.74	18.74	37.95	38.74	44.34	44.37	40.06	43.85
52.63	1.90	1.56	2.94	2.92	3.20	3.29	3.20	3.04		Clay: <1/256mm	2.75	2.53	3.79	3.74	4.49	4.52	4.19	5.17
57.77	2.09	1.75	3.06	3.02	3.27	3.38	3.35	3.13		tot sum	100.00	100.00	100.00	100.00	100.00	100.00	100.00	100.00
63.42	2.29	1.96	3.18	3.10	3.32	3.45	3.50	3.21										

Appendix

	LC1-01+02	LC1-03	LC1-04	LC1-05	LC1-06	LC2-01	LC2-02	LC2-03	LC2-04	LC2-05	LC2-06	LC3-01	LC3-02	L1-USP1.1	L1-USP1.2	L1-USP2.1	L1-USP2.2	L1-USP3.1	L1-USP3.2
	1.15	1.56	1.50	1.33	1.38	1.77	3.15	8.20	4.45	3.97	3.42	4.64	2.82	3.16	9.40	2.58	3.16	2.13	2.27
	4.95	7.57	6.02	5.20	5.73	28.78	112.27	202.97	108.28	79.21	59.24	107.49	23.88	144.29	238.99	90.86	108.59	16.07	16.59
	561.06	45.36	29.41	33.20	41.23	598.26	585.14	556.30	476.96	370.82	278.29	440.18	362.09	639.63	642.89	511.47	527.67	306.55	368.08
	4.53	7.53	6.36	5.36	5.47	543.69	429.78	287.70	201.46	193.74	144.42	284.65	12.08	465.02	342.90	364.55	361.77	9.83	10.08
0.01	7.83	4.79	4.91	5.93	5.61	4.19	2.36	1.18	1.79	1.85	2.05	1.54	2.42	2.31	0.83	2.91	2.41	3.31	3.01
1.00	14.10	9.22	10.25	12.23	11.49	7.36	4.05	2.08	3.02	3.25	3.66	2.70	4.35	4.02	1.78	4.82	4.03	6.00	5.59
2.00	11.64	8.44	9.98	11.47	10.69	5.84	3.18	1.64	2.41	2.68	3.11	2.33	3.89	3.22	1.50	3.70	3.12	5.28	5.00
3.00	9.32	7.50	9.25	10.13	9.34	4.65	2.55	1.34	1.99	2.28	2.69	2.14	3.65	2.63	1.28	2.88	2.47	4.73	4.57
4.00	7.46	6.61	8.28	8.65	7.94	3.78	2.10	1.12	1.70	1.98	2.37	1.98	3.44	2.20	1.11	2.32	2.02	4.26	4.20
5.00	6.00	5.79	7.22	7.23	6.64	3.12	1.76	0.96	1.48	1.76	2.11	1.84	3.20	1.87	0.97	1.92	1.70	3.82	3.82
6.00	4.85	5.06	6.20	5.96	5.52	2.60	1.51	0.83	1.32	1.57	1.90	1.69	2.96	1.60	0.85	1.62	1.45	3.42	3.46
7.00	3.95	4.43	5.27	4.88	4.58	2.19	1.31	0.72	1.18	1.42	1.72	1.55	2.72	1.39	0.75	1.39	1.27	3.07	3.12
8.00	3.25	3.88	4.46	3.99	3.81	1.87	1.16	0.64	1.08	1.30	1.58	1.42	2.50	1.22	0.67	1.21	1.12	2.75	2.81
9.00	2.69	3.42	3.77	3.27	3.19	1.61	1.03	0.58	0.99	1.20	1.45	1.30	2.29	1.07	0.60	1.08	1.01	2.48	2.54
10.00	12.26	19.22	16.88	13.33	14.82	8.94	6.80	3.85	7.17	8.77	10.34	8.75	15.07	6.41	3.92	6.94	6.83	15.53	15.85
20.00	3.27	7.28	3.63	2.58	4.34	4.28	4.06	2.33	4.64	5.68	6.20	4.93	7.61	3.05	2.18	4.11	4.27	7.67	7.46
30.00	1.09	3.30	1.00	0.78	1.88	2.93	3.06	1.76	3.50	4.24	4.35	3.51	4.70	2.01	1.57	3.13	3.27	4.78	4.37
40.00	0.39	4.21	0.97	1.07	3.20	14.61	20.29	20.23	26.39	27.76	30.13	21.22	18.29	17.80	16.66	21.89	21.34	17.48	14.82
150.00	11.90	6.82	7.93	8.48	6.95	32.03	44.79	60.74	41.35	34.25	26.35	43.11	22.89	49.20	65.32	40.09	43.67	15.42	19.37
2000.00																			
After C. K. Wentworth classification:																			
Sand: 2mm-1/16mm	11.90	6.82	7.93	8.48	6.95	32.03	44.79	60.74	41.35	34.25	26.35	43.11	22.89	49.20	65.32	40.09	43.67	15.42	19.37
Silt: 1/16mm-1/256mm	54.53	70.73	66.93	61.88	65.27	50.57	45.62	34.35	51.43	57.97	64.83	50.32	66.44	41.25	30.57	48.48	46.76	69.99	67.03
Clay: <1/256mm	33.57	22.45	25.14	29.63	27.78	17.40	9.59	4.90	7.22	7.78	8.82	6.57	10.67	9.55	4.11	11.43	9.56	14.58	13.60
tot sum	100.00	100.00	100.00	100.00	100.00	100.00	100.00	100.00	100.00	100.00	100.00	100.00	100.00	100.00	100.00	100.00	100.00	100.00	100.00

	L1-SOP1.1	L1-SOP1.2	L1-SOP2.1	L1-SOP2.2	L1-SOP3.1	L1-SOP3.2	L13-USP1.1	L13-USP1.2	L13-USP2.1	L13-USP2.2	L13-USP3.1	L13-USP3.2	L13-SOP1.1	L13-SOP1.2	L13-SOP2.1	L13-SOP2.2	L13-SOP3.1	L13-SOP3.2	
Channel Diameter (Lower)																			
um	3.65	3.02	2.86	3.36	8.62	8.99	2.40	2.88	2.34	2.29	2.30	2.22	3.11	4.08	2.98	3.35	4.51	5.15	
	113.08	47.86	42.20	95.64	223.06	237.19	40.42	74.69	28.03	27.14	16.98	15.34	62.36	60.30	51.98	86.02	70.98	78.56	
	719.49	400.46	497.78	613.84	651.71	701.84	467.03	507.49	319.20	306.32	261.90	327.09	540.67	462.60	498.77	613.04	477.61	435.58	
	487.08	194.46	465.61	450.44	400.80	416.84	467.17	389.34	47.74	26.79	14.83	12.01	432.08	85.21	80.82	454.30	360.52	110.01	
0.01	1.95	2.22	2.69	2.35	0.92	0.83	2.90	2.45	2.95	3.00	2.86	3.00	2.28	1.80	2.36	2.13	1.66	1.56	
1.00	3.57	4.20	4.29	3.72	1.82	1.79	5.29	4.42	5.44	5.57	5.56	5.78	4.11	3.19	4.26	3.84	2.89	2.64	
2.00	2.89	3.51	3.46	2.98	1.53	1.50	4.23	3.51	4.46	4.56	5.06	5.36	3.28	2.61	3.45	3.10	2.38	2.12	
3.00	2.39	2.96	2.96	2.52	1.30	1.29	3.45	2.85	3.70	3.78	4.55	4.86	2.70	2.24	2.85	2.53	2.08	1.82	
4.00	2.04	2.56	2.66	2.22	1.13	1.13	2.90	2.38	3.16	3.23	4.08	4.38	2.32	1.98	2.42	2.14	1.88	1.62	
5.00	1.78	2.25	2.44	1.99	1.01	1.00	2.49	2.04	2.75	2.80	3.66	3.92	2.03	1.78	2.10	1.84	1.71	1.47	
6.00	1.58	2.01	2.24	1.80	0.93	0.90	2.18	1.78	2.43	2.47	3.29	3.51	1.81	1.63	1.85	1.62	1.57	1.35	
7.00	1.42	1.81	2.07	1.63	0.86	0.82	1.93	1.57	2.17	2.20	2.97	3.16	1.63	1.50	1.65	1.44	1.46	1.24	
8.00	1.28	1.65	1.91	1.49	0.80	0.75	1.72	1.40	1.96	1.99	2.70	2.85	1.49	1.39	1.50	1.30	1.36	1.16	
9.00	1.18	1.51	1.76	1.36	0.76	0.69	1.56	1.26	1.79	1.81	2.46	2.59	1.37	1.31	1.37	1.18	1.27	1.09	
10.00	8.24	10.74	11.97	9.06	5.97	5.10	10.54	8.51	12.64	12.71	16.74	16.94	9.78	10.14	9.97	8.37	9.65	8.46	
20.00	5.00	6.72	6.50	4.88	4.01	3.29	6.22	5.04	7.90	7.82	9.19	8.65	6.01	7.07	6.55	5.25	6.43	6.10	
30.00	3.55	4.84	4.27	3.24	2.91	2.43	4.44	3.64	5.67	5.53	5.73	5.06	4.29	5.36	4.93	3.84	4.85	4.95	
40.00	16.77	23.93	20.07	17.51	16.82	16.93	22.12	22.44	24.13	23.81	16.88	13.66	21.91	26.32	24.78	20.68	26.58	30.75	
150.00	46.37	29.10	30.71	43.24	59.24	61.55	28.04	36.71	18.86	18.72	14.26	16.30	34.98	31.68	29.96	40.75	34.22	33.67	
2000.00																			
After C. K. Wentworth classification:																			
Sand: 2mm-1/16mm	46.37	29.10	30.71	43.24	59.24	61.55	28.04	36.71	18.86	18.72	14.26	16.30	34.98	31.68	29.96	40.75	34.22	33.67	
Silt: 1/16mm-1/256mm	45.22	60.97	58.85	47.71	36.49	34.33	59.54	52.90	68.30	68.15	72.26	69.56	55.35	60.71	59.97	50.19	58.84	60.01	
Clay: <1/256mm	8.41	9.93	10.44	9.06	4.27	4.12	12.42	10.39	12.84	13.13	13.49	14.14	9.67	7.60	10.08	9.06	6.93	6.32	
tot sum	100.00	100.00	100.00	100.00	100.00	100.00	100.00	100.00	100.00	100.00	100.00	100.00	100.00	100.00	100.00	100.00	100.00	100.00	100.00

8.7.4. Major elements data

sample	SiO2	TiO2	Al2O3	Fe2O3	MnO	MgO	CaO	Na2O	K2O	P2O5	LOI	Cr2O3	NiO	not_meas	new_sum	in % wt	LOI at 1050°C
LC1-01-02	53.20	0.56	21.82	5.97	0.10	2.82	0.53	1.44	6.12	0.17	7.11	0.01	0.00	0.14	100.00		
LC1-03	54.53	0.77	21.03	6.41	0.16	2.92	0.63	1.68	5.66	0.23	5.92	0.01	0.01	0.05	100.00		
LC1-04	57.37	0.74	20.35	5.75	0.17	2.44	0.72	2.11	5.68	0.24	4.31	0.01	0.00	0.10	100.00		
LC1-05	56.95	0.68	20.66	5.77	0.23	2.46	0.67	2.14	5.70	0.23	4.33	0.01	0.00	0.17	100.00		
LC1-06	55.47	0.69	20.50	6.82	0.17	2.48	0.71	2.05	5.65	0.30	4.93	0.01	0.00	0.22	100.00		
LC1-07	56.57	0.60	20.38	5.91	0.10	2.14	0.67	2.08	5.70	0.31	5.23	0.01	0.00	0.28	100.00		
LC2-01	64.47	0.44	15.52	4.40	0.08	1.75	0.69	2.07	4.18	0.23	6.05	0.01	0.00	0.12	100.00		
LC2-02	71.31	0.34	13.75	3.24	0.05	1.29	0.66	2.41	3.74	0.18	2.87	0.01	0.00	0.14	100.00		
LC2-03	73.67	0.29	13.09	2.72	0.04	1.11	0.67	2.56	3.56	0.18	1.95	0.00	0.00	0.16	100.00		
LC2-04	70.00	0.40	14.46	3.50	0.06	1.46	0.68	2.40	3.89	0.19	2.87	0.01	0.00	0.06	100.00		
LC2-05	66.20	0.53	15.90	4.40	0.08	1.83	0.77	2.23	4.13	0.25	3.54	0.01	0.00	0.13	100.00		
LC2-06	64.91	0.56	16.52	4.38	0.07	1.92	0.77	2.18	4.22	0.26	4.02	0.01	0.00	0.20	100.00		
LC2-07	64.87	0.56	16.32	4.40	0.07	1.90	0.80	2.20	4.22	0.27	3.58	0.01	0.00	0.81	100.00		
LC2-08	63.76	0.60	16.91	4.71	0.08	2.07	0.80	2.13	4.43	0.27	3.81	0.01	0.00	0.42	100.00		
LC2-09	62.25	0.65	17.34	5.14	0.09	2.32	0.80	2.01	4.35	0.27	4.23	0.01	0.00	0.55	100.00		
LC2-10	64.41	0.59	16.69	4.74	0.08	2.08	0.82	2.15	4.19	0.26	3.79	0.01	0.00	0.21	100.00		
LC2-11	63.20	0.62	16.93	4.93	0.08	2.19	0.80	2.06	4.28	0.28	4.10	0.01	0.00	0.53	100.00		
LC2-12	65.35	0.55	16.21	4.45	0.07	1.98	0.82	2.20	4.13	0.28	3.52	0.01	0.00	0.44	100.00		
LC2-13	69.54	0.42	14.79	3.37	0.05	1.46	0.80	2.45	3.94	0.26	2.55	0.00	0.00	0.37	100.00		
LC2-14	64.05	0.60	16.83	4.65	0.07	2.11	0.80	2.13	4.36	0.28	3.76	0.01	0.00	0.37	100.00		
LC2-15	62.95	0.64	17.33	5.02	0.07	2.35	0.74	1.99	4.35	0.24	4.12	0.01	0.00	0.19	100.00		
LC2-16	65.18	0.57	16.38	4.43	0.06	1.96	0.78	2.13	4.16	0.26	3.74	0.01	0.00	0.35	100.00		
LC2-17	60.40	0.68	18.08	5.29	0.08	2.27	0.77	1.94	4.54	0.29	4.95	0.01	0.00	0.69	100.00		
LC2-18	62.23	0.63	17.65	4.63	0.07	1.94	0.72	2.19	4.72	0.29	4.26	0.01	0.00	0.66	100.00		
LC2-19	63.79	0.61	17.12	4.30	0.06	1.74	0.78	2.36	4.73	0.30	3.40	0.01	0.00	0.80	100.00		
LC2-20	63.49	0.62	17.50	4.59	0.06	1.86	0.78	2.41	4.75	0.27	3.42	0.01	0.00	0.24	100.00		
LC3-01	72.65	0.26	13.78	2.27	0.05	0.83	0.58	2.61	4.25	0.22	2.27	0.00	0.00	0.22	100.00		
LC3-02	71.01	0.30	14.61	2.43	0.04	0.94	0.59	2.65	4.53	0.23	2.54	0.00	0.00	0.13	100.00		
LC3-03	71.56	0.27	14.27	2.40	0.04	0.90	0.59	2.61	4.44	0.22	2.43	0.00	0.00	0.27	100.00		
LC3-04	75.74	0.16	12.61	1.60	0.03	0.60	0.51	2.79	4.19	0.18	1.46	0.00	0.00	0.15	100.00		
LC3-05	75.43	0.16	12.70	1.69	0.03	0.61	0.52	2.74	4.19	0.20	1.55	0.00	0.00	0.20	100.00		
LC3-06	75.61	0.16	12.60	1.67	0.03	0.60	0.50	2.65	4.08	0.18	1.54	0.00	0.00	0.38	100.00		
LC3-07	75.98	0.13	12.36	1.49	0.03	0.54	0.52	2.75	4.11	0.18	1.32	0.00	0.00	0.58	100.00		
LC3-08	76.24	0.15	12.54	1.58	0.03	0.56	0.51	2.74	4.11	0.20	1.34	0.00	0.00	0.00	100.00		
LC3-10	76.48	0.14	12.13	1.51	0.03	0.54	0.47	2.71	4.00	0.17	1.30	0.00	0.00	0.52	100.00		
LC12-01	66.25	0.45	15.83	3.99	0.07	1.34	0.53	2.38	3.88	0.21	5.02	0.01	0.00	0.05	100.00		
LC12-02	64.82	0.47	16.65	4.25	0.08	1.39	0.58	2.46	3.96	0.26	5.12	0.01	0.00	-0.04	100.00		
LC12-03	63.30	0.51	17.33	4.36	0.07	1.43	0.59	2.44	4.02	0.28	5.61	0.01	0.00	0.05	100.00		
LC12-04	63.54	0.50	17.27	4.41	0.06	1.44	0.57	2.40	4.04	0.26	5.51	0.01	0.00	-0.01	100.00		
LC12-05	62.76	0.52	17.52	4.52	0.06	1.47	0.57	2.40	4.04	0.27	5.78	0.01	0.00	0.07	100.00		
LC12-06	63.34	0.50	17.32	4.46	0.06	1.46	0.58	2.41	4.04	0.27	5.60	0.01	0.00	-0.04	100.00		
LC13-01	54.70	0.65	19.30	5.28	0.04	2.24	0.36	1.36	4.59	0.28	11.09	0.01	0.01	0.07	100.00		
LC13-02	54.00	0.64	19.18	5.26	0.04	2.25	0.34	1.32	4.46	0.28	11.34	0.01	0.00	0.88	100.00		
LC13-03	54.25	0.65	19.08	5.36	0.04	2.21	0.35	1.33	4.45	0.30	11.82	0.01	0.01	0.15	100.00		
LC13-04	53.89	0.68	19.63	5.50	0.04	2.38	0.37	1.34	4.65	0.28	10.58	0.01	0.01	0.66	100.00		
LC13-05	54.39	0.74	20.24	5.66	0.04	2.48	0.40	1.42	4.81	0.27	9.40	0.01	0.01	0.13	100.00		
LC13-06	57.17	0.59	19.29	4.95	0.05	1.85	0.38	1.71	4.64	0.27	8.34	0.01	0.00	0.75	100.00		
LC13-07	57.94	0.56	19.00	4.82	0.05	1.76	0.38	1.71	4.65	0.29	8.49	0.01	0.00	0.35	100.00		
LC13-08	57.54	0.61	18.82	4.98	0.05	1.95	0.37	1.52	4.47	0.28	9.22	0.01	0.00	0.17	100.00		
LC13-09	54.83	0.68	19.09	5.27	0.04	2.29	0.34	1.18	4.36	0.29	11.55	0.01	0.00	0.07	100.00		
LC13-10	54.97	0.63	18.86	4.97	0.04	2.16	0.34	1.26	4.40	0.29	11.63	0.01	0.00	0.44	100.00		
LC13-11	55.36	0.61	18.96	4.94	0.04	2.13	0.35	1.31	4.44	0.28	11.24	0.01	0.00	0.32	100.00		
LC13-12	54.31	0.65	18.79	5.07	0.04	2.26	0.33	1.12	4.24	0.28	12.44	0.01	0.00	0.45	100.00		
LC13-13	53.65	0.64	18.45	5.06	0.04	2.26	0.32	1.05	4.11	0.30	13.59	0.01	0.00	0.51	100.00		
LC18-01	69.28	0.31	15.80	2.55	0.04	1.74	0.55	2.47	4.54	0.28	2.48	0.00	0.00	-0.04	100.00		
LC18-02	70.09	0.26	15.32	2.36	0.04	1.62	0.45	2.52	4.43	0.21	2.34	0.00	0.00	0.34	100.00		
LC18-03	65.61	0.36	17.28	3.02	0.05	2.12	0.51	2.25	4.94	0.25	3.15	0.00	0.00	0.45	100.00		
LC18-04	67.40	0.32	16.66	2.82	0.04	1.97	0.52	2.38	4.77	0.25	2.82	0.00	0.00	0.04	100.00		
LC18-05	67.70	0.30	16.62	2.73	0.05	2.01	0.48	2.39	4.78	0.22	2.69	0.00	0.00	0.02	100.00		
LC18-06	62.39	0.41	19.15	3.51	0.07	2.62	0.51	1.96	5.56	0.23	3.69	0.00	0.00	-0.08	100.00		
LC18-07	58.22	0.53	20.71	4.24	0.07	2.94	0.58	1.67	5.89	0.28	4.73	0.00	0.00	0.14	100.00		
LC18-08	59.22	0.50	20.26	4.14	0.07	2.85	0.59	1.74	5.74	0.30	4.53	0.00	0.00	0.07	100.00		
LC19-01	68.50	0.42	15.21	3.48	0.05	1.99	0.67	2.25	3.97	0.19	3.02	0.00	0.00	0.25	100.00		
LC19-02	69.80	0.41	14.85	3.40	0.05	1.94	0.65	2.29	3.84	0.19	2.59	0.00	0.00	-0.01	100.00		
LC19-03	63.63	0.52	17.48	4.30	0.07	2.49	0.62	1.93	4.68	0.21	4.00	0.01	0.00	0.06	100.00		
LC19-04	60.77	0.63	18.56	5.03	0.07	2.77	0.70	1.77	4.90	0.24	4.63	0.01	0.00	-0.07	100.00		
LC19-05	56.21	0.73	20.20	5.81	0.07	3.09	0.69	1.51	5.32	0.25	6.05	0.01	0.00	0.06	100.00		
LC19-06	58.94	0.66	19.30	5.26	0.07	2.98	0.72	1.70	5.22	0.26	4.63	0.01	0.00	0.25	100.00		
LC19-07	61.78	0.59	18.48	4.68	0.06	2.82	0.70	1.88	5.11	0.24	3.68	0.01	0.00	-0.03	100.00		

Appendix

sample	SiO2	TiO2	Al2O3	Fe2O3	MnO	MgO	CaO	Na2O	K2O	P2O5	LOI	Cr2O3	NiO	not_measured	new_sum	in % wt	LOI at 1050
LC20-01	61.25	0.67	17.66	5.42	0.11	2.64	0.87	2.09	4.08	0.25	4.95	0.01	0.01	-0.02	100.00		
LC20-02	60.35	0.69	18.18	5.57	0.19	2.74	0.80	1.98	4.40	0.24	4.89	0.01	0.00	-0.04	100.00		
LC20-03	66.72	0.53	15.63	4.38	0.10	2.08	0.73	2.29	3.81	0.24	3.31	0.01	0.00	0.17	100.00		
LC20-04	64.25	0.62	16.65	4.93	0.07	2.42	0.74	2.12	3.94	0.23	4.01	0.01	0.00	0.01	100.00		
LC20-05	59.12	0.75	18.41	6.08	0.08	2.95	0.80	1.87	4.11	0.23	5.42	0.01	0.01	0.15	100.00		
LC20-06	58.77	0.73	18.82	5.97	0.09	2.97	0.77	1.88	4.42	0.24	5.29	0.01	0.01	0.05	100.00		
LC20-07	63.46	0.62	17.17	5.10	0.07	2.51	0.74	2.14	3.99	0.21	4.02	0.01	0.00	-0.05	100.00		
LC20-08	60.22	0.70	18.42	5.66	0.08	2.84	0.77	1.98	4.37	0.24	4.80	0.01	0.00	-0.09	100.00		
LC20-09	56.01	0.79	20.00	6.52	0.09	3.22	0.77	1.76	4.87	0.25	5.69	0.01	0.01	0.00	100.00		
LC20-10	57.17	0.76	19.99	5.90	0.08	2.92	0.70	1.87	5.03	0.26	5.17	0.01	0.01	0.13	100.00		
LC20-11	57.35	0.75	20.07	5.79	0.08	2.91	0.67	1.85	5.17	0.27	5.18	0.01	0.00	-0.09	100.00		
LC20-12	59.31	0.69	19.02	5.57	0.08	2.83	0.74	1.96	4.71	0.27	4.83	0.01	0.00	-0.02	100.00		
LC20-13	58.97	0.69	19.23	5.49	0.08	2.83	0.70	1.93	4.85	0.26	4.80	0.01	0.00	0.17	100.00		
LC20-14	58.47	0.69	19.64	5.42	0.07	2.84	0.68	1.90	5.01	0.27	4.93	0.01	0.00	0.07	100.00		
LC20-15	57.45	0.75	19.50	6.08	0.08	3.06	0.77	1.84	4.73	0.27	5.37	0.01	0.01	0.07	100.00		
LC21-01	62.42	0.66	17.29	4.82	0.07	2.31	0.59	1.67	4.40	0.24	5.27	0.01	0.00	0.25	100.00		
LC21-02	63.79	0.69	17.13	4.73	0.06	2.32	0.67	1.77	4.36	0.30	4.26	0.01	0.00	-0.07	100.00		
LC21-03	62.15	0.66	17.68	5.02	0.06	2.36	0.55	1.68	4.45	0.23	5.21	0.01	0.00	-0.05	100.00		
LC21-04	57.35	0.75	18.90	5.61	0.06	2.63	0.54	1.41	4.64	0.24	7.68	0.01	0.01	0.16	100.00		
LC21-05	58.55	0.74	18.71	5.69	0.10	2.59	0.54	1.50	4.63	0.24	6.66	0.01	0.01	0.01	100.00		
LC21-06	55.69	0.79	19.69	6.20	0.10	2.82	0.53	1.39	4.86	0.25	7.45	0.01	0.01	0.22	100.00		
LC21-07	58.23	0.77	18.93	5.83	0.08	2.66	0.56	1.52	4.69	0.25	6.46	0.01	0.00	0.01	100.00		
LC21-08	59.56	0.75	18.40	5.37	0.06	2.56	0.57	1.59	4.55	0.25	5.89	0.01	0.00	0.42	100.00		
LC21-09	59.90	0.75	18.44	5.41	0.06	2.58	0.58	1.65	4.56	0.25	5.66	0.01	0.00	0.15	100.00		
LC21-10	60.58	0.74	18.26	5.29	0.06	2.52	0.58	1.62	4.55	0.26	5.37	0.01	0.00	0.17	100.00		
LC21-11	60.17	0.75	18.27	5.41	0.07	2.54	0.56	1.61	4.51	0.25	5.59	0.01	0.00	0.28	100.00		
LC21-12	60.46	0.72	18.13	5.24	0.06	2.45	0.55	1.62	4.53	0.26	5.50	0.01	0.00	0.48	100.00		
LC21-13	60.46	0.75	18.31	5.35	0.06	2.53	0.55	1.61	4.56	0.25	5.36	0.01	0.00	0.22	100.00		
LC21-14	59.99	0.76	18.27	5.40	0.07	2.54	0.55	1.59	4.54	0.25	5.57	0.01	0.00	0.47	100.00		
LC21-15	61.16	0.74	18.11	5.22	0.06	2.48	0.56	1.64	4.54	0.26	5.22	0.01	0.00	0.00	100.00		
LC22-01	55.39	0.96	18.75	8.02	0.11	3.47	1.24	1.66	4.18	0.24	5.77	0.02	0.01	0.18	100.00		
LC22-02	51.17	1.08	19.94	9.42	0.12	3.92	1.24	1.41	4.45	0.25	6.67	0.02	0.01	0.30	100.00		
LC22-03	51.45	1.07	19.97	9.15	0.16	3.94	1.25	1.43	4.52	0.25	6.20	0.02	0.01	0.58	100.00		
LC22-04	49.85	1.12	20.39	9.82	0.14	4.18	1.25	1.36	4.60	0.26	6.57	0.02	0.01	0.43	100.00		
LC22-05	51.95	1.07	19.69	8.94	0.13	3.92	1.19	1.44	4.42	0.24	6.29	0.02	0.01	0.69	100.00		
LC22-06	53.43	1.05	19.52	8.46	0.11	3.84	1.18	1.52	4.47	0.24	5.82	0.02	0.01	0.34	100.00		
LC22-07	51.34	1.07	19.99	8.98	0.11	4.03	1.16	1.41	4.58	0.24	6.42	0.02	0.01	0.63	100.00		
LC22-08	52.38	1.03	19.76	8.65	0.10	3.81	1.17	1.48	4.57	0.26	6.01	0.02	0.01	0.73	100.00		
LC22-09	50.93	1.07	20.09	9.29	0.11	4.00	1.18	1.42	4.63	0.25	6.05	0.02	0.01	0.94	100.00		
LC22-10	51.16	1.09	20.18	9.07	0.10	4.06	1.17	1.40	4.66	0.26	6.32	0.02	0.01	0.49	100.00		
LC23-01	55.06	0.62	20.90	5.05	0.07	3.17	0.60	1.51	5.72	0.22	6.42	0.00	0.00	0.67	100.00		
LC23-02	55.17	0.64	21.07	5.09	0.07	3.18	0.59	1.51	5.76	0.22	6.34	0.01	0.00	0.34	100.00		
LC23-03	54.67	0.64	21.06	5.10	0.07	3.23	0.59	1.48	5.79	0.22	6.29	0.01	0.00	0.86	100.00		
LC23-04	56.69	0.62	20.94	4.58	0.05	3.17	0.62	1.61	5.84	0.26	5.48	0.00	0.00	0.13	100.00		
LC23-05	59.95	0.51	19.57	3.91	0.05	2.88	0.62	1.84	5.56	0.29	4.36	0.00	0.00	0.48	100.00		
LC24-01	65.80	0.41	17.29	2.93	0.05	2.11	0.44	1.26	5.56	0.20	3.36	0.00	0.00	0.60	100.00		
LC24-02	64.99	0.40	18.06	3.04	0.05	2.18	0.40	1.20	5.77	0.16	3.69	0.00	0.00	0.05	100.00		
LC24-03	60.73	0.50	19.68	3.56	0.06	2.49	0.40	1.07	6.17	0.17	4.38	0.00	0.00	0.80	100.00		
LC24-04	63.52	0.46	18.53	3.31	0.06	2.32	0.44	1.18	5.86	0.18	3.86	0.00	0.00	0.27	100.00		
LC24-05	64.20	0.45	18.10	3.36	0.06	2.23	0.48	1.24	5.74	0.21	3.63	0.00	0.00	0.30	100.00		
LC24-06	63.43	0.47	18.37	3.43	0.06	2.23	0.47	1.21	5.81	0.22	3.68	0.00	0.00	0.61	100.00		
LC24-07	62.78	0.47	18.64	3.54	0.07	2.36	0.53	1.19	5.82	0.24	3.96	0.00	0.00	0.40	100.00		
LC24-08	62.66	0.47	18.39	3.61	0.06	2.40	0.53	1.22	5.68	0.23	4.09	0.00	0.00	0.68	100.00		
L1-USP1.1	73.59	0.19	12.57	1.86	0.03	0.66	0.50	2.76	3.88	0.16	3.44	0.00	0.00	0.35	100.00		
L1-USP1.2	74.41	0.21	12.81	2.03	0.04	0.70	0.52	2.66	3.72	0.18	2.28	0.00	0.00	0.44	100.00		
L1-USP2.1	69.33	0.39	14.55	3.59	0.06	1.47	0.71	2.36	3.91	0.19	3.32	0.01	0.00	0.10	100.00		
L1-USP2.2	71.34	0.33	13.57	3.19	0.06	1.24	0.70	2.44	3.66	0.19	2.58	0.01	0.00	0.67	100.00		
L1-USP3.1	66.89	0.36	16.44	3.11	0.05	1.22	0.60	2.49	4.94	0.23	3.51	0.00	0.00	0.16	100.00		
L1-USP3.2	67.41	0.38	16.10	3.12	0.05	1.22	0.59	2.48	4.84	0.22	3.30	0.00	0.00	0.28	100.00		
L1-SOP1.1	63.66	0.31	12.96	2.43	0.03	0.85	0.49	2.20	3.49	0.26	12.51	0.01	0.00	0.79	100.00		
L1-SOP1.2	60.77	0.38	14.64	3.09	0.03	1.04	0.48	2.10	3.70	0.31	13.27	0.01	0.00	0.18	100.00		
L1-SOP2.1	63.35	0.44	14.35	3.85	0.05	1.69	0.87	2.00	3.59	0.25	9.05	0.01	0.00	0.52	100.00		
L1-SOP2.2	69.32	0.36	13.51	3.19	0.04	1.35	0.77	2.36	3.56	0.21	5.04	0.01	0.00	0.28	100.00		
L1-SOP3.1	74.36	0.14	10.69	1.19	0.01	0.50	0.41	2.58	3.18	0.10	6.08	0.00	0.00	0.76	100.00		
L1-SOP3.2	74.13	0.15	10.82	1.23	0.01	0.51	0.41	2.62	3.18	0.11	6.46	0.00	0.00	0.39	100.00		
L13-USP1.1	67.86	0.32	14.69	2.94	0.04	0.94	0.41	2.24	4.19	0.23	5.76	0.01	0.00	0.38	100.00		
L13-USP1.2	70.49	0.26	13.93	2.51	0.04	0.74	0.36	2.38	4.32	0.20	4.45	0.01	0.00	0.32	100.00		
L13-USP2.1	60.80	0.54	17.16	4.29	0.06	1.63	0.42	1.72	4.35	0.26	8.60	0.01	0.00	0.17	100.00		
L13-USP2.2	60.52	0.55	17.22	4.32	0.06	1.63	0.42	1.69	4.45	0.26	8.86	0.01	0.00	0.01	100.00		
L13-USP3.1	61.56	0.51	17.72	4.57	0.09	1.70	0.39	1.90	4.67	0.25	6.50	0.01	0.00	0.12	100.00		
L13-USP3.2	61.44	0.52	17.72	4.69	0.11	1.80	0.40	1.87	4.70	0.25	6.38	0.01	0.01	0.09	100.00		
L13-SOP1.1	70.40	0.20	12.63	1.96	0.02	0.59	0.33	2.28	3.87	0.23	7.35	0.01	0.00	0.12	100.00		
L13-SOP1.2	71.67	0.20	13.60	2.06	0.02	0.52	0.31	2.40	4.20	0.22	4.20	0.01	0.00	0.59	100.00		
L13-SOP2.1	69.97	0.30	14.34	2.57	0.03	0.90	0.36	2.28	4.37	0.20	4.53	0.01	0.00	0.14	100.00		
L13-SOP2.2	73.17	0.21	13.14	2.06	0.03</												

8.7.1. Organic matter data

Sample	D13C_VPDB	Nitrogen [% wt]	Hydrogen [% wt]	TOC [% wt]	C_N	HI [mg HC/g TOC]	OI [mg CO2/g TOC]	PC [%]	RC [%]	MINC [%]	Tmax [°C]	S1 [mg HC/g]	S2a [mg HC/g]	S2b [mg HC/g]	S3
LC1-01-02	-18.70	0.040	0.801	0.81	20.33	220	323	0.22	0.59	0.10	417	0.02	1.79	0.00	2.62
LC1-03	-23.43	0.010	0.666	0.48	47.64	140	398	0.11	0.37	0.17	425	0.01	0.67	0.00	1.90
LC1-04	-26.07	0.010	0.504	0.18	18.23	122	779	0.06	0.12	0.13	424	0.01	0.22	0.00	1.42
LC1-05	-26.23	0.010	0.514	0.17	17.21	123	904	0.06	0.11	0.11	429	0.01	0.21	0.00	1.56
LC1-06	-25.88	0.010	0.576	0.27	27.21	114	646	0.07	0.20	0.14	430	0.01	0.31	0.00	1.76
LC1-07	-24.86	0.132	0.647	0.51	3.88	163	246	0.10	0.41	0.12	423	0.01	0.84	0.00	1.26
LC2-01	-18.73	0.097	0.604	1.15	11.86	244	233	0.31	0.84	0.16	410	0.02	2.81	0.00	2.68
LC2-02	-21.99	0.010	0.298	0.30	29.62	169	413	0.08	0.22	0.11	417	0.01	0.50	0.00	1.22
LC2-03	-26.97	0.010	0.209	0.08	8.31	160	686	0.03	0.06	0.13	411	0.01	0.13	0.00	0.57
LC2-04	-23.60	0.010	0.306	0.21	20.74	177	308	0.05	0.16	0.14	410	0.01	0.37	0.00	0.64
LC2-05	-25.02	0.010	0.381	0.26	25.76	125	341	0.05	0.21	0.15	424	0.01	0.32	0.00	0.88
LC2-06	-25.20	0.010	0.380	0.26	26.41	147	272	0.05	0.21	0.14	424	0.01	0.39	0.00	0.72
LC2-07	-25.33	0.095	0.428	0.26	2.71	134	267	0.05	0.21	0.15	429	0.01	0.34	0.00	0.68
LC2-08	-25.46	0.073	0.459	0.27	3.67	132	254	0.05	0.22	0.16	429	0.01	0.35	0.00	0.68
LC2-09	-25.40	0.062	0.488	0.31	5.07	135	247	0.06	0.26	0.17	429	0.00	0.43	0.00	0.78
LC2-10	-26.29	0.010	0.177	0.32	32.13	361	207	0.12	0.20	0.16	416	0.09	1.16	0.00	0.67
LC2-11	-24.87	0.041	0.473	0.31	7.56	126	254	0.05	0.26	0.17	429	0.00	0.40	0.00	0.79
LC2-12	-25.71	0.019	0.418	0.24	12.73	128	258	0.04	0.20	0.14	439	0.01	0.31	0.00	0.63
LC2-13	-27.18	0.010	0.307	0.11	11.25	127	357	0.02	0.09	0.12	427	0.00	0.14	0.00	0.40
LC2-14	-25.70	0.010	0.436	0.25	24.55	124	260	0.04	0.20	0.15	428	0.01	0.31	0.00	0.64
LC2-15	-26.01	0.010	0.204	0.32	32.30	146	232	0.06	0.26	0.16	426	0.01	0.47	0.00	0.75
LC2-16	-25.92	0.010	0.436	0.25	25.18	130	272	0.05	0.21	0.17	428	0.01	0.33	0.00	0.69
LC2-17	-24.18	0.010	0.562	0.51	51.05	158	196	0.10	0.42	0.17	430	0.01	0.81	0.00	1.00
LC2-18	-23.66	0.010	0.464	0.44	43.78	175	182	0.09	0.35	0.11	430	0.01	0.77	0.00	0.80
LC2-19	-24.92	0.010	0.406	0.21	21.28	135	272	0.04	0.17	0.12	428	0.00	0.29	0.00	0.58
LC2-20	-24.80	0.010	0.153	0.26	26.35	321	239	0.09	0.17	0.11	418	0.08	0.85	0.00	0.63
LC3-01	-21.35	0.010	0.233	0.26	25.73	213	250	0.06	0.19	0.04	407	0.01	0.55	0.00	0.64
LC3-02	-19.71	0.001	0.262	0.32	290.04	251	202	0.09	0.24	0.04	409	0.01	0.82	0.00	0.65
LC3-03	-21.36	0.010	0.243	0.24	24.03	186	242	0.05	0.19	0.03	411	0.01	0.45	0.00	0.58
LC3-04	-23.66	0.010	0.148	0.11	11.28	178	284	0.03	0.09	0.02	420	0.01	0.20	0.00	0.32
LC3-05	-22.95	0.010	0.160	0.13	12.64	176	255	0.03	0.10	0.02	417	0.01	0.22	0.00	0.32
LC3-06	-22.75	0.010	0.156	0.13	12.98	171	293	0.03	0.10	0.03	413	0.01	0.22	0.00	0.38
LC3-07	-20.67	0.010	0.145	0.10	9.56	215	218	0.02	0.07	0.02	414	0.01	0.21	0.00	0.21
LC3-08	-24.31	0.010	0.161	0.10	10.47	167	235	0.02	0.08	0.03	419	0.01	0.17	0.00	0.25
LC3-10	-25.71	0.010	0.155	0.10	10.30	170	229	0.02	0.08	0.02	448	0.01	0.18	0.00	0.24
LC12-01	-20.11	0.010	0.495	0.83	82.70	246	162	0.21	0.62	0.12	425	0.01	2.03	0.00	1.34
LC12-02	-21.44	0.010	0.543	0.83	83.18	228	178	0.20	0.63	0.12	428	0.01	1.90	0.00	1.48
LC12-03	-23.02	0.010	0.595	0.88	88.03	239	185	0.22	0.66	0.12	431	0.01	2.10	0.00	1.63
LC12-04	-22.71	0.010	0.599	0.90	89.54	239	186	0.22	0.67	0.12	431	0.01	2.14	0.00	1.66
LC12-05	-22.80	0.010	0.623	0.94	94.26	240	192	0.24	0.70	0.13	429	0.01	2.26	0.00	1.81
LC12-06	-22.88	0.010	0.436	0.90	90.21	226	196	0.22	0.68	0.13	432	0.01	2.04	0.00	1.76
LC13-01	-24.78	0.141	1.078	2.80	19.85	no data	no data	no data	no data	no data	no data	no data	no data	no data	no data
LC13-02	-24.79	0.167	1.151	3.09	18.44	335	124	0.98	2.11	0.24	419	0.16	10.34	0.00	3.84
LC13-03	-24.06	0.186	1.217	3.38	18.17	316	122	1.00	2.37	0.22	421	0.09	10.66	0.00	4.11
LC13-04	-24.65	0.140	1.094	2.61	18.68	295	124	0.73	1.88	0.18	421	0.07	7.70	0.00	3.24
LC13-05	-24.53	0.092	0.971	2.10	22.76	250	124	0.51	1.59	0.18	422	0.03	5.24	0.00	2.60
LC13-06	-24.21	0.069	0.851	1.83	26.43	244	130	0.44	1.39	0.12	427	0.03	4.46	0.00	2.37
LC13-07	-23.62	0.057	0.708	1.83	32.29	259	106	0.45	1.38	0.10	430	0.02	4.76	0.00	1.95
LC13-08	-24.56	0.097	0.778	1.91	19.64	279	115	0.50	1.41	0.15	430	0.02	5.34	0.00	2.19
LC13-09	-26.44	0.159	0.969	2.80	17.62	336	100	0.86	1.94	0.13	430	0.03	9.42	0.00	2.80
LC13-10	-27.04	0.184	0.953	2.99	16.30	353	95	0.96	2.04	0.17	430	0.04	10.56	0.00	2.86
LC13-11	-26.25	0.176	0.934	2.91	16.53	337	93	0.89	2.02	0.13	429	0.03	9.78	0.00	2.71
LC13-12	-26.47	0.296	1.084	3.33	11.22	344	91	1.04	2.29	0.12	427	0.04	11.45	0.00	3.03
LC13-13	-26.41	0.326	1.185	3.82	11.70	413	92	1.41	2.41	0.21	428	0.08	15.76	0.00	3.51
LC18-01	-23.33	0.010	0.233	0.11	11.22	197	182	0.02	0.09	0.02	413	0.01	0.22	0.00	0.20
LC18-02	-24.15	0.010	0.223	0.10	9.64	186	183	0.02	0.08	0.02	424	0.00	0.18	0.00	0.18
LC18-03	-23.10	0.010	0.289	0.16	16.13	179	187	0.03	0.13	0.02	428	0.01	0.29	0.00	0.30
LC18-04	-23.43	0.010	0.265	0.11	10.50	167	197	0.02	0.08	0.02	428	0.00	0.18	0.00	0.21
LC18-05	-24.25	0.010	0.240	0.08	8.45	172	200	0.02	0.07	0.01	419	0.00	0.15	0.00	0.17
LC18-06	-23.67	0.010	0.336	0.17	16.86	167	195	0.03	0.14	0.02	427	0.01	0.28	0.00	0.33
LC18-07	-22.96	0.010	0.410	0.32	31.50	192	166	0.07	0.25	0.03	426	0.01	0.61	0.00	0.52
LC18-08	-22.25	0.010	0.428	0.30	30.46	199	168	0.07	0.24	0.03	428	0.01	0.61	0.00	0.51
LC19-01	-18.40	0.010	0.278	0.25	25.36	257	191	0.07	0.19	0.07	417	0.01	0.65	0.00	0.48
LC19-02	-20.33	0.010	0.269	0.13	13.49	211	227	0.03	0.10	0.06	414	0.00	0.28	0.00	0.31
LC19-03	-21.94	0.010	0.388	0.32	32.46	182	185	0.07	0.26	0.08	423	0.00	0.59	0.00	0.60
LC19-04	-23.94	0.010	0.440	0.49	49.49	176	144	0.09	0.40	0.09	425	0.01	0.87	0.00	0.71
LC19-05	-23.73	0.007	0.565	0.88	128.77	197	117	0.17	0.70	0.11	426	0.01	1.73	0.00	1.03
LC19-06	-24.41	0.010	0.461	0.46	45.76	170	138	0.08	0.37	0.09	423	0.01	0.78	0.00	0.63
LC19-07	-25.15	0.010	0.347	0.21	20.76	185	176	0.04	0.17	0.07	454	0.00	0.38	0.00	0.37

Appendix

Sample	D13C_VPDB	Nitrogen [% wt]	Hydrogen [% wt]	TOC [% wt]	C_N	HI [mg HC/g TOC]	OI [mg CO2/g TOC]	PC [%]	RC [%]	MINC [%]	Tmax [°C]	S1 [mg HC/g]	S2a [mg HC/g]	S2b [mg HC/g]	S3
LC20-01	-20.38	0.010	0.233	0.48	48.32	194	258	0.11	0.37	0.15	419	0.01	0.94	0.00	1.25
LC20-02	-21.20	0.010	0.459	0.41	40.61	115	250	0.07	0.34	0.15	423	0.00	0.47	0.00	1.01
LC20-03	-23.76	0.010	0.314	0.16	15.89	24	410	0.02	0.14	0.13	419	0.00	0.04	0.00	0.65
LC20-04	-24.85	0.010	0.355	0.28	27.90	99	247	0.04	0.24	0.15	419	0.00	0.28	0.00	0.69
LC20-05	-23.68	0.010	0.253	0.50	49.75	177	209	0.10	0.40	0.16	420	0.01	0.88	0.00	1.04
LC20-06	-22.82	0.010	0.468	0.48	47.90	154	185	0.09	0.39	0.14	422	0.00	0.74	0.00	0.89
LC20-07	-23.34	0.010	0.346	0.27	26.56	97	239	0.04	0.23	0.14	421	0.00	0.26	0.00	0.63
LC20-08	-23.69	0.010	0.408	0.41	41.25	168	188	0.08	0.33	0.14	419	0.00	0.69	0.00	0.77
LC20-09	-23.43	0.010	0.493	0.51	51.03	190	174	0.10	0.41	0.12	420	0.00	0.97	0.00	0.89
LC20-10	-24.40	0.010	0.218	0.51	50.87	201	168	0.11	0.40	0.10	421	0.01	1.02	0.00	0.86
LC20-11	-23.88	0.010	0.436	0.48	47.81	183	166	0.09	0.38	0.09	424	0.00	0.88	0.00	0.79
LC20-12	-24.00	0.010	0.387	0.43	43.13	163	180	0.08	0.35	0.12	426	0.00	0.70	0.00	0.78
LC20-13	-23.90	0.010	0.379	0.41	40.52	143	210	0.07	0.33	0.13	423	0.00	0.58	0.00	0.85
LC20-14	-23.74	0.010	0.387	0.59	59.05	300	152	0.20	0.39	0.12	423	0.32	1.77	0.00	0.90
LC20-15	-24.39	0.010	0.221	0.66	66.07	296	146	0.20	0.46	0.17	418	0.10	1.95	0.00	0.97
LC21-01	-22.00	0.010	0.415	0.77	77.14	191	163	0.16	0.61	0.16	420	0.00	1.47	0.00	1.26
LC21-02	-23.10	0.010	0.326	0.36	36.00	97	250	0.05	0.31	0.15	419	0.00	0.35	0.00	0.90
LC21-03	-22.87	0.010	0.386	0.69	68.92	152	172	0.12	0.57	0.15	419	0.00	1.05	0.00	1.18
LC21-04	-20.81	0.010	0.613	1.42	141.93	212	140	0.30	1.12	0.17	423	0.00	3.01	0.00	1.98
LC21-05	-21.89	0.010	0.524	1.05	104.51	179	156	0.20	0.85	0.16	422	0.00	1.87	0.00	1.63
LC21-06	-22.25	0.015	0.601	1.26	83.22	175	154	0.24	1.02	0.17	423	0.00	2.21	0.00	1.94
LC21-07	-23.17	0.006	0.497	1.00	158.87	149	165	0.17	0.83	0.16	423	0.00	1.49	0.00	1.65
LC21-08	-23.50	0.038	0.543	0.87	22.65	162	142	0.15	0.72	0.15	425	0.00	1.40	0.00	1.23
LC21-09	-23.40	0.010	0.692	0.75	74.75	141	160	0.12	0.63	0.17	424	0.00	1.05	0.00	1.20
LC21-10	-23.85	0.010	0.663	0.63	62.60	116	190	0.09	0.53	0.17	423	0.00	0.73	0.00	1.19
LC21-11	-23.42	0.010	0.663	0.71	70.93	114	181	0.10	0.61	0.17	423	0.00	0.81	0.00	1.28
LC21-12	-23.72	0.010	0.652	0.79	79.36	123	164	0.12	0.68	0.15	426	0.00	0.98	0.00	1.30
LC21-13	-23.76	0.010	0.648	0.66	66.05	109	162	0.09	0.57	0.17	423	0.00	0.72	0.00	1.07
LC21-14	-23.65	0.010	0.675	0.72	71.80	120	178	0.11	0.61	0.16	423	0.00	0.86	0.00	1.28
LC21-15	-23.58	0.010	0.657	0.64	63.61	114	178	0.09	0.55	0.16	424	0.00	0.72	0.00	1.13
LC22-01	-23.58	0.010	0.604	0.37	36.65	95	300	0.06	0.31	0.74	418	0.00	0.35	0.00	1.10
LC22-02	-24.89	0.010	0.789	0.40	40.37	84	331	0.06	0.34	0.87	425	0.00	0.34	0.00	1.34
LC22-03	-25.76	0.010	0.712	0.37	36.91	92	313	0.06	0.31	0.76	421	0.00	0.34	0.00	1.16
LC22-04	-26.10	0.010	0.871	0.46	47.59	103	274	0.07	0.39	0.72	422	0.00	0.48	0.00	1.27
LC22-05	-26.22	0.010	0.879	0.53	53.03	117	225	0.08	0.45	0.54	425	0.00	0.62	0.00	1.19
LC22-06	-26.47	0.010	0.591	0.41	41.18	102	258	0.06	0.35	0.50	422	0.00	0.42	0.00	1.06
LC22-07	-25.89	0.004	0.788	0.53	117.72	127	223	0.09	0.44	0.48	426	0.00	0.67	0.00	1.18
LC22-08	-26.48	0.003	0.695	0.42	146.46	98	286	0.07	0.35	0.59	422	0.00	0.41	0.00	1.20
LC22-09	-26.66	0.010	1.013	0.39	38.94	90	293	0.06	0.33	0.65	424	0.00	0.35	0.00	1.14
LC22-10	-26.24	0.010	0.757	0.52	52.41	160	227	0.10	0.42	0.62	420	0.01	0.84	0.00	1.19
LC23-01	-24.06	0.009	0.669	0.82	92.10	253	142	0.21	0.61	0.07	421	0.04	2.08	0.00	1.16
LC23-02	-24.25	0.007	1.061	0.73	99.48	236	151	0.18	0.56	0.10	419	0.03	1.72	0.00	1.10
LC23-03	-23.99	0.001	0.738	0.77	1016.46	230	145	0.18	0.59	0.07	420	0.04	1.76	0.00	1.11
LC23-04	-25.05	0.010	0.664	0.62	62.06	260	121	0.16	0.46	0.06	421	0.03	1.61	0.00	0.75
LC23-05	-25.66	0.010	0.682	0.42	41.54	274	123	0.11	0.30	0.04	421	0.06	1.14	0.00	0.51
LC24-01	-25.81	0.010	0.000	0.25	24.64	379	148	0.09	0.15	0.04	406	0.09	0.93	0.00	0.36
LC24-02	-25.14	0.010	0.707	0.26	26.33	234	180	0.07	0.20	0.05	409	0.03	0.62	0.00	0.47
LC24-03	-24.64	0.010	0.692	0.40	40.39	298	151	0.12	0.28	0.06	411	0.09	1.20	0.00	0.61
LC24-04	-24.18	0.010	0.609	0.25	25.02	351	167	0.09	0.16	0.06	417	0.06	0.88	0.00	0.42
LC24-05	-23.65	0.796	0.933	0.20	0.25	450	173	0.09	0.11	0.06	415	0.05	0.90	0.00	0.35
LC24-06	-24.04	0.755	0.991	0.17	0.22	392	249	0.07	0.10	0.05	352	0.07	0.66	0.00	0.42
LC24-07	-23.70	0.745	0.937	0.20	0.27	293	221	0.06	0.14	0.06	357	0.02	0.58	0.00	0.44
LC24-08	-23.45	0.010	0.674	0.23	22.61	261	209	0.07	0.16	0.07	427	0.05	0.59	0.00	0.47
L1-USP1.1	-21.58	0.030	0.308	0.73	24.16	272	197	0.21	0.53	0.08	279	0.04	2.00	0.00	1.45
L1-USP1.2	-23.09	0.010	0.208	0.33	33.17	288	207	0.10	0.23	0.07	419	0.07	0.96	0.00	0.69
L1-USP2.1	-20.94	0.010	0.325	0.42	41.57	336	198	0.14	0.27	0.13	407	0.07	1.40	0.00	0.82
L1-USP2.2	-23.16	no data	no data	0.22	no data	no data	no data	no data	no data	no data	no data	no data	no data	no data	no data
L1-USP3.1	-19.26	no data	no data	0.50	no data	342	154	0.17	0.34	0.05	423	0.05	1.73	0.00	0.78
L1-USP3.2	-18.34	0.026	0.253	0.46	17.91	388	146	0.17	0.29	0.06	414	0.08	1.78	0.00	0.67
L1-SOP1.1	-23.56	0.261	0.815	4.47	17.14	337	163	1.46	3.01	0.22	422	0.15	15.06	0.00	7.30
L1-SOP1.2	-22.78	0.215	0.900	4.35	20.20	302	174	1.31	3.04	0.24	423	0.12	13.13	0.00	7.54
L1-SOP2.1	-25.85	0.106	0.620	2.52	23.81	302	186	0.77	1.75	0.29	280	0.11	7.63	0.00	4.70
L1-SOP2.2	-23.57	0.098	0.415	1.15	11.76	289	214	0.35	0.80	0.16	284	0.07	3.34	0.00	2.47
L1-SOP3.1	-24.67	0.069	0.364	2.04	29.34	343	187	0.69	1.35	0.11	261	0.07	6.99	0.00	3.81
L1-SOP3.2	-24.50	0.058	0.407	2.22	38.42	353	187	0.77	1.45	0.12	258	0.07	7.84	0.00	4.17
L13-USP1.1	-25.08	0.010	0.427	1.18	118.00	no data	no data	no data	no data	no data	no data	no data	no data	no data	no data
L13-USP1.2	-25.28	0.010	0.295	1.16	115.66	317	128	0.35	0.80	0.07	424	0.10	3.67	0.00	1.48
L13-USP2.1	-24.85	0.010	0.634	2.20	220.29	289	112	0.61	1.60	0.16	424	0.12	6.37	0.00	2.47
L13-USP2.2	-24.51	0.010	0.628	2.33	233.03	281	121	0.63	1.70	0.14	424	0.10	6.55	0.00	2.82
L13-USP3.1	-22.72	0.010	0.485	1.23	122.76	209	146	0.27	0.96	0.12	418	0.09	2.57	0.00	1.79
L13-USP3.2	-22.60	0.010	0.452	1.16	115.71	226	146	0.27	0.89	0.13	420	0.10	2.62	0.00	1.69
L13-SOP1.1	-23.75	0.010	0.464	2.03	203.23	254	203	0.55	1.49	0.34	416	0.06	5.16	0.00	4.12
L13-SOP1.2	-24.95	0.010	0.270	0.98	98.38	295	155	0.29	0.69	0.08	425	0.09	2.90	0.00	1.52
L13-SOP2.1	-25.32	0.010	0.297	1.03	102.55	309	126	0.31	0.72	0.14	425	0.10	3.17	0.00	1.29
L13-SOP2.2	-25.38	0.010	0.202	0.85	85.00	no data	no data	no data	no data	no data	no data	no data	no data	no data	no data
L13-SOP3.1	-24.70	0.010	0.124	0.39	39.34	357	154	0.14	0.25	0.05	418	0.10	1.40	0.00	0.61
L13-SOP3.2	-23.70	0.085	0.195	0.60	7.01	335	182	0.20	0.39	0.07	421	0.10	2.01	0.00	1.09

8.8. Bacterial spores, from ecology to biotechnology



Bacterial spores, from ecology to biotechnology

Christophe Paul^a, Sevasti Filippidou^a, Isha Jamil^a, Wafa Kooli^{a,b},
 Geoffrey L. House^b, Aislinn Estoppey^a, Mathilda Hayoz^a,
 Thomas Junier^{a,c}, Fabio Palmieri^a, Tina Wunderlin^a, Anael Lehmann^d,
 Saskia Bindschedler^a, Torsten Vennemann^d, Patrick S.G. Chain^b,
 Pilar Junier^{a,*}

^aLaboratory of Microbiology, Institute of Biology, University of Neuchâtel, Neuchâtel, Switzerland

^bBioscience Division, Los Alamos National Laboratory, Los Alamos, NM, United States

^cVital-IT group, Swiss Institute of Bioinformatics, Lausanne, Switzerland

^dLaboratory of stable isotope geochemistry, Institute of Earth Surface Dynamics, University of Lausanne, Lausanne, Switzerland

*Corresponding author: e-mail address: pilar.junier@unine.ch

Contents

1. The challenge of bacterial survival	80
2. Mechanisms of bacterial survival through cell differentiation	82
3. Investigating spores directly from environmental samples	84
4. The sporobiota: Prevalence of spores in the human microbiota	86
5. Potential spore-formers in other microbiomes	86
6. Prevalence of spore-formers in environmental samples	88
7. Spores and environmental sensing	89
8. What do spores tell us about antibiotic resistance?	91
9. Biotechnological applications of spore-forming bacteria	95
9.1 Plant growth promotion	95
9.2 Drug delivery	97
9.3 Bioremediation and biomineralization	98
10. Conclusion	102
Acknowledgments	103
References	103

Abstract

The production of a highly specialized cell structure called a spore is a remarkable example of a survival strategy displayed by bacteria in response to challenging environmental conditions. The detailed analysis and description of the process of sporulation in selected model organisms have generated a solid background to understand the cellular processes leading to the formation of this specialized cell. However, much less

is known regarding the ecology of spore-formers. This research gap needs to be filled as the feature of resistance has important implications not only on the survival of spore-formers and their ecology, but also on the use of spores for environmental prospection and biotechnological applications.



1. The challenge of bacterial survival

The unpredictability of environmental conditions in natural ecosystems represents a constant challenge to survival. In consequence, it is highly likely that during its lifetime, an individual organism will have to withstand conditions that are suboptimal for growth and reproduction. There are different responses to this phenomenon. The reduced metabolic activity that occurs in dormant cells is one of these, and dormancy therefore can allow the reduction of the fitness cost that environmental stress imposes on a population (Lennon & Jones, 2011). Although dormancy can be beneficial under fluctuating conditions, it can also be a perilous response. It bears a high biological cost, as the individual cell must invest resources in mobilizing the machinery required for the transition from an active to a dormant state (Callahan, Maughan, & Steiner, 2008; van Bodegom, 2007). It is also a risky strategy as the misinterpretation of the physiological and environmental cues that trigger dormancy or allow reactivation to an active state will result in a missed opportunity for growth and reproduction. In spite of these trade-offs, dormant cell forms have been reported in Bacteria, Eukarya, and potentially Archaea (Lennon & Jones, 2011).

Diverse survival strategies in response to challenging environmental conditions have been described for bacterial species. These strategies can constitute a complex coordinated response of the entire community (for example biofilm formation; Kreft, 2004), or favor the survival of individual cells. The latter includes processes involving morphological plasticity (Justice, Hunstad, Cegelski, & Hultgren, 2008) or post-transcriptional modifications that optimize fitness (Zhao et al., 2002). Bacterial dormancy is a well-studied survival strategy that corresponds simultaneously to both categories: community and individual survival. Dormancy can be considered a property of individuals, as not all bacterial species are able to switch from a vegetative to a dormant state. However, dormancy has been described as a community strategy that presupposes an altruistic behavior involving the communication and sacrifice of specific cells before, during and after entering this state (Buerger et al., 2012; Lennon & Jones, 2011; Wolf, Vazirani, & Arkin, 2005).

Dormant microorganisms exhibit a wide range of resting phenotypes, probably reflecting a complex evolutionary history of this trait. A comprehensive definition of dormancy includes any resting period or reversible interruption of the growth or metabolism of an organism. This definition applies both to differentiated dormant cells and to cellular states (for example viable non culturable state) that improve survival (Lennon & Jones, 2011). One of the most common ways of achieving dormancy is through the differentiation of the vegetative cells into resting structures such as spores, conidia, cysts or akinetes. This involves an obvious morphological differentiation involving reduced cell size or a special cell division that marks the formation of the dormant cell (Lennon & Jones, 2011).

Bacterial spores are a highly successful type of dormant cell. Sporulation provides a mechanism by which spore-formers can withstand unfavorable conditions, at temporal and/or spatial scale. Spores are both resistant structures that can persist in a dormant state for extended periods of time, and a vector for increasing dissemination rate, both circumventing local unfavorable conditions that prevent optimal growth (Nicholson, 2002). To date, dormancy in the form of a spore has been thoroughly investigated in four bacterial phyla, and each produces characteristic spore types: Firmicutes (endospores), Actinomycetes (exospores), Cyanobacteria (akinetes), and in the δ -Proteobacteria genus *Myxococcus* (fruiting bodies) (Barton, 2005). Collectively, research in these model groups has generated a strong foundation for exploring the prevalence and implications of this survival strategy (Hutchison, Miller, & Angert, 2014; Lennon & Jones, 2011). Likewise, predicting the ability of an organism to produce spores (or spore-like cells) is often made on the basis of the morphological and genetic information compiled in these well-studied standard model organisms. The process of dormancy in these bacteria has three general stages: initiation, resting, and resuscitation (Lennon & Jones, 2011) (Fig. 1). Initiation is the response to unfavorable changes in the environment. These changes are often detected by a tightly controlled regulatory network because of the high energetic costs of a response to a “false” signal. Therefore, in natural communities a mechanism allowing a responsive switching to initiate dormancy should be favored. The tolerance of the organism to potential stressors in their natural environment would, to a large extent, limit the triggering of responsive switching that in turn would induce dormancy. Likewise, a pathway allowing responsive resuscitation can be predicted. Indeed, dormancy is an adaptive strategy if dormant cells are able to exit it when environmental conditions are favorable and therefore, if efficient mechanisms to trigger exiting dormancy are in place (Lennon & Jones, 2011).

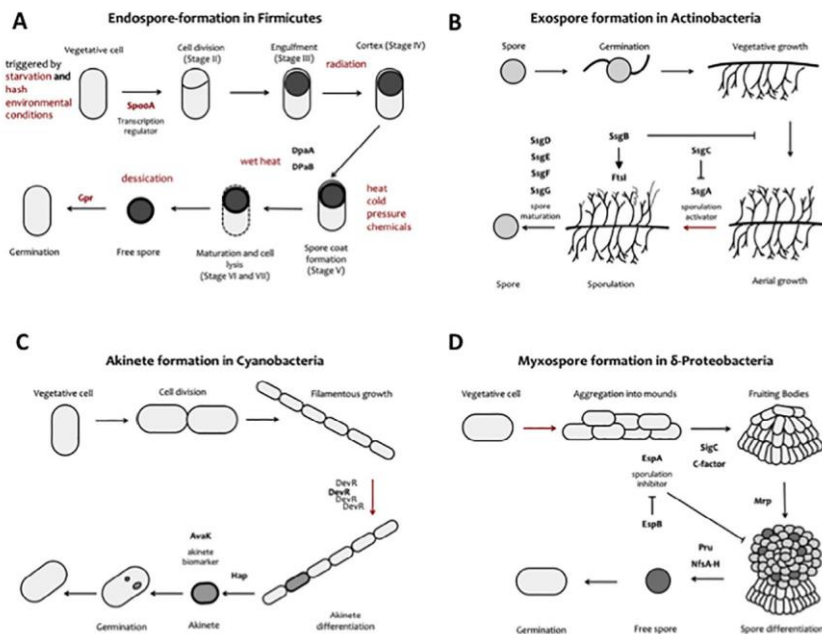


Fig. 1 Schematic representation of the sporulation process in four different bacterial taxa: (A) Firmicutes; (B) Actinobacteria; (C) Cyanobacteria; and (D) *Myxococcus* (mechanism of sporulation due to starvation by the formation of a fruiting body). The most relevant genes involved in the respective sporulation pathways are indicated. Bold arrows indicate the key step in which vegetative cells commit to sporulation.

In spite of a large amount of information obtained in model organisms in the laboratory, sporulation in the environment is only recently starting to be investigated in detail. The aim of this review is to provide a comprehensive revision of the information available in the ecology of spore-forming bacteria in natural environments and the potential uses of spore-forming bacteria in biotechnological applications.



2. Mechanisms of bacterial survival through cell differentiation

Among dormant cell forms, the best studied are endospores, which so far have only been found in Firmicutes. Endospore formation is an example of a sophisticated morphophysiological process of cell differentiation. It involves an asymmetric cell division resulting in two cells with distinct morphologies and functions (spore and mother cell), the engulfment of the

pre-spore by the mother cell, and the finally remodeling of this spore within the mother cell (Driks, 2002). Endospores are also an essential cellular state in the case of pathogens or biocontrol agents in which spores are directly involved in human disease (e.g., anthrax, botulism) (Thavaselvam & Vijayaraghavan, 2010) or pathogen control (Tetreau, 2018). In the case of other differentiated dormant cells such as exospores, myxospores or cysts, the mechanisms of formation are much less well understood (Abel-Santos, 2012), limiting our ability to perform comparative studies in order to assess their prevalence. Because of this, endospores are often used as a benchmark for a canonical resistance structure and many resistant cells are compared directly to those. Reports of dormancy involving specialized cellular structures outside these four groups are found in the literature but have often been received with skepticism. Nonetheless, over the last three decades, the formation of cyst-like resting structures has been proposed for diverse non-spore-formers (Sadasivan & Neyra, 1985; Suzina et al., 2004). Examples of resistant cyst-like-producing non-spore-forming bacteria include *Pseudomonas aeruginosa* (Zechman & Casida, 1982), *Micrococcus luteus* (Mulyukin et al., 2009), *Thioalkalivibrio versutus* (Loiko, Soina, Sorokin, Mityushina, & El-Registan, 2003), *Sinorhizobium meliloti* (Loiko et al., 2011), and *Arthrobacter globiformis* (Mulyukin et al., 2009), among others. Also, recently cyst-like cells have been found in *Serratia ureilytica* Lr5/4, a polyextreme bacterium isolated from a geothermal source in the Atacama Desert (S. Filippidou et al., submitted). However, for most of these cyst-like cells, the process of generation of the resistance structure, the genetic determinants underlying the trait, and the detailed morphology and composition of the resting cell are not yet described.

Based on the reports of resistant cells so far, one could suggest that dormancy in the form of a modified cell is prevalent among diverse bacterial phyla. This has profound evolutionary implications, and it has even been suggested that a common “sporulating” ancestor to bacteria might have existed prior to their evolutionary radiation (Tocheva, Ortega, & Jensen, 2016). Indeed, the ability to enter into a dormant and resistant cellular state would have provided a clear advantage during the evolution of bacteria in the turbulent and highly fluctuating environment early in Earth’s history that resulted in exposure to frequent meteoritic bombardments and alternating periods of boiling and freezing temperatures (Nisbet & Sleep, 2001). In order to test this evolutionary scenario, additional models need to be investigated. Therefore, one of the frontiers in research into bacteria that produce dormant cells consists of developing

tailored methods for improving the ability to enrich and culture novel spore-like-forming species (Browne et al., 2016).

The impact of improved methods to assess sporulation in environmental bacteria is remarkable. For example, even in the case of the best-studied group (Firmicutes), the ability to form spores can be discovered in so-called asporogenic (non-spore forming) species. One example of this is the deduction of spore production based on comparative genomic analysis such as in the case of the extremophile *Carboxydotherrnus hydrogenofomans* followed by the physiological demonstration of spore formation (Wu et al., 2005). Likewise, the recent isolation and characterization of novel species of *Ruminococcus*, previously regarded as a non-spore forming Firmicute genus, have demonstrated their ability to form spores (Mukhopadhyaya et al., 2018). This illustrates the large scope of work required to address what can be called the “dark spore-forming bacterial matter,” something particularly relevant in the case of non-Firmicute species. This will constitute a leap forward in our understanding of microbial physiology, and the processes of morphogenesis and cellular differentiation. Novel approaches such as single cell genomics have the potential to allow this (Miller, Weyna, Fong, Lim-Fong, & Kwan, 2016; Rinke et al., 2013) after spores are separated and enriched from the total community. Generating a method to sequence individual spores is still challenging, but should be an approach to be developed in the future.



3. Investigating spores directly from environmental samples

The previous examples considered bacteria forming spores and cyst-like cells that have been cultured and studied in the laboratory. However, it is also possible to investigate the diversity of highly resistant cells directly from environmental samples. Various culture-dependent studies of endospore-forming Firmicutes have shown an interesting distribution pattern suggesting a mismatch between the ecological optima of species and their environmental detection. For example, the revival of endospores from thermophilic endospore-forming Firmicutes species from cold sediments suggests a high dispersal potential associated with the formation of endospores (Bell, Blake, Sherry, Head, & Hubert, 2018; de Rezende et al., 2013; Hubert et al., 2010, 2009; Muller et al., 2014). In this case, dispersal in the form of a dormant endospore reduces the selective pressure

exerted by *in situ* environmental conditions. This is in contrast to the general principle of biogeographical distribution often assigned to microbial communities in which “everything is everywhere but the environment selects,” as in the case of metabolically inactive spores, the environmental conditions would not affect community structure (Martiny et al., 2006). This unique biogeographical distribution of endospore-formers as a consequence of their high dispersal potential has been also shown in soils. However, while a study in soil did not show spatial dependence or correlation with *in situ* conditions (Philippot et al., 2009), on the contrary, another one in the soil critical zone has shown a distribution associated to *in situ* environmental parameters (Tsiknia, Paranychianakis, Varouchakis, Moraetis, & Nikolaidis, 2014).

Aside from culture-dependent methods, a suite of novel approaches to study the diversity of endospore-forming Firmicutes in environmental samples have been developed (Bueche et al., 2013; Wunderlin, Junier, Roussel-Delif, Jeanneret, & Junier, 2013). This includes a new approach to carry out targeted DNA metagenomics using sporulation as a functional trait (Wunderlin, Junier, Paul, Jeanneret, & Junier, 2016; Wunderlin, Junier, Roussel-Delif, Jeanneret, & Junier, 2014). A method to enrich lysis-resistant cells was devised based on a combination of physical and chemical treatments inducing the lysis of vegetative cells. Initially developed for the isolation of endospores of Firmicutes (considered to be one of the most lysis-resistant life forms), the method has been applied to various environmental samples with unexpected results. While initial laboratory tests demonstrated a clear enrichment of endospores, results from environmental samples invariably showed extremely diverse communities including many highly abundant taxa that were previously believed to be non-spore formers. Interestingly, these previously unknown spore-formers present in the lysis-resistant fraction of the community were not a main component of the lysis-susceptible community, which indicates they were not simply contaminants due to the incomplete removal of vegetative cells (T. Junier & C. Paul, submitted). Such results suggest a potentially unsuspected diversity of organisms able to form resistant structures. This would give additional support to an evolutionary scenario that includes a widespread prevalence of sporulation (or spore-like formation pathways) in bacterial communities. This is significant considering the potential resilience that these spores and spore-like cells would give bacterial communities in surviving environmental perturbations.



4. The sporobiota: Prevalence of spores in the human microbiota

The concept of sporobiota has recently been used to characterize a particular fraction of the human microbiota that shares the characteristic of producing highly resistant endospores, which facilitates transmission of spore-formers between individuals (Tetz & Tetz, 2017). The need for defining this unique fraction is not only the consequence of the dominance of this group within the human microbiome (Browne et al., 2016), but also the unique emerging features related to the presence of highly resistant spores within this sub-community. These features include resistance to antibiotic treatment by the production of endospores, eliciting detrimental host immune responses, or the possibility of spores acting as an agent of chronic infections, among others (Tetz & Tetz, 2017). A recent human microbiome study based on the enrichment approach mentioned previously (Wunderlin et al., 2016; Wunderlin, Junier, et al., 2014) showed that these lysis-resistant cells are prone to participating in cross-host dissemination and play an important role in the re-colonization after a process affecting the stability of the human habitat (Kearney et al., 2018).

Obesity is the most representative case study in which the presence of potentially endospore-forming bacteria has been linked to health. The presence, and more importantly, a change in the relative frequency of Firmicutes versus Bacteroidetes (increase of the former relative to the latter) has been associated with the microbiota of obese mice (Clarke et al., 2012). Likewise, increases in the frequency of Firmicutes relative to Bacteroidetes have been found to correlate with body mass index in human populations (Clarke et al., 2012; Koliada et al., 2017). Additional studies have been performed in specific cohorts such as pregnant women or children (Santos-Pereira et al., 2018). In the case of children, a general pattern regarding increases in the relative abundance of Firmicutes has not been reported (Santos-Pereira et al., 2018).



5. Potential spore-formers in other microbiomes

The dominance of putative spore-forming groups, especially Firmicutes, appears to be an overarching feature in the microbiomes of mammals (Mao, Zhang, Liu, & Zhu, 2015; Nelson, 2015). A recent study has suggested that captivity affects the mammalian gut microbiome, with

Firmicutes as one of the bacterial phyla changing as a consequence of captivity (McKenzie et al., 2017). These changes can implicate either an increase or a reduction in the abundance of specific groups, and those vary for different host species. In general, captive mammals appear to harbor a higher frequency of anaerobic Bacilli and Clostridia compared to wild counterparts. In addition, other groups potentially comprising spore-forming species such as Actinobacteria and Cyanobacteria appear to also vary in response to captivity, but their prevalence is much lower than that of Firmicutes. Also, a comparison between marine and terrestrial mammals suggests the importance of Firmicutes as a predominant group associated to animals with different dietary preference and habitats. However, an exception to this appears to be a unique signature of reduced abundance of Firmicutes accompanied by increased abundance of Fusobacteria found in carnivorous marine mammals compared to terrestrial mammals (Nelson, Rogers, & Brown, 2013).

Studies considering non-mammalian hosts are currently less common. However, Firmicutes have been reported in specific proportions of the gastrointestinal tract of alligators, but in this case, Fusobacteria appears to be the most relevant phylum and to have taken over some niches usually occupied by Bacteroidetes and Firmicutes in other vertebrates. The relative proportion of Firmicutes varies with feeding-fasting regimes, seasonal feeding, and farm versus wild animals. In the case of farm animals, their feeding regime and deposition of fat appear also to be correlated to changes in the relative abundance of Firmicutes, similar to reports for obesity in other vertebrates (Keenan, Engel, & Elsey, 2013). Firmicutes are also a main component of the gut microbiota of insects, although at a lower degree than in the case of vertebrates (Engel & Moran, 2013; Yun et al., 2014). Evidence for a dynamic change in the prevalence of Firmicutes with developmental stages has also been shown for insects (Chen et al., 2016).

Recent unpublished data from our laboratory suggest that Firmicutes could also be prevalent in the microbiota of fungi. However, determining if bacteria are actually living inside fungal cells instead of closely associated with the exterior of cells can be challenging, and this needs to be investigated further. Nonetheless, by searching for genome-based signals of spore-forming genera within sequenced fungal genomes, we have identified the presence of *Bacillus* spp. in a diverse range of potential fungal hosts (Table 1). This is in agreement with the detection of *Bacillus* and related genera as endobacteria of mycorrhizal fungi (Izumi, Anderson, Alexander, Killham, & Moore, 2006).

Table 1 Signals of spore-forming *Bacillus* species recovered from the genome sequencing data of fungal isolates (291 isolates) sequenced as part of the 1000 Fungal Genomes Project.

Fungal isolate	Fungal phylum (Ascomycota or Basidiomycota) or subphylum	Best match for bacterial signal
<i>Aspergillus sydowii</i>	Ascomycota	<i>Bacillus</i> sp. CR71
<i>Cercospora zeae-maydis</i>	Ascomycota	<i>Bacillus</i> sp. IHB B 7164
<i>Dissoconium aciculare</i>	Ascomycota	<i>Bacillus cereus</i> strain CC-1
<i>Lecythophora</i> sp. AK0013	Ascomycota	<i>Bacillus coagulans</i> DSM 1 (ATCC 7050)
<i>Melanomma pulvis-pyrius</i>	Ascomycota	<i>Bacillus cereus</i> NC7401
<i>Ophiobolus disseminans</i>	Ascomycota	<i>Bacillus coagulans</i> LA204
<i>Penicillium canescens</i>	Ascomycota	<i>Bacillus velezensis</i> strain BIM B-439D
<i>Spathaspora passalidarum</i>	Ascomycota	<i>Bacillus thuringiensis</i> strain CTC
<i>Pleurotus ostreatus</i>	Basidiomycota	<i>Bacillus subtilis</i> strain 50-1
<i>Trichosporon oleaginosus</i>	Basidiomycota	<i>Bacillus cereus</i> strain M13 plasmid
<i>Phycomyces blakesleeanus</i>	Mucoromycotina	<i>Bacillus cereus</i> ATCC 10987

After quality control and stringent fungal host removal, remaining sequencing reads were assembled into contigs that were then assigned taxonomic classifications using Centrifuge (Kim, Song, Breitwieser, & Salzberg, 2016) and a custom reference database. Contigs that were at least 1000 base pairs long and had at least 80% identity to a *Bacillus* genome in the reference database were considered to have a signal of associated *Bacillus* (11 of 291 isolates). In cases where multiple *Bacillus* species were identified, only the best match is shown based on contig length and the percentage identity match. These results were validated using BLASTn against the NCBI nucleotide database, and the best scoring BLASTn bacterial species or strain is reported here.



6. Prevalence of spore-formers in environmental samples

Despite their potential for global dispersal, the prevalence of many spore-formers in molecular ecology surveys represents a paradox. An example of this current bias is the environmental detection of the phylum Firmicutes. Firmicutes are the second most abundant bacterial phylum according to previous research based on culture collections as well as whole-genome sequencing (Hugenholtz, 2002). Endospore formers are reported to live in

a wide range of environments on Earth's surface and subsurface (Nicholson, 2002; Nicholson, Munakata, Horneck, Melosh, & Setlow, 2000), and the production of endospores should allow these bacteria to be distributed in every habitat on Earth (Martiny et al., 2006). However, an initial phylogenetic assessment of bacterial communities in four metagenomic datasets revealed surprisingly few endospore formers (von Mering et al., 2007). There are at least two potential explanations for this apparently limited abundance. On the one hand, a methodological bias against molecular detection of Firmicutes could explain their under detection (Filippidou et al., 2015). Indeed, it has been shown that a tailored DNA extraction method allows for a better assessment of the presence and diversity of endospore-forming Firmicutes in environmental samples (Wunderlin et al., 2013; Wunderlin, Junier, et al., 2014). On the other hand, the limited detection of endospore-forming Firmicutes in environmental samples might accurately reflect their relative distribution. If this is the case, it is possible that the energetic demands of sporulation (Hofler et al., 2016) and other survival strategies constitute a burden that limits the prevalence of endospore-forming Firmicutes in otherwise non-limiting conditions. Indeed, results obtained from geothermal sources suggest that multiple limiting environmental conditions favor the relative presence of this group (Filippidou et al., 2016). This is consistent with studies showing that bacteria able to withstand harsh environmental conditions have extra genes or even extra chromosomes (Barton, 2005), but this additional genetic material can also be linked to a decrease in fitness under mesophilic conditions (Pope, McHugh, & Gillespie, 2010). For example, larger chromosomes that result in decreased fitness are also observed in endospore-forming bacteria: when there is no environmental pressure for sporulation, Firmicutes tend to lose their extra sporulation-related genes (de Hoon, Eichenberger, & Vitkup, 2010). This would suggest that the fitness cost to preserve the cellular machinery required for increased survival in harsh conditions is likely a better explanation of the distribution patterns of Firmicutes. However, the absence of clear molecular markers to assess the prevalence of other spore-forming clades in environmental molecular datasets limits the generalization of this trend to other groups.



7. Spores and environmental sensing

Dormant bacterial cells have the potential to be highly useful in providing records of past environmental conditions. Paleocological studies in lake sediments intend to combine physicochemical parameters with biological indicators. Typically, the latter corresponds to organisms producing

identifiable fossilized structures (e.g., pollen grains or siliceous or calcareous microfossils) that must remain unaltered in order to be preserved in the sediments and hence be analyzed at different time-scales (Gorham, Brush, Graumlich, Rosenzweig, & Johnson, 2001). Bacteria are considered as potential proxies of paleoenvironmental conditions given their large cumulative mass, their phylogenetic diversity and the wide range of different metabolisms they represent (Ariztegui, Thomas, & Vuillemin, 2015; Neelson, 1997). Nevertheless, methods for the comprehensive detection of bacterial communities are challenging, especially because of the degradation of DNA with time. Because of this, paleolimnological studies focusing on bacteria have largely been based on fossil pigments (Dressler, Huebener, Goers, Werner, & Selig, 2007; Gorham et al., 2001). An alternative to this is the use of bacterial resting states, a topic reviewed by Renberg and Nilsson (1992). Because spores are able to survive in a dormant state for centuries to thousands of years, these resistant cellular forms are a potential proxy for paleoecological studies.

The isolation and enumeration of viable cells and endospores from sedimentary archives is an old technique (Renberg & Nilsson, 1992). The first published report suggested the presence of viable *Bacillus subtilis* endospores in 320-year-old soil samples (Sneath, 1962). This initial report was then surpassed by later reports suggesting the viability of endospores of *Thermoactinomyces* from archeological excavations containing plant debris deposited between 85 and 125 AD and in 9000-year-old lake sediments (Nilsson & Renberg, 1990; Seaward, Cross, & Unsworth, 1976). A detailed study on the survival and activity of bacteria in a lake sediment core of about 7 m deposited over the past 13,000 years (Lake Constance; Rothfuss, Bender, & Conrad, 1997) shows that below 25 cm all the viable heterotrophic bacteria were present as heat-resistant endospores. Counts of viable spores decreased exponentially with depth and could not be detected below 6 m (about 8900-year-old sediment). Revival of endospores has been used in a series of studies either for paleoecological reconstruction (Bartholomew & Paik, 1966; Renberg & Nilsson, 1992; Rothfuss et al., 1997) or to demonstrate the dispersal of metabolically inactive thermophiles into cold sediments (Bartholomew & Paik, 1966; de Rezende et al., 2013; Hubert et al., 2010). However, culturing studies are biased toward a small cultivable fraction of the community (Amann, Ludwig, & Schleifer, 1995). In a culture-independent approach, the use of an endospore-specific biomarker (dipicolinic acid) suggested that endospores in sediments of the North Sea represent up to 3% of the total prokaryotic community (Fichtel, Koster, Rullkötter, & Sass, 2007). In much older sediment cores, the

abundance of endospores has been estimated to be as high as the total abundance of vegetative cells (Lomstein, Langerhuus, D'Hondt, Jorgensen, & Spivack, 2012). An alternative culture-independent molecular method has been developed, based on the identification of a specific marker for endospore-forming Firmicutes (Wunderlin et al., 2013). This marker, the stage 0 sporulation gene A (*spo0A*), is the master regulator for the sporulation pathway, and has only been reported in Firmicutes (Abecasis et al., 2013; Galperin et al., 2012). This innovative approach was successfully used (in association with other chemical measurements) to reconstruct the history of Lake Geneva, demonstrating the possible use of endospore-forming bacteria as proxies for paleoecological studies. In a first study based on a sedimentary record covering years from 1921 to 2007, changes in the composition of the endospore-forming community reflected the eutrophication process occurring in the lake between 1960 and 1990 (Wunderlin, Corella, et al., 2014). A shift from aerobic groups (*Bacillus*) and facultative anaerobes (*Paenibacillus*) to anaerobic Clostridia (*Clostridium*, *Desulfotobacterium*) was linked to a decrease in oxygen availability, low C/N values and high TOC and Fe/Mn ratio. This trend inverted after 1990, suggesting a recovery of the lake post eutrophication. Interestingly, quantification of *spo0A* gene showed its abundance (copies/gram sediment) was relatively constant with depth compared to the decrease of total DNA and 16S rRNA gene quantification, demonstrating the potential for conservation of DNA from endospore-forming bacteria in sediments. A second study based on the same sedimentary record but with a higher resolution confirmed the effect of eutrophication on community structure and highlighted episodic events of community shift (unpublished results). For example, the increasing use of fossil fuels in the 1950s and 1960s was reflected by an increase in sulfate-reducing bacteria (*Desulfotomaculum* or *Moorella*) (Fig. 2), while punctuated inputs of terrestrial organic matter (1997 and 1924) were indicated by an increase in *Brevibacillus* abundance, together with high TOC values and a C/N ratio in sediments (Fig. 3). Likewise, a cold winter recorded in 1929 was characterized by a high abundance of *Sporomusa*, a genus containing homo-acetogenic bacteria whose metabolism is commonly associated with cold anoxic environments.



8. What do spores tell us about antibiotic resistance?

It has been recently suggested that spore-forming bacteria may play an important role in the evolution and spread of antibiotic resistance, due to

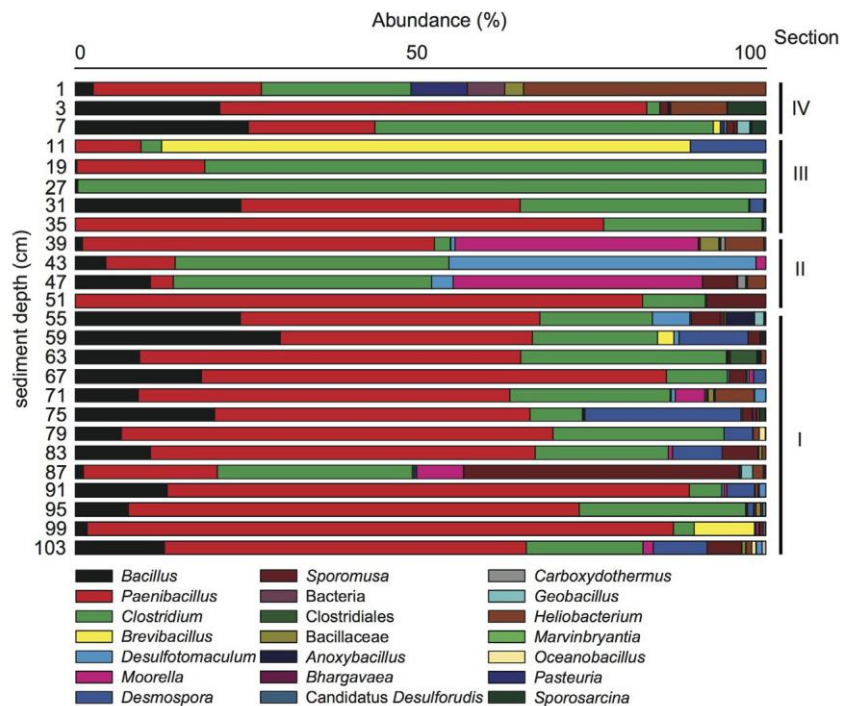


Fig. 2 Temporal changes in the community structure of endospore-forming genera in a sediment core corresponding to the last 100 years of sediment deposition in Lake Geneva. Community structure is based on the analysis of sequences from the stage 0 sporulation gene A (*spo0A*) gene. The *spo0A* sequences were clustered into operational taxonomic units (OTUs) at 97% identity and classified to genus level. The cumulative frequency (in number of sequences) of OTUs belonging to the same genus was added to calculate the percentage values represented for each genus.

their ability to withstand antibiotic treatments and their propensity for dispersal (Bengtsson-Palme, Kristiansson, & Larsson, 2018; Shoemaker & Lennon, 2018; Tetz & Tetz, 2017). Spores and spore-formers are a main component of the human microbiome (Browne et al., 2016) and encompass a wide variety of pathogens and opportunistic pathogens, especially within the group of Clostridia (Aronoff, 2013). Resistance to antibiotics has been reported for clinically relevant spore-formers (Tetz & Tetz, 2017 and references there in) and for several species isolated from the human microbiome (Tetz & Tetz, 2017). In addition, their ability to form a resting state may itself provide resistance to antibiotic treatment (Shoemaker & Lennon, 2018; Tetz & Tetz, 2017). Surviving longer, these organisms have

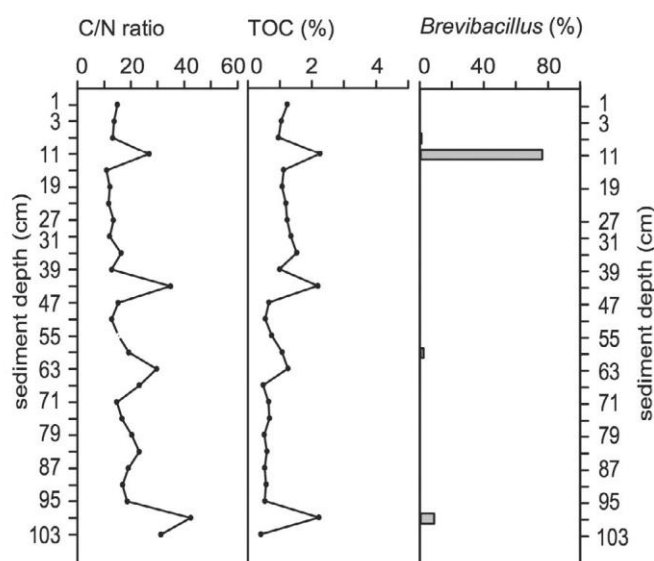


Fig. 3 Depth profile showing the correlation of C/N ratio and total organic carbon (TOC) with the relative abundance of *Brevibacillus*. Samples from a sediment core that has been validate for paleoecological studies obtained in the Rhone Delta from Lake Geneva.

more chances to acquire genetic mutations that confer antibiotic resistance (Levin-Reisman et al., 2017). Moreover, spores not only confer an advantage in the ability to survive stress (such as antibiotic treatment), but they also promote dispersal, thereby overcoming the normal limitations imposed by unfavorable environmental conditions (Bengtsson-Palme et al., 2018; Tetz & Tetz, 2017).

Highly resistant bacteria are assumed to evolve mostly in clinical and animal environments due to the extensive use of antibiotics (Baquero, Martinez, & Canton, 2008). These antibiotic resistant bacteria are notably released in natural ecosystems via sewage effluent, hospital wastewater, agricultural/farming runoff, and/or aquaculture discharge (Marti, Variatza, & Balcazar, 2014; Taylor, Verner-Jeffreys, & Baker-Austin, 2011). Aquatic ecosystems are a key system to investigate the spread of antibiotic resistance genes in human-impacted environments. Due to their uses by humans, aquatic ecosystems constitute: (1) an end-point where resistance genes can accumulate (long-term reservoir), (2) a mix zone where human and environmental organisms can meet and exchange genetic material, and

(3) a pathway for bacterial dissemination and reintroduction into human environment via drinking water supply or recreational activities (Baquero et al., 2008; Taylor et al., 2011). Using DNA extracted from spores as a biological marker, a recent study investigating the dissemination of spore-associated antibiotic resistance genes (ARG) in sediments impacted by the release of treated wastewater demonstrated that spores can be a dispersal vector for the spread of ARG in the environment (Paul et al., 2018). Given the role of spores in cross-individual transmission (Kearney et al., 2018), it appears important to pay attention to this long-lasting fraction of the community.

Although antibiotic resistance is commonly associated with clinical environments, antibiotics and their corresponding resistance mechanisms are ancestral features that evolved long before the therapeutic use of antibiotics by humans (Aminov & Mackie, 2007; Bhullar et al., 2012; D'Costa et al., 2011). Little is known about the natural background of antibiotic resistance in natural ecosystems, and how the release of antibiotics and organisms bearing resistance determinants affects the pool of resistance genes present in human-impacted environments. D'Costa, McGrann, Hughes, and Wright (2006) notably revealed an unsuspected diversity and abundance of ARG in soil microbiomes, highlighting the potential reservoir function of the environment in allowing ARG to spread through various bacterial populations. This is of particular concern since antibiotic resistance can be acquired not only by mutation but also by horizontal gene transfer, which can occur between phylogenetically distant organisms (Courvalin, 1994). The pool of ARG in the environment represents a real threat for human health, with a risk of transmission of ARG from environmental organisms to pathogens and vice versa (Perry, Westman, & Wright, 2014; Taylor et al., 2011). Investigating the environmental accumulation of ARG in sedimentary archives based on DNA-dependent methods is biased, and therefore problematic, because the preservation of DNA in sediments is taxon-dependent and is influenced by multiple biotic and abiotic factors (Boere, Sinninghe Damsté, Rijpstra, Volkman, & Coolen, 2011). Taking advantage of the ability of spores to preserve their genetic material from degradation, a recent study demonstrated a clear correlation between the historical patterns of accumulation of particular ARG within the sporobiota and the timing of medical use of their related antibiotic in lake sediments (Madueno et al., 2018). Likewise, a correlation between these accumulation patterns and specific taxa of the sporobiota was shown in the same study.



9. Biotechnological applications of spore-forming bacteria

9.1 Plant growth promotion

Different groups of beneficial bacteria in the rhizosphere have positive interactions with plants through the colonization of roots and the promotion of plant growth. These bacteria are commonly known as plant growth promoting rhizobacteria (PGPR). PGPR can enhance plant growth either directly or indirectly. Direct mechanisms include fixation of atmospheric nitrogen, solubilization of inorganic phosphorus (Zaidi & Khan, 2007), production of siderophores (Rajkumar, Ae, Prasad, & Freitas, 2010) and of phytohormone (Hayat, Hayat, Irfan, & Ahmad, 2010). Indirect mechanisms include inhibiting the growth of plant pathogens by producing or secreting various chemicals like hydrogen cyanide, phenazines, pyrrol-nitrin and tensin (Bhattacharyya & Jha, 2012), or by promoting beneficial plant-microbe symbioses (e.g., stimulation of mycorrhizae development; Glick, 2012). Among the currently recognized PGPR, *Bacillus* is one of the best-studied examples. There are many species of *Bacillus* that are well known for having plant growth promoting activities (Kumar, Prakash, & Johri, 2011), and these have been commercialized through the availability of *Bacillus*-based biofertilizer products intended to replace chemical fertilizers, for instance, Serenade, Quantum-400, Alinit, Kodiak and Rhizovital (Radhakrishnan, Hashem, & Abd Allah, 2017).

Bacillus species are known to play a vital role in helping plants to withstand the osmotic stress caused by saline water or soil by limiting the uptake of sodium and chloride ions and by enhancing plant growth and seed germination (Jeschke & Wolf, 1988; Qurashi & Sabri, 2013). For instance, *Bacillus licheniformis* A2 has been reported as a salt-tolerant PGPR when applied to peanut plants (Goswami, Dhandhukia, Patel, & Thakker, 2014). Bioinoculation with *Bacillus megaterium* and *Pseudomonas aeruginosa* diminished salt induced cell death in rice (Jha & Subramanian, 2015). Likewise, *Bacillus amyloliquefaciens* NBRISN13, another salt-tolerant PGPR, is reported to mitigate the changes in microbial diversity in the rice rhizosphere in response to salt stress (Nautiyal et al., 2013). *Bacillus* spp. can also help plants by stimulating growth through increasing nutrient acquisition or phytohormone production (Bhattacharyya & Jha, 2012). As an example, screening of 14 different bacterial strains affiliated with *Bacillus* for their plant growth promoting activities showed that 10 out of 14 were capable

Table 2 Screening of 14 endospore forming bacterial strains for plant growth promoting activities.

Bacterial strains	Nitrogen fixation	Proteolysis	Siderophore production	Auxin-like phytohormone production
<i>Bacillus thuringiensis</i> 1312	+	+	+	+
<i>Bacillus thuringiensis</i> 1310	+	+	+	+
<i>Bacillus thuringiensis</i> 1318	+	+	+	–
<i>Bacillus thuringiensis</i> 1070	–	+	+	+
<i>Bacillus thuringiensis</i> 1311	+	+	+	–
<i>Bacillus thuringiensis</i> 1321	+	+	+	–
<i>Bacillus cereus</i> 1055	+	+	+	–
<i>Bacillus cereus</i> 88	–	+	+	–
<i>Bacillus licheniformis</i>	+	+	+	+
<i>Bacillus subtilis</i>	–	+	+	–
<i>Lysinibacillus sphaericus</i>	–	+	–	–
<i>Bacillus polymyxa</i>	+	+	–	–
<i>Bacillus weihenstephanensis</i>	+	+	+	–
<i>Bacillus pumilus</i>	+	+	–	–

+ Stands for activity measured; – stands for lack of the activity.

of nitrogen fixation, whereas all 14 were able to solubilize organic nitrogen (proteolysis), and 11 out of 14 were capable of siderophore production (Table 2). In addition, four of the 14 strains were able to produce auxin-like compounds (Table 2). *Bacillus* spp. are also known to produce cytokinin, gibberellins, and indole acetic acid; all of which can directly or indirectly affect plant growth and yield (Arkhipova, Veselov, Melentiev, Martynenko, & Kudoyarova, 2005; Radhakrishnan & Lee, 2016).

The genus *Bacillus* has also been used as a biocontrol agent against plant pathogens (O'Callaghan, 2016; Widnyana & Javandira, 2016). *Bacillus* spp. can produce a wide range of antiviral, antibacterial and antifungal compounds, which may be important in their interaction with plants and other soil microorganisms. These chemicals have significant commercial potential for increasing agricultural production (Niu et al., 2011). For instance, two antifungal compounds produced by *B. amyloliquefaciens* control the development

of the soil-borne plant pathogen *Fusarium oxysporum*. Moreover, it has been reported in many studies that *Bacillus* spp. are effective biocontrol candidates against diverse fungal diseases that are caused by soil-borne *Rhizoctonia solani*, for instance tomato root rot, damping-off, sheath blight of rice, and potato black scurf (Ben Khedher et al., 2015; Solanki et al., 2012; Yang, Wang, Wang, Chen, & Zhou, 2009). In addition to their use as bio-fungicides, *Bacillus* spp. have also been widely used as bio-insecticides in sustainable agriculture. For instance, *Bacillus thuringiensis* has been used as a broad range bio-insecticide that limits the growth of larvae of pest insects by fatally damaging the midgut epithelium (Radhakrishnan et al., 2017). There are many other *Bacillus* species that have also been used in pest management systems, including *B. amyloliquefaciens*, *B. subtilis*, and *B. cereus* (Gadhav & Gange, 2016).

In spite of the potential that plant inoculation with growth-promoting microorganisms has in promoting sustainable agriculture, ensuring the success of inoculations presents many challenges (Ahmad & Kibret, 2014; Bhattacharyya & Jha, 2012; Souza, Ambrosini, & Passaglia, 2015). One of the critical issues involves the survival of bacteria acclimated under laboratory conditions to the harsh conditions in soils. Inoculated microbes have to compete with autochthonous microbial communities (Souza et al., 2015) and are also vulnerable to the relatively low nutrient availability in natural environments compared to laboratory conditions. This often results in a decline in the numbers of the bio-inoculant in the soil overtime (Souza et al., 2015; Trabelsi & Mhamdi, 2013). Moreover, the delivery of these microorganisms in an active form is an additional challenge. Application of carrier materials for the protection of bio inoculants, for instance karnolite, peat, or charcoal, is not only environmentally unfriendly (i.e., extensive mining of peat and related adverse effect on climate) but also costly, making this approach not applicable in agriculture (Arora, Tiwari, & Singh, 2014). These concerns are the incentive to identify more efficient ways of inoculating bacteria into natural environments and increasing their survival. Because of this *Bacillus* and related endospore-forming bacteria may aid development of highly efficient inoculants, as the formation of endospores in response to unfavorable environmental conditions might promote persistence of *Bacillus* in soils (Radhakrishnan et al., 2017).

9.2 Drug delivery

The area of drug delivery is one of the rapidly growing areas of research in biotechnology in which spores are considered as a potential biologically

derived delivery system (Farjadian et al., 2018). Bacterial spores can be useful carriers for drugs, but also for nucleic acids or antigens. Some studies have explored the use of bacterial endospores from Firmicutes, as well as vehicles based on proteins from the spore coat for various applications including the presentation of heterologous antigens, vaccination, and delivery of therapeutic agents, among others (Ricca & Cutting, 2003). The direct use of endospores has also been considered, but there is a significant risk associated to germination and unwanted proliferation prior to reaching the target tissue. Nonetheless, endospores from a selected number of *Clostridium* spp. (more specifically *Clostridium histolyticum* and *Clostridium novyi* NT) have been considered in the treatment of cancer, as upon germination and vegetative growth, these species induced lysis of tumor cells (Minton, 2003) or tumor regression (Roberts et al., 2014). Another approach applicable in the case of cancer treatment is the selective expression of specific enzymes upon preferential germination in hypoxic tumors (Heap et al., 2014; Lambin et al., 1998). Recombinant bacterial spores have been also used to generate thermostable vaccines (Duc le, Hong, Fairweather, Ricca, & Cutting, 2003). It appears that a combined expression on the surface of the spore, as well as upon germination, is the best way to stimulate the immune system. Tests conducted so far show that multiple applications are required for immunization (Uyen, Hong, & Cutting, 2007). However, this is an area of research in which progress can be expected as shown by recent publications (Das, Thomas, Garnica, & Dhandayuthapani, 2016; Sibley et al., 2014).

One way in which spores can be used in therapeutic applications is by selecting for spores that respond to specific molecules as inducers of germination. We have tested this approach using oxalate as a signal molecule to trigger germination. Starting from pasteurized soil samples, spores germinating in response to this compound were enriched. The first enrichment clearly showed the presence of oxalate-degrading spore-forming bacteria, which can be purified and characterized (Fig. 4).

9.3 Bioremediation and biomineralization

The term biomineralization refers to the biologically induced and controlled mineralization processes that occur in nature. Microbes are major actors in biomineralization and are responsible for the formation of a wide range of minerals, from iron oxides to carbonates and silicates (Konhauser, Lalonde, & Phoenix, 2008). Although many bacteria have been shown to

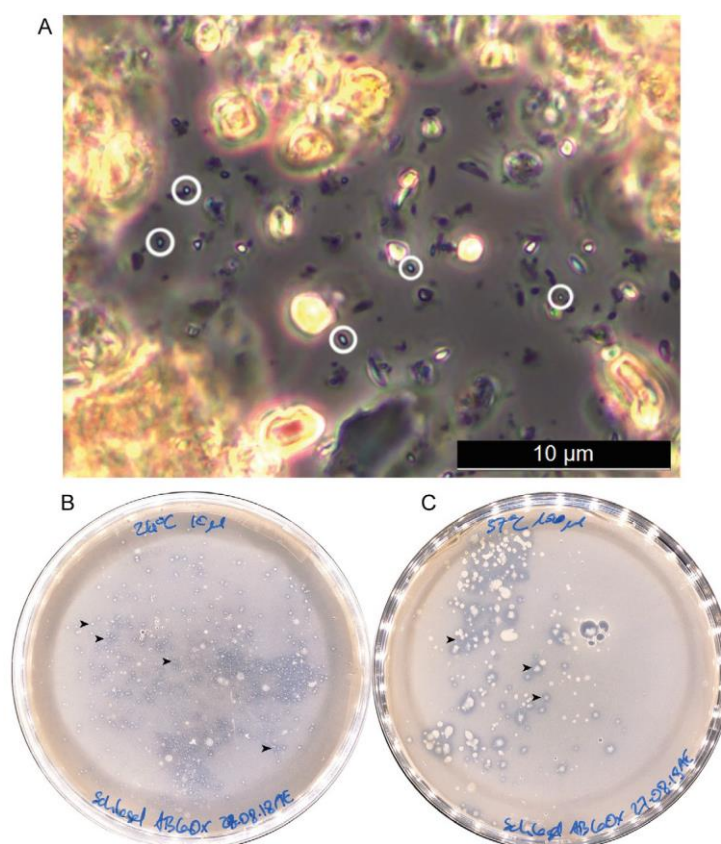


Fig. 4 Isolation of oxalotrophic endospore-forming bacteria from soil by using oxalic acid as a trigger of germination. (A) After a spore separation protocol, the presence of spores was verified by phase contrast microscopy before enrichment in liquid Schlegel AB medium with potassium oxalate as sole carbon and energy source. Spores are shown surrounded by a white circle. (B and C) Initial steps on the isolation of oxalotrophic endospore-forming bacteria on solid Schlegel AB medium with calcium oxalate as sole carbon source. Plates incubated at 24 °C (B) and 37 °C (C). Black arrows indicate the dissolution halos that confirm the presence of oxalotrophic bacteria.

be involved in biomineralization processes, only two cases of spores taking part in redox reactions have been well documented. Spores of *Bacillus* sp. can oxidize manganese (Francis & Tebo, 2002), while the anaerobe *Desulfotomaculum reducens* is able to reduce metals (uranium and iron) in its spore state (Junier et al., 2009). In the former case, this biomineralization process involves the presence of an enzyme responsible for manganese oxidation, multicopper oxidase (Francis & Tebo, 2002), which is localized at

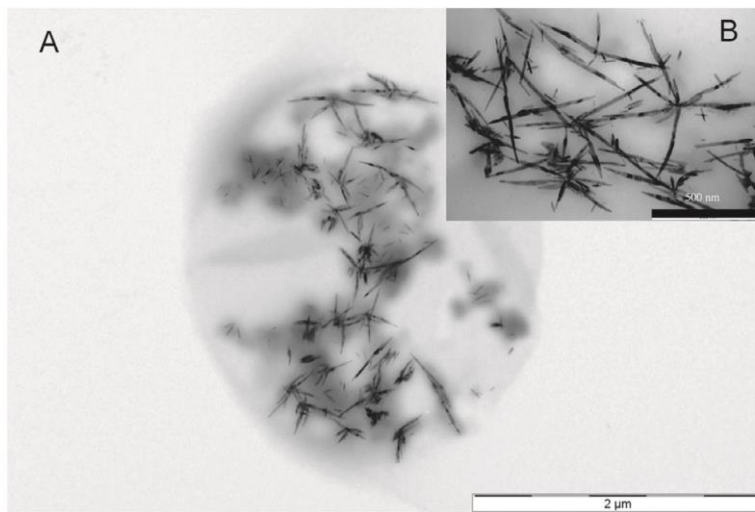


Fig. 5 Transmission electron microscopy (TEM) of Te(0) precipitates produced by *Desulfotomaculum reducens* after reduction of Te(IV). (A) Cell. (B) Close-up to the precipitate.

the exosporium layer of the spore (Francis, Casciotti, & Tebo, 2002). This enzyme was found among numerous *Bacillus* species (Dick, Torpey, Beveridge, & Tebo, 2008), and in agreement, a large fraction of spore-forming species isolated from the environment had shown the ability to oxidize manganese and to tolerate high copper concentrations (Ganesan et al., 2016). In the case of *D. reducens*, in addition of performing a redox active reaction, the spore coat was shown to act as a nucleation center for biomineralization of various metals and radionuclides (Junier et al., 2009) (Fig. 5).

Besides these two examples of reduction and oxidation of metals by spores, the vegetative cells of spore-forming bacteria can also play an important role in metal corrosion and remediation. Indeed, some studies with *Bacillus sphaericus* have shown that the proteinaceous surface layer (S-layer) interacts with uranium and other heavy metals to form nanocomplexes, which could lead to the immobilization and bioremediation of these elements (Merroun et al., 2005).

During a recent study investigating the phenomena of iron corrosion, we isolated spore-forming bacteria from the genus *Bacillus* (Fig. 6). These bacteria were obtained from iron plates that were corroded artificially in a

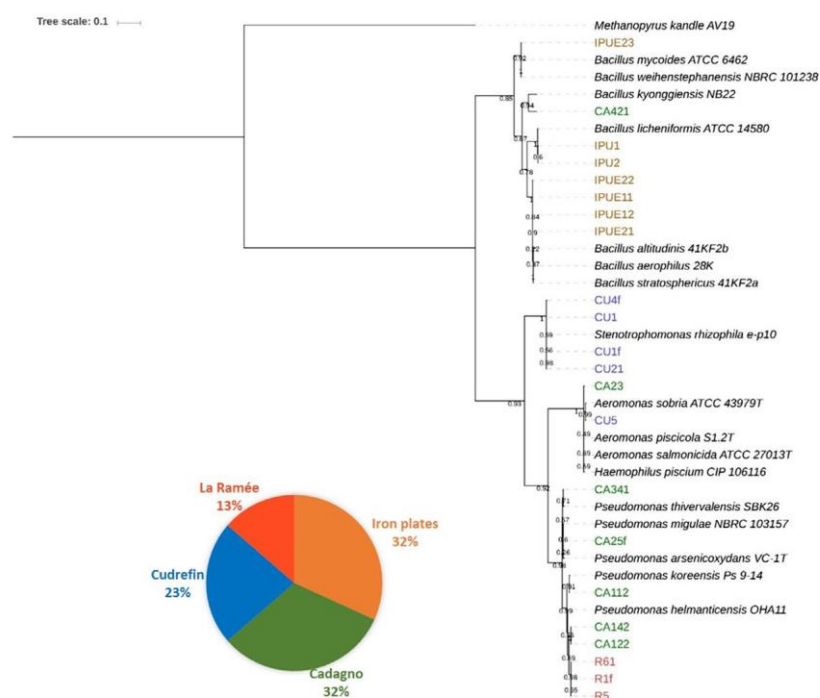


Fig. 6 Maximum likelihood phylogenetic tree describing the phylogenetic relationship between isolates obtained from corroded iron plates. Reference strains are indicated in the tree. The archaeon *Methanopyrus kandleri* was chosen as outgroup. Bootstrap values based on 100 replications were calculated and are expressed on the clades as decimal. The tree shows four main clusters: *Pseudomonas*, *Aeromonas*, *Stenotrophomonas* and *Bacillus*. All the *Bacillus* strains (code IPUE) were obtained from corroded iron plates treated with ethanol and UV. The other clades were enriched from sediments from different origins as described in the sector graph on the left where the percentage of selected isolates from each sampling location is mentioned.

marine environment and immersed in growth medium (LB) for 1 month. Prior to immersion, the plates were washed in a 70% ethanol bath and exposed for 1 h to UV light for cleaning purposes, suggesting their survival in the state of highly resistant spores. The physiological characterization of the strains showed that besides extreme tolerance to salt, most of the strains were able to partially reduce nitrate and iron (Table 3). Iron reduction was couple to the production of ferrous iron minerals, which is an additional example of the potential use of spore-forming bacteria in biomineralization and bioremediation.

Table 3 Summary of the metabolic characteristics of *Bacillus* spp. isolated from corroded iron plates.

Isolate ID	IPU1	IPU2	IPUE11	IPUE12	IPUE21	IPUE22	IPUE23
Nitrate reduction							
Growth NB + KNO ₃	+	++	+	+	+	±	+
N ₂ production	–	–	–	–	–	–	–
Nitrite production	+	+	–	+	+	+	+
Growth in NaCl (%)							
0	++	++	++	++	++	++	++
2	++	++	+	+	+++	+++	++
4	+	+	+	+	+++	+++	+
6	+	+	+	+	+	+	±
8	+	+	+	+	+	+	–
10	±	±	+	+	+	+	–
Fe(III) reduction with 2% NaCl	–	–	+	–	+	–	+
Optimal temperature (°C)	nd	nd	40	nd	40	nd	30
Optimal pH	nd	nd	6.5–7.5	nd	6.5	nd	7.5



10. Conclusion

Bacterial spores have been known since the dawn of microbiology. Although still seen largely from the perspective of their importance in disease and human health (especially in the case of endospores), bacterial survival in the form of a highly resistance cellular form is likely to be relevant in other ecosystem processes. The basic understanding of the diversity and ecology of spore-formers has direct applications in a diverse range of fields in biotechnology. Nevertheless, in order to advance in this domain, additional tailored tools combining molecular approaches and culture-based techniques are still required. The formation of spores might have been an essential part of the toolkit of early evolving bacteria and is relevant to discuss the resilience of life in a changing planet, as well as the potential existence of life beyond Earth.

Acknowledgments

The authors acknowledge funding from the Swiss National Science Foundation through grants 31003A_179297 (P.J.), CR3212_162810 (P.J., T.V.), and P2NEP3_178561 (S.F.); the Novartis Foundation through the FreeNovation program; and the U.S. Department of Energy Biological and Environmental Research Division through a Science Focus Area grant to P.S.C. and P.J. (Grant number KP1601010).

References

- Abecasis, A. B., Serrano, M., Alves, R., Quintais, L., Pereira-Leal, J. B., & Henriques, A. O. (2013). A genomic signature and the identification of new sporulation genes. *Journal of Bacteriology*, *195*(9), 2101–2115. <https://doi.org/10.1128/JB.02110-12>.
- Abel-Santos, E. (2012). *Bacterial spores: Current research and applications*. Caister Academic Press.
- Ahemad, M., & Kibret, M. (2014). Mechanisms and applications of plant growth promoting rhizobacteria: Current perspective. *Journal of King Saud University—Science*, *26*(1), 1–20. <https://doi.org/10.1016/j.jksus.2013.05.001>.
- Amann, R. I., Ludwig, W., & Schleifer, K. H. (1995). Phylogenetic identification and in situ detection of individual microbial cells without cultivation. *Microbiological Reviews*, *59*(1), 143–169.
- Aminov, R. I., & Mackie, R. I. (2007). Evolution and ecology of antibiotic resistance genes. *FEMS Microbiology Letters*, *271*(2), 147–161. <https://doi.org/10.1111/j.1574-6968.2007.00757.x>.
- Ariztegui, D., Thomas, C., & Vuillemin, A. (2015). Present and future of subsurface biosphere studies in lacustrine sediments through scientific drilling. *International Journal of Earth Sciences*, *104*, 1–11. <https://doi.org/10.1007/s00531-015-1148-4>.
- Arkhipova, T. N., Veselov, S. U., Melentiev, A. I., Martynenko, E. V., & Kudoyarova, G. R. (2005). Ability of bacterium *Bacillus subtilis* to produce cytokinins and to influence the growth and endogenous hormone content of lettuce plants. *Plant and Soil*, *272*(1), 201–209. <https://doi.org/10.1007/s11104-004-5047-x>.
- Aronoff, D. M. (2013). *Clostridium novyi*, *sordellii*, and *tetani*: Mechanisms of disease. *Anaerobe*, *24*, 98–101. <https://doi.org/10.1016/j.anaerobe.2013.08.009>.
- Arora, N. K., Tiwari, S., & Singh, R. (2014). Comparative study of different carriers inoculated with nodule forming and free living plant growth promoting bacteria suitable for sustainable agriculture. *Journal of Plant Pathology & Microbiology*, *5*, 229. <https://doi.org/10.4172/2157-7471.1000229>.
- Baquero, F., Martinez, J. L., & Canton, R. (2008). Antibiotics and antibiotic resistance in water environments. *Current Opinion in Biotechnology*, *19*(3), 260–265. <https://doi.org/10.1016/j.copbio.2008.05.006>.
- Bartholomew, J. W., & Paik, G. (1966). Isolation and identification of obligate thermophilic sporeforming bacilli from ocean basin cores. *Journal of Bacteriology*, *92*(3), 635–638.
- Barton, L. L. (2005). *Structural and functional relationships in prokaryotes*. Springer Science & Business Media.
- Bell, E., Blake, L. I., Sherry, A., Head, I. M., & Hubert, C. R. J. (2018). Distribution of thermophilic endospores in a temperate estuary indicate that dispersal history structures sediment microbial communities. *Environmental Microbiology*, *20*(3), 1134–1147. <https://doi.org/10.1111/1462-2920.14056>.
- Ben Khedher, S., Kilani-Feki, O., Dammak, M., Jabnoun-Khiareddine, H., Daami-Remadi, M., & Tounsi, S. (2015). Efficacy of *Bacillus subtilis* V26 as a biological control agent against *Rhizoctonia solani* on potato. *Comptes Rendus Biologies*, *338*(12), 784–792. <https://doi.org/10.1016/j.crvi.2015.09.005>.

- Bengtsson-Palme, J., Kristiansson, E., & Larsson, D. G. J. (2018). Environmental factors influencing the development and spread of antibiotic resistance. *FEMS Microbiology Reviews*, 42(1). <https://doi.org/10.1093/femsre/fux053>, fux053.
- Bhattacharyya, P. N., & Jha, D. K. (2012). Plant growth-promoting rhizobacteria (PGPR): Emergence in agriculture. *World Journal of Microbiology and Biotechnology*, 28(4), 1327–1350. <https://doi.org/10.1007/s11274-011-0979-9>.
- Bhullar, K., Waglechner, N., Pawlowski, A., Koteva, K., Banks, E. D., Johnston, M. D., et al. (2012). Antibiotic resistance is prevalent in an isolated cave microbiome. *PLoS One*, 7(4), e34953. <https://doi.org/10.1371/journal.pone.0034953>.
- Boere, A. C., Sinnighe Damsté, J. S., Rijpstra, W. I. C., Volkman, J. K., & Coolen, M. J. L. (2011). Source-specific variability in post-depositional DNA preservation with potential implications for DNA based paleoecological records. *Organic Geochemistry*, 42(10), 1216–1225. <https://doi.org/10.1016/j.orggeochem.2011.08.005>.
- Browne, H. P., Forster, S. C., Anonye, B. O., Kumar, N., Neville, B. A., Stares, M. D., et al. (2016). Culturing of ‘unculturable’ human microbiota reveals novel taxa and extensive sporulation. *Nature*, 533(7604), 543–546. <https://doi.org/10.1038/nature17645>.
- Bueche, M., Wunderlin, T., Roussel-Delif, L., Junier, T., Sauvain, L., Jeanneret, N., et al. (2013). Quantification of endospore-forming firmicutes by quantitative PCR with the functional gene *spo0A*. *Applied and Environmental Microbiology*, 79(17), 5302–5312. <https://doi.org/10.1128/AEM.01376-13>.
- Buerger, S., Spoering, A., Gavrish, E., Leslin, C., Ling, L., & Epstein, S. S. (2012). Microbial scout hypothesis and microbial discovery. *Applied and Environmental Microbiology*, 78(9), 3229–3233. <https://doi.org/10.1128/AEM.07308-11>.
- Callahan, H. S., Maughan, H., & Steiner, U. K. (2008). Phenotypic plasticity, costs of phenotypes, and costs of plasticity: Toward an integrative view. *Annals of the New York Academy of Sciences*, 1133, 44–66. <https://doi.org/10.1196/annals.1438.008>.
- Chen, B., Teh, B. S., Sun, C., Hu, S., Lu, X., Boland, W., et al. (2016). Biodiversity and activity of the gut microbiota across the life history of the insect herbivore *Spodoptera littoralis*. *Scientific Reports*, 6, 29505. <https://doi.org/10.1038/srep29505>.
- Clarke, S. F., Murphy, E. F., Nilaweera, K., Ross, P. R., Shanahan, F., O’Toole, P. W., et al. (2012). The gut microbiota and its relationship to diet and obesity: New insights. *Gut Microbes*, 3(3), 186–202. <https://doi.org/10.4161/gmic.20168>.
- Courvalin, P. (1994). Transfer of antibiotic resistance genes between gram-positive and gram-negative bacteria. *Antimicrobial Agents and Chemotherapy*, 38(7), 1447–1451.
- Das, K., Thomas, T., Garnica, O., & Dhandayuthapani, S. (2016). Recombinant spore delivered *M. tuberculosis* antigens elicit immune response in mice. *The Journal of Immunology*, 196(1 Supplement), 145.4.
- D’Costa, V. M., King, C. E., Kalan, L., Morar, M., Sung, W. W., Schwarz, C., et al. (2011). Antibiotic resistance is ancient. *Nature*, 477(7365), 457–461. <https://doi.org/10.1038/nature10388>.
- D’Costa, V. M., McGrann, K. M., Hughes, D. W., & Wright, G. D. (2006). Sampling the antibiotic resistome. *Science*, 311(5759), 374–377. <https://doi.org/10.1126/science.1120800>.
- de Hoon, M. J., Eichenberger, P., & Vitkup, D. (2010). Hierarchical evolution of the bacterial sporulation network. *Current Biology*, 20(17), R735–R745. <https://doi.org/10.1016/j.cub.2010.06.031>.
- de Rezende, J. R., Kjeldsen, K. U., Hubert, C. R., Finster, K., Loy, A., & Jorgensen, B. B. (2013). Dispersal of thermophilic *Desulfotomaculum* endospores into Baltic Sea sediments over thousands of years. *The ISME Journal*, 7(1), 72–84. <https://doi.org/10.1038/ismej.2012.83>.
- Dick, G. J., Torpey, J. W., Beveridge, T. J., & Tebo, B. M. (2008). Direct identification of a bacterial manganese(II) oxidase, the multicopper oxidase MnxG, from spores of several

- different marine *Bacillus* species. *Applied and Environmental Microbiology*, 74(5), 1527–1534. <https://doi.org/10.1128/AEM.01240-07>.
- Dressler, M., Huebener, T., Goers, S., Werner, P., & Selig, U. (2007). Multi-proxy reconstruction of trophic state, hypolimnetic anoxia and phototrophic sulphur bacteria abundance in a dimictic lake in Northern Germany over the past 80 years. *Journal of Paleolimnology*, 37(2), 205–219. <https://doi.org/10.1007/s10933-006-9013-x>.
- Driks, A. (2002). Overview: Development in bacteria: Spore formation in *Bacillus subtilis*. *Cellular and Molecular Life Sciences*, 59(3), 389–391.
- Duc le, H., Hong, H. A., Fairweather, N., Ricca, E., & Cutting, S. M. (2003). Bacterial spores as vaccine vehicles. *Infection and Immunity*, 71(5), 2810–2818.
- Engel, P., & Moran, N. A. (2013). The gut microbiota of insects—Diversity in structure and function. *FEMS Microbiology Reviews*, 37(5), 699–735. <https://doi.org/10.1111/1574-6976.12025>.
- Farjadian, F., Moghoofoei, M., Mirkiani, S., Ghasemi, A., Rabiee, N., Hadifar, S., et al. (2018). Bacterial components as naturally inspired nano-carriers for drug/gene delivery and immunization: Set the bugs to work? *Biotechnology Advances*, 36(4), 968–985. <https://doi.org/10.1016/j.biotechadv.2018.02.016>.
- Fichtel, J., Koster, J., Rullkotter, J., & Sass, H. (2007). Spore dipicolinic acid contents used for estimating the number of endospores in sediments. *FEMS Microbiology Ecology*, 61(3), 522–532. <https://doi.org/10.1111/j.1574-6941.2007.00354.x>.
- Filippidou, S., Junier, T., Wunderlin, T., Lo, C. C., Li, P. E., Chain, P. S., et al. (2015). Under-detection of endospore-forming Firmicutes in metagenomic data. *Computational and Structural Biotechnology Journal*, 13, 299–306. <https://doi.org/10.1016/j.csbj.2015.04.002>.
- Filippidou, S., Wunderlin, T., Junier, T., Jeanneret, N., Dorador, C., Molina, V., et al. (2016). A combination of extreme environmental conditions favor the prevalence of endospore-forming firmicutes. *Frontiers in Microbiology*, 7, 1707 (eCollection 2016).
- Francis, C. A., Casciotti, K. L., & Tebo, B. M. (2002). Localization of Mn(II)-oxidizing activity and the putative multicopper oxidase, MnxG, to the exosporium of the marine *Bacillus* sp. strain SG-1. *Archives of Microbiology*, 178(6), 450–456. <https://doi.org/10.1007/s00203-002-0472-9>.
- Francis, C. A., & Tebo, B. M. (2002). Enzymatic manganese(II) oxidation by metabolically dormant spores of diverse *Bacillus* species. *Applied and Environmental Microbiology*, 68(2), 874–880.
- Gadhav, K. R., & Gange, A. C. (2016). Plant-associated *Bacillus* spp. alter life-history traits of the specialist insect *Brevicoryne brassicae* L. *Agricultural and Forest Entomology*, 18(1), 35–42. <https://doi.org/10.1111/afe.12131>.
- Galperin, M. Y., Mekhedov, S. L., Puigbo, P., Smirnov, S., Wolf, Y. I., & Rigden, D. J. (2012). Genomic determinants of sporulation in Bacilli and Clostridia: Towards the minimal set of sporulation-specific genes. *Environmental Microbiology*, 14(11), 2870–2890. <https://doi.org/10.1111/j.1462-2920.2012.02841.x>.
- Ganesan, S., Philippidou, S., Junier, T., Rufatt, P. M., Jeanneret, N., Wunderlin, T., et al. (2016). Manganese-II oxidation and Copper-II resistance in endospore forming Firmicutes isolated from uncontaminated environmental sites. *AIMS Environmental Science*, 3(2), 220–238. <https://doi.org/10.3934/environsci.2016.2.220>.
- Glick, B. R. (2012). Plant growth-promoting bacteria: Mechanisms and applications. *Scientifica*, 2012, 15. <https://doi.org/10.6064/2012/963401>.
- Gorham, E., Brush, G. S., Graumlich, L. J., Rosenzweig, M. L., & Johnson, A. H. (2001). The value of paleoecology as an aid to monitoring ecosystems and landscapes, chiefly with reference to North America. *Environmental Reviews*, 9(2), 99–126. <https://doi.org/10.1139/a01-003>.

- Goswami, D., Dhandhukia, P., Patel, P., & Thakker, J. N. (2014). Screening of PGPR from saline desert of Kutch: Growth promotion in *Arachis hypogea* by *Bacillus licheniformis* A2. *Microbiological Research*, *169*(1), 66–75. <https://doi.org/10.1016/j.micres.2013.07.004>.
- Hayat, Q., Hayat, S., Irfan, M., & Ahmad, A. (2010). Effect of exogenous salicylic acid under changing environment: A review. *Environmental and Experimental Botany*, *68*(1), 14–25. <https://doi.org/10.1016/j.envexpbot.2009.08.005>.
- Heap, J. T., Theys, J., Ehsaan, M., Kubiak, A. M., Dubois, L., Paesmans, K., et al. (2014). Spores of *Clostridium* engineered for clinical efficacy and safety cause regression and cure of tumors in vivo. *Oncotarget*, *5*(7), 1761–1769. <https://doi.org/10.18632/oncotarget.1761>.
- Hofler, C., Heckmann, J., Fritsch, A., Popp, P., Gebhard, S., Fritz, G., et al. (2016). Cannibalism stress response in *Bacillus subtilis*. *Microbiology*, *162*(1), 164–176. <https://doi.org/10.1099/mic.0.000176>.
- Hubert, C., Arnosti, C., Bruchert, V., Loy, A., Vandieken, V., & Jorgensen, B. B. (2010). Thermophilic anaerobes in Arctic marine sediments induced to mineralize complex organic matter at high temperature. *Environmental Microbiology*, *12*(4), 1089–1104. <https://doi.org/10.1111/j.1462-2920.2010.02161.x>.
- Hubert, C., Loy, A., Nickel, M., Arnosti, C., Baranyi, C., Bruchert, V., et al. (2009). A constant flux of diverse thermophilic bacteria into the cold Arctic seabed. *Science*, *325*(5947), 1541–1544. <https://doi.org/10.1126/science.1174012>.
- Hugenholtz, P. (2002). Exploring prokaryotic diversity in the genomic era. *Genome Biology*, *3*(2), reviews0003.1–0003.8.
- Hutchison, E. A., Miller, D. A., & Angert, E. R. (2014). Sporulation in bacteria: Beyond the standard model. *Microbiology Spectrum*, *2*(5). <https://doi.org/10.1128/microbiolspec.TBS-0013-2012>, TBS-0013-2012.
- Izumi, H., Anderson, I. C., Alexander, I. J., Killham, K., & Moore, E. R. (2006). Endobacteria in some ectomycorrhiza of Scots pine (*Pinus sylvestris*). *FEMS Microbiology Ecology*, *56*(1), 34–43. <https://doi.org/10.1111/j.1574-6941.2005.00048.x>.
- Jeschke, W. D., & Wolf, O. (1988). External potassium supply is not required for root growth in saline conditions: Experiments with *Ricinus communis* L. grown in a reciprocal split root-system. *Journal of Experimental Botany*, *39*(206), 1149–1167.
- Jha, Y., & Subramanian, R. B. (2015). Reduced cell death and improved cell membrane integrity in rice under salinity by root associated bacteria. *Theoretical and Experimental Plant Physiology*, *27*(3), 227–235. <https://doi.org/10.1007/s40626-015-0047-1>.
- Junier, P., Frutschi, M., Wigginton, N. S., Schofield, E. J., Bargar, J. R., & Bernier-Latmani, R. (2009). Metal reduction by spores of *Desulfotomaculum reducens*. *Environmental Microbiology*, *11*(12), 3007–3017. <https://doi.org/10.1111/j.1462-2920.2009.02003.x>.
- Justice, S. S., Hunstad, D. A., Cegelski, L., & Hultgren, S. J. (2008). Morphological plasticity as a bacterial survival strategy. *Nature Reviews Microbiology*, *6*(2), 162–168. <https://doi.org/10.1038/nrmicro1820>.
- Kearney, S. M., Gibbons, S. M., Poyet, M., Gurry, T., Bullock, K., Allegritti, J. R., et al. (2018). Endospores and other lysis-resistant bacteria comprise a widely shared core community within the human microbiota. *The ISME Journal*, *12*, 2403–2416. <https://doi.org/10.1038/s41396-018-0192-z>.
- Keenan, S. W., Engel, A. S., & Elsey, R. M. (2013). The alligator gut microbiome and implications for archosaur symbioses. *Scientific Reports*, *3*, 2877. <https://doi.org/10.1038/srep02877>.
- Kim, D., Song, L., Breitwieser, F. P., & Salzberg, S. L. (2016). Centrifuge: Rapid and sensitive classification of metagenomic sequences. *Genome Research*, *26*(12), 1721–1729. <https://doi.org/10.1101/gr.210641.116>.

- Koliada, A., Syzenko, G., Moseiko, V., Budovska, L., Puchkov, K., Perederiy, V., et al. (2017). Association between body mass index and Firmicutes/Bacteroidetes ratio in an adult Ukrainian population. *BMC Microbiology*, 17(1), 120. <https://doi.org/10.1186/s12866-017-1027-1>.
- Konhauser, K. O., Lalonde, S. V., & Phoenix, V. R. (2008). Bacterial biomineralization: Where to from here? *Geobiology*, 6(3), 298–302. <https://doi.org/10.1111/j.1472-4669.2008.00151.x>.
- Kreft, J. U. (2004). Biofilms promote altruism. *Microbiology*, 150(Pt. 8), 2751–2760. <https://doi.org/10.1099/mic.0.26829-0>.
- Kumar, A., Prakash, A., & Johri, B. N. (2011). Bacillus as PGPR in crop ecosystem bacteria in agrobiolgy: Crop ecosystems. In D. K. Maheshwari (Ed.), *Bacteria in agrobiolgy: Crop ecosystems* (pp. 37–59). Springer Berlin Heidelberg.
- Lambin, P., Theys, J., Landuyt, W., Rijken, P., van der Kogel, A., van der Schueren, E., et al. (1998). Colonisation of Clostridium in the body is restricted to hypoxic and necrotic areas of tumours. *Anaerobe*, 4(4), 183–188. <https://doi.org/10.1006/anae.1998.0161>.
- Lennon, J. T., & Jones, S. E. (2011). Microbial seed banks: The ecological and evolutionary implications of dormancy. *Nature Reviews Microbiology*, 9(2), 119–130. <https://doi.org/10.1038/nrmicro2504>.
- Levin-Reisman, I., Ronin, I., Gefen, O., Braniss, I., Shores, N., & Balaban, N. Q. (2017). Antibiotic tolerance facilitates the evolution of resistance. *Science*, 355(6327), 826–830. <https://doi.org/10.1126/science.aaj2191>.
- Loiko, N. G., Kryazhevskikh, N. A., Suzina, N. E., Demkina, E. V., Muratova, A. Y., Turkovskaya, O. V., et al. (2011). Resting forms of Sinorhizobium meliloti. *Microbiology*, 80(4), 472. <https://doi.org/10.1134/s0026261711040126>.
- Loiko, N. G., Soina, V. S., Sorokin, D. Y., Mityushina, L. L., & El'-Registan, G. I. (2003). Production of resting forms by the gram-negative chemolithoautotrophic bacteria Thioalkalivibrio versutus and Thioalkalimicrobium aerophilum. *Microbiology*, 72(3), 285–294. <https://doi.org/10.1023/a:1024291730779>.
- Lomstein, B. A., Langerhuus, A. T., D'Hondt, S., Jorgensen, B. B., & Spivack, A. J. (2012). Endospore abundance, microbial growth and necromass turnover in deep sub-seafloor sediment. *Nature*, 484(7392), 101–104. <https://doi.org/10.1038/nature10905>.
- Madueno, L., Paul, C., Junier, T., Bayrychenko, Z., Filippidou, S., Beck, K., et al. (2018). A historical legacy of antibiotic utilization on bacterial seed banks in sediments. *PeerJ*, e4197. <https://doi.org/10.7717/peerj.4197>.
- Mao, S., Zhang, M., Liu, J., & Zhu, W. (2015). Characterising the bacterial microbiota across the gastrointestinal tracts of dairy cattle: Membership and potential function. *Scientific Reports*, 5, 16116. <https://doi.org/10.1038/srep16116>.
- Marti, E., Variatza, E., & Balcazar, J. L. (2014). The role of aquatic ecosystems as reservoirs of antibiotic resistance. *Trends in Microbiology*, 22(1), 36–41. <https://doi.org/10.1016/j.tim.2013.11.001>.
- Martiny, J. B. H., Bohannan, B. J. M., Brown, J. H., Colwell, R. K., Fuhrman, J. A., Green, J. L., et al. (2006). Microbial biogeography: Putting microorganisms on the map. *Nature Reviews Microbiology*, 4, 102. <https://doi.org/10.1038/nrmicro1341>.
- McKenzie, V. J., Song, S. J., Delsuc, F., Prest, T. L., Oliverio, A. M., Korpita, T. M., et al. (2017). The effects of captivity on the mammalian gut microbiome. *Integrative and Comparative Biology*, 57(4), 690–704. <https://doi.org/10.1093/icb/ix090>.
- Merroun, M. L., Raff, J., Rossberg, A., Hennig, C., Reich, T., & Selenska-Pobell, S. (2005). Complexation of uranium by Cells and S-layer Sheets of Bacillus sphaericus JG-A12. *Applied and Environmental Microbiology*, 71(9), 5532.
- Miller, I. J., Weyna, T. R., Fong, S. S., Lim-Fong, G. E., & Kwan, J. C. (2016). Single sample resolution of rare microbial dark matter in a marine invertebrate metagenome. *Scientific Reports*, 6, 34362. <https://doi.org/10.1038/srep34362>.

- Minton, N. P. (2003). Clostridia in cancer therapy. *Nature Reviews. Microbiology*, 1(3), 237–242. <https://doi.org/10.1038/nrmicro777>.
- Mukhopadhyay, I., Morais, S., Laverde-Gomez, J., Sheridan, P. O., Walker, A. W., Kelly, W., et al. (2018). Sporulation capability and amylosome conservation among diverse human colonic and rumen isolates of the keystone starch-degrader *Ruminococcus bromii*. *Environmental Microbiology*, 20(1), 324–336. <https://doi.org/10.1111/1462-2920.14000>.
- Muller, A. L., de Rezende, J. R., Hubert, C. R., Kjeldsen, K. U., Lagkouvardos, I., Berry, D., et al. (2014). Endospores of thermophilic bacteria as tracers of microbial dispersal by ocean currents. *The ISME Journal*, 8(6), 1153–1165. <https://doi.org/10.1038/ismej.2013.225>.
- Mulyukin, A. L., Demkina, E. V., Kryazhevskikh, N. A., Suzina, N. E., Vorob'eva, L. I., Duda, V. I., et al. (2009). Dormant forms of *Micrococcus luteus* and *Arthrobacter globiformis* not platable on standard media. *Microbiology*, 78(4), 407–418. <https://doi.org/10.1134/s0026261709040031>.
- Nautiyal, C. S., Srivastava, S., Chauhan, P. S., Seem, K., Mishra, A., & Sopory, S. K. (2013). Plant growth-promoting bacteria *Bacillus amyloliquefaciens* NBRISN13 modulates gene expression profile of leaf and rhizosphere community in rice during salt stress. *Plant Physiology and Biochemistry*, 66, 1–9. <https://doi.org/10.1016/j.plaphy.2013.01.020>.
- Nealson, K. H. (1997). Sediment bacteria: Who's there, what are they doing, and what's new? *Annual Review of Earth and Planetary Sciences*, 25(1), 403–434. <https://doi.org/10.1146/annurev.earth.25.1.403>.
- Nelson, K. E. (2015). An update on the status of current research on the mammalian microbiome. *ILAR Journal*, 56(2), 163–168. <https://doi.org/10.1093/ilar/ilv033>.
- Nelson, T. M., Rogers, T. L., & Brown, M. V. (2013). The gut bacterial community of mammals from marine and terrestrial habitats. *PLoS One*, 8(12), e83655. <https://doi.org/10.1371/journal.pone.0083655>.
- Nicholson, W. L. (2002). Roles of *Bacillus* endospores in the environment. *Cellular and Molecular Life Sciences*, 59(3), 410–416.
- Nicholson, W. L., Munakata, N., Horneck, G., Melosh, H. J., & Setlow, P. (2000). Resistance of *Bacillus* endospores to extreme terrestrial and extraterrestrial environments. *Microbiology and Molecular Biology Reviews*, 64(3), 548–572.
- Nilsson, M., & Renberg, I. (1990). Viable endospores of *Thermoactinomyces vulgaris* in lake sediments as indicators of agricultural history. *Applied and Environmental Microbiology*, 56(7), 2025–2028.
- Nisbet, E. G., & Sleep, N. H. (2001). The habitat and nature of early life. *Nature*, 409, 1083. <https://doi.org/10.1038/35059210>.
- Niu, D.-D., Liu, H.-X., Jiang, C.-H., Wang, Y.-P., Wang, Q.-Y., Jin, H.-L., et al. (2011). The plant growth-promoting rhizobacterium *Bacillus cereus* AR156 induces systemic resistance in *Arabidopsis thaliana* by simultaneously activating salicylate- and jasmonate/ethylene-dependent signaling pathways. *The American Phytopathological Society*, 24, 533–542. <https://doi.org/10.1094/MPMI-09-10-0213>.
- O'Callaghan, M. (2016). Microbial inoculation of seed for improved crop performance: Issues and opportunities. *Applied Microbiology and Biotechnology*, 100(13), 5729–5746. <https://doi.org/10.1007/s00253-016-7590-9>.
- Paul, C., Bayrychenko, Z., Junier, T., Filippidou, S., Beck, K., Bueche, M., et al. (2018). Dissemination of antibiotic resistance genes associated with the sporobiota in sediments impacted by wastewater. *PeerJ*, 6, e4989. <https://doi.org/10.7717/peerj.4989>.
- Perry, J. A., Westman, E. L., & Wright, G. D. (2014). The antibiotic resistome: What's new? *Current Opinion in Microbiology*, 21, 45–50. <https://doi.org/10.1016/j.mib.2014.09.002>.
- Philippot, L., Bru, D., Saby, N. P. A., Čuhel, J., Arrouays, D., Šimek, M., et al. (2009). Spatial patterns of bacterial taxa in nature reflect ecological traits of deep branches of the 16S

- rRNA bacterial tree. *Environmental Microbiology*, 11(12), 3096–3104. <https://doi.org/10.1111/j.1462-2920.2009.02014.x>.
- Pope, C. F., McHugh, T. D., & Gillespie, S. H. (2010). Methods to determine fitness in bacteria. *Methods in Molecular Biology*, 642, 113–121. https://doi.org/10.1007/978-1-60327-279-7_9.
- Qurashi, A. W., & Sabri, A. N. (2013). Osmolyte accumulation in moderately halophilic bacteria improves salt tolerance of chickpea. *Pakistan Journal of Botany*, 45(3), 1011–1016.
- Radhakrishnan, R., Hashem, A., & Abd Allah, E. F. (2017). Bacillus: A biological tool for crop improvement through bio-molecular changes in adverse environments. *Frontiers in Physiology*, 8, 667. <https://doi.org/10.3389/fphys.2017.00667>.
- Radhakrishnan, R., & Lee, I. J. (2016). Gibberellins producing *Bacillus methylotrophicus* KE2 supports plant growth and enhances nutritional metabolites and food values of lettuce. *Plant Physiology and Biochemistry*, 109, 181–189. <https://doi.org/10.1016/j.plaphy.2016.09.018>.
- Rajkumar, M., Ae, N., Prasad, M. N., & Freitas, H. (2010). Potential of siderophore-producing bacteria for improving heavy metal phytoextraction. *Trends in Biotechnology*, 28(3), 142–149. <https://doi.org/10.1016/j.tibtech.2009.12.002>.
- Renberg, I., & Nilsson, M. (1992). Dormant bacteria in lake sediments as palaeoecological indicators. *Journal of Paleolimnology*, 7(2), 127–135. <https://doi.org/10.1007/bf00196867>.
- Ricca, E., & Cutting, S. M. (2003). Emerging applications of bacterial spores in nanobiotechnology. *Journal of Nanobiotechnology*, 1(1), 6. <https://doi.org/10.1186/1477-3155-1-6>.
- Rinke, C., Schwientek, P., Sczyrba, A., Ivanova, N. N., Anderson, I. J., Cheng, J. F., et al. (2013). Insights into the phylogeny and coding potential of microbial dark matter. *Nature*, 499(7459), 431–437. <https://doi.org/10.1038/nature12352>.
- Roberts, N. J., Zhang, L., Janku, F., Collins, A., Bai, R. Y., Staedtke, V., et al. (2014). Intratumoral injection of *Clostridium novyi*-NT spores induces antitumor responses. *Science Translational Medicine*, 6(249), 249ra111. <https://doi.org/10.1126/scitranslmed.3008982>.
- Rothfuss, F., Bender, M., & Conrad, R. (1997). Survival and activity of bacteria in a deep, aged lake sediment (Lake Constance). *Microbial Ecology*, 33(1), 69–77. <https://doi.org/10.1007/s002489900009>.
- Sadasivan, L., & Neyra, C. A. (1985). Flocculation in *Azospirillum brasilense* and *Azospirillum lipoferum*: Exopolysaccharides and cyst formation. *Journal of Bacteriology*, 163(2), 716–723.
- Santos-Pereira, I., Rizzardi, K., Castelo, P., Ferraz, L., Darrieux, M., & Parisotto, T. (2018). Childhood obesity and Firmicutes/Bacteroidetes ratio in the gut microbiota: A systematic review. *Childhood Obesity*. <https://doi.org/10.1089/chi.2018.0040> (online).
- Seaward, M. R. D., Cross, T., & Unsworth, B. A. (1976). Viable bacterial spores recovered from an archaeological excavation. *Nature*, 261(5559), 407–408.
- Shoemaker, W. R., & Lennon, J. T. (2018). Evolution with a seed bank: The population genetic consequences of microbial dormancy. *Evolutionary Applications*, 11(1), 60–75. <https://doi.org/10.1111/eva.12557>.
- Sibley, L., Reljic, R., Radford, D. S., Huang, J. M., Hong, H. A., Cranenburgh, R. M., et al. (2014). Recombinant *Bacillus subtilis* spores expressing MPT64 evaluated as a vaccine against tuberculosis in the murine model. *FEMS Microbiology Letters*, 358(2), 170–179. <https://doi.org/10.1111/1574-6968.12525>.
- Sneath, P. H. A. (1962). Longevity of micro-organisms. *Nature*, 195(4842), 643–646.
- Solanki, M. K., Kumar, S., Pandey, A. K., Srivastava, S., Singh, R. K., Kashyap, P. L., et al. (2012). Diversity and antagonistic potential of *Bacillus* spp. Associated to the rhizosphere

- of tomato for the management of *Rhizoctonia solani*. *Biocontrol Science and Technology*, 22(2), 203–217. <https://doi.org/10.1080/09583157.2011.649713>.
- Souza, R., Ambrosini, A., & Passaglia, L. M. P. (2015). Plant growth-promoting bacteria as inoculants in agricultural soils. *Genetics and Molecular Biology*, 38(4), 401–419. <https://doi.org/10.1590/S1415-475738420150053>.
- Suzina, N. E., Muliukin, A. L., Kozlova, A. N., Shorokhova, A. P., Dmitriev, V. V., Barinova, E. S., et al. (2004). Ultrastructure of resting cells of some non-spore-forming bacteria. *Mikrobiologiya*, 73(4), 516–529.
- Taylor, N. G., Verner-Jeffreys, D. W., & Baker-Austin, C. (2011). Aquatic systems: Maintaining, mixing and mobilising antimicrobial resistance? *Trends in Ecology & Evolution*, 26(6), 278–284. <https://doi.org/10.1016/j.tree.2011.03.004>.
- Tetreau, G. (2018). Interaction between insects, toxins, and bacteria: Have we been wrong so far? *Toxins*, 10(7), 281.
- Tetz, G., & Tetz, V. (2017). Introducing the sporobiota and sporobiome. *Gut Pathogens*, 9, 38. <https://doi.org/10.1186/s13099-017-0187-8>.
- Thavaselvam, D., & Vijayaraghavan, R. (2010). Biological warfare agents. *Journal of Pharmacy & Bioallied Sciences*, 2(3), 179–188. <https://doi.org/10.4103/0975-7406.68499>.
- Tocheva, E. I., Ortega, D. R., & Jensen, G. J. (2016). Sporulation, bacterial cell envelopes and the origin of life. *Nature Reviews Microbiology*, 14(8), 535–542. <https://doi.org/10.1038/nrmicro.2016.85>.
- Trabelsi, D., & Mhamdi, R. (2013). Microbial inoculants and their impact on soil microbial communities: A review. *BioMed Research International*, 2013, 863240. <https://doi.org/10.1155/2013/863240>.
- Tsiknia, M., Paranychianakis, N. V., Varouchakis, E. A., Moraetis, D., & Nikolaidis, N. P. (2014). Environmental drivers of soil microbial community distribution at the Koiliaris Critical Zone Observatory. *FEMS Microbiology Ecology*, 90(1), 139–152. <https://doi.org/10.1111/1574-6941.12379>.
- Uyen, N. Q., Hong, H. A., & Cutting, S. M. (2007). Enhanced immunisation and expression strategies using bacterial spores as heat-stable vaccine delivery vehicles. *Vaccine*, 25(2), 356–365. <https://doi.org/10.1016/j.vaccine.2006.07.025>.
- van Bodegom, P. (2007). Microbial maintenance: A critical review on its quantification. *Microbial Ecology*, 53(4), 513–523. <https://doi.org/10.1007/s00248-006-9049-5>.
- von Mering, C., Hugenholtz, P., Raes, J., Tringe, S. G., Doerks, T., Jensen, L. J., et al. (2007). Quantitative phylogenetic assessment of microbial communities in diverse environments. *Science*, 315(5815), 1126–1130. <https://doi.org/10.1126/science.1133420>.
- Widnyana, I. K., & Javandira, C. (2016). Activities *Pseudomonas* spp. and *Bacillus* sp. to stimulate germination and seedling growth of tomato plants. *Agriculture and Agricultural Science Procedia*, 9, 419–423. <https://doi.org/10.1016/j.aaspro.2016.02.158>.
- Wolf, D. M., Vazirani, V. V., & Arkin, A. P. (2005). Diversity in times of adversity: Probabilistic strategies in microbial survival games. *Journal of Theoretical Biology*, 234(2), 227–253. <https://doi.org/10.1016/j.jtbi.2004.11.020>.
- Wu, M., Ren, Q., Durkin, A. S., Daugherty, S. C., Brinkac, L. M., Dodson, R. J., et al. (2005). Life in hot carbon monoxide: The complete genome sequence of *Carboxydotherrmus hydrogenoformans* Z-2901. *PLoS Genetics*, 1(5), e65. <https://doi.org/10.1371/journal.pgen.0010065>.
- Wunderlin, T., Corella, J., Junier, T., Bueche, M., Loizeau, J.-L., Girardclos, S. P., et al. (2014). Endospore-forming bacteria as new proxies to assess impact of eutrophication in Lake Geneva (Switzerland, France). *Aquatic Sciences*, 76(1), 103–116. <https://doi.org/10.1007/s00027-013-0329-0>.
- Wunderlin, T., Junier, T., Paul, C., Jeanneret, N., & Junier, P. (2016). Physical isolation of endospores from environmental samples by targeted lysis of vegetative cells. *Journal of Visualized Experiments*, 107, e53411. <https://doi.org/10.3791/53411>.

- Wunderlin, T., Junier, T., Roussel-Delif, L., Jeanneret, N., & Junier, P. (2013). Stage 0 sporulation gene A as a molecular marker to study diversity of endospore-forming Firmicutes. *Environmental Microbiology Reports*, 5(6), 911–924. <https://doi.org/10.1111/1758-2229.12094>.
- Wunderlin, T., Junier, T., Roussel-Delif, L., Jeanneret, N., & Junier, P. (2014). Endospore-enriched sequencing approach reveals unprecedented diversity of Firmicutes in sediments. *Environmental Microbiology Reports*, 6(6), 631–639.
- Yang, D., Wang, B., Wang, J., Chen, Y., & Zhou, M. (2009). Activity and efficacy of *Bacillus subtilis* strain NJ-18 against rice sheath blight and *Sclerotinia* stem rot of rape. *Biological Control*, 51(1), 61–65. <https://doi.org/10.1016/j.biocontrol.2009.05.021>.
- Yun, J. H., Roh, S. W., Whon, T. W., Jung, M. J., Kim, M. S., Park, D. S., et al. (2014). Insect gut bacterial diversity determined by environmental habitat, diet, developmental stage, and phylogeny of host. *Applied and Environmental Microbiology*, 80(17), 5254–5264. <https://doi.org/10.1128/AEM.01226-14>.
- Zaidi, A., & Khan, M. S. (2007). Stimulatory effects of dual inoculation with phosphate solubilising microorganisms and arbuscular mycorrhizal fungus on chickpea. *Australian Journal of Experimental Agriculture*, 47(8), 1016–1022. <https://doi.org/10.1071/EA06046>.
- Zechman, J. M., & Casida, L. E., Jr. (1982). Death of *Pseudomonas aeruginosa* in soil. *Canadian Journal of Microbiology*, 28(7), 788–794.
- Zhao, H., Msadek, T., Zapf, J., Madhusudan, Hoch, J. A., & Varughese, K. I. (2002). DNA complexed structure of the key transcription factor initiating development in sporulating bacteria. *Structure*, 10(8), 1041–1050.

9. Curriculum vitæ



LEHMANN Anaël

Géologie environnementale

“Avoir une haute capacité d’adaptation, d’analyse du terrain et une grande compréhension et intégration des spécificités naturelles régionales est un standard qui m’importe.”

“Je souhaite m’engager pour conduire des projets qui visent au suivi géologique et environnemental dans une approche multidisciplinaire et collaborative dont l’intégration régionale en est l’essence.”



13 août 1989, 31 ans
Suisse
Marié, 1 enfant



Rue des Chavannes 6
1304 Cossonay Ville



+41 78 697 30 20



lehmann.anael@gmail.com

LANGUES

- Français: Langue maternelle
- Allemand: Indépendant
- Anglais: Compétent
- Russe: Cours d’initiation

LOGICIELS

- Suite Microsoft Office
- Adobe CreativeCloud (dont Illustrator)
- SigmaPlot
- MatLab

COMPÉTENCES ET FORMATIONS EXTRA-PROFESSIONNELLES

- Cours de premiers secours en milieu isolé
- Plongée sous-marine
 - CMAS D***
 - PADI Rescue Diver and Oxygen Provider
 - TDI Advanced Nitrox
- Professeur de ski J+S 3, équivalence degré 1 SWISS SNOWSPORTS
- Membre actif du Club Alpin Moutier (BE)
- Aspirant ceinture noire 1^{er} Dan Taekwondo

EXPERIENCES PROFESSIONNELLES

DOCTORAT en sciences de la Terre, FNS

UNIL | Lausanne VD

2016 - 2021

- Étude des rivières, des lacs, de leurs sédiments, des sols ainsi que de la couverture végétale des régions Okavango-Linyanti-Chobe en Namibie et Botswana
 - Analyses pétrographiques, sédimentaires et géochimiques des sédiments et des sols
 - Analyses géochimiques de la couverture végétale
 - Analyses géochimiques des eaux de surfaces et souterraines
 - Compréhension des processus et des dynamiques environnementaux actuels tels que la dynamique des crues liées à la saison humide
 - Compréhension de la répartition de la composition géochimique de la couverture végétale selon un gradient d’accessibilité à l’eau
 - Reconstruction paléo-environnementale et paléo-climatique du lac Liambezi
- Développement et validation d’une méthode novatrice en microbiologie (séquençage ADN des bactéries sporulantes) en collaboration avec l’institut de microbiologie de l’université de Neuchâtel
 - Préparations et analyses microbiologiques

ASSISTANT DE COURS

UNIL | Lausanne VD

2014 - 2020

- Assistanat du cours degré bachelor “Introduction aux Sciences de la Terre - TP”
- Assistanat du cours degré bachelor “Géochimie générale”
- Organisation et suivi de travaux pratiques degré master traitant du suivi de la qualité des cours d’eau Sorge-Mèbre-Chamberonne ainsi que du lac Léman
- Suivi de deux travaux de master
 - Compréhension des relations végétation-sol dans la région nord-Botswana - Publication scientifique en préparation
 - Compréhension des cours d’eau région nord-Botswana, suivi de la composition et de la qualité des eaux de surfaces et souterraines au travers des saisons

ASSISTANT DE LABORATOIRE

UNIL | Lausanne VD

2013 - 2020

- Gestion des tâches journalières aux laboratoires de recherche
- Calibration et utilisation de spectromètres à gaz et autres équipements
- Mesures isotopiques (C, N, O, S) avec les spectromètres à gaz et traitement de données

MEMBRE DU CONSEIL DE L’ÉCOLE de la FGSE

UNIL | Lausanne VD

2017 - 2020

CHEF TECHNIQUE des camps de ski J+S Berne-Jura-Neuchâtel

J+S | Neuchâtel NE

2016 - 2019

- Organisation et planification des activités
- Supervision des équipes de moniteurs

STAGE DE TAILLEUR DE PIERRE

Calcaires Chappuis sàrl | L’Isle VD

2015

- Création d’une fontaine en pierre, apprentissage des techniques de taillages de pierre

SERVICE MILITAIRE OBLIGATOIRE

Armée | Explorateur d’infanterie

2008

QUALITÉS PERSONNELLES

- Autonome
- Pragmatique
- Organisé
- Méthodique et méticuleux
- Apprentissage aisé

CENTRES D'INTÉRÊTS

- Sports:
 - Plongée, ski, taekwondo, cyclisme, alpinisme, gymnastique, squash
- Culture:
 - Paléanthropologie, histoire, culture générale, géopolitique et géographie
 - Arts modestes et arts graphiques
- Développement du premier musée suisse d'Arts modestes
 - Construction d'une collection déjà riche de plusieurs centaines d'œuvres
 - Projet de site internet
 - Projet de musée

FORMATIONS

MASTER en sédimentologie et géologie environnementale

UNIL | Lausanne VD

2013 - 2015

- Étude de rivières et de dépôts sédimentaires des régions Namib-Naukluft en Namibie
 - Analyses pétrographiques, sédimentaires et géochimiques des sédiments
 - Compréhension des processus de formation et mise en place de sols et croûtes carbonatées dans les régions Namib-Naukluft

BACHELOR en géologie

UNIL | Lausanne VD

2009 - 2013

MATURITÉ GYMNASIALE bilingue français-allemand, section économie et droit

Gymnase bilingue de la Rue des Alpes | Biel/Bienne BE

2005 - 2008

- Travail de maturité portant sur l'étude des mesures de compensations écologiques et de la revitalisation de cours d'eau dans le cadre de l'A16 - Transjurane

COMPÉTENCES

- Travail géologique du terrain: cartographie et échantillonnage des roches, sols et eaux, échantillonnage de la matière organique (dans les sols, la végétation et dans l'eau)
- Analyses minéralogiques, chimiques et isotopiques des roches, sols et des eaux.
- Analyses chimiques et microbiologiques de la matière organique.
- Travail dans les laboratoires de recherche (chimiques, biologiques et isotopiques) et gestion des tâches journalières aux laboratoires de recherche.
- Préparation des échantillons (carbonates, sulfures, sulfates, matière organique) pour les mesures isotopiques de carbone, azote, oxygène, et soufre (lavage, séchage et pesage).
- Travail dans les laboratoires de géochimie isotopique (lavage des échantillons et éprouvettes, et équipement de routine dans un laboratoire de chimie avec acides faibles et eau, eau distillée).
- Mesures isotopiques (C, N, O, S) avec les spectromètres à gaz de laboratoires des isotopes stables.
- Techniques de laboratoires sédimentaires
- 1^{er} secours en milieu isolé

OUTILS

- Microscopie optique
- Microscopie électronique à balayage (MEB) (Scanning electron microscopy (SEM))
- Diffraction de rayons-X (XRD)
- Fluorescence à rayons-X (XRF)
- Spectromètre à gaz (isotopes stables)
- Méthode Rock-Eval
- Qualité et analyse de l'eau
- Manipulation et préparation d'échantillons pour la microbiologie (séquençage ADN)

DOMAINES DE COMPÉTENCE

- Minéralogie
- Amiante
- Géochimie environnementale
- Géochimie organique
- Isotopes stables comme traceurs environnementaux
- Géochimie organique moléculaire et isotopique
- Biominéralisation